SOIL CONSERVATION AND SUSTAINABLE DEVELOPMENT

21-23 August 2021
Dalian | China

LASOSU 2021
International Forum on
Land Degradation, Soil Conservation and Sustainable Development

PREFACE

The 2030 Agenda for Sustainable Development, adopted by all UN Member States in 2015, provides a shared blueprint for peace and prosperity for people and the planet through the Sustainable Development Goals (SDGs). The goals call for a deep international collaboration for the understanding of the main global problems and the search of strategic solutions, giving great importance to environmental questions. In this regard, severe soil degradation (e.g. soil erosion) has become one of the most critical phenomena affecting the Earth's surface. LASOSU2021, the International Forum on Land Degradation, Soil Conservation and Sustainable Development, 2021, will be held on 21-23 August 2021, in Dalian, China, to provide an avenue for scientists to discuss pressing issues on soil loss facing our profession and society.

LASOSU2021 was conceived in March 2020, and the first circular for session proposals was released in June 2020. Presently a total of 259 papers have been accepted, of which 66 are submitted by the first authors outside of China. More than 20 countries have been involved in the conference. The conference includes 2 slots for Keynote Speeches, 1 slot for Focus Group Discussion, and 23 slots for Parallel Sessions. We hope that LASOSU2021 will be the place where we can share our ideas, engage in debate and learn from each other. We also do hope that this event will be followed by others in the coming years. Let us work together to assure the sustainable use of precious global soil and combat the ongoing degradation of the land for an sustainable development. The proceedings are published mainly in the form of e-book publications. In order to further expand the influence of the LASOSU2021 and strengthen the academic exchanges, the papers will be published in the China National Knowledge Infrastructure.

It is worth noting that all papers/abstracts accepted in the proceedings only if their authors have signed the copyright sharing agreements.

The successful publication of this proceeding is particularly grateful to the digital publishing platform of China National Knowledge Infrastructure. Nevertheless, I am afraid that language problems still exist although we have done a great endeavor. We sincerely welcome any comments and criticisms from those who use it.

Conference team of LASOSU 2021

21 August, 2021

Yihang Li, Mingyang Liu, Tian Li, Xiangzhou Xu

Editors

LASOSU2021: International Forum on Land Degradation, Soil Conservation and Sustainable Development, 2021

This book contains the abstracts and full papers accepted in the International Forum on Land Degradation, Soil Conservation and Sustainable Development, 2021 (LASOSU2021). The conference was held with the theme of “Green Mountain & Clear Water” on 21-23 August, 2021, in Dalian, China.

Published as an e-book in August 2021.

Available at: http://meeting.dlut.edu.cn/meeting/list_en.asp?id=2710&nid=1529

Jianguo Liu   Michigan State University (USA)   Academician

Dr. Jianguo (Jack) Liu holds the Rachel Carson Chair in Sustainability, is University Distinguished Professor at Michigan State University (MSU) and serves as founding director of the Center for Systems Integration and Sustainability. Before joining MSU, he did postdoctoral study at Harvard University. Dr. Liu is a world leader in systems integration and sustainability (e.g., integration of ecology with social sciences, policy, and technologies for understanding and promoting global sustainability). He has served on numerous international committees and editorial boards, such as Science and Commission on Sustainable Agriculture Intensification. Dr. Liu also is the founder of the International Network of Research on Coupled Human and Natural Systems (CHANS-Net.org) and a past president of the U.S. Regional Association, International Association for Landscape Ecology. He has received many awards and honors, such as being elected to the American Academy of Arts and Sciences and the American Philosophical Society, Gunnerus Award in Sustainability Science from The Royal Norwegian Society of Sciences and Letters and Norwegian University of Science and Technology, Sustainability Science Award and Innovation in Sustainability Science Award from the Ecological Society of America, and CAREER Award from the U.S. National Science Foundation.

Bojie Fu   Research Centre for Eco-Environmental Sciences, Chinese Academy of Sciences   Academician

Dr Bojie Fu is a distinguished professor of landscape ecology at the State key Lab. of Urban and Regional Ecology, Research Centre for Eco-Environmental Sciences, Chinese Academy of Sciences (CAS). He is the member of Chinese Academy of Sciences, International Honorary Member of American Academy of Arts and Sciences, Fellow of the Academy of Sciences for Developing World (TWAS) and Corresponding Fellow of the Royal Society Edinburgh UK. His research areas are land use and land cover change, landscape pattern and ecological processes, ecosystem services and management. He has published more than 400 scientific papers and 12 books, including Science, Nature, Nature Geoscience and Nature Climate change. His prizes include the Alexander von Humboldt medal of EGU. China National Natural Science Prize, Outstanding Science and Technology Achievement Prize of CAS, The Ho Leung Ho Lee Science and Technology Prize-Geosciences, and Award of Distinguished Service of the International Association of Landscape Ecology.

Tingwu Lei

China Agricultural University **Professor**

Agricultural Soil-Water Engineering, Department of Hydraulic Engineering, College of Water Resources & Civil Engineering, China Agricultural University, Beijing, China. His research interests are mainly on soil erosion mechanism, monitoring of sediments and runoff from hillslopes and watersheds and efficient use of water in agriculture. He has been working infiltration measurement methods and automatic measurement system. He developed hillslope flow velocity measurement methods, including computational models and automated measurement system. He worked on the experimental and computational as well as simulation methods for rill erosion and meltwater erosion of frozen soils, and developed system for monitoring soil and water losses from runoff plots and watersheds.

Vincenzo D' Agostino

University of Padova (Italy) **Professor**

Prof. Vincenzo D'Agostino has enrolled as Full Professor of Soil conservation in mountain catchments since 2018. Since the 2019 he covers the position of Head of TESAF Department, University of Padova (UNIPD).

The research activity (more than 100 papers published) deals mainly with river dynamics, active/passive protection measures against river and hillslope erosion, innovative works for torrent control, flood modelling in mountain streams, and hazard mapping of debris flows and snow avalanches. He also performed physical modelling investigations at the Giovanni Poleni Lab. (UNIPD), at the National Sedimentation Lab. (USDA, Oxford, Mississippi), and at the National Research Center (CNR, for geo-hydrological protection). These researches are focused on local erosion downstream of a dam, on the evaluation of the bedload transport for very rough beds, and on debris-flow travel distance. Prof. D'Agostino has been involved in EU environmental research-projects (EROSLOPE I and II), DAMOCLES Project (FTP5 Programme EU) and in a number of national programs, including collaboration with local authorities in Interreg EU projects. He is now coordinating for UNIPD the LIFE Climate Governance and Information, Project LIFE 17 GIC/IT/000091 "BEWARE" BEtter Water-management for Advancing Resilient-communities in Europe (2018-2022)..

Chongfa Cai

Huazhong Agricultural University **Professor**

Dr. Chongfa Cai is currently a Professor of Soil Science at College of Resources and Environment, Huazhong Agricultural University, China. He works in the broad area of Soil Erosion and Agricultural Ecology: soil structure and interaction mechanism of Ultisols (Subtropical China), soil erosion and hydraulic processes, agroforestry models and technologies in subtropical region, soil geography and soil quality evaluation, regional agric-ecological environment, improvement of cultivated land in red soils, soil erosion mechanism and ecological restoration in hilly and mountainous areas of southern China. He also took charge of more than 20 projects of the National Natural Science Foundation Emphases Item of China and the National Science and Technology Planning Projects. He has published more than 100 papers in reviewed journals, 6 academic monographs. Dr. Cai was the president of Key Laboratory of Arable Land Conservation (Middle and Lower Reaches of Yangtze River) in Ministry of Agriculture (2010-2016), and the president of Hubei Provincial Soil and Fertilizer Society, and is one of the executive directors for Soil Science Society of China. He is an editor of ACTA PEDOLOGICA SINICA, Journal of Soil and Water Conservation and Soils.

Paulo Alexandre da Silva Pereira

Mykolas Romeris University (Lithuania) **Professor**

Geographer, Full professor at Mykolas Romeris University (Lithuania) and invited full professor at Beijing Normal University (China) is a recognized researcher in Land Degradation, Ecosystem Services and Nature-Based Solutions. He published more than 450 publications in books, peer-reviewed articles and conferences. Paulo received several international prizes (e.g., e.g., “Doctor Europeaus”, “European Geosciences Union Soil System Sciences Division Outstanding Young Scientist Award”). In 2020 was identified as one of the world most cited researchers (Clarivate Analytics Highly Cited Researcher”. In 2021 was elected as a full member of the world most prestigious scientific research honour society Sigma Xi and identified as one of the persons that achieve the highest level in his scientific field in Lithuania. He serves or served as editor in several journals of global prestige. e.g., Science of the Total Environment; Geography and Sustainability; Geoderma; Environmental Research; Current Opinion on Environmental Science and Health, Catena, Journal of Environmental Management). Presently he is working with researchers from the entire world (e.g., China, Brazil, Australia, the USA, Portugal, Spain, Croatia and Italy). He is one of the Fire Effects On Soil Properties International Network (FESP-IN) coordinators and a member of the Geography for Future Earth Coupled Human-Earth Systems for Sustainability (IGU-GFE).

Roberto A. Peiretti   Argentine No-Till Farmers Association (Argentina)   Professor

Roberto A. Peiretti is from Argentina, South America. He professionally worked in developing, adapting and promoting the adoption of the No Till System which is a highly evolved and sustainable farming system. He acted as the advisor and consultant nationally and internationally. He also acted as a very active national and international lecturer. He visited more than twenty five countries offering presentations related to No Till System in more than eighty conferences. He is a founder member of the steering committee of AAPRESID (Argentina No Till Farmers Association www.aapresid.org.ar) 1990-2005. He is a founder member and president for two terms of CAAPAS (American Confederation of No Till Farmers Associations) www.caapas.org. He wrote a large number of papers, technical publications and book chapters. He received several distinctions during his professional life, for example, the "Gold Medal" for the "Best Academic Performance " awarded by Cordoba National University, Argentina",1971. He was distinguished by WASWAC (World Association of Soil and Water Conservation) with the DEA recognition (Distinguished Extensionist Award 2016 (www.waswac.com).

Fenli Zhen   Institute of Soil and Water Conservation, Chinese Academy of Sciences   Professor

Prof. Fenli Zheng is full Prof. of Institute of Soil and Water Conservation. Currently, she is director of China-US Joint Center for Soil and Water Conservation and Environmental Protection, a member of executive board directors of World Soil and Water Conservation association, vice editor of International Soil and Water Conservation Research. She got Ph.D from Institute of Soil and Water Conservation, Chinese Academy of Sciences in 1997. Since 1986, she published more than 200 papers, nine books, and got several scientific and technological awards for different departments. Her major research fields are as follows: 1) water erosion process, mechanisms and prediction model, 2) climate change impact on agricultural soil and water environment, 3) soil erosion impacts soil productivity; 4) climate change and LUCC on river runoff and sediment. Since 1996, more than 20 research projects have been in charge, the most of projects were financial supported from Chinese Natural Science Foundation, Ministry of Sciences and Technology (MOST), Ministry of Agriculture, and Chinese Academy of Sciences. .

Chi-hua Huang

USDA-Agricultural Research Service (USA) **Professor**

Dr. Chi-hua Huang is a Soil Scientist and the Research Leader at the USDA-Agricultural Research Service (ARS) - National Soil Erosion Research Lab, West Lafayette, IN. Dr. Huang is also an Adjunct Professor of Agronomy, Purdue University. His research is focused on the quantification of surface boundary conditions affecting sediment and chemical transport on the landscape, as well as on the development of innovative research techniques for soil erosion process research. Chi-hua received BS from National Chung-Hsing University (Taiwan, China), MS from Washington State University and PhD from Purdue University, with all degrees in Soil Science. He was a Post Doc at Univ. Arizona and a Research Scientist at CSIRO (Australia) and Purdue Univ. before joining ARS in 1998. Within ARS, Chi-hua has served several acting leadership positions in ARS, i.e., Acting National Program Leader for Soil Erosion, Acting Associate Director (Midsouth Area and Midwest Area) and Acting Deputy Administrator (Natural Resources). Chi-hua has been the US Coordinator for the Sino-US Joint Centers for Soil Conservation and Environmental Protection established in 2005 between USDA and Chinese Ministry of Science and Technology. In 2017, he received the Distinguished Career Award from the Association of Chinese Soil and Plant Scientists in North America.

Baoyuan Liu

Beijing Normal University **Professor**

Dr. Baoyuan Liu is a Professor of in Beijing Normal University of China. His research interests include Soil erosion processes and prediction modeling, soil erosion research methods, regional soil erosion survey and assessment, and assessment of soil conservation measures, etc. He developed Chinses Soil Loss Equation and led National Soil Erosion Survey. He has led multiple projects such as Key projects from National Natural Science Foundation and National Science and Technology Planning Projects in China, and EU cooperation projects, and published more than 200 papers in peer reviewed journals. He is currently the director of State Key Laboratory of Soil Erosion and Dryland Farming on the Loess Plateau.

Fei Wang — Institute of Soil and Water conservation, Chinese Academy of Sciences — Professor

Professor Dr. Fei Wang, Deputy Director of Institute of Soil and Water conservation, Chinese Academy of Sciences and Ministry of Water Resources, Northwest A&F University. His research advances understanding of sustainable land management (SLM) focusing on: the environmental, economic and social impacts of land degradation and restoration, assessment and designing locally suitable technologies and approaches for SLM, and environmental policy development based on science and stakeholders involved. He is the Deputy President of the World Association of Soil and Water Conservation (WASWAC) , Director of Committee of Young Scientists, Chinese Association of Soil and Water Conservation, Co-Chair and Steering Committee Member of DesertNet International (DNI), Expert of UN Intergovernmental Science-Policy Platform on Biodiversity and Ecosystem Services (IPBES)and UNEP- the Sixth Global Environment Outlook (GEO-6), Proposal evaluator of National Natural Science Foundation of China (NSFC), Horizon2020 of European Commission, the Italian Projects of National Interest (PRIN) , the Editor-in-Chief of Bulletin of Soil and Water Conservation. He has been involved in than 20 (inter-)national projects funded by CGIAR, EU Horizon2020 and FP6, NWO Council of the Netherlands and National Natural Science Foundation of China (NSFC), MOST and CAS of China. He published more than 150 peer-reviewed articles on professional journals, such as Hydrology and Earth System Sciences, Journal of Hydrology, Science of The Total Environment, Remote Sensing, CATENA, Ecological Engineering, etc., in Chinese and English in which correspondingly for more than 80 articles.

Paolo Tarolli — University of Padova (Italy) — Professor

Personal introduction:

Paolo Tarolli is Deputy President of the Natural Hazards Division of the European Geosciences Union (EGU), and Vice President of Soil and Water Conservation Division of Italian Association of Agricultural Engineering (AIIA). Professor in Integrated Watershed Management and Water Resources Management, and Principal Investigator of Earth Surface Processes and Society research group at University of Padova (Italy). He is also Visiting Professor at Dalian University of Technology (P.R. China), and Adjunct Professor at University of Georgia (USA) and Alexandru Ioan Cuza University of Iași (Romania). Chief Executive Editor of the journal Natural Hazards and Earth System Sciences (NHESS), Associate Editor of Land Degradation & Development and Remote Sensing, Editorial Board Member of International Soil and Water Conservation Research, Earth Surface Processes and Landforms, Geography and Sustainability, Anthropocene, Journal of Mountain Science.

Scientific activity:

He is expert in digital terrain analysis, earth surface processes analysis, natural hazards, geomorphology, hydro-geomorphology, lidar, structure-from-motion photogrammetry; new research directions include the analysis of topographic signatures and impact of human activities, focusing on agricultural landscapes & land degradation. He is the author of over 350 scientific publications printed in international and national journals, and conference proceedings (Scopus, total number citations > 4700; H-index = 38). In 2020 he was ranked in the list of 100,000 top world's most cited scientists (source PLOS Biology, based on Scopus).

Altaf Ali Siyal

Mehran University of Engineering & Technology, Jamshoro (Pakistan) **Professor**

Prof. Dr. Altaf Ali Siyal is currently working as a Chairman and Director of ORIC at Sindh Agriculture University Tandojam, Pakistan. In 2011, he got Endeavour Research Fellowship funded by the Australian Government for Postdoctoral Research at CSIRO-ATSIP, Townsville, Australia. Dr. Siyal was also awarded Fulbright Fellowship to conduct Post-Doctoral Research at the University of California and the USDA-ARS Salinity Laboratory, Riverside, the USA, during 2007-8. He got his Ph.D. from Cranfield University, the United Kingdom (UK), in 2001, funded by the Ministry of Education, Government of Pakistan. He earned his Master's degree in Irrigation & Drainage and Bachelor's degree in Agricultural Engineering in 1990 from the Sindh Agriculture University Tandojam, Sindh, Pakistan.

Dr. Siyal has expertise in Remote Sensing Applications, GIS, Soil and Water Conservation, Irrigation and Drainage, Soil Salinity and Erosion, and Land Reclamation. He received training on 'GIS and Remote Sensing Applications for the Water Sector' from UNESCO-IHE, Delft Netherlands, under Netherlands Fellowship Program (NFP). He also got different training in GIS and Remote Sensing Applications from the University of Maryland USA, under Borlaug Fellowship, and from SUPARCO, Pakistan. He has published more than 60 research articles in International Journals and wrote many articles on soil, water, agriculture, and environment-related issues printed in local and national newspapers. He also has remained a consultant for Sindh Government, Pakistan on "Micro Irrigation Methods" and Asian Development Bank (ADB) for the "Sindh Coastal Resilient Project."

Duihu Ning

World Association of Soil and Water Conservation **Professor**

Prof. Duihu Ning , President of World Association of Soil and Water Conservation, Executive member of the council of Chinese Society of Soil and Water Conservation, Former Deputy Director of International Research and Training Centre on Erosion and Sedimentation. He has successively participated in administration, research and international cooperation of soil and water conservation works. Including the management of national key projects construction, the planning on key projects and on national medium and long term development, the supervision of large and medium sized construction projects, policy study of soil and water conservation in China. Since 2009 he has focused on the studies on soil and water loss classification, quantitative measurement and calculation of soil erosion caused by construction projects. Presided over the formulation of water conservancy industry standard "Guidelines for Measurement and estimation of soil erosion in Production and Construction Projects". Professor Ning is a deputy chief editor of "International Journal of Sediment Research". He founded and has been administrating the top journal on soil and water conservation--International Soil and Water Conservation Research.

Chi Zhang

Dalian University of Technology **Professor**

Chi Zhang is a professor of water resources management at Faculty of Infrastructure Engineering, Dalian University of Technology and currently the dean of the faculty. He is a recipient of the Distinguished Yong Scholar Award from the National Natural Science Foundation of China, and the ChangJiang Scholar from the Ministry of Education, China. He is the director of the Key Laboratory of Water Resources Regulation and Flood Control of Liaoning Province and serves on the Committee of China Society of Natural Resources, and the Global Water Partnership China. He is currently serving as the associated editor for Journal of Water Resources Planning and Management, and Journal of Hydrology and Environment Research.

Prof. Zhang's research focuses on developing and applying computer models, data analytics and artificial intelligence tools to tackle water challenges in reservoir operation, water environment and ecology, and smart water. His is the PI for more than 10 nation-level grants and 30 consulting projects. He has published more than 90 academic papers, and been granted two first prizes of the provincial and ministerial-level awards. The achievements have been successfully implemented in the national "South to North Water Diversion" project, and "East to West Water Diversion" project of Liaoning Province.

Weiguo Li

Water Bureau of Dalian Government **Director**

Wenlong Wang Institute of Soil and Water Conservation, Chinese Academy of Sciences Professor

Wenlong Wang, male, born in 1964, Ph.D., Professor, Doctoral supervisor. The director of the Soil Erosion Professional Committee of the Chinese Society of Soil and Water Conservation, the director of the Chinese Society of Desert Control and Sand Industry, the deputy director of the Academic Committee of the Key Laboratory of Ecological Restoration of Shaanxi Province, and the member of the Academic Committee of the Key Laboratory of the State Forestry Administration of Soil and Water Conservation and Ecological Restoration of the Loess Plateau, Invited Deputy Chief Editor of "Water Conservancy and Hydropower Technology" magazine. He has presided over more than 30 national, provincial and ministerial projects. The main researches are soil erosion process and mechanism, water and soil conservation in construction projects. He has won 3 first prizes, 1 second prize and 1 third prize for scientific and technological achievements at the provincial and ministerial level, participated in the compilation of 2 research books, and published more than 160 papers, of which more than 50 were included in SCI/EI.

Giacomo Scarascia Mugnozza Italian Society of Agricultural Engineering Professor

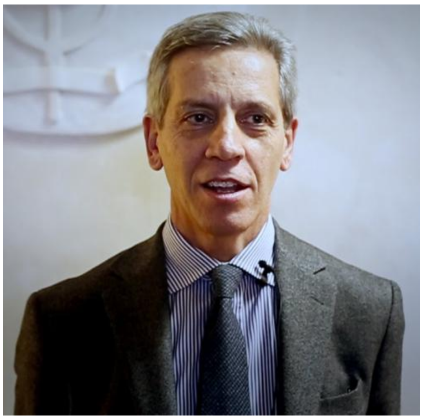

Personal introduction:

President of the Italian Association of Agricultural Engineering (AIIA). Graduated with honors in Civil Engineering, he is Full Professor of Rural Construction at the University of Bari. From 1991 to 1999 he taught at the University of Foggia and the University of Basilicata in Potenza. From 2004 to 2007 he was President of the Board of the Degree Course in "Forestry and Environmental Sciences", from 2006 to 2010 he was Director of the Inter-University Research Doctorate School, University of Bari and Polytechnic of Bari, in "Government of the Territory and of the Environment"; from 2007 to 2018 he was, first, Director of the Department of "Planning and Management of Agro-zootechnical and Forestry Systems" and, then, of the Department of "Agro-Environmental and Territorial Sciences". From 2015 to 2018 he was a member of the Academic Senate of the University of Bari Aldo Moro.

Scientific activity:

He was scientific director of numerous national and European research projects. He carried out his scientific activity in the field of Agricultural Engineering and Rural Construction and Agroforestry Territory, with particular regard to: structures, materials and systems for agricultural constructions; greenhouses for plant breeding in microgravity space; the influence and sustainability of buildings on the territory and on the agro-forestry environment; the recycling and reuse of construction materials and agricultural plastics; energy efficiency, renewable energy sources and distributed micro-generation in agriculture. He is the author of over 250 scientific publications printed in international and national journals, and conference proceedings (Scopus, total number citations > 1600; H-index = 23)..

Rui Li

Institute of Soil and Water Conservation, Chinese Academy of Sciences Professor

Professor Rui Li graduated from Department of Biology, Lanzhou University in 1970. Since 1971 he has been involved in research on soil and water conservation in Institute of Soil and Water Conservation(ISWC), Chinese Academy of Sciences CAS）and Ministry of Water Resources(MWR). His main research fields include land resources investigation and evaluation, regional impacts of soil and water loss and conservation on environment, Soil and water conseravtion planning, Remote sensing application for soil erosion monitoring. He finished more than 30 international and national research projects as leader or key scientist. He has more than 150 papers published on the journals and international conferences and 15 books published as the chief editor or co-editor.

Now he is a retired research professor of Institute of Soil and Water conservation, CAS\MWR and NWUAF, He used to be the president of World Association of Soil and Water Conservation (WASWAC) in 2011-2019 and he is the Honorary President since 2020.

Zhanbin Li

Xi' an University of Technology Professor

Professor Zhanbin Li is an Associate President and Professor of Xi'an University of Technology. His Research interests includes Catchment sediment and Eco-Hydraulics research.

Honors and Awards: "Hundred Talents Program" in Chinese Academy of Sciences; Second prize of the National Science and Technology Progress (Rank 1th)

Concurrent Academic: Associate Chairman of Soil and Water Conservation Commission of International Union of Soil Sciences (IUSS); Director of the Western Ecological Environment Collaborative Innovation Center; Chairman of State Key Laboratory of Soil Erosion and Dry-land Farming on the Loess Plateau (2011-2015); Editorial Board Member of International Journal of Soil and Water Conservation.

Academic Achievement: Published more than 10 Books; Published more than 200 International Journal papers. (1) Created catchment erosion energy theory and prediction runoff and sediment evolution in Loess Plateau (2) Catchment sediment control technology based on decentralized reduction of runoff erosion energy theory (3) Improving safety of gully remediation project and runoff and sediment utilization.

Qiangguo Cai University of Chinese Academy of Sciences Professor

Ph.D., Professor, Ph.D.advisor Key Lab of Water Cycle and Related Land Surface Processes， Institute of Geographical Sciences and Natural Resources, Chinese Academy of Sciences， University of Chinese Academy of Sciences. The State Council awarded the government science and technology special allowance. Ph.D., Physical Geography, M.S., Physical Geography, Institute of Geographical Sciences and Natural Resources Research; B.S., Geography, Peking University. Completed and undertake a number of key projects of national natural science fund, projects and major projects of the Chinese Academy of Sciences, Ministry of Science and Technology project 973, and a number of provincial ministries and research projects. Presided over the four Chinese Canadian cooperative research projects and a number of cooperation with Hong Kong research projects. Three times won the second prize of natural science, Chinese Academy of Sciences, was awarded a prize of excellent papers of the 4th Chan Ning sediment science progress award, the first prize of Science Progress of Shaanxi Province, the second prize of Science and Technology Progress of Shanxi Province, the second prize of Mountain Entrepreneurship of Hebei Province twice, and the Ministry of Water Resources awarded the national Advanced Individual of Soil and Water Conservation. Published three monographs, edited and published six proceedings, and published more than 390 academic papers at home and abroad, including 36 SCI papers and 27 EI papers. The executive director of The Chinese Society of Soil and Water Conservation, the vice chairman of the Beijing Society of Soil and Water Conservation, the honorary chairman of Cross-strait Environmental Resources and Ecological Conservation Association(CERECA), and the honorary director of the Academic Committee of shandong Provincial Key Laboratory of Soil and Water Conservation and Environmental Conservation in Linyi University. Incumbent deputy editor "China soil and water conservation science", Editorial board of "Journal of soil and water conservation", "bulletin of soil and water conservation", "Journal of Beijing forestry university", "International Journal of Sediment Research". “International Soil and Water Conservation Research”.

Guobin Liu Institute of Soil and Water Conservation, Chinese Academy of Sciences Professor

Professor Dr. Guobin Liu studied forestry at the Northwest A&F University Yangling Shaanxi, China, and holds a M.Sc. and Ph.D. in Institute of Soil and Water Conservation, Chinese Academy of Sciences and Ministry of Water Resources and got a position in the Institute since 1985, Since 1991, he was appointed as the director of Ansai Station, department of science and technology, deputy director and director of the Institute (2010-2019). He is Committee member of Science and Technology of Ministry of Water Resources, Council Member of Beijing Forestry University and Vice chairmen of Chinese Soil and Water Conservation Society

Dr. Liu Guobin has more than 35 years soil conservation and watershed management professional experience, particularly in vegetation restoration, integrated management of watershed and benefit assessment as well as strategy of regional soil conservation and rehabilitation in Loess Plateau of China. He also involved in planning of National Project and Chinese Academy of Sciences Action on soil conservation and ecological restorations, and as a principal investigator undertaken the national project from Ministry of Sciences and Technology continue for 20 years.

Xiaoying Liu International Research and Training Centre on Erosion and Sedimentation Professor

Dr. Xiaoying Liu is currently a Professor of the International Research and Training Centre on Erosion and Sedimentation(IRTCES) and the China Institute of Water Resources and Hydropower Research(IWHR). He works in the area of soil erosion, wind erosion model, mechanism of soil and water conservation effects on watershed sediment, reservoir sedimentation model(Re-RESCON Model), global and large scale key ecological project assessment model and soil and water conservation legal system and monitoring indicators. He has also been in charge of more than 50 projects of the National Science and Technology Planning Projects and UNESCO/FAO/UNDP/WB/ADB funded research projects. He has published more than 90 papers in reviewed journals, 8 academic monographs. Dr. Liu has been the Council Member and Treasurer of World Association of Soil and Water Conservation(WASWAC) since 2010 and Secretary General since 2019 and Division Chief of the IRTCES/IWHR since 2012. He is Editorial Board Member of the International Journal of Sediment Research and International Soil and Water Conservation Research. He was served as a water impact assessment expert of Beijing Municipal Bureau of Water Resources , a review expert of key research projects of the Ministry of Science and Technology, and expert of the State Forestry and Grass Administration.

Federico Preti Florence University (Italy) Professor

Personal introduction:

President of Soil and Water Conservation Division of the Italian Association of Agricultural Engineering (AIIA). President of AIPIN Italian Association Soil and Water Bioengineering and delegate for international cooperation in EFIB European Federation. Since 2015 Full Professor at the Florence University (Italy), Department of Agriculture, Food, Environment and Forestry (DAGRI), of Watershed management, Soil slope and torrent stabilization, Soil and Water Bioengineering. Deputy dean of the School of Agriculture, Florence University.

Scientific activity:

His fields of research are: agro-forestry and environmental hydraulics, mainly, processes of runoff (discharge) and transport at watershed scale, non-point pollution sources, vulnerability of soils and water bodies, transport and treatment of pollutants in natural soils, analysis of river quality, analysis of water demand and consumption and management of water resources, irrigation, rainfall-runoff and flood processes, hydraulic risk, criteria for the planning of soil slope and torrent stabilization bio-engineering He is the author of over 300 scientific publications printed in international and national journals, and conference proceedings (Scopus, total number citations > 1400; H-index = 21)...

Guanghui Zhang

Beijing Normal University **Professor**

Dr. Guang-hui Zhang, professor of Faculty of Geographic Science, Beijing Normal University. He got his bachelor degree from Northwest Agricultural University in 1992, and master degree and Ph. D. from Institute of Soil and Water Conservation, Chinese Academy of Sciences in 1995 and 1999. Zhang is the vice director of State Key Laboratory of Earth Surface Processes and Resource Ecology and also the vice director of soil erosion committee, Chinese Society of Soil and Water Conservation. He is an associate editor of International Soil and Water Conservation Research, and the editorial members of Geoderma and six Chinese Journals. His work focus on hillslope hydrology, soil erosion process and soil & water conservation. In the past several years, he was mainly working on the potential effects of vegetation restoration on soil erosion processes and their mechanisms on the Loess Plateau. In the coming five years, the potential influences of vegetation restoration on gully erosion will be studied on the Loess Plateau. The promoting approaches of degraded black soil will also be investigated in the coming years in Northeast China. Zhang has published 200 papers and the total cited number is more than 6780.

Xiangzhou Xu

Dalian University of Technology **Professor**

Prof. Dr. Xiangzhou Xu is a full professor and Ph.D. supervisor at Dalian University of Technology (China). His expertise includes resource sustainability, soil and water conservation, urban rainwater utilization, and topography measurement. His research focus lies in physical experiments in the laboratory as well as in the field. The Topography Meter developed by him opened a new way for further tracking and measuring the landslides. He is the principal investigator of over ten national, ministerial and provincial projects, including three projects funded by the National Natural Science Foundation of China and one by the Excellent Talent Programs in the Universities of Liaoning Province. He has also won two prizes of the Ministerial and Provincial-Level Science and Technology Awards as the first or third accomplisher. He is the first or corresponding author of over 50 journal articles, and first or co-author of 4 monographs. Two United States patents and 20 Chinese invention patents filed by him has been approved.

Homepage：http://faculty.dlut.edu.cn/xuxiangzhou/en/index.htm

CONTENTS

Part Ⅰ
Outstanding Papers

This section consists of the outstanding papers selected according to the anonymous reviewers.

At-many-stations hydraulic-geometry for six major rivers originated from the Qinghai-Tibet Plateau

Chao Qin*[1], Baosheng Wu[1], Guangqian Wang[1], Ge Wang[1]
1 State Key Laboratory of Hydroscience and Engineering, Tsinghua University, PR China
*Corresponding Author, e-mail: glqinchao@nwsuaf.edu.cn

Abstract
At-many-stations hydraulic geometry (AMHG) has provided a novel way to understand river network development, simulate water flow and retrieve river discharge in data-scared regions. Based on in-situ measurements of six major rivers originating from the Qinghai-Tibet Plateau (QTP), this study verifies the existence of AMHG relations along the rivers and explores AMHG relations for cross sections that are not located in the same river reach. The mainstreams and tributaries of the studied rivers in the southern and the eastern portions of the QTP have satisfactory AMHG relation strengths with $R^2 > 0.9$ for over 60% of the relations. For cross sections located in the same stream order, approximately 60% (9/15) of the AMHG relations have an $R^2 > 0.6$. AMHG strength increases with increasing stream order; this finding reflects the increasing coherence and maturity of the river networks associated with the geomorphic shaping power of increased discharge. Width-AMHG intercepts are larger than those of depth- and velocity-AMHGs for all stream orders. Most of the generated from cross sections located in middle-scale rivers (orders 7-8) are within the observed range. Congruent hydraulics generally increase with an increase in in-situ measured hydraulics when the stream order increases. The AMHG relations existing among cross sections that are not located in the same reach, which is named as cross channel AMHG, indicate linear variability of cross-sectional geometric and hydraulic similarities in the same stream order. The results break the watershed divide boundary control on AMHG and have the potential to provide background knowledge for discharge estimation in mountain rivers located in the QTP.
Keywords: Cross channel AMHG, River networks, Stream order, Qinghai-Tibet Plateau, Yarlung Zangbo River; Lantsang River

1 Introduction

The power laws that hydraulic variables and flow discharges follow are referred to as hydraulic geometry (HG), and they describe the key role of river flow on river morphology (Leopold and Maddock, 1953). These geomorphic relationships were first discovered in the early 1910s by agricultural engineers in northern India and Pakistan to maintain fluvial equilibrium in constructed division channels. The HG theory was then constructed and proposed by Leopold and Maddock in 1953. HG has many notable practical utilities, including geomorphological assessment, routing and optimizing in hydrologic models, flood monitoring, water resource management, design of channel restoration, habitat studies for aquatic organisms and discharge estimates (Shields et al., 2003; Parker et al., 2007; Rosenfeld et al., 2007; Parker and Wilkerson, 2011; Neal et al., 2012; Bieger et al., 2015; Gleason et al., 2018; Kebede et al., 2020; Song et al., 2020). Theoretical research into the practical applications of HG has recently been a hotspot in river dynamics and fluvial geomorphology studies.

At-a-station hydraulic geometry (AHG) relates river width (w), water depth (d), flow velocity (v) and discharge (Q) over the range of discharges experienced at a cross section. Downstream hydraulic geometry (DHG) focuses on a reference discharge for a given flow recurrence frequency and the corresponding width, depth and velocity for cross sections that are downstream along a river. Overall, both the AHG and DHG follow the same empirical equation set:

$$w = aQ^b \tag{1}$$
$$d = cQ^f \tag{2}$$
$$v = kQ^m \tag{3}$$

where a, c and k are hydraulic geometry coefficients and b, f and m are hydraulic geometry exponents. The coefficients and the exponents are constrained by $ack = 1$ and $b+f+m = 1$, respectively, in the equation $Q = wdv$.

Hydraulic geometry and river morphology are interrelated by the frequency of flows and the stream order considering all cross sections in a catchment boundary (Stall and Fok, 1968). Followers tried to explore basin wide hydraulic geometry in account of the idea that "cross sections of a given stream system are interrelated" (Stall and Yang, 1970; Rhodes, 1977). Basin hydraulic geometry, defines the average values of w, d, and v for a given streamflow or for a given flow duration and drainage area, reveals general characters of a given stream network in a hydrologically homogeneous basin (Singh and Broeren, 1989). Following this chain, Gleason and Smith (2014) proposed AMHG, a geomorphic phenomenon that spatially and temporally links river cross sections along a river reach (AHG coefficients and exponents statistically relating w, d, and v to Q). Linear correlations were found between AHG exponents (b, f, m) and log (AHG coefficients) (a, c, k) (e.g., $b = \alpha \log a + \beta$, $f = \gamma \log c + \mu$, and $m =$

χ log $k + \eta$). Therefore, the AMHG for a user-defined length of a river is defined as follows (Gleason and Smith, 2014):

$$w_c = a_{x1,x2,\ldots,xn} Q_{cw}{}^{b_{x1,\,x2,\ldots,xn}} \tag{4}$$
$$d_c = c_{x1,x2,\ldots,xn} Q_{cd}{}^{f_{x1,\,x2,\ldots,xn}} \tag{5}$$
$$v_c = k_{x1,x2,\ldots,xn} Q_{cv}{}^{m_{x1,\,x2,\ldots,xn}} \tag{6}$$

where subscript c refers to "congruent hydraulics", the empirically fit river-specific constants that define AMHG, $a/c/k$ and $b/f/m$ are site-specific AHG coefficients and exponents in Eq. (1)-(3) at each cross section, and subscripts $x1$, $x2$, … xn correspond to spatially indexed cross-section locations (up to n total cross-sections along a river reach).

Although not universally observed on natural rivers, AMHG is frequently verified and comprehensively reflects the relationship between the coefficients and exponents of AHG (Gleason et al., 2018). Some studies sought to verify the empirical relations across a wide range of physiographic settings, while other studies aimed to discover the theoretical basis of AMHG and apply this theory to discharge estimation. In summary, three key subjects related to AMHG research and can be summarized as follows: 1) the existence of AMHG as a geomorphological phenomenon for river reaches across various environments with differing climates, geologies, geomorphologies, soil, among others (Gleason and Wang, 2015; Shen et al., 2016; Barber and Gleason, 2018); 2) the theoretical basis for AMHG, including the calculation and proof of congruent hydraulics (Gleason and Wang, 2015; Barber and Gleason, 2018; Brinkerhoff et al., 2019); and 3) the development of river discharge and sediment estimates based on AMHG and further development of Bayesian AMHG-Manning (BAM) with and without prior in-situ measurements (Gleason et al., 2014; Gleason and Hamdan, 2017; Hagemann et al., 2017; Gleason et al., 2018; Zhao et al., 2019; Brinkerhoff et al., 2020; Flores et al., 2020).

As a geomorphic index, congruent hydraulics depict shared characteristics within a certain range of settings. AMHG suggests that there are a set of width-, depth- and velocity-discharge values that are shared by all cross sections within a river (Gleason, 2015). How to depict the mutual characteristics that are shared between individual cross sections has attracted much attention. Gleason and Smith (2014) found that the relationship between Ln (*AHG coefficients*) and *AHG exponents* of any pair of cross sections in a river reach is linear with a slope equivalent to:

$$\text{AMHG } slope = \frac{b_{x2}\text{-}b_{x1}}{\text{Ln }(a_{x2}\text{-}a_{x1})} \tag{7}$$

Exponent b and coefficient a can be replaced with exponents f, m and coefficients c, k, respectively. Eq. (7) affirms that there should be theoretical $w{\sim}Q$, $d{\sim}Q$ and $v{\sim}Q$ pairs that are shared by all cross sections along a river reach. Gleason and Wang (2015) studied the mathematical basis and geomorphological implications of AMHG. They discovered that AMHG arises from the convergence of rating curves and can be represented by congruent hydraulic pairs ($w_c{\sim}Q_c$, $d_c{\sim}Q_c$, $v_c{\sim}Q_c$), which are temporally and spatially invariable (Barber and Gleason, 2018). However, the existence of congruent hydraulics and their relationships to AMHG have not been thoroughly examined and are not well understood though a series of follow-up researches were conducted (Brinkerhoff et al., 2019). Barber and Gleason (2018) sought to establish correlations between common fluvial parameters and indices to investigate potential driving factors of AMHG for rivers with a strong AMHG presence, and they used 191 rivers in the US to perform this test. However, no correlation between AMHG strength and congruent hydraulics, or average values of in-situ measured discharge, width, depth, and velocity, has been discovered (Barber and Gleason, 2018). Brinkerhoff et al. (2019) investigated the relationships between AMHG strength and local features (cross section morphology, bed slope and boundary roughness) of individual cross sections. They found that a strong AMHG is a result of a strong slope/resistance relationship between the stations used to define AMHG. Congruent hydraulics can either be within or outside the in-situ measured range (Gleason and Wang, 2015). In Barber and Gleason's (2018) research, 118 of the 191 rivers show a strong AMHG with $R^2 > 0.6$. Specifically, over 77% of rivers with strong AMHG and only 30% of rivers with weak AMHG had a Q_c value that fell within the range of observed discharges.

More than 80% of the published papers regarding AMHG are focused on or related to the retrieval of river discharge and sediment data, relying on the applications of remote sensing or photogrammetry. AMHG allows reach-averaged discharge to be estimated where cross-sectional widths can be extracted from satellite data. Gleason et al. (2014) proposed an AMHG-based remote sensing discharge retrieval algorithm, which works for mass-conserved reaches and produced errors within 20%-30% of in-situ measured discharge in different types of rivers. Hagemann et al. (2017) developed the AMHG theory into BAM, which estimates river discharge using physical/empirical flow-law (Manning's equation) and geometric/empirical flow law (AMHG) in a probabilistic manner. Feng et al. (2019) affirmed the possibility of estimating discharge independent of ground-based measurements with BAM. Recently, geo-BAM method proposed by Brinkerhoff et al. (2020) and decile thresholding discharge estimation method developed by Mengen et al. (2020) contribute to a significant improvement in discharge estimation. However, estimation accuracy of the aforementioned method using only satellite-observed cross-sectional width data is not always guaranteed if no previous estimates were made (Hagemann et al., 2017; Brinkerhoff et al, 2020). The availability of gauge data and the accurate estimation of the AMHG can significantly improve the performance of discharge estimations (Bonnema et al., 2016).

As seen from the previous research regarding AMHG, less consideration has been taken into account for those cross sections across river reaches, although parameters across sites were linked and spatial relationships of cross-sectional morphologies were reflected in terms of the same river reach (Shen et al., 2016). This research gap prohibits a deeper understanding of river network distribution as well as the development and application of water flow simulations and estimates of river discharge in a broader scope. As the flowing water and sediment shape the river morphology to some extent, can we expect morphologies of cross sections across river reaches to be linked if they experience a similar stream order? Does AMHG exist across rivers, regions, or other configurations? Therefore, it is necessary to expand the AMHG scope (e.g. across river reaches) to facilitate research on geomorphological assessment, routing and optimizing in hydrologic models, flood monitoring and water resource management, among others.

The Qinghai-Tibet Plateau (QTP), known as Asia's Water Tower, is the origin of ten major rivers flowing through the Asian continent. This region covers a wide range of climates and underlying surface characteristics, including differing geologies, geomorphologies, and soil and vegetation types. Rivers of different stream orders show a wide variety of stream patterns from single-thread to multi-thread and from rock-constrained to free-flow. Whether the rivers in the QTP conform to the AMHG theory or if any spatial distribution can be found for AMHG relations in this region are inquiries that need to be addressed. Width, depth and velocity AMHG has been examined, with studies that have been mainly concentrated on US rivers encompassing a wide range of climate and geologic settings (Gleason and Smith, 2014; Shen et al., 2016; Barber and Gleason, 2018). Weak AMHG relations were mostly concentrated in the area of the western edge of the Rocky Mountains, while a total of five and eleven rivers along the northwest and southeast coasts, respectively, were identified as having statistically strong AMHG (Barber and Gleason, 2018). However, the weak AMHG relations of Rocky Mountains are based on limited dataset, which is worth to be further verified in other mountainous regions (Barber and Gleason, 2018). For mountain rivers located in the QTP, AMHG research is nearly nonexistent according to our literature review. The existence and spatial distribution of AMHG, which has not been confirmed but is thought to be influenced by climate and geomorphology, can be further explored in the complex environments present in the QTP (Barber and Gleason, 2018).

In summary, following are some research gaps regarding AMHG theory and application: (a) AMHG knowledge based on in-situ measurements is very limited for data-scared mountain rivers, which contributes less to understanding of river network distribution and development, and results in low accuracy of discharge estimation in these regions (Hagemann et al., 2017); (b) whether it is necessary to confine the AMHG relations to a given river reach might be questioned; (c) except for slope and flow resistance, how would the spatial features (stream order) affect AMHG strength and congruent hydraulics. Due to the limitations of previous research, this article aims to (1) verify the existence of AMHG relations for mountain rivers located in the southern and the eastern portions of the QTP; (2) explore spatial distributions of AMHG exists for cross sections across river reaches; and (3) discuss the relationships between congruent hydraulics and stream order as well as in-situ measured hydraulics.

2 Data and Methods

2.1 Studied area

The studied region, which includes basins of the upper Yellow River (YR), the Yalong River (YLR), the upper Jinsha River (JSR), the Lantsang River (LCR), the Nu River (NR) and the Yarlung Zangbo River (YLZBR), is mainly located in the southern and the eastern portions of the QTP, which is within the Qinghai, Sichuan, Gansu, and Yunnan provinces and the Tibet Autonomous Region of China (Fig. 1). The total area of the studied region is 130.787×10^4 km^2. To maintain the integrity of the upper Yellow River, portions of the connecting regions between the QTP and the Loess Plateau are included. Similarly, marginal regions that belong to the upper Jinsha River, the Lantsang River and the Nu River are also included in this study, though they are outside the southern and eastern portions of the QTP (Fig. 1). The landscape of the studied region, especially for transient regions, is highly fragmented and heavily influenced by tectonic movement and geological disasters (Qin et al., 2020). Hillslope-channel coupling (high potential of hillslope sediment delivery to streams) affects channel forms in mountainous regions (Hassan et al., 2019). But the studied cross sections of our research are mainly located in straight reaches where rarely suffered from landslides, debris flows, glacial outbursts and other extreme events. The elevation shows a decreasing trend from > 7300 m in the inland QTP to < 150 m in the southernmost area. The annual precipitation increases from 150 mm in the inland QTP to > 4000 mm near the town on Pasighat in the

Yarlung Zangbo River (Ding et al., 2007). The main discharge sources include the melting of the persistent winter snowpack, glacial deposits acting as groundwater reservoirs of the inland QTP and summer rainstorms in the remaining area.

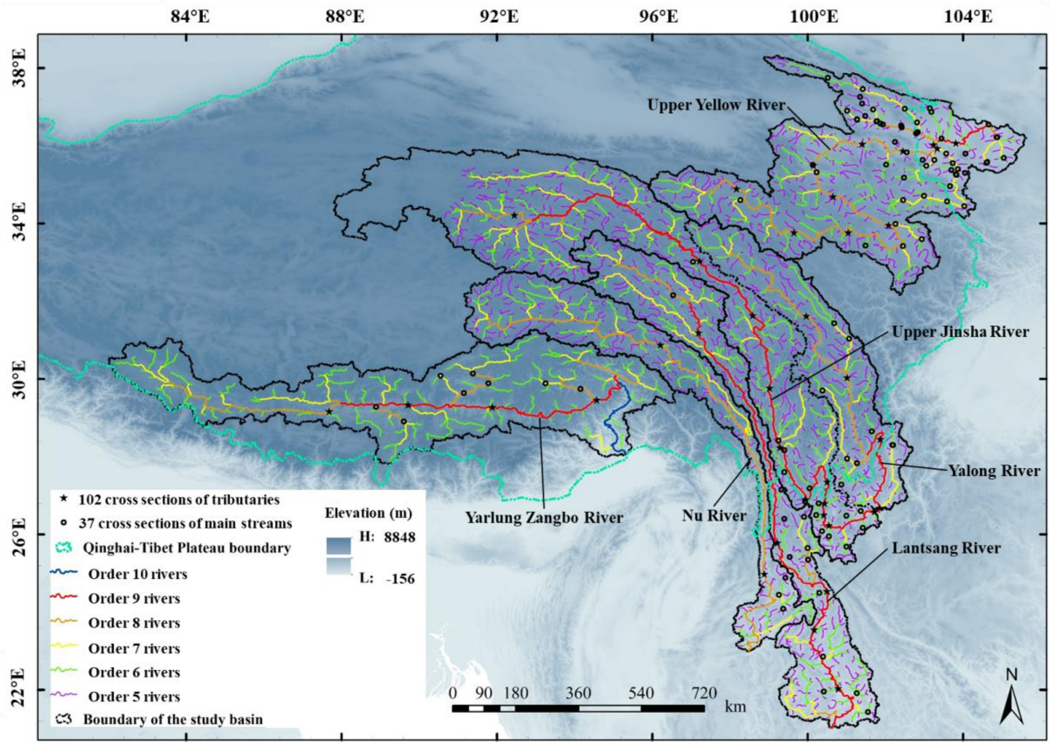

Figure 1 Location of the studied region

2.2 Data collection

The data used in this study were acquired from Annual Hydrological Reports of P. R. China (1967-2017). The measurements of flow characteristics (river width, water depth, flow velocity and flow discharge) and cross-section morphology were conducted strictly in accordance with the national standard of China, "Code for water flow measurement in open channels" (Ministry of Water Resources, P. R. China, 2016). The data set have certain representativeness of mountain rivers. Contributing area, river width, flow depth, flow velocity and flow discharge were within the ranges of 83-259177 km^2, 1.4-420 m, 0.08-21.2 m, 0.05-5.02 m s^{-1} and 0.03-10400 m^3 s^{-1}, respectively. The dataset consisted of 139 river cross sections and covered a wide range of stream patterns from single-thread (represented by straight and meandering rivers) to multi-thread (represented by braided rivers).

The SRTM 90 m DEM (can be downloaded from "http://www.gscloud.cn/") and ArcGIS 10.5 (ESRI Inc., Redlands, CA, USA) were used to generate river networks. Threshold filtering method was used to generate river networks (Mark, 1984; Martz and Garbrecht, 1992). We set a flow accumulation threshold of 40 (equals to 0.324 km^2) after trial-and-error and found that the generated river networks matched the rivers presented in Google Earth images well. The stream orders of the studied region were 1st through 10th, and only the cross sections located in order 5-9 streams were presented in this study because the available measurements were mainly concentrated in rivers of these orders (Fig. 1 and Table 1).

Table 1 Numbers of cross sections at different stream orders

River system	5	6	7	8	9	Total
Upper Yellow River	14	21	17	14	1	67
Yalong River	0	5	4	3	1	13
Upper Jinsha River	0	11	2	2	10	25
Lantsang River	3	5	2	2	5	17
Nu River	1	1	1	2	0	5
Yarlung Zangbo River	0	0	2	7	3	12
Total	18	43	28	30	20	139

2.3 Data Processing

2.3.1 Criteria for data screening

A total of 201 measured river cross sections (obtained from national and regional hydrological gauge stations) are located in the studied area, and 139 of them were selected for analysis in this study. Percentages of the selected cross sections to the total cross sections are 71%, 76%, 74%, 74%, 56% and 50% for the upper Yellow River, the Yalong River, the upper Jinsha River, the Lantsang River, the Nu River and the Yarlung Zangbo River, respectively (Table 1). The criteria for the filtering of river cross sections were as follows: the cross sections should 1) have a consecutive hydrological record length exceeding 10 years; 2) have had relatively low anthropogenic influence (e.g., no hydropower station and artificial diversion 10 km upstream and downstream of the measured cross section; located outside the backwater zone of a dam) during the study time period to maximum remove the external disturbance; 3) keep away from the region where might be affected by extreme events like glacial outbursts, landslides et al.; and 4) act as a natural riverway with perineal drainage. After initial filtering based on these four criteria, cross sections were then re-filtered based on their AHG strength, evaluated by $R^2 > 0.6$ of the power regression for $w/d/v{\sim}Q$ relations to generate reliable and representative AMHG relations and avoid possible bias of data limitations. Due to the significant effects of ice on AHG relations (Qin et al., 2020), data that were affected by border ice, slush ice run and ice cover were excluded. Finally, unrealistic fittings (cross sections with fitted AHG exponents (b, f or m) that were <0) were removed.

2.3.2 Calculation of the AMHG

Power functions depicting the relationships of $Q{\sim}w$, $Q{\sim}h$ and $Q{\sim}v$ were first fitted using the least squares method in MATLAB 2018b. The AHG coefficients, exponents and R^2 of the fittings were recorded. A minimum number of 4 cross sections was used to calculate the AMHG relations in this study. Considering the whole studied region, the AMHG fitted by 4 cross sections (Yalong River, Yarlung Zangbo River) can be regarded as a reference in analyzing spatial distributions when the AMHG relation is strong. Additionally, Barber and Gleason (2018) indicated that no correlation was found between the number of cross sections (>6) used to calculate AMHG and the AMHG strength. Finally, the AMHG of five main streams (excluding Nu River as there were only 2 measured cross sections) and one secondary tributary of the Yellow River (Datong River) were fitted (Fig. 2). The lengths of these six reaches range from 370 to 2744 km, which are longer than those used for discharge retrievals based on remote sensing images (Feng et al., 2019). Mass was not conserved, and discharge increased downstream with the confluence of tributaries.

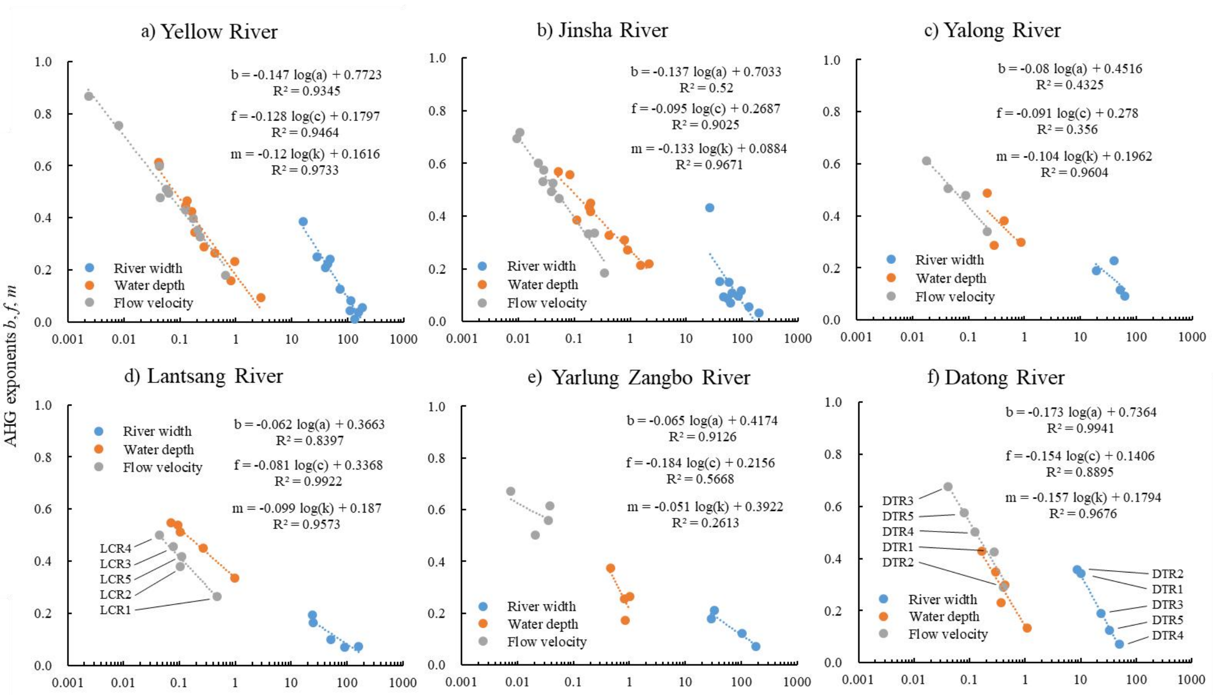

Figure 2 AMHG of five main streams (a-e) and one tributary of the Yellow River (f)

To explore AMHG relations across river reaches, five stream orders (orders 5-9) were considered in account of different clustering modes of cross sections. The following is the AMHG relations of different stream orders (revised from Gleason and Smith, 2014):

$$w_c = a_{x1,x2,\ldots,xn} Q_{cw_{O_i}}^{b_{x1,x2,\ldots,xn}} \quad (8)$$

where the subscripts $x1$, $x2$, … xn correspond to spatially indexed cross-section locations (up to n total cross sections at each stream order), O_i represents the stream order i (i = 5, 6, 7, 8, 9). Similarly, depth-AMHG and velocity-AMHG can be formulated in the same way. Cross channel AMHG, generated from cross sections that are located across river reaches but in the same stream order (Eq. 8), is defined to reflect the hydraulic self-similarity of cross sections and the consistency of AHG coefficients and exponents across reaches.

Gleason and Wang (2015) proposed that the linearity (R^2) of AMHG should be interpreted as a geomorphic index indicating the degree of convergence of AHG curves, the cross-sectional geometric variability, and the hydraulic self-similarity of a given river reach. Therefore, the strength of the AMHG can be represented by R^2 of the fitted AMHG curve. Congruent hydraulic pairs (Q_{cw}, w_c; Q_{cd}, d_c; Q_{cv}, v_c) represent the intersections of the AHG rating curves (Gleason and Wang, 2015). For rivers that exhibit strong AMHG, Q_{cw}, Q_{cd}, Q_{cv}, w_c, d_c, and v_c are given by the spatial mode of the time mean of each of these cross-sectional quantities (Gleason and Wang, 2015). To reach the minimum divergence of the rating curves, two conditions to be met: 1) sufficient variability of the AHG exponents and 2) AMHG where R^2 >0.5 (congruent hydraulics without superscript [b] in Table 2).

Table 2 Congruent hydraulics and their corresponding mean hydraulics clustered by river reaches and stream orders (of six river reaches and those in the same stream order)

Items	Log (Q_{c_w})[a]	Log (Q_{c_d})[a]	Log (Q_{c_v})[a]	Log (w_c)[a]	Log (d_c)[a]	Log (v_c)[a]	Mean Q	Mean w	Mean d	Mean v
Upper Yellow River	6.8	7.8	8.3	5.3	1.4	1.3	725.4	161.9	2.66	1.50
Upper Jinsha River	7.3	10.5[c]	7.5	5.1	2.8	0.7	2029.0	165.3	5.81	1.89
Yalong River	12.5[bc]	11.0[bc]	9.6[c]	5.6[bc]	3.1[bc]	1.9[c]	1619.2	115.6	5.97	1.88
Lantsang River	16.1[c]	12.3[c]	10.1[c]	5.9[c]	4.2[c]	1.9[c]	1857.3	140.5	6.41	2.10
Yarlung Zangbo River	15.4[c]	5.4	19.6[bc]	6.4[c]	1.2	7.7[bc]	1815.3	196.6	5.83	1.24
Datong River	5.8	6.5	6.4	4.3	0.9	1.1	172.6	54.9	1.53	1.54
Order 5 rivers	8.6[bc]	7.5[bc]	11.8[bc]	3.9[bc]	1.3[bc]	4.4[b]	10.1	13.7	0.40	0.94
Order 6 rivers	7.3[b]	8.2[c]	8.2[c]	4.1[b]	1.6[c]	2.4[c]	47.1	28.9	0.86	1.08
Order 7 rivers	8.0	6.4	7.8	4.7	0.9	1.7[c]	139.2	62.8	1.25	1.26
Order 8 rivers	9.4[c]	7.8	8.8	5.3	1.5	1.8[c]	561.7	115.2	2.51	1.45
Order 9 rivers	17.9[c]	9.2[c]	9.8	6.1[c]	1.5	2.7[c]	2139.0	166.1	6.41	1.92

[a] represents natural log, [b] represents the R^2 of the fitted AMHG is smaller than 0.5, and [c] represents the congruent value does not occur within the range of observed values.

3 Results

3.1 AMHG of the cross sections in a given river reach

Data from the six reaches, which include five main streams and one tributary of the Yellow River, were used to explore the relationships between AHG coefficients and exponents along a river reach. In terms of three AMHG relations (width-, depth- and velocity-) for all reaches, there is at least one relation for each reach that has an R^2 > 0.9 (Fig. 2). For the four reaches (Yellow River, Jinsha River, Lantsang River, Datong River) that have > 5 in-situ measured cross sections, the R^2 of the fitted AMHG relations are > 0.8, excluding the width-AMHG of the Jinsha River (Fig. 2 a, b, d, f). The outlier of the width-AMHG of the Jinsha River (shown as a blue circle in Fig. 2 b) corresponds to the Tuotuo River cross section, which is located in a braided reach, while all other cross sections of the Jinsha River (JSR2 to JSR11, Qin et al., 2020) are located in single thread reaches. Stream pattern might be a factor that influence the AMHG relation. However, due to very few cross sections are located in braided reaches, we are unable to generate AMHG relations of braided rivers alone. Cross sections located in all stream patterns are combined in the analysis. Our future work will focus on the classification of stream patterns with the help of remote sensing imagery interpretation. Then, cross sections will be clustered by single-thread and multi-thread river reaches to generate AMHG relations.

Additionally, the R^2 of the width-AMHG is usually smaller than those of the depth- and velocity-AMHGs (Fig. 2). These results agree with previous studies conducted by Gleason and Smith (2014), Gleason and Wang (2015), and Shen et al. (2016). This finding is likely due to the fact that river width is more sensitive to the variations of discharges and boundary conditions than water depth and flow velocity. Random variations of river width are evident while water depth and flow velocity show relatively stable status. Less consistent variations of river widths leads to a weaker strength of width-AMHG.

The relative relations between the depth-AMHG and the velocity-AMHG differ between the Yellow River (including its tributary) and other rivers. The curves of the depth-AMHG and the velocity-AMHG for the Yellow River and Datong River nearly overlap as shown in Fig. 2 a and f. The two curves have similar slopes and intercepts. However, the curves of the depth-AMHG for the remaining river reaches (excluding the Yarlung Zangbo River) are located to the upper right of the velocity-AMHG curves. In conclusion, AHG coefficients and exponents in the same river reach show high correlation on a spatial scale under the original definition for AMHG in the southern and eastern portions of the QTP. Both our study and Barber and Gleason's research (Barber and Gleason 2018) have focused on mountain regions. Strong AMHGs were verified in the QTP region (AMHG strength $R^2 > 0.8$, Fig. 2) while relatively weak AMHGs were observed in the Rocky Mountain area (AMHG strength $R^2 < 0.4$). One possible explanation might be attributed to that the rivers located in west Rocky Mountains own lower stream orders than those of the rivers located in the QTP. Of course, more information of local climate, geology, geomorphology, soil and vegetation et al. are needed for further comprehensive explanations.

3.2 AMHG of the cross sections in the same stream order

3.2.1 AMHG for cross sections of individual river basins

AMHG relations are fitted at different stream orders to explore the existence of AMHG for individual river basins and study the spatial distribution of the AMHGs. The Yalong River is the largest tributary of the upper Jinsha River and merges into the upper Jinsha River in Panzhihua City (26.61°N, 101.81°E) (Fig. 1). Therefore, these two rivers are combined and analyzed in Section 3.2.1 (Fig. 3).

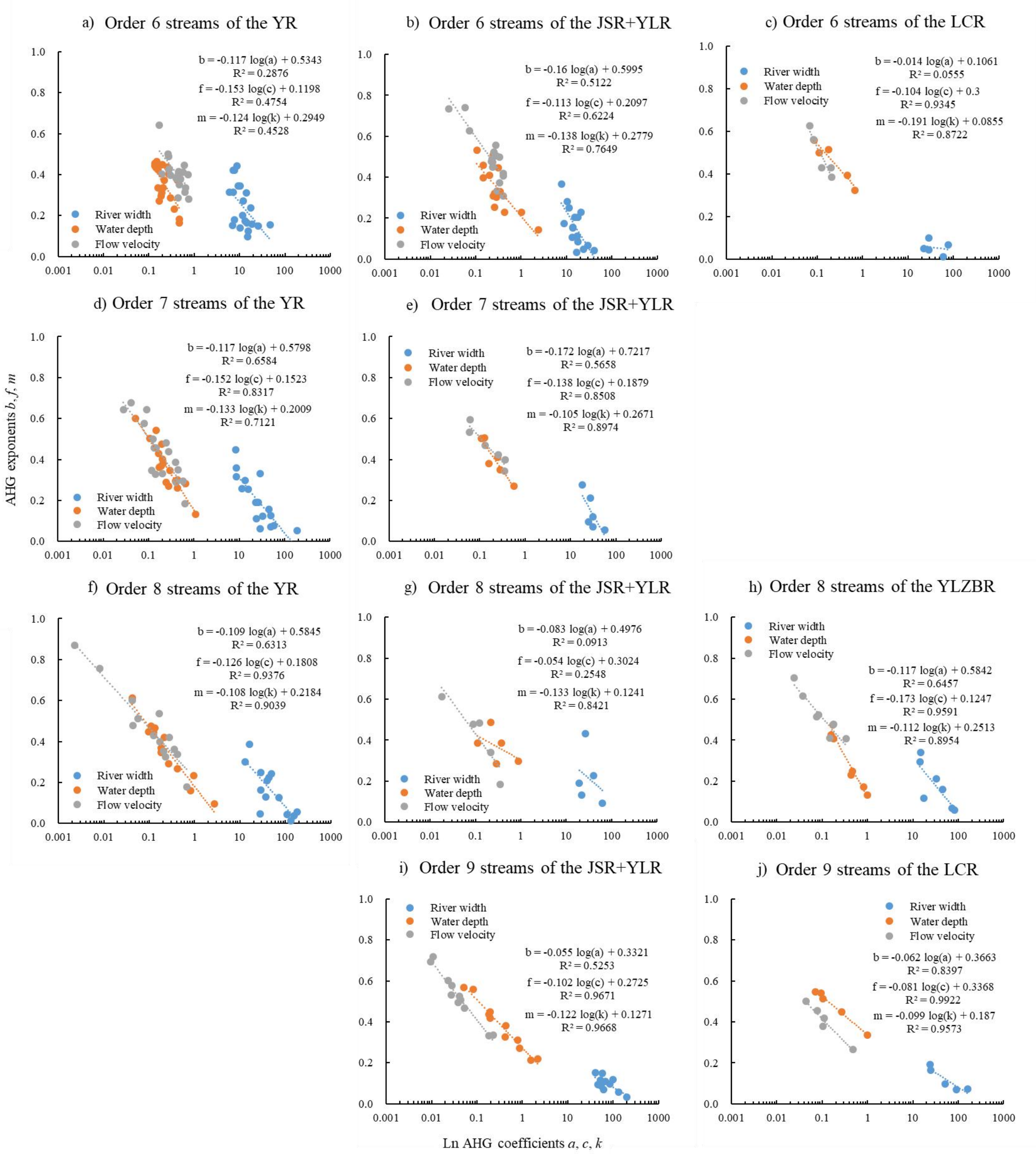

Figure 3 AMHG for cross sections located in the Upper Yellow River Basin, the Upper Jinsha River + Yalong River

Basin, the Lantsang River Basin, the Yarlung Zangbo River Basin at stream orders 6 (a-c), 7 (d, e), 8 (f-h) and 9 (i, j).

When considering the same river basin but different stream orders, the strengths of the three AMHG relations for individual river basins generally increase with increasing stream order, excluding order 8 streams of the Jinsha River + Yalong River, as shown in Fig. 3 g. When considering the same stream order but different river basins, the AMHG exhibits varied spatial distribution. The Yellow River, Jinsha River + Yalong River, and Lantsang River are located from north to south in the eastern part of the QTP. Absolute values for depth-AMHG slopes for these river basins decrease from north to south within the same stream order (Fig. 3). This pattern is potentially because the mean annual discharge generally increases from north to south, which is determined by the local climate and landscape. This result also verifies the increasing trend of Q_{c_w} for all studied reaches from north to south of the eastern QTP (Table 2). Additionally, when compared with the AMHG strength of the mainstream of the Yarlung Zangbo River, the AMHG strength of the cross sections located in order 8 streams of the Yarlung Zangbo River Basin exhibit stronger correlations (Fig. 2 e and Fig. 3 h). Specifically, the depth- and velocity-AMHG strengths of the order 8 streams of the Yarlung Zangbo River Basin are much stronger than those of the mainstream of the Yarlung Zangbo River. This finding implies that stream order may be an appropriate clustering mode for AHG coefficients and exponents.

3.2.2 AMHG for all cross sections in the studied area

Section 3.2.1 determined that AMHG relationships exist in the same stream order of individual river basins but are not belong to a single river reach. This section will extend the range and further explore AMHG relations existing in the same stream order for all cross sections in the studied area (Fig. 4). Generally, the AMHG strength increases with increasing stream order and are mostly $R^2 > 0.6$ (excluding R^2 of order 8 streams) for cross sections located at order 7 and higher streams (Fig. 4). This result can be attributed to the variability of AHG exponents (*f* and *m*), which generally increase when the stream order increases from 5 to 8 (Fig. 5 e and f). However, the width exponents of order 9 streams plot within a relatively small range (0.032-0.192) compared to those of lower order streams (Fig. 5 d), which also result in an $R^2 > 0.6$.

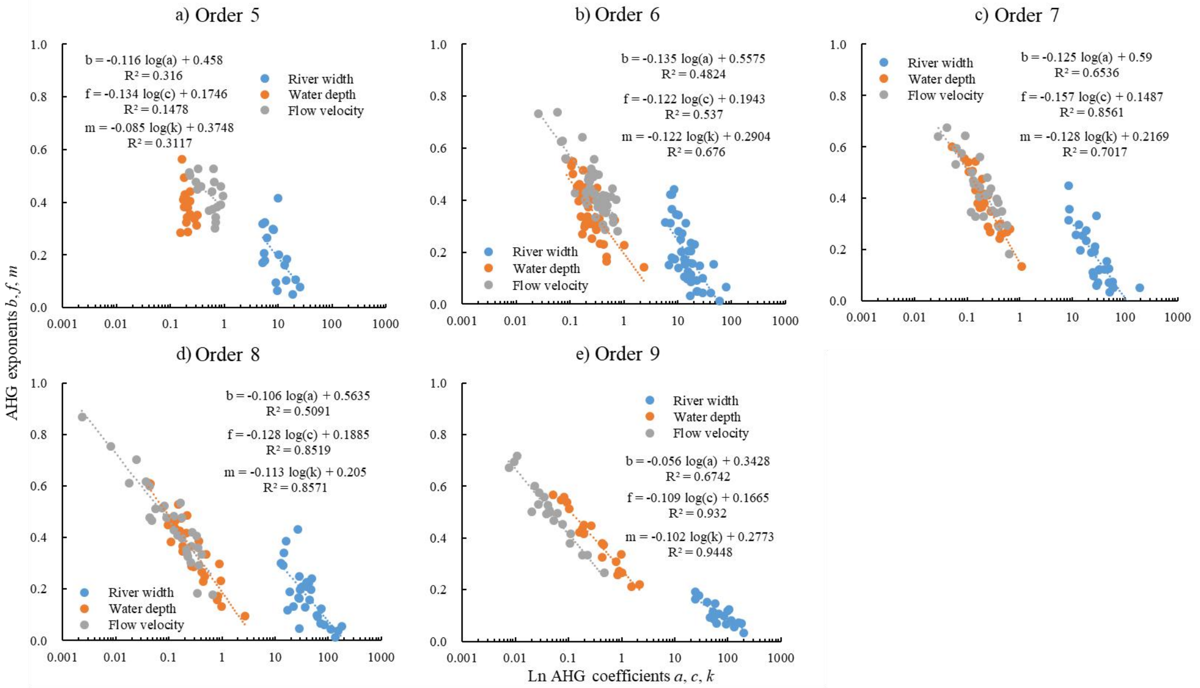

Figure 4 AMHG for all study cross sections located at different stream orders (5-9)

Similar to the AMHG relations of a given river reach (Fig. 2), the strength of the width-AMHG is generally weaker than the strengths of the depth- and velocity-AMHG relations. Compared with the AMHG strengths of the individual river basins (Fig. 3), the AMHG of all studied reaches generally shows equal or weaker strengths (Fig. 4 b-e), with a few exceptions (Figs. 3 a, c, g). Variability of the background environment within a basin is less than that of the whole studied region, which contribute to the increase in AMHG strength of the same river basin.

Relative relationships between the width-, depth-, and velocity-AMHGs change regularly with increasing stream order. Absolute values of AMHG slopes decrease with increasing stream order for all width, depth and velocity curves when the cross sections are located in the order 7-9 rivers (Fig. 4). This phenomenon can be used to explain the increase in congruent hydraulics with increased stream order (Table 2). Specifically, the depth-AMHG curve, which is located in the lower left direction relative to the velocity-AMHG curve, moves towards the upper right and finally plots to the upper right of the velocity-AMHG curve as the stream order increases from 5 to 9 (similarly, the velocity-AMHG curve moves towards the lower left direction with increasing stream order). Similar changes are found for the AMHG relations of individual river basins (Fig. 3). In addition, width-AMHG intercepts are larger than those of depth- and velocity-AMHGs for all stream orders (Fig. 4). Width-AMHG slopes of the order 5 and 6 streams are larger than those of velocity-AMHG slopes, but are smaller for the 7-9 order streams.

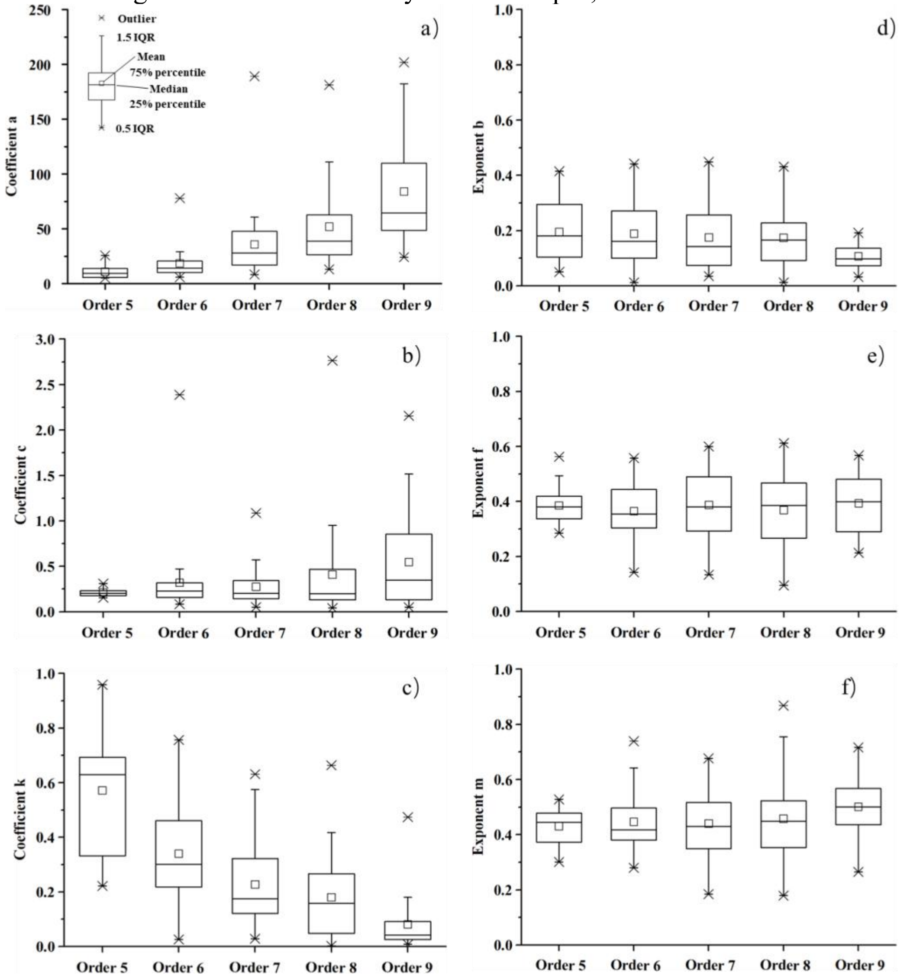

Figure 5 AHG coefficients (a-c) and exponents (d-f) for all cross sections of different stream orders

3.2.3 AMHG for cross sections located in transient regions or inside the QTP

For the cross sections that are located in different river reaches but in the same stream order, we further classified them into two types according to geomorphic units: cross sections inside the QTP and cross sections in transition regions (Table 3). We compared AMHG strengths in the same stream order for: 1) the whole studied region, 2) inside the QTP and 3) outside the QTP but in transient regions connecting the QTP and other geomorphic units (Table 3). Results indicate that AMHG strength overall increase after taking the geomorphic units into account. Compared with those generated by all cross sections, AMHG strengths generated by cross sections located in order 5, 6, 8 and 9 streams increase after taking the geomorphic units into account. For cross sections located in order 7 streams, no significant difference has been observed before and after taking the geomorphic units into account (total difference of AMHG strength (R^2) before and after taking the geomorphic units into account is -0.064). Overall, subdividing cross sections into two geomorphic units (inside the QTP or in transient regions) contributes to the increase of AMHG strength (Table 3).

3.3 Congruent hydraulics for AMHG and their geomorphic characteristics

3.3.1 Characteristics of congruent hydraulics

Stronger AMHG relationships contribute to improved estimations of congruent hydraulics (Gleason and Wang, 2015). AMHGs with an $R^2 > 0.5$ are used for the variation analysis discussed in this section (congruent hydraulics with no superscript ^{b} mark in Table 2). Generally, congruent discharges represented by width, depth and velocity

(Q_{c_w}, Q_{c_d}, Q_{c_v}) show similar variation trends in different item groups (Table 2). The mainstreams of the Yellow River, the Jinsha River, the Yalong River, the Lantsang River and the Yarlung Zangbo River were successively distributed from north to south, excluding the Datong River (Fig. 1). Q_{c_w} shows an evident increasing trend from north to south, while Q_{c_d} and Q_{c_v} exhibit exceptions to this increase in the Yellow River and the Yarlung Zangbo River (Table 2). The Yarlung Zangbo River has the largest w_c, while the Lantsang River has the largest d_c and v_c. Additionally, variations in w_c are smaller than those of d_c and v_c on a spatial scale. Excluding stream orders 5 and 6, all congruent hydraulics strictly increase with increasing stream order (Table 2).

Table 3 AMHG strengths of different stream orders and clustering modes

Stream order	Clustering modes	Strength (R^2)		
		Width-AMHG	Depth-AMHG	Velocity-AMHG
5	All cross sections	0.316	0.148	0.312
	Inside the QTP	0.540	0.431	0.406
	In transient regions	0.256	0.013	0.277
6	All cross sections	0.482	0.537	0.676
	Inside the QTP	0.348	0.705	0.618
	In transient regions	0.548	0.535	0.723
7	All cross sections	0.654	0.856	0.702
	Inside the QTP	0.492	0.811	0.409
	In transient regions	0.848	0.914	0.885
8	All cross sections	0.509	0.852	0.857
	Inside the QTP	0.511	0.894	0.822
	In transient regions	0.567	0.895	0.910
9	All cross sections	0.674	0.932	0.945
	Inside the QTP	0.694	0.976	0.924
	In transient regions	0.698	0.937	0.955

The percentage of rating curves intersecting within the observed discharge range can be used to predict the strength of AMHG (Gleason and Wang, 2015; Barber and Gleason, 2018). Among 96 congruent hydraulics (Table 2), 25% (24 out of 96 congruent hydraulics) are generated from weak AMHG strength items with $R^2 < 0.5$ (with superscript [b] mark), while 50% (48 out of 96 congruent hydraulics) are not within the observed discharge range. For those weak AMHG items, 79% (19 out of 24 congruent hydraulics, with superscript [c] mark in Table 2) are not within the observed discharge range. For those items with strong AMHG, only 40% (29 out of 72 congruent hydraulics) of them are not within the observed discharge range. These results indicate the consistency between the AMHG strength and the percentage of congruent hydraulics falling within the range of observed values for cross sections clustered by different items. Congruent hydraulics of the lower order streams (orders 5 and 6) and the higher order streams (order 9) often plot outside the observed range (Table 2 and Fig. 6). Most of the congruent hydraulics of cross sections located in stream orders 7-8 are within the observed range (Fig. 6).

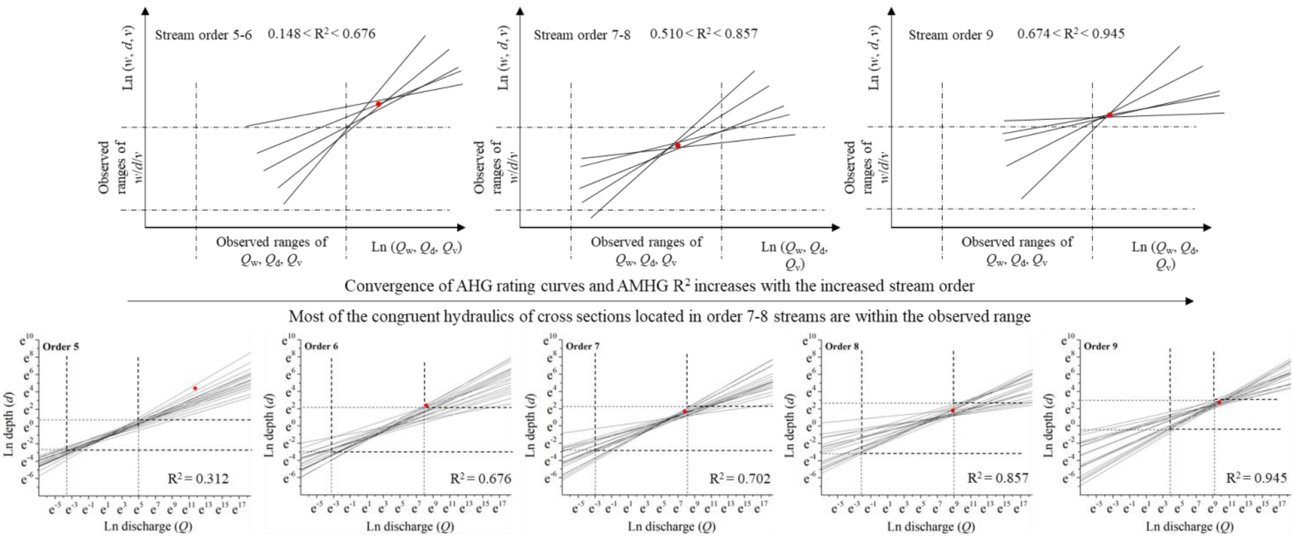

Figure 6 Schematics indicate relationships among congruent hydraulics, observed hydraulic variables and stream order (upper row); depth-AHG rating curves plotted in double logarithm coordinate systems for cross sections located in 5-9 stream orders (lower row). Red dots represent congruent hydraulics, area within dashed lines indicate the values of *w*/*d*/*v*

and Q are within the in situ measured ranges.

3.3.2 Relationships between congruent hydraulics and observed hydraulics

To further study how the congruent hydraulics vary with observed hydraulics, the *congruent hydraulics* and corresponding in-situ measured *mean hydraulics* in Table 2 were plotted as linear functions with stream order (Fig. 7). Congruent w increases significantly with an increase in in-situ measured w when stream order increases. Though this exhibits an increasing trend, the increasing degrees for congruent Q and d are not as strong as that of the congruent w (Fig. 7). The above findings verifies the slight positive trend (R=0.51) observed between mean Q and Q_c found by Barber and Gleason (2018), who determined that Q_c generally increases as the mean Q increases, though the mean Q cannot provide a reliable prediction of Q_c (R^2 = 0.26).

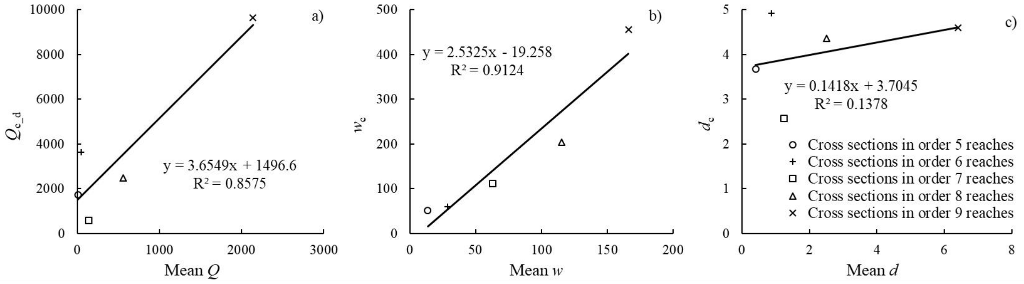

Figure 7 Congruent Q, w, d and in situ measured mean Q, w, d clustered by stream order

4 Discussions

4.1 Discussions on AMHG characteristics

Section 3.1 indicates an irregular array of AHG exponents and coefficients. Specifically, AHG exponents or coefficients along a river reach do not show a strict increasing or decreasing trend from upstream to downstream (Fig. 2 d and f). Set exponents m and coefficients k of the velocity-AHG as an example, m generally decrease with the increase of k. Based on this framework, however, increase of coefficients k and decrease of exponents m conform to the following sequence: DTR3, DTR5, DTR4, DTR1, DTR2 for the Datong River and LCR4, LCR3, LCR5, LCR2, LCR1 for the Lantsang River, respectively (Fig. 2 d and f). Not strict but an overall trends from downstream to upstream can be observed for the increase of coefficients k and decrease of exponents f along a river reach. Similar patterns can be found for coefficients (a, c) and exponents (b, f) of other river reaches (upper Yellow River and upper Jinsha River). Possible explanations might be: with the increased CA and the convergence of tributaries, Q increases downstream, which contributes to overall increasing trends of river width, water depth and flow velocity. Due to complex geology and geomorphology background for mountain rivers in the studied region, adjustments of w, d and v with Q, therefore, do not obey strict increasing law as the lowland rivers do, which leads to some irregularities of the distributions of the coefficients and exponents.

Combining Sections 3.2.1-3.2.3, AMHG does exist in cross sections of the same stream order; however, these cross sections do not belong to the same tributary or mainstream. The Jinsha, the Yalong, the Lantsang, the Nu and the Yarlung Zangbo River Basins exhibit narrow drainage basin shapes while the upper Yellow River Basin, located in northeast QTP, shows a relatively circular shape. Drainage basin shapes in the QTP and its boundary regions are largely controlled by geology and determined by geomorphology background. Large variations of the cross section morphologies in such complex region are expected, which might contribute to weak AMHG strengths. However, the results in Sections 3.2 provide evidence for AMHG as a widespread fluvial phenomenon in the same stream order. The existence of the AMHG that does not belong to a river reach indicates a hydraulic self-similarity of cross sections and a consistency of AHG coefficients and exponents that possibly exist in the same stream order. This consistency is not only shaped by flowing water but also possibly determined by the consistency of local climate, landscape, soil and vegetation. Cross channel AMHG reflects these consistency to a great extent. More tests should be conducted to see whether these AMHGs can exist in a wider geographical range and various climate types.

4.2 Factors affecting AMHG strength

AMHG strength generally increases with increasing stream order. Chi-square tests were used to verify the statistical significance of the increase in AMHG strength. In terms of the relationship between stream order and AMHG strength, the P values of the R^2 for river width, water depth and flow velocity using the chi-square test are 0.094, 0.069 and 0.014, respectively. The increasing trend of velocity-AMHG strength for stream order shows statistical significance with a P value < 0.05, while the other five increasing trends show no statistical significance (P > 0.05). Additionally, the width-AMHG strength shows a less significant increasing trend than those of the depth- and velocity-AMHG strengths.

Barber and Gleason (2018) indicated that the AMHG strength did not correlate to any available observed congruent hydraulics (Q, w, d and v) or the number of cross sections used to fit the AMHG relation. Stream order is not hydraulic parameters, but they are inherent attributes of a fluvial system and comprehensively synthesize characteristics of climate, landscape, soil and tectonic movement in the studied region. Several reasons contribute to the increase in AMHG strength with increased stream order:

1) Cross-section morphology is shaped by the geology, geomorphology, fluvial processes (water and sediment) and even tectonic movement present in the studied region. Lower-order streams (order 5 and 6 streams), representing an integrated record of past head cutting, bed incision and bank collapsing, have small CAs, which result in a small driving force and a large resistance. Discharges and stream power are small, while the boundary constraint is strong. The shaping power (river morphology and channel geometry that are shaped by flowing water and sediment) of the flowing water on the cross-section morphology is relatively small when compared to that of the higher order streams (order 7-9 streams). Geological control under a complex local landscape dominates the morphology of lower-order streams, which contributes to the high variability of cross-section morphology and less consistent variation in AHG coefficients and exponents. Outliers shown in Fig. 8 represent this inconsistency and are mainly located in lower order streams.

2) Higher-order streams have relatively large driving forces and small boundary constraints. Higher discharges and stream power indicate a greater contribution of contemporary fluvial processes to the shaping of cross-section morphology. This effect results in a relatively wide U-shaped cross section (Fig. 8; Fig. 5 a and d indicate an increase in coefficient a and a decrease in exponent b with increasing stream order, respectively). The wide U-shaped cross section corresponds to a flat channel bottom, steep banks and a relatively large shape exponent r in Dingman's cross-section geometry model (Dingman, 2007). In addition, the stream power increases along the river reach, which facilitates the regular changes in river width, water depth and flow velocity. As a result, AHG exponents vary consistently with the form of $b + f + m = 1$ in higher order streams (Fig. 8 b presents an inclined plane with some outlies located in order 5-7 streams).

In summary, the stability of cross sections increases with increasing stream order, which then contributes to the increase in AMHG strength. It can then be deduced that the AHG of cross sections located in the same stream order and shaped by discharges within similar ranges are dependent on each other but are not site specific, as previously theorized. These findings extend the AMHG theory and supports Rhodes' view (Rhodes 1977), who argued that "all cross sections of a given stream system are interrelated".

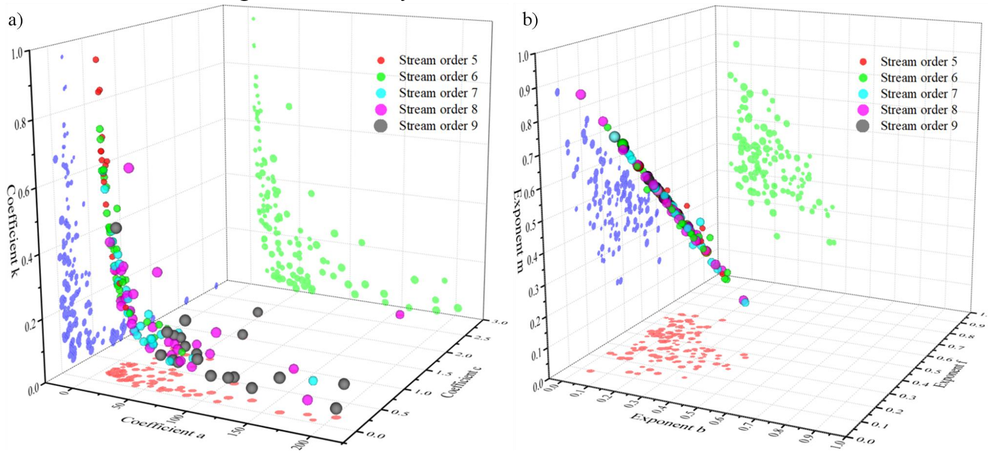

Figure 8 AHG coefficients (a) and exponents (b) for different stream orders in x-y-z coordinate systems (different sizes of shadows casted in x-y, x-z and y-z planes represent the values in different stream orders)

5 Summary and conclusions

Based on in-situ measurements of six major rivers and their tributaries originating from the QTP, this study first verified the existence of AMHG relations in the main streams of these rivers and then explored cross channel AMHG in the same stream order. Relationships among stream order and AMHG strength were studied. Congruent hydraulics and their relations to AMHG as well as in-situ measured hydraulics were tested. The following are the findings and implications of this research:

(1) AMHG exists in both main streams and cross sections located within the same stream order: a) Main streams of the Yellow River, the Datong River, the Yalong River, the Jinsha River, the Lantsang River and the Yarlung Zangbo River have at least one AMHG relation (width-, depth- or velocity-AMHG) with an R^2 > 0.9,

which supports the existence of AMHG in mountain rivers located in the southern and eastern portions of the QTP and demonstrates the power of using AMHG to predict AHG across the study river reaches. b) AMHG strength (R^2) increases with increasing stream order. The R^2 of cross sections located within order 7 and higher streams is largely > 0.6. c) Width-AMHG intercepts are larger than those of depth- and velocity-AMHGs for all stream orders. d) Congruent hydraulics generated from cross sections located in middle-scale rivers (order 7-8) are mostly within the observed range. The congruent w increases significantly with increasing in-situ measured w, while the increases of Q and d are relatively gradual as stream order increases.

(2) This study covers a large area of the eastern and southern portions of the QTP, including various environmental factors (such as climate, geology, landscape, vegetation, and soil) and stream patterns (single-thread rivers and multi-thread rivers). The findings from such complex areas indicate that AHG coefficients and exponents are functionally related and dependable between cross sections when they are in the same stream order. The cross channel AMHG is defined to reflect hydraulic self-similarity of cross sections and the consistency of AHG coefficients and exponents across reaches. The results of this research have the following implications: a) breaking the watershed divide boundary for AMHG; b) providing a basis for water and sediment simulation and research on river network structure and development; and c) providing the potential for using the AMHG theory for discharge estimation across the watershed divide, especially for data-scare mountain rivers.

(3) More testing is needed to verify the existence of AMHGs that are not located in a single river reach in complex climate, geologic and geomorphologic environments, especially for rivers in semi-arid and arid areas. The theoretical basis behind the mathematical artifact for AMHGs that existed in the same stream order should be studied further in the future.

Acknowledgement

This study was supported by the National Natural Science Foundation of China (Grant No. 51639005, 52009061, 52009062), the Postdoctoral Innovation Talents Support Program of China (Grand No. BX20190177) and the China Postdoctoral Science Foundation (2019M660656).

We appreciate the cooperation and efforts of all authors in producing the Proceedings. This will be a great symposium following the tradition of our sponsoring organizations.

References

Barber, C. A., Gleason, C. J. (2018). Verifying the prevalence, properties, and congruent hydraulics of at-many-stations hydraulic geometry (AMHG) for rivers in the continental United States. Journal of Hydrology 556, 625-633. https://doi.org/10.1016/j.jhydrol.2017.11.038

Bieger, K., Rathjens, H., Allen, P. M., Arnold, J. G. (2015). Development and evaluation of bankfull hydraulic geometry relationships for the physiographic regions of the United States. JAWRA Journal of the American Water Resources Association 51, 842-858. https://doi.org/10.1111/jawr.12282

Bonnema, M. G., Sikder, S., Hossain, F., Durand, M., Gleason, C. J., Bjerklie, D. M. (2016). Benchmarking wide swath altimetry-based river discharge estimation algorithms for the Ganges river system. Water Resources Research 52, 2439-2461. https://doi.org/10.1002/2015WR017296

Brinkerhoff, C. B., Gleason, C. J., Feng, D., Lin, P. 2020. Constraining remote river discharge estimation using reach-scale geomorphology. Water Resources Research 56, 1-24. https://doi.org/10.1029/2020WR027949

Brinkerhoff, C. B., Gleason, C. J., Ostendorf, D. W. (2019). Reconciling at-a-station and at-many-stations hydraulic geometry through river-wide geomorphology. Geophysical Research Letters 46, 9637-9647. https://doi.org/10.1029/2019GL084529

Ding, Y. J., Ye, B. S., Han, T. D., Shen, Y. P., Liu, S. Y. (2007). Regional difference of annual precipitation and discharge variation over west China during the last 50 years. Science in China Series D: Earth Sciences 50, 936-945. https://doi.org/10.1007/s11430-007-0042-8

Dingman, S. L. (2007). Analytical derivation of at-a-station hydraulic–geometry relations. Journal of Hydrology 334, 17-27. https://doi.org/10.1016/j.jhydrol.2006.09.021

Flores, J. A., Wu, J. Q., Stöckle, C. O., Ewing, R. P., Yang, X. (2020). Estimating river sediment discharge in the upper Mississippi River using Landsat imagery. Remote Sensing 12, 2370. https://doi.org/10.3390/rs12152370

Gleason, C. J. (2015). Hydraulic geometry of natural rivers: A review and future directions. Progress in Physical Geography: Earth and Environment 39, 337-360. https://doi.org/10.1177/0309133314567584

Gleason, C. J., Hamdan, A. N. (2017). Crossing the (watershed) divide: satellite data and the changing politics of international river basins. The Geographical Journal 183, 2-15. https://doi.org/10.1111/geoj.12155

Gleason, C. J., Smith, L. C. (2014). Toward global mapping of river discharge using satellite images and at-many-stations hydraulic geometry. Proceedings of the National Academy of Sciences 111, https://doi.org/4788-4791. 10.1073/pnas.1317606111

Gleason, C. J., Smith, L. C., Lee, J. (2014). Retrieval of river discharge solely from satellite imagery and at-many-stations hydraulic geometry: Sensitivity to river form and optimization parameters. Water Resources Research 50, 9604-9619. https://doi.org/10.1002/2014WR016109

Gleason, C. J., Wada, Y., Wang, J. (2018). A hybrid of optical remote sensing and hydrological modeling improves water balance estimation. Journal of Advances in Modeling Earth Systems 10, 2-17. https://doi.org/10.1002/2017MS000986

Gleason, C. J., Wang, J. (2015). Theoretical basis for at-many-stations hydraulic geometry. Geophysical Research Letters 42, 7107-7114. https://doi.org/10.1002/2015GL064935

Hagemann, M. W., Gleason, C. J., Durand, M. T. (2017). BAM: Bayesian AMHG-Manning inference of discharge using remotely sensed stream width, slope, and height. Water Resources Research 53, 9692-9707. https://doi.org/10.1002/2017WR021626

Hassan, M. A., Bird, S., Reid, D., Ferrer-Boix, C., Hogan, D., Brardinoni, F., Chartrand, S. (2019). Variable hillslope-channel coupling and channel characteristics of forested mountain streams in glaciated landscapes. Earth Surface Processes and Landforms 44, 736-751. https://doi.org/ 10.1002/esp.4527

Kebede, M. G., Wang, L., Li, X., Hu, Z. (2020). Remote sensing-based river discharge estimation for a small river flowing over the high mountain regions of the Tibetan Plateau. International Journal of Remote Sensing 41, 3322-3345. https://doi.org/10.1080/01431161.2019.1701213

Leopold, L. B., Maddock, T. (1953). The hydraulic geometry of stream channels and some physiographic implications. In "U.S Geological Survey Professional Paper 252", Washington D C.

Mark, D. M. (1984). Automated detection of drainage networks from digital elevation models. Cartographica 21, 168-178.

Martz, L. W., Garbrecht, J. (1992). Numerical definition of drainage network and subcatchment areas from Digital Elevation Models. Computers & Geosciences 18, 747-761.

Mengen, D., Ottinger, M., Leinenkugel, P., Ribbe, L. (2020). Modeling river discharge using automated river width measurements derived from Sentinel-1 time series. Remote Sensing 12, 3236. https://doi.org/10.3390/rs12193236

Ministry of Water Resources, P. R. China, (2016). Code for water flow measurement in open channels, GB 50179-2015. China Planning Press, Beijing, p. 202. (In Chinese).

Neal, J., Schumann, G., Bates, P. (2012). A subgrid channel model for simulating river hydraulics and floodplain inundation over large and data sparse areas. Water Resources Research 48, W11506. https://doi.org/10.1029/2012WR012514

Parker, G., Wilcock, P. R., Paola, C., Dietrich, W. E., Pitlick, J. (2007). Physical basis for quasi-universal relations describing bankfull hydraulic geometry of single-thread gravel bed rivers. Journal of Geophysical Research 112, F04005. https://doi.org/10.1029/2006JF000549

Parker, G., Wilkerson, G. V. (2011). Physical basis for quasi-universal relationships describing bankfull hydraulic geometry of sand-bed rivers. Journal of Hydraulic Engineering 137, 739-753. https://doi.org/10.1061/(ASCE)HY.1943-7900.0000352

Qin, C., Wu, B., Wang, Y., Fu, X., Xue, Y., Li, D., Li, M., Zhang, Y. (2020). Dynamic variability of at-a-station hydraulic-geometry for mountain rivers in the southeast Qinghai-Tibet Plateau: The cases of Yalong River and upper Jinsha River. Catena 194, 104723. https://doi.org/10.1016/j.catena.2020.104723

Rhodes, D. D. (1977). The b-f-m diagram: graphical representation and interpretation of at-a-station hydraulic geometry. American Journal of Science 277, 73-96. https://doi.org/10.2475/ajs.277.1.73

Rosenfeld, J. S., Post, J., Robins, G., Hatfield, T. (2007). Hydraulic geometry as a physical template for the river continuum: application to optimal flows and longitudinal trends in salmonid habitat. Canadian Journal of Fisheries and Aquatic Sciences 64, 755-767. https://doi.org/10.1139/f07-020

Shen, C., Wang, S., Liu, X. (2016). Geomorphological significance of at-many-stations hydraulic geometry. Geophysical Research Letters 43, 3762-3770. https://doi.org/10.1002/2016GL068364

Shields, F. D., Copeland, R. R., Klingeman, P. C., Doyle, M. W., Simon, A. (2003). Design for stream restoration. Journal of Hydraulic Engineering 129, 575-584. https://doi.org/ 10.1061/(ASCE)0733-9429(2003)129:8(575)

Singh, K. P., Broeren, S. M. (1989). Hydraulic geometry of streams and stream habitat assessment. Journal of Water Resources Planning and Management 115, 583-597. https://doi.org/10.1061/(ASCE)0733-9496(1989)115:5(583)

Song, X., Zhong, D., Wang, G., Li, X. 2020. Stochastic evolution of hydraulic geometry relations in the lower Yellow River of China under environmental uncertainties. International Journal of Sediment Research 35, 328-346. https://doi.org/10.1016/j.ijsrc.2020.02.003

Stall, J. B., Fok, Y. S. (1968). Hydraulic geometry of Illinois streams, WRC Research Report No. 15. Illinois State Water Survey, Urbanas Illinois. http://hdl.handle.net/2142/90172

Stall, J. B., Yang, C. T. (1970). Hydraulic geometry and low stream flow regimen, WRC Research Report No. 54. Illinois State Water Survey, Urbanas Illinois. https://www.isws.illinois.edu/pubdoc/CR/ISWSCR-131.pdf

Zhao, C. S., Pan, T. L., Xia, J., Yang, S. T., Zhao, J., Gan, X. J., Hou, L. P., Ding, S. Y. (2019). Streamflow calculation for medium-to-small rivers in data scarce inland areas. Science of The Total Environment 693, 133571. https://doi.org/10.1016/j.scitotenv.2019.07.377

Expansion on the loess gully sidewall: Processes and mechanisms

Yulei Ma[1], Xiangzhou Xu[1*], Peiqing Xiao[2], Qiao Yan[1], Chao Zhao[1]
1Institute of water environment, Dalian University of Technology, Dalian 116024, China
2 Key Laboratory of Process and Control of Soil Loss on the Loess Plateau, Yellow River Institute of Hydraulic Research, Zhengzhou 450003, China
*Corresponding Author, e-mail: xzxu@dlut.edu.cn

Abstract

Gully sidewall expansion is an important geomorphic natural hazard, and the expansion destroys a large extent of agricultural land in the loess regions every year. The main aim of this study was to identify the mechanisms behind gully sidewall expansion through a series of simulated rainfall experiments. The results show that land loss on the gentle slope was the result caused by the water and gravity erosions, and gravity erosion was the primary driving force. The correlation coefficient between the area of land loss on gentle slope and volume of gravity erosion on the gully sidewall was 0.93, and the correlation coefficient between the area of land loss on gentle slope and volume of water erosion was 0.71. The gravity erosion was the dominant impetus driving the change in slope gradient of the gully sidewall. The amount of gravity erosion in 17 of the 19 rainfall events causing a change greater than 5^{o} in the slope gradient of the gully sidewall accounted for more than 50% of the total amount of sidewall erosion. Furthermore, the dynamic variation of the retreat rates for the gully shoulder line showed a similar trend to that of the total volume of sidewall erosion, and exhibited an increase-decrease-increase tendency. The most significant factors affecting the change in slope gradient of the gully sidewall and retreat rate of the gully shoulder line were the rainfall duration and intensity, of which the sensitivity coefficients were 2.2 and 4.0, respectively. As a result, a combination of vegetation measures on the gentle slope, structural and ecological practices on the sidewall, and powerful structural practices, e.g., check dams, on the gully floor, is preferred for sidewalls vulnerable to expansion.

Keywords: Sidewall expansion, Gravity erosion, Water erosion, Rainfall, Landform

1 Introduction

Gully sidewall expansion, particularly in loess terrains, represents an undeniable reality both as a geomorphic process and as a type of hazard. Gully sidewall expansion—also known as gully sideward extension (Veness, 1980), gully sidewall erosion (Blong et al., 1982) and gully bank retreat (Chaplot et al., 2011)—is attributed to the combined effects of gravity erosion (landslides, avalanches and mudslides) and water erosion (by splash and runoff) (Chaplot et al., 2011). As a result of these processes, the sidewall retreats towards the gentle slope, releasing sediment to the gully, decreasing the cultivated area around the gully, and exposing new gully walls to erosion, eventually threatening local ecology and food security (Wijdenes and Bryan, 2001; Spalevic et al., 2013). According to some estimates, sidewall expansion can amount to more than 50% of the total sediment produced in gullies (Martínez-Casasnovas et al., 2004). Most studies have primarily focused on the expansion rate of the gully sidewall using remote-sensing images (Yan et al., 2014), and protection measures to mitigate gully sidewall expansion (Wang et al., 2019). Wang et al. (2019) suggested that the effectiveness of existing protection measures to control gully bank retreat was clear only in the short-term, while their long-term effectiveness remains unclear. Understanding the processes and mechanisms of gully sidewall erosion is important for implementing effective measures to reduce expansion. However, few studies have specifically addressed the processes, mechanisms and controls of gully sidewall expansion.

Gully sidewall expansion is influenced and constrained by many factors, such as slope material, topography and rainfall (Ali et al., 2014; Xu et al., 2015). Chaplot et al. (2011) indicated that raindrop runoff and splash could directly remove soil from the gully sidewall. Rainfall also indirectly causes sidewall instability by increasing the sidewall weight due to the addition of moisture (Lomtadze, 1977). The slope height and gradient are important geometric parameters of the gully sidewall. An increase in the slope height or gradient will cause stress to concentrate in a zone on the slope, resulting in soil mass displacement down from the escarpment (Lu and God, 2013). In addition, the downslope component of gravity increases as the slope gradient increases, thus reducing gully sidewall stability. Consequently, the processes and mechanisms of sidewall expansion under the influence of multiple factors are complicated.

Gully sidewall extension is an important process in gully development (Blong et al., 1982), and its dynamic nature can be assessed from changes in the gully shoulder line (Liu et al., 2016). The gully shoulder line is the line that intersects the gentle slope and gully sidewall (Fig. 2), also called the edge-line of gentle slope (Chen and Cai 2006) or line of gully boundary (Wu et al., 2008). The gully shoulder line is one of the most important landform demarcations for geomorphic analysis and land-use planning on the Loess Plateau (Yan et al., 2014). The existing research has focused on the methodology extracting the gully shoulder line, and relatively few studies have examined the factors influencing the retreat of the gully shoulder line (Qin et al., 2010; Yan et al., 2014). Thus, in this study, the direct effects of topography and rainfall on the retreat rate of the gully shoulder line were examined.

The extent of change in the slope gradient on the gully sidewall can also mirror the intensity of the sidewall expansion and the stage of gully development. The slope gradient influences the scale and intensity of material flow and energy conversion at the earth's surface (Tang et al., 2003). For instance, the infiltration, runoff and flow energy of a slope are significantly affected by the slope gradient (Assouline and Ben-Hur, 2006; Zheng and Xiao 2010). Consequently, the slope gradient directly restricts the landform morphology, runoff development and soil erosion, and also influences, to a relatively great or little extent, the evolution of natural soil and change in the land quality (Wang et al., 2005). A change in slope gradient influences the degree of the erosion of soil and migration of surface materials, and can also be interpreted as the result of space redistribution among the gully sidewall, channel floor and gentle slope. Defined development periods indicate stage-specific features for the slope gradient (Wang et al., 2005). Hence, by exploring the changing characteristics of the slope gradient on gully sidewalls and identifying the dominant mechanisms for dynamic change in sidewall slopes.

Understanding of gully sidewall expansion should be considered by further in-situ and modeling studies (Chaplot, 2013). Gravity erosion is difficult to predict due to its sudden occurrence, such process-based data of gully sidewall expansion are difficult to obtain under natural rainfall conditions. However, a physical model of a selected geomorphological feature, produced under closely controlled conditions, would be an effective way to dynamically observe the process of gully sidewall expansion in much shorter times, to search for the mechanisms behind gully sidewall expansion, and to deeply examine interacting factors and their various influences on expansion processes. Chorley (1964) identified three broad classes of physical models – segments of unscaled reality, scale models, and analog models – with the former being the most widespread in the field of soil and water conservation. In this study, the model slope was made based on field investigations and was a segment of unscaled reality.

The gully sidewall expansion on the Loess Plateau is remarkable because the gully density in the area is very large, of which 270,000 gullies are longer than 500 m (Liu et al., 2013). Loess gully sidewalls, which are gully banks usually with gradients of more than 70^{o} (Fig. 1), are prone to erosion under the action of water and gravity during rainstorms, because the slope material is mostly silty sandy loam with a loose structure, as well as being highly porous and having vertical joints (Xu et al., 2004). Usually, most soil erosion is triggered by short-burst rainfall events, where the rainfall intensity is greater than 0.5 mm min-1 and the rainfall duration ranges from 30 to 120 min (Wang and Jiao 1996; Wang et al., 2016; Jiao et al., 2001).

Sensitivity analysis has been widely utilized in soil erosion studies to reveal the relative importance of impact factors (Sánchez-Canales et al., 2015; Xu et al., 2015a). Gully sidewall expansion is a complicated process that involves a number of interactive factors. When a factor exceeds its critical value, it may become the dominant factor to trigger gully sidewall expansion (Yang et al., 2011). The method of sensitivity analysis can help in identifying the dominant factors of gully sidewall expansion, including the geology, topography and rainfall. In this study, the sensitivity of the developing features of gully sidewall expansion (i.e., variations in the slope gradient of the sidewall and retreat rates of the gully shoulder line) on the rainfall and topography have been evaluated based on the increase-rate-analysis method (Xu et al., 2015a).

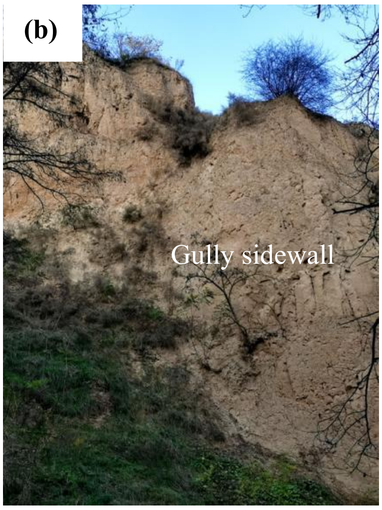

Figure 1 Photographs showing the representative loess gully sidewall on the Loess Plateau of China. (a) Gravity erosion on the gully sidewall, and (b) a typical gully sidewall with a slope gradient of more than 700.

Using a series of simulated rainfall experiments, this study aimed to understand the principal causes and mechanisms of gully sidewall expansion. The impact of gravity erosion on gully sidewall expansion was quantified, and the characteristics of gully sidewall expansion under the actions of gravity and water erosions were explored.

2 Materials and methods

A series of gully sidewall expansion experiments were conducted in 2010 and 2012 in the Joint Laboratory for Soil Erosion at the Dalian University of Technology and Tsinghua University, located in Beijing, China. Although the experiments have been completed by the corresponding author and his team for years, no similar experiments have been found by the authors in the references up to the present. The landscape simulator included a rainfall simulator, a conceptual landform and a topography meter (Fig. 2). The geometry of the conceptual landform was designed based on field investigations on the Loess Plateau. The conceptual landforms were 3 m long, 3 m wide and 1 or 1.5 m high, with a gentle slope (above the gully shoulder line) of 3° and a gully sidewall slope (below the gully shoulder line) of 70 or 80°. The test soil had a median particle diameter of 0.05 mm and a specific gravity of 2.56. Before starting each rainfall event experiment, a small intensity of rainfall was applied to the landform, and the experiment would start soon after the surface soil began to runoff generation. An SX2009 sprayer-typed rainfall simulator, designed by the authors, was used to simulate the rainfalls in the experiments. The rainfall intensities were 0.8 and 2.0 mm min^{-1}, with rainfall durations of 30 and 60 min in the experiments.

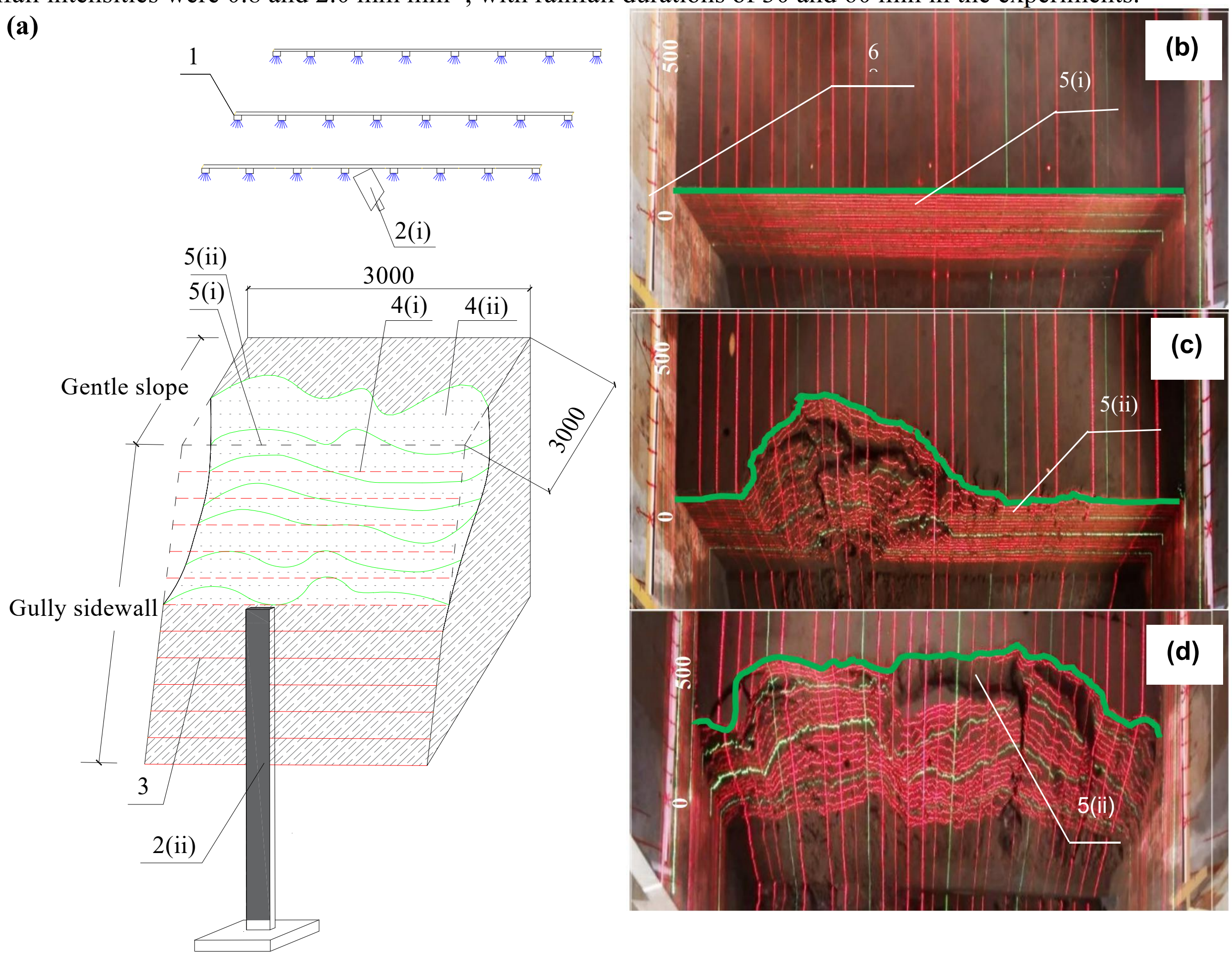

Figure 2 Landscape simulator in which the rainfall simulation experiments were conducted. All units in mm. (a) Schematic of the topography meter measurement system. (b) An image of the initial gully sidewall in experiment L6. (c, d) Images of sidewall retreat after the first and third rainfall events in experiment L6. *1* – rainfall simulator, *2* – topography meter (*i* – camera with collimator, *ii* – laser source), *3* – equidistant horizontal projections, *4* – model slope (*i* – initial model slope, *ii* – model slope after sidewall expansion), *5* – gully shoulder line (*i* – original gully shoulder line, *ii* – gully shoulder line after sidewall expansion), and *6* – positioning marks

The uniformity coefficients of the simulated rainfall exceeded 80%. Each conceptual landform was subjected to five runs of rainfall, with the interval being approximately 12 h. The experimental setup is listed in Table 1. The MX-2010-G topography meter included a set of laser sources and a camera with a collimator (Fig.2), and was applied to observe the process of sidewall expansion under the simulated rainfalls. The occurrence time and location of gravity erosion and the behavior of the sidewall expansion were recorded using a video camera. A set of parallel laser lines, equivalent to contour lines, were emitted from the topography meter to the sidewall surface, which helped to transform the target-plane figures into 3D graphs (Fig. 3). As shown in Fig. 3, after a comparison of the images of the gully sidewall, pre- and post-failure, we obtained the erosion data, including the areas of land loss on the gentle slope, the volumes of gravity erosion and total soil erosion, the retreat rates of the gully shoulder line, and the slope gradients of the sidewalls. The relative error in the volumes recorded with the MX-2010-G topography meter was less than 10% (Xu et al., 2015b).

The volume of soil erosion was calculated as follows:

$$W_{Vj} = T_{Vj} - G_{Vj} \tag{1}$$

where j is the sequence number of the rainfall event in an experiment with j = 1, 2, …, 5; W_{Vj} is the volume of water erosion in the j^{th} rainfall (cm^3); G_{Vj}, is the total volume of gravity erosion, which is the sum of the volumes of all the gravity erosion events occurring during the j^{th} rainfall in an experiment (cm^3); T_{Vj}, is the total volume of sidewall erosion, which is equal to the difference between the slope volume before and after the j^{th} rainfall in an experiment (cm^3).

The steps for extracting the area of land loss on the gentle slope were as follows. First, the picture was loaded with the control points in the software R2V, the gully shoulder line was portrayed, and then the two control points were connected below the gully shoulder line as a fixed baseline. Second, the above file was output with the format *.dxf. respectively. Third, this vector file (*.dxf) was imported into AutoCAD, vertical lines were drawn from the shoulder line to the baseline, a closed curve was formed, and then the area was calculated. Then, the total area of land endpoints of the gully loss on the gentle slope, A_R, was obtained as follow:

Table 1 Rainfall and topography conditions for experiments L1–L10. Three rainfalls, two initial slope gradients and two slope heights of the gully sidewall were considered in the experiments.

Test umber	Sidewall configuration		Rainfall		
	Height (m)	Gradient (°)	Intensity (mm min^{-1})	Duration (min)	Runs
L1	1.0	70	2.0	30	5
L2	1.0	80	2.0	30	5
L3	1.5	70	2.0	30	5
L4	1.5	80	2.0	30	5
L5	1.0	70	0.8	60	5
L6	1.0	80	0.8	60	5
L7	1.5	70	0.8	60	5
L8	1.5	80	0.8	60	5
L9	1.0	70	0.8	30	5
L10	1.0	80	0.8	30	5

$$A_R = \sum_{j=1}^{N} A_{Rj} \tag{2}$$

where A_R is the total area of land loss on the gentle slope after five rainfall events in an experiment (cm^2); A_{Rj} is the area of land loss on the gentle slope between the gully sidewall shoulder line before and after the j^{th} rainfall in an experiment (cm^2); and N is the number of rainfall events in an experiment.

The retreat rate of the gully shoulder line, V_R, can be calculated using the following formula:

$$V_R = \sum_{j=1}^{N} \frac{A_{Rj}}{Lt} \Big/ 5 = \sum_{j=1}^{N} V_{Rj} \Big/ 5 \tag{3}$$

where V_R is the average retreat rate of gully shoulder line during five rainfall events in an experiment (cm min^{-1}); V_{Rj} is the retreat rate of the gully shoulder line during the j^{th} rainfall in an experiment (cm min^{-1}); t is the rainfall duration (min); and L is the linear distance between the two endpoints of the original gully shoulder line (cm).

Only was the slope gradient of the gully sidewall discussed in the paper because hardly any erosion occurred on the gentle slope with the gradient of 3°, and all of the gravity erosions and most of the water erosions happened on the sidewall. The slope gradient of the gully sidewall was measured using the following steps. First, the block ArcScene was opened in the software ArcGIS10.6, the 3D surface models—triangulated irregular networks (TINs)—were imported and transformed into raster formats, then the slope gradients of the 3D TINs were obtained using the command *Slope* under *Raster Surface*. Second, the 3D TINs were converted into vector files using the command *Surface Slope* under *Triangulated Surface*, and the vector files corresponding to the gully sidewall were obtained by the command *Delete* under *3D Editor*. Third, the slope gradient of the gully sidewall was calculated using the vector data obtained in step 2 as clip features to clip the raster data obtained in step 1. Then, the difference in slope gradient of the gully sidewall, D_g, was obtained as follow:

$$D_g = \sum_{j=1}^{N} D_{gj} = \sum_{j=1}^{N} D_{gb}\text{-}D_{ga} \tag{4}$$

where D_g is the difference between the slope gradient of the gully sidewall before the first rainfall and that after the fifth rainfall in an experiment (°); D_{gj} is the difference in the slope gradient of gully sidewall during the j^{th} rainfall (°); and D_{gb} and D_{ga} are the slope gradient of gully sidewall before and after the j^{th} rainfall (°).

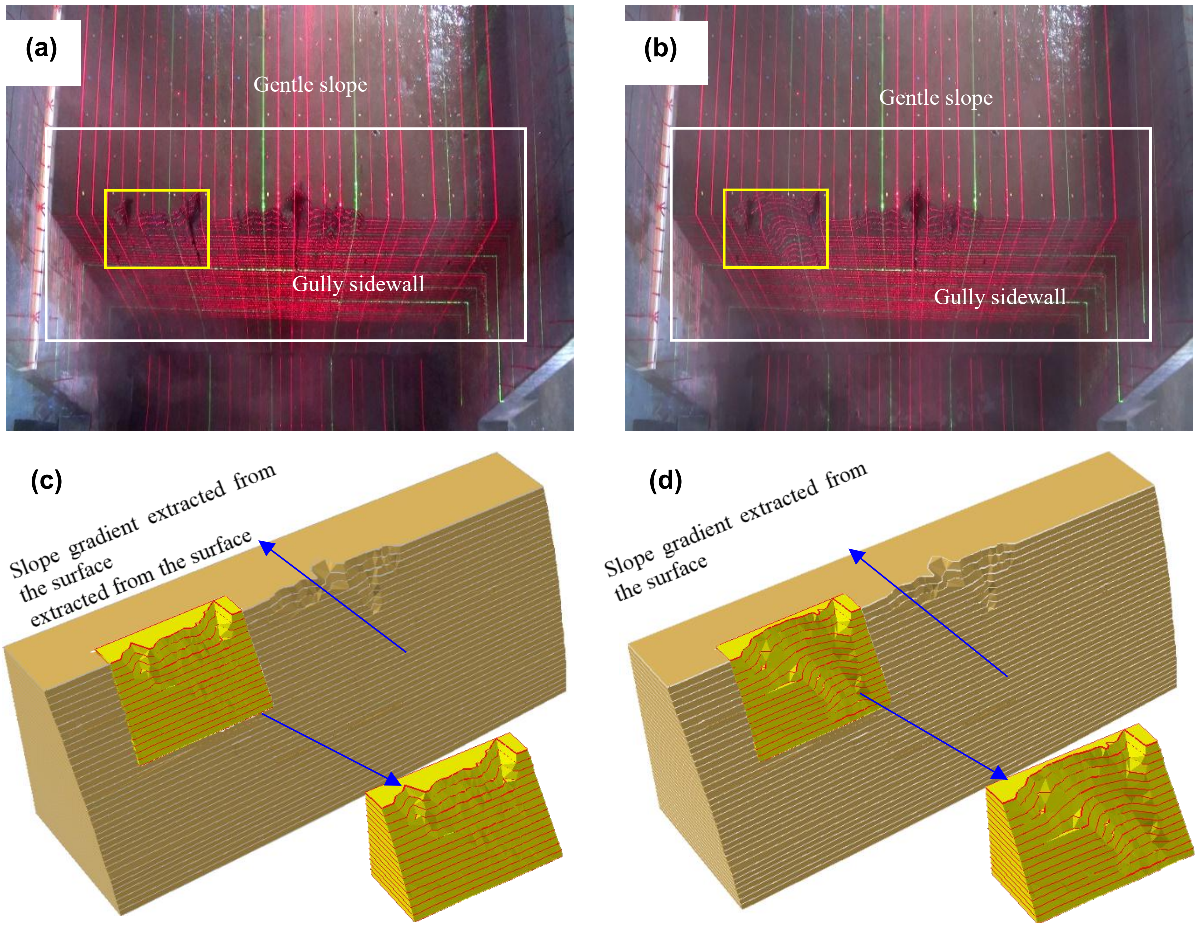

Figure 3 Comparison of the real slopes and 3D images. (a) A photo of the gully sidewall before the start of mass failure, (b) an image of the gully sidewall after a mass failure, and (c) and (d) 3D surface images corresponding to (a) and (b). The differences in the volume and gradient of the gully sidewall in the white frame have been calculated with an individual event of gravity erosion shown in the small yellow frame. The difference in volume and slope gradient of the two sidewalls shown in (c) and (d) are the total amount of soil loss and the average change in slope gradient during a rainfall event, respectively

A sensitivity coefficient, which represents the extent of change in a target value triggered by variation in a crucial factor while keeping other conditions fixed, is the ratio of the percentage change in the target value to the percentage change in the parameter (Xu et al., 2020). A relatively large sensitivity coefficient indicates that the target value is highly susceptible to changes in the influencing factor. To assess the influence of the rainfall and topography factors on D_g and V_R, we divided 10 sets of experiments into the following seven experimental groups: Ga (experiments L1, L2, L5 and L6) vs Gb (experiments L3, L4, L7 and L8), with the slope height in Ga being 1.0 m, and in Gb being 1.5 m; Gc (experiments L1, L3, L5 and L7) vs Gd (experiments L2, L4, L6 and L8), with the initial slope gradients being 70 and 80°, respectively; Ge (experiments L5 and L6) vs Gf (experiments L9 and L10), with the rainfall duration in Gc being 30 min, and in Ge being 60 min; and Gf (experiments L9 and L10) vs Gg (experiments L1 and L2), with the rainfall intensity being 0.8 and 2.0 mm min^{-1}, respectively. The average values of D_g and V_R were calculated for each experimental group ($\overline{D_g}$ and $\overline{V_R}$, respectively). We then employed the increase-rate-analysis method (Xu et al., 2015a) to evaluate the sensitivity of $\overline{D_g}$ and $\overline{V_R}$ to rainfall and topography. The sensitivity coefficients were calculated as follows:

$$S = \frac{R_t}{R_i} = \frac{(T_a - T_b)/T_b}{(I_a - I_b)/I_b} \tag{5}$$

where S is the sensitivity coefficient for assessing the susceptibility of $\overline{D_g}$ or $\overline{V_R}$ to the influencing factors; R_t is the increased ratio of $\overline{D_g}$ or $\overline{V_R}$; R_i is the increased ratio of the influencing factor; T_a represents $\overline{D_g}$ or $\overline{V_R}$ after the influencing factor was changed in an experiment group (° or cm min^{-1}); T_b represents $\overline{D_g}$ or $\overline{V_R}$ before the influencing factor was changed in an experiment group (° or cm min^{-1}); I is one of the influencing factors—initial slope gradient and height, and rainfall duration and intensity; and I_a and I_b represent the values of the influencing factors, after and before the change in an experimental group, respectively.

3 Results

3.1 Variations in the slope gradient of a gully sidewall

Changes in the slope gradients of the gully sidewalls were obvious in the experiments. Table 2 shows these changes during the five rainfall events in experiments L1–L10. After five rainfall events, the slope gradients of the gully sidewalls in experiments L1–L10 were 56.4, 54.5, 45.3, 53.3, 35.0, 37.5, 44.3, 55.6, 61.9 and 63.9°, respectively. Compared to the initial slope gradient in experiments L1–L10, the slope gradients were decreased by 13.6, 25.5, 24.7, 26.7, 35.0, 42.5, 25.7, 24.4, 8.1 and 16.1°, respectively. This implies that the landforms in experiments L5 and L6 tended to stabilize after five rainfall events, probably because the slope gradients were close to the angles of repose of dry and wet loess soil (Meng, 1996).

Table 2 Changes in the slope gradient of the gully sidewall after five rainfall events in experiments L1–L10. Compared with the initial slope gradient in experiments L1–L10, the slope gradients were decreased by an average of 24.2°.

Test number	Slope gradient of the gully sidewall (°)		D_g (°)	Test number	Slope gradient of the gully sidewall (°)		D_g (°)
	Initial	After five rainfalls			Initial	After five rainfalls	
L1	70	56.4	13.6	L6	80	37.5	42.5
L2	80	54.5	25.5	L7	70	44.3	25.7
L3	70	45.3	24.7	L8	80	55.6	24.4
L4	80	53.3	26.7	L9	70	61.9	8.1
L5	70	35.0	35.0	L10	80	63.9	16.1

Notes: D_g, namely the difference in slope gradient of the gully sidewall, means the difference between the slope gradient of the gully sidewall before the first rainfall and that after the fifth rainfall in an experiment.

Figure 4 Dynamic changes in the slope gradient of the gully sidewall in response to the volume of gravity and water erosion of a landform during five rainfall events. (a) First rainfall event, (b) second rainfall event, (c) third rainfall event, (d) fourth rainfall event, and (e) fifth rainfall event. The initial slope gradient of experiments L1, L3, L5, L7 and L9 was 70°, while the initial slope gradient of experiments L2, L4, L6, L8 and L10 was 80°

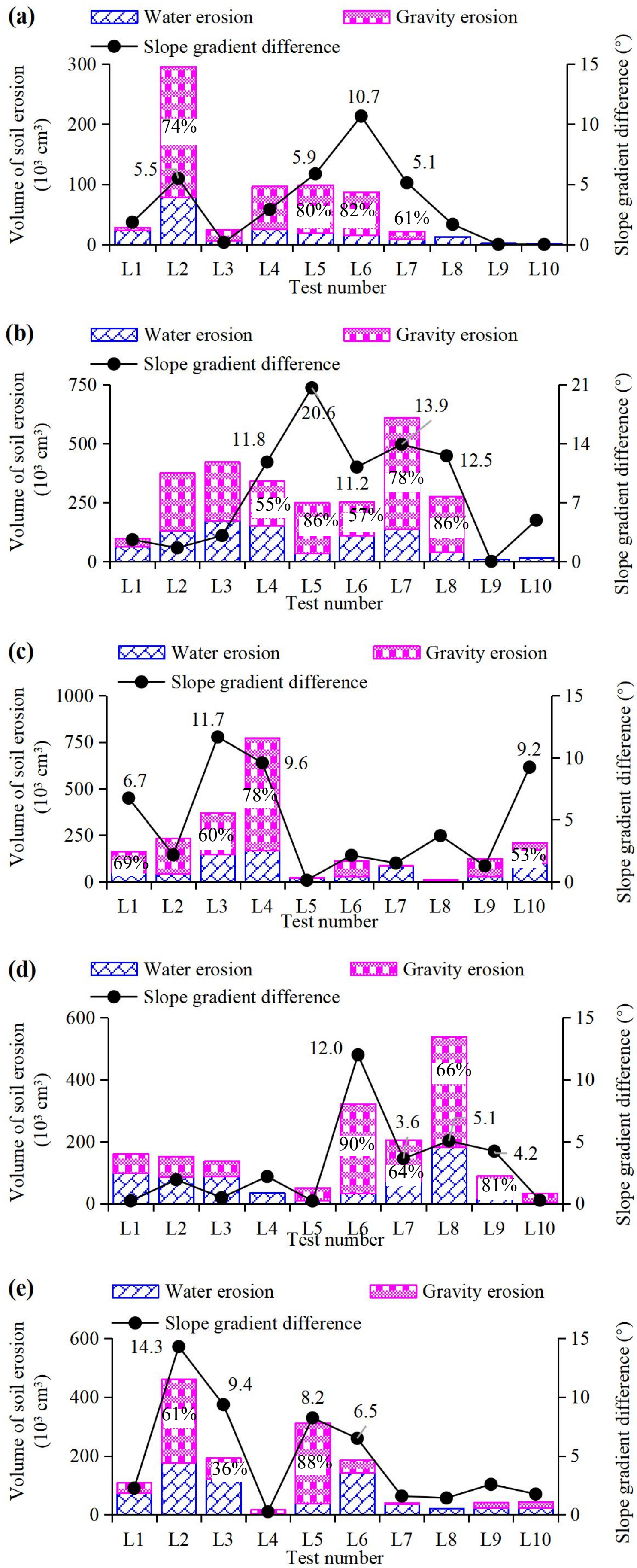

For instance, in the fourth rainfall event of experiments L1–L4, the values of changes in slope gradient of gully sidewall were 0.2, 1.9, 0.5 and 2.2°, respectively, and the corresponding volumes of water erosion accounted for 61, 57, 64 and 100% of the total volume of sidewall erosion, respectively (Fig. 4d). In addition, the volumes of water erosion in the fifth rainfall event of experiments L2 and L6 were comparable, whereas the volumes of gravity erosion in experiment L2 was 11.5 times greater than that in experiment L6, and the slope gradient of gully sidewall in experiment L2 (14.6°) decreased more significant than that in experiment L6 (6.5°) (Fig. 4e).

Gravity erosion was the primary driver influencing the change in slope gradient of the gully sidewall in the experiments. Fig. 4 illustrates the difference in the slope gradient of the gully sidewall during the five rainfall events under the actions of gravity and water erosions. The amount of gravity erosion in 17 of the 19 rainfall events causing a change greater than 5° in the slope gradient of the gully sidewall accounted for more than 50% of the total amount of sidewall erosion. For example, in the second rainfall event of experiments L4–L8, the slope gradient of the gully sidewall decreased by 11.8, 20.6, 11.2, 13.9 and 12.5°, respectively, and the corresponding volumes of gravity erosion accounted for 55, 86, 57, 78 and 86% of the total volumes of sidewall erosion, respectively (Fig. 4b). As shown in Fig. 4c, the volumes of gravity erosion accounted for 69, 60 and 78% of the total volumes of sidewall erosion during the third rainfalls of the experiments L1, L3 and L4, and their slope gradients of the gully sidewalls were reduced by 6.7, 11.7 and 9.6°, respectively. However, when the volume of water erosion during a rainfall event accounted for a large proportion of the total volume of soil erosion, the slope gradients of the gully sidewalls varied only marginally.

3.2 Retreat rate of the gully shoulder line

The gully shoulder line is always located in the most active part of a gully and its dynamics reflect the development of the gully (Liu et al. 2016). The retreat rate of the gully shoulder line mirrors not only the outward appearance of the developing gully, but also the internal mechanisms of gully development (Zhang et al. 2012). As can be seen from the experimental images (Fig. 2b–d), a retreat in the gully shoulder line was evident. Fig. 5 also illustrates the dynamic retreat of the gully shoulder line for the five rainfall events in experiment L8. After the fifth rainfall event, the maximum and minimum retreat widths of the gully shoulder line exceeded 100 and 50 cm, respectively. As shown in Fig.6, the retreat rate of the gully shoulder line and the total volume of soil erosion showed similar variations in experiments L1–L10. Additionally, the total volumes of gravity erosion in experiments L3, L6, L7 and L8 were comparable (approximately 600 × 10^3 cm^3), whereas their total volumes of water erosion were 538.0, 327.4, 338.6 and 260.9 × 10^3 cm^3, and their retreat rates of the gully shoulder line were 0.6, 0.4, 0.3 and 0.2 cm min^{-1}, respectively. This implies that the retreat rate of the gully shoulder line is related to the volume of water erosion.

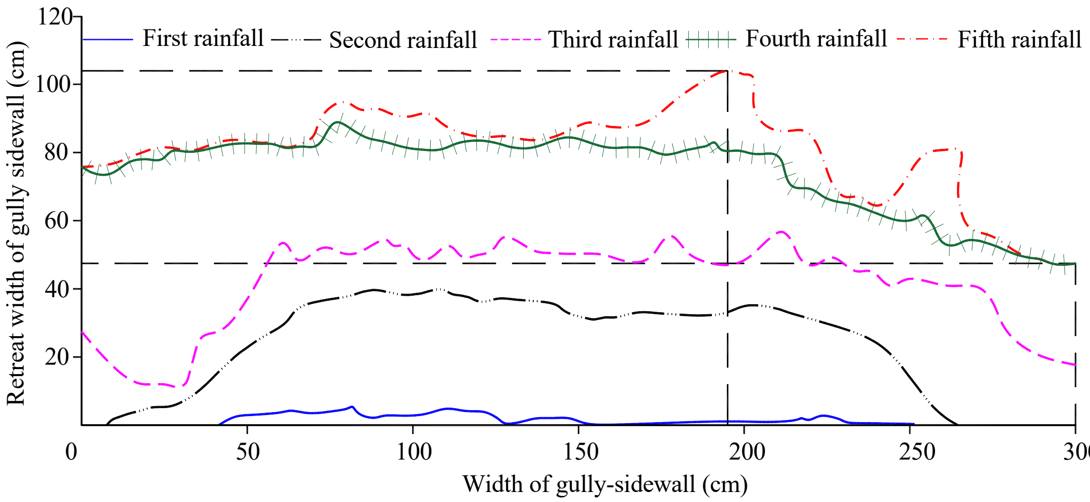

Figure 5 Dynamic changes in the gully shoulder line during five rainfall events in experiment L8. After the fifth rainfall event, the maximum retreat width of the gully shoulder line was more than 100 cm, with the minimum retreat width being more than 50 cm

The retreat rate of the gully shoulder line showed an increasing-decreasing-increasing trend during the five rainfall events in the experiments. For example, as shown in Fig. 7a, in experiment L1, the retreat rate of the gully shoulder line reached a peak value of 0.9 cm min^{-1} in the second rainfall event and reached a minimum value of 0.1 cm min^{-1} in the fifth rainfall event. The retreat rate of the gully shoulder line in experiment L2 reached the peak values in the second ($V_{R2} = 1.1\ \mathrm{cm\ min^{-1}}$) and fifth ($V_{R5} = 2.2\ \mathrm{cm\ min^{-1}}$) rainfall events, and a minimum value in the third ($V_{R3} = 0.3\ \mathrm{cm\ min^{-1}}$). As shown in Fig. 7b, the retreat rate of the gully shoulder line in experiment L7 reached the peak values of 0.6 and 0.7 cm min^{-1} in the second and fourth rainfall events, respectively. Comparing Fig. 7a and b, it can be seen that the retreat rates of the gully shoulder lines in the experimental group with a rainfall intensity of 2.0 mm min^{-1} were significantly greater than in the experimental group with a rainfall intensity of 0.8 mm min^{-1}.

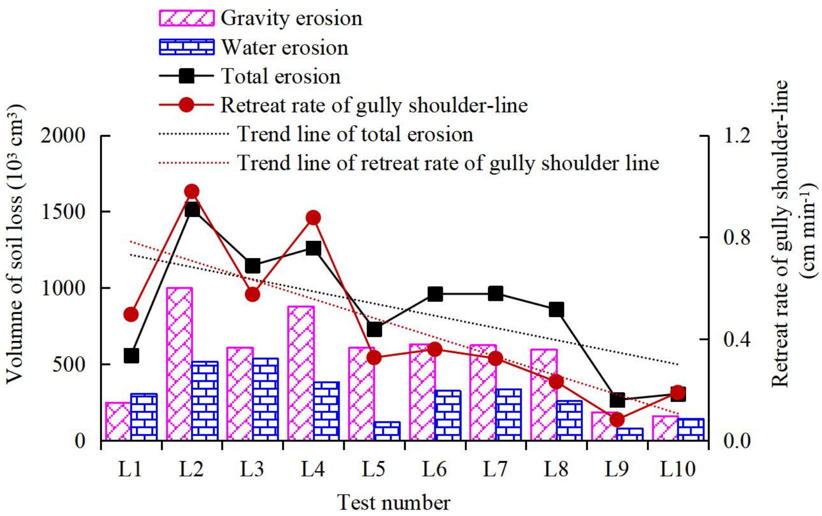

Figure 6 Retreat rate of the gully shoulder line in response to the volume and type of soil erosion after five rainfall events in experiments L1–L10. The total volume of soil erosion was equal to the sum of the volumes of the gravity and water erosion after five rainfall events for each experiment. The retreat rate of the gully shoulder line is the average retreat rate of the gully shoulder line during five rainfall events

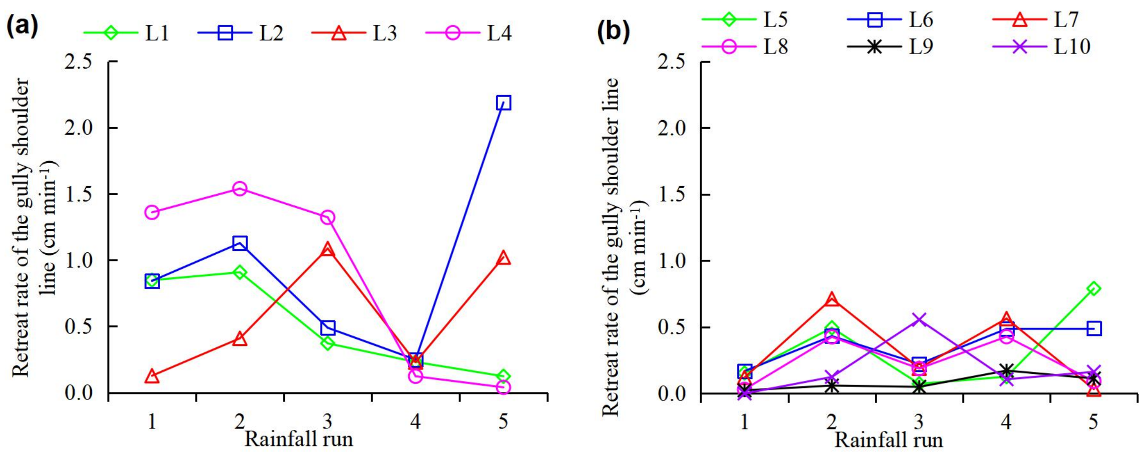

Figure 7 Retreat rate of the gully shoulder line during each rainfall event in experiments L1–L10. (a) Severe rainstorms with a density of 2.0 mm min^{-1}, and (b) gentle rainfall with a density of 0.8 mm min^{-1}

3.3 Land loss on the gentle slope

Different types of erosion may significantly influence the area of land loss on the gentle slope. In this study, we investigated the relationship between the area of land loss on the gentle slope and volumes of different types of soil erosions, namely gravity and water erosions, during the process of sidewall expansion. As shown in Fig. 8, the correlation coefficient between the area of land loss on gentle slope and volume of gravity erosion on the gully sidewall was 0.93, and the correlation coefficient between the area of land loss on gentle slope and volume of water erosion on the gully sidewall was 0.71. This shows that land loss on the gentle slope was the result caused by the water and gravity erosions, and the gravity erosion was the primary driving force. The soil on the gentle slope was separated from the slope face under the effect of gravity, accumulating on the downslope or gully bottom and resulting in an irreversible loss of land.

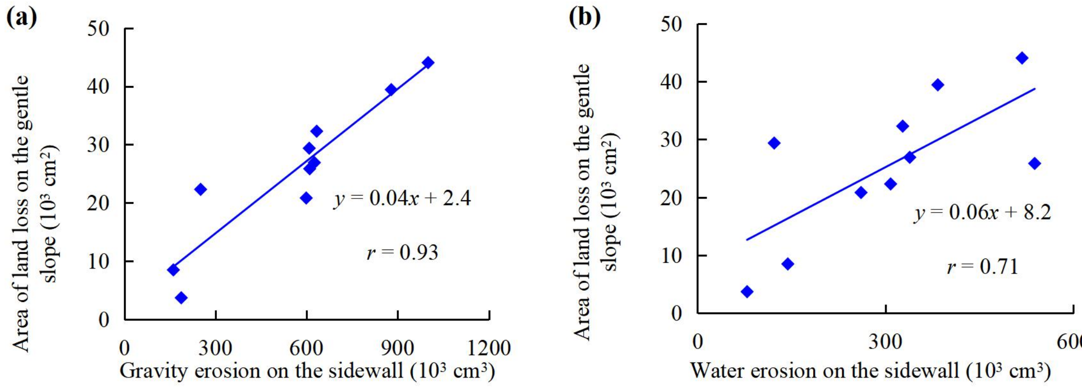

Figure 8 Correlation between the soil erosion on the sidewall and land loss on the gentle slope after five rainfall events in experiments L1–L10. (a) Gravity erosion on the sidewall vs. land loss on the gentle slope, and (b) water erosion on the sidewall vs. land loss on the gentle slope

3.4 Sensitivity coefficients

Rainfall duration and initial slope gradient significantly influenced the changes in slope gradient of the gully sidewalls in the experiments. As shown in Fig. 9, there were substantial increases in the change in slope gradient of the gully sidewall when the rainfall intensity, rainfall duration and initial slope gradient increased. In particular, when the other factors were fixed, but the rainfall duration was increased from 30 to 60 min, the change in slope gradient of the gully sidewall grew from 12.1 to 38.8°. In contrast, the change in slope gradient of the gully sidewall dropped with the increasing slope height. A sensitivity analysis was implemented to assess the influences of topography and rainfall on the change in slope gradient of the gully sidewall. The sensitivity coefficients of the change in slope gradient of the gully sidewall on rainfall duration, initial slope gradient, rainfall intensity and slope height were 2.2, 1.4, 0.4 and -0.3, respectively (Fig. 9). These results indicate that rainfall duration and initial slope gradient were the most and second-most influential factors on the changes in slope gradient of the gully sidewalls in the experiments.

Rainfall intensity and initial slope gradient were the most important sensitivity parameters affecting the retreat rate of the gully shoulder line in the experiments. Fig. 10 illustrates the variation in the retreat rate of the gully shoulder line as rainfall and topography increased. It was found that the retreat rates of the gully shoulder line increased with increasing rainfall intensity, rainfall duration and initial slope gradient. For example, when the other conditions were fixed, but the rainfall intensity was increased from 0.8 to 2.0 mm min^{-1}, the retreat rate of the gully shoulder line increased by 600% (with the retreat rate increasing from 0.1 to 0.7 cm min^{-1}). However, when the slope height increased from 1.0 to 1.5 m, the retreat rate of the gully shoulder line was maintained at approximately 0.5 cm min^{-1}. Using a sensitivity analysis with the increase-rate-analysis method, the authors found that the sensitivity coefficients of the retreat rate of gully shoulder line on rainfall intensity, initial slope gradient, rainfall duration and slope height were 4.0, 3.5, 2.0 and -0.1, respectively (Fig. 10). These results suggest that the most significant factors affecting the retreat rate of gully shoulder line were the rainfall intensity and initial slope gradient.

4 Discussion

4.1 Mechanisms of gully sidewall expansion

The variation in slope gradient of the gully sidewalls was the result of the synergetic effect of water and gravity erosions, although significant decreases in slope gradient were caused by gravitational erosion (Fig. 4). Water erosion occurred first, increasing the occurrence and development of gravity erosion during the process of sidewall expansion. The movement of topsoil towards the downslope position due to runoff was the result of increasing stress and decreasing strength at the soil surface during rainfall. This process changed the topography, such as some parts of the gully slope becoming steep, thus increasing the possibility of mass failure (Lu and Godt, 2013). Conversely, gravity

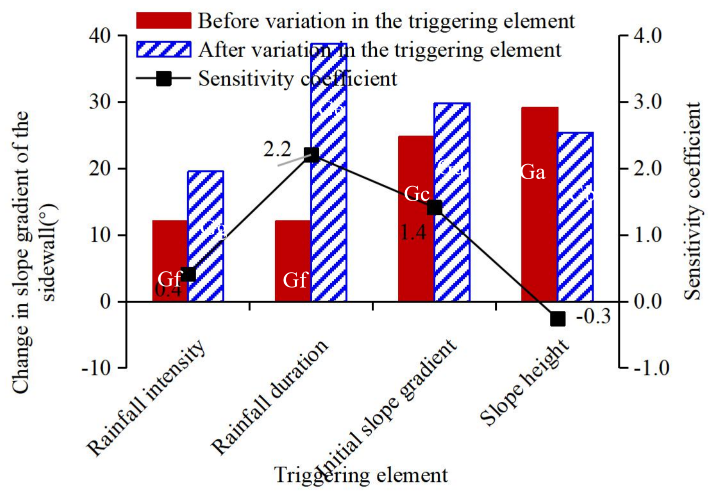

Figure 9 Sensitivity analysis of changes in the slope gradient of the gully sidewall for the triggering elements. The changes in the slope gradients of the gully sidewalls in the experimental groups Ga–Gg ranged from 12.1 to 38.8°

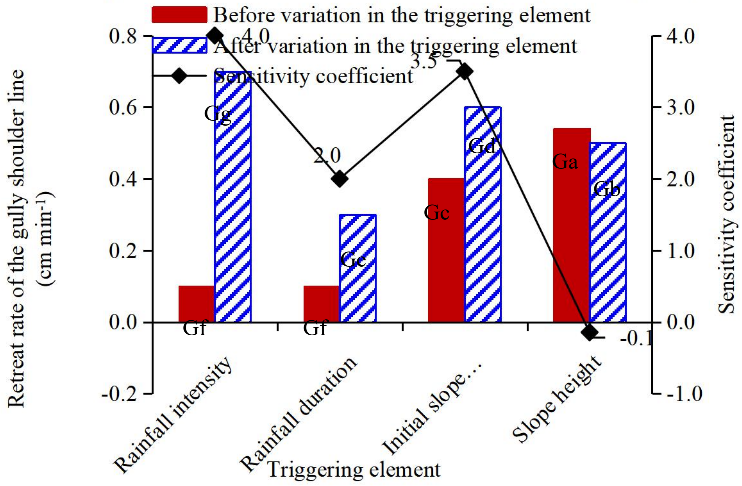

Figure 10 Sensitivity analysis of the retreat rate of the gully shoulder line for the triggering elements. The average retreat rates of the gully shoulder line in experimental groups Ga–Gg ranged from 0.1 to 0.7cm min^{-1}

erosion destroyed the original structure of the soil as the structure became loose, providing a major source of water erosion. In the experiments, the slope gradient of the gully sidewalls was significantly reduced owing to the occurrence of large-scale failure or a large number of small-scale failures that allowed for temporary stability of the gully sidewall. Water erosion then became the main erosion pattern of the gully sidewall, as evidenced with the erosion from the gully sidewall caused by surface runoff and that from the soil accumulation caused by channel flow. Because much of the material produced by the gravity erosion remained at the toe of the gully sidewall, the deposition may have increased the instability of the gully sidewall. Liu and Wu (1993) also suggested that the processes of water and gravity erosions mutually influence each other in the gully development.

The retreat of the gully shoulder line was also influenced by a combination of gravitational and hydraulic erosion. The gully shoulder is a heavily eroded area, characterized with the rapid retreat of the gully shoulder line. In the experiments, soil erosion started from the gully shoulder (Fig. 3a and b). The rapid retreat of the gully shoulder line is likely due to two reasons. First, the formation of runoff provides a driving mechanism for soil erosion (Lu and Godt, 2013). After the formation of infiltration-excess runoff on the loess gentle slope, the runoff flows through the gully shoulder, eroding it, with the intensity of the erosion gradually decreasing from the gully shoulder to the downslope. In addition, with an increase in rainfall duration, the stress distribution in a slope is dynamic, whether caused by water movement or mass gravity. Tensile cracks form at the top of the slope, owing to a decrease in the cohesion and an increase in the downslope component of gravity in the gully sidewall, as the soil water content increases under rainfall infiltration. Pore water pressure is generated after rainwater enters these tension cracks, causing tension crack propagation and coalescence, followed by the formation of a potential slip surface. When the strength at the slip surface decreases with an increase in pore water pressure (Orense, 2004), gravity erosion occurs, accompanied with retreat of the gully shoulder line.

4.2 Effects of parameters on gully sidewall expansion

Changes in rainfall and topography significantly influence the process of sidewall extension, such as dynamic changes in erosion patterns and slope gradients (Thornes and Alcantara-Ayala, 1998; Sánchez-Canales et al., 2015). In this study, rainfall duration and initial slope gradient had significant influences on changes in slope gradient of the gully sidewalls (Fig. 9). When the rainfall intensity was constant, but the duration was increased, the dynamic and hydrostatic pressure caused by rainfall infiltration had an adverse effect on slope stability (Tu et al., 2009). In addition, the matric suction decreased or even disappeared with an increase in water content during rainfall infiltration, resulting in a decrease in soil shear strength, eventually leading to the occurrence of gravity erosion (Lomtadze et al., 1977; Tu et al., 2009). An increase in the initial slope gradient results in the concentration of shear stress at the sidewall toe and tension stress at the gully shoulder (Pei et al., 2013), leading to an increase in the absolute values of shearing forces, followed by slope failure. This indicates that mass failure led to a remarkable change in slope gradient during sidewall expansion. This result supports the finding of Claessens et al. (2013), which also proved that mass movement on the sidewall may be responsible for sudden and significant changes in the slope angle. In addition, the change in the slope gradient of the sidewall was negatively correlated with initial slope height in the experiments. The reason for this phenomenon may be that a higher slope height requires a greater amount of infiltration and more time for the rainfall to move from the top to the bottom of the soil profile on the gully sidewall.

Our results also indicate that the most significant factors affecting the retreat rate of the gully shoulder line were rainfall intensity and initial slope gradient (Fig. 10). The main reason for this is that runoff velocity rises with increasing slope gradient and rainfall intensity (Chen and Cai, 1990; Wang et al., 2013), which leads to the component of the tractive force of flowing water parallel to the slope surface to be greater than the soil resistance, eventually causing retreat of the gully shoulder line, leading to gully widening (Xiao and Tang, 2007). Demissie et al. (2019) also suggested that heavier and longer-lasting rainfall events had a substantial influence on channel width. As the initial slope gradient increases, the retreat rate of the gully shoulder line also increases. It is likely that the steep slope gradients encouraged the concentration of tension stresses at the top, which in turn led to the formation of tension cracks in the gentle slope near the gully shoulder line, and subsequent mass failure.

4.3 Hazards and defense scenarios

Gully sidewall expansion always causes land loss on the gentle slope. It is only when gullies threaten humankind that they represent a hazard (Ionita et al., 2015). The evolution of gullies has reduced the extent of agricultural land, which can diminish crop yields (Frankl et al., 2011; Zgłobicki et al., 2015). Before the ‘Grain-for-Green’ program in China, the Loess Plateau had been facing severe land loss due to sidewall expansion. For example, from 1958 to 1978, the average rate of sidewall retreat was 0.84 m a-1 in the Xingzi River Catchment in Yan'an City, and the annual loss of the inner-gully area was approximately 1886.7 hm2 (Meng, 1996). Recently, several studies have shown that land loss on the gentle slope, caused by sidewall expansion, is still severe on the Loess Plateau. Li et al. (2015) found that, from 2003 to 2010, the maximum retreat rates of gullies in 30 investigated catchments in the southeastern part of the Loess Plateau ranged between 0.23 and 1.08 m a-1, with an average of 0.51 m a-1. It has been understood that, both before and after the 'Grain-for-Green' program in China, there was severe land loss on the gentle slope, caused by gully sidewall expansion. Qin et al. (2018) indicated that gully widening constituted approximately 80% of the total soil loss. Gully development caused by sidewall expansion is one of the greatest threats to land loss not only in China but also in other countries (Kuhnert et al. 2010). A field investigation in the Umbulo Catchment of southern Ethiopia indicated a rapid, downslope development of gullies in the past 30 years, with an average soil loss rate of between 11 and 30 t ha-1 a-1 (Moges and Holden, 2008). If gully sidewall expansion had not been controlled, gully expansion would have reached its maximum extent, forcing farmers to retreat, and reduce the cultivated area around the gullies (Yitbarek et al., 2012).

Only after the mechanisms of gully sidewall erosion have been understood, can effective measures be designed to reduce their expansion. Gully sidewall expansion results from the combined actions of water and gravity erosions. The importance of vegetation in controlling water erosion is widely accepted (Bochet et al., 2006). Vegetation plays a crucial role in intercepting rainfall and runoff, increasing infiltration capacity, stabilizing soil through root growth, protecting the soil surface against the direct impact of raindrops, and trapping sediment (Wei et al., 2009). In this study, the gully shoulders were eroded by rainfall and surface runoff, which promoted the occurrence and development of gravity erosion. Vegetation planted on gully shoulders could stabilize the gully and decrease runoff erosion (Nyssen et al., 2007). However, vegetation does not have a significant effect on controlling gravity erosion on the gully sidewall (Guo et al., 2019). With vegetation restoration on the Loess Plateau of China, the amount of soil erosion on the gentle slope has decreased, but the amount of soil erosion on the gully sidewall has become more prominent (Yang et al., 2011). The reasons are some unfavorable influences of vegetation on gully slope stability, including the relatively high near-surface water content both during and after rainfall events (Simon and Collison, 2002). Our findings suggest that mass failure was the main cause of gully sidewall expansion, which is in agreement with the findings of Lohnes (1991) and Rowland et al. (2009). Consequently, treatment of the gravity erosion is the key to control gully sidewall expansion. Control measures for gully sidewall expansion cannot be effective, especially in the long term, if the gravity erosion is not considered to be the dominant mechanism in the gully sidewall expansion. For example, a structural practice implemented in the Yanwachuan Catchment of the Dongzhiyuan tableland on the Loess Plateau, involving simply filling the gully head with loess, was proved to be not effective (Wang et al., 2019). Simple gully landfill combined with drainage measures were also proved to be ineffective because the surface drainage on the downslope side always collapsed, triggered by washing and erosion. However, as a way to mitigate the risk of sidewall expansion, combining gully landfill and drainage with ecological slope protection can effectively control the mass failures (Wang et al., 2019). In addition, from a long-term perspective, the check dam has become an effective practice to control mass failure in gully areas on the Loess Plateau. The expansion of gully sidewall will be mitigated when the thalweg in the upper reach of the gully is increased and the height of the sidewall behind the check dam is reduced as a result of siltation behind the check dam (Xu et al., 2020). Thus, a combination of vegetation measures on the gentle slope, structural and ecological practices on the sidewall, and powerful structural practices, e.g., check dams, on the gully floor, is preferred for sidewalls vulnerable to expansion.

4.4 The way forward

In this study, rainfall and topographic factors were taken into account in an examination of gully sidewall expansion, although vegetation may influence and constrain such sidewall expansion. Although the Loess Plateau is characterized by low vegetation cover, the vegetation on the slope has recovered well in some areas through implementation of the 'Grain-for-Green' program. The roots of trees, shrubs, grasses and other plants play an important role in slope stability. Living plant roots can provide mechanical reinforcement to the soil (Chirico et al., 2013), which can resist the generation of tensile cracks, or can be converted into shear strength to resist shear stress. However, several studies have reported that vegetation can promote the initiation of mass movement on gully sidewalls during rainfall (Guo et al., 2019; Gao et al., 2020). For instance, Wang (2014) reported that sheet and rill erosion on the gentle slope was mitigated effectively through vegetation restoration, but that there was severe gravity erosion on gully sidewalls during a rainstorm in the Yanhe watershed on the Loess Plateau. Consequently, in future experiments, the effect of vegetation on gully sidewall expansion should be assessed.

New techniques can supplement traditional fieldwork that is based on visual observations and the use of erosion pins or stakes (Martínez-Casasnovas et al., 2004). On one hand, detailed studies and long-term monitoring activities on lateral gully expansion are neither frequent nor adequately documented in the existing literature, mainly because of the difficulties involved in investing human and economic resources on these phenomena, which are often considered a low hazard risk (Pasuto and Soldati, 2013). On the other hand, innovative monitoring techniques, such as the global positioning system (i.e., GPS) (Magri et al., 2008) and light detection and ranging (i.e., LiDAR) (Vianello et al., 2009), have already been used successfully in several studies dealing with ground deformation due to their high accuracy and reliability. Hence, to understand the kinematics, evaluate and mitigate the hazards, and predict evolutionary scenarios of gully sidewall expansion, there is a need to couple traditional monitoring with innovative monitoring techniques.

5 Conclusions

Land loss on the gentle slope was the result of the effect of water and gravity erosions, and gravity erosion was the primary cause. A strong positive correlation was found between the area of land loss on the gentle slope and the volume of gravity erosion (r_1 = 0.93), and the area of land loss on the gentle slope and the volume of water erosion also exhibited a positive correlation (r_2 = 0.71).

The gravity erosion is the major impetus of the change in slope gradient of the gully sidewall during the process of sidewall expansion in the experiments. As mentioned above, the amount of gravity erosion in 17 of the 19 rainfall events causing a change greater than 5° in the slope gradient of the gully sidewall accounted for more than 50% of the total amount of sidewall erosion. The retreat rate of the gully shoulder line showed a similar change with the total volume of sidewall erosion, exhibiting an increase-decrease-increase trend in the experiments. In addition, the retreat rate of the gully shoulder line was related to the volume of water erosion.

The rainfall duration and initial slope gradient had a significant influence on the change in slope gradient of the gully sidewall in the experiments. Meanwhile, the retreat rate of the gully shoulder line was highly susceptible to the rainfall intensity and initial slope gradient. The sensitivity coefficients of the change in slope gradient of the gully sidewall on the rainfall duration and initial slope gradient were 2.2 and 1.4, and the sensitivity coefficients of the retreat rate of the gully shoulder line on the rainfall intensity and initial slope gradient were 4.0 and 3.5, respectively.

Acknowledgments

This study was supported by the National Key R & D Project (2016YFC0402504), National Natural Science Foundation of China (No. 51879032), and Open Research Fund Program of Key Laboratory of Process and Control of Soil Loss on the Loess Plateau (201903).

References

Ali, A., Huang, J., Lyamin, A. V., Sloan, S. W., Cassidy, M. J. (2014). Boundary effects of rainfall induced landslides. Computers and Geotechnics, 61, 341–354.

Assouline, S., Ben-Hur, M. (2006). Effects of rainfall intensity and slope gradient on the dynamics of interrill erosion during soil surface sealing. Catena, 66, 211–220.

Blong, R. J., Graham, O. P., Veness, J. A. (1982). The role of sidewall processes in gully development; some NSW examples. Earth Surface Processes & Landforms, 7, 381–385.

Bochet, E., Poesen, J., & Rubio J. L. (2006). Runoff and soil loss under individual plants of a semi-arid Mediterranean shrubland: influence of plant morphology and rainfall intensity. Earth Surface Processes & Landforms, 31, 536–549.

Chaplot, V., Brown, J., Dlamini, P., Eustice, T., Janeau, J. L., Jewitt, G., Lorentz, S., Martin, L., Nontokozo-Mchunu, C., Oakes, E., Podwojewski, P., Revil, D., Rumpel, C., & Zondi, N. (2011). Rainfall simulation to identify the storm-scale mechanisms of gully bank retreat. Agricultural Water Management, 98, 1704–1710.

Chen, H., Cai, Q. G. (2006). Impact of hillslope vegetation restoration on gully erosion induced sediment yield. Science in China, Series D – Earth Sciences, 49, 176–192.

Chirico, G. B., Borga, M., Tarolli, P., Rigon, R., Preti, F. (2013). Role of vegetation on slope stability under transient unsaturated conditions. Procedia Environmental Sciences, 19, 932–941.

Chorley R. J. (1964). Geography and analog theory. Annals of the Association of American Geographers, 54(1): 127-137.

Claessens, L., Temme, A. J. A. M., Schoorl, J. M. (2013). Mass-movement causes: changes in slope angle. In J. Shroder (Ed. in Chief), R. A. Marston, & M. Stoffel (Eds.), Treatise on Geomorphology, vol. 7, Mountain and hillslope geomorphology. Academic Press, San Diego, pp. 212–216.

Demissie, B., Eetvelde, V. V., Frankl, A., Billi, P., Asfaha, T. G., Haile, M., Nyssen, J. (2020). Dynamics of ephemeral streams at the foot of degraded catchments in northern Ethiopia. Land Degradation & Development, 31, 591–606.

Frankl, A., Nyssen, J., Dapper, M. D., Haile, M., Billi, P., Munro, R. N., Deckers, J., Poesen, J. (2011). Linking long-term gully and river channel dynamics to environmental change using repeat photography (Northern Ethiopia). Geomorphology, 129, 238–251.

Gao, H., Xu, X. Z., Zhang, H. W., Jiang, Y. Z., Zhao, T. Q. (2020). How effective is vegetation in reducing gravity erosion on loess gully sidewall under intense rainfalls? Land Degradation & Development, 23, 157–166.

Guo, W. Z., Chen, Z. X., Wang, W. L., Gao, W. W., Zhao, M. (2019). Telling a different story: the promote role of vegetation in the initiation of shallow landslides during rainfall on the Chinese Loess Plateau. Geomorphology, 350, 106879.

Ionita, I., Fullen, M. A., Zgłobicki, W., Poesen, J. J. N. (2015). Gully erosion as a natural and human-induced hazard. Natural Hazards, 79, 1–5.

Jiao, J. Y., Wang, W. Z. (2001). Non-uniformity of the spatial distribution of rainfall on the Loess Plateau. Hydrology, 21, 20–24. (in Chinese).

Kuhnert, P. M., Henderson, A. K., Bartley, R., Herr, A. J. E. (2010). Incorporating uncertainty in gully erosion calculations using the random forests modelling approach. Environmetrics, 21, 493–509.

Li, Z., Zhang, Y., Zhu, Q. K., He, Y. M., & Yao, W. J. (2015). Assessment of bank gully development and vegetation coverage on the Chinese Loess Plateau. Geomorphology, 228, 462–469.

Liu Q., Wang Y., Zhang J. (2013). Filling Gullies to Create Farmland on the Loess Plateau. Environmental Science & Technology, 47(14): 7589-7590.

Liu, B. Z., Wu, F. Q. (1993). Gully erosion and its development on the loess plateau. Journal of the Northwest Forestry University, 8, 7–15. (in Chinese)

Liu, H., Deng, Q. C., Zhang, B., Li, X., Wang, L., Luo, M. X., Qin, F. C. (2016). Influences of different surveying and mapping methods on fractal characteristics of gully-head shoulder lines. Physical Geography, 37, 1–22.

Lohnes, R. A. (1991). A method for estimating land loess associated with stream channel degradation. Engineering Geology, 31, 115–130.

Lomtadze, V. D. (1977). Regularities of development of gravitational processes and their prediction. Bulletin of Engineering Geology and the Environment, 15, 9–12.

Lu, N., Godt, J. W. (2013). Hillslope Hydrology and Stability. Cambridge University Press, Cambridge, UK.

Magri, O., Mantovani, M., Pasuto, A., Soldati, M. (2008). Geomorphological investigation and monitoring of lateral spreading along the north-west coast of Malta. Geografia Fisica e Dinamica Quaternaria, 31, 171–180.

Martínez-Casasnovas, J. A., Ramos, M. C., Poesen, J. (2004). Assessment of sidewall erosion in large gullies using multi-temporal DEMs and logistic regression analysis. Geomorphology, 58, 305–321.

Meng, Q. M. (Ed.). (1996). Soil and Water Conservation on the Loess Plateau. Water Resources Press of the Yellow River, Zhengzhou, China, pp. 166–167. (in Chinese)

Moges, A., Holden, N. M. (2008). Estimating the rate and consequences of gully development, a case study of the Umbulo catchment in Southern Ethiopia. Land Degradation & Development, 19, 574–586.

Nyssen, J., Descheemaeker, K., Haregeweyn, N., Haile, M., Deckers, J., Poesen, J. (Eds.). (2007). Lessons learnt from 10 years research on soil erosion and soil and water conservation in Tigray. Tigray Livelihood Papers No. 7, Mekelle Zala-Daget Project, Mekelle University, K. U. Leuven, Relief Society of Tigray, Africa museum and Tigray Bureau of Agriculture and Rural Development, pp. 50.

Orense, R. P. (2011). Slope failures triggered by heavy rainfall. Philippine Engineering Journal. 25, 73–90.

Pasuto, A., Soldati, M. (2013). Lateral Spreading. In J. Shroder (Ed. in Chief), R. A. Marston, M. Stoffel (Eds.), Treatise on Geomorphology, vol. 7, Mountain and hillslope geomorphology. Academic Press, San Diego, pp. 239–248.

Pei, Q. T., Li, H. B., Liu, Y. Q., Jiang, J. G. (2013). Influence of slope gradient on distribution rule of geostress field in river valleys. Applied Mechanics and Materials, 404, 365–370.

Qin, C., Zheng, F. L., Wells, R., Xu, X., Wang, B., Zhong, K. (2018). A laboratory study of channel sidewall expansion in upland concentrated flows. Soil & Tillage Research, 178, 22–31.

Qin, W., Zhu, Q. K., Zhao, L. L., Qi, G. M. (2010). Topographic characteristics of ephemeral gully erosion in loess hilly and gully region based on RS and GIS. Transactions of the CSAE, 26, 58–64. (in Chinese).

Rowland, J. C., Dietrich, W. E., Day, G., Parker, G. (2009). Formation and maintenance of single-thread tie channels entering floodplain lakes: Observations from three diverse river systems. Journal of Geophysical Research, 114, F02013.

Sánchez-Canales, M., López-Benito, A., Acuña, V., Ziv, G., Hamel, P., Chaplin-Krame, R., & Elorza, F. J. (2015). Sensitivity analysis of a sediment dynamics model applied in a Mediterranean river basin: global change and management implications. Science of the Total Environment, 502, 602–610.

Simon, A., Collison, A. J. C. (2010). Quantifying the mechanical and hydrologic effects of riparian vegetation on streambank stability. Earth Surface Processes and Landforms, 27, 527–546.

Spalevic, V., Nyssen, J., Curovic, M., Lenaerts, T., Kerckhof, A., Annys, K. Van Den Branden, J., Frankl, A. (2013). The impact of land use on soil erosion in the river basin Boljanska Rijeka in Montenegro. Proceedings Agrosym 2013, Keynote Papers, pp. 54–63.

Tang, G. A., Zhao, M. D., Li, T. W., Liu, Y. M., Xie, Y. L. (2003). Modelling slope uncertainty derived from DEMs in loess plateau. Acta Geographica Sinica, 58, 824–830. (in Chinese).

Thornes, J. B., Alcantara-Ayala, I. (1998). Modeling mass failure in a Mediterranean mountain environment: climatic, geological, topographical and erosional controls. Geomorphology, 24, 87–100.

Tu, X. B., Kwong, A. K. L., Dai, F. C., Tham, L. G., Min, H. (2009). Field monitoring of rainfall infiltration in a loess slope and analysis of failure mechanism of rainfall-induced landslides. Engineering Geology, 105, 134–150.

Veness, J. A. (1980). The role of fluting in gully extension. Journal of Soil Conservation Service of New South Wales, 36, 100–108.

Vianello, A., Cavalli, M., Tarolli, P. (2009). Lidar-derived slopes for headwater channel network analysis. Catena, 76, 97–106.

Wang, C., Tang, G. A., Zhang, T., Li, Z. B., Wang, L., Wu, L. C. (2005). The study with high precision and high resolution of spatial variation of slope at small loess watershed with the erosion of rainfall. Journal of Mountain Research, 23, 589–595. (in Chinese).

Wang, L. Q., Liang, T., Zhang, Q. (2013). Laboratory experiments of phosphorus loss with surface runoff during simulated rainfall. Environmental Earth Sciences, 70, 2839–2846.

Wang, W. Z., Jiao, J. Y. (1996). Statistic analysis of the variation of rainfall and runoff-sediment yield process on slope surface in Loess Plateau Region. Bulletin of Soil and Water Conservation, 5, 21–28. (in Chinese)

Wang, X. F., Huo, A. D., Zhu, X. H., Zhao, Y. B., Jiang, C., Zheng, X. L. (2019). Study on governance mode of gully consolidation and highland protection project in East Gansu. Yellow River, 41, 106–109. (in Chinese).

Wang, Z. J. (2014). Characteristics of Vegetation and Erosion Sediment Yield in the Yanhe Watershed. Yangling: Research Center for Soil and Water Conservation and Ecological Environment, Chinese Academy of Sciences and Ministry of Education. (in Chinese)

Wang, Z. J., Jiao, J. Y., Rayburg, S., Wang, Q. L., Su, Y. (2016). Soil erosion resistance of Grain for green vegetation types under extreme rainfall conditions on the Loess Plateau, China. Catena, 141, 109–116.

Wei, W., Chen, L. D., Fu, B. J., Lv, Y. H., Gong, J. (2010). Responses of water erosion to rainfall extremes and vegetation types in a loess semiarid hilly area, NW China. Hydrological Processes, 23, 1780–1791.

Wijdenes, D. J. O., Bryan, R. B. (2010). Gully-head erosion processes on a semi-arid valley floor in Kenya: a case study into temporal variation and sediment budgeting. Earth Surface Processes & Landforms, 26, 911–933.

Wu, Y. Q., Zheng, Q. H., Zhang, Y. G., Liu, B. Y., Chen, H., & Wang, Y. Z. (2008). Development of gullies and sediment production in the black soil region of northeastern China. Geomorphology, 101, 683–691.

Xiao, C. C., Tang, G. A. (2007). Classification of valley shoulder line in loess relief. Arid Land Geography, 30, 646–653. (in Chinese).

Xu, X. Z., Liu, Z. Y., Xiao, P. Q., Guo, W. Z., Zhang, H. W., Zhao, C., Yan Q. (2015a). Gravity erosion on the steep loess slope: Behavior, trigger and sensitivity. Catena, 135, 231–239.

Xu, X. Z., Ma, Y. L., Yang, W. J., Zhang, H. W., Tarolli, P., Jiang, Y. Z., Yan, Q. (2020). Qualifying mass failures on loess gully sidewalls using laboratory experimentation. Catena, 187, 104252.

Xu, X. Z., Zhang, H. W., Wang, W. L., Zhao, C., Yan, Q. (2015b). Quantitative monitoring of gravity erosion using a novel 3D surface measuring technique: Validation and case study. Natural Hazards, 75, 1927–1939.

Xu, X. Z., Zhang, H. W., Zhang O. Y. (2004). Development of check-dam systems in gullies on the Loess Plateau, China. Environmental Science & Policy, 7, 79–86.

Yan, S. J., Tang, G. A., Li, F. Y., Zhang, L. (2014). Snake model for the extraction of loess shoulder-line from DEMs. Journal of Mountain Science, 11, 1552–1559.

Yang, J. S., Yao, W. Y., Ma, X. P., Shao, H., Wang, L. L. (2011). Progress of the gravity erosion and sediment yield study in the Loess Plateau. Yellow River, 33, 77–79. (in Chinese).

Yitbarek, T. W., Belliethathan, S., Stringer, L. C. (2012). The onsite cost of gully erosion and cost-benefit of gully rehabilitation: A case study in Ethiopia. Land Degradation & Development, 23, 157–166.

Zgłobicki, W., Baran-Zgłobicka, B., Gawrysiak, L., Telecka, M. (2015). The impact of permanent gullies on present-day land use and agriculture in loess areas (E. Poland). Catena, 126, 28–36.

Zhang, L., Tang, G. A., Li, F. Y., Xiong, L. Y. (2012). A review on research of loess shoulder-line. Geography and Geo-Information Science, 28, 44–48. (in Chinese)

Zheng, F. L., Xiao, P. Q. (2010). Gully erosion and sediment yield on the Loess Plateau. Beijing Science Press, 7 pp. (in Chinese)

Part Ⅱ
Abstracts

This section contains all the abstracts that has been signed copyrighted sharing agreement and accepted by LASOSU2021

2.1 Keynote Speeches

Metacoupling: Framework and Applications

Jianguo (Jack) Liu
Michigan State University (USA)

Abstract

The United Nations aims to achieve all the Sustainable Development Goals "everywhere" by 2030. However, the impacts of global human-interactions across space on achieving the goals are largely unknown, because previous research efforts often focused on specific places separately and paid inadequate attention to human-nature interactions with other places nearby and faraway. To address such crucial knowledge gaps, this talk will first introduce the integrated framework of metacoupling (human-nature interactions within as well as between adjacent and distant places). Then, the talk will present examples of applying the framework to the UN Sustainable Development Goals, international trade, food-energy-water-CO2 nexus, and global land use and food security. Finally, the talk will highlight challenges and opportunities in applying the framework, benefits of metacoupling research, and implications of the framework for land degradation, soil conservation, and sustainable development.

China's Ecosystem Restoration and Management

Bojie Fu
Research Centre for Eco-Environmental Sciences, Chinese Academy of Sciences

Abstract

China is working to achieve ecosystem protection and restoration, and Eco-civilization is the guiding philosophy of this process, which is centered on the idea of respecting nature, conforming to nature, and protecting nature. Historically, due to the complex and diverse ecosystems and the uneven distribution of population and resources, China's socio-economic development has caused several ecological problems, including dust storms, soil erosion, land desertification, and over-exploitation of resources. Through a series of ecological restoration projects implemented at the national and local levels, such as the Chinese Ecosystem Research Network, Natural Forest Conservation Program, Grain to Green Program, and Ecological Conservation Red Line at the national level, as well as the Wind and Sand Source Area Control Program, the Three-River Sources Ecological Program, and the Rocky Desertification Control Program at the local level, the area of soil erosion decreased by 5.6%, land desertification decreased by 6%, and land stone desertification decreased by 4.7% between 2000 and 2010, and vegetation restoration also greatly contributed to carbon sink and soil protection. However, China is also beginning to face new ecological challenges from urbanization, over-exploitation of water resources, coastal wetland loss. Additionally, the future ecological restoration will need to shift from an increase in vegetation area to an improvement in ecosystem quality through landscape restoration and management

.

Soil Infiltration: Physics Math & Experiments

Tingwu Lei
China Agricultural University

Abstract

Soil infiltration is an important component in overland hydrological process, to affect soil water budgets, overland surface water runoff and soil erosion, as well as ground water recharge. There are numerous traditional methods to measure soil infiltration, such as rain simulator, and signal and double ring infiltriometers. They are featured with difficulties to install in the field and to produce high errors in measured infiltration rate. Soil infiltration is physically and mathematically comparable to capacitance electric circuit as well as to rill erosion process, which share very similar principals. An electric capacitance needs time to recharge to full so does an eroding rill need distance to reach the transport capacity. American Society of Testing Materials recommend that soil infiltration is recommended to be measured every 15 min during the initial hour and 30 min or longer later on. Too short a measurement time duration produces high measurement error. Long time duration to make measurement reduces random error and middle point assignment reduces systematic error. Soil infiltration can be measured with rainfall runoff method. The rainfall intensity and runoff generation slope length produce defined runoff intensity. The runoff intensity covers ever-increasing wetted area, to supply a way to compute soil infiltration rate, with a convenient measurement procedure. In point source method, when water flow of given discharge is supplied, the wetted soil surface area can be automatically measured to mathematically compute the soil infiltration. The automatic system and the computational method make the measurement accurate and convenient. Physic method was used to stop soil preferential flow to measure soil matrix infiltration. Therefore it is used to determine the soil preferential flow rate by the total soil infiltration subtracting its matrix infiltration rate. All those methods are of great important for over land runoff estimation.

Challenges for land and soil protection in mountain areas

Vincenzo D'Agostino
University of Padova (Italy)

Abstract

The context of steep mountain catchments is presented by analysing the related main challenges posed by this highly erosive and unstable environment. Here, during flood events, different forms of intense sediment flows occur in the mountain river network ("torrents" in Europe). These forms range from bedload transport to debris flood to debris flow and they demand specific actions for the land protection. The anthropic action in the next years should be addressed increasingly by locking for protective solutions under the umbrella of sustainability at global watershed scale. Some insights are provided highlighting the milestones, which might drive scientist and local authorities for soil protection in mountain areas: i) controlling the sediment transport via a morphological-oriented approach (e.g usage of boulders to imitate natural step pools and rapids); ii) managing vegetation and large wood in channels by dosing the priorities (e.g., river habitat preservation versus hydraulic efficiency need); iii) planning the maintenance of protection works as well as assessing their functionality and life expectancy; iiii) providing right communication of expected hazards to inhabitants (even in presence of existing protection works); last but not least: iiiii) dedicating more efforts to a correct planning of the urban development also recovering past mistakes (e.g., decreasing the presence of buildings and roads in morphologically evident floodplain areas).

Benggang erosion in southern China: challenges and research needs

Chongfa Cai
Huazhong Agricultural University

Abstract

Benggang, a spectacular fragmented erosional landform, has been highlighted as a national concern in China due to its serious impacts on ecosystem and social services in tropical and subtropical regions. Benggang is a composite erosion formed by hydraulic scour and gravitational collapse. An effective control of Benggang is always technically difficult or extremely expensive, due to the complication in erosion process and randomization in erosion development. Whether Benggang is a unique erosion type and only distributes in southern China still remains inconclusive. Given the unclear of erosion mechanism and unsatisfied erosion control of Benggang, this presentation is devoted to highlighting soil erosion in southern China in a global perspective. Herein, relevant works including the spatial distribution of Benggang, similar erosional landforms around the world, driving forces, erosion process and mechanisms of Benggang have been addressed briefly. According to our existing studies, some useful conclusions and suggestions have been made. Overall, to facilitate the investigation and preventation of Benggang, it is necessary to establish a global research network of gully erosion that includes Benggang.

Land Degradation, Wildfires and Ecosystem Services

Paulo Alexandre da Silva Pereira
Mykolas Romeris Univeristy (Lithuania)

Abstract

Land Degradation is a pervasive natural and man-made phenomenon that affects, directly and indirectly, the environment, society and economy. Fire is a natural element of the ecosystems; however, climate change and land abandonment increased wildfire severity and recurrence in the last years, with detrimental effects on the ecosystems and human goods. This is a global catastrophe, as 2021 is shown in different parts of the world (e.g., Siberia, California).

In the immediate period after the wildfire, the ecosystems are vulnerable (window of disturbance) to meteorological agents, increasing land degradation risk. This degradation can be even high if the wildfires have a high recurrence or human interventions damage the soil (e.g., salvage logging). A high fire recurrence and unsustainable management practices reduce the capacity of the fire-affected areas to supply ecosystem services. In this context, post-fire management is a crucial aspect of minimising the wildfire effects and restoring the supply of Ecosystem Services in these areas. In this key lecture, the effects of wildfires on land degradation and ecosystem services will be discussed

.

The Conservation Agricultural Model based on the No till system

Roberto A. Peiretti
Argentine No-Till Farmers Association (Argentina)

Abstract

Since agriculture begun around ten thousand years ago, the process was based in some kind of soil tillage. In modern times and drive by the mechanization growth, tillage was intensified mostly based in soil inversion using the moldboard ploughs as well as other tillage tools. The soil deterioration and degradation were quickly accelerated by means of wind and water run-off erosion as well as by oxidation of the soil organic matter. Here a new farming system able to offer a valid answer to the restrictions was designed and step by step adapted and adopted around the world. The new System is based in three main principles; namely: avoidance of tillage, soil covered as much and as long as possible and crop rotation and diversity. The three main principles are valid universally, however they have to be adapted to local conditions. Carbon plays a central key role within the new farming paradigm. Conservation Agriculture based on the No Till System, truly represents a Paradigmatic change and evolution of the farming system that could reach and benefit any agro-ecosystem around the world and hence the whole humanity.

2.2 Focus Group Discussion

Global Soil Conservation and Food Production

Fenli Zheng
Institute of Soil and Water Conservation, Chinese Academy of Sciences

Abstract

The FGD is a hot discussion related to the topic entitled Global Soil Conservation and Food Production. Six outstanding scientists from 4 different countries are involved in the discussion.

USDA-ARS' Vision for Future Erosion Research and Model Development

Chi-hua Huang
USDA-ARS National Soil Erosion Research Lab (SUA)

Abstract

In the fall of 2019 and spring of 2020, a group of USDA-ARS scientists developed a strategic plan for future soil erosion research and model development. An article describing this plan has been published in the Journal of Soil and Water Conservation: https://doi.org/10.2489/jswc.2020.0805A The background for this development and the anticipated outcomes will be presented in the Focus Group Discussion during LASOSU2021.

Surveying and Mapping of Northeastern Black Soil and its Conservation

Baoyuan Liu
Beijing Normal University

Abstract

The protection of black soil is of general concern to President Xi and the entire country. How large is the black soil area, where is it distributed, what is the current situation, and what are the prospects for sustainable use...etc. These are the premises of the effective protection of black soil. The distribution of black soil is discontinuous, it is interleaved with other soil and ground components. Digital survey and mapping are beneficial to make statistics on the area, and draw up the distribution map, therefore, the "central gravitational agglomeration method" has been proposed, and the distribution map of black soil is prepared, to provide reference for planning of the protection of black soil. It is delineated that: the Northeast black soil area is 556,000 km^2, and the typical black soil area is 333,000 km^2. According to the current conditions and erosion forecast of black soil, the risk of soil erosion and degradation is obtained, proposing that the key projects of soil and water conservation is 89,000 km^2, and the prioritization object is 78,000 km^2.

Current Global Food Crises and Soil Conservation

Fei Wang
Institute of Soil and Water conservation, Chinese Academy of Sciences and Ministry of Water Resources, Northwest A&F University

Abstract

Soil erosion worldwide increases continuously in last several decades, and it will be worse with the population growth, climate change and regional conflicting very likely. The wind and water erosion will make the soil degradation threating to land, freshwater and food security and that will aggravate the malnutrition. There was more than 820 million people in hungry in 2019 reported by WFP and enhanced by the COVID-19 pandemic since 2019 over more than 48 countries. The global soil erosion rate and hungry people distribution matches quite well in 2010's and arises the task of soil and water conservation for food production.

It is necessary to pay more attention to soil erosion and food crises if we considering the facts of less people for field working, much poorer to purchase food, shortage of world food supply induced by COVID-19 and extreme climate events and its relating disasters of drought and flooding. What's is the future of hungry people in the soil erosion area is standing upon of us. It is time to find solutions to improve the soil quality for food and encourage the people to conquer this hard stage together.

Earth, Agriculture, and Society: towards sustainable development in the Anthropocene

Paolo Tarolli
University of Padova (Italy)

Abstract

The unsustainable intensification of agriculture driven by the rapid population growth of the last half past century has led, for some regions in the world, to a strong acceleration in the rate of erosion (and in general land degradation) to the extent that the soil is lost at a greater magnitude than it is produced by mechanisms of regeneration. The 2030 Sustainable Development Goals (SDGs) aim to end poverty, combat inequality, build peaceful societies, and fight climate change, promoting sustainable socioeconomic progress. SDG2 "End hunger, achieve food security and improved nutrition and promote sustainable agriculture", purposes to eliminate hunger around the world, which is often linked to environmental degradation, drought, and loss of biodiversity (United Nations 2020). According to SDG2, the sustainability of an agricultural practice must be assessed in the economic, social, and environmental context. It must combine the themes of productivity, profitability, resilience, land/water management, decent work, and well-being, in order to capture its multidimensional nature (FAO 2020). Intensification needs to be sustainable; unsustainable agriculture has a significant impact on soil. When we are talking about sustainable agriculture we need also to include an adaptation to different climate regimes; wrong actions, especially in drylands could create more critical scenarios and further accelerate land degradation. Humans started to cultivate land thousands years ago, and in some region, soil conservation / agricultural practices shaped the landscapes in an unique way creating a virtuous equilibrium with nature; these are terraces, considered cultural heritage, cultural ecosystem services, that need to be protected. Therefore when we provide solutions, these should be not only focused at soil/land protection, but also to people and their traditions.

This talk provides an overview, in support of the discussed topic, of some useful case studies located on high-steep agricultural landscapes of the World. Such environments offer a perspective in helping to guide future research for better management of socio-economically relevant agricultural landscapes, and therefore guarantee sustainable food production.

The role of Check Dam on the Pothohar Plateau of Pakistan

Altaf Ali Siyal
Sindh Agriculture University Tandojam (Pakistan)

Abstract

The Pothohar Plateau of Pakistan has a severe soil erosion issue due to scarce vegetation and an erodible underlying soil surface.

Unsustainable farming practices for since long, combined with huge population pressures and soil erosion, have led to severe environmental degradation in these areas. As a key measure for soil and water conservation in this area, check dams have achieved remarkable results. Check dams are small dams constructed across small streams to reduce the runoff velocity, prevent soil erosion and recharge the groundwater. About 1,000 check-dams are in Pothohar Plateau, while more than 100,000 check dams have been built on the Loess Plateau since the 1950s. The climatic, underlying soil conditions, and the proportion of the agricultural population in the Pothohar Plateau of Pakistan are very similar to those of the Loess Plateau of China. In Pakistan, Farmers of Pothohar are suffering from food shortages. The check dams, constructed in collaboration with the Chinese Government, play an important role in solving local food, erosion, and groundwater recharge issues in the Pothohar plateau. Collaborative research between Pakistan and China can improve the management level and efficient use of water and sediment technology in both areas, especially in the Pothohar plateau

2.3 Parallel Sessions

Hydraulic Tests and Interpretation of Test Data for Erosion Protection Systems in Open Channel Flow

Paolo Di Pietro*[1], Nicola Mazzon[2], Fuding (Frank) Xu[3], Baiying (Calipso) Zhang[4]
1 Corporate Business Unit Senior Specialist, Officine Maccaferri S.p.A., Italy
2 R&D Manager, Maccaferri Innovation Center (M.I.C.), Italy
3 Technical Marketing Director, Maccaferri Changsha, China
4 DT Business Development, Maccaferri Changsha, China
*Corresponding Author, e-mail: p.dipietro@maccaferri.com

Abstract

The stability of erosion control systems depends both on the ability to prevent soil loss underneath, as well as to maintain their integrity under the effects of the flow. This work is about a comprehensive research study aimed at studying performance of revet mattresses and of geosynthetic mats as lining systems in open channels. Geomats were tested on a 0.6 x 20m flume at 2.7%, laid on soil bed at variable discharge rates, in accordance with ASTM D6460. For revet mattresses, tests were done on a 1 x 10m size flume where units were placed on a 0.30m soil layer. The performance against erosion was evaluated by assessing the effect of the stone motion inside the mattress, in relationship to its thickness and stone size, under variable hydraulic flow regimes. While confirming the design method typical for revet mattresses (commonly referred to the tractive force theory using Shield parameters), research allowed to define a new performance limit based on incipient soil erosion underneath by monitoring soil settlements due to the flow. The study for the mattresses was aimed at defining whether different types of partition diaphragms in mattresses provide different results against stability. Research also established a range of applicability between geomats and rock filled mattress systems, in order to define a criterion based on performance. Tests on geomats were performed both in unvegetated and vegetated condition

Keywords: Revet mattresses, Erosion control, Open channel, Shear stress, Velocity

Utilization of arbuscular mycorrhizal fungi for controlling soil erosion

Hongguang Liu*[1], Lichao Zhang[2], Faxing Shen[1]
1 Institute of Soil and Water Conservation, Jiangxi Academy of Water Science and Engineering, Nanchang, China
2 Institute of Water resources Planning and Development, Jiangxi Academy of Water Science and Engineering, Nanchang, China
*Corresponding Author, e-mail: Hongguangliu0791@hotmail.com

Abstract

Plant measure is a vital alternative for controlling soil erosion and promoting sustainable development. The contribution of soil microbiome associated with plant roots for soil erosion control is largely neglected. Arbuscular mycorrhizal fungi (AMF) could establish mutualistic symbiosis with roots of over 90% of terrestrial plants, and facilitate the formation and stabilization of soil aggregates. However, it is far from utilizing AMF in soil erosion conservation. We found the AMF community diversity indices are higher in smaller than in large sizes of soil aggregates, but with consistent community composition, associated with grasses commonly used for control soil erosion. Soil phosphorus, pH and potassium are the main factors correlated with AMF diversity changes at aggregate level. Inoculation with single AMF significantly enhanced the plant growth and root architecture parameters of clover, and associated soil aggregate stability. However, the impact of AMF inoculation followed host-AMF pattern. The suppression of indigenous AMF using benomyl significantly increased the sediment yield and phosphorus loss, emphasizing the importance of AMF for reducing phosphorus loss on sloping land. We therefore propose the two ways of utilizing AMF for controlling soil erosion: i inoculating soil conservation plants with synthetic AMF consortia to maximize its benefits for the areas deficient of AMF propagule; ii optimizing the management practices (such as no tillage, lower P fertilizer and cover grass) to nourish the indigenous AMF.

Keywords: Soil microbe, Erosion control, Plant measure, Phosphorus loss

Estimation of soil erosion and its response to land use change predicted with RMMF model in karst regions of northwest Guangxi, southwest China

Hongsong Chen*[1,2], Jinjiao Lian[1,2], Teng Feng[3], Chengzhi Li[1,2]

1 Key Laboratory of Agro-Ecological Processes in Subtropical Region, Institute of Subtropical Agriculture, Chinese Academy of Sciences, Changsha 410125, China

2 Huanjiang Observation and Research Station for Karst Ecosystems, Chinese Academy of Sciences, Huanjiang 547100, China

3 School of Resource & Environment and Safety Engineering, Hunan University of Science and Technology, Xiangtan 411201, Hunan, China

*Corresponding Author, e-mail: hbchs@isa.ac.cn

Abstract

Rock desertification is caused by deforestation and subsequent severe soil erosion in karst regions with fragile eco-environment. However, due to the differences of lithology and human influence intensity, the spatial distribution of soil loss and its relationship with land uses are still unclear at regional scale. Based on the revised Morgan-Morgan-Finney (RMMF) model and ArcGIS technology, this study aimed to simulate surface soil erosion in 1990, 2000 and 2010, and to investigate its response to land use changes from 1990 to 2010 in northwest Guangxi, southwest China. The simulated results showed that most areas suffered from slight degree of soil erosion. For karst area, the soil erosion modulus (SEM) in 1990, 2000, and 2010, was 17.97 t km^{-2} a^{-1}, 12.00 t km^{-2} a^{-1} and 18.85 t km^{-2} a^{-1}, respectively, but for non-karst area it was 311.45 t km^{-2} a^{-1}, 180.19 t km^{-2} a^{-1} and 309.90 t km^{-2} a^{-1}, respectively. The mean annual soil erosion amount (SEA) was 1056.86×104 t in non-karst area and 49.01 ×104 t in karst area. This indicated that the non-karst area was the main source of soil loss. Furthermore, for land use type, the mean annual SEA greatly came from sparse woodland (460.28×104 t) in non-karst area, but dry land (25.01×104 t) in karst area. In consideration of the same rainfall condition as 1990, SEA changed from 1233.54 ×104 t in 2000 to 1146.10 ×104 t in 2010 in non-karst area, and it varied from 57.11 ×104 t in 2000 to 56.99 ×104 t in 2010 in karst area. This suggested that “Grain for Green” Plan had reduced SEA, mostly in non-karst area. This study may help to assess the soil-water conservation effectiveness in karst region.

Keywords: Soil erosion, RMMF model, Karst area, Non-karst area, Land use type

An experimental investigation of the uncertainties of lacustrine-delta morphology driven by water inflow

Xiaolong Song*[1,2], Haijue Xu[1,2], Yuchuan Bai[1,2]

1 State Key Laboratory of Hydraulic Engineering Simulation and Safety, Tianjin University, Tianjin 300350, China

2 Institute for Sedimentation on River and Coastal Engineering, Tianjin University, Tianjin 300350, China

*Corresponding Author, e-mail: xlsong@tju.edu.cn

Abstract

The development of lacustrine-delta systems possesses some stochastic characteristics even under slow-varying external conditions. In this study, two sets of repeated physical modeling experiments were conducted to tentatively explore the uncertain effects of the upstream river-inflow on the lacustrine-delta morphology. The quantitative analysis of the geometrical characteristics of the obtained quasi-periodically similar deltaic channels and sedimentations, on one hand, revealed some fresh information of bifurcation instability of channels in terms of the deterministic position indicator of bifurcation node and the factor of flow turbulence, and the non-deterministic noise factors of sediment properties; on the other hand, demonstrated that within the Runs-Repeated works, the unbalanced sediment transportation along the quasi-equiprobable anticlockwise-clockwise diverging directions from the polar perspective resulted in the remarkably negative relationships of both the average amplitude of the indicator of sedimental center and average frequency of the indicator of sedimental height versus the corresponding average values, in low-discharge cases; while, the uncertainties of the indicator of sedimental width always become prominent accompanied by the weakening of flow instability, in high-discharge cases. This study innovatively interprets a new probabilistic way of understanding the lacustrine-delta morphology.

Keywords: Lacustrine-delta morphology, Water inflow; Quasi-periodically similar, Bifurcation instability, Unbalanced sediment transportation

Rock fragment sizes regulate the effects of rock coverage on soil erosion

Xinli Li*[1], Suhua Fu[1], Yaxian Hu[2], Baoyuan Liu[1,2]
1 Faculty of Geographical Science, Beijing Normal University, Beijing 100875, PR China
2 State Key Laboratory of Soil Erosion and Dryland Farming on the Loess Plateau, Institute of Soil and Water Conservation, Northwest A&F University, Yangling 712100, PR China
*Corresponding Author, e-mail: lixinli1995@163.com

Abstract

Soil erosion can cause environmental, economic and social problems. The presence of rock fragments can change land cover, resulting in tremendous impacts on soil erosion process. Many studies investigated the effects of rock fragments coverage and contents on soil erosion, but the effects of rock fragment size on soil erosion need further investigation. Therefore, the purpose of this study is to identify the impacts of rock fragment size on runoff, sediment concentration and soil loss. A series of simulated rainfall experiments were applied to erosion plots with two initial soil moisture contents (dry run and wet run) and two rock fragment coverage (30 % and 60 %). To be specific, each erosion plot was covered with rock fragments of the same size, and in total seven different fragment sizes were selected to form the two rock fragment coverage: 0.7, 1.1, 3.0, 5.5, 12.0, 18.8 and 36.0 cm. The results show that runoff, sediment concentration and soil loss increased with rock fragment size and the rock fragment size and soil loss ratio followed a power function (R^2 = 0.96). The sediment concentration and soil loss were greater under the 30% coverage than that under the 60% coverage. The erosion plots with wet run generated greater runoff, sediment concentration and soil loss. Our findings can help to advance our current understanding of soil erosion process and soil erosion control management for rocky regions where rock fragments are abundantly available and thus often used to cover soil surface to prevent soil erosion.

Keywords: Rock fragment, Soil moisture, Soil erosion, Runoff, Land cove

Effects of Acanthopanax senticosus cultivation on soil physical properties of abandoned slope farmland in warm, cool and humid mountainous areas

Yizi Duan*[1], Kezhuang Wang[1], Haili Ru[1], Fu Wang[1]
1 Pingliang Research Institute of soil and water conservation. Pingliang. GanSu
*Corresponding Author, e-mail: 876728963@qq.com

Abstract

In this study, typical field investigation and indoor analysis were used to select the representative Acanthopanax senticosus concentrated cultivation site. The results showed that with the increase of soil depth, the soil bulk density of Acanthopanax senticosus and corn land also increased. In 0-60cm soil layer, the non capillary pore of Acanthopanax senticosus forest land was 15.24%, and that of corn leisure land was 9.78% The results showed that the air permeability of Acanthopanax senticosus forest land was better than that of corn fallow land; the soil particles > 5mm in 2-year-old Acanthopanax senticosus forest land accounted for 35.74% of the total weight of soil samples, the soil particles 2-5mm accounted for 32.97%, the soil particles < 0.5mm accounted for 31.3% of the total weight of soil samples, and the soil particles < 0.25mm only accounted for 5.6%, and the sand content in the soil was higher; the soil particles > 5mm in 3-year-old Acanthopanax senticosus forest land accounted for 88.4% of the total weight of soil samples, and the soil particles < 0.5mm accounted for 5.6% of the total weight of The total root length was 1.9 times of that in 20-30cm soil layer and 9.8 times of that in 30-40cm soil layer, accounting for 59.6% of the total root weight; the length and quantity of hairy roots less than 1mm were greater than those in other soil layers, accounting for 66.7% of the total root length and 85.7% of the total root number It is mainly distributed in 0-20cm soil layer, showing the growth and development characteristics of shallow rooted shrubs, which is conducive to improving the surface soil structure, improving soil porosity, and increasing the storage and utilization capacity of precipitation and surface runoff.

Keywords: Warm, Cool and humid mountainous area abandoned farmland Acanthopanax senticosus cultivation soil physical properties

Slop threshold for overland flow resistance on sandy soils

A. Nicosia*[1], V. Pampalone[1]
1 Department of Agricultural, Food and Forest Sciences, University of Palermo, Palermo, Italy
*Corresponding Author, e-mail: alessio.nicosia@unipa.it

Abstract

In this paper, using measurements available in literature carried out in sandy soils by flume characterized by gentle and steep slopes, a theoretical overland flow resistance equation based on the integration of the power velocity distribution, is tested.The main aim of this paper is to deduce a relationship between the velocity profile parameter Γ, the channel slope *s*, the Reynolds number *Re* and the Froude number *F* using a data base characterized by a wide range of hydraulic conditions, for sandy soils having a gentle slope (5.2%- 13.2%) and a steep slope (17.4% - 42.3%).The analysis demonstrated that: 1) the velocity profile parameter can be accurately estimated by the proposed equation in which the exponents of Re, F and s can be assumed independent of the slope condition, while the scale coefficient a is equal to 0.8750 for the gentle slope condition and 0.8984 for the steep slope; 2) the Darcy-Weisbach friction factor estimates by the theoretical flow resistance law are accurate and characterized by errors ≤+ 5% for 97.2% of cases, and 3) in the range of steep slope, the flow resistance law calibrated for the gentle slope condition systematically overestimates the Darcy-Weisbach friction factor. Finally, the distinction between gentle and steep slope condition allows to properly consider the effect of sediment transport on the estimate of the friction factor for overland flow.

Keywords: Flow resistance, Overland flow hydraulics, Soil erosion, Gentle hillslopes, Steep hillslopes

Multifractal characteristics of soil particle-size distribution under different land-use types in an area with high frequency debris flow

Songyang Li[1,2,3], Jingyuan Lin[1], Jiahong Pan[1], Hang Yu[1,2,3], Ruoyun Gao[1,2,3], Liusheng Yang[1,2,3], Yongming Lin*[1,2,3], Daojie Wang[2,4], Jian Li[1,3]
1 College of Forestry, Fujian Agriculture and Forestry University, China;
2 Key Laboratory of Mountain Hazards and Surface Processes, Chinese Academy of Sciences, China
3 Key Laboratory for Forest Ecosystem Process and Management of Fujian Province, China; 4 Institute of Mountain Hazards and Environment, Chinese Academy of Sciences and Ministry of Water Conservancy, China
*Corresponding Author, e-mail: monkey1422@163.com

Abstract

Aiming to reveal the influence of different land use types on soil particle size distribution in the area with frequent debris flow, the multifractal characteristics of soil particle size distribution in the area with frequent debris flow were studied. Four typical land use types, including bare land, meadow, shrubs, and woodlands, were selected to collect soil samples of 5 soil layers from 3 soil profiles in each land use type for particle size analysis. The laser diffraction method was used to measure soil particle size distribution. We calculated multifractal parameters based on multifractal theory. ① Land use type has significant impact on the soil particle distribution. The volume fraction of silt particles in shrubs, forest is significantly larger than bare land, meadow, while the total volume fraction of sand particles is bare land, meadow is significantly larger than shrub, forest. The soil depth has no significant effect on soil particle size distribution in the depth range of 0-50 cm. ② In this study, the generalized dimensions spectra curves of soil particle distribution in bare land, meadow, shrub and forest are inverse "S" curve, while the singular spectrum function of the soil particle size is an asymmetric upward convex curve, indicate indicating that the soil particle size distribution at different depths of the plots has multifractal characteristics. The multifractal parameters of soil particle size distribution have significant differences in different land use types. The soil texture gradually becomes thinner following the sequence from bare land to woodlands. The heterogeneity of soil particle size distribution gradually decreases following the sequence of bare land − meadow − shrubs − woodlands. This study provided a theoretical basis for the evaluation of soil structure improvement and vegetation restoration effects in areas with frequent debris flow.

Keywords: High-frequency debris flow area, Soil particle-size distribution, Multifractal, Soil texture

Interactive effects of rainfall and flow depth on the resistance characteristics of sheet flow

Enshuai Shen[1,2,3], Gang Liu*[1,2], Chenxi Dan[2], Chengbo Shu[2]
1 State Key Laboratory of Soil Erosion and Dryland Farming on the Loess Plateau, Institute of Soil and Water Conservation, Chinese Academy of Sciences and Ministry of Water Resources, Yangling 712100, China
2 Institute of Soil and Water Conservation, Northwest A&F University, Yangling, 712100, China
3 University of Chinese Academy of Sciences, Beijing 100049, China
*Corresponding Author, e-mail: gliu@foxmail.com

Abstract

The rainfall and sheet flow (SF) under the gentle slope always appear concurrently. However, the interactive effects of rainfall and flow depth on SF resistance is still unclear on gentle slopes. In this study, two sets of experimental (upstream inflow and rainfall + upstream inflow) were conducted to investigate resistance characteristics of SF. The results that in the flow depth alone conditions, the Darcy-Weisbach resistance (*f*) and Manning coefficient (*n*) decreased with increasing flow depth with the power function. When the Reynolds number (*Re*) is less than 1200, the *n* and *f* decreased with increasing *Re* in power function. Under the interactive condition of rainfall and flow depth, rainfall increased the *n* and *f* at low flow velocity and energy and reduced resistance at high flow velocity and energy. Both the *n* and *f* increased with increasing rainfall intensity. The effects of rainfall on the *f* and *n* were obvious in the laminar zone under interactive effects of rainfall and flow depth. Both the *f* and *n* decreased with increasing the ratio of flow depth and raindrop size (H/D50) in the laminar zone. It indicated that the deeper flow could dissipate more raindrop energy. Meanwhile, the fitted equations among the *Re* (< 1200), and H/D50 were established to predict the *n* and *f*. This study is helpful to understand the effect of the interactive rainfall and flow depth on SF resistance characteristics.

Keywords: Sheet flow, Rainfall intensity, Raindrop size, Flow resistance, Reynolds number

High-resolution topography for nested parameterization and validation of physically based soil erosion models

Lea Epple*[1], Andreas Kaiser[2], Marcus Schindewolf[3], Anette Eltner[4]
1 Department of Physical Geography, Institute for Geography, Friedrich-Schiller University Jena, Germany
2 Administrative Department for Climate and Sustainable Mobility, District Administration Siegen- Wittgenstein, Germany
3 Department of Plant Production, Thuringian State Institute of Agriculture, Jena, Germany
4 Institute of Photogrammetry and Remote Sensing, Technical University Dresden, Germany
*Corresponding Author, e-mail: lea.epple@uni-jena.de

Abstract

Information on soil erosion, transport and deposition as well as accurate erosion rate assessment is important to support sustainable management, soil protection and recovery strategies.In this study we use temporal and spatial high resolution time-lapse imagery to measure soil erosion from the micro-plot to the micro-watershed scale. The data will be implemented in physically based soil erosion models to improve the process mapping and validate predicted surface changes across scales. At the micro-plot scale (3 m²) we use eight to eleven cameras at time-lapse intervals of 20 seconds to monitor rainfall simulations. To capture soil surface changes during rainfall events at the hillslope scale, we installed a permanent rain-gauge triggered setup – three rigs at three slope positions, equipped with five synchronized RGB cameras. Furthermore, we take UAV-imagery before and after rainfall events to assess soil surface changes at the small catchment scale (4 ha).The observations are used for parameterization and validation of physically based soil erosion models. The adjustments of erosion models should enable cross-scale validation and displaying of scale-dependent processes and provide new perspectives on the relationship between event frequency and magnitude as well as connectivity.

Keywords: Physically-based soil erosion model, Time-lapse photogrammetry, Across-scale

Experimental study on the microstructure and mechanical properties of Pisha sandstone under wet-dry cycles

Feng Qu*[1], Caiqian Yang[1,2], Yanbing Zhao[1], Zhishui Liang[1], Zhiren Wu[3]
1 Key Laboratory of Concrete & Prestressed Concrete Structures of the Ministry of Education, Southeast University, Nanjing, 211102, China
2 College of Civil Engineering& Mechanics, Xiangtan University, Xiangtan, 411105, China
3 School of Environment and Safety Engineering, Jiangsu University, Zhenjiang, 212013, China
*Corresponding Author, e-mail: qufeng@seu.edu.cn

Abstract

The effects of the wet-dry cycles on the chemical compositions and mechanical properties of the Pisha sandstone were experimentally investigated in atmosphere conditions. The evolutions of the mineral compositions, microstructure characteristics were confirmed by X-ray diffraction (XRD) and scanning electron microscope (SEM). In addition, uniaxial compression tests were conducted to validate damage from a macro perspective. Experiment results indicated that the Pisha sandstone displayed extremely unstable performances in both chemical and physical properties when exposed to wet-dry cycles. The decompositions of easily weathering feldspar and calcite resulted in a dramatic increase in the proportion of secondary clay minerals, which increased by 54% in comparison to the initial condition. Consequently, the microstructures of the Pisha sandstone severely deteriorated and porosity increased by 177%. The compression properties (uniaxial compression strength) of the Pisha sandstone were sensitive to the wet-dry effects, which also linearly correlated with the porosity.

Keywords: Pisha sandstone, Microstructure, Mineral compositions, Uniaxial compression, Wet-dry cycle

Reducing soil erodibility of mine dump slope by biochar combined with Inoculated vegetation in the Loess Plateau, China

Yanfeng Zhu[1,2], Jing Ma[1], Qi Zhang[1,3], Zhanbin Luo[4], Jiao Zhao[2], Chen Fu*[1,2]
1 Engineering Research Center of Ministry of Education for Mine Ecological Restoration, Xuzhou 221116, China
2 Low Carbon Energy Institute, China University of Mining and Technology, Xuzhou 221008, Jiangsu, China
3 School of Public Policy & Management, China University of Mining and Technology, Xuzhou, China
4 College of Natural Resources and Environment, Northwest A&F University, Yangling, Shaanxi 712100, China
*Corresponding Author, e-mail: chenfu@cumt.edu.cn

Abstract

Soil erosion is a worldwide problem. Mining activities have destroyed the original terrain and vegetation, and aggravated the local soil erosion. In order to effectively prevent soil erosion on the slope of the mining area, the present research established a rainfall simulation-runoff plot observation experiment 39 treatments with 50*100cm sample plots on a slope of ~30%., using a three-dimensional laser micro-topography scanner (DEM) and a finite element analysis simulation model (ABAQUS) for discussing the effects of adding straw biochar (SBC) and inoculating arbuscular mycorrhizal fungi (AMF) on slope soil splash erosion and rill erosion under 3 kinds of ryegrass coverage. The results showed that: (1) SBC significantly increased the splash erosion of all treatment groups, and reduced the soil loss and sand content due to rill erosion. (2) The runoff, runoff coefficient and soil loss in the SBC+AFM treatment group were significantly reduced, and the runoff and sediment yield were 1.9 and 2.3 times that of the control group (CK) and SBC treatment group, respectively. (3) The results of DEM showed that compared with the CK and SBC treatment groups, the SBC+AFM treatment had balanced light and heat resources on the slope surface after rainfall, with low slope distortion and lower erosion than the CK and SBC treatment groups. The ABAQUS results show that SBC+AFM has improved the pore pressure, displacement, and saturation in the slope seepage, improved the water retention capacity of the slope, and slowed down the slope erosion process and the degree of soil erosion. The entire results can provide scientific parameters for the prevention and control of geological disasters slope soil erosion and shallow landslides in mining areas.

Keywords: Mine dump slope, Biochar, Arbuscular mycorrhizal fungi, Composite microtopography, Corrosion resistance

Double Turbulence Sources and its′ influence for Rainfall-Runoff Movement Process on High Steep Slopes

Xinghua Li[1], Zhe Gao[1], Jianen Gao*[1,2,3,4], Zihao Guo[3], Yan Yin[2], Xingchen Zhang[3], Pengcheng Sun[2] , Ji Mingjuan[2]
1 College of Water Resources and Architectural Engineering, Northwest A&F University, Yangling, Shaanxi, 712100,China.
2 Institute of Soil and Water Conservation, Northwest A&F University, Yangling, Shaanxi, 712100, China
3 Institute of Soil and Water Conservation, Chinese Academy of Sciences and Ministry of Water Resources, Yangling, Shaanxi, 712100, China
4 Research Center on Soil & Water Conservation Ministry of Water Resources, Yangling,712100, China
*Corresponding Author, e-mail: gaojianen@126.com

Abstract

A large number of high and steep slopes appear in the Yellow River basin for land regulation, often leading to serious storm runoff erosion. Aiming at the bigger calculation error of hydrodynamic parameters of rainfall runoff on high-steep slope, the interaction mechanism of rainfall and bed-facing to runoff was explored. The results are that the rainfall runoff movement of slope was affected by the double turbulence sources of bidirectional action of raindrops splash and bed roughness. The dispersed motion wave model proposed by the original hydraulic approach did not consider the sheet flow simultaneously affected by double turbulent sources, which led to poor calculation accuracy. In this study, based on the "double turbulent source sheet flow model of high and steep slopes", a new calculation method was proposed and verified by test data of indoor and field. The new model could be used to calculate hydraulic parameters of the slope runoff, and its accuracy was greatly improved, and it still could be used for calculations of slope flow processes. This is of great significance to the safety design of various high and steep slope and soil loss prevention in the Loess Plateau.

Keywords: Rainfall-Runoff Movement, Double Turbulence Sources, High and Steep Slopes

Geostatistical characterization of soil clay patterns in a typical watershed of cultivated black soil

Zhihu Sun[1], Enheng Wang[1], Xiangyou Xia[1], Xiangwei Chen*[1]
1 School of Forestry, Northeast Forestry University, Harbin, 150040, China
*Corresponding Author, e-mail: chenxwnefu@163.com

Abstract

Soil clay influences a range of processes including vertical and lateral redistribution of water, runoff, and erosion. Knowledge of the spatial pattern of soil clay content (SCC) in cultivated soil region is important. The objective of this study was to determine the degree of spatial variability of SCC across depths in a cultivated black soil region, northeastern China. Data collected from each of 58 sites on a regular grid of 50 by 50 m were analyzed both statistically and geostatistically to describe the spatial distribution. The SCCs between different segments in soil profiles were significant difference. The 0- to 65-cm soil profile could be clustered into 3 segments: 0- to 30-cm, 30- to 35-cm, and 35- to 65-cm layers.The standard deviation (SD) and coefficients of variation (CV) for SCC of 30- to 35-cm segment were greatest. Experimental semivariograms of SCC were best fitted by spherical models. Nugget-to-sill ratios indicated a strong spatial dependence for SCC at other depths except 40- to 45-cm and 60- to 65-cm segments. The 35- to 40-cm layer had the largest spatial dependency compared with the other layers. Cross-validation of the kriging map showed that prediction of SCC using semivariogram parameters was better than assuming mean of observed value for any unsampled location. The mapping displayed heterogeneity of SCC across the experimental site and revealed higher SCC close to tail of eroded gully and lower SCC neighbouring eroded gully margins. The fragmentation degree and clay-enriched patch amount increased from near-surface down to 65cm depth, suggesting the higher evenness of SCC in cultivated layer than that in the tillage pan.

Keywords: Black soil, Clay, Spatial pattern, Variogram

Massive evaluation of soil and water conservation in 50 Italian steep-slope vineyards by a systematic remote sensing-based approach

Anton Pijl[1], Paolo Tarolli*[1], Eugenio Straffelini[1], Wendi Wang[1]
1 Dept. of Land, Environment, Agriculture and Forestry, University of Padova, Legnaro (PD), Italy
*Corresponding Author, e-mail: paolo.tarolli@unipd.it

Abstract

Terracing is an important historical heritage in northern Italy agriculture, particularly in steep-slope wine production where their presence signifies cultural vineyard landscapes. Several different types of terraces are commonly used in this part of the world, each with unique characteristics in terms of soil and water conservation (SWC). There is an emerging need to understand and quantify the land degradation challenge of these steep cultivation systems, to ensure sustainable future viticulture. In this study, we aim to deliver an evaluation of 5 different terraced and non-terraced cultivation types in terms of SWC impact. For this purpose, we analysed 50 individual vineyards in northern Italy by workflow of high-resolution LiDAR data and physical modelling of water flow and sediment transportation. Simulations were systematically analysed to statistically compare and rank the 5 different practices in terms of soil and water movement using a predefined set of performance criteria. This work, relying on a workflow of big data, provides a reliable representation of the most common SWC systems in this part of the world. Our results thus lead to practical recommendations for improving sustainable management and planning in steep-slope cultivation systems.

Keywords: Remote sensing, Terracing, Steep-slope agriculture, LiDAR data, Modelling

Digital terrain analysis and geomorphometry for land degradation analysis

Giulia Sofia[1]
1 Department of Civil & Environmental Engineering University of Connecticut 261 Glenbrook Rd Storrs, CT 06269
*Corresponding Author, e-mail: giulia.sofia@uconn.edu

Abstract

In recent years, the wealth of technological development revolutionised our ability to collect data in geosciences. Due to the unprecedented level of detail of these datasets, researchers are facing new challenges, giving more in-depth answers to a broad(er) range of fundamental questions across the full spectrum of land degradation analysis. This contribution builds on the existing literature of geomorphometry (the science of quantitative land-surface analysis) and feature extraction (translate land surface parameters into extents of geomorphological elements). It offers examples of methodologies for mapping degrading land i.e. areas susceptible to land slide, flood damage and drought so that proper plans can be made for sustainable development of the land. It further highlights existing opportunities to develop GIS and Remote Sensing capabilities for land degradation assessment, computerized agro-zoning and sustainable land management planning, and the challenges of providing 'Training for the trainers'. It provides evidence of critical themes as well as emerging fields of future research in the digital realm, supporting the likely effectiveness of geomorphometry and feature extractions as they are advancing the theoretical, empirical and applied dimension of land degradation studies.

Keywords: LiDAR data, Modelling, Geomorphometry, DEM

Zero to thirty trillion: Advancing surface process studies with open access to high resolution topography

Ramon Arrowsmith*[1], Christopher J. Crosby[2], Viswanath Nandigam[3]
1 School of Earth and Space Exploration, Arizona State University, Tempe, AZ 85287-6004, USA
2 UNAVCO, 6350 Nautilus Drive, Boulder, CO 80301-5394, USA
3 SDSC - UC San Diego, 9500 Gilman Drive, La Jolla, CA 92093-0505,USA
*Corresponding Author, e-mail: ramon.arrowsmith@asu.edu

Abstract

High-resolution topography (HRT) is a powerful observational tool for studying the Earth's surface, vegetation, and urban landscape, with broad scientific, engineering, and education-based applications. Sub-meter resolution imaging is possible when collected with laser and photogrammetric techniques using ground, air, and space-based platforms. Open access to these data and a cyberinfrastructure platform that enables users to discover, manage, share, and process them increases the impact of investments in data collection and catalyse scientific discovery. Furthermore, open and online access to data enables broad interdisciplinary use of high-resolution topography across academia and in communities such as education, public agencies, and the commercial sector. Computation of topographic metrics, interactive analysis, and differencing of topographic data has great value for the characterization of land degradation. Open access to rapidly growing collections of multitemporal HRT promises to advance synoptic and objective understanding of landscape change.

Keywords: Geomorphology, Topography, Surface processes, Cyberinfrastructure, Geoinformatics

Monitoring the state of soil degradation in arid areas in algeria-case of the wilaya of djelfa-by studting the multi-temporal dynamics of spectral indices

Saida*[1], AMGHAR Fateh[1], BACHARI Nour El Islem[2]
1 Department of Biology, Faculty of sciences, University M'Hamed Bougara of Boumerdes, Algeria
2 Department of Biology, Faculty of sciences, University of sciences and Technology Houari Boumediene
*Corresponding Author, e-mail: s.sadi@univ-boumerdes.dz

Abstract

According to the statistical data of the National Scheme of Soil Conservation and Combating Desertification, the area affected by desertification in Algeria is estimated at 20 million hectares of steppe rangelands. These steppes play a fundamental role in the agro-pastoral economy of the country. Unfortunately, these spaces are currently very threatened by the phenomenon of desertification, a very complex process, which results from anthropic action, particularly overgrazing, aggravated by variations in climatic factors (drought). Desertification can cause changes in the vegetation cover, water and soil degradation, the dominant element of arid and semi-arid ecosystems. The latter is manifested in particular by a modification of the surface component, impairment of physico-chemical properties, silting, loss of organic matter etc. Faced with this challenge, the monitoring of changes in the dynamics of steppe landscapes remains a relevant approach that relies on diachronic studies, and this, in order to detect the changes and their rhythms, understand the relationships and interactions between natural and human factors. The objective of this paper is to characterize the state of the soil surface considered as a good indicator to understand the dynamics of degradation and highlight the degraded areas in the study area, based on the use of Landsat multi-date satellite data of 30 m resolution after a series of processing that was applied on satellite images of Landsat TM 1987 and OLI 2020 taken in the same season of peak vegetation production (April-May). These radiometric indicators helped to understand the changes of sensitive steppe landscapes and to understand the predominant factor in these dynamic.

Keywords: Desertification, Landscapes, Spectral indices, Remote sensing, Dynamic

REQUALIFE: A Web-App to Assess and Predict the Eco-Morphological Quality of Water Courses

Paolo Di Pietro*[1], Nicola Mazzon[2], Fuding (Frank) Xu[3], Baiying (Calipso) Zhang[4]
1 Corporate Business Unit Senior Specialist, Officine Maccaferri S.p.A., Italy
2 R&D Manager, Maccaferri Innovation Center (M.I.C.), Italy
3 Technical Marketing Director, Maccaferri Changsha, China
4 DT Business Development, Maccaferri Changsha, China
*Corresponding Author, e-mail: p.dipietro@maccaferri.com

Abstract

This work aims at presenting the main features of an innovative Web-App platform named REQUALIFE. The application provides an objective quantitative assessment of the current eco-morphological quality of a watercourse or alternatively, in case of a new intervention, can provide a forecast of the potential improvement over time. REQUALIFE web application is based on the WEQUI evaluation method, which results from further developments of other existing and widely used ones. WEQUI shares with these methods a multidisciplinary and objective evaluation approach, based on 15 technical-environmental indicator values. Each option is associated to a score that follows an exponential scale from 1 to 16. In addition to the indicators commonly used in most evaluation methods, REQUALIFE also introduces the Carbon sequestration and Carbon footprint, with the purpose of considering the carbon cycle of a riverbank stabilization. The Carbon sequestration indicator, as well as others included in WEQUI method, highlight the role of a riparian and floodplain vegetation, the importance of which plays a key role for both terrestrial and aquatic ecosystems. In this way the level of subjectivity and uncertainty during the compilation of WEQUI indicators is minimized.

Keywords: Eco-morphological quality, Indicators, Carbon sequestration, Carbon footprint, Channel morphology

A participatory-based methodology for the selection of sustainable land and water management practices in rural Myanmar

G. Castelli*[1], V.Re[2], W. M. Oo[3], A.di Maggio[4], L. Fellin[5], E. Bresci[1]
1 Department of Agriculture, Food, Environment and Forestry (DAGRI), University of Florence, Italy
2 Earth Sciences Department, University of Pisa, Italy
3 Water Supply and Sanitation Section, Department of Rural Development (DRD), Ministry of Agriculture, Livestock and Irrigation of Myanmar, Myanmar
4 Fondazione LINKS – Leading Innovation & Knowledge for Society, Italy
5 Fondazione Edmund Mach, Italy
*Corresponding Author, e-mail: giulio.castelli@unifi.it

Abstract

Besides providing water for irrigation, rural development efforts in Myanmar should target rural water security in terms of safe water supply and sanitation, and of mitigation of water-related hazards. However, very few studies are currently available on the topic, and consequently on suitable practical solutions for water-related development. This work presents a participatory methodology undertaken involving 45 rural development officers of the Department of Rural Development (DRD) of the Ministry of Agriculture, Livestock and Irrigation (MOALI), aimed at identifying suitable sustainable land and water management (SLWM) practices to be developed in rural areas of the country. Adoption of water safety plans (WSP), water harvesting, and soil and water bioengineering were identified as key SLWM practices, while the need for improving water sanitation, especially in the marginal areas of the country, was made evident. Insights of the participatory process confirmed that the poorest regions of Myanmar have also the worst water management structures. The results of the present work can represent a baseline information and a needs assessment for future rural development projects in the country. In any case, there is still a strong need of more studies and reports targeting marginalized rural contexts of Myanmar, to support equitable development. The present abstract is based on: Castelli, G., Oo, W. M., Maggio, A. di, Fellin, L., Re, V., & Bresci, E. (2020). Participatory analysis of sustainable land and water management practices for integrated rural development in Myanmar. Journal of Water, Sanitation and Hygiene for Development.

Keywords: Erosion, Expert participation, Public engagement, Soil and water bioengineering, Water harvesting

Explore Landscape Change in the Loess Plateau of China through Repeat Photography

Hailong He*[1], Lanmin Liu[1], Junru Chen[1]
1 College of Natural Resources and Environment, Northwest A&F University, Yangling 712100, China
*Corresponding Author, e-mail: hailong.he@nwafu.edu.cn

Abstract

The Loess Plateau of China has witnessed remarkable evolution in terms of significantly reduced soil erosion and soared vegetation coverage by the ecological restoration programs over the past decades. The Loess Plateau has become the model for soil and water conservation and ecological restoration in the world with numerous reports on this in the literature. However, there is a lack of visualized evidences depicting the effectiveness of the ecological restoration in the Loess Plateau. This objective of this study was to explore the landscape change associated with the ecological restoration using the repeat photography that compared historical and current photos of the same venue. The first collection of repeat photography is established with numerous photo pairs taken over the past decades across the Loess Plateau. The study provides a unique opportunity to investigate landscape change over time that would be difficult to discern by other approaches.

Keywords: Afforestation revegetation, Grain for Green project, Re-photography, Before-and-after photos, Photo pairs

Land degradation and the development of soil conservation measures in the moldavian plateau,eastern Romania: a case study from racova catchment

Lilian Niacsu*[1], Ion Ionita[1], Claudia Samoila[1], Georgel Grigoras[1], Ana Maria Blebea-Apostu[2]
1 Department of Geography, Faculty of Geography & Geology, "Alexandru Ioan Cuza" University of Iași, Romania
2 “Horia Hulubei” National Institute for Physics and Nuclear Engineering, Bucharest – Magurele, Romania
*Corresponding Author, e-mail: lilianniacsu@yahoo.com

Abstract

Land degradation by soil erosion, gullying and landslides and reservoir sedimentation is a major environmental threat in the Moldavian Plateau of eastern Romania. This paper reviews both land degradation and the development of soil conservation measures in a representative 32,908 ha catchment located in the Central Moldavian Plateau. Previous studies focused on larger areas and provided insufficient detailed information about land degradation and land improvements. The mean value of soil erosion was estimated at 22.7 t ha^{-1} y^{-1}. Gully erosion is very limited in extent (covering 3% of the catchment area), but has considerable impacts in terms of reactivating landslides and sediment detachment and transport. The 1:5,000 scale landslide distribution maps shows that 56% of Racova Catchment is covered by landslides. Traditional agriculture in the Moldavian Plateau focused on ‘up-and-down slope’ farming on small plots. However, soil conservation measures were actively undertaken over a 20-year period (1970-1989). More recent legislation (No. 18/1991 Agricultural Real Estate Act) includes two provisions that discourage maintaining and extending soil conservation practices. Hence, the former contour farming system has been abandoned in favor of the traditional, inadequate farming methods. The mean annual sedimentation rate in reservoirs is moderate at 2.7 cm y^{-1} in the upper Racova Catchment and almost double that rate in Puscasi Reservoir at the catchment outlet. Consequently, land degradation remains a serious problem in the study area and effective soil conservation is urgently needed.

Keywords: Soil erosion, Gully erosion, Landslides, Conservation practices, Reservoir sedimentation

Effects of ecological restoration measures with a fire disturbance on soil organic carbon improvement for degraded land in the agro-pasture ecotone in North China

Zhuo Pang[1], Haiming Kan[1], Junliang Zou[1], Guofang Zhang[1], Xiaodong Ma, Juying Wu*[1]
1 Research and Development Centre for Grass and Environment, Beijing Academy of Agriculture and Forestry Sciences, China
*Corresponding Author, e-mail: pangzh-84@163.com; wujuying@grass-env.com

Abstract

To improve soil organic carbon content of degraded lands in the agro-pasture ecotone in North China, ecological restoration measures, including revegetation with *Bromus inermis* and *Medicago sativa*, have been widely implemented. Soil organic carbon (SOC), water soluble organic carbon (WSOC) and hot-water extractable organic carbon (HEOC) were measured and soil respiration rate (Rs) was monitored continuously from April to October in grasslands of *Bromus inermis* and *Medicago sativa* from 2014 to 2020, with a fire disturbance occurred in 2017. The results showed that during the six years, SOC, WSOC and HEOC improved significantly in both types of grassland. Initially, SOC was decreased but WSOC and HEOC were increased in both grasslands in 2015 due to the grassland establishment practice. Moreover, fire disturbance in 2017 suppressed the increasing trend of SOC but had no effect on WSOC and HEOC, however, the fire disturbance triggered a sharp increase in WSOC and HEOC thereafter. Finally, Rs did not differ significantly among years and between types of grassland, however fire disturbance depressed Rs in *Medicago sativa* grassland, which became lower than that in *Bromus inermis* grassland thereafter. These findings suggest that revegetation with *Bromus inermis* and *Medicago sativa* can effectively improve SOC to neutralize land degradation and fire disturbance renders SOC in *Medicago sativa* grassland more stable with lower Rs.

Keywords: Degraded land management, Ecological restoration, Soil organic carbon, Fire event, Agro-pasture ecotone

Fluvial sediment fluxes response to climate change in a cold basin on the Tibetan Plateau

Dongfeng Li*[1], Xixi Lu[1], Ting Zhang[1]
1 Department of Geography, National University of Singapore, Kent Ridge 117570, Singapore
*Corresponding Author, e-mail: dongfeng@u.nus.edu

Abstract

Sediment flux in cold environments is a crucial proxy to link glacial, periglacial, and fluvial systems and highly relevant to hydropower operation, water quality, and the riverine carbon cycle. However, the long-term impacts of climate change on sediment flux changes in cold environments remain insufficiently investigated. Here we examine the multi-decadal changes in the in-situ observed fluvial sediment fluxes from a cold pristine basin, the Tuotuohe headwater of the Yangtze River, on the Tibetan Plateau. Results show that the fluvial sediment fluxes have substantially increased over the past three decades (i.e., a net increase of 135% from 1985–1997 to 1998–2017) due to the warming and wetting climate. We also quantify the relative impacts of air temperature and precipitation on the increased sediment fluxes with a novel attribution approach and find that climate warming and intensified glacier-snow-permafrost melting is the primary cause of the increased sediment fluxes, with precipitation increase and its associated pluvial erosion processes being the secondary driver. In an expected warming and wetting climate for the region, we predict that the sediment fluxes in the pristine headwaters of the Tibetan Plateau will likely continue to increase throughout the 21st century.

Keywords: Discharge, Sediment flux, Climate change, Tibetan Plateau

Effect of biochar on the soil structure and hydraulic characteristics of the sloping farmlands in the black soil region

Guoxin Shi[1,2,3], Yu Wu[4] , Qiang Fu*[1,2,3], Tianxiao Li[1,2,3], Yongxia Wei[1,2]
1 School of Water Conservancy and Civil Engineering, Northeast Agricultural University, Harbin, Heilongjiang 150030, China
2 Key Laboratory of Effective Utilization of Agricultural Water Resources of Ministry of Agriculture, Northeast Agricultural University, Harbin, Heilongjiang 150030, China
3 Heilongjiang Provincial Key Laboratory of Water Resources and Water Conservancy Engineering in Cold Region, Northeast Agricultural University, Harbin, Heilongjiang 150030, China
4 Heilongjiang Province Hydraulic Research Institute, Harbin, Heilongjiang 100050, China
*Corresponding Author, e-mail: fuqiang0629@126.com

Abstract

Biochar has been widely applied as a soil conditioner, but currently it is mostly used in short-term applications, and there is a serious lack of research on soil structure and hydraulic properties in the medium and long term. To examine the medium-to-long-term biochar effects on soil structure and hydraulic properties, farmland runoff plots with a slope of 3° in the black soil area of Northeast China were selected as the research object, and 4-year observations were conducted. By examining the influence of different biochar application amounts (0, 25, 50, 75, and 100 t/hm^2) on soil structure characteristic parameters, soil water retention curves, unsaturated hydraulic conductivity and unsaturated water diffusivity over 4 consecutive years, the optimal biochar application mode was determined. The results showed that the biochar application amount, year and their interaction imposed significant effects on soil structure and moisture characteristic parameters. Biochar application for 4 consecutive years increased the surface soil water content. When the water content was less than a certain value (0.24-0.28 cm^3·cm^{-3}), biochar yielded little effect on soil hydraulic conductivity. When the water content exceeded a certain value, biochar improved the soil hydraulic conductivity. In regard to black soil, biochar inhibited the horizontal diffusion of water, while Pearson correlation analysis indicated that soil structure improvement encouraged soil water holding capacity enhancement. Based on analysis of the soil structure and hydraulic characteristics of biochar over time, the best biochar application mode for water and soil improvement of the sloping farmlands in the black soil area was proposed, namely, biochar application at 50 t·hm^{-2} for two consecutive years. The research results provide theoretical support for actual production improvement.

Keywords: Biochar, Soil structure, Water conductivity, Water diffusion, Application mode

Contributions of vegetation restoration and climate change to spatiotemporal variation in the energy budget in the Loess Plateau of China

Linjing Qiu*[1], Zhaoyang Shi[1], Yuting Chen[1], Qingyue Xue[1]
1 Department of Earth and Environmental Science, Xi'an Jiaotong University, China
*Corresponding Author, e-mail: qiulinjing@xjtu.edu.cn

Abstract

Anthropogenic land cover change (ALCC) can modify energy exchanges and further alter the regional climate. Due to the complexity of land-atmosphere energy exchange processes and limited observation networks, the influence of ALCC on the energy balance remains unclear. The Loess Plateau (LP) of China has experienced evident land surface change due to the implementation of the Grain for Green vegetation restoration program. Under this program, a large amount of cropland has been converted to grassland and forestland, which will inevitably result in surface energy balance changes. However, due to their complexity and lack of in situ observations, it is a challenge to quantify the spatial-temporal dynamics of energy balance changes associated with the GFGP. Here we first investigated the changes in surface energy partitioning in the LP region during the period of 1980–2018. Then we modified the land cover characteristics for each plant functional type in the LP based on multiple sources of observations to improve the representations of historical vegetation in the model. Finally, we performed a series of sensitivity simulation experiments to quantitatively identify the contribution of vegetation restoration and climate change to energy balance component changes.

Keywords: Energy exchange, Land cover change, Scenario simulation, Earth system model

Effects of raindrop temperature on the contribution of slaking and mechanical striking to aggregate disintegration during splash erosion

Hairu Li*[1,2], Ju Gu[1,3], Gang Liu*[1,2], Mohamed A. M. Abd Elbasit[4], Feinan Hu[1,2], Tingrun Zou[5], Liang Wang[5]
1 State Key Laboratory of Soil Erosion and Dryland Farming on the Loess Plateau, Institute of Soil and Water Conservation, Northwest A&F University, Yangling 712100, China
2 Institute of Soil and Water Conservation, Chinese Academy of Sciences and Ministry of Water Resources, Yangling 712100, China
3 Yangtze Ecology and Environment Co. Ltd., Wuhan 430000, China
4 Agricultural Research Council, Institute for Soil, Climate & Water, Private Bag X79, Pretoria 0001, South Africa
5 College of Natural Resources and Environment, Northwest A&F University, Yangling 712100, China
*Corresponding Author, e-mail: gliu@foxmail.com

Abstract

In this study, the effects of raindrop temperatures on aggregate disintegration of three loessal soils with different textures were investigated by using simulated rainfall. Deionized water and ethanol (95%) were employed as raindrop materials to quantify the effects of raindrop temperature on the contribution rate of slaking and mechanical striking to splash erosion. Three raindrop temperatures were set to 2℃, 10℃ and 20℃, and the rainfall height was set to 0.5 m, 1.0 m and 1.5 m with a rainfall intensity of 60 mm h-1. The results showed that the sensitivity of soils to slaking was greater than to mechanical striking. The resistance of clay loam and loamy sand to slaking decreased with increasing temperature. As the raindrop temperature increased, the breakdown rate of the three soils caused by mechanical striking decreased significantly. The soil erosion rate under deionized water tests was larger than that under ethanol for the three soils at the same raindrop temperature. Slaking contributed more to aggregate disintegration at 10 ℃ and 20 ℃, while mechanical striking was the primary contributor at 2℃. This study improves the understanding of splash erosion and provides a theoretical basis for the development of a soil erosion prediction model.

Keywords: Splash erosion, Raindrop temperature, Slaking, Mechanical striking, Soil aggregates

Effects of biochar and straw application on soil structure and gas transport characteristics in seasonally frozen soil areas

Ping Xue[1], Qiang Fu*[1], Tianxiao Li*[1], Dong Liu[1], Renjie Hou[1], Qinglin Li[1], Yi Ji[1], Mo Li[1]
1 School of Water Conservancy and Civil Engineering, Northeast Agricultural University, Harbin, Heilongjiang 150030, China
*Corresponding Author, e-mail: fuqiang0629@126.com; litianxiao@neau.edu.cn

Abstract

In this study, freeze-thaw cycles (FTCs) were used as boundary conditions and three typical soils in Songnen Plain were used: black soil, baijiang soil and meadow soil;Four treatments including biochar addition (B1), straw addition (S1), biochar combined with straw addition (B1S1) and untreated control group (CK) were set; The proportion of soil water-stable aggregates, total porosity (TP), soil water retention curve (SWRCS), soil dissolved organic carbon (DOC) and soil air permeability (PL) were measured; The effects of biochar and straw on soil structure and gas transport characteristics under FTCs were analyzed. The results showed that straw and biochar had a certain regulating effect on the structure of the three types of soil, and the aggregates with large (2mm-0.5mm), medium (0.5-0.25mm) particle size increased significantly in the three types of soil. The stability indexes of soil aggregates were better than CK, and the three-phase ratio of soil gradually tended to be ideal. The regulation effect of different regulation modes on black soil was particularly obvious, and the generalized soil structure index (GSSI) reached 95.59, 94.36 and 98.74, respectively. There was a certain interaction between biochar and straw, the regulation effect of B1S1 was better than other treatments, and the increase of total porosity (TP) was the most significant. Soil water holding capacity was improved ($FC=0.317cm^3 \cdot cm^{-3}$). FTCs increased the content of soluble organic carbon in soil and promoted soil carbon mineralization. Under B1S1 treatment, the contents of dissolved organic carbon in black soil, baijiang soil and meadow soil were 160.78mg/kg,272.828mg/kg and 271.912mg/kg, respectively. At the same time, the combination of biochar and straw can effectively reduce the fluctuation of soil air permeability under FTCs, and improve the long-term stability of soil structure

Keywords: Freeze-thaw cycles, Biochar, Straw, Soil structure, Characteristics of soil gas transport

Spatial distributions and temporal variations of the near-surface soil freeze state in Northeast China and its disparity under different land use types

Song Xu[1], Qiang Fu*[1], Tianxiao Li*[1], Dong Liu[1], Renjie Hou[1], Qinglin Li[1], Yi Ji[1], Mo Li[1]

1 School of Water Conservancy and Civil Engineering, Northeast Agricultural University, Harbin, Heilongjiang 150030, China

*Corresponding Author, e-mail: fuqiang0629@126.com; litianxiao@neau.edu.cn

Abstract

The near-surface soil freeze state has undergone significant changes with the global warming, and the soil freezing depth plays an important role in the evaluation of water resource balance, surface energy exchange and biogeochemical cycle changes in frozen regions. Based on the daily soil freezing/thawing depth data from 31 meteorological stations in Heilongjiang Province during 1960-2016, the spatial and temporal distribution characteristics of 8 soil freezing-thawing state variables (maximum seasonally frozen depth, first date of freezing/thawing, last date, freezing period days, thawing period days, duration and actual freezing days) in Heilongjiang Province were analyzed using Sen's Slope, Hurst exponent and Mann-Kendall trend analysis and combined with land use data, we further analyzes the difference of frozen soil degradation trend under different land use types. On average across Heilongjiang province over the study period, the maximum seasonally frozen depth decreased by 48±6 cm with a rate of 0.85±0.13 cm/year, the first date of freezing was delayed by approximately 10±1 days with a rate of 0.18±0.02 days/year, the first date of thawing and the last date advanced by 6±1 and 27±3 days with rates of 0.11±0.02 and 0.48±0.04 days/year, respectively, the freezing period days and the thawing period days shortened by 17±2 and 21±3 days with rates of 0.30±0.03 and 0.38±0.04 days/year, respectively, and the duration and the actual freezing days decreased by 38±4 and 34±4 days with rates of 0.68±0.07 and 0.61±0.06 days/year, respectively. The Hurst exponent indicates that the frozen soil variables at most stations in the future will keep the same trend as at present and the trend of frozen soil variables is the smallest in the forest area and the largest in the settlement area.

Keywords: Freeze state, Spatiotemporal variation, Northeast China, Climate warming, Land use types

Future climate zone shifts could threaten steep-slope agriculture

Wendi Wang[1], Paolo Tarolli*[1], Anton Pijl[1]

1 Department of Land, Environment, Agriculture and Forestry, University of Padova, Legnaro (PD)

*Corresponding Author, e-mail: paolo.tarolli@unipd.it

Abstract

Food security is one of the critical issues for human in the 21st century due to projected future climate change. Steep-slope agricultural landscapes play an important role in food productivity (feeding about 10% of global population) as well as cultural and heritage with 50 ancient agricultural systems in steep slope are well protected by UNESCO World Heritage Sites and FAO Globally Important Agricultural Heritage System (GIAHS). However, these special landscapes are under threaten due to climate change and water scarcity. To better understand how growing aridity affects steep slope agricultural system in the future, we aim to (1) produce a high-resolution map of global distribution of steep slope farmland based on GIS technique; (2) compare present (1980-2016) distribution of steep slope agricultural areas with the future (2071-2100) distribution at different climatic regions; and, (3) quantify the fraction of steep slope agricultural areas will be affected by future climate zone shifts. Our findings provide a guideline for climate adaptation to improve the resilience for agricultural system in steep slopes.

Keywords: Steep slope, Climate change, Agricultural systems, Food security

Effects of biochar on key processes of soil nitrogen cycle and its regulatory mechanism under freeze-thaw conditions

Xuechen Yang[1], Qiang Fu*[1], Tianxiao Li*[1], Dong Liu[1], Renjie Hou[1], Qinglin Li[1], Yi Ji[1], Mo Li[1]
1 School of Water Conservancy and Civil Engineering, Northeast Agricultural University, Harbin, Heilongjiang 150030, China
*Corresponding Author, e-mail: fuqiang0629@126.com; litianxiao@neau.edu.cn

Abstract

Freezing and thawing cycle is an important factor affecting nitrogen cycle in terrestrial ecosystems, which mainly affects the transport and transformation of nitrogen in soil by changing the physical and chemical properties of soil.As a new soil conditioner, biochar has become a regulatory approach for agricultural emission reduction, yield increase and efficiency increase due to its special physical and chemical properties.Biochar under the condition of considering the freezing and thawing soil improvement research is relatively small, in order to explore applying biochar in seasonal frozen soil nitrogen cycle regulation mechanism of key processes and mechanisms, based on the black soil on the Songnen plains of China as an example, the indoor simulation of soil column freeze-thaw cycling test, freeze-thaw cycle was studied under the interaction of soil and biological carbon change characteristics of the physical and chemical properties and the nitrogen cycle index, and then explores the soil nitrogen cycle key process response to environmental factors. The results showed that :(1) Freezing and thawing times, soil moisture, soil temperature and soil aggregate stability significantly affected the nitrogen conversion process, and the change of soil physical and chemical properties was the main reason for the increase of soil available nitrogen, N_2O emission flux and nitrogen conversion rate.(2) Biochar can improve soil physical structure, accelerate soil nitrogen transformation, effectively conserve soil nutrients and reduce greenhouse gas emissions, and different treatment conditions have significant effects on soil nitrogen indicators ($P < 0.05$).This study reveals the regulation mechanism of biochar in the process of soil nitrogen transformation.

Keywords: Freeze-thaw cycle, Biochar, Nitrogen cycle, Influence mechanism, Regulation mechanism

Effect of Snow cover on soil moisture in Spring in Songhua River Basin

Yanxin Li2, Qiang Fu1, Tianxiao Li1, Dong Liu1, Renjie Hou, Qinglin Li1, Yi Ji1, Mo Li1
1 School of Water Conservancy and Civil Engineering, Northeast Agricultural University, Harbin, Heilongjiang 150030, China
2 Key Laboratory of Effective Utilization of Agricultural Water Resources of Ministry of Agriculture, Northeast Agricultural University, Harbin, Heilongjiang 150030, China
3 Heilongjiang Provincial Key Laboratory of Water Resources and Water Conservancy Engineering in Cold Region, Northeast Agricultural University, Harbin, Heilongjiang 150030, China
4 Heilongjiang Province Hydraulic Research Institute, Harbin, Heilongjiang 100050, China
*Corresponding Author, e-mail: fuqiang0629@126.com; litianxiao@neau.edu.cn

Abstract

Soil moisture is an important index to characterize farmland drought and waterlogging, and snow cover is an important replenishment resource of spring soil moisture in seasonal permafrost areas, but few studies have been done to quantitatively analyze the relationship between snow cover and spring soil moisture. This study quantifies for the first time the influence of snow parameters in the Songhua River Basin above the control section of Jiamusi Hydrological Station on soil moisture in spring. Based on the model simulation and the use of snow remote sensing products, the temporal and spatial distribution characteristics of snow parameters and soil moisture in the Songhua River basin were analyzed. According to the correlation, a unitary linear regression model based on snow parameters to predict spring soil moisture was constructed. The optimal model is selected to predict the probability of drought and flood in spring in the Songhua River basin. The results show that there is an obvious positive correlation between snow cover and soil moisture in spring, and the correlation between snow cover and soil moisture in May is better than that in April, and the maximum snow depth is the most suitable snow parameter to predict drought and flood in May. If 55% Mel 75% is the suitable moisture range of the soil, the probability of spring drought prediction of the linear model in May is 71.56%, and the probability of suitable moisture and spring waterlogging prediction is also more than 50%. This study quantifies the effect of snow cover on soil moisture in spring on the watershed scale, which provides a theoretical basis for the rational use of snow resources to solve the problem of spring drought, and provides a new way for the prediction of soil moisture in spring.

Keywords: Snow cover, Soil moisture, VIC model, Farmland, Spring drought

Transport characteristics of snowmelt in cold and arid regions: regulatory mechanism of biochar

Yutian Zuo[1], Qiang Fu*[1], Tianxiao Li*[1], Dong Liu[1], Renjie Hou[1], Qinglin Li[1], Yi Ji[1], Mo Li[1]
1 School of Water Conservancy and Civil Engineering, Northeast Agricultural University, Harbin, Heilongjiang 150030, China
*Corresponding Author, e-mail: fuqiang0629@126.com; litianxiao@neau.edu.cn

Abstract

This study simulated the soil structure characteristics and spring snowmelt water transport process of farmland black soil under the conditions of different gradient biochar application amounts in spring thawing period after 9 freezing-thawing cycles, and further explored the response mechanism of snowmelt water transport characteristics. The results showed that :(1) The application of biochar could increase the total porosity of soil, increase the proportion of medium porosity, and reduce the proportion of soil voids and extremely micro pores.(2) Under the condition of carbon application, the stability of soil aggregates increased firstly and then decreased with the increase of the amount of carbon application. The influence of biochar on medium and silt clayey aggregates was more significant. The stability index of medium-size aggregates was consistent with that of silt&clay aggregates, while the stability index of silt&clay aggregates was opposite.Similarly, GSSI and STPSD also show a similar pattern.(3) With the increase of the amount of biochar applied, the saturated water conductivity of soil increased, while for frozen soil, the effect of the opposite effect was shown.In order to effectively reveal the mechanism effect of different biochar amounts on snow melt water transport, this paper proposed XI to evaluate soil infiltration performance in thawing period based on soil saturation water conductivity. XI has a good correlation with snow melt water transport index, which provides a new idea for future research on water transport law in thawing period.(4) Evaporation, infiltration and runoff in snowmelt period also showed a trend of improving first and then producing negative effects with the increase of carbon application amount.

Keywords: Farmland in cold region, Freeze-thaw cycle, Biochar, Soil structure, Transport of snowmelt.

Initial recovery characteristics and variability of soil carbon, nitrogen, and phosphorus in the damaged forests under disaster disturbance

Hang Yu[1,2,3], Qinghu Luo[1,2,3], Songyang Li[1,2,3], Yongming Lin*[1,2,3], Daojie Wang[4]
1 College of Forestry, Fujian Agriculture and Forestry University, Fuzhou 350002, China
2 Key Laboratory of Mountain Hazards and Surface Processes, Chinese Academy of Sciences, Chengdu 610041, China
3 Key Laboratory for Forest Ecosystem Process and Management of Fujian Province, Fuzhou 350002, China
4 Institute of Mountain Hazards and Environment, Chinese Academy of Sciences and Ministry of Water Conservancy, Chengdu 610041, China
*Corresponding Author, e-mail: 5665309598@163.com

Abstract

In this study, two different kinds of forest land destroyed by major floods were selected for the determination of soil organic carbon (SOC) content, total nitrogen (TN) content and total phosphorus (TP) content of surface soil in different sample plots (damaged area, recovered area, and undamaged area), and then the initial recovery characteristics and variability of SOC, TN, TP of damaged forests were analyzed. The results showed that: (1) Disaster caused severe damage to the secondary broad-leaved forest and *Cunninghamia lanceolata* forest. The contents of SOC, TN and TP in all plots decreased as the vegetation coverage, following the rule of “undamaged area > recovered area > damaged area”, indicating that damaged forests had not recovered to the pre-disaster level after seven years of natural recovery. (2) Only TP content of the recovered area was significantly higher than the damaged area in secondary broad-leaved forest, while the content of SOC and TP of the recovered area were both significantly higher than the damaged area in *Cunninghamia lanceolata* forest, and the recovery rate of soil nutrients in *Cunninghamia lanceolata* forest was higher than secondary broad-leaved forest, indicating that the early fertilization had a positive promoting effect on the natural restoration of soil nutrients in *Cunninghamia lanceolata* forest. (3) C:P value was mainly affected by SOC, C:N and N:P values were mainly affected by TN in the damaged forests, and only C:P value of recovered area was significantly higher than the damaged area in *Cunninghamia lanceolata* forest.

Keywords: Soil nutrient, Ecological restoration, Variable coefficient, Fujian, Nanping

Sediment yield trend in loess Plateau since Last Deglaciation and anthropic stress

Yu An[1], Niannian Fan*[1], Junping Wang[2], Yunzhen Chen[3], Chengshan Wang[4], Xingnian Liu[1]
1 State Key Laboratory of Hydraulics and Mountain River Engineering,College of Water Resource &Hydropower, Sichuan University, Chengdu, China
2 College of Resource Environment and Tourism, Capital Normal University, Beijing, China
3 Yellow River Institute of Hydraulic Research, Zhengzhou, China
4 State Key Laboratory of Biogeology and Environmental Geology, China University of Geosciences, Beijing, China
*Corresponding Author, e-mail: fanniannian@scu.edu.cn

Abstract

The Loess Plateau is the most serious area suffered from erosion all over the world, however, the role of natural and anthropic influence in erosion is still controversial due to lack of studies from fluvial deposition in the scale of 10-20 ka.As one of the rivers with the highest sediment yield through the loess area, the watershed of Yongding River mainly locates in the North China Craton and is partially covered by Quaternary loess. Here we report the measurement of mineral composition and detrital zircon ages from a section in the Guanting Canyon in the middle reaches of the Yongding River, which records multiple paleo-flood events from 17.8ka to 1939AD. Our study shows the proportion of loess in sediment yield declined gradually after 17.8 ka, however it suddenly increased at 1.0 ka, and then went back to the natural trend. We propose that since the Last Deglaciation, the sediment yield from loess has been declined gradually naturally. Strongly agriculture activities at 1.0 ka accelerated loess erosion,nevertheless, this change would attenuate rapidly within hundreds of years.

Keywords: Loess Plateau, Sediment yield, Last Deglaciation, Anthropic stress

Experience and Perspectives on Acceptance Review of Soil and Water Conservation Facilities and Water Conservancy Engineering—Taking the reinforcement of PanZhuang Yellow River Diversion Sluice as Example

Li Li*[1,2], Xiaodong Zhao[3], Xueyuan Wei[1]
1. Yellow River Institute of Hydraulic Research, Yellow River Conservacy Commission, China
2 Key Laboratory of Soil and Water Conservation on the Loess Plateau of Ministry of Water Resources, China
3 Construction Center of Yellow River Shandong Bureau, China
*Corresponding Author, e-mail: 14578126@qq.com

Abstract

In 2017, the State Council changes the acceptance of soil and water conservation facilities from administrative acceptance to self-acceptance which is organized by implementer of these project. The acceptance report will be prepared by the institutions who were not involved in the project. Take the PanZhuang reinforcement project of the Yellow River Diversion Sluice as example, this article briefly introduces the characteristics of acceptance processes of soil and water conservation facilities in water conservancy engineering. The invited institutions who is responsible for acceptance quality implement the acceptance based on information received from UAV remote sensing. UAV remote sensing technology has been widely applied to monitor situation of soil and water conservation project due to its advantages of quick collecting and extracting effective information, improving the accuracy and reliability of relevant indicators, and providing more intuitive and reliable results, which could support acceptance of soil and water conservancy facilities. Self-acceptance of soil and water conservation project could focus on the analysis and evaluation of soil erosion prevention and control of the scope of responsibility changes, completion of soil and water protection measures, quality assessment of soil and water conservation engineering , soil and water-keeping effect, Draw definitive conclusions whether to meet the criteria and conditions in acceptance soil and water conservation facilities by owners. The paper also summarized the existing challenges on project self-acceptance and proposes countermeasures, which might provide reference to the similar projects acceptance.

Keywords: Water conservancy engineering, Yellow River Diversion Sluice, Soil and Water Conservation Facilities, Independent check and acceptance

High-efficiency cultivation model of Xanthoceras Sorbifolia bunge in Gully region of Loess Plateau

Xiaoling Yan*[1], Ying Zhang[2]
1 Yellow River water and Soil Conservation Supervision Bureau of Xifeng District Administration, Qingyang, Gansu
2 Ziwuling Forestry Administration, Heshui branch, Lianjia Bian forest farm, Qingyang, Gansu
*Corresponding Author, e-mail: hwxfyxl@163.com

Abstract

Xanthoceras Sorbifolia bunge has very high edible value, medicinal value, ornamental value and ecological value. It is an efficient soil and water conservation plant with ecological, ornamental and edible uses, its high-efficiency cultivation mainly includes suitable land for trees, reasonable close planting, planting at the right time, shaping and pruning, field management, seed harvesting and other links. Gansu is also one of the most suitable provinces for the growth of Xanthoceras Sorbifolia bunge. As early as 2008, Gansu was incorporated into the State Forestry Administration of the People's Republic of China and established a 73,000 hm2 production base for Xanthoceras Sorbifolia. The popularization of Xanthoceras Sorbifolia bunge has a bright future in controlling soil and water loss, improving ecological environment, developing Xanthoceras Sorbifolia bunge industry, adjusting agricultural structure and revitalizing rural areas.

Keywords: Gully region of Loess Plateau, Xanthoceras Sorbifolia, High-efficiency cultivation model, Development prospect

Study on comprehensive soil and water conservation measures and their effects on runoff in Nanxiaohegou watershed

Zhongping Tuo*[1], Ying Hao[1]
1 Yellow River water and Soil Conservation Supervision Bureau of Xifeng District Administration, Qingyang, Gansu
*Corresponding Author, e-mail: xftzp@163.com

Abstract

Taking the Nanxiaohegou watershed in Xifeng district, Qingyang city, Gansu Province as the experimental area, this paper expounds in detail the main factors causing soil and water loss in the watershed, and puts forward the "three lines of defense" comprehensive control model for the tableland slope gully, the experience and effect of comprehensive harness in Nanxiaohegou watershed are summarized. The impact of soil and water conservation measures on runoff is analyzed, and the organic combination of pest control and profit-making can maximize the utilization degree of precipitation resources and promote the coordinated and sustainable development of all industries in the basin, it provides theoretical basis for promoting the ecological civilization construction in the Some Random Place Somewhere region, coordinating the thought of landscape, forest, Lake, grass and sand control, high quality development in the Yellow River Basin, rural revitalization strategy and sustainable development of social economy.

Keywords: Nanxiaohegou watershed, Soil and Water Conservation, Comprehensive measures, Runoff

Sustainable soil tillage and energy savings: first subsoiling tests of compacted soils with an innovative machine

R. Tomasone*[1], M. Pagano[1], C. Cedrola[1], A. Assirelli[1]
1 Research Center for Engineering and Agro-Food Processing, CREA, Italy
*Corresponding Author, e-mail: roberto.tomasone@crea.gov.it

Abstract

The repeated passage of agricultural machinery in the field is a major cause of soil compaction, negatively affecting the soil's macro-porosity. This article describes the subsoiling tests carried out to assess the operational performance (energy required by the machine, operative performance and quality of work) of this particular subsoiler, linked to a 110 kW tractor. The only exception was the specific traction force, which was slightly higher in the OFF test. The power demand on the tractor's PTO, to drive the eccentric, was extremely low. Tractor slippage was higher with the oscillating device in operation. Work times, recorded at the same forward speed, were the same for the two trials. Soil cloddiness analysis confirmed that tillage with the activate plate was more effective, with about 70% of the total cloddiness falling in the large size class (>25 mm), compared to 55% in the OFF test. The profiles of the soil cross-sections were similar for both trials. The elevation of the tilled soil relative to ground level was not particularly excessive. The oscillating plate elevates the soil producing a “double windrow” profile, with an elevation of about 20 cm, on both sides of a small central furrow created by the vertical shaft. The effectiveness of the subsoiling operation along the inter-row of orchards or vineyards is strongly influenced by soil conditions, because in case of extremely compacted soils, the tractor's slippage would be excessive, and the working depth must be reduced. The proper setup of the equipment can reduce the demand for power and therefore for energy, improving overall operating performance. The correct execution of subsoiling can improve the deep structure of the soil by facilitating aeration, rainwater infiltration and drainage.

Keywords: To be supplemented

Landslide and gully water and sediment connectivity: insights from high-resolution DEMs at the hill slope scale

Nicușor Necula*[1], Mihai Niculiță[1], Mihai Ciprian Mărgărint[1], Valeriu Stoilov-Linu[1], Georgiana Văculișteanu[1], Mihai-Cosmin Ciotină[1], Paolo Tarolli[2]
1 Department of Geography, Faculty of Geography and Geology, Alexandru Ioan Cuza University of Iași, Romania
2 Department of Land, Environment, Agriculture and Forestry, University of Padova, Italy
*Corresponding Author, e-mail: neculanicusor93@gmail.com

Abstract

High-resolution centimetric topography was calculated through SfM of visible imagery acquired by UAV in 2019, and the derived orthophoto imagery was used further on for geomorphological mapping. Geomorphic change detection was derived using the LiDAR data from 2012. The gully system and its related landslides are reducing the surface connectivity flow of water and sediment through the drainage network at the hillslope scale. Microtopography, especially in landslided areas, introduces dis-connectivity in water and sediment fluxes. In the case of dryer areas, the lack of running water (at all or the right amount) does not allow the sediment to pass from the hillslope into the channel, even for landslides that reach the slope bottom. Sediment will accumulate along the hillslope and move into the fluvial system only when gullies will evolve over the landslided area. Moreover, the geomorphic change detection also reveals the eroded patches and the sediment sinks on landslide hummocky topography. The water and sediment dis-connectivity favor the piping process, while the cracks related to landslide evolution increase the subsurface flow. Based on our investigations, high-resolution topography seems to provide crucial information that can reveal patterns of sediment connectivity and dis-connectivity at the hillslope scale.

Keywords: High-resolution topography, Dis-connectivity, Gully, Landslide, Piping

Surface water ponding in lowland agriculture: a rapid mapping approach using UAV-SfM

Eugenio Straffelini*[1], Sara Cucchiaro[1,2], Paolo Tarolli[1]
1 Department of Land, Environment, Agriculture and Forestry, University of Padova, Italy
2 Department of Agricultural, Food, Environmental and Animal Sciences, University of Udine, Italy
*Corresponding Author, e-mail: eugenio.straffelini@unipd.it

Abstract

Surface water ponding is defined as a surplus of water that remains in terrain depressions after prolonged rainfall due to soil saturation. It is a major threat in lowland agricultural landscapes and worsened by soil compaction as a result of heavy mechanization. As water ponding affects crops and management, it is important to map the areas with potential water-ponding risk to help understand the phenomena and develop sustainable solutions to mitigate the risk. The advance in technology and remote sensing, such as Uncrewed Aerial Veichels (UAV) combined with the Structure-from-Motion (SfM) technique, provides great potential in surface processes investigation. This study aims to present a novel approach in surface water ponding mapping using high-resolution Digital Elevation Models (DEMs). The Relative Elevation Attribute (REA) index is used to identify terrain concavities and map the potential extension/depth of stagnant water. A method for assessing the results based on field observations is also proposed. The findings provide stakeholders with useful guidance for improved lowland agricultural management quickly and at a low-cost.

Keywords: Water ponding, UAV-SfM, DEM

Modelling splash erosion under vegetation using the Vegetation Splash Factor and airborne laserscanning data

Johannes A. Senn*[1], Fabian Ewald Fassnacht[2], Zahra Hosseini[2,3], Jannika Schäfer[2], Steffen Seitz[4]
1 School of Engineering, Newcastle University, Newcastle upon Tyne, United Kingdom of Great Britain – England, Scotland, Wales.
2 Institute for Geography and Geoecology, Karlsruhe Institute of Technology, Karlsruhe, Germany.
3 Department of Forestry, Faculty of Agricultural and Natural Resources, Lorestan University, Khorramabad, Iran.
4 Institute of Geography, Department of Geosciences, Universität Tübingen, Tübingen, Germany.
*Corresponding Author, e-mail: j.senn@newcastle.ac.uk

Abstract

Due to small-scale variation in vertical and horizontal vegetation structure in many forest ecosystems, it is challenging to adequately capture these relationships over larger spatial extent and therefore these processes have not yet been sufficiently integrated into spatial erosion models. Here, we present the vegetation splash factor (VSF) which was designed to close this gap. The VSF attempts to quantify the influence of vegetation structure on TKE using continuous information on vegetation structure as available in lidar point clouds collected from airborne devices. The results from the splash cup measurements demonstrated that adult beech trees induced about 70 % less TKE than young Oak trees. Among the individual splash cup positions on the transect, the lowest energy values were measured for splash cups positioned under canopy openings and were hence representing freefall kinetic energy (FKE). Splash cups positioned in locations covered by intermediate height young growth and shrub layer showed medium values. In near-trunk and other positions without intermediate layers, we measured TKE values more than twice as high as FKE. The microscale runoff plots showed that this kinetic energy is sufficient to result in significant sediment removal beneath the tree layer when the ground covering litter layer is removed. This agrees with studies from other non-European forest ecosystems. A first comparison of the VSF with the TKE measured by the splash cups showed reasonable agreements, particularly when focusing on high intensity rainfall events. These initial results confirm the potential of the VSF to capture the influence of vegetation structure on TKE. More detailed analyses of the data to adjust and calibrate the VSF model to the data are currently underway.

Keywords: Splash erosion, Vegetation, Airborne laserscanning, Remote sensing

UAV-SfM 4D mapping of landslides activated in a steep terraced agricultural area

Luca Mauri*[1], Eugenio Straffelini[1], Sara Cucchiaro[1,2], Paolo Tarolli[1]
1 Department of Land, Environment, Agriculture and Forestry, University of Padova, Legnaro (PD)
2 Department of Agricultural, Food, Environmental and Animal Sciences, University of Udine, Italy
*Corresponding Author, e-mail: luca.mauri.2@phd.unipd.it

Abstract

The presence of roads is linked with the activation of land degradative phenomena such as landslides. Recent developments in digital photogrammetry (e.g., Structure from Motion; SfM) paired with Uncrewed Aerial Vehicles (UAV) systems increased our possibilities to realize low-cost and recurrent topographic surveys. This can lead to the development of multi-temporal (4D) high-resolution Digital Elevation Models (DEMs), so as to analyse geomorphological features and quantify processes at the fine spatial and temporal resolutions. This research proposes a multi-temporal comparison of geomorphometric indicators describing a landslide-prone terraced vineyard, to assess the observed high-steep slope failures. The investigation of the evolution of landslides' geomorphic features in a steep agricultural system through a high-resolution and 4D comparison of such indicators is a challenge to be explored. The dynamics of the landslides were firstly monitored by repeated DEMs comparison. The road participation in superficial water flows alterations was proved by the elaboration of the Relative Path Impact Index (RPII). Finally, the multi-temporal comparison of indicators and features extraction underlined the geomorphological changes affecting the study area. The accuracy of features extraction was analysed through the Quality Index computation. This work could be a starting point for further studies of landslide-susceptible zones on wider scales.

Keywords: Landslides, Roads, Agricultural systems, Uncrewed Aerial Vehicles, Geographical Information System

Is diffuse soil erosion quantifiable under field conditions?

Simone Ott*[1], Bastian Steinhoff-Knopp[1]
1 Institute of Physical Geography & Landscape Ecology, Leibniz University Hannover, Germany
*Corresponding Author, e-mail: ott@phygeo.uni-hannover.de

Abstract

The complexity and discontinuity of erosion processes on cultivated farmland make it difficult to quantify the amount of soil material that is relocated. High-resolution measurement methods like UAV-photogrammetry or terrestrial laser scanning (TLS) have already been used in different studies to estimate soil erosion under controlled conditions (Eltner et al. 2013; Eltner et al. 2016; Meinen and Robinson 2020; Cândido et al. 2020). In this study we aim at the quantification of especially diffuse soil erosion (sheet and interrill erosion) on cultivated cropland, using TLS within a high-frequency multi-temporal approach. The study area is located on farmland which is part of a long-term soil erosion monitoring program in Northern Germany (Steinhoff-Knopp and Burkhard 2018). Four plots were selected based on previously recorded erosion events considering different gradients in the microtopography within a thalweg. To reduce masking by other surface processes, which is not trivial especially when investigating diffuse soil erosion, we use a higher observation frequency on weekly basis from spring to early summer and record further parameters like rainfall, bulk density and soil moisture. The presentation will highlight results from the measurements and challenges within the field trials.

Keywords: Soil erosion, Terrestrial laser scanner, Farmland, Multi-temporal, Sheet erosion, Interrill erosion

Classification crops types using Sentinel 2 satellite data in the NE of Romania

Alexandra Petronela STOLERIU*[1], Iuliana Gabriela BREABAN[1,2]
1 Institute of Interdisciplinary Research - ICI-UAIC, Integrated Center of Environmental Science Studies in the North Eastern Region - CERNESIM, Iasi, Romania
2 Faculty of Geography and Geology, "Alexandru Ioan Cuza" University of Iasi, Romania
*Corresponding Author, e-mail: iulianab2001@gmail.com

Abstract

The main purpose of this study was to conduct an assessment of crop types over a two years' period and to see what was the role of soil properties in crop development and how it was affected by land-use changes. The characteristics of the catchment, including soil type, soil moisture and land-use, affect both the quantity and quality of crops. These differences can be explained by changes in the history of agricultural land uses and the low correlation between soil class and crop type. In order to have knowledge concerning the proper optimum crop or land-use suitable for each soil unit, both the soil class and physico-chemical soil properties have equally importance. The environmental attributes taken into consideration are multi-temporal Sentinel 2 imagery bands and indices and LULC. For crop monitoring has been used Soil and Vegetation Indices, such as NDVI and NDWI, that involves the SWIR and NIR parts of the electromagnetic spectrum close related to the water content property of plants, while BI, CI, RI, SBL, GOSAVI, SAVI, SARVI, and PSRI, have the purpose to highlight the vegetation and soil signal, by enabling accurate crop discrimination and minimization of the contribution of solar irradiance and soil background. Random forest algorithm has been used for crops classification providing a higher overall accuracy and measures for most of the covariates included in the model. For the model validation field data from 42 locations with different crops and land use management have been used. Overall, the present study demonstrates accuracy of the model is high and provides good results for crop type mapping, making this research a particularly suitable approach when in-field adjustments are needed, as in the case of soil complexes involving degraded land.

Keywords: Sentinel 2, Soil and vegetation indices, Crop classification, Random forest

Spatial heterogeneity of microtopography and its effect on soil erosion under simulated rainfall

Jian Luo[1,2], Zicheng Zheng*[1], Tingxuan Li[1], Paolo Tarolli[2]
1 College of Resources Science, Sichuan Agricultural University, China
2 Department of Land, Environment, Agriculture and Forestry, University of Padova, Italy
*Corresponding Author, e-mail: zichengzheng@aliyun.com

Abstract

Microtopography is widely recognized as an important factor influencing water erosion processes. Currently, the effect of microtopography on soil erosion is still unclear. Methods employed included a rainfall simulator and the use of a laser scanner to generate a digital elevation model. Three artificial tillage practices were used to simulate different microrelief patterns. The spatial heterogeneity of microtopography was characterized by directional derivatives, semi-variogram, and multifractal model in terms of morphology and quantity. And we identified the temporal variability characteristics of runoff and sediment yield based on wavelet and rescaled range (R/S) analyses. Microtopography and drainage networks have strong multifractal behaviors, and the temporal sequences of runoff and sediment of tillage practices showed a long-range positive range and multi-time scale characteristics. Microtopography remarkably influenced the temporal evolution of soil erosion. The effect of microrelief on soil erosion was double-edged. Contrasting phenomena were found among the experiments, that is, microrelief can increase or decrease soil erosion simultaneously during water erosion processes. We established a model for forecasting soil erosion on sloping farmland using a multifractal approach. This work help clarify the effect of microtopography on soil erosion and provide a theoretical foundation to guide future tillage practices on sloping farmland of purple soil.

Keywords: Microtopography, Multifractal model, Temporal sequences analysis, Soil erosion, Purple soil

Modeling rill network evolution and its effect on erosion processes on steep hillslopes with upslope earthen dike terraces

Nana Wang[1], Zicheng Zheng[1*], Tingxuan Li[1], Shuqin He[2]
1 College of Resources Science, Sichuan Agricultural University, China
2 College of Forestry, Sichuan Agricultural University, China
*Corresponding Author, e-mail: zichengzheng@aliyun.com

Abstract

Rill morphology is a key factor for evaluating the quantity of rill erosion and the stages in rill evolution. Soil erosion processes on downslope areas are largely affected by upslope inflow. A study of rill network evolution and its effect on erosion processes was undertaken based on flume scouring experiments. Experiments using three upslope terrace areas (measuring 0.15 m^2, 0.30 m^2, and 0.45 m^2) were run with purple soil and an upslope inflow of 6 L min^{-1} on a 15° slope. We characterized the spatial variation in rill morphology based on the rill cross-section curve and rill morphological indicators. The results showed that rill erosion process was composed of four stages: drop-pits development, intermittent rill, headward erosion and rill stabilization. The number of rills gradually decreased with increasing upslope terrace area, and rill erosion intensity in the upper and middle slope was greater than that on the downslope. Rill cross-section depths reached their maximum during the rill stabilization stage and declined with increasing upslope terrace area. Cross-section morphology changed from V-shape to U-shape during the rill erosion process. The mean of rill average length (A_l), width (A_w), depth (A_d), and tortuosity complexity (c) at the entire course of rill development gradually decreased with increasing upslope terrace area, while the width-depth ratio ($R_{w/d}$) and rill density (ρ) increased initially and then decreased. The values of A_l, A_w, and A_d were significantly lower under 0.45 m^2 upslope terrace area than 0.15 m^2 area, decreasing by 2.78%, 20.67%, and 33.68%, respectively. Soil and water loss due to rill erosion decreased with increasing upslope terrace area. Our study found that ρ and A_d were the optimal indicators to estimate rill erosion.

Keywords: Rill morphology, Rill erosion, Upslope terrace areas, Flume scouring experiment

Forested catchments affected by fluvial or large infrequent disturbances: forest cover changes and large wood recruitment into the channel network

L. Picco*[1,2,3], L. Martini[1], G. Pellegrini[1], R. Rainato[1], A. Iroumé[4]
1 Department of Land, Environment, Agriculture and Forestry, University of Padova, Italy
2 Universidad Austral de Chile, Faculty of Engineering, Chile
3 Universidad Austral de Chile, RINA – Natural and Anthropogenic Risks Research Center, Chile 4 Universidad Austral de Chile, Faculty of Forest Sciences and Natural Resources, Chile
*Corresponding Author, e-mail: lorenzo.picco@unipd.it

Abstract

Forested catchments and vegetated rivers can be affected by flood events and large infrequent disturbances (LID) such as windstorms, wildfires, and volcanic eruptions. All these types of disturbances are able to rapidly change the forest cover stability and extension, promoting not only soil erosion, but also the recruitment of huge amounts of large wood (LW) into the channel network. Once in the channel network, LW exerts both positive and negative effects that must be carefully considered in the frame of forest management approach. With this work, we want to present our results on the relationship among forested areas affected by disturbance and the subsequent in-channel dynamic. Wood recruitment, load and dynamics are presented, considering forested catchments affected by ordinary flood (Piave River, Italy), artificial flood (Spöl River, Switzerland), subsequent wildfires (Rio Toro, Chile), extreme windstorm (Rio Cordon, Italy) and volcanic eruption (Rio Blanco, Chile). Different stressors produced different dynamics also related to the intrinsic differences of the morphological settings of the basins. Our results demonstrated, once again, how important it is to exert a holistic approach combining intervention of risk mitigation and forest management plans.

Keywords: Forested catchment, Disturbances, Large wood recruitment, Wood load, LW budget

Mechanisms of Soil Erosion in subtropical Chinese Forest Ecosystems

Steffen Seitz*[1], Christian Geissler[1], Philipp Goebes[1], Xuezheng Shi[2], Zhengshan Song[1,2], Thomas Scholten[1]
1 Institute of Geography, Department of Geosciences, Universität Tübingen, Tübingen, Germany
2 State Key Laboratory of Soil and Sustainable Agriculture, Institute of Soil Science, Chinese Academy of Sciences, Nanjing, PR China
*Corresponding Author, e-mail: steffen.seitz@uni-tuebingen.de

Abstract

Soil erosion is a severe environmental problem in many parts of the world. It is also a serious challenge in subtropical China, and has even been observed in woodlands after disturbances. Forests provide a multi-storey canopy layer which largely influences rain throughfall patterns. Furthermore, soil covering layers on the forest floor affect raindrop impact and modify water flows. It is also well conceivable that species identity and richness plays a role under such forest stands regarding soil erosion control. This study investigated the effects of tree species diversity, species traits, leaf litter with fauna and biocrusts on initial soil erosion in a subtropical forest ecosystem. It made use of micro-scale runoff plots under natural and simulated rainfall and splash cups to measure rainfall kinetic energy. Measurements took place in a forest biodiversity and ecosystem functioning experiment (BEF China). Results showed effects of neighborhood diversity on TKE, and positive trends of tree species richness on sediment discharge, runoff and TKE. Patterns clearly changed with ongoing successional stage of the plantation, where young trees showed more homogenous functionality than older trees. Furthermore, species-specific traits of trees and leaves influenced initial soil erosion processes under forest. High crown cover and leaf area index reduced soil erosion, whereas it was slightly increased by increasing tree height. TKE could be effectively minimized by low LAI, low tree height, simple pinnate leaves, dentate leaf margins, a high number of branches and a low crown base height. Therefore, the appropriate choice of tree species during the establishment of plantations plays a major role for erosion control. Bryophyte-dominated biocrusts importantly mitigated sediment delivery and runoff generation in this mesic forest environment and their ability to quickly colonise soil surfaces after disturbance were of particular importance.

Keywords: Soil erosion, Splash erosion, Forest ecosystems, Biodiversity, Biocrusts

Exploring the factors influencing the hydrological response of soil after fire of different severity and post-fire treatments in Mediterranean forests

Manuel Esteban Lucas-Borja[1], Pedro Antonio Plaza-Alvarez[2], Xiangzhou Xu[3], Bruno Gianmarco Carra[2], Demetrio Antonio Zema*[2]
1 Country Department of Agroforestry Technology and Science and Genetics, Campus Universitario s/n, E-02071, Albacete, Spain
2 Mediterranean University of Reggio Calabria, Department “AGRARIA”, Località Feo di Vito, I-89122 Reggio Calabria, Italy
3 Institute of Environmental and Water Resources, School of Hydraulic Engineering, Dalian University of Technology, 2 Ling Gong, Ganjingzi, Dalian, 116024, China
*Corresponding Author, e-mail: dzema@unirc.it

Abstract

The effects of fire on the hydrological response of forest soil depend on fire severity and changes exerted on its physico-chemical and biological properties. To explore this influence and weight of each factor on the runoff and erosion rates in Mediterranean pine forests, this study has applied the Principal Component Analysis to a set of covers (shrub vegetation, litter, bare soil and ash) and properties (water repellency, hydraulic conductivity and organic matter content) of soil as well as to two key hydrological variables (runoff coefficient and sediment concentration), which have been monitored at lot scale 1.5 years after fire of different severity (prescribed fire and wildfire, in the latter case also after post-fire mulching) in two forests of Central Eastern Spain. Moreover, multiregression models have been tested, using the most influencing factors detected by the PCA, to predict water runoff and soil loss. The highest runoff coefficients and sediment concentrations were mainly associated to high soil repellency and low hydraulic conductivity in soils burned by both prescribed fire and wildfire, and to low vegetation cover and ash percentage in wildfire-affected soils. The multiregression analysis gave powerful equations that were able to predict accurately predict water runoff and soil erosion based on three of the factors mentioned above.

Keywords: Hydrological monitoring, Water runoff, Soil erosion, Principal component analysis, Multiregression models.

Environmental and social advantages to on-site and local vermicomposting of food and agricultural waste

Ellen B, Sandbeck*[1], Tara VanToai[2]
1 President, Laverme's Worms, U.S.A.
2 USDA Agricultural Research Service, U.S.A.
*Corresponding Author, e-mail: ellen.sandbeck@gmail.com

Abstract

This is a distillation of thirty-plus years of experience, experimentation, and observations, gleaned while designing, setting up, running, and refining, indoor vermicomposting systems. The objectives of this study are to reduce the volume of food waste going into the waste stream; produce high quality organic fertilizer; improve soil health; reduce waste-hauling costs; encourage community members to move away from using chemical fertilizers, herbicides, and pesticides, in their gardens. We set up vermicomposting bins and systems for individual households, schools, businesses, and institutions, train people to run their system, wait for phone calls, do troubleshooting when problems arise. Learn from everyone's mistakes. This has been, essentially, a long-term, crowd-conducted, wide-ranging, and ongoing experiment. As a result, indoor vermicomposting of food waste is a simple process, but only if the system is designed and run in a way that maximizes the health and comfort of the worms. If the system is designed mainly for human convenience, it is almost certain to fail. Hence, the design of a system is important, but the way it is run is more important. For some people, prison inmates, for example, learning to run a vermicomposting system, can be life- and mind-altering.

Keywords: Vermicomposting, Waste reduction, Fertilizer production

Tillage erosion and its effect on soil organic carbon in black soil region of China

Enheng Wang*[1]
1 School of Forestry, Northeast Forestry University, Harbin, China
*Corresponding Author, e-mail: erxin222@163.com

Abstract

The black soil region of Northeast China is characterized by flat to gentle undulating topography; it is ideally suitable for tillage with machines and has become the forefront for the expansion of agricultural mechanization in China. As a result, the potential risk of soil erosion has been inevitably increased with the increases of tractor power, tillage speed, and depth. Thus, this study aims to 1) provide direct measurements of tillage translocation due to moldboard plowing; and 2) analyze the effect of tillage erosion on the spatial variation of soil organic carbon (SOC). Tillage translocation was determined in a plot experiment using stone chips as tracers. The tillage erosivity, expressed in terms of tillage transport coefficient, was 234 kgm^{-1} tillage $pass^{-1}$. High soil loss occurred in the top and lower section of slope, whereas the middle- and bottom section areas reflected soil accumulation. The spatial pattern of SOC exhibited an approximately opposite trend as tillage erosion in the study field, and SOC concentrations were negatively correlated with tillage erosion rates. The findings suggest that tillage erosion could be a major cause of soil redistribution and C dynamics on sloping farmland in the black soil region of Northeast China.

Keywords: Tillage erosion, Soil redistribution, Soil organic carbon, Black soils

Study on Climate Change Character in Black Soil Region of Northeast China

Fengyuan Zhang[1], Yuanhang Su*[1]
1 School of Forestry, Northeast Forestry University, Harbin, China
*Corresponding Author, e-mail: 468357182@QQ.com

Abstract

The average temperature, the maximum temperature and the minimum temperature in the black soil region have risen significantly, and the minimum temperature has risen more obviously, resulting in a decrease in the temperature difference between day and night. Radiation goes through a process of decreasing first and then rising. Research has found that the frequency of extreme rainfall in the black soil region of Northeast China has increased, while the frequency of small rainfall has decreased. The increase in extreme rainfall may aggravate the degree of soil erosion in the black soil region and cause the loss of black soil resources. The decrease in rainfall frequency may lead to short-term droughts. The average wind speed in the black soil region showed a significant downward trend. This climate change may have an impact on agricultural production and the process of soil erosion, and further research is needed.

Keywords: Temperature, DTR, Rainfall, Wind speed

Evaluation on the Spatial Configuration of Soil Conservation Practices in a Small Catchment of the Black Soil Region, Northeast China

Haiyan Wang*[1,2]
1 Key Laboratory of Water Cycle and Related Land Surface Processes, Institute of Geographic Sciences and Natural Resources Research, Chinese Academy of Sciences, Beijing 100101, China
2 University of Chinese Academy of Sciences, Beijing 100049, China
* Corresponding author. E-mail address: fanghy@igsnrr.ac.cn

Abstract

Because severe soil erosion has occurred in the black soil region, northeastern China, large scale soil conservation practices were implemented to control soil loss. Evaluation of the efficiencies of an individual and/or comprehensive practice in controlling soil loss is urgently required for better configuring soil conservation practices. In the present study, based on current land use condition, 24 land use scenarios were supposed, which includes different soil conservation practices on different slope gradients or at different sites. The soil conservation measures include contour tillage, hedgerow planting, terrace, trench at the edge of forest and cultivated land on slopes, and check dam, reservoir in gullies/rivers. Soil erosion and sediment yield under different land use scenarios were predicted based on the WaTEM/SEDEM (Water and Tillage Erosion Model and Sediment Delivery Deposition Model). Results found that the configuration of contour tillage at slopes with gradient less than 3 degree, hedgerow at slopes with gradients between 3 to 5 degrees, terracing at slopes with gradients between 5 to 8 degree, and forestation at slopes with gradient larger than 8 degree coupled with trench at the edge of forest and dams in gullies/on rivers was the best to control soil loss, with soil loss rate less than the tolerable value of 200 t km^{-2} yr^{-1}. This study further improved the effect of the three defensing lines in reducing soil loss.

Keywords: Soil erosion, Soil conservation practice, Spatial configuration, Black soil region

Influence of cultivation duration on soil mechanical properties: A case study from black soil region of Northeast China

Lin Lin[1,2], Shaojie Han[1], Chengcheng Zhang[3], Enheng Wang*[1]
1 School of Forestry, Northeast Forestry University, Harbin, China
2 Department of Environment - Soil Physics Unit, Ghent University, Gent, Belgium
3 College of Civil engineering, Northeast Forestry University, Harbin, China
*Corresponding Author, e-mail: erxin222@163.com

Abstract

It is important to understand how soil properties such as organic matter content (SOC), clay content (CC), water content (WC), and bulk density (BD) are related to soil mechanical properties. We hypothesized that the soil properties changes caused by tillage practices would cause corresponding variations in the soil mechanics. The natural and manipulated soils were tested to determine how the cultivation duration affected the compression and rebound behavior of black soil in Northeast China, and to explore the main factors that affected compaction and resilience, from the perspective of soil mechanics rather than soil physico-chemical properties. Undisturbed soil samples were collected from fields for different periods (0, 17, 30, and 40 yr). Meanwhile, the manipulated samples were remolded to obtain soils with 3 different organic matter contents (44.9 g kg^{-1}, 69.1 g kg^{-1}, and 93.1 g kg^{-1}), 3 different clay contents (18.6 %, 29.4 %, and 56.3 %), and 2 different water contents (20 % and 30 %). The compression index and rebound index were determined by the fast oedometer test. As the cultivation duration increased, SOC gradually decreased, but CC and BD increased; The compression and rebound indexes of all the soils decreased after cultivation. Compressibility increased if the SOC and CC increased, and the soil would be less resilient if the CC was higher. In a word, the compressibility and resilience of soils with long-term cultivation duration were poor due to the decrease of SOC and increase of CC. SOC was further found more significant than CC on influencing compression and rebound behavior of black soils.

Keywords: Tillage, Organic matter content, Clay, Compression index, Rebound index, Mollisol

Soil Health Assessments in Biofuel Cropping Systems

Michael L. Thompson*[1], Fritzie Chen[2], Mostafa Ibrahim[3], Ala Khaleel[1]
1 Agronomy Department, Iowa State University, Ames, IA, USA
2 Monty's Plant Food, Louisville, KY, USA
3 Actagro LLC, Research & Development, Kerman, CA, USA
*Corresponding Author, e-mail: mlthomps@iastate.edu

Abstract

Cropping systems designed to produce feedstock for cellulosic-based fuels include both annual and perennial crops. In this study, we explored the impacts of long-term production of cellulosic feedstocks on several parameters related to soil health and collectively referred to as the Haney tests of soil health. The four cropping systems of interest in central Iowa are: continuous corn, continuous corn with a cover crop, reconstructed prairie with no fertilization, and N-fertilized reconstructed prairie. We measured short-term CO_2 evolution (soil respiration), organic carbon (OC), total nitrogen (TN), particulate organic matter (POM), and water-extractable organic carbon and nitrogen (WEOC and WEON) in soils under both annual and perennial cropping systems managed for biomass production. Compared to soil supporting the annual bioenergy crops (maize in the continuous corn and continuous corn with cover-crop treatments), soil in the fertilized, multispecies, reconstructed prairie cropping system had significantly greater CO_2 respiration rates, greater concentrations of POM, more water-extractable organic carbon, and a higher soil health index. Most soil health indicators were higher for fall-collected samples than for samples collected in the spring of each year. Overall, the fertilized reconstructed prairie had the highest soil health indices, and the continuous corn treatment had the lowest soil health indices over the three-year period.

Keywords: Haney soil health index, Particulate organic matter, Short-term carbon respiration

Soil degradation and morphological change in low relief, "high clay" Mollisol pedons, Iowa

Lee Burras C. *[1], Xiiangyou Xia[2], Enheng Wang[2]
1 Department of Agronomy, Iowa State University, Iowa, USA
2 Department of Soil & Water Science, School of Forestry, Northeast Forestry University, China
*Corresponding Author, e-mail: lburras@iastate.edu

Abstract

Iowa is located in the center of North America's Mollisol region that extends from west central Canada through the USA's Great Plains into northeastern Mexico. Not surprisingly, this means Iowa is also centrally located in North America's most intensely cropped region. As a result, many of Iowa's Mollisols experienced significant degradation throughout the 20th century as farming practices intensified. This project longitudinally examines soil degradation (and/or regeneration) that occurred between 1950 and 2020 in low relief (i.e., slopes less than 3%) in five high clay, upland Mollisol soil series from central Iowa. Low relief conditions are examined in order to understand soil change that occurs when erosion is not the primary degrader. "High clay" soils are of interest to allow best comparison between Iowa and Northeast China. Data comes from a combination of USDA-NRCS pedons and ISU research pedons. Pedological properties examined are epipedon, B horizon and sola thickness, color, soil organic matter content and structure. Updated interpretations derived from those pedological properties are revised Soil Taxonomic classifications (Suborder through the family level), CSR2 (Iowa's soil productivity rating) and comparison of corn yields expected on the "original" soil as well as its modern analog.

Keywords: Endoaquoll, Hapludoll, Morphology, Pedons

Dynamics of soil organic carbon and soil nutrients following tillage and water erosion in an agricultural landscape

Pengzhi Zhao*[1], Enheng Wang[2]
1 Earth and Life Institute, Georges Lemaître Centre for Earth and Climate Research, Université Catholique de Louvain, 1348 Louvain-la-Neuve, Belgium
2 School of Forestry, Northeast Forestry University, Harbin, China
*Corresponding Author, e-mail: pengzhi.zhao@uclouvain.be

Abstract

Soil degradation from accelerated erosion in the northeast China, the Chinese breadbasket, has become a critical threat to national food security. A mechanistic understanding spatial redistribution of soil particles and associated nutrients associated with the erosion process is required to formulate precision soil conservation measures. Using the directional tillage erosion model and revised universal soil loss equation in combination with measurements of the soil organic carbon (SOC) and soil nutrients from 112 surface soil samples (0–20 cm) on a sloping farmland, we explored the distribution of SOC fractions, total nitrogen (TN) and total phosphorus (TP) attributed to tillage and water erosion. Results showed that the sensitivity of TP distribution is more responsive to water erosion than tillage erosion. In comparison, no significant relation between TN and tillage erosion or water erosion could be found on any slope position. We found that water erosion played a greater role in controlling dissolved organic C than tillage erosion, whereas particulate organic C distribution was more sensitive to tillage erosion than water erosion. In addition, we observed a contrasting relationship between microbial biomass C and water erosion rates for the mild (averaged 17.42 t ha^{-1} y^{-1}, $r = -0.43$, $P < 0.05$) vs. intense erosion scenario (averaged 54.60 t ha^{-1} y^{-1}, $r = 0.38$, $P < 0.05$). This clear shift indicates a possible dual role of soil microbes in SOC cycling: water erosion depletes microbial biomass and contributes to SOC mineralization in mild erosion scenarios, whereas intense water erosion may lead to a shift in microbial activity and composition thus promoting the dynamic replacement of SOC at eroding sites. Further data is needed to confirm this hypothesis.

Keywords: Tillage erosion, Carbon fractions, Soil nutrients, Microbial biomass carbon, Black soil

Soil Tillage and Crop Planting Timing Effects on Soil Erosion

Enheng Wang[1], Rick Cruse*[2], Daryl Herzmann[2], Brian Gelder[2], David James[3]
1 School of Forestry, Northeast Forestry University, Harbin 150040, China
2 Department of Agronomy, Iowa State University, Ames, IA 50011, USA
3 USDA-ARS National Laboratory for Agriculture and the Environment, Ames, IA50011, USA
*Corresponding Author, e-mail: rmc@iastate.edu

Abstract

Soil surface conditions, especially residue cover, and rainfall characteristics control soil erosion losses on sloping land. Because rainfall characteristics vary with season and time of year, the timing of tillage and crop planting, which reduces crop residue cover, potentially impact soil erosion losses. The objective of this study is to determine the impact of tillage and planting dates on estimated sheet and rill soil erosion losses. Using the Daily Erosion Project (DEP) modeling system multiple spring planting dates were imposed across a ten-year period and resulting soil erosion estimates were determined with all tillage dates experiencing documented and archived precipitation through the simulation period. For the Central US continental climate conditions, soil erosion increased monotonically with delayed tillage and planting. Early season planting seems the most favorable for soil conserving purposes.

Keywords: Erosion, Daily Erosion Project, Tillage timing, Planting timing, Rainfall intensity

Root Exudation Rates Decrease with Increasing Latitude in Some Tree Species

Liu Yang[1], Xiuwei Wang*[1]
1 Key Laboratory of Sustainable Forest Ecosystem Management-Ministry of Education, Northeast Forestry University, Harbin 150040, China; yangliuin1996@163.com
*Correspondence, e-mail: wxgreat@nefu.edu.cn

Abstract

Understanding of the spatial variation of root exudation on a regional scale can help understand the response of plant adaptability to environmental changes. Although root exudation has become an important topic in belowground ecology, its relationship with root traits and environmental factors is poorly understood. Our objective was to explore how root traits and environmental factors influence root exudation. We used a multi-factorial design consisting of three tree species spanning across sites located at three latitudes to assess root exudation dynamics, which was measured using a syringe-basis incubation system. The strongest and clearest effect observed in our study was a decrease in root exudation rates of Korean pine (*Pinus koraiensis* Sieb. et Zucc.) and larch (*Larix gmelinii* (Rupr.) Kuze.) at sites located in higher latitudes. Root exudation rates were positively related to mean annual temperature, mean annual precipitation, and negatively related to soil total organic carbon. Root exudation in coniferous species decreased at sites located in higher latitudes. Despite differences in root exudation rate among sites located at different latitudes and species with suitable variation in root morphological traits and environmental factors, we could not identify consistent influencing factors on root exudation rates.

Keywords: Root exudates, Fine-roots, Root morphological traits, Environmental factors, Regional scale

Effect of freeze–thaw cycles on phosphorus availability in biochar-amended black soil

Ying Han*[1]
1 College of Geography and Environmental Science, Hainan Normal University, China
*Corresponding Author, e-mail: hanying0729@126.com

Abstract

The black soil region in northeast China has been one of the most important crop production areas in the country owing to the productive physical and chemical capacity of black soil. However, substantial soil phosphorus (P) losses often occur in the black soil region owing to soil freeze-thaw cycles (FTCs). Presumably, biochar amendment is an efficient method of conserving P and sustaining agricultural production in the black soil region of northeast China. To better understand how biochar interacts with FTCs to affect soil P availability in black soil, we aim to (1) sift optimum biochar preparations to enhance phosphorus availability; (2) identify the regular pattern of biochar-amended soil P adsorption/desorption and P fractions with FTCs; (3) reveal the interactions among FTC treatments and soil moisture conditions on P availability after biochar amendment. Our findings provide a guideline for sustainable development of black soil resources.

Keywords: Biochar, Freeze-thaw cycles, Mollisol, Adsorption and desorption, Phosphorus fractions

A new method for weakening slaking of collecting eroded aggregates by water erosion

Fu Yu*[1]
1 School of Forestry, Northeast Forestry University, Harbin, China
*Corresponding Author, e-mail: aily_fy@163.com

Abstract

In most of previous studies about aggregate breakdown caused by water erosion, a critical process that water inevitably fragments the eroded aggregates by water erosion again is generally ignored. This will reduce the accuracy of research results. Hence, alcohol has been added to the collecting device of eroded aggregates to weaken the slaking of eroded aggregates by the researchers, but the optimal alcohol-to-water ratio for protecting the size fraction distribution of eroded aggregates remains unclear. Aggregates with a size fraction of 2-5 mm obtained by dry sieving of Black soil in Northeast China were selected as the research object to analyse the effects of five alcohol-to-water ratios on aggregate characteristics and their variation with soaking time. The results showed that the size distribution in terms of mass percentage under different soaking times was similar. For the same soaking time, the mass percentage of 2-5 mm aggregates gradually decreased with decreasing alcohol ratio, but the aggregates with the second-highest mass percentage were gradually distributed among smaller size fractions. A percentage of aggregate destruction (*PAD*) of 20% served as the dividing line to evaluate the stability of soil aggregates. In this case, eroded aggregate collection should be completed within 12 min at an alcohol-to-water ratio of 1:1. Alternatively, eroded aggregate collection should be completed within 6 min at an alcohol-to-water ratio of 2:3. The above results can provide a reference for improving the accuracy of data collection regarding eroded aggregates.

Keywords: Slaking breakdown, Mean weight diameter, Percentage of aggregate destruction, Alcohol

Improvement of resistance to mechanical disturbance by adding organic materials to black soil

Miaomiao Wang[1], Enheng Wang*[1]
1 School of Forestry, Northeast Forestry University, Harbin, China
*Corresponding Author, e-mail: erxin222@163.com

Abstract

The black soil region is an important commodity grain production base with the highest degree of agricultural mechanization across China. During long-term and frequent mechanical production, the tillage equipment can directly apply to the soil, which results in less stability of soil aggregates and further aggravates the risk of soil erosion. To find out whether exogenous organic materials can enhance the ability of black soil to resist mechanical disturbance, this study added three kinds of exogenous organic materials (straw, biochar, swine manure) with different content gradients to the cultivated soil; and the responses of soil aggregate stability (MWD) to mechanical disturbance were analyzed by using constant temperature and humidity culture experiment and simulating mechanical disturbance. After adding organic materials, soil aggregate stability was improved by different degrees with an order of straw > swine manure > biochar. The addition of straw and swine manure can significantly improve MWD, and the improvement effect was getting better with the increase of the addition amount; however, the MWD gradually decreased with the increase of disturbance intensity. The anti-mechanical disturbance ability of soil was affected by the type of material, the amount of material, and the intensity of disturbance; and the improvement effect of adding straw is the best. Straw returning not only plays the traditional role of increasing soil water storage and carbon, and regulating soil temperature, but also improves the ability of cultivated black soil to resist mechanical disturbance. Thus, straw returning could be one of the optimal conservation tillage measures in black soil region.

Keywords: Black soil, Straw, Biochar, Wine manure, Mechanical disturbance, Soil aggregate stability

Effect of subsoiling operations on the recovery of compacted black soil

Qianqian Lu[1*]
1 College of Earth Sciences, Guilin University of Technology, China
*Corresponding Author, e-mail: luqq0404@163.com

Abstract

With the advancement and development of modern agriculture, the widespread application of large-scale mechanical operation will not only improve the production efficiency and economic benefits, but also have different degrees of impact on the structure of cultivated soil, and the problem of soil compaction is becoming increasingly prominent. Subsoiling operations can directly affect soil bulk density and porosity, and then the seasonal freeze-thaw characteristics of soil, which may promote the natural recovery of compacted soil structure. To better understand how the influences of subsoiling operations before overwintering on the mechanical compacted black soil, we aim to (1) prove subsoiling operations will affect the soil structures and seasonal freeze-thaw characteristics; (2)compare the different effects of subsoiling operations at different depths (15cm and 30cm); (3)discuss how subsoiling before overwintering is beneficial to the recovery of compacted black soil. Our findings provide a theoretical basis for the restoration of compacted black soil.

Keywords: Black soil, Mechanical compaction, Subsoiling operations, Freeze-thaw characteristics, Micro-aggregates

Applicability Research of Four Runoff and Sediment Sampling Methods in Black Soil Region of Northeast China

Sidiaihemaiti Yusupu[1], Enheng Wang*[1]
1 School of Forestry, Northeast Forestry University, Harbin, China
*Corresponding Author, e-mail: erxin222@163.com

Abstract

Accurate measurement of sediment concentration in the collection tanks of runoff plot is the key to monitor soil erosion and estimate the soil loss amount of sloping farmland. The research on measurement accuracy, influencing factors and applicability of runoff plot observation method is the basis of soil erosion evaluation in black soil area of northeast China. In this study, the black soil was taken as the research object. the accuracy of four sampling methods (manual stirring sampling, mechanical stirring sampling, mechanical stirring + full profile sampling, and full profile sampling) under different sediment concentrations (1, 5, 10, 50, 100, and 500 kgm-3) and different water and sediment volumes (30, 50, and 90 L) was compared by indoor simulation test, and the measurement results were modified. The results show that: 1) When the volume of water and sediment is 50 L with different sediment concentrations, the measurement error of mechanical stirring + full profile method is the lowest in general; 2) The higher the sediment concentration, the greater the measurement error; Under different sediment concentrations, the influence of water and sediment volume on the measurement error is different. When the sediment concentration is less than 50 kgm-3, the water and sediment volume has no significant effect on the measurement accuracy of mechanical full section sampling method. 3) When the sediment concentration is less then 10 kgm-3, the artificial mixing method is suitable for field runoff plot observation; when the sediment content is larger than 100 kgm-3, the full profile sampling method is suitable for field runoff plot observation. Mechanical stirring method and mechanical stirring + full section sampling method can be directly used in field runoff plot observation. The research results can provide a basis for sampling and measurement of runoff and sediment in the catchment bucket in black soil region.

Keywords: Collection tanks, Sampling method, Sediment concentration, Measurement error

Forms and availability of soil phosphorus around the stumps and coarse roots in black soil region

Xiuli Men*[1]
1 School of Forestry, Northeast Forestry University, Harbin, China
*Corresponding Author, e-mail: 1032647163@qq.com

Abstract

Vegetation restoration might be an important practice to control soil degradation, and thus improve soil productivity in black soil region. The stumps and coarse roots, as a component of ecosystem, could affect the soil nutrients status in the microsites. To explore the effect of Larix stumps and coarse roots decomposition on soil phosphorus forms and availability,the topsoil (0-10cm) around stumps and coarse roots with four different decay classes (Ⅰ -Ⅳ) were collected for analyzing phosphorus content, fractionations and availability. Organic P is the major fraction for four different microsites and sodium hydroxide extractable organic P (NaOH-Po) representing moderately labile organic phosphorus is predominant in the microsite with decay class Ⅰ ,which accounts for 7.9% of total P. The more labile fractions, H2O-Pi and NaHCO3-Po are less, only accounting for 2.4% and 0.7% of the total P content, respectively. Except for NaHCO3-Po, all the other P fractions correlate with each other, and they also show significant correlations with soil organic matter. Leaving the stumps and coarse roots in situ not only can reduce the disturbance of soil thus decrease soil erosion, but also can improve the availability of soil phosphorus, improving the soil nutrient availability.

Keywords: Black soil, Soil nutrient, Phosphorus fractionation, Phosphorus availability, Organic phosphorus

Interaction of Tillage and Water Erosion on Soil Aggregate Stability in Black Soil Region

Yongjiang Li[1], Enheng Wang*1
1 School of Forestry, Northeast Forestry University, Harbin, China
*Corresponding Author, e-mail: liyongjiang@nefu.edu.cn

Abstract

Mechanical tillage and water erosion are two main factors that aggravate soil quality degradation in black soil slope farmland. Previous studies focused on the individual effect of tillage disturbance or water erosion on the structure, anti-erodibility, and nutrient loss of black soil, and there were few studies on the interaction of the two processes. To further investigate the coupled damage mechanism of tillage disturbance and water erosion on the stability of black soil aggregates, we simulated the disturbance of mechanical tillage (T) and three water erosion processes with different damage mechanisms (F= fast wetting, representing rainstorm and heavy rain; S= slow wetting, representing moderate rain and light rain; V= mechanical damage of water, representing runoff) and the interaction of the two processes. Soil aggregate mean weight diameter (MWD) and aggregate size distribution (ASD) were measured and analyzed. Compared with tillage disturbance and water erosion separately, the interaction of tillage disturbance and water erosion significantly reduced MWD. The effect of water erosion after tillage disturbance on MWD was enlarged with an amplitude of V > S > F. The effect of T or F on ASD was similar, which mainly broke 2-10 mm aggregates, and the interaction of T and F can further break 1-2 mm aggregates. S or V had no significant effect on ASD, but the interaction with T (S*T, V*T) could also significantly broke 2-10 mm aggregates. The interaction of tillage disturbance and water erosion reduced the stability of black soil aggregates, mainly by crushing 2-10 mm large aggregates and increasing the proportion of < 0.25 mm small aggregates.

Keywords: Black soil, Tillage, Water erosion, Soil aggregate stability, Aggregate size distribution

Opinion: Using eDNA fingerprinting in high mountain environments to support soil restoration and hazard control

A. Frankl*[1,2], O. Evrard[3], E. Verleyen[4], E. Cammeraat[5], A. Stokes[1]
1 INRAE, AMAP, IRD, CIRAD, CNRS, University Montpellier, France
2 Department of Geography, Ghent University, Belgium
3 Laboratoire des Sciences du Climat et de l'Environnement (LSCE/IPSL), Unité Mixte de Recherche 8212 (CEA/CNRS/UVSQ), Université Paris-Saclay, France
4 Department of Biology, Ghent University, Belgium
5 Institute for Biodiversity and Ecosystem Dynamics, University of Amsterdam, The Netherlands
*Corresponding Author, e-mail: Amaury.Frankl@cirad.fr

Abstract

Mitigating erosion, mass movements, and geohazards in high mountains is increasingly conceived within frameworks of ecological restoration, that is, recovering the form and function of ecosystems that have been damaged by degradation. Vegetation may be the most distinctive feature of high mountains, where the underlying lithology is heterogeneous and soils are mainly shallow and poorly developed. Because there are strong interrelations between land cover and geomorphological processes in high mountain environments, the use of land cover-based sediment tracers would be particularly meaningful. eDNA has the highest source discrimination potential in that regard, providing information up to the species level and reflecting changes in vegetation on over short timescales. Furthermore, eDNA signals in sediments will be strongest from areas experiencing higher erosion rates and which are highly connected with the hydrographic network. The use of eDNA sediment source fingerprinting would thus allow the investigation of complex and often poorly understood relationships between vegetation cover, restoration activities, and geomorphological response at the catchment scale. To improve the success rates of restoration activities, collaboration between scientists and stakeholders can accelerate technology transfer rates. However, time and budget constraints often hamper in-situ monitoring of soil and water bioengineering applications, and very few monitoring programs exist. Knowledge of success rates is, however, essential for restoration. To this end, sediment source fingerprinting has been shown to provide a valid framework for supporting soil restoration activities. We opinionate that eDNA fingerprinting – as an emerging technique – could be particularly useful to support soil restoration and hazard control in high mountain environments.

Keywords: Landslides, Sediment source fingerprinting, Soil Erosion, Vegetation

Nature-based Solutions for water management and conservation: the case study of the LIFE BEWARE project

Bettella F*[1], Bortolini L.[1], D'Agostino V.[1]
1 Department of Land, Environment, Agriculture and Forestry, University of Padova, Agripolis, Viale dell'Università 16, 35020 Legnaro, Italy
*Corresponding Author, e-mail: francesco.bettella@unipd.it

Abstract

The EU LIFE funded project BEWARE "Better Water Management for Advancing Resilient-communities in Europe" promotes the diffusion of Nature-based Solutions (NBS) for a better management of the rainwater in order to increase the resilience of the territory to flooding and drought. In particular, seven NBS were implemented in the Altovicentino area (Vicenza Province, Veneto Region, northeastern Italy), six of them in urban areas and one in a rural area. A description of the adopted NBS is reported. These interventions have show a good ability to manage rainwater by all the implemented NBS, allowing to overcome local flooding. The NBS implemented in the rural area enables to better cope with drought improving the crop yields.

Keywords: Flooding mitigation, Low impact development, Sustainable urban drainage systems, Climate change adaptation

Slope stability analysis on the vegetated hillslopes on Carrara Marble quarries

First C. Mauriello[1], A. Errico[2], Y. Giambastiani[2,3], F. Preti*[1]
1 DAGRI Department, University of Florence, Italy
2 Blue Biloba Srl, Florence, Italy
3 CNR National Research Council of Italy - Institute of BioEconomy (IBE)
*Corresponding Author, e-mail: minomauriello@gmail.com

Abstract

The present work was carried out on the Apuan Alps in the surroundings of Carrara and Colonnata (MS), one of the biggest marble extraction areas of the planet. The aim of the research was to determine the effect of spontaneous vegetation on the stability of marble dump deposits originated by the marble extraction and processing, named "ravaneti". In fact, these deposits represent a severe hazard for the settlements located downstream, due to the high potential of failure and sediment production that can cause the obstruction of riverbeds and bridges. The vegetation of these deposits can contribute to contrast these phenomena, but a detailed estimation of this contribution has never been carried out before. The calculation of the stability factor was carried out by applying the model proposed by Greenwood (2006), also known as Slip4ex - Slope and stability analysis. A destructive sampling campaign allowed the determination of shape and size of the root systems of the forest species growing on these deposits. Results showed that the contribution of shrubs and trees on the stability of ravaneti is significant, especially for the shallower layers, which are typically the most affected by failure during severe rainstorms in the Apuan Alps area. The results of the present research provided useful information for the planning of vegetation management activities on ravaneti dump deposits, suggesting that a progressive revegetation of abandoned deposits can contribute significantly to their stability. In this perspective, these findings can be used also for the design of soil bioengineering techniques for restoration purposes.

Keywords: Ravaneti, Root reinforcement, Slip4Ex

Landslide and rockfall risk assessment and natural-based solutions for risk mitigation: a case study in Sardinia (Italy)

F. Giadrossich*[1], D. Cohen[2], I. Murgia[3], Y. Giambastiani[4], M. Schwarz[5]
1 Dipartimento di Agraria, Università di Sassari, Italy
2 Department of Earth and Environmental Science, New Mexico Tech, Socorro, NM, USA
3 Dipartimento di Architettura, Design e Urbanistica, Università di Sassari, Italy
4 CNR-IBE—Consiglio Nazionale della Ricerca, Istituto di BioEconomia, 50019 Florence, Italy
5 Bern University of Applied Sciences, Bern, Switzerland
*Corresponding Author, e-mail: fgiadrossich@uniss.it

Abstract

For several years Bonorva has been subjected to continuous warnings about the risk of landslides and rockfalls. Periodically, as a result of heavy seasonal rainfalls, signs on the slope appear as cracks in the soil, showing triggers of the incipient landslide. Moreover, large boulders resting on top of a hill above the city are becoming more and more unstable. Despite these dangers, no tragic event has occurred yet. This study analyzes at the slope scale the probability of landslide occurrence in this unstable area using specific tools for the analysis of slope stability. In addition, probabilistic analysis was performed on the trajectory and affect the impact of large boulders on the town. The analyses were conducted through field surveys and the use of software SOSlope and Rockyfor3D. SOSoslope is a hydro-mechanical model that computes the factor of safety at the and includes the effects of vegetation root structure and composition. Rockyfor3D is a probabilistic model that quantifies the probability of rockfall with the possibility to consider the effect of vegetation at the slope scale and localizes potential areas where forest protection can be improved. Results allowed the evaluation of the stability factor under critical rainfall. The quantification of critical thresholds for slope stability allowed the identification of natural-based solutions for risk mitigation. The presence of vegetation can in the long-term lead to a substantial improvement in the stability factor. Besides, the risk of impact against sensitive targets for people and property is significantly mitigated. These results are useful information for land use planning and decision-making on hazard mitigation actions.

Keywords: Slope stability, Protection forests, Root reinforcement, Land planning

An overview of constructed wetlands for wastewater treatment in mountain areas: performance and floristic evolution in several case studies in Val Camonica (North Italy)

R. Stentella[1], E. Bona[2], G. Calvi[2], L. Giupponi[3], A. Cislaghi[1,3], G.B. Bischetti[1,3], L. Rossi *[1]
1 Department of Agricultural and Environmental Sciences, Production, Landscape and Agroenergy (DiSAA), University of Milan, Milan, Italy
2 Adamello Regional Park, Breno (BS), Italy
3 Centre of Applied Studies for the Sustainable Management and Protection of Mountain Areas, (Ge.S.Di.Mont.), University of Milan, Edolo (BS), Italy
*Corresponding Author, e-mail: lmw.rossi@gmail.com

Abstract

In the last half century, CWs have become increasingly popular solutions in mountainous areas, given the inherent harshness of this environment. The most prominent problems are: (i) the lack of space and the steep slope for the construction; (ii) the climatic conditions that do not promote growth of plant species traditionally used in phytoremediation systems; (iii) the supply of meteoric inflows (stormwater) washing and diluting the greywater supply (reducing efficiency); and (iv) the difficulty in finding adequately trained staff with appropriate means for frequent maintenance. The aim of this study is to propose guidelines for CWs design employing subsurface flow beds (to improve performance under cold climatic conditions) and enhancing the resulting ecosystem services (biodiversity, landscape, recreational experience). We carried out several activities on six CWs :1. monitoring the treatment efficiency in two high-altitude sites;2. monitoring the floristic evolution of plant communities from construction to the actual conditions;3. estimating the treatment efficiency as a function of substrate through a scientific review. The results showed a good treatment efficiency in the monitored sites, highlighting how the combination of zeolite and gravel favors pollutant abatement also in harsh mountainous environment. Substrate clogging remains the operational challenge for the maintenance. We propose a series of technical, engineering and botanical measures to improve the design and maintenance of the CWs, to increase the wastewater treatment efficiency and exploiting the multi-functionality of these areas.

Keywords: Constructed wetlands, Wastewater treatment, Floristic evolution

Transferability analysis as a supporting tool for the implementation of soil and water bioengineering techniques to unknown areas

M Maxwald*[1,2], C Crocetti[3], R Ferrari[3], A Petrone[1], H P Rauch[2] F Preti[1,3]

1 Department of Agricultural, Food, Environmental and Forestry Sciences and Technologies (DAGRI), University of Florence, 50144 Firenze, Italy

2 Institute of Soil Bioengineering and Landscape Construction (IBLB), University of Natural Resources and Life Sciences, 1190 Vienna, Austria

3 AIPIN (Soil and Water Bioengineering Italian Association), Via del Monte, 2, 34122 Trieste TS, Italy

*Corresponding Author, e-mail: melanie.maxwald@unifi.it; melanie.maxwald@boku.ac.at

Abstract

Soil and water bioengineering as a nature-based solution to protect and secure natural, as well as artificial slopes, banks or shorelines, gained worldwide popularity among urban and regional planning within the last decades. Sources confirm that this old method was used frequently during the Roman Imperial period in Europe, as well as to control torrential flood waters in Asian countries 2000 BC by employing biological components. It aims to define the general applicability of policies from a Leading Site to a Take-Up Site and tries therefore to show the external validity of the concept independently from situation or time. The transfer of a policy can be carried out in various grades: (1) a complete transfer (copying), (2) the transfer of the ideas behind the policy (emulation), (3) a fusion of different policies (combinations) and (4) taking inspiration from a policy with a different jurisdiction, whereby the final outcome does not draw on the original idea [4]. For the actual assessment regarding the transferability of SWBE in step 4 main phases have been classified from the Leading Sites: (a) Planning Phase, (b) Construction Phase,(c) Use Phase, as well as (d) End of Life Phase of a construction. These categories were subdivided by the following components: (a) know-how of soil and water bioengineering techniques, local climate conditions, botany, hydraulics, pedology; (b) materials, qualified labor, equipment and mechanical instruments, economic resources; (c) monitoring, efficiency, sustainability, maintenance; (d) replicability. The assessment of these components allows therefore to determine key barriers and key support factors regarding the transfer of SWBE techniques to unknown areas, helping the planning and executing parties at the Take-Up Sites, as well as the discipline itself to grow.

Keywords: Soil and Water Bioengineering, Transferability analysis, Sustainable erosion control, Nature-based solutions

Stabilization of the sediment transport dynamics in the Cristo Gully system (Tudela, Navarra, Spain)

Sangalli Paola*[1,2], Tardio, Guillermo Carcar[2], Mónica[3], Bergara. Ignacio[2]

1 SCIA, EFIB, Spain

2 AEIP, Consultant engineer. Spain

3 Ypatia ingeniería, Spain

4 Navarra Govern, Spain

*Corresponding Author, e-mail: sangalli@sangallipaisaje.com

Abstract

El Cristo gully system is one of the basins near the Tudela town, located at the north of the urban center. This basin has an area of 60 hectares and the El Cristo hermitage is placed within it. Besides, the gully bed runs under a road through a long culvert which, when intense rainfalls take place and because of the active transport dynamics present in the gully system, becomes blocked. In these situations, the road itself becomes impracticable. The Cristo gully basin is formed of tertiary deposits in which clays and silts are the predominating materials. This explains the high erodibility of the system as well as the overall scarcity of plant cover (above all over the slopes). These circumstances, together with the torrential rainfall regime of this area of Navarra, trigger a high activity of the gully system which, in turn, generates many problems to the aforementioned railway and road. For addressing this situation, the Tudela municipality requested the Government of Navarra the elaboration of a project with the aim of reducing the sediment transport intensity of the gully system. The use of Nature Based Solutions and soil bioengineering frameworks was included as a condition in the project development. It has been the first experience of the River restoration section of the Navarra Govern in such an extreme landscape and arid conditions. In this paper we show the followed strategy and the objectives achieved.

Keywords: Sediment traps, Gully stabilization, Soil and Water Bioengineering

Soil and Water Bioengineering (SWB)in Europe: 25 Years of the EFIB

Sangalli, Paola*[1], Eva Hacker[2], Rosmarie Stang [3]
1 President EFIB, Spain and Austria
2 Vicepresident EFIB
3 Secretariat / Management
*Corresponding Author, e-mail: efibioengineering@gmail.com

Abstract

Soil and Water Bioengineering, (SWB) with the use of native plants as a building material, offers sustainable solutions face to the challenges of mitigation and adaptation to climate change. The development, although not homogeneous in all European countries, is proceeding rapidly thanks to the introduction of the Green Infrastructure as a planning concept and the use of NBS as constructive solutions. SWB as an applied discipline, was born in Central Europe at the beginning of the last century, mainly in the field of hydraulic-forestry arrangements integrated with civil engineering techniques. Subsequently, in the forties, it will begin its development in other fields (coastal area, mining, linear infrastructures).and started to spread into the Mediterranean countries in the eighties, with the decisive role of the Associations through numerous courses, conferences and publications , from the eighties. This development resulted in the creation in 1996 at the Institute of Soil and Water Bioengineering in the University of Boku in Vienna of the European Federation for Soil and Water Bioengineering (E.F.I.B). In this paper we want to present the evolution of our discipline through the history of the European federation of Soil and Water Bioengineering

Keywords: Native plants, NBS solutions

Soil and Water Bioengineering in fluvial areas the Cantabrian basin within the EU Interreg Poctefa project H_2Ogurea (Navarra, Spain)

Sangalli Paola*[1],Tardio, Guillermo[2],Luis Sanz[3]
1 SCIA SL, EFIB, Spain
2 AEIP, Consultant engineer. Spain
3 Navarra Govern, Spain
*Corresponding Author, e-mail: sangalli@sangallipaisaje.com

Abstract

Execution of different Soil and Water Bioengineering techniques in the Cantabrian basin within the European Interreg Poctefa H2O Gurea project. The most relevant problem is the erosion of the margins, with different types of erosion near the inhabitant areas. Morphological changes have occurred due to the introduction in the fluvial system of transversal structures, that have produced modifications of the morpho dynamic behavior of the section. In the Baztan river and in the Bidasoa river various SWB Bioengineering solutions are applied during the project and a practical training workshop and a technical manual is held with the cooperation of the Specifically, the actions promote the recovery of the hydraulic section and the defense of the banks. In addition, the native riparian vegetation was reinforced, and some examples of alien vegetation were eliminated. Several techniques used like vegetated crib walls, brush matters, brush layers During the presentation, we want to present this and other successfully cases of the use of SWB techniques and their results after several years.

Keywords: Bank protection, H2O Gurea project, Crib wall

Ecosystem Kickstarter: affordable and sustainable erosion control for restoring desertification-prone agro-ecosystems

Teun A. Vogel*[1], Anton Pijl[2], Jantiene Baartman[3], Martine van der Ploeg[4]
1 Cambisol Environmental Consultancy, Wageningen, The Netherlands
2 Dept. of Land, Environment, Agriculture and Forestry, University of Padova, Legnaro (PD), Italy
3 Soil Physics and Land Management group, Wageningen University, Wageningen, The Netherlands
4 Hydrology and Quantitative Water Management group, Wageningen University, Wageningen, The Netherlands
*Corresponding Author, e-mail: teun@cambisol.com

Abstract

Worldwide, vast areas are subjected to land degradation with severe impacts on soil ecosystems and fertility. Although soil erosion is naturally part of the dynamics of healthy ecosystems, perturbations such as drought or extreme rainfall can trigger accelerated land degradation. This can lead to a desertification state through a positive feedback loop of nutrient removal, diminishing vegetation, and the loss of water storage capacity. We designed and tested an innovative low-cost erosion control measure, specifically aiming at reverting the process of desertification by offering a first kickstart to restore healthy ecosystems. By offering both soil stability and plant seeds, the Ecosystem Kickstarter provides an initial chance for sediment trapping, water storage, and pioneering vegetation. Soil consolidation is gradually taken over by the recovering ecosystem itself, as the fully biodegradable honey-comb structure of the Ecosystem Kickstarter becomes dissolved. Field experiments in Uganda and Kenya have shown a 79% reduction of erosion and 38% increase in soil water storage as a result of implementation, while its nature based design ensures a long-lasting impact. This innovation offers an affordable soil and water bioengineering solution to farmers in degraded areas, thanks to the use of low-cost material and transferable production techniques.

Keywords: Soil restoration, Nature based solutions, Erosion control, Innovation, Ecosystem recovery

Erosion processes and their spatial interactions within the large, complex gully systems in an experimental watershed of the Chinese Loess Plateau

Tongxin Zhu[1]
1 University of Minnesota-Duluth, Duluth, MN 55812, USA
*Corresponding Author, e-mail: Email: tzhu@d.umn.edu

Abstract

Gully erosion is of importance in sediment production and land degradation in many parts of the world, which has attracted an increasing number of studies over the past few decades. Most of the previous studies on gully erosion are focused on the measurement of gully growth rates and their controlling factors, sediment production and empirical modeling. There have been fewer studies on the erosion processes within gullies, and even less on the spatial interactions of different erosion processes. An understanding of the erosion processes within the gullies is the prerequisite to develop a process-based gully erosion model and to design effective measures for gully erosion control. In this study, a comprehensive investigation of erosion processes within the large gully systems was conducted in a semi-arid, complex-terrain watershed, Wangjiagou (WJG), on the Loess Plateau of China. A total of 704 gullies/ephemeral streams, 547 mass movements, and 967 tunnel inlets were identified in the field. In addition, more than 5000 soil shear strength measurements were taken in situ within the watershed. By using GIS, the spatial patterns of erosion processes and their interactions were analyzed. Furthermore, statistical analysis was conducted to analyze the relationships between gully erosion processes and their controlling factors. The results showed tunnel formation plays an important role in the development of headwater gullies and hillside gullies, but not in valleyside gullies and ephemeral stream channels. Although the types of mass movement are varied among different types of gullies, they all drastically reduce soil shear strength and thereby increase soil erodibility. The study results suggest that a combination of different measures, such as increasing vegetative cover on the gully sideslopes and bottoms, converting slopelands to terraces above gully edges as well as building check-dams at the outlet of gullies, may achieve optimal effectiveness in gully erosion control.

Keywords: Gully systems, Mass movement, Tunnel erosion, Spatial interaction, Loess Plateau

PlaNet – An international research network on plant-based solutions to mitigate climate-induced geo-hazards

Vittoria Capobianco*[1,2], Stine Olsen[1]
1 Natural Hazards, Norwegian Geotechnical Institute (NGI), Norway 2 Member of AIPIN (Italian Association of Naturalistic Engineering)
*Corresponding Author, e-mail: vittoria.capobianco@ngi.no

Abstract

The Norwegian Geotechnical Institute (NGI) coordinates PlaNet, and the network has 5 research organisations and 7 universities as initial core partners. PlaNet is multidisciplinary, encompassing a wide range of expertise areas, such as geotechnical engineering, hydrology, soil science, plant ecology, biodiversity, and agronomy. The objectives of PlaNet are to share research on how vegetation-based solutions can be used to mitigate climate changes, influence policy nationally, internationally prepare the grounds for a European policy to be adopted by future research programmes and to foster multidisciplinary and international research-exchange and facilitate participation of industry and entrepreneurs. This forum does not only benefit researchers but also provide the knowledge needed for policy makers, entrepreneurs and suppliers, and to the general public for education and information. Activities in the network include knowledge dissemination, through filming and distributing virtual laboratory/site tours to real case study sites where NBS have been implemented, to generate interest and enhance the impact of PlaNet beyond the "research" boundaries. As well as to promote the international presence of Norwegian PlaNet partners. Activities also include publishing articles in national and international professional journals and magazines. PlaNet contributes to encourage Norwegian researchers to participate more widely in, and exert greater influence on, global research on climate and the environment and it contributes to Norway gaining a leading position in Europe for development and use of nature-based solutions. It also contributes to strengthen the international relationship among Norwegian research institutes and universities developing expertise in different aspects of nature-based solutions. It promotes and supports research on vegetation-based solutions for mitigating climate- induced geohazards and contributes to the use of nature-based solutions and ecological restoration.

Keywords: Network, Nature-based solutions, Multidisciplinary thinking, Vegetation, Natural hazards

NBS and traditional erosion and landslide mitigation measures in LaRiMiT database: pooling of expert scores

Vittoria Capobianco*[1,2], Bjørn Kalsnes[1]
1 Natural Hazards, Norwegian Geotechnical Institute (NGI), Norway 2 Member of AIPIN (Italian Association of Naturalistic Engineering)
*Corresponding Author, e-mail: vittoria.capobianco@ngi.no

Abstract

Landslides represent one of the most common natural hazards worldwide. With the effect of climate change on the frequency and intensity of extreme weather events, climate-driven landslides are expected to become more frequent. Nature-based solutions (NBS) are "solutions supported by nature, that simultaneously provide environmental, social and economic benefits and help build resilience. NBS applied to landslide hazard mitigation are mostly soil bio-engineering practices, including vegetation and the use of natural materials, are sustainable techniques for managing erosion and mitigate shallow landslides. Selecting the most suitable measure is complicated by both technical and non-technical factors such as site-specific conditions, local knowledge and resources, socio-economic constraints, and environmental considerations. LaRiMiT (Landslide Risk Mitigation Toolbox) is a web-based database and user portal for identifying and selecting mitigation measures assisted by an embedded expert scoring system. This work presents the database of mitigation measures in LARIMIT, including newly implemented NBS, and then the framework used to collect, interpret and implement the expert's scoring of the mitigation measures available in LaRiMiT. An Analytic Hierarchy Process resident in the toolbox provides a ranked list of suitable mitigation measures for that specific case. The quantitative scores reflect the input relevance weights and option scores. The results from this first pooling are discussed and analyzed, and the scores of 56 measures were updated on the basis of the pooling answers. However, due to the small number of respondents so far, it was not possible to give a full statistical significance of the scores. LaRiMiT will be dynamically updated as more expertise becomes available.

Keywords: Web-toolbox, Nature-based solutions, Decision making, Mitigation measures, Soil bio-engineering

Is the runoff coefficient increasing or decreasing after ecological restoration on China's Loess Plateau?

Haiyan Zheng[1], Chiyuan Miao*[1], Guanghui Zhang[1], Xiaoyan Li[1], Shuai Wang[1], Jingwen Wu[1], Jiaojiao Gou[1]
1 Chiyuan Miao, State Key Laboratory of Earth Surface Processes and Resource Ecology, Faculty of Geographical Science, Beijing Normal University, Beijing 100875, China.
*Corresponding Author, e-mail: miaocy@vip.sina.com

Abstract

The "Grain for Green" project (GGP) was launched in 1999 on China's Loess Plateau to reduce soil erosion, which had far-reaching impacts on the local eco-hydrological processes. In this study, we use monthly runoff depth and precipitation datasets spanning 1961 to 2015 for 16 primary basins of the plateau to reveal changes in runoff generation capacity before and after the GGP. We use a Budyko-based elasticity method to calculate the runoff depth (R_1) and runoff coefficient (C_1) exclusively attributable to land use/cover change. Results indicate that the mean annual runoff coefficients (C_0) decline by 26%–76% from the periods 1961–1999 to 2000–2015. The annual observed runoff depth (R_0) and C_0 for 75% of basins show significant downward trends during 1961–1999; after implementation of the GGP, both annual R_0 and annual C_0 for over 50% of basins show upward trends. The study further finds that the increase of erosive rainfall during the period 2000–2015, whose mean increasing rate reaches 4.6 mm/year, is the main reason for upward trends of R_0 and C_0. After removing the effect of precipitation variation during this period, we find that 11 out of 16 basins show decreased trends for C_1, with the downward rate between 2.4% and 6.0% per year. The reduction rate in semi-arid areas is about four times the rate in semi-humid areas. The results remind us to consider the carrying capacity of local water resources when implementing the soil and water conservation measures across the Loess Plateau.

Keywords: Loess Plateau, Precipitation, Runoff coefficient, Budyko-based elasticity method, Land use/cover change

Remote sensing and field-based approach in understanding soil erosion mitigation through grass cover in steep vineyards

Eugenio Straffelini*[1], Anton Pijl[1], Stefan Otto[2], Enrico Marchesini[3], Simone Gottardi[3], Paolo Tarolli[1]
1 Department of Land, Environment, Agriculture and Forestry, University of Padova, Italy
2 National Research Council, Institute for Sustainable Plant Protection, Italy
3 Agrea s.r.l, Italy
*Corresponding Author, e-mail: eugenio.straffelini@unipd.it

Abstract

Steep viticulture is a common practice in the Mediterranean basin. These complex agricultural systems are very fragile and one of the main problems is soil erosion during extreme rainfall events. Also, soil compaction by mechanization, climate change and land abandonment worsen this condition. A common solution for soil erosion mitigation involves the use of grass cover. Indeed, it provides active protection from the kinetic energy of water droplets, reduces the surface runoff and increases the infiltration capacity of the soil, thus improving ecosystem services in the vineyard. This work aims to evaluate the effectiveness of different types of grass cover in reducing erosion and runoff generation in steep slope viticulture. To do this, a combined remote sensing/field-based approach is proposed. We collect and compare the water and sediment downstream of an experimental vineyard managed with different grass cover using specifically-designed collection boxes. We further analyse and simulate the erosion processes in a GIS environment using DEMs from UAV-SfM survey and the physical model SIMulated Water Erosion (SIMWE). The integrated techniques allow efficient mapping of erosion and deposition processes providing useful information to stakeholders for better soil and land use management.

Keywords: Vineyard, Soil erosion, UAV-SfM, DEM, Modelling

The Coupling Effects of Soil Internal and External Forces on Rainfall Splash Erosion

Jingfang Liu*[1,2], Feinan Hu*[1,2,3], Shiwei Zhao[1,2,3]
1 State Key Laboratory of Soil Erosion and Dryland Farming on the Loess Plateau, Northwest A&F University, Yangling, China;
2 College of Natural Resources and Environment, Northwest A&F University, Yangling, China;
3 Institute of Soil and Water Conservation, Chinese Academy of Sciences and Ministry of Water Resources, Yangling, China
*Corresponding Author, e-mail: hufn@nwafu.edu.cn

Abstract

Soil erosion is the number one threat to our planet's soils. Hence, clarifying the mechanism of rainfall splash erosion is very important for soil erosion prevention and environmental safety. Rainfall splash erosion mainly includes two processes: soil aggregate breakdown and soil fragment movement. Aggregate breakdown is the first key step of splash erosion. Recent studies have found that soil internal forces, such as electrostatic repulsive force, hydration repulsive force and van der Waals force, are the main intrinsic factors affecting the aggregates stability, thereby will certainly have an important impact on the splash erosion. However, the current research on the splash erosion mainly focuses on external forces such as raindrop impact force, and little is known about the effects of soil internal forces on splash erosion. Therefore, to investigate the effect of soil internal force on splash erosion, and gain the contribution of soil internal force to splash erosion, ethanol and electrolyte solution were used as rainfall material to determine the solo effect of raindrop impact force and the combined effect of internal force and raindrop impact force on splash erosion of Lou soil, separately. The results showed that: (1) with increasing soil net repulsive force, the mean weight diameter (MWD) decreased, and the splash erosion rate (SER) increased. SER had a negative linear relationship with MWD (R2=0.92), and a positive linear relationship with the < 0.15 mm fragment content (R2=0.93), which indicated that soil internal forces can influence splash erosion through its effect on the size distributions of fragments from aggregate breaking. (3) SER increased exponentially with the increase of rainfall kinetic energy, suggesting that splash erosion was also affected by the raindrops impact force. (4) The contribution rate of soil internal forces on splash erosion was > 65% at a low electrolyte concentration (< 10−2 mol L−1), indicating that internal forces exerted higher contribution to rainfall splash erosion than raindrop impact force under most field conditions. Our results suggesting that splash erosion could be due to the coupling effects of soil internal forces and the raindrop impact force. soil internal forces initiate soil aggregate breakdown and then releases of fine soil particles, supplying the original material for splash erosion. Furthermore, the raindrop impact force is the driving mechanism causing soil particle movement.

Keywords: Rainfall splash erosion, Electrostatic repulsive force, Hydration repulsive force, Van der Waals force, Raindrop impact force

Practical rainfall thersholds for separating non-reosive and erosive storms in the umbria region (Central Italy)

L. Vergni*[1], A. Vinci[1], Todisco[1]
1 Department of Agricultural, Food and Environmental Sciences, University of Perugia, Italy
*Corresponding Author, e-mail: lorenzo.vergni@unipg.it

Abstract

In this work, 522 rainfall events recorded at the Masse experimental site (central Italy), were analyzed to identify rainfall thresholds capable of classifying erosive and non-erosive events. The thresholds were derived solely from the 30-min hyetographs and describe both overall (e.g, total depth and duration) and pattern (e.g., number and depth of bursts) rainfall characteristics. The thresholds' performances were evaluated based on different accuracy measures. The thresholds obtained from the 30-min rainfall datasets were compared with those obtained in a previous analysis based on a 5-min dataset. Results indicate that the types of threshold providing the best accuracy based on the 5-min database are usually the best also working on the 30-minute data. Of course, larger threshold values are found passing from the shorter to the longer time resolution. The best 30-min thresholds identified at the Masse experimental station were therefore applied to seventeen stations of the Umbria region in the period 1999-2020 to analyze the spatial variability of the return periods associated with erosive events.

Keywords: Erosive event classification, Return period, Soil erosion risk

New quantitative geomorphometric approach to estimate soil volumes stored in agricultural terraces

Sara Cucchiaro[1,2*], Guido Paliaga[3], Daniel J. Fallu[4], Ben R. Pears[5], Kevin Walsh[6], Pengzhi Zhao[7], Kristof Van Oost[7], Lisa Snape[8], Andreas Lang[8], Antony G. Brown[4, 5], Paolo Tarolli[2]
1 Department of Agricultural, Food, Environmental and Animal Sciences, University of Udine, Italy
2 Department of Land, Environment, Agriculture and Forestry, University of Padova, Italy
3 Research Institute for Geo-Hydrological Protection, National Research Council, Italy
4 Natural Sciences, Tromso University Museum, Arctic University of Tromsø, Norway
5 Department of Geography and Environmental Science, University of Southampton, UK
6 Department of Archaeology, University of York, UK
7 Georges Lemaître Centre for Earth and Climate Research, Earth and Life Institute, UCLouvain, Belgium
8 Department of Geography and Geology, University of Salzburg, Austria
*Corresponding Author, e-mail: sara.cucchiaro@uniupd.it

Abstract

Geomorphometric information can be exploited to study the future preservation of agricultural terrace landforms in a world increasingly affected by anthropogenic activities. High-resolution topographic techniques allow the mapping and characterization of geomorphological features with wide-ranging perspectives through high-resolution Digital Terrain Models (DTMs). By using riser bases as well as terrace edges (riser tops) and through the computation of geomorphometric parameters, it is possible to obtain environmentally useful information on these agricultural systems such as terrace soil thickness and volumes. This work aims to realize and test an innovative and rapid methodological workflow to estimate the minimum anthropogenic reworked and moved soil of terrace systems. We mapped and extracted geomorphological features, from which the original theoretical slope-surface of terrace systems were derived. Differences between actual and theoretical terraces from DTM and excavation evidence have been used to estimate the minimum soil volumes and masses used to remould slopes. Moreover, geomorphometric analysis through indices such as sediment connectivity permitted also to quantify the volume of sediment transported downstream, with the associated and mobilized C, after a collapsed terrace. The quantification of terrace volumes can provide extremely useful benchmarks for soil erosion models and offer a measure of the effect of these agricultural systems on soil organic carbon (SOC) sequestration.

Keywords: Volume computation, Agricultural terrace systems, High-resolution topography, Geomorphological features

The changes of the structure and function in black soil after 16 years of conservation tillage

Jianye Li[1], Xingyi Zhang*[1]
1 Key Laboratory of Mollisols Agroecology, Northeast Institute of Geography and Agroecology, Chinese Academy of Sciences, Harbin 150081, China
*Corresponding Author, e-mail: zhangxy@iga.ac.cn

Abstract

The black soil region in Northeast China is one of the four largest black soil regions in the world. However, the black soil in Northeast China has been seriously degraded and its structure and function was deteriorated after long-term cultivation. This study took corn-soybean rotation black soil as the research object, set up 4 tillage treatments (conservation tillage: NT, RT; traditional tillage: MT, Rot), and explored the different growth periods of soybean (seedling stage: SS, flowering stage: FLS, filling stage: FiS, maturity stage: MS) The dynamic changes of soil bulk density, porosity, water status, and water-stable aggregate content in response to tillage methods. The results of the study showed that (1) Conservation tillage improved and stabilized the soil structure. During the whole growth period of soybean, the soil surface field capacity under NT treatment was 4.56% ~ 23.07% higher than that of traditional tillage. NT improves soil water infiltration, and the initial infiltration rate is 1.26 to 1.63 times that of other treatments. (2) Conservation tillage significantly increased the accumulation of soil surface organic carbon. The soil surface organic carbon content under NT treatment was 32.60%, 30.28% and 25.79% higher than MT, RT and Rot treatments, respectively. (3) No-tillage increases soybean production. In short, long-term conservation tillage significantly affects soil structure and organic carbon accumulation. This study can provide a theoretical basis for exploring the long-term effects of conservation tillage in the black soil area of Northeast China.

Keywords: Conservation tillage, Soil structure , Soil organic carbon, Crop yield, Growth Period

Variation of runoff and sediment in typical tributaries of the upper reaches of the Yangtze River and its influencing factors

Yin Chen*[1,2], Yangui Wang[1,2]
1 International Research and Training Centre on Erosion and Sedimentation, Beijing, China
2 China Institute of Water Resources and Hydropower Research, Beijing, China
*Corresponding Author, e-mail: 896178065@qq.com

Abstract

In recent years, the human activities are frequent in the Yangtze River, such as soil and water conservation, reservoir construction and river sand dredging. According to incomplete statistics, the cumulative amount of controlled soil loss area is 390 thousand km^2, and more than 90 large reservoirs have been built in the Yangtze River by the end of 2015. Human activities have caused the variation of runoff and sediment load in the Yangtze River, especially the average annual sediment production has greatly decreased. For example, the sediment discharge of Datong station has decreased from 5.04×10^8t in 1950s to 1.23×10^8t in the last decade (2006-2015), and it decreased by 75.79%. Runoff and sediment variation and their influence factors is one of the hot spots in hydrological science, but the research results are different because of the differences in methods and data, so it is necessary to do further research in this field.

Keywords: The upper Yangtze River, Silt trapping of reservoir, Soil and water conservation, Sediment transport modulus (STM)

Analysis on the influences of grazing and fencing on vegetation benefit of soil and water conservation in northern sandy region

Qiankun Guo*1, Shuangwu Yu1,2, Yuxuan Chen2, Yan Zhang2, Wei Qin1, Zhijie Shan1
1 China Institute of Water Resources and Hydropower Research, Beijing 100048, China
2 School of Soil and Water Conservation, Beijing Forestry University, Beijing 100083, China
*Corresponding Author, e-mail: guoqiankun@iwhr.com

Abstract

As one of the main erosion regions in China, the northern sandy region suffered from serious erosion caused by fragile natural environment and human disturbance, it is of great significance to quantitatively evaluate the ecological influences of grazing on the grassland, and the ecological benefits of soil conservation measures such as fencing. Therefore, a large number of literatures were collected for meta-analysis to explore the effects of grazing intensity, grazing period and fencing period on above-ground biomass and vegetation coverage in typical steppe and desert steppe. The results indicated: 1) in both desert steppe and typical steppe, the relative aboveground biomass and relative vegetation coverage decreased significantly with the increase of grazing intensity; 2)the negative effect of grazing period on the relative aboveground biomass is very significant; 3)in both desert steppe and typical steppe, the aboveground biomass and vegetation coverage increased significantly as the fencing period increases. These results illustrate the impact of grazing and fencing on the vegetation benefits of soil and water conservation in the northern sandy region. It also points out the shortcomings of the current research and the direction that should be paid more attention to.

Keywords: Northern sandy region; Fencing period, Grazing intensity, Grazing period, Aboveground biomass, Vegetation coverage

Height-diameter models for *Pinus sylvestris* var. *mongolica* sand-fixing plantations in Horqin Sandy Land, Northeast China

Fengyan Zhou[1], YanGang Han*[1,2,3]
1 Liaoning Technology University, China
2 CAS Key Laboratory of Forest Ecology and Management, Institute of Applied Ecology, Chinese Academy of Sciences, China
3 University of Chinese Academy of Sciences, China
*Corresponding Author, e-mail: hyghan@163.com

Abstract

Height-diameter (H-D) model is important in predicting forest dynamic. Nevertheless, the H-D models are still not available for *Pinus sylvestris* var. *mongolica* in "three north" shelterbelt plantations. In order to develop accurate height prediction model, we analyzed the H-D relationship using investigation data collected from *P. sylvestris* even-aged stands in Zhanggutai of Liaoning province. The original nonlinear least squares (OLS) and nonlinear mixed effects models with and without stand variables were employed to predict height. In addition, mixed-effects models were calibrated by different sampling designs and sampling sizes. In the selected stand variables, adding dominant height (DH) into H-D model significantly improved model prediction accuracy. The goodness-of-fit of OLS generalized model was obviously higher than OLS basic model. Inclusion of random effects improved the prediction accuracy. However, difference between generalized mixed-effects and generalized OLS H-D model was not obvious. Measuring two tree height randomly select from a plot is relative economical accurate for tree prediction using mixed effects models calibration. Our work can be used for height prediction of *P. sylvestris*, which needs low cost and have higher accuracy.

Keywords: Height-diameter, Mixed-effects model, Dominant height; Model calibration, *Pinus sylvestris* var. m*ongolica*

Ectomycorrhizal fungal characteristics of *Pinus sylvestris* var. *mongolica* and their effect on the seedlings

Guanglei Gao*[1,2], Mishan Guo[1,2]
1 Yanchi Research Station, School of Soil and Water Conservation, Beijing Forestry University, Beijing 100083, China
2 Key Laboratory of State Forestry and Grassland Administration on Soil and Water Conservation, Beijing Forestry University, Beijing 100083, China
*Corresponding Author, e-mail: gaoguanglei@bjfu.edu.cn

Abstract

Pinus sylvestris var. *mongolica*, a widely planted tree species, is facing long-lasting, unresolved degradation in desertified northern China. Ectomycorrhizal fungi (EMF) are closely related to the stand status, because they participate in ecological processes of terrestrial forest ecosystems. EMF may be key to solving the introduction recession. Therefore, we performed DNA sequencing of *P. sylvestris* root samples from plantations and natural forest as control to characterize the EMF from semi-arid and dry sub-humid regions, using ITS Illumina sequencing and conventional soil physicochemical index determination. The results indicated that (1) the dominant EMF genera were *Suillus*, *Rhizopogon*, and *Wilcoxina* in the Hulunbuir, Mu Us and Horqin Sandy Lands, respectively. Their dominance kept along the stand ageing. (2) Plantation EM fungal diversity differs significantly among the three sandy lands, and was significantly lower than in natural forest. The diversity varied along stand age with distinct trends at the local scale. (3) At the regional scale, the mean annual sunshine times and the soil organic carbon content affects EMF diversity. The community composition and structure were more characterized by temperature and precipitation. At the local scale, besides the soil organic carbon content, the EM fungal community composition and structure were correlated with total nitrogen and phosphorus content (Hulunbuir), the total phosphorus content (Mu Us), and the pH and total soil porosity (Horqin). The EM fungal community composition and structure have the obvious geographical distribution variation, they were strongly correlated with the meteorological elements and soil nutrients at the regional scale. At the local scale, they were jointly driven by stand age and soil properties. This improved information contributes to increased understanding of the interaction between EMF and forest ecosystems.

Keywords: *Pinus sylvestris* var. *mongolica*, Ectomycorrhizal fungi, Stand age, Soil properties

Forest Ecological Restoration: Lessons Learned from the Southern United States

Ge Sun*[1]
1 Eastern Forest Environmental Threat Assessment Center, Southern Research Station, USDA Forest Service, USA
*Corresponding Author, e-mail: Ge.Sun@usda.gov

Abstract

Ecosystem restoration is the process of assisting the recovery of an ecosystem that has been degraded, damaged, or destroyed. The US forest Service's national strategic plan calls "to sustain the health, diversity, and productivity of the nation's forests and grasslands to meet the needs of present and future generations." There are specific restoration needs: reducing the risk from catastrophic wildland fire, reducing the impacts from invasive species, and improving watershed conditions. Indeed, protecting forest resources and restoring degraded lands were the primary reasons for creating the Forest Service and establishing the national forests and grasslands in 1904. The Organic Act (1897), Weeks Act (1911), Multiple Use–Sustained Yield Act (1944), National Forest Management Act (1976), and other statutes governing the management of the national forests and grasslands provide legal foundations for forest restoration and protection. The Forest Service recommends 10 principles of restoration: 1) Seek and set goals for restoration only as societal choices; public involvement is key; 2) Make operational decisions at the lowest possible levels in an organization; 3) Consider the effects of restoration at local and landscape levels; 4) Give priority to restoring ecosystem processes, such as hydrologic pulses for rivers and streams or prescribed burning for fire-dependent ecosystems; 5) Establish objectives for the long term; 6). Recognize that ecosystems are dynamic, and that change is inevitable; avoid "static endpoint" thinking; 7) Use multiple sources of relevant information, such as historical records, scientific studies, practical experience, and indigenous knowledge; 8) Deal with uncertainty by using adaptive approaches to restoration; 9) Design and implement monitoring as part of restoration; 10) Learn as you go. The science of restoration is still emerging and application the principles emphasizes multiple spatial scales, integrating the ecological and social sciences, and restoring processes that provide for ecosystem health, integrity, and sustainability. Research is still needed on the processes leading to degradation, determining realistic goals and measures of success, developing methods for implementing the goals and incorporating them into land management and planning strategies, and monitoring the restoration to assess its success. This paper will review the history of forest restoration research efforts in the southern U.S such as reforestation for erosion control, water quality improvement, and forest hydrological vegetation manipulation experiments, and contemporary forest restoration efforts such as longleaf pine *(Pinus palustris)* and oak forest restoration under a changing climate.

Keywords: Ecological Restoration, Erosion Control, Forests

Considerations of Stream Restoration – A Case Study of a Coastal Creek in the San Francisco Bay Area

Guoyan Li*[1]
1 Water Resources Engineering, Stetson Engineers Inc., USA
*Corresponding Author, e-mail: GuoyuanLi@gmail.com

Abstract

This presentation talks about the policies, procedures, and challenges of the stream restoration projects in the west coast of the United States. An ongoing channel restoration project on a San Francisco Bay Area coastal creek is used as an example for this talk. The creek flows through an urbanized area before entering the San Francisco bay. The project is to remove parts of the downstream end of the Army Corps of Engineers concrete flood control channel to restore as much natural functioning aquatic, tidal, transitional, and riparian upland habitat as possible within site constraints, in a manner that is adaptive to future sea level rise. Policy considerations include the environmental regulatory permits, right-of-way, easements, and agreements. Procedures include the vegetation reconnaissance, ecological analysis, topographic and boundary survey, hydrologic and hydraulic modeling, geomorphic channel design, geotechnical investigation, and construction. Challenges include both the technical such as the potential sedimentation issue and political such as obtaining permits and agreements.

Keywords: Stream Restoration, Modeling, Design, Policy

Effects of soil microbial films on sand fixation and water retention characteristics of aeolian soils

Hongyu Cao[1,2,3], Yujia Du[1,2,3], Guanglei Gao*[1,2,3], Liangyi Rao[2,3], Lihua Chen[2,3], Guodong Ding[1,2,3], Ying Zhang[1,2,3], A Lasa[1,2,3], Zhenting Liu[2,3]

1 Yanchi Research Station, School of Soil and Water Conservation, Beijing Forestry University, Beijing 100083, China

2 Key Laboratory of State Forestry and Grassland Administration on Soil and Water Conservation, Beijing Forestry University, Beijing 100083, China

3 Engineering Research Center for Forestry Ecological Engineering, Ministry of Education, Beijing Forestry University, Beijing 100083, China

*Corresponding Author, e-mail: gaoguanglei@bjfu.edu.cn.

Abstract

In natural environment, soil microorganisms usually exist in the form of microbial aggregates rather than the free single microbial cell by secreting extracellular polymeric substances on the surface of soil particles, which are known as soil microbial films. More and more people are realizing that soil microbial films potentially contribute to the anti-erodibility and water retention improvement of aeolian soils. However, due to the mechanism of this improved process remains unclear, these knowledge gaps have been hindering soil microbial films to be an alternative for desertification combating. In this study, the controlled experiment was conducted in a greenhouse using the common aeolian soils and soil bacteria (*Bacillus subtilis* and *B. pumilus*). 6 microbial agents (0, 1, 3, 5, 7 and 10 g/kg) were involved to test various soil properties and to identify the ecological function of soil microbial films. The results indicated that 1) Soil microbial films were successfully and largely induced by the microbial agents. In this process, soil microbial biomass carbon, nitrogen and polysaccharide were 2.41%-8.82%, 0.79%-8.60%, and 13.25%-55.13% higher than control, respectively. 2) Soil porosity, soil moisture, soil aggregates, and soil pH were increasing significantly (P<0.05) affected by soil microbial films. 3) Soil polysaccharide was the most critical factor affecting aeolian soils with the highest interpretation rate (47%). In conclusion, soil microbial films effectively improve aeolian soils involving anti-erodibility and water retention. We highly recommended that the suitable microbial agents were 1-5 g/kg which can be optimized to alleviate and curb soil salinization. Our research provided a better understanding of the mechanism of soil microbial films affecting sand fixation and soil moisture, eventually and substantially contribute to a firm theoretical basis and scientific & technological support for the new technology exploration of desertification combating in a soil microbial approach.

Keywords: Soils, Sand consolidation, Microbial films, *Bacillus*; Extracellular polymeric substance, Aeolian soil, Water retention

Ecological restoration of water-level-fluctuation zone in Three Gorges Reservoir area

Liangyi Rao*[1,2], SiYuan Li[1]

1 School of Soil and Water Conservation, Beijing Forestry University, Beijing,P.R. China

2 Key Laboratory of State Forestry Administration on Soil and Water Conservation, Beijing Forestry University, Beijing 100083, P.R. China

* Corresponding Author, e-mail: raoliangyi@bjfu.edu.cn

Abstract:

The water-level fluctuation zone is formed by periodically storing water of reservoir. The original soil and vegetation have been seriously damaged due to the long-term impact of water and waves, leading to serious soil and water losses, which makes the ecological environment of the transitional zone very fragile. The fluctuation zone formed by the periodical drawdown and impoundment of the Three Gorges Reservoir is as high as 30 meters, thus adversely affecting the local ecological environment. Therefore, it is urgent to restore the ecosystem of the hydro-fluctuation belt in the Three Gorges Reservoir area, which is necessary for the sustainable development of the local society and economy. This paper aims to introduce the ecological environmental issues of the water-level fluctuation zone in the Three Gorges Reservoir area, the application of biological treatment technology, as well as the industrial mode of ecological restoration. We anticipate that our research could help better understand the environmental issues and provide practical experience and enlightenment on the restoration and sustainable management in the TGR area.

Keywords: Ecological restoration, Water-level fluctuation zone, Three Gorges Reservoir area

Pathways to persistence: plant root traits alter carbon accumulation in different soil carbon pools

Lorenzo M.W. Rossi*[1,2], Zhun Mao[1], Luis Merino-Martín[1,3], Catherine Roumet[3], Florian Fort[4], Olivier Taugourdeau[5], Hassan Boukcim[5], Stéphane Fourtier[1], Maria Del Rey-Granado[3], Tiphaine Chevallier[6], Rémi Cardinael[7,8,9], Nathalie Fromin[c], Alexia Stokes[1]

1 Univ Montpellier, AMAP, INRAE, CIRAD, CNRS, IRD, Montpellier, France
2 Department of agricultural and environmental science, Univ. degli studi di Milano, Milan, Italy
3 Univ Montpellier, CEFE, CNRS, EPHE, IRD, Univ Paul Valéry Montpellier 3, Montpellier, France
4 Univ Montpellier, CEFE, Montpellier SupAgro, CNRS, EPHE, IRD,Univ Paul Valéry Montpellier 3, Montpellier, France
5 Valorhiz, 1900, Boulevard de la Lironde PSIII, Parc Scientifique Agropolis F-34980 Montferrier sur Lez, France
6 Univ Montpellier, Eco&Sols, IRD, CIRAD, INRA, Montpellier SupAgro, Montpellier, France Eco&ols
7 CIRAD, UPR AIDA, Harare, Zimbabwe
8 Univ Montpellier, AIDA, CIRAD, Montpellier, France
9 University of Zimbabwe, Crop Science Department, Box MP167, Mt. Pleasant, Harare, Zimbabwe
*Corresponding Author, e-mail: lmw.rossi@gmail.com

Abstract

Soil C storage is a key component in a framework of climate change mitigation and, in the Anthropocene era, the highly disturbed and anthropized soils can play an important role as “carbon sponges. To efficiently use these embankments as “C sponges” is fundamental to select the best species for revegetation. For species selection, we propose an approach based on the use of root traits as indicators for C storage potential in terms of C quantity but also C quality, in terms of its stability in soil. Twelve herbaceous species were grown for 37 weeks in monocultures. Root elongation rate (RER) was measured throughout the experiment. At the end of the experiment, we determined morphological and chemical root traits, as well as substrate induced respiration (SIR) as a proxy for microbial activity. Carbon was measured in four different soil fractions, following particle-size and density fractionation. In N2-fixing Fabaceae species, root biomass, RER, root diameter, hemicellulose content and SIR, were all positively correlated with increased C in the coarse silt fraction. Root diameter and hemicellulose content were also negatively correlated with C in the POM fraction, that was greater under non N2-fixing Poaceae species, characterized by lignin-rich roots with a high carbon:nitrogen ratio that grew slowly. The accumulation of C in different soil pools was mediated by microbial activity. Our results show that root traits determine C input into different soil pools, mediated primarily by microbial activity, thus determining the fate of soil organic C, with N2-fixing species increasing the stable C in the MAOM fraction. We also highlight that C in different soil pools, and not only total soil organic C, should be reported in future studies to better understand its origin, fate and dynamics.

Keywords: Particulate organic matter, Mineral-associated organic matter, Carbon stabilization, Root traits, Geotechnical soils revegetation

Exploring heat- and drought-tolerant plants from the Southwest U.S.

Mengmeng Gu[1]

1 Department of Horticultural Sciences, Texas A&M AgriLife Extension Service, TAMU 2134, College Station, TX 77843, USA
*Corresponding Author, e-mail: mgu@tamu.edu

Abstract

The Southwest United States is known for its hot weather and drought conditions. There could be many days with temperatures over 38 °C. In recent years, the area has experienced record high temperatures. Many areas have annual precipitation less than 50cm. There are many unique plant germplasms in the Southwest U.S., which have adapted to the hot and dry conditions. Many plants, including trees, shrubs, perennials and annuals, have very high ornamental values and could be used for both ecological reclamation and landscape beautification.

Keywords: Aesthetics, Landscape plants

Remote sensing-based carbon and water data facilitates sustainable ecological restoration

Yongzhe Chen*[1,2], Xiaoming Feng[1,2], Bojie Fu[1,2]
1 State Key Laboratory of Urban and Regional Ecology, Research Center for Eco-Environmental Sciences, Chinese Academy of Sciences, Beijing, PR China
2 College of Resources and Environment, University of Chinese Academy of Sciences, Beijing, PR China
*Corresponding Author, e-mail: yongzhechen@126.com

Abstract
The changes in vegetation carbon stock, carbon sink and water availability has always been a major concern in assessing the benefits and sustainability of a restoration program, especially in cold or arid regions. We have developed several datasets on the temporal changes in carbon and water at global scale using remote sensing. The first is observational-based continuous irrigation water simulation, which revealed an increase in irrigation water consumption in arid regions around the world under climate warming and intensive farming, calling for a more sustainable water allocation between food production and natural environment. Second, we published a temporally-consistent global surface soil moisture dataset by calibrating and fusing multiple microwave-based retrievals, which can help monitor the long-term change in soil water availability, especially in relatively arid regions under vegetation restorations. Third, by spatially mapping the vegetation optimum growth temperature and maximum light use efficiency, we suggested an underestimation of gross primary production in arid and cold regions, indicating that the restorations' carbon benefits should be re-evaluated. Finally, by separating the climatic and anthropogenic effects on carbon flux, we discovered that ecological restoration played the leading role, while improved climatic after 2010 also supported an accelerated increase of carbon uptake in China.
Keywords: Remote sensing, Carbon, Water, Ecological restoration.

Ecological management technology in Pisha stone area of the Yellow River Basin

Zhenzhou Shen[1], Wenyi Yao[1], Liangyi Rao[2], Peiqing Xiao[1], Yan Wu[1], Jishan Yang[1]
1 Key Laboratory of Soil and Water Conservation on the Loess Plateau of Ministry of Water Resources, Yellow River Institute of Hydraulic Research, Zhengzhou 450003
2 School of soil and water conservation, Beijing Forestry University, Beijing 100083, China
*Corresponding Author, e-mail:wyyao@yrihr.com.cn

Abstract
The national strategy of ecological protection and high quality development of the Yellow River Basin points out that the Yellow River basin governance should adhere to the concept that green water and green mountains are golden mountains and silver mountains, and focus on strengthening ecological protection and governance, promoting the implementation of a number of major ecological protection, restoration and construction projects, among which the Pisha Sandstone Area in the middle reaches of the Yellow River is one of the areas that should focus on ecological comprehensive governance. Based on the analysis of the previous management theory and practice in Pisha Sandstone Area, this paper carried out the research and development of ecological comprehensive management technology in Pisha Sandstone area covered with sand, including slope top runoff high-efficiency storage and utilization technology, slope top economic forest fruit industry mode, block gravity erosion polymer grouting technology, slope anti erosion and promoting growth comprehensive management technology, channel flexible dam Pisha Sandstone modified material valley Through the research and development and integration of erosion control technology of the slope top and check dam, the ecological comprehensive management mode of the sand covered Pisha Sandstone Area was finally summarized: slope top ditch network vertical and horizontal water blocking, irrigation and grass mixing to improve efficiency; steep slope grouting consolidation, gentle slope protection with shrub and grass; ditch bottom modified material gufangtang dam irrigation and grass flexible dam; gully mouth Pisha Sandstone modified check dam, sediment detention, flood reduction and silting to increase efficiency, and the project was put into practice The model of comprehensive ecological management was tested and demonstrated. The comprehensive ecological management mode of Pisha Sandstone can provide strong technical support for ecological protection and high-quality development of the Yellow River Basin.
Keywords: Pisha stone Area, Comprehensive ecological management; Model

Spatio-temporal variation characteristics of soil organic carbon in the vegetation restoration area on the Loess Plateau

Zixu Jia*[1,2], Xiaoming Feng[1], Jiahao Ma[2]
1 State Key Laboratory of Urban and Regional Ecology, Research Center for Eco-Environmental Sciences, Chinese Academy of Sciences, Beijing, PR China
2 Chang'an University, Xi'an, PR China
*Corresponding Author, e-mail: 2020127019@chd.edu.cn

Abstract

Vegetation restoration and the construction of check-dams are important measures for soil and water conservation in the Loess Plateau, and are also important driving factors for the carbon cycle of the Loess Plateau. In this paper, WaTEM/SEDEM model was used to simulate the soil erosion, sedimentation, and siltation in the dam control area of the Loess Plateau in the 1980s, 1990s, 2000s, and 2010s. Through Meta-analysis and data integration method, a data set of surface soil organic carbon content in different periods of the Loess Plateau was constructed and spatio-temporal patterns of the effects of vegetation restoration and check-dams construction on soil organic carbon storage were discussed. The results showed that (1) soil erosion and sediment decreased by 19.8% and 15.8% from the 1980s to 2010s. Meanwhile, the amount of sediment deposition in the control area of check-dams was decreasing year by year, reaching the lowest value in the 2010s. Spatially, the areas with high erosion deposition amounts were mainly distributed in the southwest and east of the Loess Plateau, while the areas with low erosion deposition amounts were mainly distributed in the northwest of the Loess Plateau. (2) The organic carbon content in surface soil showed an increasing trend from the 1990s to 2010s but decreased from the south to north in space. (3) The effect of vegetation restoration on soil organic carbon storage increased in different times, and the carbon sinks in the 1990s, 2000s, and 2010s were 0.19 Tg yr^{-1}, 1.82 Tg $yr^{-1,}$ and 2.04 Tgyr^{-1}, respectively. The carbon sink effect of the check-dams first increased and then stabilized with the values being 0.66 Tg yr^{-1}, 1.19 Tg yr^{-1}, and 1.03 Tg yr^{-1} in the 1990s, 2000s, and 2010s, respectively. In the spacial domain, the areas where vegetation restoration significantly increased soil organic carbon storage were mainly distributed in the southwestern Loess Plateau, the northern Shanxi Basin of the Hekou-Tongguan section, the central and northern basins of the Shaanxi section, and the Lanzhou-Hekou section. The significant areas affected by organic carbon storage in the dam control area of the check-dams were mainly distributed in the southwest of the Loess Plateau, the Lanzhou-Hekou interval, the central watershed of the Hekou-Tongguan interval, the northern part of the Shanxi section, and the upper Fenhe River.

Keywords: Soil erosion, Vegetation restoration, Check-dams construction, Soil organic carbon storage

Advances on the ecological restoration of saline land

Qian Yue[1,2], Liangyi Rao*[1,2], Siyuan Li[1,2]
1 School of Soil and Water Conservation, Beijing Forestry University, Beijing,P.R. China
2 Key Laboratory of State Forestry Administration on Soil and Water Conservation, Beijing Forestry University, Beijing 100083, P.R. China
* Corresponding Author, e-mail: raoliangyi@bjfu.edu.cn

Abstract

As one of the major soil degradation threats occurring in the world, soil salinization has negatively affected soil characteristics and ecological functions. Human activities such as unreasonable irrigation measures in agriculture as well as climate change have played an important role in soil salinization. The ecological restoration of saline land has become a common concern around the world. According to the most recent literatures, this paper summarized the research methods on the dynamic changes of water and salt in saline lands, modeling, monitoring methods as well as key indicators for soil salinity. Furthermore, an overview of the ecological restoration technologies for salinization control is presented. Finally, the deficiencies in current research and key topics for the future saline soil hardness were pointed out.

Keywords: Saline land, Ecological restoration, Advances

Soil Moisture Variability in Newly Implemented Agricultural Bench Terraces in Tigray Region, Ethiopia

G Castelli*[1], S Mesfin[2], L A Almeida Oliveira[3], E Bresci[1], E Yazew[4]
1 Department of Agriculture, Food, Environment and Forestry (DAGRI), University of Florence, Italy
2 Department of Land Resource Management and Environmental Protection, Mekelle University, Ethiopia
3 Department of Agricultural Engineering (DEA), University Campus, Federal University of Viçosa, State of Minas Gerais, Brazil
4 Institute of Water and Environment, Mekelle University, Ethiopia
*Corresponding Author, e-mail: giulio.castelli@unifi.it

Abstract

The effectiveness of radical bench terracing in reducing drought risk is dependent on its correct implementation. However, it is still not clear how proper or improper terracing implementation can impact the landscape capacity of holding soil moisture. In addition to this, the spatial patterns of Soil Water Content (SWC) within the same terraced hillslope are understudied. The present work analyses the variability of SWC in four newly implemented terraced hillslopes in Tigray Region, Northern Ethiopia. In all sites, terraced areas show SWC significantly higher than non-terraced ones, with the lowest part of the terraced hillslope more humid than the others. A Multiple Linear Regression (MLR) analysis highlighted significant dependency of SWC from the date of sampling, the position in the terraced slope, and its significant positive correlation with the percent of Water Stable Aggregates (WSA). Since high soil disturbance can induce low soil aggregates stability, this result shows how low soil disturbance can significantly increase SWC of radical terraces. Overall, the results of the present study testify the good performances of bench terraces in Northern Ethiopia in terms of soil water conservation and can represent a guideline for informing future terracing implementation in some arid and semi-arid agricultural areas of the world.

Keywords: Drought risk, Dry stone walls, Terracing, Terracing implementation, Soil water content

Runoff and soil erosion after prescribed fire and mulching with fern in Mediterranean forests

Bruno Gianmarco Carrà[1], Giuseppe Bombino[1], Manuel Esteban Lucas-Borja*[2], Demetrio Antonio Zema[1]
1 Mediterranean University of Reggio Calabria, Department “AGRARIA”, Località Feo di Vito, I-89122 Reggio Calabria, Italy
2 Country Department of Agroforestry Technology and Science and Genetics, Campus Universitario s/n, E-02071, Albacete, Spain
*Corresponding Author, e-mail: ManuelEsteban.Lucas@uclm.es

Abstract

Prescribed fire is a valid tool to prevent damage by widlfires in Mediterranean forests. However, the soil left bare after burning may expose hillslopes to runoff and soil erosion in the short term. Mulching with straw has been widely experimented as soil conservation measure in the “window of disturbance” after fire. However, the use of straw can be expensive due to transport costs and furthermore may introduce alien species in forest . In contrast, fern is a native plant species and widely available inside in more humid forests locations. Until now, no experiences are found in literature about the hydrological effects of fern in Mediterranean forests. This study has evaluated surface runoff and soil erosion after prescribed fire in small plots installed in three forest stands (*Quercus frainetto*, *Pinus pinaster*, and *Castanea sativa*) of Southern Italy. Six plots were burned with low-intensity fire, of which three were treated with fern mulching; other three unburned plots were considered as control. Precipitation, runoff volumes and sediment concentrations were monitored throughout one year after fire (June 2019 - May 2020). For the seven erosive events measured in this monitoring period, in the burned plots runoff and erosion was higher compared to control up to October, and, subsequently, the hydrological response of the burned soil returned to the pre-fire level, except for the oak forest. In pine and chestnut stands, mulching was effective in reducing runoff and erosion of burned soils until the control values or slightly higher; in the oak forest, the pre-fire erosion rates was not recorded, but mulching was able to noticeably reduce soil loss due to fire.

Keywords: Hydrological monitoring, Soil loss, Low-intensity fire, Soil conservation practices

Eco-environmental effects of soil and water conservation measures in Northern Rocky Mountain area of China

Liangyi Rao*[1,2], Lei Gao[1]
1 School of Soil and Water Conservation, Beijing Forestry University, Beijing,P.R. China
2 Key Laboratory of State Forestry Administration on Soil and Water Conservation, Beijing Forestry University, Beijing 100083, P.R. China
* Corresponding Author, e-mail: raoliangyi@bjfu.edu.cn

Abstract

Eco-environmental effects of soil and water conservation have been highly paid attention in recent years. Based on the standard runoff plots observation data in Baima small watershed of Northern China, the runoff and sediment yield effects of soil and water conservation measures were studied. The results showed that the heavy rain and storm rain were the main rainfall types that could lead to soil and water losses in rocky mountain areas. Runoff yield of slop plots under moderate rainfall intensity and the high rainfall intensity accounted for up to 71.94%-73.60% of the total runoff respectively, while the sediment yield of that accounted for up to 80.78%-90.35% respectively. Bare land has the highest runoff and sediment yield under different rainfall intensity, and then the natural slope. While the runoff and sediment yield of arbor plot was lower than that of shrub and grass. Soil moisture of different slope runoff plots were basically identical, and there was a good consistency between soil moisture and rainfall variation. Shrub and arbor forest could effectively reduce runoff and sediment yield so as to control soil and water losses in this areas.

Keywords: Soil and water conservation measures, Eco-environmental effects, Northern Rocky Mountain area

A dynamic modeling framework of sediment trapping by check-dam networks: a case study of a typical watershed on the Chinese Loess Plateau

Pengcheng Sun*[1,2], Yiping Wu[1]
1 Department of Earth & Environmental Science, Xi'an Jiaotong University, Xi'an, Shaanxi Province, 710049, China
2 Yellow River Institute of Hydraulic Research, Yellow River Conservancy Commission
*Corresponding Author, e-mail: sunpech@163.com

Abstract

Check dam construction is one of the most effective and popular methods for sediment trapping in the Yellow River Basin and other places of the world prone to severe soil erosion. Quantitative estimation of the dynamic sediment trapping by check dams is necessary for evaluating the effects of check dams and for planning new check dams as well. In this study, we proposed a new framework, SWAT-DCDam (Soil and Water Assessment Tool-Dynamic Check Dam), for modeling sediment deposition caused by check dams dynamically by integrating the widely-used SWAT model and a newly developed module, DCDam. We then applied this framework to a typical loess watershed, the YanRB (Yan River Basin), to assess the time-varying effects of check dam networks along past 60 years (1957-2016). The DCDam module generates a specific check dam network to conceptualize the complex connections at each time step (monthly), and streamflow and sediment load simulated by the SWAT model were used to force the sediment routing in the check dam network. The evaluation results showed that the SWAT-DCDam framework performed satisfactorily in simulating sediment trapped by check dams when compared to the field survey of sediment deposition. In the YanRB, our study suggested that the designed structural parameters of check dams have evolved during the past 60 years, with higher dam but smaller controlled area in recent years. Sediment trapped by check dams increased with the intensity of soil erosion, but their relationship varied in different time periods. Further, annual amount of sediment deposition increased with the available storage, and their relationship is clearer when the available storage is less than 115×10^6 m^3, which may be a critical storage for the YanRB, and sediment trapped by check dams could be restricted when the available storage is below the critical level. Besides, our simulation results showed that more than 75% check dams in the YanRB are almost full, indicating the demand for new check dams in this watershed. In brief, our developed framework can be a promising tool for check-dam effects study, and the study can provide valuable information and support to decision making for soil and water conservation and check dam planning and management.

Keywords: Check dams, Dynamic Check Dam (DCDam), Loess Plateau, Sediment trapping, SWAT

Study on Interface Shear Characteristics between Polyurethane Treated Pisha Sandstone and Original Pisha Sandstone under Dry-Wet Cycles

Xuan Zhou*[1], Caiqian Yang[1,2], Zhishui Liang[2], Wenbo Ma[1]
1 College of Civil Engineering and Mechanics, Xiangtan University, Xiangtan, Hunan 411105, China
2 College of Civil Engineering, Southeast University, Nanjing, Jiangsu 211189, China
*Corresponding Author, e-mail: mawenbo@xtu.edu.cn

Abstract

Currently utilization of hydrophilic polyurethane (W-OH) materials for slope protection in arid areas has proved to be a cost-effective protocol. The treatment effect highly depends on the interface performance between the W-OH treated Pisha sandstone and the original sandstone. This study aims to investigate the shear characteristics between the Polyurethane treated Pisha sandstone and the original Pisha sandstone and its durability under dry-wet cycles in the arid area. The results from the direct shear test indicate the interface shear strength increases with the increase of W-OH solution concentration and decreases with the increase of water content of the original Pisha sandstone. Further investigations under dry-wet cycles indicate the interface cohesion is obviously deteriorated by the dry-wet cycles, while the influence on the internal friction angle is not obvious. The correlation between the degradation level and the dry-wet cycles can be well fitted with the "S" curve using two combined exponential functions. Furthermore, the EVA content is utilized to enhance the interface cohesion and the resistance to dry-wet cycles. It is found the EVA can not only improve the bonding property and the resistance to dry-wet cycles. The shear zone after dry-wet cycles will become much flatter with the EVA modification. The results of this study can serve as solid base for the application of W-OH materials in the arid region.

Keywords: W-OH polyurethane, Pisha sandstone slope, Dry-wet cycles, Direct shear test; Interface strength, Ethylene-vinyl acetate (EVA)

Effect of municipal sludge on soil improvement and plant growth of weathered Pisha sandstone

Zhishui Liang*[1], Haiying Gao[1], Haowei Liu , Yanbing Zhao[1], Zhiren Wu[2]
1. School of Civil Engineering, Southeast University, Nanjing 210002, China
2 School of the Environment and Safety Engineering, Jiangsu University, Zhenjiang 212013, China
*Corresponding Author, e-mail: zs_liang@seu.edu.cn

Abstract

The special property of Pisha sandstone and vegetation degradation are the main reasons causing the serious soil erosion in Pisha sandstone area. Pisha sandstone is easily to be eroded by water and changes into mud and small particle. However, it consist little organics and nutrients, leading to the land degradation and decreased vegetation coverage. So far, serval measures have been tried to protect the Pisha sandstone slopes and improve the weathered or eroded Pisha sandstone, and some of them have achieved a good result and the Pisha sandstone has been recourse utilization. Additionally, based on the high organic content in the municipal sludge, it can be used in land utilization to improve soil fertility. Therefore, it is used to improve the characteristics of weathered Pisha sandstone, making it suitable for vegetation growth. In order to study the improvement effect of sludge on weathered Pisha sandstone soil, the municipal sludge from the sewage treatment plant was mixed with weathered Pisha sandstone, and the improvement effect was evaluated by the changes of its physical and chemical indexes and fertility levels. After selecting the appropriate sludge addition amount, the pot experiment was used to study the effect of different mixed soils on plant biomass. The results showed that: (1) The addition of sludge can effectively improve the physical and chemical properties of the weathered sandstone soil and its fertility level, and the sludge addition amount of 10% is the most suitable; (2) In the pot experiment, the fresh weight, dry weight and plant height of the plants growing on improved Pisha sandstone were all ameliorated comparing with the plants on the weathered Pisha sandstone, in which the biomass of Alfalfa and Elymus growing in the mixed soil of 10% sludge was the largest, but the Sweet clover grew best in the mixed soil of 5% sludge. The research results will provide new ideas for soil improvement and vegetation restoration in Pisha sandstone area.

Keywords: Pisha sandstone, Land application of sludge, Pot experiments, Soil improvement

Ecological rehabilitation practice of production and construction projects in ecologically fragile area——Taking the construction of Qinghai Tibet ± 400kV DC Power Transmission Interconnection Project as an example

Jing Huang*[1], Xinxin Hou[1]
1 Key Laboratory of Soil and Water Conservation on the Loess Plateau of Ministry of Water Resources, Yellow River Institute of Hydraulic Research, China
*Corresponding Author, e-mail:huangjing_hky@163.com

Abstract

Ecological rehabilitation in ecologically fragile areas is an important part of the 14th Five-Year Plan. The Qinghai-Tibet Plateau is characterized by high and cold terrain, harsh climate, harsh natural conditions, sparse vegetation, and obvious soil erosion phenomena such as wind erosion, water erosion, frost erosion, etc. Moreover, the construction of production and construction projects is likely to destroy the surrounding ecological environment. It is too difficult to ecological rehabilitation in ecologically fragile areas. Taking Qinghai ~ Tibet ±400kV DC power transmission interconnection project as an example, this paper investigated and analyzed the impact of temporary protection of soil and water conservation, plant measures and engineering measures on ecological rehabilitation in the process of project construction, and discussed the ecological rehabilitation schemes of production and construction projects in the ecologically fragile area.

Keywords: Ecologically fragile area, Ecological rehabilitation, Production and construction projects

Spatio-temporal variability and driving factors of urban household water consumption in arid and semi-arid areas of Northwest China

Lin Li[1], Xiaohu Dang[1,*], Liangxin Fan[2], Peng Li[3], Xiaoshu Cao[4], Jiaxin Tian[1]
1 College of Geology and Environment, Xi'an University of Science and Technology, Xi'an 710054, China
2 Research Centre of Arable Land Protection and Urban-Rural High-Quality Development of Yellow River Basin, Henan Polytechnic University, Jiaozuo, Henan, 454003, China
3 State Key Laboratory of Eco-hydraulics in Northwest Arid Region of China, Xi'an University of Technology, Xi'an 710048, China
4. Academy of Natural Resources and Territorial Space, Shaanxi Normal University, Xi'an 710062, China
*Corresponding Author, e-mail: 1004149699@qq.com

Abstract

Given increasing water demand, cities in arid and semi-arid areas are facing increasingly severe water scarcity in China. Understanding the spatio-temporal pattern of water consumption and its socio-economic drivers is of importance to alleviate urban water crisis in arid and semi-arid areas. In this study, influencing factors of water consumption in 42 cities in Northwest China were identified by cluster tree analysis and multivariate regression. Results showed that from 2000 to 2017, the per capita domestic water consumption in Northwest China decreased by 9.5%. 17 cities out of 42 cities were low water consumption cities (<100L/d), 12 cities of which had changed significantly (8 increased cities and 4 decreased cities); 14 cities were high-consumption cities (>190L/d), 6 cities of which had changed significantly (5 increased cities and 1 decreased city); and remains were medium water-consumed. Daily water consumption per capita was found positively correlated with household income, water supply capacity, and built-up area, and negatively correlated urban population, people engaging in social services, and water saving and reuse efficiency. Among the high water-consumed cities, the expansion of built-up area is the main factor that causes high water consumption; and in low and medium water-consumed cities, residential water use is restricted by water supply and household income. The findings of this work suggested that improving water-use efficiency in high-water-consumed cities and increasing water supply capacity in low-water-consumed cities should be considered in urban water management strategies in Northwest China.

Keywords: Urban water use; Socio-economic driver; Cluster analysis; Water resource management; Arid and semi-arid area

Sediment connectivity and natural disturbances: insights from two Chilean study cases

L Martini*[1], L Picco[1,2,3], A Iroumé[4], M Cavalli[5]
1 Department of Land, Environment, Agriculture and Forestry, Italy
2 Universidad Austral de Chile, Faculty of Engineering, Chile
3 Universidad Austral de Chile, RINA – Natural and Anthropogenic Risks Research Center, Chile
4 Universidad Austral de Chile, Faculty of Forest Sciences and Natural Resources, Chile
5 National Research Council, Research Institute for Geo-Hydrological Protection, Italy
*Corresponding Author, e-mail: lorenzo.martini.2@phd.unipd.it

Abstract

Chile is often affected by wildfires and volcanic eruptions that are capable of disrupting an entire catchment, affecting the forest cover, increasing the runoff, sediment availability and mobilization. The Rio Toro (18 km^2) and the Rio Blanco catchment (70 km^2) were affected by two wildfires and volcanic eruption, respectively. To study the variation in sediment transfer pathways after these disturbances, the Index of Connectivity (IC) is used to investigate the potential role of land cover changes on sediment connectivity. To represent impedance to sediment fluxes, i.e. the W factor in the IC formula, the Manning's n was used and applied thanks to a combination of field surveys, remote sensing products and indices. The results show that the IC increased after both disturbances due to a massive reduction in forest cover. However, in both areas two main constraints prevent sediment to be transferred downstream: in the Rio Blanco catchment the flat and wide valley bottom prevents the transfer of sediment fluxes from the hillslopes to the outlet; in the Rio Toro the fast forest recolonization reduced the variation in sediment connectivity after the wildfires. The IC has proven a useful tool to investigate the effect of natural disturbances and to provide the basis for predicting evolutionary scenarios.

Keywords: Chile, Disturbances, Catchment, Connectivity, Sediment

Diverse flood magnitude in an alpine watershed: evidence of responses over different spatial and temporal scales

Riccardo Rainato*[1], Giacomo Pellegrini[1], Lorenzo Martini[1], Lorenzo Picco[1,2,3]
1 Department of Land, Environment, Agriculture and Forestry, University of Padova, Italy
2 Universidad Austral de Chile, Faculty of Engineering, Chile
3 Universidad Austral de Chile, RINA – Natural and Anthropogenic Risks Research Center, Chile
*Corresponding Author, e-mail: riccardo.rainato@unipd.it

Abstract

A sustainable watershed management cannot be separated from an accurate evaluation of the basin responses to flood events. In this sense, an appropriate management of the hydrological and geomorphic processes should be based on a good understanding of how they can change according to different floods magnitudes. The achievement of such an understanding is particularly difficult in mountain basin due to their high complexity. An evidence of this is given by the fact that, in literature, few studies analyzed the effect induced by flood events in small mountain watersheds, especially when considering direct field-data collection. This work investigated over three decades of water and sediment fluxes measured by the long-lasting monitoring program of the Rio Cordon basin (5 km^2, Northeast Italy). Thirty-three flood events were analyzed, permitting to highlight how they act on different temporal and spatial scales, depending on their magnitude. Large and infrequent events (RI > 30 y) accentuated the erosion processes over the entire basin, inducing observable long-term effects. Interestingly, also under-bankfull floods produced disturbances, which were detected at lower spatial and temporal scales.

Keywords: Mountain basin, Field data, sediment fluxes, Large flood, Under-bankfull event

Spatial temporal evolution pattern and driving mechanism of soil erosion in the Yellow River Basin based on LMDI model and Geodetector

Hongwei Wu[1], Cuixia Wei[1], Bing Guo*[1]
1 School of Civil Architectural Engineering, Shandong University of Technology, Zibo 255000, Shandong, China
*Corresponding Author, e-mail: guobingjl@163.com

Abstract

Under the influences of global change, soil erosion in the Yellow River Basin has changed dramatically. However, it is a significant challenge to analyze the impacts of climate vegetation and land use as well as their combined effects on soil erosion. Based on RUSLE model and multi-source data, this study aims to retrieve the annual soil erosion modulus of the Yellow River Basin, and use LMDI model and geographic detector to identify the dominant driving factors of soil erosion evolution in different historical periods and regions at pixel scale and landscape scale. Results showed that: (1) In recent 40 years, the average soil erosion was 2,255 $t \cdot km^{-1} \cdot a^{-1}$, which belonged to mild erosion. The serious (intensive, extreme intensive and severe) erosion areas are mainly distributed in the Loess Plateau, while the slight and mild erosion areas are mainly distributed in the Hetao Plain, Ordos Plateau, Ningxia plain and Guanzhong Plain; (2) In the last 40 years, the soil erosion modulus of Loess Plateau has a decreasing trend, mainly manifested in the area of stability and reduction area in the study area is 78.63%. During the study period, the gravity center of soil erosion moved from southwest to northeast, which indicated that the increment and increasing rate of soil erosion in the northeast of the Yellow River Basin were higher than that of the southwestern areas; (3) During the past 40 years, the increased soil erosion due to the R factor (ISER) was the most widely distributed, accounting for 79.21% of the area where soil erosion increased, while the decreased soil erosion due to the C factor and the R factor was the most widely distributed, accounting for 49.15% of the area where soil erosion decreased； (4) Before 2000, precipitation, vegetation and soil types were the dominant factors affecting the evolution pattern of soil erosion in the study area. With the increase of human activities, such as returning farmland to forest or grassland, the explanatory power of land use change in the evolution pattern of soil erosion was increasing. The research results can provide important decision support for the control of soil erosion in the Yellow River Basin.

Keywords: Soil erosion, Evolution pattern, LMDI model, Geographic detector, Driving mechanism

Multi-temporal modeling of road-induced overland flow alterations in a terraced landscape characterized by shallow landslides

Luca Mauri*[1], Eugenio Straffelini[1], Paolo Tarolli[1]
1 Department of Land, Environment, Agriculture and Forestry, University of Padova, Legnaro (PD)
*Corresponding Author, e-mail: luca.mauri.2@phd.unipd.it

Abstract

The presence of roads in high steep agricultural systems is associated with landslides occurrence. The aim of this research is to propose a multi-temporal modeling of road induced overland flows changes in a terraced vineyard affected by shallow landslides. The combined use of Uncrewed Aerial Vehicles (UAV) and photogrammetric techniques (e.g. Structure from Motion; SfM) allowed to elaborate multi-temporal (4D) high-resolution Digital Elevation Models. Hydrological analyses of water flow's depth alterations due to the road presence were performed adopting the SIMulated Water Erosion model (SIMWE), focusing on different scenarios considering the presence of the road and assuming its absence trough DEM smoothing procedures. The computation of 4D hydrological simulations at hillslope scale in the investigation of roads role in water flows alterations is still a challenge to be deeply investigated. Results proved the role played by the road in water overland flows alterations above the two observed shallow landslides. No-road simulations not revealed significant water deviations towards landslide zones, underlining that the absence of the road network would avoid relevant changes in water flow paths toward the collapsed surfaces. This work could be a solid starting point for similar analysis at wider scales and for planning mitigation interventions able to reduce the occurrence of similar future scenarios.

Keywords: Terraced landscape, Road, Landslide, Remote sensing, DEM

Remote sensing, field data to describe and monitoring the impacts and the ongoing processes of a large natural disturbance

Giacomo Pellegrini*[1], Lorenzo Martini[1], Riccardo Rainato[1], Luca Mao[2,3], Lorenzo Picco[1,4,5]
1 Department of Land, Environment, Agriculture and Forestry, University of Padova, Italy
2 School of Geography and Lincoln Centre for Water and Planetary Health, University of Lincoln, UK
3 Instituto de Geografía, Pontificia Universidad Católica de Chile, Chile
4 Universidad Austral de Chile, Faculty of Engineering, Chile
5 Universidad Austral de Chile, RINA – Natural and Anthropogenic Risks Research Center, Chile
*Corresponding Author, e-mail: giacomo.pellegrini@phd.unipd.it

Abstract

Remote sensing is a valuable tool to investigate land degradation and the impacts of natural disturbances in the environment. This work focuses on the Vaia storm (October 2018), a high-magnitude/low-frequency event that has severely impacted most northeast Italian Alpine catchments. In this context, the exploitation of LiDAR-derived products such as Digital Terrain Models and ortophotos, allowed i) a reliable detection of the hillslope instabilities (i.e. landslides, debris flows and windthrows) and ii) the application of a new integrated IC (Index of connectivity)-DoD (Dem of Difference) approach to identify the sediment routing and to estimate the volume of the eroded and deposited sediment along two Italian mountain basins. Furthermore, the site-specific monitoring of suspended sediment transport (using multiparameter sonde) allowed to infer the long-term cascading processes following a large infrequent disturbance. Preliminary results show different responses between areas affected and not affected by the event, and further analysis to cover different type of flood events (i.e. snowmelt, summer-autumn storms) are ongoing.

Keywords: Vaia storm, Mountain catchment, Remote sensing, Suspended Sediment

Understanding the challenge of terrace failure from an aerial vs. a field perspective

Anton Pijl[1], Edoardo Quarella[1], Teun A. Vogel[2], Vincenzo d'Agostino[1], Paolo Tarolli*[1]
1 Dept. of Land, Environment, Agriculture and Forestry, University of Padova, Legnaro (PD), Italy
2 Cambisol Environmental Consultancy, Wageningen, The Netherlands
*Corresponding Author, e-mail: paolo.tarolli@unipd.it

Abstract

While terraces are generally favourable for mitigating land degradation on cultivated hillslopes, several factors can trigger terrace failure. Growing rainfall aggressiveness in many parts of the world is challenging terrace stability, but also the specific design of a terraced plot can strongly induce surface flow accumulation in critical sections. In this work, we studied the possible causes of several observed terrace failures in a north-Italian vineyard, comparing two distinct methodologies. Firstly, we mapped the spatial distribution of soil moisture content (SMC) through multi-temporal field surveys under wet and dry conditions using Time Domain Reflectometry (TDR). Secondly, we performed an Uncrewed Aerial Vehicle (UAV) survey to obtain a high-resolution topographic model, serving as input for terrain-based and physical flow simulations. Either approach revealed valuable information that allows an understanding of the terrace failure phenomenon. The field-based survey provided a novel indication of terraces at risk, while the remote sensing survey clearly indicated the upstream formation of preferential pathways in the vineyard, constituting the terrace failure downstream. This case study holds a wider relevance for other terraced landscapes around the world, by illustrating the merits and limitations of methods tested, while also providing key insights for mitigating land degradation processes in this context.

Keywords: Agricultural terraces, Soil moisture, Remote sensing, Physical modelling, Land degradation

At-many-stations hydraulic-geometry for six major rivers originated from the Qinghai-Tibet Plateau

Chao Qin*[1], Baosheng Wu[1], Guangqian Wang[1], Ge Wang[1]
1 State Key Laboratory of Hydroscience and Engineering, Tsinghua University, PR China
*Corresponding Author, e-mail: glqinchao@nwsuaf.edu.cn

Abstract

At-many-stations hydraulic geometry (AMHG) has provided a novel way to understand river network development, simulate water flow and retrieve river discharge in data-scared regions. Based on in-situ measurements of six major rivers originating from the Qinghai-Tibet Plateau (QTP), this study verifies the existence of AMHG relations along the rivers and explores AMHG relations for cross sections that are not located in the same river reach. The mainstreams and tributaries of the studied rivers in the southern and the eastern portions of the QTP have satisfactory AMHG relation strengths with $R^2 > 0.9$ for over 60% of the relations. For cross sections located in the same stream order, approximately 60% (9/15) and 53% (8/15) of the AMHG relations have an $R^2 > 0.6$. AMHG strength increases with increasing stream order; this finding reflects the increasing coherence and maturity of the river networks associated with the geomorphic shaping power of increased discharge. Width-AMHG intercepts are larger than those of depth- and velocity-AMHGs for all stream orders. Most of the congruent hydraulics generated from cross sections located in middle-scale rivers (orders 7-8) are within the observed range. Congruent hydraulics generally increase with an increase in in-situ measured hydraulics when the stream order increases. The AMHG relations existing among cross sections that are not located in the same reach, which is named as cross channel AMHG, indicate linear variability of cross-sectional geometric and hydraulic similarities in the same stream order. The results break the watershed divide boundary control on AMHG and have the potential to provide background knowledge for discharge estimation in mountain rivers located in the QTP.

Keywords: Cross channel AMHG, River networks, Stream order, Qinghai-Tibet Plateau, Yarlung Zangbo River, Lantsang River

Changes in runoff energy, surface landform and sediment yielding during the bank gully erosion process in Dry-hot Valley Region, Southwest China

Donghong Xiong[1], Baojun Zhang[1]
1 Key Laboratory of Mountain Hazards & Earth Surface Processes, Institute of Mountain Hazards & Environment, Chinese Academy of Sciences, Chengdu 610041, China
*Corresponding Author, e-mail: dhxiong@imde.ac.cn

Abstract

Gully erosion is one of the major contributors to severe land degradation in the Yuanmou Dry-hot Valley Region, Southwest China. To quantify the changes in flow energy, sediment yield and surface landform impacted by headcut height during bank gully erosion, five experimental platforms were constructed with different headcut heights ranging from 25 to 125cm within an in situ active bank gully head. A series of scouring experiments were conducted under concentrated flow and the changes in flow energy, sediment yield and surface landform were observed. The results showed that great energy consumption occurred at gully head compared to the upstream area and gully bed. The flow energy consumption at gully heads and their contribution rates increased significantly with headcut height. Gully headcuts also contributed more sediment yield than the upstream area. The mean sediment concentrations at the outlet of plots were 2.3 to 7.3 times greater than those at the end of upstream area. Soil loss volume at gully heads and their contribution rates also increased with headcut height significantly. Furthermore, as headcut height increased, the retreat distance of gully heads increased, which was 1.7 to 8.9 times and 1.1 to 3.2 times greater than the incision depth of upstream area and gully beds. Positive correlations were found between energy consumption and soil loss, indicating that energy consumption could be used to estimate soil loss of headcut erosion. Headcut height had a significant impact on flow energy consumption, and thus influenced the changes in sediment yield and landform during the process of gully headcut erosion. Headcut height was one of the important factors for gully erosion control in this region. Further studies are needed to identify the role of headcut height under a wide condition.

Keywords: Flow energy consumption, Sediment yield, Surface landform change, Bank gully erosion, Dry-hot Valley region

The distribution and intensity of gully erosion in Hengduan Mountain area based on the Google Earth Images

Yifan Dong*[1], Xingwu Duan[1], Yong Nie[2], Shuxian Cheng[1], Ji Yang[1], Donghong Xiong[2]
1 Institute of International Rivers and Eco-Security, Yunnan University, Kunming, 650091, PR China
2 Key Laboratory of Mountain Hazards& Surface Process, Institute of Mountain Hazards and Environment, Chinese Academy of Sciences, Chengdu, 610041, PR China
*Corresponding Author, e-mail:yifan@ynu.edu.cn

Abstract

Gully erosion was one of the key processes of soil erosion in Hengduan mountain area, which belonged to the eastern part of Qinghai-Tibet Plateau with dramatic changes in both horizontal and vertical direction. The aims of this study were to investigate the gully distribution and density in Hengduan mountain area, and find out the key factors that influenced the susceptibility and intensity of gully erosion in different regions of Hengduan mountain area. Totally 2242 investigation quadrats were randomly set with the size of 1 km × 1 km to check whether the occurrence and the density by Google Earth images. The ratio of gully occurrence (GR) was 25.5%, and the average gully density (GD) and gully number (GN) was 2.20 km km^{-2} and 20.38 of Hengduan mountain area. The gully prone to distributed in the sites with lower annual precipitation and higher land surface temperature (LST), and the gully density clearly influenced by the vegetation cover (NDVI). There were 65.1% of the Q_{eg} were located in the grassland. The dry red soil, cinnamon soil and dark felty soils were observed high susceptibility of gully erosion, but the average GD of dark felty soils sites were smaller than the average GD of Hengduan mountain area, which was significant different with that in dry red soil and cinnamon soil sites.

Keywords: Gully erosion, Google Earth, Hengduan mountain area

Changing Land Management Institution and Its Effect on the Development of Gully Erosion in Black Soil Area of Northeast China

Jiuchun Yang*[1], Shuwen Zhang[1], Liping Chang[1]
1 Northeast Institute of Geography and Agro-Ecology, Chinese Academy of Sciences, China
*Corresponding Author, e-mail: yangjiuchun@iga.ac.cn

Abstract

Land management institution is the integral human decision made based on assessing quantitatively land system change and its ecological effects, which is prerequisite to understand and propose sustainable land management strategies. The evolution process of land management institution, experienced army-owned farms (A1) and collectively owned People's Commune (B1) (1947-1956), to state-owned farms (A2) (after 1956) and household contract responsibility system (B2) (after 1978), to the farmer specialized cooperatives (B3) (after 2006), which could be reflected by the types of farmers. The boundary of army owned and state-owned farms were delineated based on the thematic map. Other region outside the farms was tilled by individual farmers. The gully data in the study area were extracted by interactive human-machine interpretation method, based on remote sensed images of the Corona images centered the year of 1965 with spatial resolution of about 3m, Spot5 images centered the year of 2005 with spatial resolution of 5m and GF-1 images with 2m spatial resolution obtained in 2015. Through the analysis with comparing the number, speed and erode area of gullies developed respectively under the institutions of A and B, the results showed that erosion gullies increased during the period of 1965- 2005. The increasing speed of number, length and erode area of gullies under B was 5.25, 6.77 and 12.8 times of those under A. For the area of individual farmland was nearly 4 times larger than the area of state-operated farms, we then normalized the value. The results indicated when land management institution of B1 was implemented in 1965, the number, length and erode area of gullies outside state-operated farms was 6.60, 7.79 and 8.55 times of those inside the state-operated farms. While land management institution of B2 was implemented in 2005, the times of the number, length and erode are of gullies outside state-operate farms decreased to 1.39, 1.77 and 3.03. Compared to the land management institution of B, the level of mechanization, management, input and environmental awareness under A were much better to prevent effectively the development of gullies. However, compared to B1, the land management institution of B2 could arouse the enthusiasm and initiative of individual farmers to better manage the farmland. The results would provide a reference to the readjustment of agricultural structure and decision making of sustainable agricultural institution.

Keywords: Land management institution, Gully erosion, Remote sensing, The Black Soil Area

Expansion on the loess gully sidewall: Processes and mechanisms

Yulei Ma[1], Xiangzhou Xu[1*], Peiqing Xiao[2], Qiao Yan[1], Chao Zhao[1]
1Institute of water environment, Dalian University of Technology, Dalian 116024, China
2 Key Laboratory of Process and Control of Soil Loss on the Loess Plateau, Yellow River Institute of Hydraulic Research, Zhengzhou 450003, China
*Corresponding Author, e-mail: xzx@dlut.edu.cn

Abstract

Gully sidewall expansion is an important geomorphic natural hazard and the expansion destroys a large extent of agricultural land in the loess regions every year. The main aim of this study was to identify the mechanisms behind gully sidewall expansion through a series of simulated rainfall experiments. The results show that land loss on the gentle slope was the result caused by the water and gravity erosions, and gravity erosion was the primary driving force. The correlation coefficient between the area of land loss on gentle slope and volume of gravity erosion on the gully sidewall was 0.93, and the correlation coefficient between the area of land loss on gentle slope and volume of water erosion was 0.71. The gravity erosion was the dominant impetus driving the change in slope gradient of the gully sidewall. The amount of gravity erosion in 17 of the 19 rainfall events causing a change greater than 5° in the slope gradient of the gully sidewall accounted for more than 50% of the total amount of sidewall erosion. Furthermore, the dynamic variation of the retreat rates for the gully shoulder line showed a similar trend to that of the total volume of sidewall erosion, and exhibited an increase-decrease-increase tendency. The most significant factors affecting the change in slope gradient of the gully sidewall and retreat rate of the gully shoulder line were the rainfall duration and intensity, of which the sensitivity coefficients were 2.2 and 4.0, respectively. As a result, a combination of vegetation measures on the gentle slope, structural and ecological practices on the sidewall, and powerful structural practices, e.g. check dams, on the gully floor, is preferred for sidewalls vulnerable to expansion.

Keywords: Sidewall expansion, Gravity erosion, Water erosion, Rainfall, Landform

Infiltration and bulk density dynamics:Rain simulation experiments

F Todisco*[1], L Vergni[1], D Torri[2]
1 Department of agriculture, food and environmental sciences, University of Perugia, Italy
2 Senior associate researcher, CNR-IRPI, Perugia, Italy
*Corresponding Author, e-mail: francesca.todisco@unipg.it

Abstract

Experiments with simulated rain on interrill plots were set up to study the cumulative effects of the processes affecting the soil surface and top layer and to which extent the drying period separating successive rainfalls allow the soil to recover. The modifications were characterized in terms of the random roughness, bulk density, porosity, and infiltration dynamics. Every event was characterized by observations conducted before the rainfall event, then when runoff was close to start, and when rainfall ceased. Runoff was measured along the rain. Each experiment consisted of three subsequent simulated rainfall episodes carried out in the range of few weeks in a silty-clay loam soil, manually harrowed at the beginning of each experiment. The data confirm a quick and consistent decrease of porosity. Bulk density data show a dynamic with an increase during rainfall followed by a decrease between successive rainfalls. Roughness too decreases exponentially with cumulated rainfall and energy but shows a partial recovery during the in-between-rains interval. The knowledge of the initial condition resulted enough for the studied soil to predict the roughness decay. From a literature model on macropore dynamics, a family of functions expressing the pore dynamics were derived. Those functions were then adapted to be used with the data of total porosity extracted from the bulk density data. Using the pore size and the total porosity decrease within a simple porous media hydraulic formula it was possible to interpolate well the infiltration data. This study underlines that adequate data are needed to generate algorithms able to evaluate the recovery behavior of the soil as it affects the total porosity, the bulk density, and the initial roughness when following rainfall occur.

Keywords: Modelling, Rainfall sequence, Soil crust, Runoff

Research on mining method of spatial and temporal distribution information of soil erosion in small watershed

Jing Huang*[1,2], Xinxin Hou[1,2]
1 Key Laboratory of Soil and Water Conservation on the Loess Plateau of Ministry of Water Resources, China
2 Yellow River Institute of Hydraulic Research, China
*Corresponding Author, e-mail:huangjing_hky@163.com

Abstract

The process of soil erosion in small watershed is a typical nonlinear dynamic processes, its internal erosion development and evolution process is very complex, so spatial and time distribution information of soil erosion in small watershed need to be mined, but using current algorithms for mining the information of small watershed soil erosion, only focus on the space distribution information mining of soil erosion, which results in the inefficient minting of spatial and time information. This paper proposes a space-time distribution information mining method for small watershed soil erosion based on density track clustering. The method firstly use water and soil loss equation to form the model for small watershed soil erosion, calculate rainfall erosivity, soil erodibility factor, slope length factor of small watershed area, on the basis of spatial and temporal information included in small watershed soil erosion trajectory, spatial and time neighborhood density of soil erosion is clustered to dig out the temporal and spatial distribution pattern information of soil erosion. The simulation proved that spatial and time distribution information mining method for small watershed soil erosion based on the density cluster of tracks has a high value in the field of soil erosion.

Keywords: Small watershed, Soil erosion, Data mining

Precipitation and soil and water conservation measures intensity-runoff evolution law in semi-arid areas

Yanting Hu*[1], Fu Zhang[1], Zhuzhu Luo[2,3], Feng Jin[4], Rui Zhou[5], Xiulan Zhao[1], Bingchen Bao[1]
1 College of Forestry, Gansu Agricultural University, Lanzhou 730070, Gansu, China
2 Gansu Key Laboratory of Aridland Crop Science/ Gansu Agricultural University, Lanzhou 730070, Gansu, China
3 College of Resources and Environmental Sciences, Gansu Agricultural University, Lanzhou 730070, Gansu, China
4 Gansu Provincial Department of Water Resources, Lanzhou 730000, Gansu, China;
5 Gansu Institute of Soil and Water Conservation Science, Lanzhou 730000, Gansu, China
*Corresponding Author, e-mail: fuzhang001@163.com

Abstract

The evolution law and cause analysis of runoff in a climate change, principally the quantitative analysis of the impact of precipitation and soil and water conservation measures on runoff, are still hot issues in the current hydrology and water resources research. This study uses Tyson polygons, Morlet wavelet analysis, regression analysis to study the evolution of precipitation, measures, and runoff under different periods and soil and water conservation measures in Anding District, Gansu, China. The results depicted that (1) the annual runoff exhibits a decreasing trend from 1957 to 2016 (P<0.001). (2) With the advancement of soil and water conservation work, the intensity of soil and water conservation measures such as terraces, artificial afforestation, artificial grass planting, and enclosure gradually increase to 36.14, 25.26, 11.56, and 3.22 $hm^2 \cdot km^{-2}$, respectively. (3) The influence of precipitation on runoff modulus was about less than 40% and the impact of measure intensity was about 60% higher. This shows that the impact of the intensity of measures on runoff exceeds the driving force of the precipitation factor. This study provides support for scientific and rational adjustment of land use structure, deployment of soil and water conservation measures, and construction of ecological environment.

Keywords: Evolution law, Precipitation, Soil and water conservation measures intensity, Runoff

Spatial distribution and influencing factors of gully erosion in the Red River Basin

Shuxian Cheng[1], Yifan Dong*[1], Xiaoli Wen[1], Yang Ji[1]
1 Institute of International Rivers and Eco-Security, Yunnan University, China
*Corresponding Author, e-mail: yifan@ynu.edu.cn

Abstract

To find out the spatial distribution of gully erosion in the Red River basin, reveal the main environmental factors controlling gully erosion development. The study area was divided into small basins as investigation units by ArcGIS 10.3 software, and 360 investigation units were set randomly. Based on field surveys and high-resolution satellite remote sensing images, two types of erosion channels were extracted by manual visual interpretation. The average density of ancient erosion gully is 2.63 $km \cdot km^{-2}$, and the modern erosion gully is 0.77 $km \cdot km^{-2}$. Gully erosion is concentrated at an altitude of 835-2098m. The gully density tends to decrease with the increase of altitude and is larger when rainfall is 1000mm. The correlation between NDVI and gully erosion is stronger. The modern gully density of medium coverage grassland was 3.96, which was significantly higher than that of other land use. The gully density was higher in red soil, purplish soil, and lateritic soil. The area of severe erosion is concentrated in the upper reaches and the dry-hot valley of the mainstream of the Yuanjiang, and the distribution of gully erosion was affected by precipitation, NDVI, altitude and soil type.

Keywords: Gully erosion, Large scale, Influencing factors, Dry-hot valley

Land use types influence soil microbial community through effects on soil properties in the dry-hot valley region in southwestern China

Taicong Liu[1], Zhe Chen[2], Li Rong*[1], Xingwu Duan*[1]
1 Yunnan Key Laboratory of International Rivers and Trans-boundary Eco–security, Kunming, Yunnan Province 650091, China
2 Institute of International Rivers and Eco–security, Yunnan University, Kunming, Yunnan Province 650091, China
*Corresponding Author, e-mail: rongli@ynu.edu.cn; Xingwu xwduan@ynu.edu.cn

Abstract

Land use changes can cause physical, chemical and biological variations of soils. In particular unsuitable land use can accelerate soil degradation. However, how land uses affected the soil microbial community compositions is still not fully understood due to the response of soil microbial communities to changes in land use was controlled by multiple factors. We focused on four typical land uses in the dry hot valley to investigate the mechanism underlying in land use on microbial communities. The results showed that land uses altered bacterial and fungal community composition on phylum level. In sugarcane land (SL) and (BL), the respective absence of a kind of fungi at phylum the level *Zoopagomycota* and *Blastocladiomycota*. The abundances of several bacterial phyla such as *Gemmatimonadets* and *Acidobacteria* associated with promoting mineralization in SL were higher than that in other three land uses. Structural equation model (SEM) showed that land use had direct and indirect effects on bacterial composition, but only indirect effects on fungal composition. Land use indirectly affected bacterial composition through negative effects on soil moisture, clay and available potassium contents, whereas through negative effects on clay and available potassium for fungal composition. Bacteria were more sensitive to land use changes compared to fungi in the dry-hot valley. Considering the low level of total potassium in soil under SL and CT, adding potassium fertilizer is expected to be a beneficial pathway to improve soil microbial composition and soil nutrients in the dry hot valley.

Keywords: Land use, Soil microbial community, Dry-hot valley, Soil properties, Structural equation model

Effects of Vegetation Restoration on Soil Carbon and Nitrogen in Gully Development Area of Yuanmou Dry-hot Valley

Xiaoli Wen[1], Yifan Dong*[1], Ji Yang[1], Xingwu Duan[1]
1 Institute of International Rivers and Eco-Security, Yunnan University, Kunming
*Corresponding Author, e-mail: yifan@ynu.edu.cn

Abstract

Gully erosion results in an unstable state of surface morphology with significant changes. Natural restoration of vegetation through prohibition is one of the main modes of gully management in Yuanmou Dry-hot valley. However, under the comprehensive effect of continuous restoration of gully vegetation and significant development of gully, the changing trend of soil carbon and nitrogen content in gully remains to be clearly defined. In this study, 81 samples of 1 m*1 m were randomly arranged in a typical gully in Yuanmou Dry-hot valley. The vegetation index, elevation changes caused by the erosion/sedimentation process, and soil physical and chemical properties were measured during the early dry seaon in 2012 and 2017, respectively. The results showed that: during the period of prohibition, the gully development area is dominated by sedimentation. Although the vegetation recovered significantly, the soil carbon and nitrogen did not improve significantly. The severity of topographical changes in the gully is significantly higher than that of surface erosion, and it has a significant impact on the carbon and nitrogen of the surface soil of the gully. This study will help to identify the comprehensive effects of vegetation restoration and gully development on soil carbon and nitrogen, and provide support for the restoration of the degraded gully ecosystem in Dry-hot valley.

Keywords: Vegetation restoration, Gully erosion, Soil carbon and nitrogen, Elevation change, Dry-hot valley

The influence of topographical conditions on the asymmetry of the rill cross-section

Xingli Gu[1], Lei Wang[1], Bin Zhang*[1], Hui Liu[1], Jun Luo[1], Qingchun Deng[1], Fachao Qin[1], Jianzhong Wuqiang[1]
1 School of Land and Resources, China West Normal University, Nanchong 637009, China
*Corresponding Author, e-mail: envgeo@163.com

Abstract

Topographical condition is the main factor that control the development and evolution of asymmetrical rill cross-section, and is the key to study rill morphology and rill erosion. In order to study the influence of topographical conditions on the asymmetry of the rill cross-section, the morphological characteristics of 712 rill cross-sections were obtained through field survey in Yuanmou dry-hot valley, and the topographic factor parameters were extracted by using GIS method. The results showed that: (1) rill slope ratio, average slope gradient, rill curvature coefficient, rill curvature coefficient at section position, rill turning angle at section position, rill both sides area ratio at section position and rill depth were all less than 2, all of them can be used as the main parameters to study the effect of topography on rill cross-section asymmetry ratio;(2) rill slope ratio, average slope gradient and rill depth were significantly negatively correlated with cross-sectional asymmetry ratio; rill curvature coefficient, curvature coefficient at section position, rill turning angle at section position and rill both sides area ratio at section position were significantly positively correlated with cross-sectional asymmetry ratio; (3) the relationship between the topographic factors and the asymmetry ratio of the rill cross sections were the results of the interaction of multiple topographic factors. This study will deepen the understanding of morphological characteristics of rill cross sections and provide theoretical guidance for the development of soil and water conservation.

Keywords: Asymmetric, Correlation coefficient; Topographic factors, Dry-hot valley

Dry-hot valley distribution in Hengduan Mountains Region

Yang Deng[1], Xingwu Duan[1,2], Ronghua Zhong*[1,2]
1 Institute of International River and Eco-Security, Yunnan University, Kunming 650091, PR China
2 Yunnan Key Laboratory of International Rivers and Trans-boundary Eco-security, Yunnan University, Kunming 650091, PR China
*Corresponding Author, e-mail: ronghuazhong@ynu.edu.cn

Abstract

Dry-hot valley (DHV) refers to the geographical landscape with high temperature and low humidity which formed by the foehn effect and other factors. The DHV is a typical fragile ecosystem with prominent water-heat conditions, low vegetation coverage and serious soil and water loss. Thus, once the DHV is damaged, it is difficult to restoration and governance. Clarifying the boundary of DHV and its spatial distribution is the prerequisite for scientific research. However, the boundary of DHV in Hengduan Mountainous Region (HMR) has not been clearly defined over the past few decades, which seriously blocking the related scientific research of this zone. Therefore, based on the previous research (Zhang et al., 1992), the present study extracted the DHV boundary and analyzed its spatial distribution pattern according to the data sets, such as the Google Earth remote image data, 1 km resolution 2017-2019 national monthly average temperature, rainfall, soil type and DEM data, and combined with field investigation. The results showed that the DHV of HMR covers a total area of 18852.80 km^2 with a total length of 1327.34 km along the main stream of Jinsha River, Yuanjiang River, Nu River and Lancang River. The distribution region of DHV including 52 counties in Yunnan Province and Sichuan Province. The area of DHV in Yuanjiang River, Lancang River, Nu River and Jinsha River is 4113.79 km^2, 251.60 km^2, 1910.22 km^2 and 12577.17 km^2, respectively. The elevations of DHV ranges from 174 m to 3421 m, and the area with an altitude of 500 m- 2000 m accounted for 91.35% of the total area of DHV. The DHV has a deep steep valley, in which the steep slope over 15° accounts for area 65.15% of the total area of DHV. The current research results can provide the basic data for the eco-environment related research of DHV and helpful for the management and restoration of different degraded ecosystems in HMR.

Keywords: Hengduan Mountain Region, Dry-hot vally, Boundary; Spatial distribution range

Spatial distribution characteristics of gravity erosion on Loess Gully Slope

Shi Jiao Dong[1], Xiang Zhou Xu[1]
1 Institute of water environment, Dalian University of technology, Dalian 116024, China

Abstract

To explore the influence of rainfall and geomorphic factors on the spatial distribution characteristics of gully slope gravity erosion can provide the basis for monitoring and controlling the gravity erosion disaster in the Loess Plateau. The sensitivity analysis method based on variable growth rate was used to analyze the geomorphology and rainfall influencing the gravity erosion near the gully edge line. The results show that. (1) The top of the gully slope is the erosion prone area, the middle of the gully slope is the second, and the slope toe is the weakest. The average ratio of the erosion volume at the top, middle and toe of the gully slope to the total erosion volume is 48%, 33% and 19% respectively. (2) The spatial distribution characteristics of collapse, landslide and mud flow on the loess gully slope are closely related to rainfall and underlying surface. With the increase of rainfall duration, the distribution of landslide erosion on the top and middle of the gully slope increases, which aggravates the development degree of landslide erosion on the top and middle of the slope, and expands the scope of mud flow erosion from the upper part of the gully slope to all parts of the gully slope. With the increase of slope, the volume of collapse erosion increases in the middle and toe of the slope, which aggravates the collapse in the middle and lower part of the gully slope, and the mud flow is mainly concentrated on the top of the slope, which aggravates the development degree of the mud flow on the top of the slope. （3) The sensitivity of different gravity erosion types near the gully edge line to rainfall duration and gully slope geomorphic change is different. In terms of the total amount of gully edge line erosion, collapse, landslide and mudflow are the most sensitive to rainfall duration, and the corresponding sensitivity coefficients are 0.6, 34.2 and 9.1. From the maximum single collapse of the gully edge line, the landslide and mud flow are most sensitive to the rainfall duration change, and the sensitive corresponding sensitivity coefficient is 13.8 and 6.5, and the collapse is the most sensitive to the change of slope height, and the sensitivity coefficient is 0.6

Keywords: Gravity erosion, Rainfall simulation test, Loess gully sidewall, Sensitivity analysis, Gully edge line

Study on gully erosion in the Dry-hot Valley Region of Jinsha River, Southwest China

Donghong Xiong*[1,2], Zheng'an Su[1,2], Yifan Dong[1,2], Baojun Zhang[3], Dan Yang[4], Su Zhang[1,2]
1 Key Laboratory of Mountain Hazards & Surface Process, Chinese Academy of Sciences, Chengdu, 610041, China
2 Institute of Mountain Hazards & Environment, Chinese Academy of Sciences, Chengdu, 610041, China
3 Faculty of Geographical Science, Beijing Normal University, Beijing, 1000875, China
4 School of Land and Resources, China West Normal University, Nanchong, 637009, China
*Corresponding Author, e-mail: dhxiong@imde.ac.cn

Abstract

Gully erosion is very intense in the Dry-hot Valley Region of Jinsha River, and the study on its occurrence mechanism, sediment production process and effects have been still of urgent needs. In recent years, the research group led by Prof. XIONG Donghong from Institute of Mountain Hazards & Environment, CAS has conducted the related research on the background conditions for gully development, the kinetic process and its effects on sediment production, and the sediment control mechanism in gully beds *et al*.. Research results concluded that the lithological properties with low erosion resistance is one of the important material basis for gully developing, gully heads belt is the chief sediments contributors and the headcut height is one of the important factors influencing energy transformation of surface flow and sediment yield. Moreover, the distance between the vegetative buffer strips growing in gully bed and the gully head were found to be one of the important indicator which greatly influence the flow energy reduction and sediments deposition. The above results and conclusions are of significance for furtherly revealing the occurrence mechanism of gully erosion and can offer theoretical guidance for the practice in controlling it.

Keywords: Gully Erosion, Lithological Properties, Hydrodynamics, Gully Headcut, Vegetative Buffer Strip, Dry-hot Valley Region of Jinsha River

Part III
Full papers

This section contains the full papers that was carefully reviewed and accepted by LASOSU21

Hydraulic Tests and Interpretation of Test Data for Erosion Protection Systems in Open Channel Flow

Paolo Di Pietro*[1], Nicola Mazzon[2], Fuding (Frank) Xu[3], Baiying (Calipso) Zhang[4]
1 Corporate Business Unit Senior Specialist, Officine Maccaferri S.p.A., Italy
2 R&D Manager, Maccaferri Innovation Center (M.I.C.), Italy
3 Technical Marketing Director, Maccaferri Changsha, China
4 DT Business Development, Maccaferri Changsha, China
*Corresponding Author, e-mail: p.dipietro@maccaferri.com

Abstract

The stability of erosion control systems depends both on the ability to prevent soil loss underneath, as well as to maintain their integrity under the effects of the flow.

This work is about a comprehensive research study aimed at studying performance of revet mattresses and of geosynthetic mats as lining systems in open channels. Geomats were tested on a 0.6 x 20m flume at 2.7%, laid on soil bed at variable discharge rates, in accordance with ASTM D6460. For revet mattresses, tests were done on a 1 x 10m size flume where units were placed on a 0.30m soil layer. The performance against erosion was evaluated by assessing the effect of the stone motion inside the mattress, in relationship to its thickness and stone size, under variable hydraulic flow regimes.

While confirming the design method typical for revet mattresses (commonly referred to the tractive force theory using Shield parameters), research allowed to define a new performance limit based on incipient soil erosion underneath by monitoring soil settlements due to the flow.

The study for the mattresses was aimed at defining whether different types of partition diaphragms in mattresses provide different results against stability.

Research also established a range of applicability between geomats and rock filled mattress systems, in order to define a criterion based on performance. Tests on geomats were performed both in unvegetated and vegetated conditions.

Keywords: Revet mattresses, Erosion control, Open channel, Shear stress, Velocity

1 Introduction

The stability of erosion control systems depends on their ability to prevent soil loss underneath, maintaining their integrity under the effects of the flow. This report provides an overview of a comprehensive research program aimed at evaluating performance of Maccaferri Reno Mattresses in open channels. Mattresses were preliminarily tested on a 0.20m (8inch) soil layer in a 0.60x20m (2ft x 60ft) flume, and on a 0.30m (12inch) soil layer in a 0.90x10m (3ft x 30ft), at increasing flow rates and at varying slopes. Mattress performance against erosion was evaluated by quantifying the limit condition when erosion underneath starts developing and assessing the effect of the stone motion inside the compartments as a function of its size, grading uniformity, the thickness of the mattress.

The test procedure used was in accordance with ASTM D6460.

Results indicated that the shear and velocity values used in design, following earlier research studies commonly referred to the tractive force theory (CSU test report 1984), could be achieved and considerably exceeded by introducing a new improved connection between base panel and lid, and by optimizing the configuration of the cells and of the stone filling. This research allowed to define a limit of performance by combining effects due to incipient soil erosion under the mattress and stone settlements and at increasing flow rates.

An additional scope of the study was to analyse performance response by varying mattress diaphragm spacing and type of partition. The analysis of the effects due to the stone motion inside the mattress, and relative soil erosion resistance underneath, led to a formulation of a design approach based on mattress specific properties. Performance is determined as a function of the type of diaphragm partition, on proper installation, and on grading and uniformity of the stone fill.

This report provides testing description and results completed up until December 2019 by Colorado State University.

The Project was articulated in an initial 4 stage (or tasks) research.

The experimental study aimed at monitoring erosion underneath the mattress, until a soil loss threshold under the protection was detected. Furthermore, the principle of monitoring stone movement inside the cell was also utilized. This approach is suitable for erosion protection systems, whose primary function is to avoid soil loss.

2 C.S.U. Hydraulics Lab

Laboratory testing was performed at the Colorado State University (CSU) Hydraulics Laboratory located at CSU's Engineering Research Centre (ERC) in Fort Collins, CO. The hydraulics lab is comprised of many indoor and outdoor facilities that allow for a wide variety of hydraulics research. Water supply to both outdoor and indoor research facilities is furnished by Horsetooth Reservoir, which is adjacent to the ERC as shown in Fig. 1 Outdoor facilities are gravity fed from Horsetooth Reservoir with a capacity of approximately 170,000 acre-feet of water and a maximum static pressure of approximately 760 kPa (110 psi) providing up to 5.7 m3/s (200 cfs) at some facilities. Indoor facilities are fed by a connected sump and recirculating pump system allowing for research year-round.

Figure 1 Aerial view of Horsetooth Reservoir and the Engineering Research Center (E.R.C.)

3 Preliminary Investigations

Three preliminary tasks were setup to determine the best performing configuration to use for the last and final Task.

Task 1 consisted of tests on 0.30m (12inch) thick mattresses without the stone fill. The objective was to firstly assess how much contribution would the wire mesh alone provide to the flow dissipation within the mattress thickness.

Tasks 2 and 3 were performed to measure the reduction of velocity within mattresses, filled with stone fill of different diameter and uniformity and with different configurations. The aim was to measure the dissipation effect through the mattress layer. Discharges were released to keep the flow depth constantly right above the mattress at different flume inclinations (Fig. 2). Average velocities were also measured with sensor measurements through the testing.

A lesser flow rate would correspond to a higher dissipation effect of the flow through the structure. Results showed that the smaller the rock size, and the less the flow could travel through the mattress.

Figure 2 Profile view of the flume in preliminary investigations

Comparing trends between tests, it was possible to observe how smaller rocks provide an increased dissipation to the flow through the mattress. The coarser material with larger size lets more water seep through the mattress structure. Different diaphragm spacing did not significantly affect the flow in the mattress.

A relevant influence was observed by the uniformity C_u of the grading for the same d_{50}. The mattress with 0.10m (4inch) rock and C_u=1.5 performed less to flow dissipation through the structure than the mattress with 0.10m (4inch) and C_u=1.0. Rock uniformity was therefore more affecting performance than the rock size. These observations on the influence of rock size and of uniformity led to the decision to select as ideal stone range for Task 3, a filling with a rock size of d_{50}= 0.95m (3.75inch), that is slightly smaller than the 0.10m (4inch) size, and C_u=1.0.

3 Hydraulic Performance of Reno Mattresses

Based on results obtained during preliminary investigation, the final task was performed on a 1.20m (4ft) wide, 10m (30ft) long flume on a soil bed, at varying flow rates up to 0.65m^3/s (23cfs) and at variable slopes (15% up to 50%) to test performance limit conditions of the most representative configuration (Fig. 2). Mattresses were manufactured with a 6x8 steel wire mesh type, made with wire diameter 2.2mm nominal steel wire, coated with a high abrasion resistance polymer (branded as Polimac®) with a nominal thickness of 0.5mm, resulting in a 3.2mm outer diameter. Mattress units were partitioned at 1m (3.3ft) spacings in longitudinal direction, by pleating the base and connecting the bottom corners by wire rings, in order to form each partition as a double wall.

Reno Mattress units fabricated with this manufacturing, by double pleating the base. Reno Mattress units were installed with the best grading of rockfill, corresponding to a D_{60}/D_{10} = 1. The scope was to test the mattress when filled with the best available performing rock grading, despite the value conventionally assumed in the design practice as D_{60}/D_{10} = 1.5. Results allowed to obtain the values of shear stress within a range (min/max) as a function of the rock, in size and grading.

Tests were performed in line with the requirements of ASTM D6460. A brief summary of test configurations is reported in Table 1.

Mattress configurations are schematically illustrated in Fig. 3 In two of the three tests, base and lid were secured with an especially firm vertical wire connection, in a pattern of 2 wire bracings per m^2.

Mattresses used are schematically illustrated in Fig. 3. Mattresses used in Test A, were with pleated diaphragms and no vertical bracings, while Mattresses used in Test B and C had 2 vertical bracings per sqm. Mattress units are shown in Fig. 4

Table 1 Testing matrix

Test	Mattress Properties				Stone Properties	
	Thickness	Mattress Width	Diaphragm Spacing	Vertical Ties (X-Ties)	d_{50}	$C_u=D_{60}/D_{10}$
A	0.17m (6inch) Reno Mattress	1m (3.3ft)	1m (3.3ft)	No	100mm (3.75inch)	1
B	0.17m (6inch) Reno Mattress Plus	1m (3.3ft)	1m (3.3ft)	Yes	100mm (3.75inch)	1
C	0.30m (12inch) Reno Mattress Plus	1m (3.3ft)	1m (3.3ft)	Yes	100mm (3.75inch)	1

Figure 3 Sieves used for preparing rock gradations

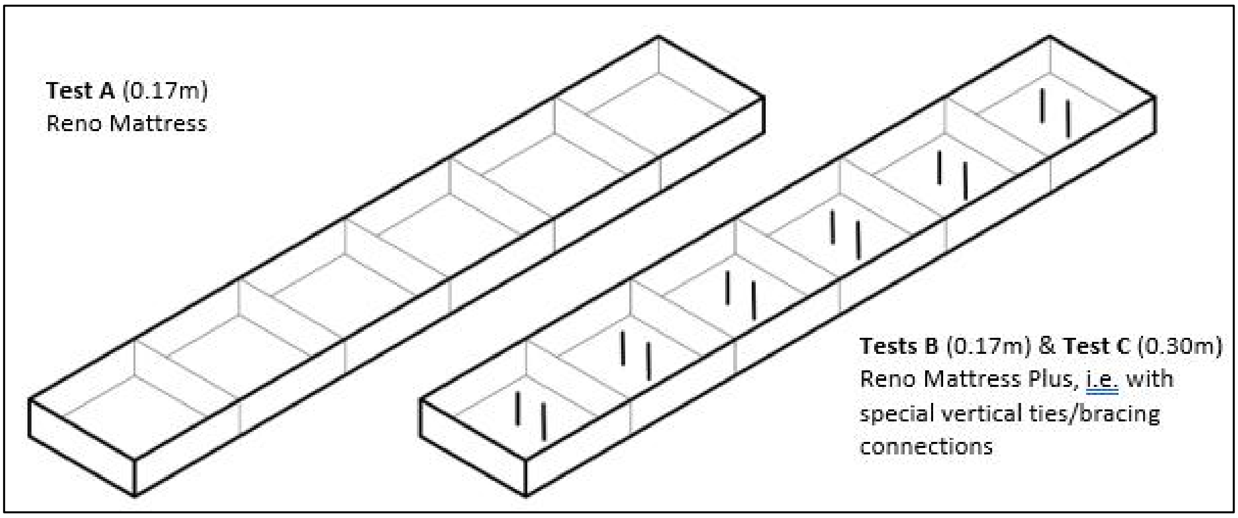

Figure 4 Overview of mattress configurations

Figure 5 Reno mattress units 0.17m (left) and 0.30m (right)

Figure 6 Views f the flume during testing

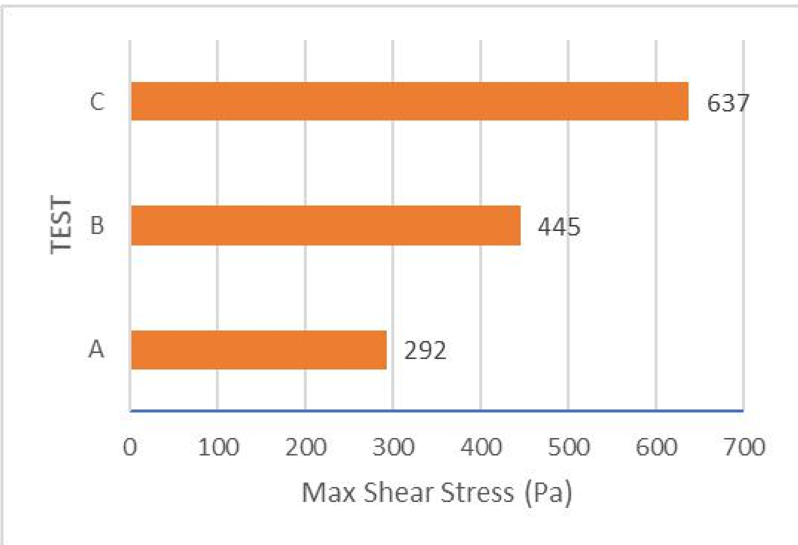

Figure 7 Max shear stress values recorded

Shear stress values reached during the test of 3 configurations with small rock with d_{50}=100mm (3.75inch) and C_u=1 show a significant reduction of erosion underneath. A summary of shear stresses reached during the tests is reported in Fig. 6

4 Summary and interpretation model

In literature, the design of a riverbank protection with Gabions or Reno mattresses made of double twisted wire mesh considers the lining to be stable when minimal or no movement of individual stones occur inside the gabion or mattress compartment, so keeping the protective function.

The experimental study was carried out with mattresses with a “pleated” double layer of mesh in each compartment, filling the units with more selected rock and, most importantly, installing vertical bracings to firmly connect the lid to the base of the unit. Tests were performed in accordance with ASTM D6460.

The test campaign allowed to define new performance values for these erosion protection systems.

The experimental results show an increase in the limit values compared to those obtained in 1984. This difference may be attributed to the new mattress configuration and to a different interpretation of the threshold values.

Shear stress values calculated in tests carried out in 1984, and values recorded in 2019 are summarized in the Table 2 below.

Along with the new interpretation model, this difference in performance can be attributed to:

1) the use of vertical connections,
2) the use of a double pleated diaphragms,
3) the use of different rockfill (both in size and in uniformity).

The values on the left end of the range for “Castoro” Reno Mattresses and for Reno mattresses Plus indicate the max allowable shear stress for units filled with coarse graded rock (C_u=1.5). The right end of the range indicates the max allowable shear stress for mattresses filled with uniformly graded rock (C_u=1.0).

Table 2 Max shear stress values recorded at CSU in 1984 and recorded in 2019

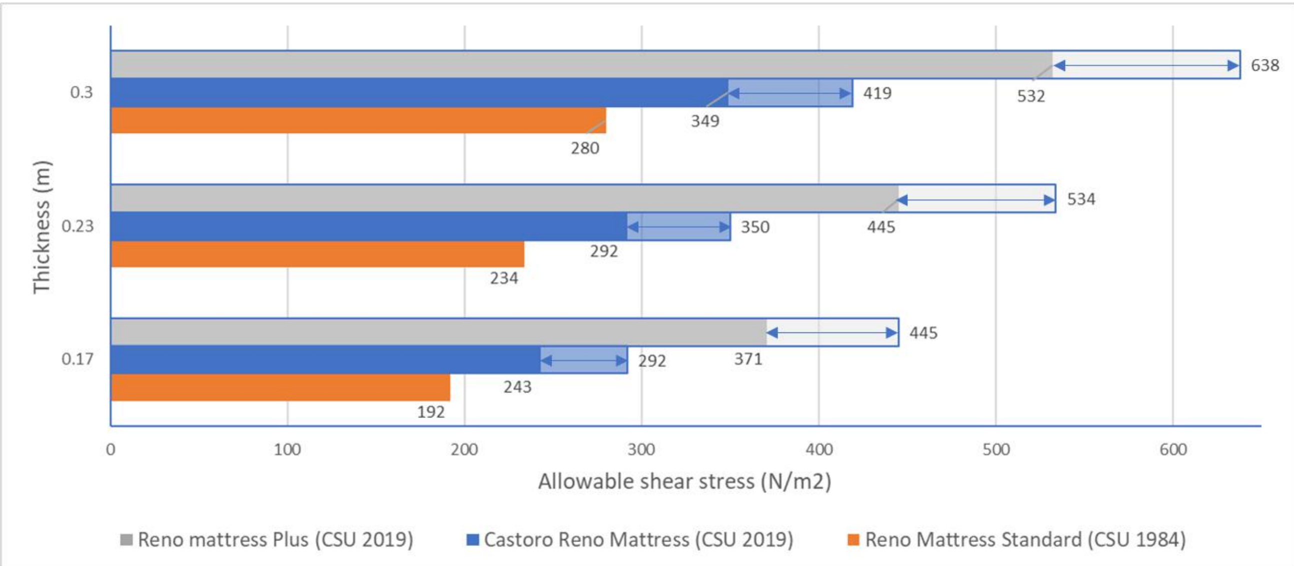

Among the variables, a fundamental new improvement in the performance is due to the presence of vertical connections. The experimental program involved the use of a double connection. Such connection was later converted in an industrially manufactured component, named X-Tie, where vertical bracing components are connected in a special U-Shape characterized by an even higher stiffness than the tested double connection. This system component, named as X-Tie, is part of the new Reno mattress Plus.

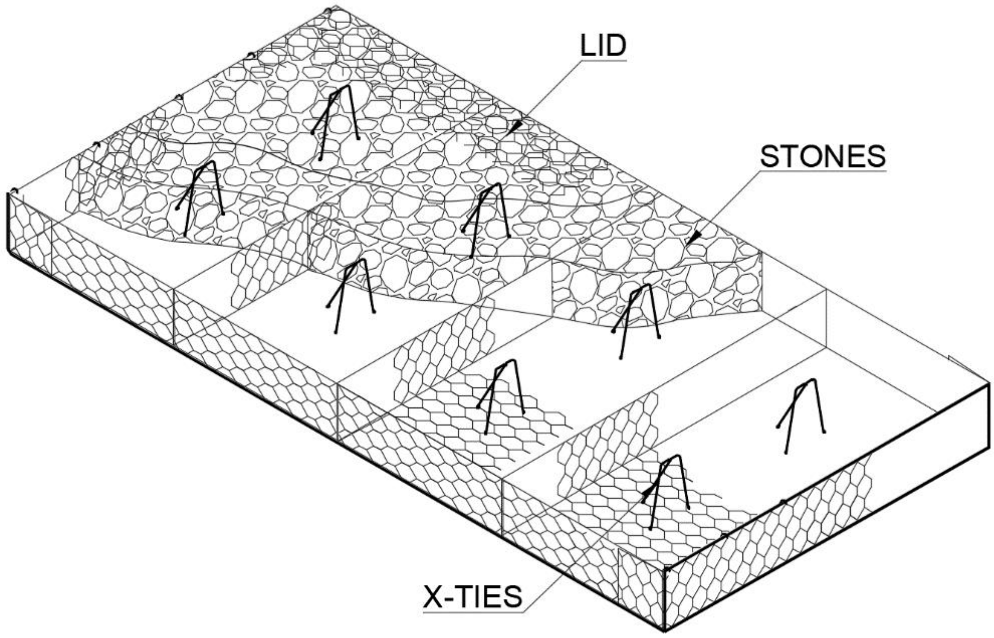

Figure 8 View of Reno Mattress Plus

5 References

Daryl Simons, Yung Hai Chen, Lawrence J. Swenson (Simons, Li & Associates) (1984) Hydraulic Tests to Develop Design Criteria for the Use of Reno Mattresses, Civil Engineering Department – Engineering Research Center, Colorado State University -Fort Collins, CO

ASTM D 6460-19 American Standard for Testing Materials, Standard Test Method for Determination of Rolled Erosion Control Products (RECP) Performance in Protecting Earthen Channels from Stormwater-Induced Erosion, (Dec. 5, 2013).

AFNOR NF P 94-325-2 Association Française de Normalisation, Execution des travaux geotechniques speciaux "Ouvrages en gabions en grillage metallique a maille hexagonale double torsion, Partie 2: Ouvrages en site aquatique, (Nov. 2006)

Ven Te Chow, PhD, Open Channel Hydraulics, McGraw Hill (1988)

HEC 20, Hydraulic Engineering Circular No.20, Stream Stability at Highway Structures, FHWA-HIF-12-004, Apr. 2012

HEC 15, Hydraulic Engineering Circular No.15, III Edition, Design of Roadside Channels with Flexible Linings, Sept. 2005

NCHRP Report 568, National Cooperative Highway Research Program, Riprap Design Criteria, Recommended Specifications, Quality Control, Transportation Research Board, Sept. 2006

R.Agostini, A.Conte, G.Malaguti, A.Papetti, Flexible linings in Reno mattress and gabions for canals and canalized watercourses, Officine Maccaferri S.p.A., Jan. 1985

Effects of Acanthopanax senticosus cultivation on soil physical properties of abandoned slope farmland in warm, cool and humid mountainous areas

Yizi Duan[1]*, Kezhuang Wang[1], Haili Ru[1], Fu Wang[1]
1 Pingliang Research Institute of soil and water conservation, Pingliang, Gansu, China
*Corresponding Author, e-mail: 876728963@qq.com

Abstract

With the rapid development of urbanization, industrialization and agricultural modernization, A large number of rural laborers have turned to cities, resulting in abandonment of slope farmland, soil compaction, nutrient loss, changes in physical and chemical properties, and rill erosion and surface erosion on local slopes, resulting in new soil erosion. Therefore, soil and water conservation of abandoned farmland has become a new topic of efficient use of agricultural farmland after urbanization and new rural construction. Based on the Huating medicinal material base in Gansu Province, we selected representative abandoned farmland, acanthopanax senticosus concentrated cultivation land of different age classes, abandoned farmland for re cultivation of corn land, selected representative plots in the experimental demonstration site by profile sampling method and ring knife method, and excavated 0.6m deep soil profile, Soil samples were taken every 20cm with the ring knife method (to keep the soil structure in the ring knife from being damaged), covered and taken back to the laboratory for determination. Refer to "Determination of Forest Soil Moisture-Physical Properties" (LY/T 1215—1999) to determine and calculate the soil bulk density, maximum water holding capacity, capillary water holding capacity, non-capillary porosity, and capillary tube Soil physical properties such as porosity and total porosity; Select the representative Acanthopanax senticosus standard wood from the standard land, use the excavation harvesting method to sample, remove the floating soil beside the root system, dig the whole Acanthopanax senticosus roots, observe the root color, traits, size, distribution and other characteristics and make records.Measure 0-10cm, 10-20cm, 20-30cm, 30-40cm root width, length, thickness, quantity, fresh weight and other data with vernier caliper, tape measure and balance. After the measurement, bring it back and put it in the oven at 85. Bake at ℃ for 48h to constant weight, measure the dry biomass of roots; select a standard sample plot with a 1.2m soil drill and sample in 20cm layers, repeat twice for each layer, weigh it and bring it back to the laboratory and bake it in an oven at 105℃ for 12h To a constant temperature, weigh the dry weight and calculate the average soil moisture content; apply the dry sieve method to determine the soil mechanical composition.At the same time, a 60 cm deep soil profile was excavated from a representative plot of Acanthopanax senticosus test demonstration site, and 1000 g of mixed soil was taken back to the laboratory. After air-drying, the soil samples were shaken up and down by hand with 5 mm, 2 mm, 1 mm, 0.5 mm and 0.25 mm aperture soil sieves at 30 times / min for 5 min to determine the weight of soil samples on each aperture sieve. The results showed that the standardized strip cultivation of Acanthopanax senticosus, an economic shrub for soil and water conservation in warm, cool and humid mountainous areas, enriched the local medicinal materials, expanded the root level, maintained the physical properties of shallow soil, and improved the soil structure significantly; In 0-60cm soil layer, the non capillary porosity of 2-year-old Acanthopanax senticosus forest land was 15.24%, that of 3-year-old Acanthopanax senticosus forest land was 18.89%, and that of corn fallow land was 9.78%; The total root length was 1.9 times of that in 20-30 cm soil layer and 9.8 times of that in 30-40 cm soil layer, accounting for 59.6% of the total root quantity. The hairy root length and root quantity less than 1 mm were larger than those in other soil layers, accounting for 66.7% of the total root length and 85.7% of the total root number, showing the growth and development characteristics of shallow rooted shrubs; The surface soil of 2-year-old Acanthopanax senticosus forest land is loose, and the total porosity of soil is 13.3% higher than that of corn land. The average total porosity of 3-year-old Acanthopanax senticosus forest land is 74.22%, 25.58% higher than that of corn land, and 24.5% higher than that of 2-year-old Acanthopanax senticosus forest land. As the depth of the soil layer increases, the total porosity of the soil shows a downward trend. The standardized cultivation of Acanthopanax senticosus on abandoned cultivated land is conducive to cultivating characteristic leading industries and optimizing land use structure. It not only protects the local ecological environment, but also promotes stable income growth of farmers, and has a good ecological and economic prospect.

Keywords: Warm, Cool and humid mountainous area, Abandoned farmland, Acanthopanax senticosus, Cultivation, Soil physical properties

With the development of society and economy, my country's new urbanization, industrialization and agricultural modernization have accelerated, leading to a large number of rural laborers turning to cities. This has led to the phenomenon of abandonment of slope farmland in mountainous areas due to insufficient labor, resulting in soil hardening and nutrient accumulation Erosion, physical and chemical properties have changed, rill erosion and surface erosion have gradually increased, causing more serious soil erosion.Therefore, soil and water conservation of abandoned arable land has become a new issue for the efficient use of agricultural arable land after urbanization and new rural construction. For this reason, for many years, Huating City has relied on the medicinal material base and made use of the local good temperature, cool and humid climate and soil conditions, and successively planted Chuanxiong, Duhuo, Pinellia, Astragalus and Pueraria lobata and Chinese medicinal materials have achieved significant economic benefits, providing a model for local people to get rid of poverty and enrichment, and improve the efficiency of land resource utilization. While showing good economic benefits, Chinese medicinal materials also store water and soil and reduce soil erosion on sloping farmland. , Improve the soil has played a good role.

In early 2018, Yangan village of Ankou Town, based on Farmers' cooperatives, demonstrated the cultivation of 2 hm2 Acanthopanax senticosus medicinal economic shrub for soil and water conservation. By picking tender leaves, buds, root bark and other measures, the economic benefits of Acanthopanax senticosus were improved, and the surrounding villages were gradually driven to expand the cultivation area. On this basis, we rely on this base to study the growth of Acanthopanax senticosus on abandoned farmland and its influence on soil physical and chemical properties, in order to optimize the cultivation and management measures of Acanthopanax senticosus, improve the utilization efficiency of land resources, further expand the cultivation area of Acanthopanax senticosus in abandoned farmland, and provide technical support for local sustainable and stable poverty alleviation and rural industrial revitalization.

1 The general situation of the study area and the economic effect of Acanthopanax senticosus

The study area is located in Yangan village, Ankou Town, Huating City, Gansu Province. It is located in the intersection of Loess Hilly and gully area and earth rock mountain area. The terrain is high in the West and low in the East, with an average altitude of 1942m, a frost free period of 164d and an average annual temperature of 7.9 ℃ . The annual extreme minimum temperature is - 22 ℃, the extreme maximum temperature is 26 ℃, the active accumulated temperature of ≥ 10 ℃ is 3200 ℃, the annual sunshine hours is about 2100h, and the annual average precipitation is 625mm, mostly concentrated in July, August and September. The climate is cool and humid, the groundwater level is high, and the water resources are rich. The soil is mainly gray cinnamon soil, and the regional vegetation coverage rate reaches 30%. In recent years, the village has learned from the experience of planting Chinese herbal medicine in Maxia,Cedi and other townships in the city (Duan et al., 2018), and tried to standardize and concentrate the cultivation of wild Acanthopanax senticosus, relying on the development of herbal medicine base to build an ecologically beautiful village, providing a typical example for the regional economic development with characteristics of warm, cool and humid mountainous areas and the achievement of stable poverty alleviation and prosperity.

Acanthopanax senticosus (Rupr. Maxim.) harms is a perennial shrub of Acanthopanax senticosus (Rupr. Maxim.) harms. It is 1-6m high and has many branches. It likes warm and humid climate. It is resistant to cold and shade. It has the effects of anti inflammation and sterilization, enhancing immunity, reducing blood pressure, eliminating dampness and pain, regulating body disorder, tonifying the middle and essence, promoting blood circulation and removing blood stasis, strengthening stomach and diuresis. Its seeds can extract oil and make soap, The buds are edible, and they are high-quality wild vegetables and raw materials for tea making. The roots and rhizomes or stems are harvested in spring and autumn. The extract and glycosides of Acanthopanax senticosus root have anti fatigue effect, can antagonize the immunosuppressive effect of lobotoxin C, and have special antiviral immunity to tick borne encephalitis. The extract can increase the defense ability of capillaries under low pressure, and reduce the incidence frequency caused by cold and the content of hemoglobin in blood.

2 Materials and methods

2.1 Research methods

Based on the methods of field investigation and indoor analysis, the representative plots were selected in the dormancy period of Acanthopanax senticosus before spring branch sprouting in March 2020 and after defoliation in November 2020: (1) concentrated cultivation of Acanthopanax senticosus, with an average slope of 12 °, It is cultivated in the same height belt with the width of 0.5-0.8m, the belt spacing of 1.2m and the plant spacing of 0.1-0.3m. In the spring of 2018, the artificial wild transplanting and centralized cultivation methods were adopted to plant on the abandoned slope farmland of Yang'an village. The branches on the ground were cut off and the soil was covered with 5-10cm to facilitate the normal overwintering（2) Corn was planted in abandoned farmland, and corn fallow land was used as control.

2.2 Determination content

2.2.1 Determination of soil physical properties

According to the cultivation time and growth situation of Acanthopanax senticosus, a representative plot was selected in the experimental demonstration site, and a 0.6m deep soil profile was excavated. Soil samples were taken every 20cm by the ring knife method for bulk density, total porosity, capillary porosity and field water capacity. According to the soil occurrence level or every 10cm by the ring knife method (to keep the soil structure in the ring knife from being damaged), Use a sharp soil knife to flatten the surface of the ring knife, cover it and take it back to the laboratory for determination. Refer to "Determination of Forest Soil Moisture-Physical Properties" (LY/T 1215—1999) to determine and calculate the soil bulk density, maximum water holding capacity, capillary water holding capacity, non-capillary porosity, and capillary tube Soil physical properties such as porosity and total porosity (Song et al., 2019).

2.2.2 Underground biomass determination of Acanthopanax senticosus

Select the representative Acanthopanax senticosus standard wood from the standard land, use the excavation and harvest method to sample, carefully remove the floating soil next to the root system to avoid damage to the root system.After excavation, observe the root color, character, size, distribution and other characteristics and make records. Use vernier caliper, tape measure and balance to measure the root width, length and thickness of 0-10cm, 10-20cm, 20-30cm, 30-40cm ,quantity, fresh weight and other data, after the end of the measurement, bring it back and put it in an oven at 85 ℃ for 48h to constant weight, then measure the root dry biomass.

2.2.3 Determination of soil moisture

Select the standard sample plot and use a 1.2m soil drill to sample in 20cm layers. Repeat two for each layer. After weighing, take it back to the laboratory and bake it in an oven at 105°C for 12 hours to a constant temperature. Weigh its dry weight and calculate the average soil moisture content.

2.2.4 determination of soil mechanical composition

The mechanical composition of soil was determined by dry sieving method. A soil profile with a depth of 60cm was excavated from a representative plot in the experimental demonstration site, and 1000g of mixed soil was taken back to the laboratory. After air drying, the soil samples were shaken up and down for 5min by hand with aperture of 5mm, 2mm, 1mm, 0.5mm and 0.25mm at 30 times / min to determine the weight of soil samples on each aperture sieve.

3 Results and analysis

3.1 Analysis of soil physical properties of Acanthopanax senticosus forest land

3.1.1 Soil bulk density and soil porosity

Soil bulk density and soil porosity are the basis of soil physical properties, and are also important indicators to evaluate soil firmness and structural characteristics. The more obvious the soil bulk density is, the more porous the soil is (Wang et al., 2019), the more loose the soil is, the better the structure is, and the soil moisture, air and heat are in good condition, which is conducive to the growth of plant roots and underground biomass. It can be seen from table 1 that with the increase of soil depth, soil bulk density of Acanthopanax senticosus and corn land also increases, but soil bulk density of Acanthopanax senticosus forest land in 0-40 cm soil layer is less than that of corn land; With the increase of soil depth, the total porosity of soil in Acanthopanax senticosus and corn land decreased. The total porosity and capillary porosity of soil in 0-20cm and 40-60cm soil layers of Acanthopanax senticosus forest land and corn land changed little, but the total porosity of soil in 20-40cm Acanthopanax senticosus forest land increased by 13.3% compared with corn land. The average total porosity of 3-year-old Acanthopanax senticosus forest land reached 74.22%, which was 25.58% higher than corn land, It was 24.5% higher than that of 2-year-old Acanthopanax senticosus forest. The comprehensive analysis of soil porosity and soil bulk density showed that the surface soil of 0-40cm Acanthopanax senticosus forest was loose, the soil aggregate structure was significantly better than that of the control corn field, and the bottom soil porosity of 40-60cm had little change. This was because Acanthopanax senticosus was a two-year-old plant, and its growth and development roots were mainly distributed in 0-40cm soil layer, With the increase of growth years, the root system of Acanthopanax senticosus expanded horizontally, and the root quantity also increased. Its effect on maintaining the physical properties of shallow soil and improving soil structure will be gradually obvious.

Table 1 Soil Physical Properties of 0-60cm soil layer

Land type	Soil depth （cm）	Soil bulk density （g/cm^3）	Non capillary pores （volume%）	Capillary space （volume%）	Total porosity （volume%）	Soil aeration （volume%）
Acanthopanax senticosus (2 years old)	0-20	1.18	3.97	51.65	55.63	53.39
	20-40	1.34	7.34	45.07	52.41	49.86
	40-60	1.67	3.92	37.21	41.14	37.96
	average	1.4	5.08	44.65	49.72	47.07
Acanthopanax senticosus (3 years old)	0-20	1.07	7.2	69.7	77.0	72.1
	20-40	1.30	3.11	67.19	70.30	64.46
	40-60	1.34	3.46	71.92	75.39	69.35
	average	1.24	4.60	69.62	74.22	68.65
Corn field (contrast)	0-20	1.22	3.11	52.95	56.05	53.91
	20-40	1.41	2.85	43.41	46.26	43.77
	40-60	1.48	3.82	39.78	43.60	41.12
	average	1.37	3.26	45.38	48.64	46.26

3.1.2 Soil water content and soil water storage

Soil water is the most important part of soil and the main source of water for plant growth and development (Yan et al., 208). It can be seen from table 2 that the average maximum soil water holding capacity, soil water storage capacity and soil volume water content in 0-60cm soil layer of Acanthopanax senticosus plantation are greater than those in corn field. With the increase of soil depth, the maximum soil water holding capacity, soil water storage capacity and soil volume water content also increase. In 0-40cm soil layer, the maximum soil water holding capacity of 2-year-old Acanthopanax senticosus plantation reaches 864.9g/kg, 15g / kg in corn field; The results showed that the average soil water content of Acanthopanax senticosus was 16.7% in 0-40 cm soil layer and 17.8% in corn field. The surface soil water content of Acanthopanax senticosus forest was lower than that of corn field. This is because the soil porosity of Acanthopanax senticosus forest land is larger, the soil permeability is good, acanthopanax senticosus plants sprout and grow, and the soil water evapotranspiration is greater than that of corn fallow land. The non capillary porosity of Acanthopanax senticosus forest land in 0-60cm soil layer was 15.24%, and that of corn fallow land was 9.78%.

Table 2 Physical properties of soil in soil layer of 0-60cm

Land type	Soil depth（cm）	Volumetric water content （volume%）	Soil water storage （mm）	Maximum water holding capacity （g/kg）	Capillary capacity （g/kg）
Acanthopanax senticosus (2 years old)	0-20	22.40	1344.24	473.36	439.64
	20-40	25.50	1530.13	391.53	336.55
	40-60	31.81	1908.75	246.41	222.85
	average	26.57	1594.37	370.44	333.02
Corn field (contrast)	0-20	21.45	1287.29	461.10	435.55
	20-40	24.96	1497.78	327.06	306.86
	40-60	24.79	1487.69	311.72	284.75
	average	23.74	1424.25	366.62	342.39

3.1.3 Soil mechanical composition

Based on the analysis of 0-60cm air dried soil samples from Acanthopanax senticosus plantation, the soil particles with diameter > 5mm accounted for 35.74% of the total weight of soil samples, the soil particles with diameter 2-5mm accounted for 32.97%, the soil particles with diameter < 0.5mm accounted for 31.3%, the soil mechanical composition of 0-60cm soil layer with diameter 0.25-2mm accounted for 29.05% of the total weight, and the soil particles with diameter < 0.25mm only accounted for 5.6%; The results show that the soil porosity of 3-year-old Acanthopanax senticosus forest land is higher than that of 2-year-old Acanthopanax senticosus forest land.The proportion of soil weight with different particle sizes in 0-60cm soil layer is shown in Table 3.

3.2 Root vertical distribution characteristics of Acanthopanax senticosus

The distribution characteristics of plant roots not only depend on their own genetic characteristics, but also are greatly affected by the soil environment (Zhang et al., 2009). It can be seen from table 4 that with the increase of soil depth, the fine root biomass of Acanthopanax senticosus changed greatly. The root quantity and length of different diameter classes in 10-20cm soil layer were larger than those in other soil layers, and the total root length was 1.9 times of that in 20-30cm soil layer and 9.8 times of that in 30-40cm soil layer, accounting for 59.6% of the total root quantity; From different diameter classes, the length and quantity of hairy roots less than 1 mm were greater than other diameter classes. The root length accounted for 66.7% of the total root length, and the number of roots accounted for 85.7% of the total. It further showed that the root system of Acanthopanax senticosus was mainly distributed in 0-20 cm soil layer, showing the growth and development characteristics of shallow rooted shrubs. The distribution of soil root system in this layer was more conducive to improving the surface soil structure and soil environment, Increase soil porosity, increase the storage and utilization capacity of forestland for precipitation and surface runoff.

Table 3 Proportion of different particle sizes of 100g soil weight in 0-60cm soil layer

Mesh size class（mm）	Soil weight（g）		Proportion（%）	
	Acanthopanax senticosus cultivation site（2 years old）	Acanthopanax senticosus cultivation site（3 years old）	Acanthopanax senticosus cultivation site（2 years old）	Acanthopanax senticosus cultivation site（3 years old）
＞5	35.74	56.66	35.74	56.66
2-5	32.97	24.77	32.97	24.77
1-2	7.34	6.97	7.34	6.97
0.5-1	14.55	8.98	14.55	8.98
0.25-0.5	3.81	1.54	3.81	1.54
＜0.25	5.60	1.08	5.60	1.08

Table 4 Statistical table of root distribution characteristic values of 2-year-old Acanthopanax senticosus with different diameter classes

Soil depth（cm）	category	Diameter class（mm）					Air dried root weight（g）	Proportion %
		<1	1-3	3-5	≥5	total		
0-10	Root length（cm）	156			10	166	11	9.2
	Number of roots（slips）	6			1	7		
10-20	Root length（cm）	1188	302.6	94.9	282	1867.5	71	59.6
	Number of roots（slips）	95	18	3	7	123		
20-30	Root length（cm）	708.86	116.1		150	974.96	21.2	17.8
	Number of roots（slips）	138	9		2	149		
30-40	Root length（cm）	81.2	33.5		75	189.7	15.9	13.4
	Number of roots（slips）	36	3		3	42		
total	Root length（cm）	2134.06	452.2	94.9	517	3198.16	119.1	100
	Number of roots（slips）	275	30	3	13	321		

3.3 Growth of Acanthopanax senticosus branches

After planting wild Acanthopanax senticosus in the early spring of 2018, the aboveground part of Acanthopanax senticosus was stubbled to reduce the ineffective water consumption of aboveground plants and affect the growth and survival rate of underground roots. According to the typical investigation, the average growth length of branches in that year is 70cm, and that in 2019 is 110cm. There are 3-5 tillering branches in two-year-old cluster, and the average crown width is 0.95cm. Therefore, with the growth and development of root system, the growth of aboveground part of Acanthopanax senticosus also increased.

4 Conclusion and discussion

(1) With the increase of soil depth, soil bulk density of Acanthopanax senticosus forest increased; The horizontal expansion range and rooting amount of Acanthopanax senticosus roots increased with the growth years, which showed good effect in maintaining the physical properties of shallow soil and improving the soil structure. However, the effect of Acanthopanax senticosus roots on the physical and chemical properties of deep soil should be further studied according to its growth years. The soil bulk density of Acanthopanax senticosus forest land in 0-40 cm soil layer was lower than that of corn land; The total porosity of 20-40cm Acanthopanax senticosus forest land was 13.3% higher than that of corn land. The average total porosity of 3-year-old Acanthopanax senticosus forest land was 74.22%, 25.58% higher than that of corn land, and 24.5% higher than that of 2-year-old Acanthopanax senticosus forest land. The surface soil of 0-40cm Acanthopanax senticosus forest was loose, and the soil aggregate structure was significantly better than that of the control corn field, while the porosity of 40-60cm bottom soil changed little.

(2) With the increase of soil depth, the maximum soil water holding capacity, soil water storage capacity and soil volume water content also increased. In 0-40cm soil layer, the maximum soil water holding capacity of 2-year-old Acanthopanax senticosus forest land was 864.9g/kg, and that of corn land was 788.15g/kg; The results showed that the average soil water content of Acanthopanax senticosus in 0-40 cm soil layer was 16.7%, that of corn land was 17.8%, that of non capillary pore in 0-60 cm soil layer was 15.24%, and that of corn fallow land was 9.78%.

(3) In 0-60cm air-dried soil samples, the content of sand in the soil is relatively high. As the depth of the soil layer increases, the biomass of the fine roots of the two-year-old Acanthopanax senticosus varies greatly, among which the amount and length of roots of different diameters in the 10-20cm soil layer all are larger than other soil layers, the total root length is 1.9 times that of the 20-30cm soil layer and 9.8 times that of the 30-40cm soil layer, and the root mass accounts for 59.6% of the total root mass; According to different diameter classes, the length and quantity of hairy roots less than 1 mm were greater than other diameter classes, and the root length accounted for 66.7% of the total root length, and the number of roots accounted for 85.7% of the total, which showed the growth and development characteristics of shallow rooted shrubs. It was beneficial to improve the surface soil structure, improve the soil environment, improve the soil porosity, and increase the storage and utilization capacity of precipitation and surface runoff.

(4) With the increase of growth years, the aboveground and underground biomass of Acanthopanax senticosus increased correspondingly. The average branch growth length of Acanthopanax senticosus planted in early spring of 2018 was 70cm in that year and 110cm in 2019. The number of two-year-old cluster tillering branches was 3-5, and the average crown width was 0.95cm. With the growth and development of root system, the growth of the aboveground part of Acanthopanax senticosus also increased, and the crown width increased.

(5) Acanthopanax senticosus, as a medicinal shrub species for soil and water conservation, enriches the local varieties of traditional Chinese medicine, and plays a typical role in helping local people to get rid of poverty and enrich people, increasing farmers' economic income, building ecological beautiful countryside, and optimizing land use structure. At the same time, the strip cultivation of Acanthopanax senticosus in the gentle slope abandoned farmland is conducive to layer by layer retaining the surface runoff and sediment on the upper slope, making it a compound economic plant for soil and water conservation in warm, cool, cloudy and humid mountainous areas, which has a good prospect for ecological and economic development. The situation of surface runoff and sediment on different slope positions needs further observation and analysis.

5 References

Duan Yizi, Wang Anmin, Wang Kezhuang,K(2018).“The present situation and Countermeasures of the construction of beautiful countryside with characteristics of Nanyu in Huating”. Modern agricultural science and technology,11,290-293.

Song Zhihong, Zhang haitao, Sun Dongxue, etc,K（2019）.“Effect of honeysuckle on soil erosion on gneiss slope under simulated rainfall”.Journal of soil and water conservation,33,43-48.

Wang Meng, Li Gang Tie, Dang Hong Zhong, etc,K（2019）.“Soil water holding characteristics of apple orchard in gully region of Loess Plateau”.Chinese Journal of soil and water conservation, 17 ,19-26.

Yan Hui, Su Yinquan, Li Jiping, etc,K(2008).“Vertical distribution of fine roots and its relationship with soil nutrients in Robinia pseudoacacia Plantation on the northern slope of Qinling Mountains”.Soil and water conservation research, 15, 65-68.

Zhang Yuanrun, Dong Liguo, Cai Jinjun, etc,K(2009). “Characteristics of soil physical and chemical properties under different land use patterns in Semi-arid Degraded Mountainous Areas”. Bulletin of soil and water conservation, 29 ,65-68.

Multifractal characteristics of soil particle-size distribution under different land-use types in an area with high frequency debris flow

Songyang Li[1,2,3], Jingyuan Lin[1], Jiahong Pan[1], Hang Yu[1,2,3], Ruoyun Gao[1,2,3], Liusheng Yang[1,2,3], Yongming Lin[1,2,3*], Daojie Wang[2,4], Jian Li[1,3]

1 College of Forestry, Fujian Agriculture and Forestry University, China

2 Key Laboratory of Mountain Hazards and Surface Processes, Chinese Academy of Sciences, China

3 Key Laboratory for Forest Ecosystem Process and Management of Fujian Province, China

4 Institute of Mountain Hazards and Environment, Chinese Academy of Sciences and Ministry of Water Conservancy, China

*Corresponding Author, e-mail: monkey1422@163.com

Abstract

Aiming to reveal the influence of different land use types on soil particle size distribution in the area with frequent debris flow, the multifractal characteristics of soil particle size distribution in the area with frequent debris flow were studied. Four typical land use types, including bare land, meadow, shrubs, and woodlands, were selected to collect soil samples of 5 soil layers from 3 soil profiles in each land use type for particle size analysis. The laser diffraction method was used to measure soil particle size distribution. We calculated multifractal parameters based on multifractal theory. ① Land use type has significant impact on the soil particle distribution. The volume fraction of silt particles in shrubs, forest is significantly larger than bare land, meadow, while the total volume fraction of sand particles is bare land, meadow is significantly larger than shrub, forest. The soil depth has no significant effect on soil particle size distribution in the depth range of 0-50 cm. ② In this study, the generalized dimensions spectra curves of soil particle distribution in bare land, meadow, shrub and forest are inverse "S" curve, while the singular spectrum function of the soil particle size is an asymmetric upward convex curve, indicate indicating that the soil particle size distribution at different depths of the plots has multifractal characteristics. The multifractal parameters of soil particle size distribution have significant differences in different land use types. The soil texture gradually becomes thinner following the sequence from bare land to woodlands. The heterogeneity of soil particle size distribution gradually decreases following the sequence of bare land – meadow – shrubs – woodlands. This study provided a theoretical basis for the evaluation of soil structure improvement and vegetation restoration effects in areas with frequent debris flow.

Keywords: High-frequency debris flow area, Soil particle-size distribution, Multifractal, Soil texture

1 Introduction

Soil particle-size distribution refers to the percentage of soil particles with different particle sizes (particle groups) in soil, which has significant effects on soil bulk density, porosity, soil organic matter and cation exchange capacity (Wang et al., 2019; Bieganowski et al., 2013). Soil is a kind of porous medium, the soil particle-size distribution has obvious fractal characteristics (Zhang et al., 2017). Therefore, based on fractal theory, domestic and foreign scholars studied the variation characteristics of soil particle-size distribution under different soil parent materials (Jiang et al., 2017), different land use types (Xia et al., 2013) and different vegetation types (Xia et al., 2020), which proved the practicability of soil fractal theory. At present, the fractal characteristics of soil particle-size distribution are mostly studied by single fractal dimension (Wang et al., 2019; Luo et al., 2019). The results can only obtain the overall or average characteristics of soil particle size distribution, and can not clearly understand the local heterogeneity of soil particle size distribution (Guan et al., 2011; Bai et al., 2012). Therefore, some scholars use single fractal and multifractal theory to describe soil particle-size distribution at the same time. The results showed that multifractal parameters can be used together with single fractal parameters to completely describe the characteristics of soil particle-size distribution (Sun et al., 2015; Li et al., 2018). At present, the multifractal theory is widely used in the study in semi-arid desert area (Wang et al.,2018), loess hilly area (Wang et al., 2014), and abandoned tailings reclamation area (Min et al., 2017), but it is rarely involved in high frequency debris flow areas.

Affected by special climate and terrain conditions, debris flow disasters occur frequently in Jiangjiagou gully of Yunnan Province, which is a representative debris flow gully in southwest China (Huang et al., 2015). The study of soil particle size distribution in high frequency debris flow areas can further understand the soil structure characteristics of debris flow provenance, which is helpful to deepen the understanding of the occurrence mechanism of debris flow. Predecessors have done a lot of research on soil particle-size distribution in debris flow area using fractal dimension theory. The fractal dimension characteristics of soil particle size of different coverage meadow in Jiangjiagou gully were described. The relationship between fractal dimension and soil structure, bulk density and organic matter (Xie et al., 2011) was discussed by using fractal theory. Fractal theory is used to analyze the particle size distribution of gravel soil in debris flow source area, and the relationship between fractal dimension and soil particle composition (Huang et al., 2012) is discussed. The fractal characteristics of soil particles of five different vegetation types in Jiangjiagou gully, and the relationship between fractal dimension and soil nutrients were analyzed (Chen et al., 2016). The above studies have deepened the understanding of the relationship between soil particle size distribution and soil properties in high frequency debris flow areas. However, these studies only used single fractal dimension to analyze, and lacked the understanding of the local variation characteristics of soil particle-size distribution in different land use types, and cannot accurately determine the response mechanism of soil texture when land use type changes. Therefore, our study uses multifractal theory to analyze the soil particle-size distribution characteristics of four main land use types (bare land, meadow, shrub, forest) in high frequency debris flow areas, and studies the relationship between multifractal parameters and soil texture, aiming to reveal the influence of land use types on soil particle-size distribution in high frequency debris flow areas, and provide theoretical support for ecological restoration and land use optimization in disaster-prone areas.

2 Material and methods

2.1 Study area

Our study area was the Jiangjiagou Gully (26°13′-26°17′N, 103°6′-103°13′E), located in Dongchuan District, Kunming City, Yunnan Province, southwest of China. Its elevation ranges from 1042m to 3269m above sea level(asl). Jiangjiagou gully is a high mountain canyon landform with large elevation difference (Guo et al.,2011), rainfall concentrated in May-October, showery rain and rainstorm are the main types of rainfall in this area. Due to severe soil and water loss, viscous debris flows have occurred frequently in Jiangjiagou Gully since the early Late Pleistocene. As a result of the natural and artificial factors, original vegetation has been replaced by artificial forest, Forest land, shrubs, meadow, bare land and cultivated land are the main land use types in the study area. The main soil types in this area are dry red soil, red yellow soil and gravel soil (Guo et al., 2012)

2.2 Study subjects and soil sample collection

In July to August, 2019, four typical land use types, including bare land, meadow, shrubs, and forest lands, were selected as the study objects (Table 1). Three quadrats were selected in each of the four sample plots (Forest land, shrubs, meadow, and bare land). In each selected quadrat, at least five soil samples were collected from the 0–10 cm, 10–20 cm, 20–30 cm,30-40 cm, and 40-50 cm soil layers. The soil samples were taken to the lab and air-dried in shady and cool areas for later use. A total of 60 soil samples were collected from the four land use types.

Table 1 Characteristics of all plots

Land use type	soil types	Longitude	Latitude	Elevation/(m)	Aspect	Slope/(°)	Coverage/(%)	Main vegetation species
Bare land	Red-yellow soil	103°08′11″E	26°14′46″N	1356	NE	24	5	/
Meadow	Red-yellow soil	103°07′34″E	26°14′55″N	1288	NE	20	40	*Heteropogon contortus, Ageratina adenophora*
Shrub	Red-yellow soil	103°08′01″E	26°14′53″N	1337	SW	19	80	*Desmodium racemosum, Heteropogon contortus*
forest	Red-yellow soil	103°08′04″E	26°14′44″N	1347	NE	20	90	*Leucaena leucocephala, Sophora davidii, Coriaria sinica, Themeda japonica, Arthraxon lancif olius*

2.3 Determination of the soil particle size distribution of the soil samples

The soil particle composition was measured using a laser particle analyzer (Mastersizer 2000, Malvern Company, UK). The plant roots and litter were removed from the air-dried samples before they were passed through a 2.0 mm sieve. A 10% H_2O_2 solution was added to each 0.3 g soil sample to remove organic matter, and a 10% HCl solution was added to remove carbonate salts. Deionized water was added and the liquid supernatant was then removed. Subsequently, the pH was adjusted to 6.5-7. The 0.1 mL/L sodium hexametaphosphate was added, and after ultrasonic vibration for 10 min, the laser particle analyzer was used to measure the percentage volume of soil particles in the range 0.02–2000μm.

2.4 Calculation of the multifractal parameters

The measurement interval I = [0.02, 2000] of the laser particle size analyzer is divided into 64 smaller intervals $I_i = [\varphi_i, \varphi_{i+1}]$, $I = 1, 2\ldots, 64$, with constant $\lg(\varphi_{i+1}/\varphi_i)$. A new dimensionless $J = [0, 5.3]$ can then be created. A number $N(\varepsilon) = 2^k$ of cells with equal size $\varepsilon = 5.3 \times 2^{-k}$ for k is set up ranging from 1 to 5 (i.e., ε= 2.65 to 0.165625). We created a certain measure μ that distributes over the interval of sizes I and each cell $\mu_i(\varepsilon)$ is contained in available data. $N(\varepsilon)$ is taken as the number of samples when the scale is ε; and $\mu_i(\varepsilon)$ is the probability density (percentile) of the ith subinterval (J_i), namely the sum of all measurements in the sub interval J_i. The generalized fractal dimension D_q is defined as follows:

$$D_q = \lim_{\varepsilon\to 0}\frac{1}{q-1}\frac{\lg\left[\sum_{i=1}^{N(\varepsilon)}\mu_i(\varepsilon)^q\right]}{lg\varepsilon}(q \neq 1) \tag{1}$$

$$D_1 = \lim_{\varepsilon\to 0}\frac{\sum_{i=1}^{N(\varepsilon)}\mu_i(\varepsilon)\lg\mu_i(\varepsilon)}{lg\varepsilon}(q = 1) \tag{2}$$

The singularity spectrum may be computed through a parameter q by:

$$\alpha(q) = \lim_{\varepsilon\to 0}\frac{\sum_{i=1}^{N(\varepsilon)}\mu_i(q,\varepsilon)\lg\mu_i(\varepsilon)}{\lg\varepsilon} \tag{3}$$

$$f(\alpha) = \lim_{\varepsilon\to 0}\frac{\sum_{i=1}^{N(\varepsilon)}\mu_i(q,\varepsilon)\lg\mu_i(q,\varepsilon)}{\lg\varepsilon} \tag{4}$$

Using the formula (1) ~ (4), in the range of $-10 \leq q \leq 10$, the fitting calculation is carried out with 1 as the step size to get $D(q)$, $\alpha(q)$ and $f(\alpha)$. When $q = 0$, D_0 is the capacity dimension, also called box-counting dimension, it reflects the range of a continuous distribution. When $q = 1$, D_1 is the entropy dimension of the measure, providing a measure of the heterogeneity of soil particle size distribution. When $q = 2$, D_2 is the correlation dimension that can capture some of the inner details of the particle-size distributions. D_1/D_0 can be used to quantitatively describe the dispersion degree of soil particle size distribution (Guan et al., 2011).

$\alpha(q)$ and $f(\alpha)$ can characterize local multifractal characteristics of soil particle size distribution, α_0 is the average value of multifractal singular spectrum, The greater the α_0, the smaller the local density of soil particle size distribution. $\Delta\alpha = \alpha_{max}-\alpha_{min}$ is the width of multifractal singular spectrum, it represents the spatial heterogeneity of soil particle size distribution. $\Delta f = f(\alpha_{min})- f(\alpha_{max})$ reflects the shape of multifractal singular spectrum, when $\Delta f(\alpha) > 0$, $f(\alpha)$ is a left hook upper convex curve (Tian et al., 2020).

2.5 Data analysis

Correlation and significance analysis were carried out using the IBM SPSS Statistics 23. Data processing and charting used Microsoft Excel 2018 and Origin 2018. All data in all tables are mean ± standard error.

3 Results

3.1 Characteristics of soil particle-size distribution

The soil particle size distribution particle size distribution of all land use types followed the order of silt (35.18%-74.04%) > sand (12.73%-59.10%) > clay (5.51%-14.94%) (Table 2). The volume fraction distribution of silt and sand was high under the bare land and meadow. The sand content of the bare land and meadow was dominated by middle sand. The volume fraction distribution of silt was high under the shrub and forest, lacked coarse sand and very coarse sand. The soil texture of bare land and meadow is loam, shrub and forest is silt loam based on USDA classification system of soil texture (Wu et al., 2019).

For different soil layer under the same land use type the content of clay, silt and sand had no significant different, but for different land use type under the same soil layer, the volume fraction of silt in shrub and forest was significantly higher than bare land and Meadow ($P < 0.05$). The total volume fraction of sand in bare land and meadow was significantly higher than shrub and forest.

Table 2 Volume percentage of soil particle-size Distribution

Land use type	Soil depth (h/cm)	Clay (r/%) (< 2 μm)	Silt (r/%) (2-50μm)	Sand					Sand (r/%) (50-2000 μm)
				Very fine sand (r/%) (50-100 μm)	Fine sand (r/%) (100-250 μm)	Medium sand (r/%) (250-500 μm)	Coarse sand (r/%) (500-1000 μm)	Very Coarse sand (r/%) (1000-2000 μm)	
Bare land	0-10	7.10 ± 0.37^{Acd}	48.48 ± 5.86^{Ab}	15.26 ± 6.23^{Aa}	11.56 ± 2.39^{Aa}	14.25 ± 8.78^{Aa}	3.33 ± 3.67^{Aa}	0.02 ± 0.01^{Aa}	43.73 ± 4.79^{Aa}
	10-20	6.85 ± 0.72^{Ab}	43.86 ± 0.83A^{Bb}	11.53 ± 0.20^{Aa}	10.66 ± 2.33^{Aa}	19.26 ± 1.86^{Aa}	7.47 ± 3.57^{Aa}	0.35 ± 0.34^{Aa}	49.28 ± 1.48^{Aa}
	20-30	6.13 ± 0.76^{Aa}	39.81 ± 8.68^{ABb}	11.44 ± 0.67^{Aa}	11.38 ± 2.81^{Aa}	21.32 ± 3.75^{Aa}	7.59 ± 3.10^{Aa}	0.34 ± 0.29^{Aa}	50.37 ± 9.67^{Aa}
	30-40	5.87 ± 0.10^{Ac}	38.69 ± 3.21^{Bb}	12.38 ± 1.34^{Aa}	13.12 ± 2.85^{Aac}	20.88 ± 0.73^{Aa}	8.39 ± 0.77^{Aa}	0.09 ± 0.03^{Aa}	53.91 ± 3.36^{Aa}
	40-50	5.51 ± 0.11^{Ad}	35.18 ± 2.83^{ABb}	11.54 ± 0.12^{Aab}	12.30 ± 0.65^{Ab}	22.75 ± 1.38^{Aa}	11.92 ± 0.63^{Aa}	0.59 ± 0.71^{Aa}	59.10 ± 2.54^{Aa}
Meadow	0-10	8.08 ± 0.65^{Abd}	46.38 ± 5.20^{Ab}	13.64 ± 1.69^{Aa}	13.16 ± 2.77A^{Ba}	15.57 ± 1.99^{Aa}	3.33 ± 2.20^{Aa}	0.04 ± 0.03^{Aa}	43.28 ± 2.41^{Aa}
	10-20	7.59 ± 0.21^{Ab}	45.84 ± 7.09^{Ab}	13.01 ± 2.45^{Aa}	10.57 ± 0.97^{Ba}	17.00 ± 5.13^{Aa}	5.90 ± 1.87^{Aa}	0.09 ± 0.05^{Aa}	43.71 ± 4.50^{Aa}
	20-30	7.52 ± 1.11^{Ab}	42.67 ± 4.90^{Ab}	11.56 ± 1.26^{Aa}	10.04 ± 1.14^{Ba}	15.16 ± 0.31^{Aa}	6.46 ± 3.15^{Aa}	0.80 ± 0.35^{Aa}	44.02 ± 2.90^{Aa}
	30-40	9.06 ± 0.57^{Ab}	47.08 ± 11.83^{Ab}	12.35 ± 0.14^{Aa}	14.18 ± 3.24^{ABa}	15.50 ± 4.47^{Aab}	2.32 ± 1.98^{Ab}	0.00 ± 0.00^{Aa}	44.36 ± 8.84^{Ab}
	40-50	7.44 ± 0.23^{Ac}	39.92 ± 0.90^{Ab}	14.44 ± 0.13^{Aa}	16.77 ± 3.09^{Aa}	13.36 ± 3.83^{Ab}	0.19 ± 0.08^{Ab}	0.00 ± 0.00^{Ab}	44.76 ± 7.07^{Aa}
Shrub	0-10	10.45 ± 1.36^{Ab}	72.13 ± 5.83^{Aa}	7.34 ± 2.83^{Ab}	5.34 ± 2.67^{Ab}	4.45 ± 0.98^{Ab}	0.30 ± 0.28^{Ab}	0.00 ± 0.00^{Aa}	18.42 ± 7.19^{Ab}

	10-20	10.51 ± 0.68^{Aa}	71.52 ± 1.21^{Aa}	9.41 ± 0.99^{Aa}	6.08 ± 0.91^{Aa}	2.42 ± 0.75^{Ab}	0.08 ± 0.07^{Ab}	0.00 ± 0.00^{Ab}	17.99 ± 0.55^{Ab}
	20-30	10.50 ± 1.23^{Ab}	66.50 ± 4.09^{Aa}	10.1 ± 1.81^{Aa}	6.70 ± 2.22^{Ab}	3.31 ± 2.22^{Ab}	0.07 ± 0.06^{Ab}	0.00 ± 0.00^{Ab}	20.09 ± 7.51^{Ab}
	30-40	10.91 ± 0.46^{Aab}	65.61 ± 0.50^{Aa}	9.64 ± 0.36^{Aa}	8.22 ± 1.79^{Abc}	5.14 ± 0.98^{Aa}	0.33 ± 0.28^{Ab}	0.00 ± 0.00^{Aa}	23.32 ± 1.12^{Ac}
	40-50	10.92 ± 0.74^{Ab}	65.15 ± 5.10^{Aa}	10.08 ± 0.32^{Ab}	7.20 ± 0.37^{Ac}	4.93 ± 2.43^{Ac}	0.47 ± 0.40^{Ab}	0.00 ± 0.00^{Ab}	22.67 ± 4.93^{Ab}
Forest	0-10	12.91 ± 1.90^{Aa}	74.04 ± 5.78^{Aa}	7.06 ± 0.68^{Ab}	3.10 ± 0.86^{Ab}	2.42 ± 0.42^{Ab}	0.14 ± 0.07^{Ab}	0.00 ± 0.00^{Aa}	12.73 ± 2.24^{Ab}
	10-20	13.43 ± 1.92^{Aa}	62.51 ± 12.78^{Aab}	8.58 ± 3.35^{Ab}	9.83 ± 7.22^{Aa}	6.51 ± 5.01^{Ab}	0.14 ± 0.13^{Ab}	0.00 ± 0.00^{Ab}	25.06 ± 15.64^{Ab}
	20-30	14.94 ± 0.32^{Aa}	73.98 ± 3.64^{Aa}	7.31 ± 0.74^{Ab}	8.86 ± 5.61^{Aa}	11.34 ± 8.43^{Aa}	0.74 ± 0.50^{Ab}	0.00 ± 0.00^{Ab}	13.09 ± 3.96^{Ab}
	30-40	13.23 ± 1.62^{Aa}	61.22 ± 10.45^{Aab}	8.92 ± 0.92^{Aa}	7.52 ± 4.20^{Aac}	8.65 ± 6.99^{Aab}	2.21 ± 2.03^{Ab}	0.01 ± 0.00^{Aa}	13.42 ± 1.17^{Ad}
	40-50	13.14 ± 0.41^{Aa}	72.15 ± 4.78^{Aa}	7.06 ± 2.07^{Ab}	3.19 ± 0.77^{Ac}	1.83 ± 1.33^{Ac}	0.08 ± 0.07^{Ab}	0.00 ± 0.00^{Ab}	14.47 ± 1.91^{Ac}

Different capital letters in the same column indicate significant differences between different soil depth of the same land use type ($P < 0.05$); different lowercase letters in the same column indicate significant differences between different land use types of the same soil depth ($P < 0.05$).

2.2 Multifractal characteristics of soil particle-size distribution

Using eqs. (1) and (2), Rényi dimensions spectra $D(q)$ were calculated for $-10 \leq q \leq 10$ at 1 lag increment (Fig. 1). The generalized dimensional spectrum of the soil particle-size distribution under different land use types decreased in an inverse "S" pattern (Fig. 1), which can be described by sigma-shape curve (Paz et al., 2010). The multifractal parameters, followed the order of $D_0 > D_1 > D_2$ for each land use type, indicating that the particle-size distribution of each land use type is nonuniform and can be subjected to multifractal analysis.

With the increase of soil depth, D0, D1, D1/D0 and D2 of bare land decreased first and then increased in the depth range of 0-40 cm, and the maximum values appeared in the 30-40 cm soil layer. The maximum values of D0, D1, D1/D0 and D2 in meadow all appeared in 40-50 cm soil layer. D0, D1, and D2 of shrub increased first and then decreased, and D1/D0 decreased gradually. D0, D1, D1/D0 and D2 of forest increased first and then decreased.

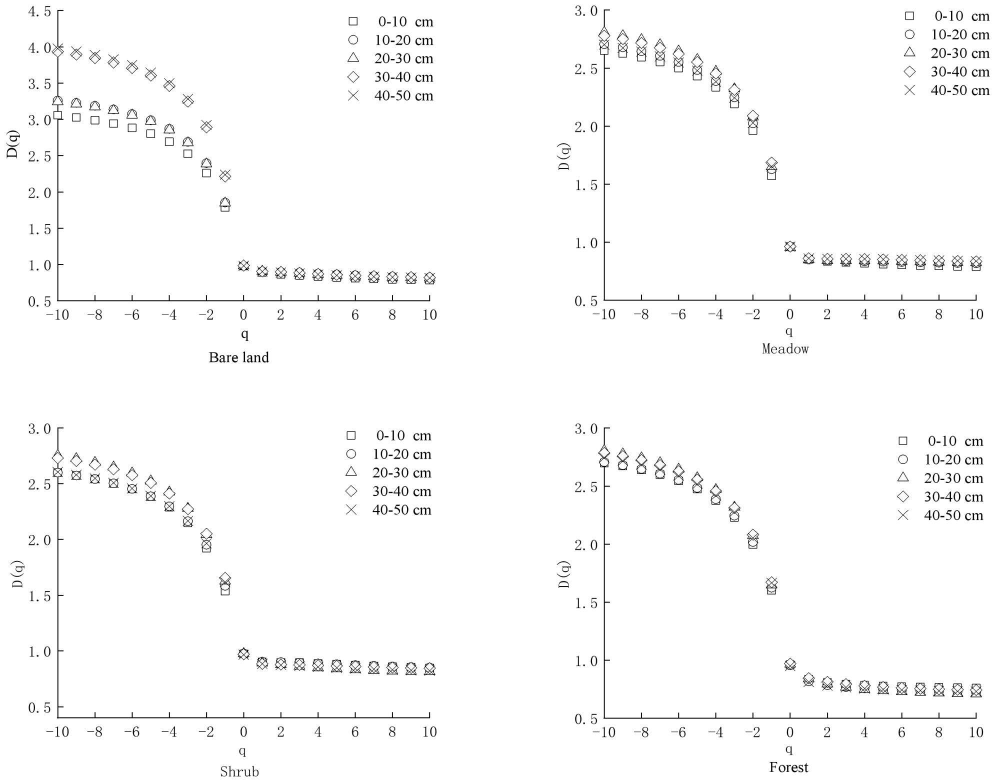

Figure 1 Generalized dimensions spectra for soil particle size distribution under different land use types

As seen in Fig. 1 and Fig. 2, Capacity dimension (D0) were ranked as forest > shrub > bare land > meadow. It shows that the range of soil particle-size distribution in forest and shrub is wider than that in bare land and meadow. The values of D1, D1/D0 and D2 were ranked as forest > shrub >meadow >bare land. Indicating that the heterogeneous of soil particle-size distribution were ranked as forest > shrub >meadow >bare land.

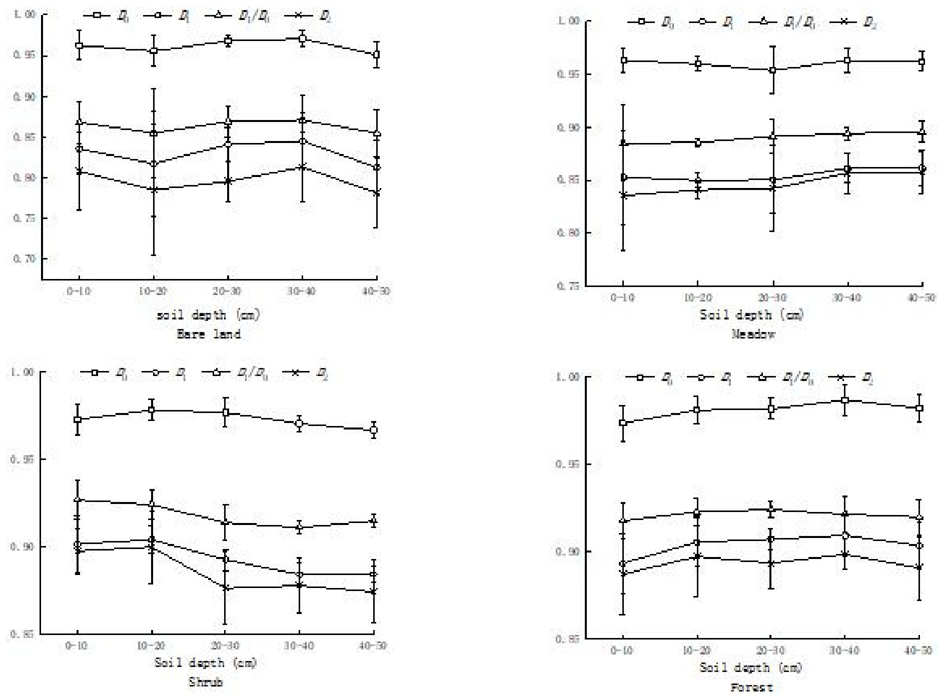

Figure 2 Multifractal generalized spectra parameters for soil particle size distribution under different land use types

Using eqs. (3) and (4), Multifractal singularity spectra function were calculated (Fig. 3). The f(α) - α plots in Fig. 3 have a strong non-symmetric parabolic downward shape, indicating that the soil layers at different depths in all land use types showed heterogeneous characteristics and multifractal characteristics. In addition, all samples showed singularity spectra with a clear left branch, and all Δf values are greater than 0, indicating that the large probability subset was dominant in soil.

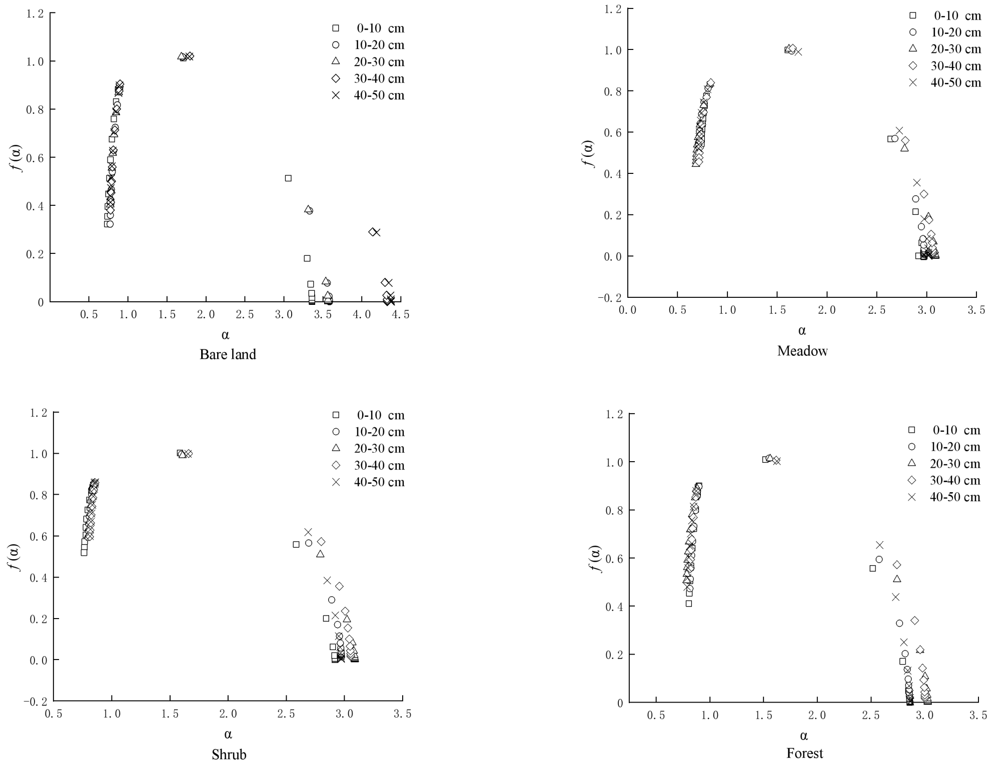

Figure 3 Multifractal singularity spectra function for soil particle size distribution under different land use types

As seen in Table 3, the α 0 of bare land gradually increased with the increase of depth in the range of 0-50 cm, indicating that the local density of soil particle-size distribution gradually increased with the increase of depth, and the α 0 was the largest at the depth of 30-40 cm. The value of Δα gradually increased with the increase of depth, indicating that the unevenness of soil particle size distribution gradually increased with the increase of soil depth. The value of α 0 showed a gradual increase trend in meadow, shrub and forest, and Δα increased first and then decreased, with a maximum value in 20-30 cm soil layer. The value of α 0 in different land use type followed the order of bare land (1.686-1.795) > meadow (1.606-1.711) > shrub (1.587-1.661) >forest (1.517-1.624), The value of Δα in different land use type followed the order of bare land (2.626-3.600) > meadow (2.231-2.402) > shrub (2.155-2.286) >forest (2.043-2.245).

2.3 Relationship between soil texture and multifractal parameters

Table 4 compares Pearson correlations between soil texture and multifractal parameters of soil particle-size distribution. We found that the volume fraction of clay was significantly negatively correlated with very fine sand and sand ($P < 0.01$). The volume fraction of silt was significant positive correlation with multifractal parameters D_0, D_1 and α_0 ($P < 0.05$), and extremely significant positive correlation with $\Delta\alpha$ and Δf. There was no significant relationships between the volume fraction of fine sand, very fine sand, medium sand and multifractal parameters. There was a significant negative correlation between coarse sand and α_0, a extremely significant negative correlation between extremely coarse sand and α_0, and a significant negative correlation between extremely coarse sand and Δα. The volume fraction of total sand content was significantly negatively correlated with D_0, D_1 and Δf.

Table 3 Parameters of multifractal spectrum for soil particle size distribution under different land use types

Land use type	Soil depth (h/cm)	α_0	α_{max}	α_{min}	$\Delta\alpha = \alpha_{max}-\alpha_{min}$	$f(\alpha_{max})$	$f(\alpha_{min})$	$\Delta f = f(\alpha_{max})-f(\alpha_{min})$
Bare land	0-10	1.709 ± 0.034	3.362 ± 0.086	0.736 ± 0.096	2.626	1.013 ± 0.013	0.000 ± 0.000	1.012
	10-20	1.700 ± 0.019	3.586 ± 0.012	0.771 ± 0.051	2.815	1.017 ± 0.008	0.000 ± 0.000	1.017
	20-30	1.686 ± 0.012	3.569 ± 0.034	0.773 ± 0.051	2.796	1.017 ± 0.006	0.000 ± 0.000	1.017
	30-40	1.795 ± 0.025	4.326 ± 0.029	0.776 ± 0.029	3.550	1.021 ± 0.009	0.000 ± 0.000	1.021
	40-50	1.788 ± 0.027	4.374 ± 0.068	0.775 ± 0.061	3.600	1.018 ± 0.008	0.000 ± 0.000	1.018
Meadow	0-10	1.606 ± 0.060	2.970 ± 0.031	0.739 ± 0.073	2.231	0.998 ± 0.018	-0.001 ± 0.002	0.999
	10-20	1.646 ± 0.122	2.978 ± 0.056	0.703 ± 0.087	2.275	0.994 ± 0.012	0.007 ± 0.011	0.986
	20-30	1.618 ± 0.023	3.087 ± 0.085	0.685 ± 0.056	2.402	1.004 ± 0.007	-0.001 ± 0.002	1.004
	30-40	1.655 ± 0.034	3.062 ± 0.148	0.714 ± 0.046	2.348	1.006 ± 0.010	0.009 ± 0.013	0.997
	40-50	1.711 ± 0.074	3.019 ± 0.015	0.710 ± 0.046	2.310	0.989 ± 0.016	0.000 ± 0.002	0.989
Shrub	0-10	1.587 ± 0.086	2.917 ± 0.057	0.762 ± 0.076	2.155	1.001 ± 0.008	0.000 ± 0.001	1.002
	10-20	1.600 ± 0.018	2.975 ± 0.051	0.796 ± 0.010	2.179	0.995 ± 0.007	0.014 ± 0.000	0.981
	20-30	1.609 ± 0.024	3.088 ± 0.024	0.803 ± 0.052	2.286	0.989 ± 0.022	0.011 ± 0.000	0.979
	30-40	1.661 ± 0.029	3.055 ± 0.121	0.811 ± 0.027	2.243	0.999 ± 0.012	0.015 ± 0.011	0.984
	40-50	1.656 ± 0.015	2.972 ± 0.014	0.814 ± 0.023	2.159	0.998 ± 0.009	0.003 ± 0.000	0.995
Forest	0-10	1.517 ± 0.015	2.860 ± 0.014	0.805 ± 0.045	2.056	1.008 ± 0.009	0.000 ± 0.000	1.008
	10-20	1.551 ± 0.017	2.857 ± 0.042	0.814 ± 0.075	2.043	1.014 ± 0.006	0.014 ± 0.000	1.000
	20-30	1.561 ± 0.026	3.028 ± 0.070	0.783 ± 0.098	2.245	1.013 ± 0.008	0.001 ± 0.000	1.011
	30-40	1.617 ± 0.052	3.003 ± 0.097	0.817 ± 0.077	2.186	1.006 ± 0.005	0.017 ± 0.018	0.990
	40-50	1.624 ± 0.015	2.866 ± 0.042	0.789 ± 0.085	2.077	1.002 ± 0.005	0.003 ± 0.000	1.000

2.3 Relationship between soil texture and multifractal parameters

Table 4 compares Pearson correlations between soil texture and multifractal parameters of soil particle-size distribution. We found that the volume fraction of clay was significantly negatively correlated with very fine sand and sand ($P < 0.01$). The volume fraction of silt was significant positive correlation with multifractal parameters D_0, D_1 and α_0 ($P < 0.05$), and extremely significant positive correlation with $\Delta\alpha$ and Δf. There was no significant relationships between the volume fraction of fine sand, very fine sand, medium sand and multifractal parameters. There was a significant negative correlation between coarse sand and α_0, a extremely significant negative correlation between extremely coarse sand and α_0, and a significant negative correlation between extremely coarse sand and $\Delta\alpha$. The volume fraction of total sand content was significantly negatively correlated with D_0, D_1 and Δf.

Table 4 Correlation analysis between soil textures and multifractal parameters

	Clay	Silt	Very fine sand	Fine sand	Medium sand	Coarse sand	Very Coarse sand	Sand	D_0	D_1	D_1/D_0	D_2	α_0	$\Delta\alpha$	Δf
Clay	1														
Silt	0.063	1													
Very fine sand	-0.296**	0.027	1												
Fine sand	-0.125	0.015	0.009	1											
Medium sand	-0.092	-0.148	-0.227*	0.136	1										
Coarse sand	0.086	0.093	-0.021	-0.169	-0.068	1									
Very Coarse sand	-0.051	-0.054	-0.049	-0.053	0.028	0.177	1								
Sand	-0.461**	-0.057	0.139	0.105	0.217*	0.104	-0.042	1							
D_0	0.022	0.222*	0.018	-0.011	-0.066	-0.052	-0.161	-0.234*	1						
D_1	0.021	0.225*	-0.021	0.042	-0.017	-0.079	-0.198	-0.217*	0.879**	1					
D_1/D_0	0.016	0.193	-0.042	0.072	0.019	-0.087	-0.197	-0.173	0.686**	0.950**	1				
D_2	0.006	0.205	-0.005	0.005	0.039	-0.052	-0.185	-0.115	0.718**	0.904**	0.909**	1			
α_0	0.109	0.213*	-0.040	0.168	0.100	-0.224*	-0.375**	-0.064	0.155	0.245*	0.269*	0.282**	1		
$\Delta\alpha$	-0.052	0.279**	0.034	0.082	0.104	-0.082	-0.231*	-0.046	0.194	0.260*	0.266*	0.256*	0.826**	1	
Δf	-0.015	0.328**	-0.014	0.149	-0.061	0.067	0.075	-0.244*	0.177	0.188	0.168	0.130	0.246*	0.538**	1

* means significantly correlated at the 0.05 level, ** means significantly correlated at the 0.01 level.

3 Discussion

Soil particle size distribution can affect the structure and properties of soil. Different land use types are one of the important reasons for the difference of soil particle size distribution (Gui et al., 2011). In this study, the volume fractions of clay and silt in shrub and forest soil were significantly increased compared with those in bare land and meadow ($P < 0.05$), and the sand content was significantly decreased. The homogeneous degree of soil particle-size distribution followed the order of bare land > meadow > shrub > forest, this result is consistent with the findings of Liu et al (Liu et al., 2017), this is because in our study, the roots of shrub (*Desmodium racemosum*) and forest (*Leucaena leucocephala*) were more developed than those of grassland (*Heteropogon contortus*) (Zheng, 2015), plant root system has stronger improvement effect on soil. Jiangjiagou gully is located in the lower reaches of Jinsha River, and the main soil erosion pattern is hydraulic erosion (Li et al., 2012). The different intensities of runoff and sediment yield in different land use types is also one of the reasons for the differences in soil particle-size distribution. Due to the absence of vegetation cover, under the interaction of rainfall and runoff, a large number of fine soil particles are lost in the bare land, resulting in uneven soil particle-size distribution. Previous studies suggest that shrub and forest have stronger sediment reduction capacity than meadow (Ai et al., 2013). In this study, the trees in forest had a large canopy. Although the shrub also had a certain canopy, the canopy of the forest had a stronger ability to intercept rainfall. The understory vegetation of forest was rich, and it had a hierarchical structure of trees, shrubs and herbs. The ability to reduce the river valley wind and surface runoff was stronger than that of the shrub, reducing the splash and runoff erosion. Therefore, compared with the shrub and meadow, the forest had a more homogeneous soil particle size distribution. In the depth range of 0-50 cm, there was no significant difference in soil particle-size distribution at different depths of the same land use type, which was similar to the results of Zhou et al (Zhou et al., 2009), but different from the results of Xia et al (Xia et al., 2020). This is because all land use types in this study are perennial landslide deposits, the soil parent material sources and soil texture of each soil layer in the same land use type soil profile are basically the same, and the vegetation restoration period is only 6-15 years, which confirms the previous conclusion that vegetation restoration within 40 years has no significant effect on soil texture at different depths (Qi et al., 2018). In different land use types, with the increase of soil depth, the range and homogeneous degree of soil particle-size distribution changed greatly in bare land. However, meadow, shrub and forest changed little, which may be because the growth of vegetation reduced the erosion of rainfall and runoff on surface soil particles, maintained the original state of surface soil particle size distribution, and had little difference from deep soil.

In this study, the volume fraction of silt was significantly or extremely significantly correlated with D_0, D_1, α_0, $\Delta\alpha$ and Δf, indicating that the volume fraction of silt had a significant impact on the multifractal parameters of soil particle size distribution, which was different from the results of Wang et al (Wang et al., 2018) and Sun et al (Sun et al., 2015) that the volume fractions of sand and fine sand were the main influencing factors of multifractal parameters. In this study, the values of Δf were all greater than 0, indicating that soil particles with large probability size had a major impact on soil particle size distribution. The soil textures of bare land and meadow were loam, and the silt content was close to the total sand content, which was much larger than the clay content. The soil textures of shrub and forest were silt loam, and the silt volume fraction was much larger than the clay and sand. Meanwhile, the volume fraction of silt in our study was 35.18 %-74.04 %, which was much higher than Wang et al (Wang et al., 2018) (35.94 % -42.89 %) and Sun et al (Sun et al., 2015)(7.84 % -17.05 %). Therefore, the volume fraction of silt had a significant impact on the multifractal parameters of soil particle size distribution. Different land use types had significant effects on soil multifractal parameters, which confirmed the results of Qi et al (Qi et al., 2018).

4 Conclusions

In our study, we analyzed the differences between soil particle size distribution and multifractal parameters, which promoted the understanding of water and soil conservation capacity of different land use types and provided theoretical basis for ecological restoration of debris flow basin. There were significant differences in soil particle-size distribution among different land use types. The volume fractions of clay and silt followed the order of forest > shrub > meadow > bare land, while the volume fraction of sand was opposite. Correlation analysis showed that different land use types had significant effects on soil particle volume fraction and multifractal parameters of soil particle size distribution, indicating that different land use types had different ability to change soil structure, affecting the erosion and accumulation of soil particles. Vegetation restoration in high frequency debris flow areas could increase fine particles in soil, which was helpful to improve soil texture.

The soil particle size in our study area is nonhomogeneous distributed and has multifractal characteristics. The analysis results of multifractal parameters are consistent with the measured soil particle size distribution, indicating that multifractal theory can reveal the small difference of soil volume fraction when land use changes in the high frequency debris flow area.

The volume fraction of silt has a great influence on the local density and heterogeneity of soil particle-size distribution in the study area. Therefore, in the process of soil improvement in Jiangjiagou gully, we should pay attention to the influence of the volume fraction of silt in soil.

References

Ai, N., Wei, TX.. Zhu, QK. (2013). “The effect of rainfall for runoff-erosion-sediment yield under the different vegetation types in Loess Plateau of northern Shaanxi province”. Journal of Soil and Water Conservation, 27 (2), 26-30+35.

Bieganowski, A., Chojecki, T., Ryżak, M., Sochan, A., & Lamorski, K. (2013). “Methodological aspects of fractal dimension estimation on the basis of particle size distribution”. Vadose Zone Journal, 12(1), 1-9.

Bai, YR,, Wang, YK. (2012). “Monofractal and multifractal analysis on soil particle distribution in hilly and gully areas of the loess plateau”. Transactions of the Chinese Society for Agricultural Machinery, 43(3), 43-48+42.

Chen, AM., Deng, HJ., Yan, SW., Lin, YM., Zhang, GS., Du, K. (2016). “Fractal features of soil and their relation with soil fertility under five vegetation in Jiangjiagou gully”. Mountain Research , 34(3), 290-296.

Guan, XY., Yang, PL., Lv, Y. (2011). “Analysis on spatial variability of soil properties based on multifractal theory”. Journal of Basic Science and Engineering, 19(5), 712-720.

Yang, PL., Lv, Y. (2011). “Relationships between soil particle size distribution and soil physical properties based on multifractal”. Transactions of the Chinese Society for Agricultural Machinery, 42(3), 44-50.

Guo, XJ., Cui, P., Zhu, XH. (2011). “Flow simulation in a typical debris flow basin of Jiangjia canyon”. Bulletin of Soil and Water Conservation, 31(1), 175-179.

Guo. XJ., Cui, P., Zhu, XH.(2012). “Soil infiltration and runoff generation characteristics in Jiangjia gulley with frequent debris flow”. Mountain Research,. 30(5), 585-591.

Gui, DW., Lei, JQ., Zeng, FJ., Mu, GJ., Li, KF. (2011). “Characteristics of soil particle size distribution in different land-use types of Oasis Rim”. Scientia Silvae Sinicae, 47(1), 22-28.

Huang, Y., Ding, MT., Miao, C., Wang, J., Zhou, P. (2015). “Characteristics and evolution of debris flow motion in Jiangjia gully in Yunnan province”. Resources and Environment in the Yangtze Basin, 24 (8): 1434-1442.

Huang, Q., Chen, NS., Zhu, YH., Lu, Y., Lv, LQ. (2012). “Particle size fractal characteristics of the gravel soil in original area of debris flow valleys”. Mountain Research, 30(5), 578-584.

Jiang, K., Qin, HL., Lu, Y., Jia, CJ., Liu, HY., Cui, QC. (2016). “Fractal demension of particle-size distribution for soils derived from diffirent parent materials in Guangdong province”. Journal of Soil and Water Conservation, 30(6), 319-324.

Luo, QH., Wu, JZ., Cui, Y., Sun, F., Lin, YM., Wang, DJ., Wu, CZ. (2019). “Characteristics of soil properties and fractal dimensions of destroyed and naturally restored forest land under flood disaster disturbance”. Chinese Journal of Applied and Environmental Biology, 25(1), 29-37.

Li, K., Yang, H., Han, X., Xue, L., Lv, Y., Li, J., ... & Zhang, Y. (2018). “Fractal features of soil particle size distributions and their potential as an indicator of Robinia pseudoacacia invasion 1”. Scientific reports, 8(1), 1-13.

Liu, ZQ., Gao, JX., Tian, MR., Li, ZF., Wang, YP. (2017). “Fractal dimension characteristics of soil particle size under different plant communities in ecological restoration area”. Chinese Journal of Ecology, 36(2), 303-308.

Li, B., Tang, Y. (2012). “Impacts of Human Activities on Soil Erosion in the Lower Jinsha River Basin”. Mountain Research, 30(3), 299-307.

Min, XY., Li, XJ., Li, QC. (2017). “Influence of mechanical compaction on reclaimed soil particle size distribution multifractal characteristics”. Transactions of the Chinese Society of Agricultural Engineering, 33(20), 274-283.

Qi, F., Zhang, R., Liu, X., Niu, Y., Zhang, H., Li, H., ... & Zhang, G. (2018). “Soil particle size distribution characteristics of different land-use types in the Funiu mountainous region”. Soil and Tillage Research, 184, 45-51.

Sun, Z., Wang, YB., Liu, GH., Gao, ZY. (2015). “Heterogeneity analysis of soil particle size distribution in the process of degradation of alpine meadow in the permafrost regions based on multifractal theory”. Journal of Glaciology and Geocryology, 37(4), 980-990.

Xiafei, T., Fenghuan, S., Xiaojun, G., Jingjing, L., & Yong, L. (2020). “Material sources supplying debris flows in Jiangjia Gully”. Environmental Earth Sciences, 79(13), 1-20.

Wang, J., Zhang, J., & Feng, Y. (2019). "Characterizing the spatial variability of soil particle size distribution in an underground coal mining area: An approach combining multi-fractal theory and geostatistics". Catena, 176, 94-103.

Wang, L., Yang, R., Zhang, S., Zhang, G., & Liu, X. (2019). "Fractal features and infiltration characteristics of the soil from different land uses in a small watershed in a rocky, mountainous area in Shandong Province". Journal of Forestry Research, 1-8.

Wang, Y., Meng, ZJ., Siqingbilige., Ding, YL., Wang, ZY., Wan, F., Wu, XL.(2018). "The research of surface soil particle size distribution characteristics based on multifractal in Semi-arid farmland". Soils, 50(4), 826-831.

Wang, JM., Zhang, M., Bai, ZK., Yang, RX., Guo, LL. (2014). "Multi-fractal characteristics of reconstructed soil particle in opencast coal mine dump in loess area". Transactions of the Chinese Society of Agricultural Engineering, 30(4), 230-238.

Wu, KN., Zhao, R. (2019). "Soil texture classification and its application in China". Acta Pedologica Sinica, 56 (1), 227-241.

Xia, JB., Zhang, SY., Wang, RR., Zhao, YY., Sun, JK., Liu, JT., Liu, Q.(2013). "Water ecology and fractal characteristics of soil particle size distribution of three typical vegetations in Shell Island". Acta Ecologica Sinica, 33(21), 7013-7022.

Xia, J., Ren, R., Chen, Y., Sun, J., Zhao, X., & Zhang, S. (2020). "Multifractal characteristics of soil particle distribution under different vegetation types in the Yellow River Delta chenier of China". Geoderma, 368, 114311.

Xie, XJ., Wei, FQ (2011). "Characteristics of soil particle fractal dimension under different coverage grassland of the area with high-frequency debris flow". Journal of Soil and Water Conservation, 25(4), 202-206.

Zhang, JR., Wang, JM., Zhu, YC., Li, B., Wang, P (2017). "Application of fractal theory on pedology: a review". Chinese Journal of Soil Science, 48(1), 221-228

Zheng, LW. (2015). "Effect of root system on soil properties". Beijing: Beijing Forestry University.

Zhou, XF., Zhao, R., Li, YY., Chen, XY (2009). "Effects of land use types on particle size distribution of reclaimed alluvial soils of the Yangtze Estuary". Acta Ecologica Sinica, 29(10), 5544-55

REQUALIFE: A Web-App to Assess and Predict the Eco-Morphological Quality of Water Courses

Paolo Di Pietro*[1], Nicola Mazzon[2], Fuding (Frank) Xu[3], Baiying (Calipso) Zhang[4]
1 Corporate Business Unit Senior Specialist, Officine Maccaferri S.p.A., Italy
2 R&D Manager, Maccaferri Innovation Center (M.I.C.), Italy
3 Technical Marketing Director, Maccaferri Changsha, China
4 DT Business Development, Maccaferri Changsha, China
*Corresponding Author, e-mail: p.dipietro@maccaferri.com

Abstract

This work aims at presenting the main features of an innovative Web-App platform named REQUALIFE. The application provides an objective quantitative assessment of the current eco-morphological quality of a watercourse or alternatively, in case of a new intervention, can provide a forecast of the potential improvement over time. REQUALIFE web application is based on the WEQUI evaluation method, which results from further developments of other existing and widely used ones. WEQUI shares with these methods a multidisciplinary and objective evaluation approach, based on 15 technical-environmental indicator values. Each option is associated to a score that follows an exponential scale from 1 to 16. In addition to the indicators commonly used in most evaluation methods, REQUALIFE also introduces the Carbon sequestration and Carbon footprint, with the purpose of considering the carbon cycle of a riverbank stabilization.

The Carbon sequestration indicator, as well as others included in WEQUI method, highlight the role of a riparian and floodplain vegetation, the importance of which plays a key role for both terrestrial and aquatic ecosystems. In this way the level of subjectivity and uncertainty during the compilation of WEQUI indicators is minimized.

Keywords: Eco-morphological quality, Indicators, Carbon sequestration, Carbon footprint, Channel morphology

1 Introduction

This work aims at presenting the main features of an innovative Web-App platform named REQUALIFE. The application provides an objective quantitative assessment of the current eco-morphological quality of a watercourse or alternatively, in case of a new intervention, can provide a forecast of the potential improvement over time. REQUALIFE web application is based on the WEQUI evaluation method, which results from further developments of other existing and widely used ones.

The WEQUI (Water Eco-morphological QUality Index) method was developed to create an index that defines the quality of the morphology and the ecosystems of watercourses. Special attention is paid to the role of riparian and floodplain vegetation. This method deals with the evaluation of the current conditions of the watercourse.

REQUALIFE was developed within a Research and Development Project funded by the ERDF 2014-2020 Program of the Autonomous Province of Bolzano in Italy, in collaboration with Naturstudio Srl, MavTech Srl and the University of Bolzano.

The WEQUI matrix was arranged to be applicable to a rather wide range of watercourses, with the exception of mountain streams in their upper part. The matrix has a list of indicators with various options/answers. Sometimes the identification of most appropriate answer for each indicator is not straightforward. In der to facilitate the choice, some practical indications are provided to minimize subjectivity and uncertainty during the compilation.

The relevance and environmental characteristics to be considered for each indicator are provided.

2 The WEQUI method main features

The WEQUI method is a further development of other existing and widely used methods based on a multidisciplinary approach using indicator values.

This method was developed to assess watercourses where river stabilization measures were used in the past and/or will be used in the future, with the scope of defining both the current quality status of a river stretch and to estimate the long-term eco-morphological quality in case of a future interventions. In the first case, the method allows to quantify the eco-morphological quality status of the watercourse, guiding the design choices towards an improvement of the overall quality.

In the second case, the method can be used to compare different design alternatives and to identify those able to support high-quality ecosystems.

In addition to indicators common to other evaluation methods, WEQUI introduces Carbon sequestration and Carbon footprint. The last one allows to include environmental cost in terms of CO2 emissions associated in the analysis for the production and installation of a riverbank protection. The carbon sequestration allows the calculation of the CO2 absorption capacity associated to vegetation grown on the structures. The CO2 absorption is a fundamental compensatory aspect of the carbon footprint; therefore, the use of both indicators allows somehow to perform a balance of CO2 emissions to and from the atmosphere.

The vegetation is included in WEQUI through specific criteria, as riparian vegetation is an important element for ecological quality with direct consequences on the fauna biodiversity.

3 The WEQUI Matrix

The WEQUI method consists of 15 technical-environmental indicators of different nature that allow the evaluation of ecological and morphological aspects. Each indicator has 5 alternative options to choose from. Each option is associated to a score that follows an exponential scale from 1 to 16 with a pitch of 2, so that there is a clear gap between a high score indicating medium-high quality and a low score indicating medium-low quality.

The matrix is shown in Table 1 with the list of indicators to be used for assessing the eco-morphological quality of the watercourse.

Indicators have been verified and validated on watercourses located in temperate climate zones.

Table 1 Matrix for the eco-morphological quality assessment according to WEQUI method

N	INDICATOR	LEFT BANK	CHANNEL	RIGHT BANK
1	**LAND USE (LATERAL ZONE)**			
a.	Prevailing arboreal-shrubby vegetation	16		16
b.	Prevailing shrubby-herbaceous vegetation	8		8
c.	Prevailing agricultural land use, synanthropic vegetation	4		4
d.	Prevailing suburban areas with green expanses	2		2
e.	Prevailing urban areas with impermeable soil	1		1
2	**LATERAL CONTINUITY**			
a.	Full continuity channel-lateral zone	16		16
b.	Good continuity channel-lateral zone	8		8
c.	Limited continuity channel-lateral zone	4		4
d.	Low continuity channel-lateral zone	2		2
e.	No continuity channel-lateral zone	1		1
3	**VERTICAL CONTINUITY (CHANNEL AND BANK PERMEABILITY)**			
a.	Natural vertical continuity	16	16	16
b.	Good vertical continuity	8	8	8
c.	Limited vertical continuity	4	4	4
d.	Low vertical continuity	2	2	2
e.	No vertical continuity	1	1	1
4	**LONGITUDINAL CONTINUITY (TRANSVERSE HYDRAULIC STRUCTURES)**			
a.	Unaltered longitudinal continuity		16	
b.	Good longitudinal continuity		8	
c.	Limited longitudinal continuity		4	
d.	Low longitudinal continuity		2	
e.	No longitudinal continuity		1	
5	**CHANNEL MORPHOLOGY**			

a.	Natural or natural-like morphology, rich morphology		16	
b.	Quite rich morphology		8	
c.	Quite poor morphology		4	
d.	Poor morphology		2	
e.	Very poor morphology		1	
6	**ORGANIC-MATTER RETENTION CAPACITY**			
a.	Stable retention structures		16	
b.	Unstable retention structures		8	
c.	Stable, very sparse retention structures		4	
d.	Very sparse retention structures, unstable during floods		2	
e.	No retention structures		1	
7	**FLOW REGIME**			
a.	No modifications to the natural flow rate		16	
b.	Minimal modifications to the natural flow rate		8	
c.	Significant modifications to the natural flow rate		4	
d.	Heavy flow-rate control, hydropeaking phenomena; environmental flow complied		2	
e.	Artificial hydrological regime; environmental flow not complied		1	
8	**CHEMICAL WATER QUALITY**			
a.	Unpolluted water		16	
b.	Slightly polluted water		8	
c.	Polluted water		4	
d.	Highly polluted water		2	
e.	Highly polluted water, with specific pollutants		1	
9	**MACROBENTHIC COMMUNITY**			
a.	Well-organised and heterogeneous macrobenthic community		16	
b.	Sufficiently-heterogeneous macrobenthic community, with modified organisation		8	
c.	Poorly-heterogeneous and poorly-balanced macrobenthic community		4	
d.	No organised macrobenthic community, few taxa (mainly pollution-tolerant)		2	
e.	No macrobenthic community		1	
10	**FISH SUITABILITY**			
a.	High fish suitability		16	
b.	Good fish suitability		8	
c.	Limited fish suitability		4	
d.	Very low fish suitability		2	
e.	No fish suitability		1	
11	**VEGETATION OF RIPARIAN ZONE/FLOODPLAIN**			
a.	Arboreal riparian/floodplain vegetation	16		16
b.	Shrubby riparian/floodplain vegetation	16		16
c.	Heliophilous vegetation, peat bogs, hygrophilous herbaceous vegetation	8		8
d.	Fallow land, grassland, grazing land, synanthropic formations	4		4
e.	Agricultural crops	2		2
f.	No vegetation	1		1
12	**WIDTH OF RIPARIAN/FLOODPLAIN VEGETATIVE ZONE (only for 11a. and 11b.)**			

a.	Vegetative zone width: > 30 m	16		16
b.	Vegetative zone width: 10-30 m	8		8
c.	Vegetative zone width: 6-10 m	4		4
d.	Vegetative zone width: 3-6 m	2		2
e.	Vegetative zone width: < 3 m	1		1
13	**CONTINUITY OF RIPARIAN/FLOODPLAIN VEGETATIVE ZONE (only for 11a. and 11b.)**			
a.	Vegetative zone length: > 80% of the investigated length	16		16
b.	Vegetative zone length: 60-80% of the investigated length	8		8
c.	Vegetative zone length: 40-60% of the investigated length	4		4
d.	Vegetative zone length: 20-460% of the investigated length	2		2
e.	Vegetative zone length: < 20% of the investigated length	1		1
14	**CARBON SEQUESTRATION**			
a.	No hydraulic structures supporting vegetation regeneration/growth very well	16		16
b.	Hydraulic structures supporting vegetation regeneration/growth	8		8
c.	Hydraulic structures hindering vegetation regeneration/growth slightly	4		4
d.	Hydraulic structures hindering vegetation regeneration/growth significantly	2		2
e.	Hydraulic structures not integrated in the natural environment	1		1
15	**CARBON FOOTPRINT**			
a.	No or poor presence of hydraulic structures with low carbon footprint	16	16	16
b.	Hydraulic structures with low carbon footprint	8	8	8
c.	Hydraulic structures with medium carbon footprint	4	4	4
d.	Presence, in several points, of hydraulic structures with high carbon footprint	2	2	2
e.	Presence, in the whole area, of hydraulic structures with high carbon footprint	1	1	1

As shown in Table 1, some indicators refer only to the *banks*, others refer to the *channel* or *both banks and channel*: in the first case, the indicators should be assessed separately for the two banks; in the second case, indicators refer to the river corridor as a whole; in the third case, the assessment should be carried out by dividing the river corridor into three areas.

Once all the 15 indicators have been compiled, i.e., after the scores have been assigned to the indicators with reference to the proper zone, the total score is computed. The calculation is done separately for each of the two banks, proceeding as follows:

1. all the indicator scores referred to the *channel* are added up, to obtain the sum s_0;
2. all the indicator scores referred to the *left bank* are added up, to obtain the sum s_L;
3. s_0, s_L are added to obtain S_{left}, i.e. the total score of the eco-morphological state of the *left bank*;
4. all the indicator scores referred to the *right bank* are added up, to obtain the sum s_R;
5. s_0, s_R are added together to obtain S_{right}, i.e., total score of eco-morphological state of *right bank.*

The S_{left} and S_{right} total scores range from a minimum value of 27 to a maximum value of 272. Scores may be different for the two banks of the same reach.

The S_{left} and S_{right} scores are then classified in terms of eco-morphological quality classes. The classification criteria adopted are shown in Table 2, where the score range is divided into classes in an almost homogeneous way.

Table *2* also shows the nomenclature of the quality classes and the corresponding colouring, inspired by the classification of the ecological status contained in the Water Framework Directive 2000/60/CE.

Table 2 Criteria for the classification of the eco-morphological quality and level of functionality of the area

WEQUI METHOD TOTAL-SCORE CLASSIFICATION CRITERIA			
min	**max**	**Eco-morphological quality class**	**Level of functionality**
225	272	high	I
175	225	good	II
125	175	moderate	III
70	125	poor	IV
15	70	bad	V

4 Relevance of indicators

More generally, alongside a watercourse many relevant elements can affect the eco-morphological quality. Typically:

- *water quality* (supply of nutrients, fertilisers, and polluted substances),
- *hydrology* (surface runoff can be particularly rapid and intense in the presence of impermeable surfaces),
- *morphology* (the presence of structures and artificial elements can modify the morphology of the sections and impede the channel mobility),
- *vegetation* (certain land uses can change biodiversity, facilitate the growth of invasive species, limit the vegetation growth),
- *fauna* (biodiversity and riparian/river habitats can be affected positively or negatively).

Each indicator will be characterized by an assigned set of impact coefficients, depending on the type of structures present in the river reach under evaluation. Table 3 shows the classification of structures which may be selected, where an impact factor to each structure type has been assigned.

Table 3 Coefficients for the calculation of the equivalent impact and classification

	STRUCTURE TYPE CODE	STRUCTURE TYPE DESCRIPTION
CLOSED TRANSVERSE STRUCTURES	T1	Gabion sill
	T2	Permeable sill with boulders
	T3	Cemented-stone sill
	T4	Concrete sill
	T5	Stony ramp
	T6	Gabion weir
	T7	Gabion sloped weir
	T8	Wooden and stony weir
	T9	Dry-stone weir
	T10	Cemented- or fastened-stone weir
	T11	Concrete weir
TRANSVERSA L	T12	Self-cleaning wire dam
	T13	Wire dam
	T14	Slit dam
	T15	Slot dam with horizontal rectangular openings
	T16	Filtering dam with steel bars
AL	S1	Natural riparian vegetation
	S2	Natural floodplain vegetation

	S3	Widespread willow coverage
	S4	Planted riparian shrubs
	S5	Vegetated geomat
	S6	Geomat
	S7	Vegetated Reno mattresses
	S8	Reno Mattresses
	S9	Double live wooden cribwall
	S10	Live wooden cribwall with cylindrical gabion
	S11	Green Terramesh
	S12	Terramesh
	S13	Green gabions
	S14	Gabions
	S15	Green drystone bank covering
	S16	Drystone bank covering
	S17	Tied drystone bank covering
	S18	Cemented-stone bank covering
	S19	Palisade with l-beams and cross-beams
	S20	Stone covering, rip rap
	S21	Concrete covering
	S22	Drystone bank wall
	S23	Cemented-stone bank wall
	S24	Concrete bank wall
RIVERBED COVERING	R1	Geosynthetic covering
	R2	Gabions/Reno mattresses covering
	R3	Woody covering
	R4	Drystone covering
	R5	Cemented stone covering
	R6	Concrete covering
GROYNES	P1	Groyne with wooden stake
	P2	Gabion groyne
	P3	Wooden and rocky groynes
	P4	Drystone groyne
	P5	Cemented boulders groyne
	P6	Mixed-masonry groyne
	P7	Concrete groyne
OTHER WORKS	I1	Railway
	I2	Powerline
	I3	Paved road
	I4	Dirt road
	I5	Cycle lane
	I6	Trail
	I7	Bridge (piles in the channel)

	I8	Bridge (no piles in the channel)
	I9	Ford
	I10	Barrage
	I11	Dam

This analytical procedure has been implemented within an automatic algorithm and incorporated in the web platform. The algorithm requires the data related to the structures and the infrastructures present in the lateral zone under analysis to be entered before it does the calculation and automatically selects the related option.

5 REQUALIFE: the software structure

The Software is mainly characterized as *Open-source* technology based on multi-tier architecture, as shown in Fig. 1

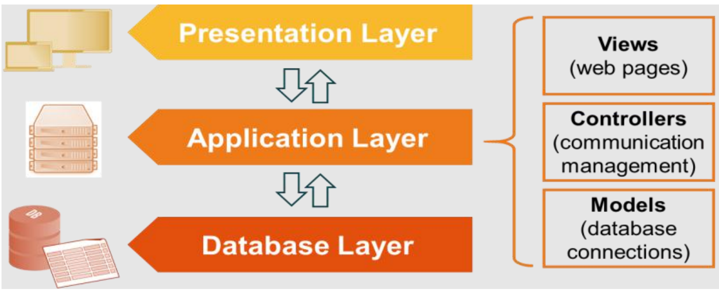

Figure 1 Scheme of the multi-tier architecture

The function process, thus, includes the *presentation layers*, the *application layer*s, and the *database layers* through which, the compilation of the assessment, can be done. Application layer are being illustrated as “arrows” through which an intuitive guidance is provided.

With the guided procedure of REQUALIFE the user will be able to either evaluate the current eco-morphological state of a watercourse or to evaluate the eco-morphological expected enhancement a few decades after an intervention with hydraulic structures. These options are called ***Monitoring*** and ***Forecast,*** respectively.

The software starts with a homepage providing a menu of menu functionalities, a map navigation, and evaluation procedures.

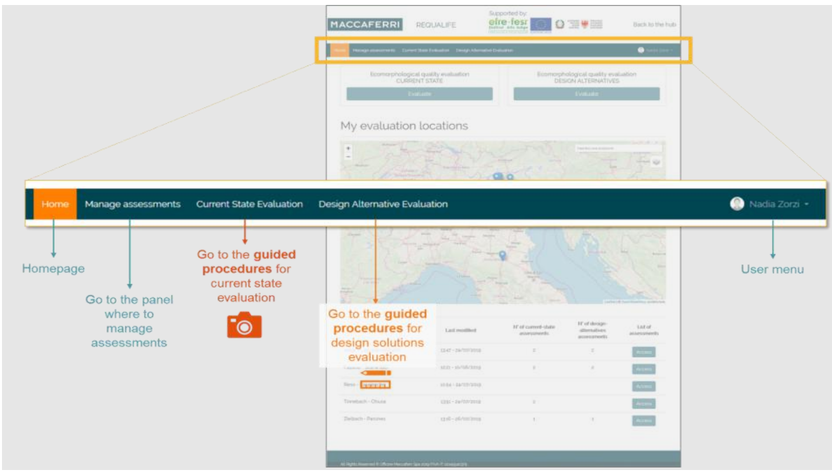

Figure 2 Main menu (home page)

The homepage includes two access evaluation procedures. To create new evaluations, the user may click on one of the tabs available based on his/her approach demands.

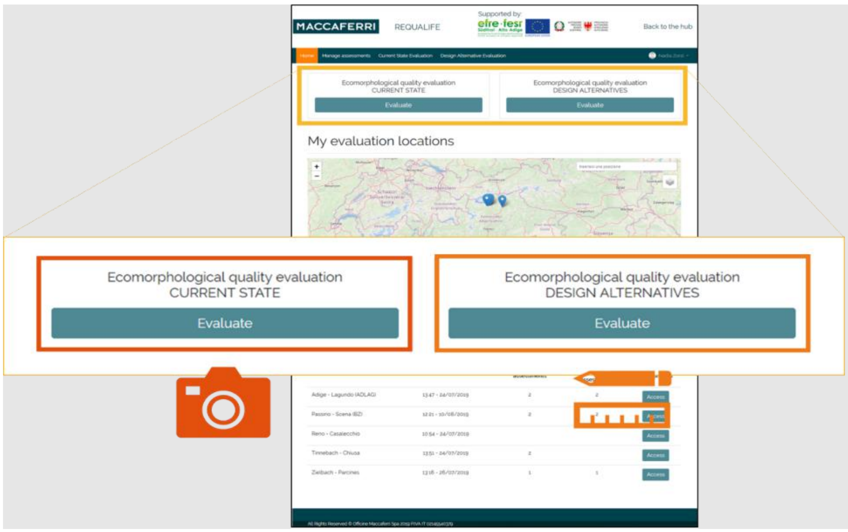

Figure 3 View of the two options (Current state and Design) accessible from the home page

6 REQUALIFE: Self Evaluation Procedure

In the self-evaluation procedure the user shall compile the questionnaire of 15 indicators. This procedure requires an understanding of the WEQUI method, and knowledge of the river ecology and morphology.

Following *Self-evaluation*, the procedure begins with the evaluation details and continues with the questionnaire modulus as shown in the figures below.

Clicking on the "Next" button the compilation form pops out, where the evaluation method shall be performed.

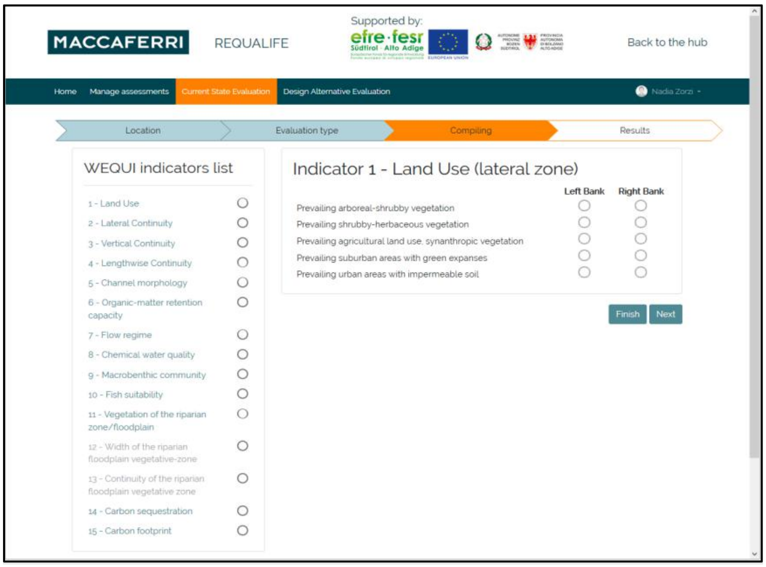

Figure 4 View of first page of the Evaluation method (Indicator 1)

Each indicator offers 5 answer options to be assigned either to the banks (Left and Right) and/or in the channel, as shown in the example below.

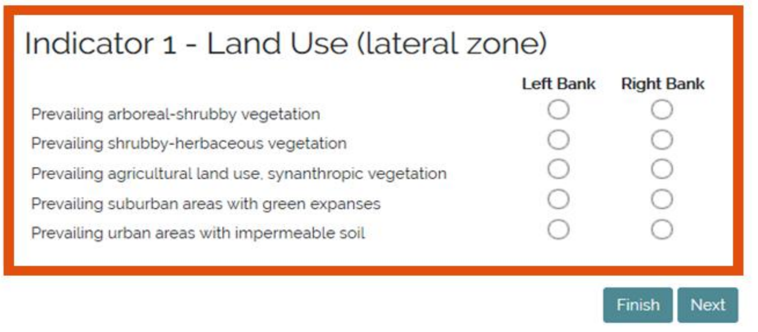

Figure 5 View of the options available for each Indicator

The process continues with the indicators list modulus, through which the user can navigate the indicators. A traffic light emphasizes the compilation status as *compiled*, *incomplete* or *to be compiled*.

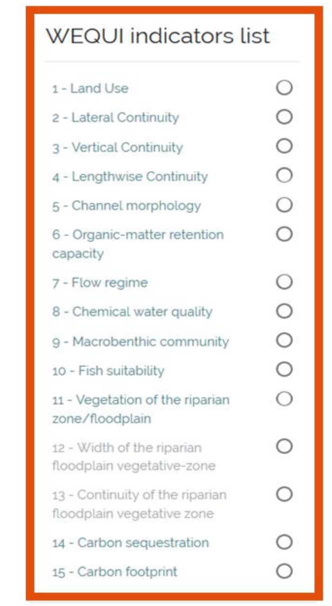

Figure 6 View of the full Indicator List available at the end of the data entry

The output of the *Self-evaluation* can be displayed in the "Results" tab, where a score system has been implemented to provide a mark for each answer option assigned in the previous phase either on the banks or on the channel.

Afterwards the final score is being displayed on the interface, compared with the upper maximum value defined. The total score provides also an eco-morphological investigation as shown in the Fig. 7

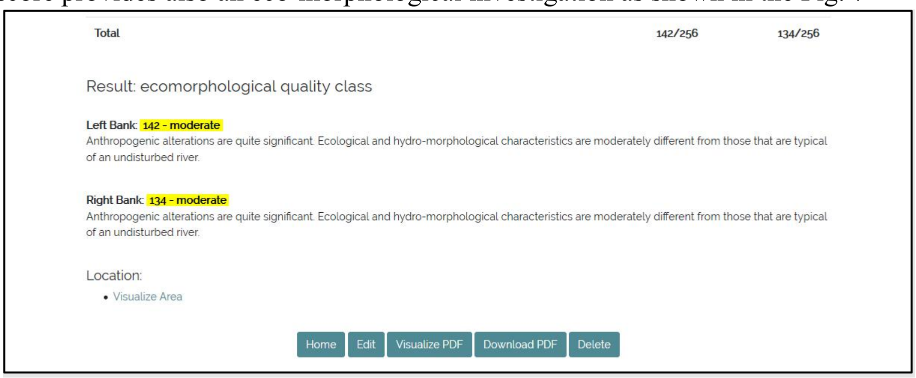

Figure 7 Results of the self-evaluation Eco-morphological investigation

7 REQUALIFE: Guided Evaluation Procedure

The Guided Evaluation Procedure is recommended for unexperienced users. The user is guided through a series of questions. This allows several indicators to be filled in automatically. To complete the procedure though, some data in the sideways will be required.

During the Guided Evaluation Procedure, the following indicators will be displayed. Analyzing the compilation fields, some brief explanations and descriptions of each indicator have been attached to the figures below, showing graphically a straightforward illustration of the current procedure:

a) Watercourse morphology
b) Channel sediment,
c) Channel retention structures.
d) Riparian floodplain,
e) Organic-matter retention capacity,
f) Flow regime,
g) Chemical water quality,
h) Macro-benthic community,
i) Land use (lateral zone),
j) Existing infrastructures (roads, railways, power lines, reservoirs, etc. within the study area), relevant for the analysis,
k) Existing hydraulic structures (within the study area).

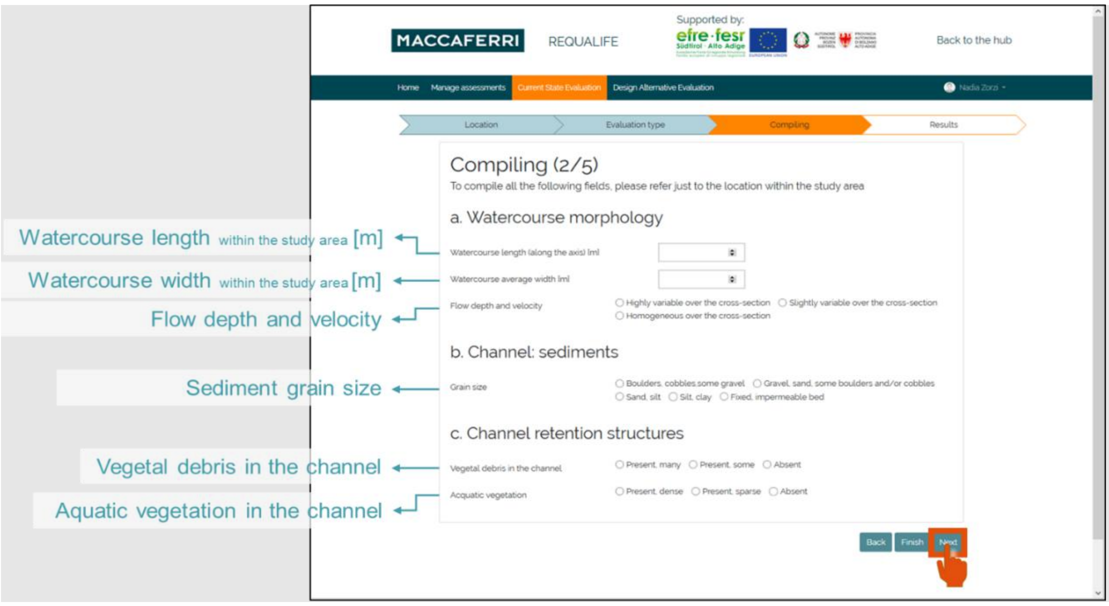

Figure 8 Example of Guided Evaluation Procedure Data Entry Page for a), b), and c)

8 REQUALIFE: Analysis of Results

The final step of the web platform application is the analysis of the results, which consist in checking in the worldwide map provided the list of evaluations made.

The user can browse through a list of assessments, sorted in alphabetical order, and access each one separately for a potential inspection or investigation. By clicking on the assessment list, a detailed evaluation table will be displayed with all the information regarding that river reach.

9 Conclusions

REQUALIFE is the web-app platform resulting after a 3 years (2017-2020) research project funded by the Province of Bolzano, where private companies (Maccaferri Innovation Center, MAVTech and Naturstudio) and the University of Bolzano (https://www.unibz.it) decided to concretely address an extremely current theme: the sustainable development of the territory. The project ended with a successful achievement of all expected results and it involved a high grade of complexity due to the high-level of activities required.

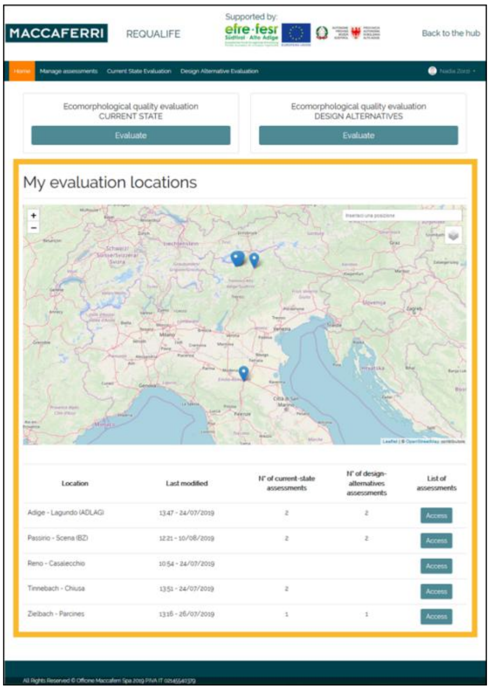

Figure 9 Example of evaluations stored in the Worldwide Map

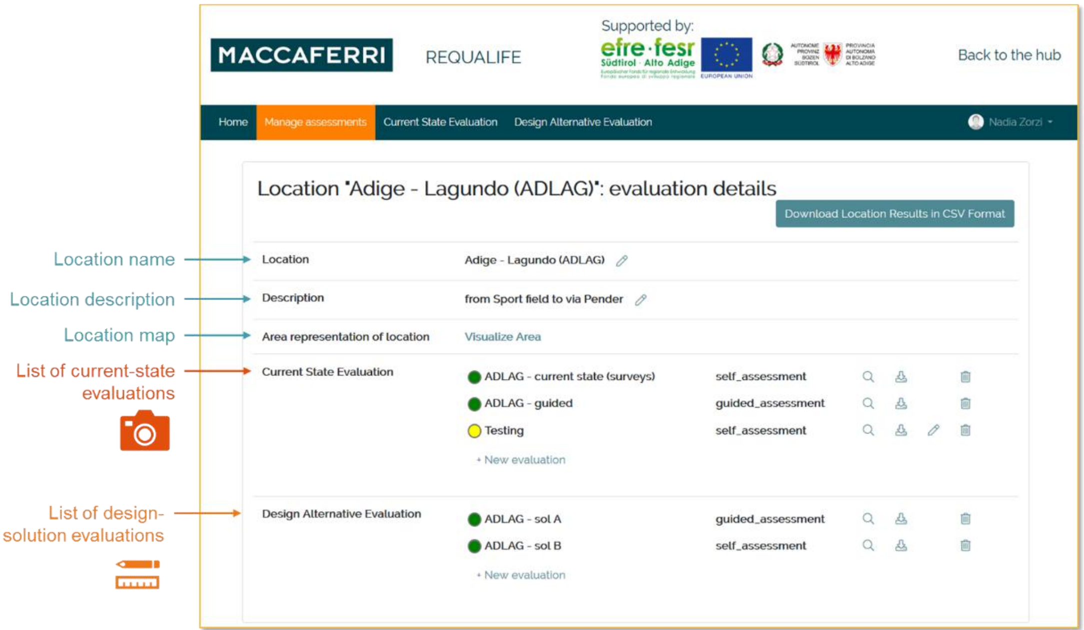

Figure 10 Example of an evaluation in the form of a summary table

The project adopted the recommendations of the European Commission in the field of Green Infrastructures, and project partners worked closely together to create a web-based system that supports the design of interventions to improve and better safeguard watercourses.

REQUALIFE is created as a simple and practical tool to assist design engineers, project managers, public authorities, and institutional stakeholders to use an integrated territorial approach, promoting the protection of fluvial ecosystems.

The online tool implements an analytical procedure that requires the evaluation of various parameters. These parameters allow to frame hydraulic structures and solutions in relation to their real capacity to contribute to the good management of the territory and the containment of environmental impacts. Some of these parameters can be obtained through automated survey techniques and using remote-sensing data captured by drones.

As a part of the project, drones were designed, built, and equipped with high-tech sensors, which, in a short time, allow to collect large amounts of data of the territory. The use of similar tools reduces the workload in the field, gives objectiveness in the analysis supporting decision makers in the sustainable design of future interventions.

Acknowledgement

As special thanks to the University of Bolzano who provided the scientific support and the equipment for the advanced analyses carried out with the drones, and to the project partners and who were all pro-actively involved collaborating to the whole and full development of the project. This strong interaction allowed all the objectives to be achieved, thanks to the specific know-how provided by each partner.

References

Belletti, B., M. Rinaldi, A. D. Buijse, A. M. Gurnell, and E. Mosselman. 2014. 'A Review of Assessment Methods for River Hydromorphology'. *Environmental Earth Sciences* 73 (5): 2079–2100. https://doi.org/10.1007/s12665-014-3558-1.

Bourne, Christina M., Dan G. Kehler, Yolanda F. Wiersma, and David Cote. 2011. 'Barriers to Fish Passage and Barriers to Fish Passage Assessments: The Impact of Assessment Methods and Assumptions on Barrier Identification and Quantification of Watershed Connectivity'. *Aquatic Ecology* 45 (3): 389–403. https://doi.org/10.1007/s10452-011-9362-z.

Beffagni, Andrea, S. Erba, Sebastian Birk, M. Cazzola, C. Feld, T. Ofenböck, John Murray-Bligh, et al. 2005. *Towards European Inter-Calibration for the Water Framework Directive: Procedures and Examples for Different River Types from the E.C. Project STAR*. Vol. Quad. Ist. Rome: IRSA. https://doi.org/10.1097/00005768-200105000-00017.

Canadian Council of Ministers of the Environment. 2017. *Canadian Water Quality Guidelines for the Protection of Aquatic Life: CCME Water Quality Index, User's Manual 2017 Update*.

Chutter, Francis Mark. 1998. *Research on the Rapid Biological Assessment of Water Quality Impacts in Streams and Rivers*. Water Rese. Pretoria.

D'Agostino, Vincenzo, and M.A. Lenzi. 1998. 'La Massimizzazione Della Resistenza Al Flusso Nei Torrenti Con Morfologia a Step-Pool'. In *XXVI Convegno Di Idraulica e Costruzioni Idrauliche*, 281–92. Catania: CUECM.

Environmental Agency. 2005. 'A Refined Geomorphological and Floodplain Component to River Habitat Survey (GeoRHS)'. Bristol.

EPA - Environmental Protection Agency. 2001. *Parameters of Water Quality: Interpretation and Standards*. Environmental Protection Agency, Ireland.

Gonzáles del Tánago, Marta, and Diego García de Jalon. 2011. 'Riparian Quality Index (RQI): A Methodology for Characterising and Assessing the Environmental Conditions of Riparian Zones'. *Limnetica* 30 (2): 235–54.

Karr, James R. 1981. 'Assessment of Biotic Integrity Using Fish Communities'. *Fisheries* 6 (6): 21–27. https://doi.org/10.1577/1548-8446(1981)006<0021:AOBIUF>2.0.CO;2.

Kleynhans, CJ, JA Mackenzi, and MD Louw. 2007. 'Module F: Riparian Vegetation Response Assessment Index (VEGRAI)'. *River EcoClassification: Manual for Ecostatus Determination (Version 2)*.

Muhar, Susanne, Michaela Schwarz, Stefan Schmutz, and Mathias Jungwirth. 2000. 'Identification of Rivers with High and Good Habitat Quality: Methodological Approach and Applications in Austria'. In *Assessing the Ecological Integrity of Running Waters*, 422/423:343–58. Dordrecht: Springer Netherlands. https://doi.org/10.1007/978-94-011-4164-2_28.

Petersen, Robert C. 1992. 'The RCE: A Riparian, Channel, and Environmental Inventory for Small Streams in the Agricultural Landscape'. *Freshwater Biology* 27 (2): 295–306. https://doi.org/10.1111/j.1365-2427.1992.tb00541.x.

Richter, Brian D., Jeffrey V. Baumgartner, Jennifer Powell, and David P. Braun. 1996. 'A Method for Assessing Hydrologic Alteration within Ecosystems'. *Conservation Biology* 10 (4): 1163–74. https://doi.org/10.2307/2387152.

Rosgen, D. L. 2007. *Watershed Assessment of River Stability and Sediment Supply (WARSSS)*. Wildland H. Fort Collins, CO.

Sear, David, Malcolm Newson, Christopher Hill, Jo Old, and Julia Branson. 2009. 'A Method for Applying Fluvial Geomorphology in Support of Catchment-Scale River Restoration Planning'. *Aquatic Conservation: Marine and Freshwater Ecosystems* 19 (5): 506–19. https://doi.org/10.1002/aqc.1022.

Shiau, Jenq-Tzong, and Fu-Chun Wu. 2008. 'A Histogram Matching Approach for Assessment of Flow Regime Alteration: Application to Environmental Flow Optimization'. *River Research and Applications* 24 (7): 914–28. https://doi.org/10.1002/rra.1102.

Xia, Ting, Wei Zhu, Pei Xin, and Lei Li. 2010. 'Assessment of Urban Stream Morphology: An Integrated Index and Modelling System'. *Environmental Monitoring and Assessment* 167 (1–4): 447–60. https://doi.org/10.1007/s10661-009-1063-x.

Effects of ecological restoration measures with a fire disturbance on soil organic carbon improvement for degraded land in the agro-pasture ecotone in North China

Zhuo Pang[1], Haiming Kan[1], Junliang Zou[1], Guofang Zhang[1], Xiaodong Ma and Juying Wu*[1]
1 Research and Development Centre for Grass and Environment, Beijing Academy of Agriculture and Forestry Sciences, China
*Corresponding Author, e-mail: pangzh-84@163.com; wujuying@grass-env.com

Abstract

To improve soil organic carbon content of degraded lands in the agro-pasture ecotone in North China, ecological restoration measures, including revegetation with *Bromus inermis* and *Medicago sativa*, have been widely implemented. Soil organic carbon (SOC), water soluble organic carbon (WSOC) and hot-water extractable organic carbon (HEOC) were measured and soil respiration rate (Rs) was monitored continuously from April to October in grasslands of *Bromus inermis* and *Medicago sativa* from 2014 to 2020, with a fire disturbance occurred in 2017. The results showed that during the six years, SOC, WSOC and HEOC improved significantly in both types of grassland. Initially, SOC was decreased but WSOC and HEOC were increased in both grasslands in 2015 due to the grassland establishment practice. Moreover, fire disturbance in 2017 suppressed the increasing trend of SOC but had no effect on WSOC and HEOC, however, the fire disturbance triggered a sharp increase in WSOC and HEOC thereafter. Finally, Rs did not differ significantly among years and between types of grassland, however fire disturbance depressed Rs in *Medicago sativa* grassland, which became lower than that in *Bromus inermis* grassland thereafter. These findings suggest that revegetation with *Bromus inermis* and *Medicago sativa* can effectively improve SOC to neutralize land degradation and fire disturbance renders SOC in *Medicago sativa* grassland more stable with lower Rs.

Keywords: Degraded land management, Ecological restoration, Soil organic carbon, Fire event, Agro-pasture ecotone

1 Introduction

The ecologically fragile agro-pasture ecotone in North China (APENC) is subject to increasingly severe land degradation, because of anthropogenic disturbance and climatic change (Huang et al., 2007; Xu et al., 2010). As APENC supports millions of population and serves as the ecological shelters of Beijing and Tianjin, neutralizing land degradation to restore ecosystem functions is urgent and important in this area (Guo et al., 2013; Wang et al., 2015; Cowie et al., 2018). Among the ecological restoration measures, revegetation with herbaceous plants is more reasonable and widely used due to their multiple morphological, physiological and functional traits (Fort et al., 2017; Gao et al., 2018), especially for the semiarid APENC.

Improvement of soil organic carbon (SOC) content is essential and pivotal to degraded land neutralization, in that higher SOC results in stronger water holding capacity, retention ability of available nutrients, soil biological and enzymatic activities, and hence prevents soil erosion (Campbell et al., 1999; Ghani et al., 2003). Compared with the gradually changed SOC, water soluble organic carbon (WSOC) and hot-water extractable organic carbon (HEOC), with higher solubility and turnover rare, are more sensitive to climate and management practice (Ghani et al., 2003; Guigue et al., 2015). WSOC plays a significant role in soil carbon transport, transformation and redistribution as a result of leaching with various forms of dissolved nitrogen (Kramer Marc et al., 2012; Chang et al., 2018). While HEOC closely relates to soil microbial biomass, micro aggregation and CO2 evolution (Ghani et al., 2003). Increase in SOC also shows the potential of sequestering atmospheric CO2 and mitigating global warming (Belay-Tedla et al., 2009), however, soil respiration (Rs), releasing soil carbon to atmosphere, undermines and threats SOC improvement due to the positive feedback loop (Yan et al., 2020).

In addition, as one of the most important disturbance to restoration of degraded land, wildfire plays critical roles in affecting soil carbon as well (Chen et al., 2019; Raiesi and Pejman, 2021). Fire disturbance, commonly exacerbated by long-term drought and high temperatures, can directly convert SOC to pyrogenic CO2 through topsoil heating (van der Werf et al., 2006), and indirectly perturb soil functions by destructing plant communities (Strong et al., 2017), reshaping interactions/feedbacks between plants and soil microbes (Yang et al., 2019), changing soil enzyme activities related to SOC decomposition (Gutknecht et al., 2010), and impacting the source components of soil respiration (Chen et al., 2019). However, the comprehensive information about the effects of fire disturbance on SOC, labile components of SOC and soil carbon release during degraded land restoration is limited.

Bromus inermis and *Medicago sativa* (alfalfa) have been widely applied to restore degraded land in APENC, because they can not only stabilize the loose topsoil by dense roots and strong rhizomes (Otfinowski et al., 2007) and regenerate soil fertility and productivity by plentiful organic residues and biological nitrogen fixation (Vanek et al., 2020), but also ensure a supply of high-quality forage and increase income of local inhabitants. The objectives of this study were to: 1) identify SOC improving effect of revegetation with herbaceous plants to restore degraded land, 2) quantify the influence of fire disturbance on SOC, labile components of SOC, and Rs, 3) investigate the difference in neutralization of degraded land between grasslands of *Bromus inermis* and *Medicago sativa*.

2 Methods

2.1 Site description

The study site located at the southeast border of APENC in Yanqing District Beijing City of China (40°27′53″N, 115°50′23″E) (Fig. 1). As the floodplain of Gui River, the study site has a thin and sandy soil layer, with 7% clay (<0.002 mm), 22% silt (0.002-0.02 mm) and 71% sand (0.02-2 mm). The semi-arid continental monsoon climate (mean air temperature is 8.4 ° C, mean annual precipitation is 466 mm, concentrating on the period between May and September) (Wu et al., 2016) facilitates the occurrence of wind erosion and dust-storm in spring and early summer in this region, due to strong wind, sparse vegetation and scarce rainfall (Guo et al., 2013).

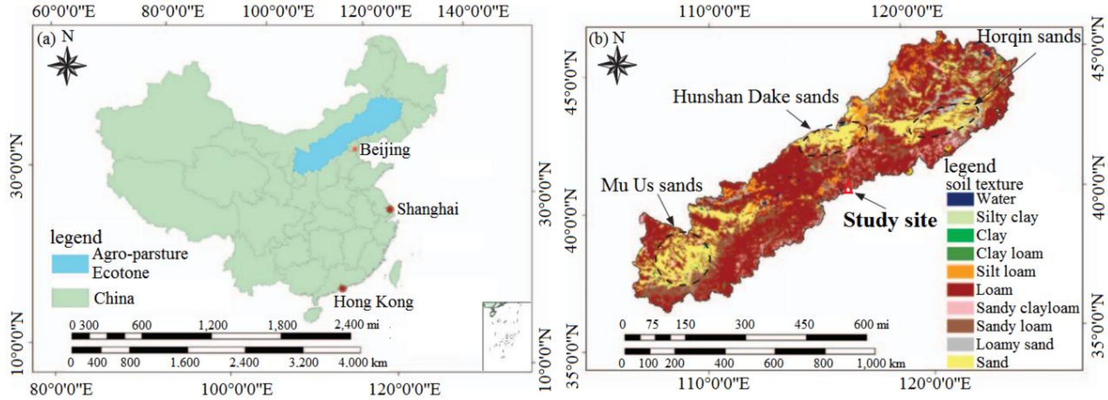

Figure 1 Location of study site. The agro-pasture ecotone in North China (a) and the study site (b)

To control dust-storm caused by wind erosion and neutralize regional land degradation, Beijing-Tianjin Sandstorm Source Control program was implemented and summer maize farmland was revegetated with perennial *Bromus inermis* and *Medicago sativa* in 2014 in APENC. The grasslands of had been left to develop naturally without anthropogenic disturbance (no irrigation, fertilization and harvesting) after germination of seeds since August 2015, until the untoward fire event in early May 2017. This mishap burnt the accumulated herbaceous fuels and the grasslands became more verdant in the rainy season of 2017. The above-ground parts have been harvested in early winter every year since the fire event.

2.2 Sample collection

The sampling campaigns were carried out in contiguous grasslands of Bromus inermis and Medicago sativa with similar plant density of ~1800 ind • m-2. Four randomly selected sampling plots (2 m × 2 m) were established in each type of grassland. Three 0-10 cm soil cores were collected with a 7 cm-diameter soil auger and well mixed in each sampling plot. The sample collection was implemented in May every year, before the seed sowing in 2014 and after the fire event in 2017.

2.3 Measurement and analysis

Each soil sample was divided into two parts. One part was air-dried and sieved through a 0.25 mm sieve. SOC was then measured with the traditional potassium dichromate oxidation method. The other part was used to measure WSOC and HEOC according to the method from Ghani et al., 2003. Briefly, the fresh soil was firstly sieved through a 4 mm sieve, then was extracted in distilled water, centrifuged, filtered and analyzed for WSOC. Distilled water was further added to the sediments, after the water-sediment system was shaken, incubated in 80 °C hot-water for 16 h, shaken again, centrifuged, filtered and analyzed for HEOC.

The hourly soil respiration (Rs, in μmol $CO_2 \cdot m^{-2} \cdot s^{-1}$) rates were simultaneously measured in grasslands of *Bromus inermis* and *Medicago sativa* with a Li-8100A automated soil CO_2 flux system equipped with eight long-term chambers (four in each types of grassland) (Li-COR Inc., Lincoln, NE, USA). Measurement details were in accordance with Wu et al., 2016. The Rs monitoring period covered April to October every year, except for 2014 and 2017 disturbed by seed sowing activity and fire event.

2.4 Statistical analysis

Regression analysis was performed to examine the temperature sensitivity of soil respiration (Q_{10}) using SPSS 16.0 software for Windows (SPSS Inc., Chicago, IL, USA). Q_{10} was obtained from Eq. (1).

$$Rs = Rs_0 \times Q_{10}^{Ts/10} \tag{1}$$

Where, Rs_0 is soil respiration rate at 0 °C, referred to as basic soil respiration; Q_{10} is temperature sensitivity of soil respiration, or increasing times of soil respiration rate with temperature increase of 10 °C; Ts is soil temperature.

Two-way repeated measures analysis of variance (ANOVA) followed by Tukey's least significance difference post-hoc test, with significance specified as $p < 0.05$, were carried out in GraphPad Prism v.7.0 to compare values between the grassland types as well as between the years.

3 Results

3.1 Changes of soil organic carbon contents

The soil organic carbon content in *Bromus inermis* and *Medicago sativa* grasslands exhibited identical temporal trend of increase, decrease, increase again and decrease again (Fig. 2) After 6 years' revegetation, both types of grassland significantly improved SOC ($p < 0.05$). The greatest improvement of SOC occurred in 2019. SOC did not differ significantly between the two types of grassland initially in 2014, and thereafter SOC in *Medicago sativa* grassland was significantly higher than that in *Bromus inermis* grassland in 2016, 2017 and 2018, but showed no significant difference for the remain 3 years (i.e. 2015, 2019 and 2020).

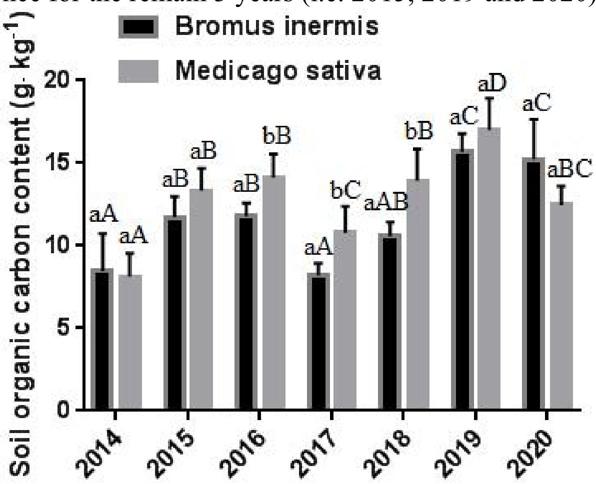

Figure 2 Trends of soil organic carbon content in two types of grasslands. Different lowercase and uppercase letters indicate significant difference ($P < 0.05$) between grassland types and among years, respectively.

Fire disturbance significantly depleted SOC of both types of grassland in 2017, and the negative effect was more serious in *Bromus inermis* grassland than in *Medicago sativa* grassland. Additionally, the recovering of SOC after the fire event was more rapid in *Bromus inermis* grassland than in *Medicago sativa* grassland as well (Figure 2).

3.2 Changes of labile components of soil organic carbon contents

Water soluble organic carbon content did not differ significantly between Bromus inermis and Medicago sativa grasslands from 2015 to 2020. WSOC also exhibited the same temporal trend and the initial increase was insignificant in 2015 for the two types of grassland (Fig. 3). Nevertheless, the fluctuation of WSOC with year was more complicated and significant in Bromus inermis grassland than in Medicago sativa grassland.

In both types of grassland, fire event did not significantly changed WSOC in 2017 from that in 2016, however, a sharp increase in WSOC followed in 2018, and thereafter WSOC regressed to the earlier level (Fig. 3). Fire disturbance showed a hysteretic and short-lived priming effect on WSOC.

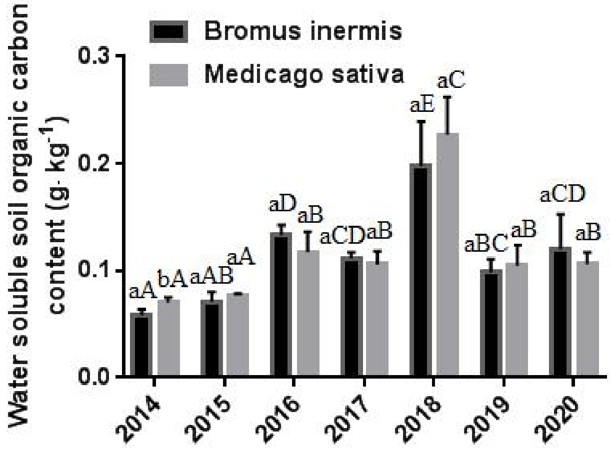

Figure 3 Trends of water soluble soil organic carbon content in two types of grasslands. Different lowercase and uppercase letters indicate significant difference ($P < 0.05$) between grassland types and among years, respectively.

Hot-water extractable organic carbon also did not differ significantly between *Bromus inermis* and *Medicago sativa* grasslands except in 2015 (Fig. 4). In accordance with WSOC, fire disturbance presented a hysteretic and short-lived priming effect on HEOC as well.

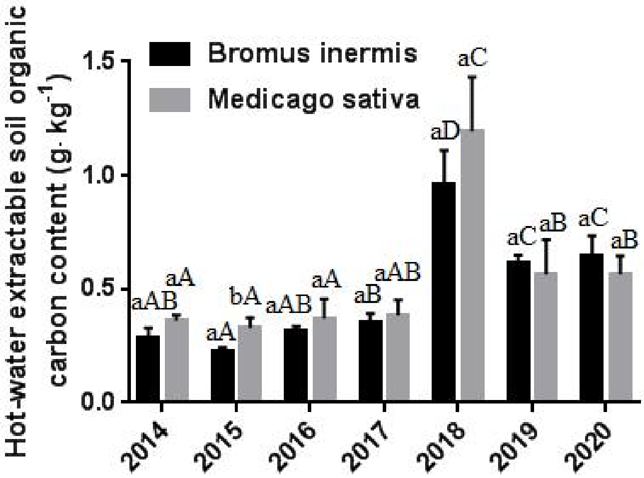

Figure 4 Trends of hot-water extractable soil organic carbon content in two types of grasslands. Different lowercase and uppercase letters indicate significant difference ($P < 0.05$) between grassland types and among years, respectively.

3.3 Changes of soil respiration and its temperature sensitivity

Soil respiration exhibited different temporal trends between *Bromus inermis* and *Medicago sativa* grasslands (Fig. 5). Rs increased, decreased, and increased again in *Bromus inermis* grassland, but increased and decreased in *Medicago sativa* grassland.

The fire event exerted different influence on Rs (Fig. 5). After fire disturbance, Rs was stimulated in Bromus inermis grassland with higher temperature sensitivity (Q_{10}) than before fire event in 2017, but was repressed in *Medicago sativa* grassland (Table 1; Fig. 5).

Table 1 Characteristic values of temperature sensitivity of soil respiration

Grassland type	Year	SR_0	Q_{10}	R^2
	2015	0.4905	1.3993	0.0855
	2016	0.3941	1.6620	0.1511
Bromus inermis	2018	**0.1934**	**2.5396**	**0.4722**
	2019	**0.2231**	**2.0876**	**0.2481**
	2020	**0.3447**	**2.0320**	**0.3990**
	2015	0.3593	1.6537	0.1428
	2016	0.3869	1.6787	0.1451
Medicago sativa	2018	**0.2933**	**1.6307**	**0.1140**
	2019	**0.2726**	**1.7092**	**0.1543**
	2020	**0.2831**	**1.7160**	**0.1608**

Notes, bold type indicates values after the fire disturbance in 2017.

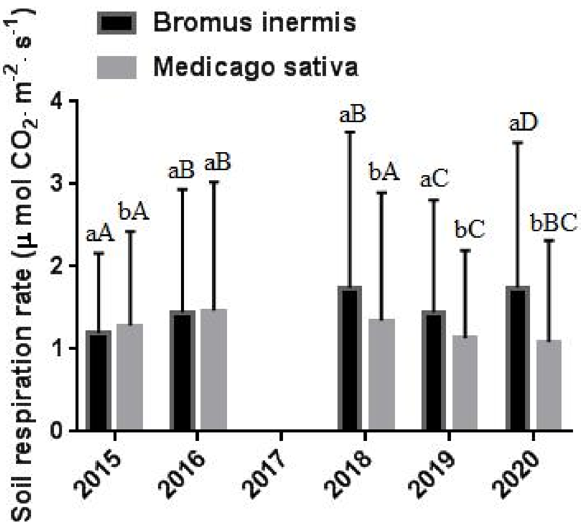

Figure 5 Trends of soil respiration rates in two types of grasslands. Different lowercase and uppercase letters indicate significant difference ($P < 0.05$) between grassland types and among years, respectively.

4 Discussion

4.1 Adaptability of ecologically restoring species for SOC improvement

As to species selection for restoration of degraded land, it is necessary to multiply consider climatic, edaphic and economic factors for soil regeneration, and the socio-ecological niches determines the acceptability and sustainability of ecological restoration measures (Ojiem et al., 2006). Specifically, the species should be able to reduce disease, cover soil surface rapidly, produce abundant organic residue and provide animal forage (Vanek et al., 2020).

Both *Bromus inermis* and *Medicago sativa* as revegetating species can effectively improve SOC and its labile components, indicating that they are adaptable to the climate and soil conditions of APENC. Moreover, both species are high-quality forage as well.

4.2 Effects of fire disturbance on soil carbon cycle

Fire has become a more and more prevalent and important disturbance for ecologically fragile areas with land degradation, in that fire frequency and intensity will further increase in the coming century (Westerling et al., 2006). The priming effect of fire event on WSOC and HEOC may be caused by the stimulation of fine root production and soil microbial growth, due to the short-term increase of N availability (Reich et al., 2001; Adersson et al; 2004; Strong et al., 2017).

Fire disturbance has distinct influence on soil respiration between *Bromus inermis* and *Medicago sativa* grasslands. As soil respiration is closely associated with soil microbial biomass and soil moisture, the discrepant responses to fire event may be resulted from the different taxonomic and functional composition of soil microbial communities (Chen et al., 2019; Yang et al., 2019).

4.3 Limitations

This study has focused on the influences of revegetating species and fire disturbance on soil carbon pools (SOC, WSOC and HEOC) and soil carbon release (Rs), however, the impacts on soil carbon input still need to be explored. It has been reported that living root inputs or root-derived inputs are major contributors to soil organic carbon formation and are sensitive to climate change and human disturbance (Sokol et al., 2018; Keller et al., 2021). So it is necessary to incorporate soil carbon input processes into the monitoring regime to comprehensively understand the soil carbon cycle.

5 Conclusions

We show that, in agro-pasture ecotone in North China, the degraded land revegetated with *Bromus inermis* and *Medicago sativa* effectively and significantly improved SOC. Fire disturbance significantly depleted SOC, and the negative effect and aftermath of fire disturbance was more serious in *Bromus inermis* grassland than in *Medicago sativa* grassland. Fire disturbance exerted priming effect on WSOC and HEOC. Fire disturbance stimulated Rs in *Bromus inermis* grassland but suppressed Rs in *Medicago sativa* grassland. Our results thus collectively point to the importance of *Medicago sativa* as ecological restoration species for SOC improvement in APENC. We highlight two key areas for future work, based on our results. First, the response of Rs to fire disturbance is so different between *Bromus inermis* and *Medicago sativa* grasslands, it is important to determine how plants with different soil microbial communities will alter the temperature sensitivity of Rs. Second, including the soil carbon input into consideration will be critical to deepen our understanding of the mechanisms underpinning the SOC improving pathway and the plant traits with which they are associated during degraded land restoration.

Acknowledgement

This work was supported by the Beijing Academy of Agriculture and Forestry Sciences [No. KJCX20200301, KJCX20190404] and Natural Science Foundation of Beijing Municipality [No. 5204031].

References

Andersson, M., Michelsen, A., Jensen, M., Kjøller, A. (2004). “Tropical savannah woodland: effects of experimental fire on soil microorganisms and soil emissions of carbon dioxide”. Soil Biology and Biochemistry, 36(5), 849-858.

Belay-Tedla, A., Zhou, X.H., Su, B., Wan, S.Q., Luo, Y.Q. (2009). “Labile, recalcitrant, and microbial carbon and nitrogen pools of tall grass prairie soil in the US Great Plains subjected to experimental warming and clipping”. Soil Biology & Biochemistry, 41, 110–116.

Campbell, C.A., Biederbeck, V.O., McConkey, B.G., Curtin, D., Zentner, R.P. (1999). “Soil quality-Effect of tillage and fallow frequency. Soil organic matter quality as influenced by tillage and fallow frequency in a silt loam in South Western Saskatchewan”. Soil Biology & Biochemistry, 31, 1–7.

Chang, R., Li, N., Sun, X., Hu, Z., Bai, X., Wang, G. (2018). “Nitrogen addition reduces dissolved organic carbon leaching in a montane forest”. Soil Biology & Biochemistry, 127, S0038071718303018-. DOI: 10.1016/j.soilbio.2018.09.006

Chen, J., Zhang, Y.F., Luo, Y.Q., Zhou, X.H., Jiang, Y., Zhao, J., Chen, Y.Z., Wang, C., Guo, L., Cao, J.J. (2019). “Contrasting responses after fires of the source components of soil respiration and ecosystem respiration”. European Journal of Soil Science, 70, 616-629.

Cowie, A.L., Orr, B.J., Castillo Sanchez, V.M., Chasek, P., Crossman, N.D., Erlewein, A., Louwagie, G., Maron, M., Metternicht, G.I., Minelli, S., Tengberg, A.E., Walter, S., Welton, S. (2018). “Land in balance: the scientific conceptual framework for Land Degradation Neutrality”. Environmental Science & Policy, 79, 25-35.

Fort, F., Volaire, F., Guilioni, L., Barkaoui, K., Navas, M.L., Roumet, C. (2017). "Root traits are related to plant water-use among rangeland Mediterranean species". Functional Ecology, 31, 1700-1709.

Gao, X., Liu, Z., Zhao, X., Ling, Q., Huo, G., Wu, P. (2018). "Extreme natural drought enhances interspecific facilitation in semiarid agroforestry systems". Agriculture Ecosystems & Environment, 265, 444-453.

Ghani, A., Dexter, M., Perrott, K. W. (2003). "Hot-water extractable carbon in soils: a sensitive measurement for determining impacts of fertilisation, grazing and cultivation". Soil Biology & Biochemistry, 35(9), 1231-1243.

Guigue, J., Lévêque, J., Mathieu, O., Schmitt-Kopplin, P., Lucio, M., Arrouays, D., Jolivet, C., Dequiedt, S., Chemidlin Prévost-Bouré, N., Ranjard, L. (2015). "Water-extractable organic matter linked to soil physico-chemistry and microbiology at the regional scale". Soil Biology & Biochemistry, 84, 158-167.

Guo, Z., Zobeck, T.M., Zhang, K., Li F. (2013). "Estimating potential wind erosion of agricultural lands in northern China using the Revised Wind Erosion Equation (RWEQ) and GIS". Journal of Soil and Water Conservation, 68, 13-21.

Gutknecht, J.L.M., Henry, H.A.L., Balser, T.C. (2010). "Inter-annual variation in soil extra-cellular enzyme activity in response to simulated global change and fire disturbance". Pedobiologia, 53(5), 283-293.

Huang, D., Wang, K., Wu, W.L. (2007). "Dynamics of soil physical and chemical properties and vegetation succession characteristics during grassland desertification under sheep grazing in an agro-pastoral transition zone in Northern China". Journal of Arid Environments, 70, 120-136.

Keller, A.B., Brzostek, E.R., Craig, M.E., Fisher, J.B., Phillips, R.P. (2021). "Root-derived inputs are major contributors to soil carbon in temperate forests, but vary by mycorrhizal type". Ecology Letters, 24, 626-635.

Kramer Marc, G., Sanderman, J., Chadwick Oliver, A., Chorover, J., Vitousek Peter, M. (2012). "Long-term carbon storage through retention of dissolved aromatic acids by reactive particles in soil. Global Change Biology, 18, 2594-2605.

Ojiem, J.O., de Ridder, N., Vanlauwe, B., Giller, K.E. (2006). "Socio-ecological niche: a conceptual framework for integration of legumes in smallholder farming systems". International Journal of Agricultural Sustainability, 4, 79–93.

Otfinowski, R., Kenkel, N.C., Catling, P.M. (2007). The biology of Canadian weeds. 134. *Bromus inermis* Leyss. Canadian Journal of Plant Science, 87, 183-198.

Raiesi, F., and Pejman, M. (2021). "Assessment of post-wildfire soil quality and its recovery in semi-arid upland rangelands in central iran through selecting the minimum data set and quantitative soil quality index". Catena, 201, 105202.

Reich, P. B., Peterson, D. W., Wedin, D. A., Wrage, K. (2001). "Fire and vegetation effects on productivity and nitrogen cycling across a forest–grassland continuum". Ecology, 82(6), 1703-1719.

Sokol, N.W., Kuebbing, S.E., Karlsen-Ayala, E. Bradford, M.A. (2018). "Evidence for the primacy of living root inputs, not root or shoot litter, in forming soil organic carbon". New Phytologist, 221, 233-246.

Strong, A.L., Johnson, T.P., Chiariello, N.R., Field, C.B. (2017). "Experimental fire increases soil carbon dioxide efflux in a grassland long-term multifactor global change experiment". Global Change Biology, 23, 1975-1987.

van der Werf, G.R., Randerson, J.T., Giglio, L., Collatz, G.J., Kasibhatla, P.S., Arellano, A.F., Jr. (2006). "Interannual variability in global biomass burning emissions from 1997 to 2004". Atmospheric Chemistry and Physics, 6, 3423–3441.

Vanek, S.J., Meza, K., Ccanto, R., Olivera, E., Scurrah, M., Fonte S.J. (2020). "Participatory design of improved forage/follow options across soil gradients with farmers of the Central Peruvian Andes". Agriculture Ecosystems & Environment, 300, 106933.

Wang, C., Gao, Q., Wang, X., Yu, M. (2015). "Decadal trend in agricultural abandonment and woodland expansion in an agro-pastoral transition band in Northern China". PLoS One, 10, e0142113.

Westerling, A.L., Hidalgo, H.G., Cayan, D.R., Swetnam, T.W. (2006). "Warming and earlier spring increase western US forest wildfire activity". Science, 313(5789), 940-94

Wu, J.Y., Pang, Z., Sun, T.J., Kan, H.M., Hu, W., Li, X.N. (2016). "Soil respiration simulation based on soil temperature and water content in artificial smooth brome grassland". Rangeland Journal, 38, 579-589.

Xu, Z., Wan, S., Zhu, G., Ren, H., Han, X. (2010). "The influence of historical land use and water availability on grassland restoration". Restoration Ecology, 18, 217-225.

Yan, C., Yuan, Z., Shi, X., Lock, T.R., Kallenbach, R.L. (2020). "A global synthesis reveals more response sensitivity of soil carbon flux than pool to warming". Journal of Soils and Sediments, 20(3). DOI: 10.1007/s11368-019-02513-1

Yang, S.H., Zheng, Q.S., Yang, Y.F., Yuan, M.T., Ma, X.Y., Chiariello, N.R., Docherty, K.M., Field, C.B., Gutknecht, J.L.M., Hungate, B.A., Niboyet, A., Roux X.L., Zhou, J.Z. (2019). "Fire affects the taxonomic and functional composition of soil microbial communities, with cascading effects on grassland ecosystem functioning". Global Change Biology, 26(2), 431-442.

Initial Recovery Characteristics and Variability of Soil Carbon, Nitrogen, and Phosphorus in the Damaged Forests under Disaster Disturbance

Hang Yu[1,2,3], Qinghu Luo[1,2,3], Songyang Li [1,2,3], Yongming Lin[1,2,3]*, Daojie Wang[4]

1 College of Forestry, Fujian Agriculture and Forestry University, Fuzhou 350002, China;

2 Key Laboratory of Mountain Hazards and Surface Processes, Chinese Academy of Sciences, Chengdu 610041, China;

3 Key Laboratory for Forest Ecosystem Process and Management of Fujian Province, Fuzhou 350002, China;

4 Institute of Mountain Hazards and Environment, Chinese Academy of Sciences and Ministry of Water Conservancy, Chengdu 610041, China）

Abstract

In June 2010, heavy floods induced large-scale landslides in Nanping City, Fujian Province, causing severe damage to forests in the area. In this study, two different kinds of forest land (*Cunninghamia lanceolata* forest and secondary broad-leaved forest) destroyed by major floods were selected for the determination of soil organic carbon (SOC) content, total nitrogen (TN) content and total phosphorus (TP) content of surface soil in different sample plots (damaged area, recovered area, and undamaged area), and then the initial recovery characteristics and variability of SOC, TN, TP of damaged forests were analyzed. The results showed that: (1) Disaster caused severe damage to the secondary broad-leaved forest and *Cunninghamia lanceolata* forest. The contents of SOC, TN and TP in all plots decreased as the vegetation coverage, following the rule of "undamaged area > recovered area > damaged area", indicating that damaged forests had not recovered to the pre-disaster level after seven years of natural recovery. (2) Only TP content of the recovered area was significantly higher than the damaged area in secondary broad-leaved forest, while the content of SOC and TP of the recovered area were both significantly higher than the damaged area in *Cunninghamia lanceolata* forest, and the recovery rate of soil nutrients in *Cunninghamia lanceolata* forest was higher than secondary broad-leaved forest, indicating that the early fertilization had a positive promoting effect on the natural restoration of soil nutrients in *Cunninghamia lanceolata* forest. (3) C:P value was mainly affected by SOC, C:N and N:P values were mainly affected by TN in the damaged forests, and only C:P value of recovered area was significantly higher than the damaged area in *Cunninghamia lanceolata* forest. (4) TN had the maximum variability, followed by SOC and TP in the damaged forests, but the recovery rate of soil nutrients was contrary to the above conclusions, indicating that disaster had the greatest impact on TN of the damaged forests. The results indicated that soil nutrients had been severely damaged by disaster, and the natural recovery process of soil nutrients was slow and the recovery effect was poor. Therefore, appropriate artificial measures should be carried out to promote the recovery of damaged forests, especially secondary broad-leaved forests. The research results can provide a scientific basis for the prediction of the succession process and mechanism, soil erosion control, and the optimization of restoration measures of the damaged forests.

Keywords: Soil nutrient, Ecological restoration, Variable coefficient, Fujian, Nanping

1 Introduction

In recent years, all kinds of disasters such as floods, storms, and heavy rains have often occurred, which not only seriously damaged infrastructure, but also lead to a series of ecological environmental issues (Van et al., 2017; Zhang et al., 2011). Secondary disasters such as landslides, collapse, mudslides caused by continuous heavy rainfall, resulting in an ectopic or restructuring of the original soil layer, a large area of natural vegetation was buried or disappeared, and it was easy to form a secondary naked place (Liu et al., 2013). From the perspective of soil's microstructure, soil aggregates and micro-aggregates reduced, reducing the soil's anti-corrosion ability (Gburek et al., 1998), with the increase of rainfall erosion and surface runoff, the amount of eroded sediment increases after the soil structure and stability were destroyed, nutrients on the surface of aggregates and small particles flowed in large amounts with sediment and runoff (Liu et al., 2013), reduced the supply of the plant, thereby limited the productivity of vegetation communities, this lead to the reduction of biodiversity, and the ecological chain was easily interrupted by disasters, and the stability, anti-interference ability and self-recovery ability of the ecosystem deteriorated, which lead to further degradation of the ecological environment (Zeng et al., 2013; Yu et al., 2002; Wang et al., 2004). At present, natural recovery characteristics and mechanisms have been widely concerned by the academic disaster interference. Domestic and foreign scholars have studied the soil nutrients before and after the earthquake, found that the soil nutrient content of the landslide induced by continuous precipitation after the earthquake was significantly lower than that of adjacent areas where no landslide occurred. With the increase of the ecological restoration period of vegetation, the soil nutrient content of the landslide body shows a significant increase trend, and the regional habitat conditions have also been significantly improved (Wu et al., 2012;

Arunachalam et al., 2000). Therefore, restoring and improving the ecosystem in disaster-disturbed areas and giving full play to its ecological functions are not only the basic guarantee and important support for the healthy and stable development of the ecosystem, but also the key link and inevitable way to effectively prevent the occurrence of secondary disasters.

In the early stage of ecosystem restoration, soil nutrients, especially soil organic carbon (SOC), total nitrogen (TN), and total phosphorus (TP), whose storage was closely related with the growth and development of plants, the stability of the surface ecosystem, and the recovery process of the ecosystem (Yi et al., 2019). However, during the natural recovery of vegetation, due to the change in surface cover caused the heterogeneity of the local litter quantity, soil surface temperature and humidity, organic matter decomposition ability, and due to different vegetation types had different selection and absorption capacities of soil nutrients, and differences in soil structure and texture, Lead to different degrees of variability in the physical and chemical properties of the soil (Yang et al., 2012; Leuschner et al., 2013). Therefore, a correct understanding of the distribution pattern and restoration process of soil nutrients in damaged forests after floods can provide a theoretical basis for scientific management of soil nutrients and quantitative evaluation of the ecological restoration benefits of damaged ecosystems. However, the current domestic research on ecosystems in flood-affected areas was mainly focused on management and governance measures (Jin et al., 2013; Zhang et al., 2015), and there were relatively few studies on the restoration characteristics and variability of the main nutrients in damaged forest soils, especially for small-scale slopes, the variation characteristics caused by disasters were rarely reported, and it was difficult to summarize targeted recovery measures

Fujian Province is located in the southeast coastal area of my country, there are many storms and rains in summer, mountains and hills account for more than 80% of the total area of the province. The environmental background is potentially unstable (Lin et al., 2015), and the total area of soil erosion reaches 1.2×10^4 km^2, about 10% of the province's land area (Wang et al., 2017). The catastrophic floods and secondary disasters that occurred in June 2010 caused extensive damage to the main woodlands (secondary broad-leaved forests, fir forests, etc.) in Nanping City in northern Fujian Province, and the local vegetation-soil ecosystem was greatly damaged. Nanping City is one of the most serious regions of soil erosion in the southern red soil area (Yao et al., 2016), analyzing the damaged forest soil nutrients and recovery characteristics caused by its disasters can not only deepen the understanding of the disaster's effect on forest destruction, but also has important guiding significance for further formulating soil and water conservation plans, optimizing forest soil improvement measures, and implementing disaster impact assessment. In view of this, this paper selects the damaged forest land (secondary broad-leaved forest and fir forest) under the disturbance of flood disasters in Nanping City as the research object. The soil in the damaged area was sampled in July 2010, the recovered area and the undamaged area were sampled in July 2010, analyzed the main nutrient variation, restoration characteristics, and chemical measurement characteristics of soil in disaster interference damage forest, aims to provide data reference for the judgment of the main restrictive soil nutrient factors in the area and the protection, restoration and reconstruction of damaged forest ecosystems.

2 Material and methods

2.1 Site characteristics

The study area (Fig. 1a) is located in Nanping City, northern Fujian Province, with a humid subtropical monsoon climate, abundant forest resources, and covers up to 76.5%. The low mountains and hills in Nanping are widely distributed, with strongly affected by tectonic movement, the mountainous area is obviously cut and the topography is large. In addition, there are many rivers in the area, the runoff is large, the river courses are steep, and flood disasters are prone to occur. In June 2010, the heavy rainfall in Nanping City caused major floods such as landslides and mudslides. The number of forest landslides accounted for 64% of the total number of landslides. Among them, the two main types of local forests (secondary broad-leaved forest and fir forest) were the most severely damaged (Yu et al., 2016). Both forest types were affected by shallow landslides. The soil structure of 20~30 cm on the surface of the soil was severely damaged. The vegetation on the slope was buried or removed, and the original soil layered structure disappeared and formed a weak air layer. Therefore, in this study, two forests of secondary broad-leaved forest and fir forest were selected (Table 1) as the research objects

The fir forest (Fig. 1b) is located in Yuankeng Town, Shunchang County. In 2017, the undamaged Chinese fir forest was 22 years old, and it was a pure Chinese fir forest, and the main understory plants were covered with *Maesa japonica*, *Ageratum houstonianum* and *Kadsurae caulis* in undamaged area, and *Sapium discolor*, *Miscanthus floridulus* and *Rhus chinensis* in recovered area. Before the landslide occurred, the local people applied calcium-magnesium-phosphate fertilizer 749.63 kg·ha^{-1} and urea 224.89 kg·ha^{-1} on the undamaged and damaged plots of Chinese fir every year. The secondary broad-leaved forest plot (Fig. 1c) is located in Mangdang Town, Yanping District. Among them, the undamaged forest land was a natural secondary broad-leaved forest. Since 1958, there has been no human disturbance. The existing vegetation was multi-layered, and the first sublayer of the arbor layer was *Castanopsis carlesii*, *Castanopsis fargesii*; second sublayer of that was *Altingiagracilipes* and *Cyclobalanopsis glauca*; The third sublayer was mixed with the shrub layer, mainly including *Castanopsis carlesii*, *Arthraxon lancifolius* and *Angiopteris fokiensis*. The main vegetation of damaged natural restoration forest land included *Acidosasa longiligula*, *Alchornea davidii* and *Dicranopteris linearis*. The slopes of the undamaged sample plots of the two forest types had not been artificially modified, and the slope shape was complete and the degree of undulation was small.

In this experiment, due to the overall movement or reversal of the soil layer, the soil layers of the damaged sample plots affected by the landslide in the two forest types were flattened under the action of the post-disaster rainfall. The slope shape was relatively complete and uniform during sampling. Although there were residual vegetation in some areas, it is not in the sampling square, and the continuity and consistency of the slope shape are maintained between adjacent squares of each slope position to ensure the uniformity of sample collection. Disturbed by disasters, vegetation coverage was low, mainly distributed *Conyza canadensis* and *Miscanthus floridulus*. Fig. 2 showed the comparison before and after natural recovery of the secondary broad-leaved forest landslide.

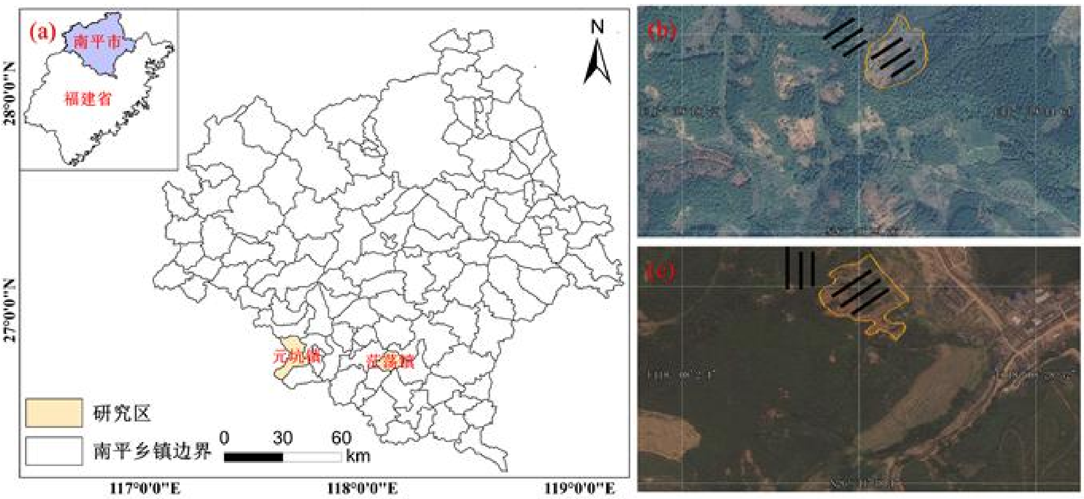

Figure 1 Location of the study area and sample plot: (a) Schematic map of study area; (b) Remote sensing image of Cunninghamia lanceolata forest in Yuankeng town in 2010; (c) Remote sensing image of Secondary broad-leaved forest of Mangdang town in 2010

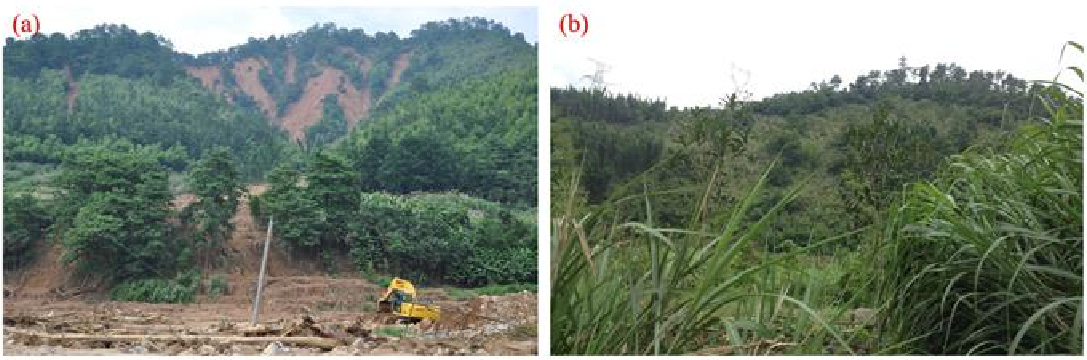

Figure 2 Comparison of Mangdangshan landslide in Nanping City before and after natural recovery

Table 1 Characteristics of sample plots

Forest types	Plot types	Longitude	Latitude	Altitude/m	Slope/°	Coverage/%
Secondary broad-leaved forest	Recovered area	118°08′35″	26°41′39″	173	40	60
	Undamaged area	118°08′31″	26°41′42″	188	36	88
	Damaged area	118°08′35″	26°41′39″	173	40	20
Cunninghamia lanceolata forest	Recovered area	117°39′45″	26°50′33″	226	32	52
	Undamaged area	117°39′44″	26°50′36″	238	34	72
	Damaged area	117°39′45″	26°50′33″	226	32	10

2.2 Research method

2.2.1 Plot setting with sample collection

In July 2010, one damaged plot of 40 m×30 m was set up in the secondary broad-leaved forest and fir forest. With an interval of 10m, three slope positions were set up from top to bottom for each plot, and three 2 m×2 m squares were selected for each slope position, and the interval between the squares was about 5 m. Take soil samples at a depth of 20 cm at the diagonal center of each plot, and bring them back to the laboratory for air-drying and pass through a soil sieve with a diameter of 0.149 mm for determination of soil nutrient content.

Set up undamaged plots of the same area near the damaged plots of various forest types, closed for management but no sampling. Second sampling was carried out in July 2017. The same method was used to sample the blocked undamaged sample plot and the original damaged sample plot as the soil samples for undamaged plots and natural recovery plots (7a). A total of 54 soil samples were collected from all plots.

2.2.2 Sample analysis

SOC content adopted sulfuric acid-potassium dichromate external heating method; TN content adopted sulfuric acid-semi-trace Kjeldahl method; TP content adopted molten alkali-molybdenum antimony colorimetric method (Ge et al., 2012).

2.2.3 Calculation method

(1) Soil recovery rate formula (Liu et al., 2019):

$$R = D/U \quad (1)$$

R is the recovery rate of soil SOC, TN, TP (%), D is the content of SOC, TN, TP in the damaged recovery area ($g·kg^{-1}$), U is the content of SOC, TN, TP in the undamaged area ($g·kg^{-1}$)

（2) Variation Coefficient Formula (Liu et al., 2019):

$$C.V = SD/\bar{x} \quad (2)$$

C.V is the coefficient of variation of soil SOC, TN, and TP (%), *SD* is the standard deviation of SOC, TN, and TP content (g·kg-1), and $\bar{x}$ is the average of SOC, TN, and TP content ($g·kg^{-1}$).

2.2.4 Data processing

Used Excel 2016 for data processing, and used SPSS 19.0’s one-way analysis of variance (LSD test was performed when the significance level of the difference between variables was P <0.05) to compare SOC, TN, TP content and stoichiometric ratio in different sample plots.

3 Results and analysis

3.1 Comparison of SOC, TN, and TP content in two different forest types

Analyze the measurement data of soil samples from different forest types of research areas in Nanping City(Table 2). The contents of SOC, TN, and TP in the two forest types were all expressed as undamaged area> recovered area> damaged area. Among them, The SOC and TP of the secondary broad-leaved forest were significantly different between different sample plots (*P* <0.05), while TN was not significantly different between the recovered area and the damaged area (*P*> 0.05). The SOC of Chinese fir forest were significantly different between different locations (*P* <0.05), while TN had no significant difference between the recovered area and the damaged area (*P*> 0.05). TP was in the damaged recovery area and the undamaged area, TN was not significantly different between the recovered area and the undamaged area

Table 2 SOC, TN, TP content and the P-value in different sample plots of the two forest types.

Forest types	Plot types	SOC/ $g \cdot kg^{-1}$	TN/ $g \cdot kg^{-1}$	TP/ $g \cdot kg^{-1}$
Secondary broad-leaved forest	Recovered area	10.18±0.17bc	0.57±0.04b	0.58±0.01b
	Undamaged area	23.64±0.82a	1.76±0.04a	0.78±0.01a
	Damaged area	4.51±0.21c	0.12±0.00b	0.22±0.00c
Cunninghamia lanceolata forest	Recovered area	16.97±0.43b	0.75±0.04b	0.55±0.00b
	Undamaged area	18.59±0.70a	1.64±0.04a	0.59±0.01b
	Damaged area	4.38±0.15c	0.24±0.01b	0.34±0.01c

Note: Different lowercase letters indicate the difference reaches a significant level of 0.05.

3.2 Differences in soil restoration rates of different forest types

It can be seen from Table 3 that the average recovery rate of SOC, TN and TP in the fir forest were higher than secondary broadleaf forest. Overall, both forest types showed the highest recovery rate of TP, followed by SOC, and the lowest recovery rate of TN.

Table 3 Average recovery rates of SOC、TN and TP in different forest types

Forest types	SOC/%	TN/%	TP/%
Secondary broad-leaved forest	43.06	32.39	74.36
Cunninghamia lanceolata forest	91.29	45.73	93.22

3.3 Stoichiometric ratio of soil C, N, P in two forest types

According to Table 4, comparing the recovered area and the undamaged area of the two forest types, it can be found that C:N in the damaged recovery area was significantly higher than the undamaged area only in the Chinese fir forest (*P* <0.05), C: P in the undamaged area was significantly higher than the recovered area only in the secondary broad-leaved forest (*P* <0.05), and N:P in the undamaged area was significantly higher than the damaged recovery area in both forest types (*P* <0.05).

Comparing the recovered area and the damaged area of the two forest types, it can be found that, except for C:P in the damaged recovery area was significantly higher than the damaged area in the Chinese fir forest, (*P*

<0.05). C:N, C:P and N:P showed no significant difference between the recovered area and the damaged area of the two forest types (P> 0.05).

Table 4 Soil stoichiometric ratio in different sample plots of the two forest types

Forest types	Plot types	Stoichiometric ratio		
		C:N	C:P	N:P
Secondary broad-leaved forest	Recovered area	23.04±1.23ab	17.82±0.41b	0.95±0.05b
	Undamaged area	13.18±0.22b	30.44±1.03a	2.28±0.05a
	Damaged area	39.04±1.89a	20.34±0.90b	0.54±0.01b
Cunninghamia lanceolata forest	Recovered area	24.26±0.61a	31.23±0.84a	1.38±0.07b
	Undamaged area	11.68±0.46b	31.52±1.09a	2.82±0.08a
	Damaged area	20.09±0.97ab	12.93±0.46b	0.70±0.02b

Note: Different lowercase letters indicate the difference reaches a significant level of 0.05.

3.4 Coefficient of variation of soil carbon, nitrogen, and phosphorus in two different forest types

The strength of soil variability can be classified according to the size of the coefficient of variation: C. V ⩽ 20% is weak variability; 20% < C. V < 50% is moderate variability; C. V ⩾ 50% is a strong variability (Wu et al., 2019).

It can be seen from Table 5 that SOC was moderately variable in the two forest types, and its coefficient of variation was shown as the damaged area > damaged recovery area; TN had strong variability in the restored areas of the two forest types, belonged to medium variation and below in other plots. and its coefficient of variation was shown as damaged recovery area > damaged area in both forest types. The coefficient of variation of TP showed weak variability in each of the two forest types, the scope of change was not large, indicating that its content in the soil was relatively stable.

Table 5 Change of SOC, TN, TP variation coefficient in different sample plots of the two forest types

Forest types	Plot types	SOC/%	TN/%	TP/%
Secondary broad-leaved forest	Recovered area	15	58	16
	Undamaged area	31	19	13
	Damaged area	42	23	13
Cunninghamia lanceolata forest	Recovered area	23	42	6
	Undamaged area	34	23	6
	Damaged area	31	28	14

4 Discussion

4.1 Variation characteristics of soil nutrient content in damaged forests

SOC, TN and TP are the main nutrient elements of plant growth, and soil nutrients as part of the soil environment (Cheng et al., 2003; Chander et al., 1998; Morrison et al., 2001), which reflects the recovery level of the entire soil system (Zhao et al., 2018; Yu et al., 2009). In this study, the SOC, TN and TP of secondary broad-leaved forests and fir forests were expressed as undamaged area> recovered area> damaged area, similar to the change trend of vegetation coverage in various plots, it indicated that the main soil nutrient content was consistent with the degree of vegetation restoration, which was consistent with the research results of most scholars (Li et al., 2018; Liu et al., 2014). The flood and its induced secondary disasters had damaged local forests to a certain extent, resulting in an increase in the degree of flushing erosion of the soil. Surface runoff carried nutrient-carrying sediment particles and converges to the river channel, which lost nitrogen, phosphorus and organic matter in the sediment. The nutrient content of other soils was higher than that of topsoil, resulting in poor forest soil nutrients (Wu et al., 2019). With the increase of ecological restoration years, vegetation restoration can not only change the characteristics of vegetation community, increase root exudates and the amount of litter material input into the soil (Yang et al., 2012), but also change the living environment of microorganisms and affect the decomposition rate of plant residues (Fang et al., 2001). Chen Xiaoqing and others believe that the vegetation in good vegetation areas had a relatively complete combination of arbor, shrub, and grass, and its roots can anchor a large amount of soil from shallow to deep, so that the soil was reinforced by vegetation and the soil structure was gradually improved, which helped microorganisms obtain a stable living environment, which was conducive to their activities and reproduction, and increase the rate of decomposition of organic matter (Chen et al., 2006; Jason et al., 2005). In this study, the contents of SOC, TN, and TP in the recovered areas of the two forest types were higher than those in the damaged area, indicating that the initial natural restoration of the ecosystem had a significant effect on the accumulation of major soil nutrients, but only the TP content of the secondary broad-leaved forest showed that the recovered area was significantly higher than the damaged area. The SOC and TP content of the damaged recovery area of Chinese fir forest were significantly higher than those of the damaged area, and the recovery rate of SOC, TN and TP of the Chinese fir forest was higher than that of the secondary broadleaf Forest, indicating that the natural restoration of soil nutrients in fir forests was better, which was mainly affected by the combined effects of fertilization treatment, forest land slope, soil texture: First of all, the fertilization in the early stage of the Chinese fir forest disaster can effectively increase the nutrient content of the soil, make the plant root system more developed, and provide a basis for the restoration of soil nutrients after the disaster (Liu et al., 2014), and at the same time, it was beneficial to promote the reproduction of microbial populations, promote nutrient cycling and biological effectiveness (Sun et al., 2004); Secondly, the smaller slope of the damaged recovery area of fir forest can enable the vegetation and microorganisms in the area to obtain a relatively stable living environment; Furthermore, the soil of the fir forest plot involved in this study was doped with more small gravel, which was conducive to reducing soil bulk density and improving soil porosity, which in turn was conducive to plant root growth and promotes nutrient cycling and transformation (Luo et al., 2019). Therefore, it is recommended to strengthen the ecological management of the damaged area of the secondary broad-leaved forest in the later restoration and management process to improve the soil structure and promote nutrient cycling.

4.2 Variability of soil nutrients in damaged forests

The soil erosion caused by flood disasters will not only directly destroy the surface vegetation, but also lead to changes in soil nutrients, exhibiting different degrees of variability (Li et al., 2016). Research on the coefficient of variation of SOC, TN, and TP in two forest lands, the results show that the coefficient of variation of SOC in all forest lands was shown as damaged area> recovered area, indicating that the soil structure in the damaged area was severely damaged due to soil erosion, and the soil surface nutrient loss was serious, and the heterogeneity of SOC also increased with the degree of soil damage. The difference from the above rules was that the coefficient of variation of TN in each forest lands shown as recovered area > damaged area. This was mainly because: (1) When the forest was just damaged, due to the amino acid nitrogen, the nitrate nitrogen in the NH_3-N and inorganic nitrogen components were easily lost with sediment and surface runoff, resulting in the loss of soil surface nitrogen, resulting in greater variability in the region (Zhao et al., 2010; Wang et al., 2000) (coefficient of variation performance was: damaged area> undamaged area); (2) Nitrogen is the main restrictive element for plant growth, the demand for nitrogen in the early stage of plant growth far exceeds that of other nutrients such as phosphorus (Wang et al., 2000). Coupled with the random expansion and reproduction of herb communities in the early stage of restoration, increased the degree of heterogeneity of TN content in the soil, leading to a high degree of heterogeneity in its spatial distribution (Garner et al., 1989; Paul et al., 1991; Epstein et al., 1998). TP showed weak variability in both forest lands, which may be related to the form of phosphorus in the soil. The soil phosphorus in the southern red soil area is mainly controlled by the minerals contained in the soil parent material, which is relatively stable and not easy to leaching and loss (Wang et al., 2002), so the variability was weak.

4.3 C:N:P stoichiometric ratio of damaged forest soil

The stoichiometric ratio of soil C:N:P is an important indicator to measure the balance characteristics of soil carbon, nitrogen, and phosphorus, reflecting the synergy of soil nutrient elements in the damaged forest ecosystem and its changing trend (Liu et al., 2019).

The soil C:N value reflects the change trend between carbon and nitrogen. In this study, except for the undamaged area, the soil C:N value of the damaged area and the recovered area in two forest types was higher than the C:N level range of mountainous soil in Fujian Province (11.7 ~ 18.2) (Tian et al., 2010). Due to the easy mobility of nitrogen in the soil, it is easily leached and lost (Zhao et al., 2010), resulting in the average recovery rate of TN in the two forest types being lower than that of SOC. Compared with SOC, TN is in a more deficient state, which caused the soil C:N value to increase, indicating that the floods and secondary disasters in this area had severely damaged the soil carbon and nitrogen cycles, leading to the instability of the input and output balance mechanism of SOC and TN in the initial stage of restoration, damaged areas still need long-term ecological restoration to achieve a more stable soil carbon-nitrogen ratio.

Soil C:P reflects the ability of microbial mineralized soil organic matter to release phosphorus or absorb and hold phosphorus from the environment. It is an important indicator to measure the availability of soil phosphorus. The lower the value, the higher the effectiveness of soil phosphorus (Chen et al., 2012). The study area was red-yellow soil. The TP content in the surface layer of each forest type was significantly lower than that of the national soil surface layer (0.78 $g \cdot kg^{-1}$) (Paul et al., 1991), but the soil C:P value was significantly lower than that of the subtropical soil C: The P value (78) (Batjes, 2014), showed that although the soil in the study area had less phosphorus (Lai et al., 2018), its available phosphorus content can meet the needs of plant growth, and the soil C:P value was mainly affected by SOC. In addition, because the recovery rate of SOC in secondary broad-leaved forest (43%) was significantly lower than that of fir forest (91%), the soil C:P in the secondary broad-leaved forest was significantly higher in the undamaged area than in the damaged recovery area, and there was no significant difference between the two regions of Chinese fir forest.

Soil N:P is used to determine the threshold of soil nitrogen and phosphorus nutrient limits (Zhu et al., 2013). The TN and TP values of the two forest lands in this study were lower than the TN (1.86$g \cdot kg^{-1}$) and TP (0.78$g \cdot kg^{-1}$) contents of the national soil surface (Wang et al., 2002), indicating that there was a serious lack of nitrogen and phosphorus in this study area. In addition, the average N:P value of the damaged and restored areas of the two forest types was lower than that of the undamaged area. This was mainly because the recovery rate of TN was much lower than that of TP, indicating that the N:P value of soil in this area was mainly affected by TN.

Comparing the recovered area and the damaged area of the two forest types, it can be found that, except for C: P of the damaged recovery area was significantly higher than the damaged area in Chinese fir forest,, and C: N, C: P and N: P shown no significant differences between the recovered area and the damaged area of the two forest types, indicating that the SOC of the two forest types and the TN of the secondary broad-leaved forest did not achieve significant recovery during the natural recovery process, and there was still a large gap compared with the damaged area, indicating that the natural restoration effect of soil nutrients in this area was poor. It is recommended that artificial measures be used to promote vegetation restoration and improve soil fertility in the later period.

5 Conclusion

In summary, landslides caused by flood disasters not only caused extensive damage to vegetation and serious soil erosion, but also caused a large amount of loss of SOC, TN and TP. On the whole, the loss of TN was the most serious, followed by SOC, and the loss of TP is the smallest in the damaged forest soil in Nanping City. It is recommended that nitrogen fertilizer and carbon fertilizer be appropriately applied in the later treatment to improve the overall nutrients of the soil, which is beneficial to the overall ecological restoration of the region. In addition, the scope of this study was in an area with insufficient phosphorus. It is recommended to appropriately apply phosphate fertilizer or biological phosphate solubilizing bacteria fertilizer to ensure the supply and balance of the main nutrients in the soil, avoid the restriction of P in the next stage of restoration process, so as to promote better restoration of vegetation-soil ecosystem. In addition, the stoichiometric ratios of soil nutrients in the disaster-stricken forests were all in a serious imbalance. Soil C:P was mainly affected by SOC, soil C:N and N:P were mainly affected by TN. Overall, TN has the largest variability, followed by SOC, TP has the least variability. From the perspective of the degree of soil nutrient restoration, the SOC and TP content in the recovered area of fir forest were significantly higher than that in the damaged area, while the only the TP content was significantly higher than that in the damaged area secondary broad-leaved forest. The recovery rates of TN, TP and TP in secondary broad-leaved forest were higher than those of secondary broad-leaved forests, indicating that the early fertilization of fir forests had a good effect on the natural restoration of soil nutrients. It is recommended that the ecological restoration of secondary broad-leaved forests should be strengthened in the later management process. In addition, although vegetation restoration had increased the SOC, TN and TP nutrient contents of the disaster-disturbed soil as a whole, there was still a certain gap compared with the undamaged area, indicating that the soil nutrient in this area had not been restored to the original level, and the natural restoration process was slow and the effect is poor. It is recommended that the damaged forest be properly managed manually in the later stage, such as closing hills for afforestation, planting artificial forests or adopting engineering technical measures to promote its recovery as soon as possible

Acknowledgement

We thank Pu, S. L., Bai, P. B., Zhang, Y. L., Lu, Z. S. and the staff of Dongchuan Debris Flow Observation and Research Station for help with collecting and analyzing data.

References

Arunachalam, A., Arunachalam, K., Bhattacharjee, A., et al. (2000). "Natural revegetation on landslides in humid tropical Arunachal Pradesh: community dynamics and soil properties." Journal of Tropical Forest Science, 12(4): 682-696.

Batjes, N. H. (2014). "Total carbon and nitrogen in the soils of the world." European Journal of Soil Science, 65(1): 10-21.

Chander, K., Goyal, S., Nandal, D. P., et al. (1998). "Soil organic matter, microbial biomass and enzyme activities in a tropical agroforestry system." Biology and Fertility of Soils, 27(2): 168-172.

Epstein, H. E., Burke, I. C., Mosier, A. R. (1998). "Plant effects on spatial and temporal patterns of nitrogen cycling in shortgrass steppe." Ecosystems, 1(4): 374-385.

Chen, F. S, Xue, F., Chao, L. (2012). "Endogenous versus exogenous nutrient affects C, N, and P dynamics in decomposing litters in mid-subtropical forests of China." Ecological Research, 27(5): 923-932.

Chen, X. Q., Cui, P., Wei, F. Q.. (2006). "Study of control debris flow in high-covered vegetation region." Mountain Research, 24(3): 333-339.

Cheng, X. L., An, S. Q., Li, Y., et al. (2003). "The individual distribution patterns and soil elements hetero-geneity during the degradation of grassland in Ordos." Acta Phytoecologica Sinica, 27(4): 503-509.

Fang, C., Moncrieff, J. B. (2001). "The dependence of soil CO_2 efflux on temperature." Soil Biology and Biochemistry, 33(2): 155-165.

Garner, W., Steinberger, Y. (1989). "A proposed mechanism for the formation of 'Fertile Islands' in the desert ecosystem." Journal of Arid Environments, 16(3): 257-262.

Gburek, W. J., Sharplry, A. N. (1998). "Hydrologic controls on phosphorus loss from upland agricultural watersheds." Journal of Environmental Quality, 27(2): 267-277.

Ge, X. G., Xiao, W. F., Zeng, L. X., et al. (2012). "Relationships between litter substrate quality and soil nutrients in different-aged *Pinus massoniana* stands." Acta Ecologica Sinica, 32(3): 852-862.

Leuschner, C., Wulf, M., Bauchler, P., et al. (2013). "Soil C and nutrient stores under Scots pine afforestations compared to ancient beech forests in the German Pleistocene: the role of tree species and forest history." Forest Ecology and Management, 310(1): 405-415.

Li, N. N., Zhang, G. H., Wang, H., et al. (2018). "Properties of vegetation succession on shallow landslide deposits in loess hilly and gully region and the related response of Soil nutrient." Mountain Research, 36(5): 669-678.

Jason, G. V., Valentine, D. W., Roger, W. R. (2005). "Soil and root respiration in mature Alaskan black spruce forests that vary in soil organic matter decomposition rates." Canadian Journal of Forest Research, 35(1): 161-174.

Jin, Z. F. (2013). "Yushu seismic landslide characteristics and formation mechanism and its control measures." Building Structure, 43(S2): 686-689.

Lai, Z. J., Liu, J., Yu, K. Y., et al. (2018). "Spatial variability of Soil nutrients in typical *phyllostachys pubescens* growing areas in South China--*Takmg phyllostachys heterocycla cv.pubescens* forest management area in Shunchang county, Nanping city, Fujian province as example." Journal of North-East Forestry University, 46(3): 63-68.

Li, Y., Pei, Z. Y., Qin, W., et al. (2016). "Regional clear cutting operation on Soil nutrient of *salix psammophila* forest short-term disturbance characteristics." Science Technology and Engineering, 16(18): 161-165.

Lin, J. (2015). "Practice and exploration of soil and water loss control in Fujian province." Soil and Water Conservation in China, (10): 27-28.

Liu, F. (2014). "A study on fertilization effects and changes of soil nutrient contents in 2 year-old Chinese fir plantation." Fuzhou: Fujian Agriculture and Forestry University, 1-6.

Liu, Y., Song, T. Q., Cai, D. S., et al. (2014). "Soil fertility characteristics under different land use patterns in depressions between karst hills." Chinese Journal of Applied Ecology, 25(6): 1561-1568.

Liu, Y., He, J. W., Wu, J. Z., et al. (2019). "Soil recovery rate and spatial heterogeneity in the process of ecological restoration in an earthquake-affected area." Chinese Journal of Applied & Environmental Biology, 25(4): 823-830.

Luo, Q. H., Wu, J. Z., Cui, Y., et al. (2019). "Basic soil properties and fractal dimensional characteristics of damaged naturally restored forest land disturbed by flood and waterlogging disasters." Chinese Journal of Applied & Environmental Biology, 25(1): 29-37.

Morrison, I. K., Foster, N. W.. (2001). "Fifteen-year change in forest floor organic and element content and cycling at the Turkey Lakes watershed." Ecosystems, 4(6): 545-554.

Paul, B. H., Ingrid, C. B., Lauenroth, W. K. (1991). "Heterogeneity of soil and plant N and C associated with individual plants and openings in North American shortgrass steppe." Plant and Soil, 138(2): 247-256.

Sun, R. L., Zhu, L. S., Zhao, B. Q., et al. (2004). "Effects of long-term fertilization on soil microorganism and its role in adjusting and controlling soil fertility." Chinese Journal of Applied Ecology, 15(10): 1907-1910.

Van, O. K., Quine, T. A., Govers, G., et al. (2007). "The impact of agricultural soil erosion on the global Carbon cycle." Science, 318(5850): 626-629.

Wang, B. Q., Dai, M. J. (2000). "Simulated study on movement features of soil nitrogen in different forms in soil profile." Research of Soil and Water Conservation, 7(4): 117-122.

Tian, H. Q., Chen, G. S., Zhang, C., et al. (2010). "Pattern and variation of C:N:P ratios in China's soils: a synthesis of observational data." Biogeochemistry, 98(1/3): 139-151.

Wang, J., Fu, B. J., Qiu, Y., et al. (2002). "Spatial heterogeneity of soil nutrients in a small catchment of the Loess Plateau." Acta Ecologica Sinica, 22(8): 1173-1178.

Wang, S. J., Liu, Q. M., Zhang, D. F. (2004). "Karst rocky desertification in southwestern China: geomorphology, landuse, impact and rehabilitation." Land Degradation & Development, 15(2): 115-121.

Wang, S. Q., Yu, G. R. (2008). "Ecological stoichiometry characteristics of ecosystem carbon, nitrogen and phosphorus elements." Acta Ecologica Sinica, 28(8): 3937-3947.

Wang, Z. P., Wang, X. Q., Zeng, S. J., et al. (2017). "Analysis of soil and water loss in Fujian province." Bulletin of Soil and Water Conservation, 37(5): 169-175.

Wu, C., Wang, J. N., Lu, T., et al. (2012). "Effect of Wenchuan earthquake on soil physical and chemical properties of the Longmen mountain, southwestern China." Chinese Journal of Applied & Environmental Biology, 18(6): 911-916.

Wu, P., Cui, Y. C., Zhao, W. J., et al. (2019). "Characteristics of soil stoichiometric in natural restoration process of Maolan karst forest vegetation, southwestern China." Journal of Beijing Forestry University, 41(3): 80-92.

Yang, H. F., Mu, S. J., Li, J. L. (2012). "Effects of climate change on soil organic carbon storage of grassland ecosystem." Pratacultural Science, 29(3): 392-399.

Yang, X. Y., Guo, P. Y., Han, Y. Z., et al. (2012). "Effects of cutting disturbance on spatial heterogeneity between root biomass of the herb and Soil environment in *larix principis-rupprechtii* forests in Guandi Mountain." Journal of Wuhan Botanical Research, 30(6): 545-551.

Yao, X., Yu, K. Y., Liu, J., et al. (2016). "Spatial and temporal changes of the ecological vulnerability in a serious soil erosion area, Southern China." Chinese Journal of Applied Ecology, 27(3): 735-745.

Yi, Z., Peng, L., Liu, X. J., et al. (2019). "Effects of farmland conversion on the stoichiometry of carbon, nitrogen, and phosphorus in soil aggregates on the Loess Plateau of China." Geoderma, 351:188-196.

Yu, B. (2009). "Study on spatial heterogeneity of soil nutrients in different degradation stages of *seriphidium* desert grassland." Urumqi: Xinjiang Agricultural University, 2-6.

Yu, K. Y., Liu, J., Yang, P., et al. (2016). "The impact of forest management forest management process on the landslide." Journal of Central South University of Forestry & Technology, 36(4): 5-10.

Yu, L. F., Zhu S. Q., Ye J. Z., et al. (2002). "Evaluation on degradation of Karst forest community and human disturbance." Chinese Journal of Applied Ecology, 13(5): 529-532.

Zeng, D. P., Jiang, L. L., Zeng, C. C., et al. (2013). "Reviews on the ecological stoichiometry characteristics and its applications." Acta Ecologica Sinica, 33(18): 5484-5492.

Zhang, D. G. (2015). "Effect of deforestation and landslide on soil of *Rhododendron* shrub ecosystem in the eastern Qilian mountains." Acta Prataculturae Sinica, 2002, 11(3): 72-75.

Zhang, J. D., Hull, V., Xu, W. H., et al. (2011). “Impact of the 2008 Wenchuan earthquake on biodiversity and giant panda habitat in Wolong Nature reserve, China.” Ecological Research, 26(3): 523-531.

Zhao, M. X., Zhou, J. B., Yan, Z. L. (2010). “Adsorption characteristics of soluble organic Carbon and Nitrogen in different layer of cultivated soils.” Chinese Journal of Soil Science, 41(6): 1328-1332.

Zhao, Y., Luo, Z. J., Liao, M. X., et al. (2018). “Study on the spatial distribution of Soil nutrients and its influencing factors in the cultivated land of Taihe county.” Journal of Soil and Water Conservation, 32(5): 296-303.

Zhu, Q. L., Xing, X. Y., Zhang, H., et al. (2013). “Soil ecological stoichiometry under different vegetation area on loess hilly gully region.” Acta Ecologica Sinica, 33(15): 4674-4682.

Experience and Perspectives on Acceptance Review of Soil and Water Conservation Facilities and Water Conservancy Engineering
—Taking the Reinforcement of Panzhuang Yellow River Diversion Sluice as an Example

Li Li*[1,2], Zhaoxiao Dong[3], Xueyuan Wei[1]
1 Yellow River Institute of Hydraulic Research, Yellow River Conservancy Commission, China
2 Key Laboratory of Soil and Water Conservation in the Loess Plateau, MWR, China
3 Construction Center of Yellow River Shandong Bureau, China
*Corresponding Author, e-mail: 14578126@qq.com

Abstract

In 2017, the State Council changed the acceptance of soil and water conservation facilities from administrative acceptance to self-organized acceptance by project implementation unit. The acceptance report will be prepared by the organization not involved in the project. Taking the Panzhuang reinforcement project of the Yellow River Diversion Sluice as an example, the paper briefly introduces the characteristics of the acceptance process of soil and water conservation facilities in water conservancy engineering. The invited organization is responsible for the acceptance quality, and the acceptance is based on the received UAV remote sensing information. UAV remote sensing technology has been widely used in monitoring the status and supporting the acceptance due to its advantages of rapid collection and extraction of adequate information. It improves the accuracy and reliability of relevant indicators and provides more intuitive and reliable results. Independent acceptance of soil and water conservation project focuses on analyzing and evaluating changes in responsible range, completion of soil and water conservation measures, quality assessment of soil and water conservation engineering, effects of soil and water conservation, etc., so as to draw a conclusion whether the acceptance by owners meets the standard. The paper finally summarizes the existing challenges on independent acceptance and proposes countermeasures, which might provide reference for independent acceptance of similar projects.

Keywords: Water Conservancy Engineering, Yellow River Diversion Sluice, Soil and Water Conservation Facilities, Independent Check and Acceptance

1 Introduction

As the special acceptance before the completion acceptance of production and construction projects, the acceptance of soil and water conservation facilities is the precondition for the smooth operation of production and construction projects. It is consistent with the rule that soil and water conservation facilities must be put into operation simultaneously. The acceptance is an important inspection process to check whether the production and construction units fulfill the obligation of soil and water loss prevention in accordance with the law, and whether the prevention effect meets the standards and requirements of soil and water conservation plan.

In 2017, the Ministry of Water Resources issued a notice to strengthen the supervision during and after work and standardize the independent acceptance of soil and water conservation facilities for production and construction projects (Ministry of Water Resources, 2017). It is stipulated that the acceptance of soil and water conservation facilities for production and construction projects shall be conducted by the project legal person independently rather than the water administrative department. The legal person shall organize a third party to prepare the acceptance report.

As central budget investment projects, water conservancy projects are slightly different from ordinary production and construction projects in terms of construction management, capital use and acceptance evaluation. Taking the reinforcement of Panzhuang Yellow River Diversion Sluice Project in the lower Yellow River as an example, this paper analyzes the acceptance characteristics of soil and water conservation facilities for water conservancy projects, then summarizes the experience in the independent acceptance of soil and water conservation facilities. Based on these, the paper also analyzed problems existing in the independent acceptance and puts forward the countermeasures, so as to provide some reference for the water conservancy project builders in the undertaking of independent acceptance.

2 Project Overview

Sluice is a controlling hydraulic structure built on the river, which belongs to the water conservancy infrastructure and is an integral part to the flood control system of rivers and lakes (Yan, 2012). Located in the lower reaches of the Yellow River, the Panzhuang Yellow River Diversion Sluice mainly introduces the water of the Yellow River and undertakes the task of local industrial, agricultural and domestic water supply, as well as the task of emergency water supply to Tianjin City. After years of operation, it was rated as Class IV and needs to be reinforced due to safety problems such as seepage stability, energy dissipation and anti-scouring that cannot meet the requirements, rusting and cracking of the gate chamber and cavity, aging of the equipment， etc. This will eliminate the hidden danger of engineering safety, thereby ensuring the flood control safety of the Yellow River Levee.

Panzhuang Yellow River Diversion Sluice is strengthened by demolishing the original sluice and rebuilding in the new site to maintain the original project scale, grade and flood control standards. The design diversion flow is $100m^3/$ s, the engineering grade is grade 1, the main building grade is grade 1, and the design flood standard is $11000m^3/$ s. The project consists of main engineering zone, construction, production and living area, construction road zone, borrow site and temporary stockyard. It covers an area of $26.23hm^2$, of which $0.23hm^2$ is occupied permanently and $26hm^2$ is occupied temporarily. The project will be started on January 18, 2017 and completed on May 20, 2019, with a total construction period of 28 months.

3 Characteristics of Acceptance

(1) The layout of sluice reinforcement project is relatively concentrated, and its construction area is mainly located at or near the original sluice location, with relatively low disturbance intensity.

(2) Soil and water conservation measures of water conservancy projects are divided into two types, one is that the main body already has the soil and water conservation facilities, the other is that new measures are added to the soil and water conservation scheme. The investments approved by the Ministry of Water Resources in the soil and water conservation scheme and by the State Development and Reform Commission in the preliminary design stage are new investments in soil and water conservation measures. Therefore, when carrying out the acceptance assessment, the quantities of soil and water conservation measures in the main works should be verified on site, and the completion and effect should be evaluated, which are not regarded as the investment statistics of soil and water conservation.

(3) In the preliminary design stage, the reclamation of the borrow site and the topsoil stripping and re-covering for the occupied farmland are specially considered for the immigrants of the main engineering. They are not listed repeatedly. In the acceptance assessment, these measures are incorporated in the existing ones of the main engineering, only for on-site verification and evaluation, and not included in soil and water investment.

(4) The project belongs to the central government budgetary investment based on the investment estimates approved by the National Development and Reform Commission. The soil and water conservation is an independent unit project. The development unit and the construction unit sign a contract for soil and water conservation project, in which the construction requirements and payment procedures of the soil and water conservation project are specified.

(5) The project has a large amount of excavation and backfilling. Loam and clay need to be filled for the construction of new sluice. Silt and construction materials dismantled are wastes. Therefore, the soil yard and the destination of the waste are the key assessment scope of the project acceptance.

(6) The data is collected from different departments, mainly from participant units, while the temporary land occupation and earth volume are from the Demolition and Relocation Office. Therefore, it is necessary to verify each data source and corroborate each other to ensure the accuracy of the data.

4 Analysis and Evaluation on Acceptance of the Third-party Organization

Third-party organizations are commissioned to prepare acceptance reports of soil and water conservation facilities as project legal persons. Considering the characteristics of the project, the main contents of acceptance and evaluation are to verify the responsible range for soil and water loss prevention, the location of borrow site and measures to protect them, the completion of soil and water conservation measures and investment, the evaluation of soil and water conservation project quality, and the effect of soil and water conservation, etc. All the above contents are evaluated truthfully, and a clear conclusion is drawn as to whether the acceptance criteria and conditions of soil and water conservation facilities are met (Peng, 2020).

Unmanned Aerial Vehicle (UAV) technology is a comprehensive technology that acquires data information by sensors and processes image data by computer. It has developed rapidly in many fields with advantages of high spatial resolution, good automation process, convenient carrying and fast reaction speed (Liao, 2018). In this project, UAV technology is used to obtain data information such as area, length, vegetation coverage, volume, shape and slope of the measuring object by means of graphics vectorization, spatial three-dimensional calculation and field aerial photography. Comprehensive management of acquired data and information by Ovi Map software can realize continuous comparison of prevention and control effects and determine the implementation of various measures in different construction periods of the project, thus providing more reliable and convenient technical methods for project completion acceptance, especially for the image information with high accuracy and within the scope of key verification. UAV technology can obtain more intuitive and reliable analysis results, so as to the requirements of comparative analysis of data information during acceptance of soil and water conservation facilities (Shi, 2019).

4.1 Responsible range for soil and water loss prevention

After aerial photography, data processing and information extraction of the site with UAV technology, the three-dimensional modeling of Panzhuang Yellow River Diversion Sluice (2017-2019) is shown in Fig. 1-3. The approval and actual range for soil and water loss prevention of Panzhuang Yellow River Diversion Sluice are detailed in Table 1.

Figure 1 3D modeling of Panzhuang Yellow River Diversion Sluice (2017)

Figure 2 3D modeling of Panzhuang Yellow River Diversion Sluice (2018)

Figure 3 3D modeling of Panzhuang Yellow River Diversion Sluice (2019)

4.2 Implementation of soil and water conservation measures

The problems lie in whether the soil erosion can be effectively prevented and controlled in the construction process, and whether the built soil and water conservation facilities can exert a long-term influence in soil and water conservation. The integrity of soil erosion control system and the reliability of engineering quality are the most important basic guarantee (Jiang, 2018). Based on the approved soil and water conservation scheme, preliminary design and construction contract, Table 2 shows the soil and water conservation measures determined by UAV technology combined with field investigation.

Table 1 Responsible Range of Soil and Water Loss Prevention

Project composition	Area type	Approval range(hm^2)		Actual range(hm^2)	
		Construction area	Range of prevention	Construction area	Range of prevention
Main engineering zone	Permanent			0.23	0.23
	Temporary	1.73	1.73	2.37	2.37
Construction, production and living zone	Temporary	0.48	0.52	1.18	1.18
Temporary stockyard	Temporary	3.53	3.93	3.71	3.71
Construction road zone	Temporary	0.85	0.94	1.34	1.34
Borrow site	Temporary	15.16	16.84	17.40	17.40
Overall		21.75	23.96	26.23	26.23

As can be seen from Table 1, the actual range of soil and water loss prevention is 26.23hm^2, including permanent land occupation of 0.23hm^2 and temporary land occupation of 26hm^2.

After investigation and verification, the measures system implemented in this project is reasonable and complete, the soil and water conservation function of each measure is not reduced, and the trace land recovery of temporarily occupied land is protected to the maximum, reflecting the principle of comprehensive management and focus on effectiveness. The water conservation measures of the main body are verified and evaluated. For example, tree, shrub and grass greening implemented in free area after new gate, No.17 dam of Panzhuang Perilous Dam and No.21 dam head area is a change in the design of the main project, while performs the function of soil and water conservation. The quantity and the effect of prevention are included in the special acceptance evaluation of soil and water conservation, while the investment is not included in the soil and water conservation investment.

Through field verification, UAV technology has better practicability and reliability. It can simultaneously obtain orthophoto image and three-dimensional point cloud data, then quantify the accuracy and reliability of related indexes, thus completing the comprehensive and rapid evaluation of soil and water conservation facilities acceptance (Zhu, 2017). It is significantly superior to the traditional survey method in determining the responsible range, implementation, quantity and effect of soil and water conservation prevention.

4.3 Quality evaluation for soil and water conservation

According to the Code for Quality Assessment of Soil and water Conservation Projects (SL336-2006), the quality assessment of soil and water conservation projects should be divided into three levels: unit project, division project and separated item project.

The unit project should be divided by type based on easy management. Combined with the characteristics of the project, there is a separate construction contract for the soil and water conservation project, which is a relatively independent part for the project. Therefore, it is a single unit project, namely the third bid section of Shandong Yellow River Sluice Reinforcement Project in 2016.

Combined with the characteristics of various soil and water conservation measures, the division project can be divided into five parts based on the same type and relatively independent function, including site regulation, blocking, drainage, covering and patchy vegetation.

The separated item project is divided according to the prevention zone and the implementation location of the project. For example, the land consolidation project is divided according to the area of each prevention zone and every 0.1-1 hm^2 is regarded as a separated item project. The coverage is divided according to the area of each prevention zone and every 100-1000m^2 is a separated item project. The temporary retaining is divided according to the retaining length of bagged soil, and a unit project is divided every 50-100m. The temporary drainage is divided according to the length of drainage ditch, and a unit project is divided every 50-100m. Planting trees and sowing grass seeds are divided according to the area of each control area. Every 0.1-1 hm^2 of design spot is divided into a unit project.

The project legal person organizes relevant construction units to accept the unit project of soil and water conservation. According to the self-assessment of construction unit, supervision unit review and identification of project legal person, the project involves 1 unit project, 5 division projects and 115 separated item projects. All separated items are qualified with 100% passing rate. The 3 division projects are excellent, and the overall quality of soil and water conservation projects is qualified.

Table 2 Completed Quantities of Soil and Water Conservation Measures

Prevention zone		Type of measure	Project name	Unit	Quantity of work	
					Existing	Newly added
Main engineering zone	Newly built silting zone	Vegetation	Planting suitable forest			1409
			Planting dike protection forest			450
			Sowing grass	hm^2		1.2
	Greening of management office		Planting cedar			53
			Planting buxus microphylla			462
			Sowing seed grass	hm^2		0.06
	Greening of sluice		Planting cedar		246	
			Planting sabina chinensis		4600	
			Planting ligustrum vicaryi		760	
Construction, production and living zone		Engineering	Topsoil stripping and re-covering	m^3		1518.3
		Vegetation	Silt area tree planting			803
			Sowing grass	hm^2		0.5
		Temporary	Temporary drainage ditch	m^3		284.1
			Temporary covering	m^2		523.9
			Bagged soil blocking	m^3		37.5
Construction road zone		Engineering	Land consolidation	hm^2		1.2
		Vegetation	Silt area tree planting			1838
			Sowing grass	hm^2		1.14
		Temporary	Temporary drainage ditch	m^3		607.5
Temporary stockyard		Engineering	Topsoil stripping and re-covering	m^3	7040	
		Vegetation	Silt area tree planting			5716
			Sowing grass	hm^2		3.5
		Temporary	Temporary covering	m^2	18560.7	
			Bagged soil blocking	m^3	274.6	
Borrow site		Engineering	Land reclamation	hm^2	17.4	
		Temporary	Temporary covering	m^2		6174.1
			Bagged soil blocking	m^3		164.2

4.4 Effect evaluation for soil and water conservation

After the completion of the project, soil and water conservation projects and plant measures will play their due roles. The intensity of soil and water loss prevention within the responsible range decreases significantly, the total degree of soil and water loss control reaches 97.9%, the rate of disturbed land control reaches 97.83%, the ratio of soil loss control reaches 1, the rate of sediment retaining reaches 99.07%, the rate of forest and grass vegetation recovery reaches 98.65%, and the rate of forest and grass cover reaches 27.83%.

All 6 prevention objectives all reach the program design standard, indicating that the new soil and water losses have been effectively controlled, the ecological environment has been protected to the maximum extent, the environment has been significantly improved, the soil and water conservation facilities are operating normally, safe and effective, and the acceptance conditions are met.

5 Experience of Independent Acceptance by Project Legal Person

(1) Strong organizational leadership is essential to soil and water conservation. It is necessary to fulfill the responsibility of construction management so as to implement soil and water conservation measures. It is suggested that a soil and water conservation construction management system should be formed with project legal person as the core, Project Office (field management organization) as the management extension, design unit, construction unit, supervision unit and soil and water conservation monitoring unit as members. The responsibilities of each unit are clearly divided. Among them, the project legal person is responsible for the management of soil and water conservation in the project construction. In the management of soil and water conservation, the project legal person shall strictly follow the relevant regulations of the Ministry of Water Resources, the Yellow River Conservancy Commission and the Provincial Bureau, and play a core role in the quality, progress and fund management of the project. Project Office, as the management organization assigned by the construction center to the construction site, performs the construction management responsibilities of the project legal person on the construction site. It is necessary to set up a leading group of soil and water conservation work to directly manage the quality, progress and investment control of soil and water conservation measures and to take direct management responsibility for soil and water conservation management. Each member unit has set up a leading group which specializes in the implementation of soil and water conservation of the project.

(2) According to the requirements of Regulations on Project Management of Water Conservancy Projects, the system of project legal person responsibility, tendering and bidding, construction supervision and contract management are strictly implemented, and a series of management rules and regulations are formulated in combination with the actual construction of the Yellow River Project. For example, "Implementation Measures for Legal Person Acceptance of Soil and water Conservation in Shandong Yellow River Construction (Trial Implementation)" and "Notice on Printing and Distributing Key Points of Soil and water Conservation and Environmental Protection Management of the Yellow River Water Conservancy Project in Shandong Province " are used as basis and management requirements for acceptance by legal person to guide and standardize the work of soil and water conservation.

(3) At the beginning of the project construction, in order to comprehensively promote soil and water conservation work and improve the level of soil and water conservation construction management, the project legal person holds training courses on soil and water conservation and conducts business training on soil and water conservation for each participating unit. During this training, the contents, requirements and completion standards of soil and water conservation work were clearly defined, and the awareness of soil and water conservation was significantly increased, especially the implementation of temporary protection measures for soil and water conservation.

(4) The project legal person has timely entrusted the third-party organization to intervene in the work. The supervision unit, monitoring unit, and the third-party organization can effectively cooperate with each other to find out the problems in time and solve them in a timely manner, thus providing an effective guarantee for the smooth implementation of the independent acceptance in the later period.

6 Existing Problems and Solutions

(1) There lacks special supervision on soil and water conservation. The main supervision unit is in charge of the supervision of soil and water conservation of the project. Despite the fact that relevant business training has been conducted, the supervision unit still lacks professional supervision technicians for soil and water conservation. For this reason, it fails to effectively cooperate with the acceptance work in soil and water conservation quality assessment division, as well as verification of soil and water conservation facility engineering quantity and investment, thus making it difficult to ensure the accuracy of the information and affecting the overall progress of the project node and even affect the acceptance quality. Therefore, some measures should be taken in terms of the supervision unit's lack of professional supervision personnel for soil and water conservation. Firstly, it is imperative to carry out special bidding in the bidding stage, and make it clear in the document that other participants should be subject to the supervision management. Secondly, it is necessary to formulate the supervision system of soil and water conservation during the construction of the project, and the professional personnel shall carry out their special responsibilities. Thirdly, it is imperative to strengthen management means, keep the data of the construction process, and formulate a joint plan of soil and water conservation management so that supervision work on soil and water conservation will be effectively implemented (Li, 2020).

(2) The construction unit lacks an accurate understanding of the process and procedures of soil and water conservation design changes. In recent years, the technical standards, specifications, and related documents on soil

and water conservation have proposed higher requirements for the soil and water conservation scheme and subsequent design. For water conservancy projects, the preliminary design and construction drawing design of soil and water conservation are relatively detailed, and the measures and plans of the scheme can develop in the direction of easy operation and practical feasibility based on the actual engineering. However, it is still difficult to implement some measures in the actual implementation process. Under the circumstances that the soil and water conservation measures fail to be implemented according to the design for various reasons, the construction unit still has no knowledge of how to implement the change procedure to meet the procedure requirements. It is suggested that the construction unit should assign special personnel to be in charge of the relevant work, communicate with the supervision unit, monitoring unit, and third-party organization in a timely manner, and accomplish timely feedback of the problems on the site.

(3) The production and construction unit lack professional soil and water conservation technical personnel and needs to further improve the professional competence. Acceptance of soil and water conservation facilities is policy-based and professional work, but the construction unit provides only a limited number of special soil and water conservation personnel. When managing multiple projects, some personnel are unfamiliar with the relevant laws, regulations, and standards of soil and water conservation and lack experience in conducting the acceptance of soil and water conservation facilities and in key work contents, acceptance procedure, and key data, thereby finally leading to insufficient working ability, passive implementation and affecting the quality of acceptance work (Shen, 2020). It is suggested that the construction unit should enhance the technical level of the personnel in charge of soil and water conservation by strengthening the study, publicity, implementation, and training of relevant documents, strengthening communication and coordination with the local water administration departments, and establishing a long-term mechanism for personnel training, so as to solve the problems of brain drain and work connection.

7 Conclusions

(1) During the construction of the project, the construction unit has seriously implemented the requirements of the approved soil and water conservation plan and subsequent design, as well as various measures for soil and water conservation, and ensured the targeted use of the special fund for soil and water conservation. Consequently, the soil and water loss has been effectively controlled, and the ecological environment has been improved step by step within the scope of prevention and control responsibility. Based on the evaluation by the third-party organization, the project has reached the prevention and control objectives determined by the soil and water conservation plan and has implemented the responsibility for management and protection. Meanwhile, the soil and water conservation facilities have met the acceptance criteria and conditions.

(2) The third-party organization should fully grasp the latest policies, standards, and specifications, constantly improve the professional technical level, carry out technical evaluation work based on new technologies and methods, and put forward rectification and treatment suggestions on existing problems, thus providing good technical support to ensure independent acceptance of the construction unit.

(3) Acceptance of soil and water conservation facilities plays an important part in the completion of the project. Thus, the construction unit should carefully study and understand the principle of relevant documents issued by the Ministry of Water Resources from an overall perspective. It is encouraged to constantly explore the practice, summarize the experience so as to improve relevant systems and contribute to the sustainable development of the society in the new era.

References

Ministry of Water Resources. (2017). Notice on Strengthening the Supervision during and after Work and Standardizing the Independent Acceptance of Soil and Water Conservation Facilities for Production and Construction Projects

Yan, F. X. (2012). "Cost Control of Sluice Reinforcement Project in Design Stage." Water Conservancy Construction and Management, 01, 14-15.

Peng, Z. W. (2020). "Discussion on Problems and Countermeasures of Acceptance of Soil and Water Conservation Facilities in the New Period." City Construction Theory Research, 20, 105-106.

Liao, R. Z. (2018). "Application of UAV Technology in Soil and Water Conservation Monitoring." Technology Style, 23, 29.

Shi, R, Y. (2019). "Application of UAV Technology in Acceptance of Soil and Water Conservation Facilities." Heilongjiang Hydraulic Science and Technology, 47, 03, 131-34.

Jiang, D. W. (2018). “Discussion on the Work of the Third-party in the Acceptance of Soil and Water Conservation Facilities.” China Soil and Water Conservation, 02, 4-8.

Zhu, K. (2017). “Research on Ways and Technical System of Soil and Water loss Prevention in Haicheng City.” Technology of Soil and Water Conservation, 06, 33-35.

Li, Y. F. (2020). “Discussion on the Acceptance of Soil and Water Conservation Facilities in High Speed Railway Construction Projects under the New Situation.” Subtropical Soil and Water Conservation, 32, 02, 66-67.

Shen, X. Q. (2020). “Discussion on Problems Related to Independent Acceptance of Soil and Water Conservation Facilities by Production and Construction Units.” China Soil and Water Conservation, 11, 12-13.

High-efficiency cultivation model of Xanthoceras sorbifolia Bunge in Gully regionof Loess Plateau

Xiaoling Yan[1], Ying Zhang[2]
1 Yellow River water and Soil Conservation Supervision Bureau of Xifeng District Administration, Qingyang, Gansu 745000
2 Ziwuling Forestry Administration, Heshui branch, Lianjia Bian forest farm, Qingyang, Gansu 745000
*Corresponding Author, e-mail: hwxfyxl@163.com

Abstract

Xanthoceras sorbifolia Bunge has very high edible value, medicinal value, ornamental value and ecological value. It is an efficient soil and water conservation plant with ecological, ornamental and edible uses, its high-efficiency cultivation mainly includes suitable land for trees, reasonable close planting, planting at the right time, shaping and pruning, field management, seed harvesting and other links. Gansu is also one of the most suitable provinces for the growth of Xanthoceras sorbifolia Bunge. As early as 2008, Gansu was incorporated into the State Forestry Administration of the People's Republic of China and established a 73,000 hm2 production base for Xanthoceras Sorbifolia. The popularization of Xanthoceras sorbifolia Bunge has a bright future in controlling soil and water loss, improving ecological environment, developing Xanthoceras sorbifolia Bunge industry, adjusting agricultural structure and revitalizing rural areas.

Keywords: Gully region of Loess Plateau, Xanthoceras sorbifolia Bunge, High-efficiency Cultivation Model, Development prospect

1 The characteristics and value of Xanthoceras sorbifolia Bunge

1.1 The morphological and biological characteristics of Xanthoceras sorbifolia Bunge

Xanthoceras sorbifolia Bunge is an exclusive species of Xanthoceras sorbifolia Bunge, a special woody oil tree species in the north of China. The branches of Xanthoceras sorbifolia Bunge are purple-brown in young and gray-brown in later, and are arbor in good site condition and sufficient soil water and fertilizer, the tree height can reach 7cm~ 10m. Leaves are odd-pinnate, alternate, up to 20cm~ 25 cm long, 9 ~ 19 leaflets, sessile, many opposite, long elliptic to slope needle-shaped, 2cm~ 6 cm long, the edge was sharply serrate, dark green leaves, generally smooth and hairless, some leaves have short silvery gray hairs on the back. The flowers and leaves of Xanthoceras sorbifolia Bunge Bloom simultaneously. Flowers are racemes, usually 15cm ~ 25cm long, up to 30 cm long, slender, erect pedicel, yellow-white flowers gradually into Lilac, a few of the base for red-purple. Pedicel diameter is about2cm, 5petals, petals are yellow, purple, White, red and other four colors, flowering period about4-5months, flowering duration for more than 20 days; The fruit has five shapes, such as round, triangular, heart-shaped, oval and cylindrical. The color of the fruit is yellow-white, with about 3 ~ 4 cells, 4 ~ 6 seeds per cell.

1.2 Ecological characteristics of Xanthoceras sorbifolia Bunge

Xanthoceras sorbifolia Bunge is light-loving and suitable for planting on sunny slopes with sufficient light. It has strong cold resistance and can survive the winter even in extremely low temperatures. It has a strong adaptability to soil and can grow even in areas with low annual precipitation, it can also grow in soil and rock mountainous area, sandy land and saline-alkali land. However, the most suitable environment for Xanthoceras sorbifolia Bunge is fertile soil with Ph value between 7.5 and 8.0, sufficient water resources, sunny and leeward. It should be noted that Xanthoceras sorbifolia Bunge are afraid of waterlogging and can not be planted in low-lying wetlands. The Xanthoceras Sorbifolia bunge planted in the north usually blooms in May, but it usually blooms more and bears less fruit.

2 Ecological and economic value of Xanthoceras sorbifolia Bunge

2.1 Economic value

Xanthoceras sorbifolia Bunge is not only an excellent woody oil tree species in China, but also a precious ornamental plant for tourism. The seed oil content of Xanthoceras sorbifolia Bunge was 35% — 40% , and the kernel oil content was 62.8% — 73% . Xanthoceras sorbifolia Bunge oil is a high-grade medicine, edible oil, Xanthoceras sorbifolia Bunge oil up to 94% , easy to be absorbed and digested by the human body, has the effect of lowering cholesterol, softening blood vessels, can effectively prevent unsaturated fat. Xanthoceras sorbifolia Bunge oil is rich in brain gold nerve acid (2.6% ~ 5%) , is the heart and brain and nervous system health of the main elements. At present, linoleic acid dropping pills have been developed in China, which are specially used to prevent and treat hypertension, hyperlipemia and other diseases. In addition to fruit, leaves can be developed into health tea. Xanthoceras sorbifolia Bunge tea has the functions of sterilization, anti-inflammation, hemostasis, diuresis, digestion, elimination of Fat, anti-oxidation, anti-aging, etc. can treat insomnia, gout, gastroenteritis, Prostatitis and "fall three high" , weight loss. Vigorously developing Xanthoceras sorbifolia Bunge fruit industry can make the land green and the farmers rich, can solve the ecological crisis, edible oil crisis, and promote the harmonious and healthy development of ecological, economic and social benefits.

2.2 Ecological value

In the Gully region of the Loess Plateau, the topography is broken, the gullies are vertical and horizontal, the drought is few, the soil erosion is serious, the ecology still presents the partial management, the overall deterioration tendency. Afforestation is the most effective means to improve the ecological environment, and Xanthoceras sorbifolia Bunge as one of the ecological tree species, which is of great significance to the development and improvement of the ecological environment. The development of Xanthoceras sorbifolia Bunge fruit industry is an important breakthrough to adjust the local rural industrial structure, control soil erosion and increase farmers'income. In the Loess Plateau and Gully region where the natural conditions are harsh, the ecological environment is fragile and the economic development is relatively backward, the development of Xanthoceras and fruits industry will help to improve the ecological environment, adjust the structure of agricultural industry and promote the increase of farmers'income, new Green and new energy industry will be promoted to achieve the goal of multi-win economic, social and ecological benefits.

2.3 The development prospect of Xanthoceras sorbifolia Bunge in the Loess Plateau and Gully region

Xanthoceras sorbifolia Bunge is a unique tree species in China and an excellent woody oil tree species unique to the north. Xanthoceras sorbifolia Bunge has low requirements for soil, is drought-resistant and salt-tolerant. Seeds can be pressed for oil and leaves can be used for tea, Xanthoceras sorbifolia Bunge is an elegant ornamental plant. Its flowering period can last about 1 month. It is one of the ideal tree species for urban landscaping, river banks, highway and railway construction, can also be used as a garden, House front and rear ornamental plants, bonsai plants, with high ornamental value. Xanthoceras sorbifolia Bunge has strong cold resistance,-41 °C can survive the winter safely. Xanthoceras sorbifolia Bunge is also a kind of nectar source plant, which can be used as nectar source plant in early spring. The Loess Plateau Gully region is one of the most suitable areas for the growth of Xanthoceras sorbifolia Bunge. The distribution of wild Xanthoceras sorbifolia Bunge can be seen everywhere on the sunny slope and the steep cliffs of Yangshan. As early as 2008, Gansu was incorporated into the State Forestry Administration of the People's Republic of China and established a 73,000 hm2 canopy fruit raw material base. In 2016, Zhenyuan County, Gansu, which is located in the Loess Plateau Gully region, introduced Shenzhen Baolihongyuan Enterprise Development Co. , Ltd. to invest in building 200,000 mu of the Xanthoceras sorbifolia Bunge woody oil industry base, leading to the transformation of rural industries, to turn what was once a pile of wasteland into a farmer's playground. The fruit of Xanthoceras sorbifolia Bunge has a yield of 300 kg/mu, seed kernel of 10 yuan/kg, yield of 3,000 Yuan/mu, deep processing of seed, oil yield of 60% , can be used as high-level health care edible oil and clean biodiesel.

The characteristics of climate, soil, elevation, landform and geomorphology in the Gully region of the Loess Plateau are not consistent with the characteristics of Xanthoceras sorbifolia Bunge. Suitable for large-scale cultivation. And there are large areas of abandoned farmland, sloping terraced fields due to the planting of common native tree species to become uncultivated grassland, as well as large areas of uncultivated hillsides are suitable for cultural crown fruit. In recent years, more and more scientific and technical personnel have been engaged in the study of Xanthoceras sorbifolia Bunge, and its planting techniques have become more and more mature, it makes the root system of the seedling intact and the plant develop robustly, overcomes the shortcoming of root injury of the Xanthoceras sorbifolia Bunge seedlings, and solves the difficult problem of low survival rate of transplanting. At the same time, it takes the substrate to transplant, the survival rate is high, not restricted by season, and can be planted in spring, summer and Autumn Festival In cultural management of Xanthoceras sorbifolia Bunge, the fatal problems of "a thousand flowers and one fruit" were solved by reasonable close planting, shaping and pruning, fertilization before and after flowering, thinning flowers and fruits and strengthening management during fruit expansion period.

3 key techniques of high-efficiency cultivation mode of xanthoceras Sorbifolia

3.1 Suitable site and suitable tree

Following the principle of suitable site and suitable tree species is the mutual adaptation of site conditions and tree species characteristics, which is a basic principle for selecting afforestation tree species. The Xanthoceras Sorbifolia bunge has strong adaptability and can grow and develop normally in sandy grassland, abandoned land, Rocky Mountain area, Loess Plateau and Gully, sloping terraced field, Ridge and mound, and even on the side of mountain, half shade tolerance, strong adaptability to soil, poor tolerance, salt tolerance, cold resistance, drought resistance, in the annual rainfall of only 150 mm area there are scattered trees, but Xanthoceras Sorbifolia are not resistant to waterlogging, afraid of the wind, it is not suitable for planting in low-lying areas with poor drainage, heavy saline-alkali land and unfixed sand land. Should choose (1) high-lying Tableland, Sichuan Platform; (2) arid, semi-arid mountain terraced fields, slope farmland, Ridge, hillside ditch side; (3) rural residents in front of the House space behind.

3.2 Proper close planting

The cultivation methods of Xanthoceras sorbifolia Bunge were different for different purposes. As a soil and water conservation forest, the main purpose is to close the surface of the earth, so high density cultivation should be adopted and planted at a distance of 1m× 1.5 m per plant, and as a ridge shelter forest, it has the function of strengthening ridge, preventing collapse and reducing soil and water loss, according to the plant row spacing 2m× 2m, and can obtain certain economic yield. Proper close planting can increase early yield and increase benefit. Specific close planting should be based on site conditions. Plots with fertile soil and irrigation conditions should be sparse, while plots with poor soil and no irrigation conditions should be dense. Under the condition of dry land, 2m× 2m row spacing could be used to plant 2500 plants/hm^2, or 3m× 2m row spacing could be used to plant 1670 plants/hm^2. The plot with irrigation condition can be designed by 3 m ×3 m plant row spacing and planted with 1110 plants/hm^2.

3.3 Planted at the right time

Xanthoceras sorbifolia Bunge can be transplanted and planted in Spring and autumn. In the Gully region of the Loess Plateau, the spring is usually from the middle to the late march, at the latest in the early April, and after the fall of Xanthoceras sorbifolia Bunge leaves (mid-late october to early november) , especially the large area development and does not have the watering condition the mountain area, the autumn planting does not need to irrigate the survival rate also to be able to be 80% above. Early planting in spring is also a key technology to improve the survival rate, the depth of soil thawing up to 30 cm can be planted. The survival rate of Xanthoceras Sorbifolia Bunge was over 85% .

3.4 Plastic pruning

young trees planted in time to set the stem, stem height of about 40 cm, fertility, watering some appropriate high. Adventitious stem with seedling height less than 40 cm. In mid-june of the same year, 3 ~ 4 main branches, one central branch and the other branches were pruned in summer, and 5 ~ 10 cm high-yield branches were reserved. In early July of the same year, root tillers were found and the buds under the main branches were cut off in time so as to concentrate nutrients to supply the selected branches and promote their growth. The main branches should be evenly distributed, open at an angle, each other in a neat manner. That year winter plastic pruning only as an auxiliary means, not re-cut. The selected main branch should be released to promote its growth as long as its height is the same, and if it is too strong, it should be retracted to make its height basically the same as other main branches. Summer cut short branches, fruit and specifically reserved for early hanging, should continue to release, promote growth and development, and strive for early flowering. Xanthoceras sorbifolia Bunge is a tree with terminal buds that blossom and bear fruit. It is essential to keep the terminal buds of both small and large trees. The second year pruning task is to cultivate the branch group, adjust the tree shape, promote flowering. Summer pruning usually begins in mid-june. The central trunk should be opened to allow full upward growth. The main branch can be removed generally heart processing, promote the growth of side branch. The remaining branch group is not generally treated, promoting flower buds. If the branches are too dense, they can be appropriately cut off to avoid competition. Second summer pruning in mid-july, found that the main branch on the back of the branch, the erect branch, are generally cut off. Other branches should not be too much head, to promote its development. Three-year-old trees, at this time the task is to control the lateral growth, prevent the closure, stay two main branches, form a good tree, as early as possible to improve yield. The distance between the main branch of the second layer and the first layer is about 40 cm. The branches on the central trunk of interlayer can be retracted by half and cultured into fruiting branch group. The first layer of main branches should continue to head, promote the growth of branches. The closed place should be appropriately dredged or retracted. Later pruning should be carried out according to the principle of "shaping according to trees and promoting high yield" . After four or five-year-old trees can form a large number of flower buds every year, a large number of spring flowering, but the drop of flowers and fruit is very serious. At this point should be moderate cut off flower bud, so that the concentration of nutrients, improve fruit setting rate.

3.5 Field management

Xanthoceras sorbifolia Bunge fruit drop flower drop fruit serious, there are "a thousand flowers a fruit" said. The key to prevent fruit drop is to strengthen management, apply foot-bottom fertilizer, apply fertilizer in time, prevent pests and rats, and strengthen tree vigor. Spraying 50 mg/L Sodium naphthylacetate and 0.3% ~ 0.5% urea at full flowering stage could effectively improve the fruit setting rate. Increasing the rate of fruit setting is an important means of increasing income. To solve the problem of falling flowers and fruits has obvious effect on improving the rate of setting fruit and increasing the yield.

3.6 Harvested in good time

As a fresh fruit, can be harvested and sold when the kernel contents have become turbid and have become semi-milk-like. The seeds can no longer be harvested after they become astringent. As an oil plant, it is necessary to wait for the pericarp to turn yellow, the pericarp to turn black, and the seeds to be harvested at full maturity. After recovery, the sun cracking, to be reduced by less than 13% moisture storage for sale. Sun seed should be in the shop or grass curtains, matting, can not be in the cement, slate drying, in order to prevent the impact of seed vitality.

References

Hu Jianzhong. Configuration, development and utilization of plant resources for efficient soil and water conservation in China. BEIJING: China Water Conservancy and hydropower press, 2016.13.

Yan Xiaoling, Hu Jianzhong, Yin Liqiang. High-efficiency cultivation model of daylily in Gully region of Loess Plateau[J]. Soil and water conservation in China, 2017(11)46-49.

Study on comprehensive soil and water conservation measures and their effectson runoff in Nanxiaohegou watershed

Zhongping Tuo[1], Ying Hao[1]
1 Yellow River water and Soil Conservation Supervision Bureau of Xifeng District Administration, Qingyang, Gansu 745000
*Corresponding Author, e-mail: E-mail: xftzp@163.com

Abstract

Taking the Nanxiaohegou watershed in Xifeng district, Qingyang city, Gansu Province as the experimental area, this paper expounds in detail the main factors causing soil and water loss in the watershed, and puts forward the "three lines of defense" comprehensive control model for the tableland slope gully, the experience and effect of comprehensive harness in Nanxiaohegou watershed are summarized. The impact of soil and water conservation measures on runoff is analyzed, and the organic combination of pest control and profit-making can maximize the utilization degree of precipitation resources and promote the coordinated and sustainable development of all industries in the basin, it provides theoretical basis for promoting the ecological civilization construction in the Some Random Place Somewhere region, coordinating the thought of landscape, forest, Lake, grass and sand control, high quality development in the Yellow River Basin, rural revitalization strategy and sustainable development of social economy.

Keywords: Nanxiaohegou watershed, Soil and Water Conservation, Comprehensive measures, Runoff 1 General Situation of Nanxiaohegou watershed

1.1 Basic situation

Nanxiaohe gully is located in the west edge of Dongzhi Tableland, located in Xifeng district of Qingyang City, 13 km from the city of Qingyang. It is a typical Loess tableland gully area with a watershed area of 36.30 km 2. Is a tributary of the Left Bank of Po Ho, a secondary tributary of the Jing River River. It is located in East Longitude 107º30′03″ ~ 107º37′26″ , north latitude 3740′51″ ~ 3544′55″ , altitude 1050 ~ 1423 m, relative height difference 373 m, average specific drop of main gully 2.8% , gully density 2.68 km/km2, and 183 tributaries in the basin, the relative height difference from Gully bottom to tableland surface is 150 ~ 200m. The watershed geomorphology can be divided into three types according to the erosion form: Plateau, slope and Gully. Water erosion is the main factor in Nanxiaohegou watershed, and gravity erosion is the second. According to the research results, the slope soil and water conservation area of the watershed is 20.94 km2, and the treatment degree is 56.45% . There are 2 small reservoirs with a total capacity of 2.9 million M3,3 silt dams, a total capacity of 1.56 million M3,9 pond dams, 341 water cellars, 9 Gully head protection, 70 Gufang, 41 manholes and 65 waterlogging ponds.

1.2 Geology and geomorphology

The geological structure of Nanxiaohegou basin is relatively simple, except for the Cretaceous sandstone layers at the bottom of the lower valley, the rest are all covered by quaternary loess with a total thickness of 250m. Due to the geological age of Loess Formation and the different physical and chemical properties, Mechanical Properties, particle composition, expansion coefficient, permeability coefficient, porosity and collapsible uplift of loess in different parts, the texture is different, and the erosion resistance and erosion resistance are different, therefore, the impact on soil erosion is also different. The most serious erosion occurred at the bottom of the gully, especially in the middle reaches of the Gully, where clay bodies were deposited at the foot of the gully. The other part belongs to the late pleistocene alluvium, which is a two-or three-stage platform composed of loess-like sub-clay and sub-sandy soil layers. The slope is steeper, generally over 45, and in some places it is a cliff with vertical walls, or by the infiltration of groundwater and earthquake,
resulting in a large number of collapse phenomenon.

The landform of Nanxiaohegou watershed consists of tableland, slope and Gully, the proportion of which is 57% , 16% and 27% respectively. Among them, the tableland surface is flat and open, the slope is relatively gentle, generally between 0 ~ 3, is the center of production, life and other activities, the vast majority of villages and farmlands are distributed on the tableland surface, the slope surface topography is broken mostly presents the ridge and mound Tsui, the slope is steeper, mostly between 10 and 20. The Ravine gradient is steeper, mostly above 45, mostly presents the cliff vertical wall.

1.3 Meteorological and hydrological characteristics

Nanxiaohegou is an arid and semi arid region of the monsoon. It is characterized by four distinct seasons, with little rain in winter and spring and moderate rainfall in summer and autumn. The average annual precipitation is 561.5 mm, of which the precipitation from July to September accounts for more than 60% of the annual precipitation, the average temperature is 8.3 °c, the average sunshine time is 3060 hours, the total radiation is 548 kj/cm2, the frost-free period is 162 days, and the accumulated temperature ≥10 °C is 2700 ~ 3300 °C.

2.The process of management of Nanxiaohegou watershed

2.1 Characteristics of soil erosion

2.1.1 Major types and modes of erosion

Water erosion is the main erosion in this basin, followed by gravity erosion. The annual average erosive rainfall is 199.88 — 276.4 mm, which is 45% — 63% of annual rainfall and 54% — 67% of June — September rainfall. The 137 CS tracer technique was used to study the soil erosion in the farmland of Nanxiaohegou. The results showed that the soil erosion generally fluctuated with the change of slope length, and it was relatively strong in the middle part of the slope, reached the peak value, and then decreased gradually with the increase of slope length, the foot of the slope is usually piled up.

This area is a typical highland gully area, the runoff comes from the tableland surface, the sediment comes from the gully. There are nearly 30% of the tableland surface in this area, but its runoff accounts for 67% of the total runoff in the basin. Gully erosion has resulted in gully landforms in the region, gully erosion system is based on dry gully, most of the dry gully has cut into bedrock, gully and gully are modern erosion gully, and most of them are developed in Loess Stratum, the former is 5% — 7% , the latter is more than 20% , most of these valleys are "v" shaped, showing incisions, lateral erosion, and active expansion of the head of the gully. Rills and shallow ditches are mainly distributed on slopes with slope gradient less than 250, and large shallow ditches are mainly distributed on barren slopes. The lower part of the rills is often connected with the suspended ditches, which is the most common combined form of gully erosion in the area, it's causing a lot of erosion. The erosion of clay clay on the slope of 450 ~ 750 red soil layer near the gully bed is the most serious erosion mode in this area, its area only accounts for 8.74% of the slope area, but the amount of erosion accounts for 92.4% of the total erosion.

The thickness of red soil in the exposed valleys of the nanxiaohegou watershed is 15 ~ 20m, the slope of the red soil is more than 400, and there is no grass at all. In the Nanxiaohegou watershed, there is little rain in spring and concentrated rainfall in flood season, which brings strong power to the gully erosion and makes the red soil piled up in the gully completely washed away by the water flow. The investigation shows that the slope of the landslide is between 400 and 600. The area of clay clay is only 2.47% of the total area of the basin, but the amount of soil erosion accounts for 25.5% of the total amount of soil erosion.

According to the investigation, there are more than 100 landslides and collapses in this small watershed before the dam is built. Every year, landslides and collapses occur, causing serious soil and water loss. After the construction of the dam and reservoir, the landslide and collapse decrease with the increase of sediment deposition.

2.1.2 Spatial and temporal distribution of soil erosion

According to the research results, in the initial stage of harnessing, the runoff amount on the surface of the tableland is 67.4% of the total runoff amount in the whole basin, the runoff amount in the gully is 24.0% of the total runoff amount in the whole basin, the sediment amount in the tableland is only 12.3% of the total sediment amount in the whole basin, the sediment amount in the gully is 86.3% of the total sediment amount in the whole basin, the average annual runoff modulus is 8994.0 m3/km2, and the soil erosion modulus is 4350.0 t/km2. Soil erosion in july-august is the most, the total amount of erosion in the other months is less than 20% of the total amount of erosion, and the number of soil erosion is only 20% of the total amount of erosion. According to the types of erosion, from top to bottom, it is as follows: Slope Gully erosion zone —— Slope Gully Gully Erosion Zone gravity erosion zone; from watershed to valley bottom, it is as follows: Slope rill erosion zone —— slope rivulet erosion zone, shallow gully erosion transitional zone —— Slope Gully erosion zone —— -- Modern Gully and gully erosion zone.

2.2 Governance processes for the Nanxiaohegou watershed

Since the Nanxiaohegou watershed was brought under control, the larger process has been divided into four stages. The first phase, from 1951 to 1959, was a trial run. In 1954 and 1956, the water and soil conservation plan for the whole basin was formulated twice, and the control direction of the Gully area in the highland was defined to protect the tableland and fix the ditch, and make use of the gully for afforestation, planting grass and building orchard. Specific control measures: Three Defense Lines were laid on the tableland surface, and the first defense line was as follows: deep tillage, Alfalfa Belt, water dustpan and bank on the land edge The main measures of the Second Village Road Defense Line are flood pond, water cellar and water storage dam, saving water and controlling it by stages, and the third gully head defense line is called as gully edge and gully head protection, so that the water on the tableland surface does not fall into the ditch. Gully control measures are building horizontal terraces, trying to build mountain orchards, build slope forest, slope planting Alfalfa and so on. In the Valley of the middle reaches of the main gully, 18 mu-tai and Huaguoshan reservoirs and several warping dams have been built, and Tugufang, Liugufang and anti-erosion forest at the bottom of the gully have been built in the branch gully. Basically to water not under the tableland, not out of the ditch mud. But the edge Ridge and water dustpan are only transitional measures, which can not solve the problem of water and soil conservation completely. In the second stage, from 1964 to 1966, horizontal strip fields were established on the tableland surface of the valley, mountain orchards were established, and reservoirs and ponds were built in the middle reaches of the valley. Every branch of furrow forest grows well because of tending and protecting. In the third stage, from 1970 to 1979, under the promotion of the Central "North Agriculture" conference and the Yan 'an conference on water and soil conservation, large areas of terraced fields were built on the tableland surface, and large-scale Afforestation of poplar trees were carried out on all sides, the waste Hutong, waterlogging pond and soil pit are used to build small forest fields, and the forest net fields are formed on the tableland. The whole basin management effect is remarkable. In the fourth stage, since 1980, the study of plant measures in soil and water conservation has been carried out vigorously, and the main tree species for afforestation in soil and water conservation have been determined. A study on the classification of different site types and the suitable site for trees in the Loess Plateau Gully region was carried out, and it was determined that the first-class (extremely drought-tolerant) tree species are Sophora Viciifolia, platycarya Chinensis and Xanthoceras sorbifolia Bunge, the drought-resistant tree species of grade 2 are hippophae rhamnoides and Caragana Korshinskii. These drought-resistant tree species are the main afforestation species on hilly and gully slopes. In 2003, with the full implementation of the National Program for conversion of farmland to forests and the construction project of the Qijiachuan demonstration area of the Yellow River for water conservation and ecological engineering, scientific management was carried out on the basis of rational planning of the Nanxiaohegou watershed, it has realized the combination of rapid governance and high efficiency, and has created a model for similar areas.

3 Experience of comprehensive management of Nanxiaohegou watershed

3.1 According to the law of soil and water loss, the comprehensive control model of "three lines of defense" is put forward

Based on the observation of 76 runoff fields and 11 rainfall stations with different slope, aspect, vegetation and site conditions in Nanxiaohegou watershed, it is preliminarily concluded that 67.4% of the runoff comes from the tableland surface, 86.3% of the sediment comes from the gully, and 77.9% of the total erosion takes place under the water, thus, the management policy of "fixing gullies on the plateau" is put forward, in practice, the comprehensive management mode of "three-line defense" is put forward, which is "farmland improvement and gully head protection project on the tableland surface, afforestation on the gully slope, development of orchard and planting of Herbage, construction of retaining project and establishment of anti-erosion forest on the gully" .

3.2 Make full use of land resources, build grain production base on the surface of the tableland and grass production base in the ravine

3.2.1 To build a grain production base on the surface of the tableland

There are 16.88 KM2 of farmland in the basin, 95% of which is tableland. After the level terrace is built, the water conservation, soil conservation, fertilizer conservation, yield increase is remarkable.

3.2.2 To establish forest, garden and pasture bases in ravines

One is planting grass and planting fruit trees on the large area of steep slope farmland and small piece of farmland, the other is building up a level terrace on the abandoned slope land of 0.1 km2, planting fruit trees and establishing a mountain orchard with an average fruit yield of 50000kg per year Third, the Yangjiagou, zhangtashan ditch, Fan Jiagou slope protection forest.

After many years of comprehensive treatment, Nanxiaohegou watershed has achieved remarkable results in the production and water retaining and sediment reduction. After key treatment, the control degree reached 80.9% , including 82.8% of the tableland, 53.7% of the gully, and 38.1% of the forest and grass coverage. After treatment, the average annual runoff modulus is 6199.3 m3/km2, which is 23.3% less than before treatment, and the average annual erosion modulus is 55.8% less than before treatment. After treatment, the land use structure becomes more reasonable and the land use ratio is 3.71% higher than before treatment, grain production increased by 90.3 percent, and per capita income from production increased by a large margin.

4 Harness effect of Nanxiaohegou watershed

Generation after generation of soil and water conservation workers have carried out nearly 60 years of regulation in the Nanxiaohegou Basin. Now the Nanxiaohegou is known as "an emerald on the Some Random Place Somewhere" . The first dam built in the early stage of regulation has silted more than 10 HM2 of land, it is a solid barrier to control the soil and water loss of nanxiaohe ditch completely.

In the management of the Nanxiaohegou watershed, the mountain apple orchard with "the First Garden in Longdong" was built in Huaguo Mountain, the Robinia pseudoacacia forest was built in Yangjiagou, and the theory and technology of imitating natural forest was followed in the cross section of the main gully, from the Sunny Ridge mound slope, the sunny gully slope, to the cloudy Gully Slope, the cloudy Ridge Mound Slope, successively distributed with Platycladus Orientalis, juniper, Pinus Tabulaeformis, Robinia PSEUDOACACIA, Nitraria, Rosa xanthina, Caragana, Elaeagnus pungens, hippophae rhamnoides, Sumac, Pinus Tabulaeformis, Populus Davidiana, Armeniaca Vulgaris, etc. , the Whole Valley has realized "spring view of flowers, summer view of green, autumn view of fruit, winter view of snow" ecological and cultural landscape. In addition, the 18-mu-tai reservoir and Huaguoshan Reservoir, with the first dam in Longdong, have been selected as a water conservancy scenic spot in 2011 and become important places for Chen Dong to visit, it has played a good role in education, science popularization and demonstration of soil and water conservation resources.

Through the implementation of the construction project of the Qijiachuan demonstration area of the Yellow River water and soil conservation ecological engineering, first, according to the law of soil and water loss that the gully under the surface runoff of the tableland in the Gully region will increase the erosion modulus by 79% , in the existing tableland underwater gully head construction gully head protection project, the tableland surface construction terrace, has realized the plateau protection goal; Third, projects such as the newly-built Gully Runoff Tableland, water-logging pool on the tableland surface and water cellar, while basically solving the problem of drinking water for people and livestock in rural areas, have carried out water-saving irrigation for fruits, vegetables and other crops, and promoted the adjustment of agricultural structure, fourth, the water-saving irrigation and high-yield cultivation techniques of fruit trees, plastic film mulching planting techniques, drought-resistant afforestation techniques of Evergreen (Pinus Tabulaeformis and Platycladus Orientalis) , the organic combination of ecological benefit and economic benefit has been realized.

5 Impact of soil and water conservation measures on runoff

Great achievements have been made in soil and water conservation in Nanxiaohegou watershed since soil and water conservation was carried out. According to the characteristics of runoff, measures should be taken according to local conditions, and measures should be combined with biological measures and engineering measures, as well as slope and gully control. Water and soil conservation forests are built on the surface of the tableland, terraced fields on the slope, horizontal ditches and fish-scale pits, etc. . The main ditches are built with silt dams, reservoirs, etc. , all measures are closely combined, from top to bottom, layer upon layer of fortification, block and store, giving full play to the protective role of group measures. In order to evaluate the benefits of soil and water conservation in the small watershed of Nanxiaohegou, the water and soil conservation benefits of Yangjiagou and Dongzhuanggou were analyzed.

The effects of soil and water conservation on runoff and sediment in Nanxiaohegou watershed were studied by setting Yangjiagou as control gully and Dongzhuang gully as contrast gully. The topography, physiognomy, soil and vegetation of Yangjiagou and Dongzhuanggou before harness are basically similar. The watershed area is 0.87 KM2 and 1.15 KM2 respectively, the main ditch length is 1500 m and 1600 m respectively, and the specific drop of channel is 8.46% and 8.93% respectively. In Yangjiagou area, many forest-based measures have been taken to control soil and water loss in different types of land.

5.1 Benefits of water storage

The characteristics of rainfall runoff in Yangjiagou and Dongzhuang Gully in the Loess Plateau are shown in Table 1.

Table 1 Runoff characteristics of Yangjiagou and Dongzhuang gully in different year types

Projects	Flood Frequency			Flood rainfall（mm）			Runoff modulus（m^3/km^2）			Annual runoff coefficient（%）		
	Withered	Flat	Abundance	Withered	Flat	Abundance	Withered	Flat	Abundance	Withered	Flat	Abundance
Yangjiagou	7.3	10.8	18.0	186.7	280.0	448.4	2910	6016	13197	0.69	1.08	1.74
Dong Zhuanggou	9.8	14.2	20.7	211.7	305.6	519.4	6519	11503	21367	1.53	2.06	2.84

Analysis Table 1, compared with Dongzhuanggou (contrast ditch) , Yangjiagou (governance ditch) watershed: (1) slightly reduced flood rainfall. The average annual flood yield in Yangjiagou is 280 mm, the average annual flood yield in Dongzhuanggou is 305.6 mm, the decrease is 25.6 mm, the difference is 71 mm. (2) the number of floods is obviously reduced. The average annual flood production in Yangjiagou is 10.8 times, that in Dongzhuanggou is 14.2 times, and the annual flood production is reduced by 24% . Especially in the middle period of management, the average flood production is reduced by 28% . In different precipitation years, the low water year is reduced by 26% , and the high water year is reduced by 13% . (3) the surface runoff modulus decreases and the water storage capacity increases. The average annual runoff depth of Yangjiagou is 6.0 mm, the runoff modulus is 6016 m3/km2, and the average annual runoff depth of Dongzhuanggou is 11.5 mm, the runoff modulus is 11503 m3/km2. The storage period of Yangjiagou watershed is increased by 5.5 mm and 47.8% , while the storage period of Dongzhuanggou watershed is increased by 55.5% . The annual average runoff coefficient is 1.08 in Yangjiagou and 2.06 in Dongzhuang Gully, 0.69 and 1.53 in dry years, 1.74 and 2.84 in wet years, the runoff Coefficient of Yangjiagou is 2.15, Dongzhuanggou is 3.76, the difference is 1.61. (4) the annual variation of flood-producing rainfall, flood-producing times and runoff modulus increased after harnessing. The annual variation of precipitation and runoff in Yangjiagou and Dongzhuanggou are shown in Table 2.

Table 2 Annual variation characteristics of precipitation and surface runoff in Yangjiagou and Dongzhuanggou

Drainage area	Projects	Annual rainfall (mm)	Flood Frequency	Floods Rainfall	Annual Runoff Modulus	Annual diameter Flow depth	runoff coefficient year（%）	runoff coefficient of floods（%）
Yangjiagou	average	558.5	10.8	280.0	6016	6.02	1.08	2.15
	C_0	0.23	0.50	0.58	0.80	0.80	0.60	0.78
Dong Zhuanggou	average	558.5	14.2	305.6	11503	11.5	2.06	3.76
	C_0	0.23	0.43	0.39	0.69	0.69	0.56	0.64

Compared with Dongzhuanggou, the flood rainfall and runoff modulus of Yangjiagou watershed are small, and the annual variation of flood rainfall, flood production times and runoff modulus is different. The effect of soil and water conservation makes runoff decrease most significantly in dry year and small in high water year, which leads to the increase of interannual variation range and the increase of interannual variation coefficient of runoff.

5.2 Benefits of arresting typical storm runoff

The characteristics of flood runoff in 11 typical precipitation processes in Yangjiagou and Dongzhuanggou basins are shown in Table 3

Table 3 Flood characteristics of small watersheds during typical precipitation

Secondary rainfall (mm)	Average rain intensity (mm/h)	Yangjiagou		Dong Zhuanggou		Storage Benefits (%)
		modulus of runoff (m^3/km^2)	runoff coefficient %	modulus of runoff (m^3/km^2)	runoff coefficient %	
27.0	5.5	2862	10.60	5180	19.19	45
30.6	4.2	187	0.61	1157	3.78	84
13.8	8.0	51	0.37	2758	19.99	98
59.9	4.4	167	0.28	1743	2.91	90
11.8	22.5	69	0.59	449	3.82	8
98.9	5.0	2423	2.45	7065	7.14	66
69.2	1.2	231	0.33	1695	2.45	86
33.7	33.8	695	2.06	3257	9.66	79
8.7	2.2	119	1.37	649	7.46	82
132.8	1.5	590	0.44	3099	2.33	81
36.0	5.0	1283	3.56	2962	8.23	57
47.5	8.5	789	2.06	2729	7.91	77
0.83	1.21	1.26	1.47	0.73	0.80	0.20

The results show that the ability of storm interception is improved, and the benefit of storm storage is increased by 45-98% , with an average of 77% . The effect of Soil and water conservation measures is different for different rainstorm. The less the intensity of rainstorm, the less the precipitation, the more significant the effect of interception and the smaller the modulus of runoff. When the average rainfall is less than 4 MM/H, the runoff decreases by 40 ~ 50% , the average rainfall is 4 ~ 10 mm/h, and the runoff decreases by 45 ~ 55% .

From the runoff coefficient, the average runoff coefficient in Yangjiagou watershed was 1/4 of that in Dongzhuanggou watershed, and the average runoff coefficient was 98% of that in dongzhuanggou watershed, but 92% in dongzhuanggou watershed. Under the same rainfall condition, the secondary runoff rheologic rate of Yangjiagou is obviously larger than that of Dongzhuanggou. The Coefficient of variation of secondary runoff modulus of Yangjiagou is 1.26,73% higher than that of Dongzhuanggou. The maximum to minimum ratio is 56 in Yangjiagou and 16 in Dongzhuanggou, the management makes the surface runoff change violently.

6 Conclusion

6.1 Effect of comprehensive management on surface runoff in Nanxiaohegou watershed

In the Gully region of the Loess Plateau, compared with the unharnessed small watershed, the integrated management of the small watershed reduced the number of flood and the runoff modulus and coefficient, especially in the dry years the most significant. The relationship between forest and grass and annual runoff in the Gully region of Loess Plateau is analyzed. The rainfall is large but the runoff is small, the runoff coefficient is small. The Comprehensive Management makes the annual change rate of surface runoff modulus of small watershed increase, the instantaneous flow and peak flow decrease and disappear, so as to reduce flood flow, reduce flood damage and prevent soil erosion, soil and water conservation can delay the beginning time of runoff yield and shorten the duration time of runoff.

6.2 Effect of comprehensive harness in Nanxiaohegou watershed

In the management of the Nanxiaohegou watershed, the mountain apple orchard with "the First Garden in Longdong" was built in Huaguo Mountain, the Robinia pseudoacacia forest was built in Yangjiagou, and the theory and technology of imitating natural forest was followed in the cross section of the main gully, from the Sunny Ridge mound slope, the sunny gully slope, to the cloudy Gully Slope, the cloudy Ridge Mound Slope, successively distributed with Platycladus Orientalis, juniper, Pinus Tabulaeformis, Robinia pseudoacacia, Nitraria, Rosa xanthina, Caragana, Elaeagnus pungens, hippophae rhamnoides, Sumac, Pinus Tabulaeformis, Populus Davidiana, Armeniaca Vulgaris, etc. , the Whole Valley has realized "spring view of flowers, summer view of green, autumn view of fruit, winter view of snow" ecological and cultural landscape. In addition, the 18-mu-tai reservoir and Huaguoshan Reservoir, with the first dam in Longdong, have been selected as a water conservancy scenic spot in 2011 and become important places for Chen Dong to visit, it has played a good role in education, science popularization and demonstration of soil and water conservation resources.

Ectomycorrhizal fungal characteristics of Pinus sylvestris var. mongolica

Guanglei Gao 1,2,*, Mishan Guo 1,2
1 College of Soil and Water Conservation, Key Laboratory of State Forestry Administration on Soil and Water Conservation, Beijing Forestry University, Beijing 100083, China;
2 Yanchi Research Station, School of Soil and Water Conservation, Beijing Forestry University, Beijing 100083, China
*Corresponding Author, e-mail: gaoguanglei@bjfu.edu.cn

Abstract

Pinus sylvestris var. mongolica, a widely planted tree species, is facing long-lasting, unresolved degradation in desertified northern China. Ectomycorrhizal fungi (EMF) are closely related to the stand status, because they participate in ecological processes of terrestrial forest ecosystems. EMF may be key to solving the introduction recession. Therefore, we performed DNA sequencing of P. sylvestris root samples from plantations and natural forest as control to characterize the EMF from semi-arid and dry sub-humid regions, using ITS Illumina sequencing and conventional soil physicochemical index determination. The results indicated that (1) the dominant EMF genera were Suillus, Rhizopogon, and Wilcoxina in the Hulunbuir, Mu Us and Horqin Sandy Lands, respectively. Their dominance kept along the stand ageing. (2) Plantation EM fungal diversity differs significantly among the three sandy lands, and was significantly lower than in natural forest. The diversity varied along stand age with distinct trends at the local scale. (3) At the regional scale, the mean annual sunshine times and the soil organic carbon content affect EMF diversity. The community composition and structure were more characterized by temperature and precipitation. At the local scale, besides the soil organic carbon content, the EM fungal community composition and structure were correlated with total nitrogen and phosphorus content (Hulunbuir), the total phosphorus content (Mu Us), and the pH and total soil porosity (Horqin). The EM fungal community composition and structure have the obvious geographical distribution variation, they were strongly correlated with the meteorological elements and soil nutrients at the regional scale. At the local scale, they were jointly driven by stand age and soil properties. This improved information contributes to increased understanding of the interaction between EMF and forest ecosystems.

Keywords: Ectomycorrhizal fungi, Pinus sylvestris var. mongolica, Sand age, Sandy land, Soil properties

1. Introduction

Ectomycorrhizal fungi (EMF) are widely found in forest ecosystems (Steidinger et al., 2018). The EMF mycelium infects vegetative roots of trees and forms symbiotic structures(Anderson et al., 2010). Through this symbiosis, EMF obtain carbon from host plants for growth, and host plants increase the absorption and utilization of soil moisture and mineral nutrients (Smith et al. 2008). Ectomycorrhizae (EM) can improve host plant resistance to environmental changes and stress, thus maintaining forest ecosystem stability (Courty et al., 2009).

Pineaceae was the oldest known EM plant taxon in the word and widely distributed in the boreal forests (Tedersoo et al., 2012). Lots of EMF were identified in the pine forests. In China, more than 30% of the reported EMF were pine-associated. *Pinus sylvestris* var. *mongolica* (*P. sylvestris* for short below) is native to the Hulunbuir Sandy Land. It is the most widely planted evergreen arbor in desertified northern China (Li et al., 2016). At first, plantations were generally successful, but many introduction areas experienced large-scale decline and death over time. Currently, this is a critically unresolved issue hindering development and ecological restoration in China.

P. sylvestris is a typical ectomycorrhizal-dependent species (Zhu et al., 2017). EMF have a mutually beneficial relationship with *P. sylvestris*. Some scholars believe that EMF loss is a major reason for the decline of *P. sylvestris* plantations as their crucial function throughout the pine life cycle, including the role of promoting the host resistance to drought, diseases and other poor surroundings. Moreover, the EMF also play an irreplaceable role in the natural regeneration and seedling establishment and survival (Hohmann et al., 2017). The positive role of EM in the tree physiology and ecosystem function is widely known. Conversely, the EM fungal community variation will also retroact to plant health and ecosystem stability (Scott et al., 2012). Consequently, EMF should not be neglected in studies of the sustainable management of *P. sylvestris* plantations, because the disrupted EMF symbiosis may have significant effect on the *P. sylvestris* growth and metabolism.

Soil EMF have numerous species and geospatial variabilities which are driven by the host, the environment and geographical distance. In northern China, *P. sylvestris* were all introduced from the Hulunbuir Sandy Land, so genetic variation among trees is small (Miao et al., 2017). Therefore, environmental elements, rather than the host species, likely influences the EM fungal community. Generally, the geographical climate has directly and indirectly shaped and regulated EMF. Soil physical and chemical factors alter the community composition and EMF structure. At the regional scale, the fungal dispersal process which was limited by geographical distance played an important role in the EM fungal distribution (Wurzburger et al., 2017). At the same time, EM fungal community succession occurs with aging of the host plant (Gao et al., 2015). In addition, mycorrhizal functional traits themselves modulate and stabilize EMF geographic pattern and ecosystem functions, for example, the role of nutrient capture may regulate the community distribution along the biogeochemical pattern. Consequently, differences in ectomycorrhizal fungal populations between introduced and native areas may be key factors affecting the vigorous growth of *P. sylvestris*. However, the connection between EMF and *P. sylvestris* decline remain largely unknown.

We investigated how *P. sylvestris*-associated EM fungal communities respond host ageing and bioclimatic zones. We tried to find out the key impact factors of EM fungal communities in different scales during the introduction and forest development. It contributes to the further study to identify relevant functional relationships between EM fungal community and *P. sylvestris* plantation degradation. We hypothesized that 1) the natural forest has rich EM fungal diversity which should also be higher in the original habitat among plantation, and the EM fungal diversity increased with the plantation stand ageing. 2) climate factors drive EMF communities at the regional scale, with variable EMF composition driven by soil environmental factors at the local scale.

2. Material and methods

2.1 Study site

The study was conducted in *P. sylvestris* origin and introduction areas (Fig. 1). Natural forest plot was located in Honghuaerji Forest Park (Inner Mongolia Autonomous Region). The introduction areas include Hailar Forest Park (Inner Mongolia Autonomous Region), Hongshixia Sandy Botanical Park (Shaanxi Province), and Zhanggutai Sandy Land Forest Park (Liaoning Province). The plantations selected were afforested by the same method, and there is no manual management after planting. The Hulunbuir Sandy Land (6400 km^2) is the origin area of *P. sylvestris*. Honghuaerji and Hailar Forest Parks are located in the Hulunbuir Sandy Land, which has a semi-arid area continental climate (Table 1). The dominant shrub and herb vegetation mainly include *Artemisia desertorum*, *Salix kochiana*, and *Saussurea japonica*. The Hongshixia Sandy Botanical Park is located in the Mu Us Sandy Land, and has a semi-arid continental monsoon climate (Table 1). The Mu Us Sandy Land is the westernmost sandy land in China (42,200 km^2), and it is one of the most important *P. sylvestris* introduction areas. The dominant shrub and herb vegetation types mainly include *A. desertorum, S. cheilophila,* and *Agropyron cristatum.* The Zhanggutai Sandy Land Forest Park is located in the Horqin Sandy Land, which has a dry sub-humid continental monsoon climate (Table 1). The Horqin Sandy Land is the largest sandy land in China (63,600 km^2). It is the first *P. sylvestris* introduction area in China. The *P. sylvestris* recession was first found here. The dominant shrub and herb vegetation mainly include *A. desertorum, Lespedeza bicolor,* and *Artemisia argyi.*

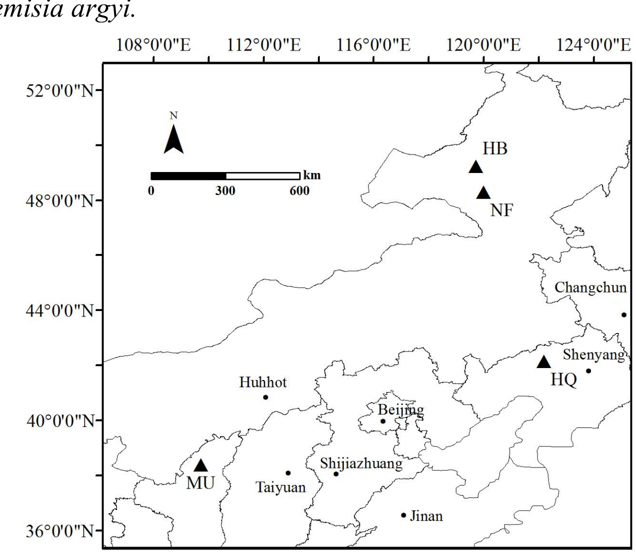

Figure 1 The location of study sites. *NF*: natural forest; *HB*: Hulunbuir Sandy Land; *MU*: Mu Us Sandy Land; *HQ*: Horqin Sandy Land

2.2. Sample Collection

Soil-roots samples were collected from July-August 2017 during the peak of plant biomass production and soil microbial activity. Plantations of three age groups (half-mature, nearly mature, and mature forest) without manual management in each sandy land area were selected for study (Tang et al., 2018). The natural *P. sylvestris* origin forest was used as a control (Table 1). Fine *P. sylvestris* roots were excavated along the base of the standard tree trunk. Roots and accompanying soil were pooled into a plastic bag, but litter, herbs roots, and undergrowth humus layers were excluded. There was at least 10 m apart between each sampling tree. Five composite samples (consisting of three replicate root samples each one) were collected each stand. All the composite samples ((3 sandy lands ×3 stand ages + NF) ×5=50 composite samples) were stored at 4 ºC for transport to the lab for analysis. The general soil samples from 0-20 cm into the soil layer were collected to analyze physical and chemical soil properties. The undisturbed soil samples were collected with cutting rings additionally.

Table 1 General information of study and sampling sites

	Hulunbuir Sandy Land				**Mu Us Sandy Land**			**Horqin Sandy Land**		
plots	**NF**	**HBh**	**HBn**	**HBm**	**MUh**	**MUn**	MUm	HQh	HQn	HQm
Geographic coordinates	N47°36′-48°35′, E118°58′-120°32′	N49°07′-49°13′, E119°21′-119°44′			N38°16′-38°20′, E109°12′-109°43′			N42°37′-42°50′, E122°11′-122°40′		
The mean annual temperature (ºC)	-0.69	-1.05			9.42			8.15		
The mean maximum temperature (ºC)	26.98	27.13			29.64			29.37		
The mean minimum temperature (ºC)	-31.94	-31.10			-13.57			-17.09		
The mean annual precipitation (mm)	343.66	353.38			499.91			517.29		
The mean annual sunshine times (h)	239.82	218.29			228.61			210.27		
Soil type	aeolian sandy soil				aeolian sandy soil			aeolian sandy soil		
Stand age (a)	6-56	24	33	42	26	32	43	26	33	43
Average tree height (m)		11.98±1.62	12.63±1.71	13.40±2.36	12.48±3.69	13.95±2.38	14.14±1.84	10.26±1.47	10.61±1.03	11.12±1.74
Average DBH (cm)		14.66±3.40	18.36±2.42	22.74±1.98	11.76±3.72	13.58±3.44	19.95±3.03	16.93±2.81	14.06±2.44	21.07±1.02
Canopy density	0.83	0.75	0.82	0.71	0.79	0.86	0.73	0.72	0.75	0.68
Stand status	Stable growth with multiple age class	normal growth, natural regeneration			decline with partial deadwood and no-regeneration			decline with partial deadwood and no-regeneration		

NF: natural forest; HB: Hulunbuir Sandy Land; MU: Mu Us Sandy Land; HQ: Horqin Sandy Land; h: half-mature; n: nearly-mature; m: mature.

2.3 DNA extraction and PCR amplification

The sampled EM roots were cleaned under running water prior to DNA extraction. DNA was purified using a Powersoil DNA Isolation Kit (MoBio, USA). Extracted DNA concentration was quantified on a NanoDrop spectrophotometer (Thermo Scientific, USA). EMF ITS regions were amplified using the common fungal primers ITS1F (5-GGAAGTAAAAGTCGTAACAAGG-3) and ITS2 (5-TCCTCCGCTTATTGATATGC-3). The PCR mixtures were as follows: 4 µl 5× FastPfu Buffer, 1 µl of each primer (5 µM), 2 µl of dNTP mixture (2.5 mM), 2 µl template DNA, and 10 µl H_2O. The PCR amplification program consisted of an initial denaturation at 95ºC for 2 min, followed by 30 cycles of 95 ºC for 30 secs, 55 ºC for 30 secs, 72 ºC for 30 secs, and a final extension at 72 ºC for 5 min. PCR amplification was performed in triplicate to account for potentially heterogeneous amplification from the environmental template for each sample. PCR products were purified using an AXYGEN Gel Extraction Kit (QIAGEN, Germany). An equimolar mix of all three amplicon libraries was used for sequencing at Allwegene Technology Inc. China, using an Illumina MiSeq sequencing system (Illumina, USA).

2.4. Sequencing data analysis

The original sequences were processed using the Mothur (v1.30.1, https://www.mothur.org) Sequences with quality scores > 30 and longer than 200 bp were used for analysis. Chimeric sequences were removed using the software package Usearch (Version 8.1.1861, http://www.drive5.com/usearch/). The remaining high-quality sequences were classified as an operational classification unit (OTU) with more than 97% similarity using Uclust. In order to ensure that the coverage of all samples was as high as possible, and to reduce the error caused by the different data size, the data size of all samples was homogenized to 120,204 sequences. Singleton tags were removed first when the data was processing. Taxonomic assignment was performed using the Ribosomal Database Project (RDP) classifier. Assigned taxa were verified by NCBI BLAST (https://www.ncbi.nlm.nih.gov/). The non-EM fungal sequences were removed base on the guilds output using FUNGuild v1.0 (http://www.stbates.org/guilds/app.php) (Klute 1986), the EM fungal OTU sequences were submitted to the NCBI GenBank (Accession number in Table S1). EM fungal OTU richness (Chao1), Shannon, Simpson and Pielou indices were computed using the vegan package in R (version 3.4.3).

2.5. Soil properties and climate data analysis

The general soil samples were air-dried for 2 days. Roots and stone debris were removed, and soil pH was measured using 1:1 soil and distilled water mixture by a PHS-3E pH meter (INESA, China). The total soil porosity (TSP) was gravimetrically determined after the undisturbed soil samples soaking in water for 8 h (Walkley 1934).

The total soil organic carbon (SOC) was determined using the dichromate oxidation method. Total nitrogen (TN) and total phosphorus (TP) content were analysed with a Smartchem Discrete Auto Analyzer (AMS, Italy) with the indophenol-blue spectrophotometric method and Mo-Sh anti-colorimetric analysis methods, respectively.

Climate data from 2007-2016 for each site were obtained from the China Meteorological Data Sevice Center (CMDC, http://data.cma.cn/en). The mean annual temperature (Ta), mean annual precipitation (Pa), and the mean annual sunshine times (St) was calculated by averaging the annual value (the sum of average monthly value) over ten years. The average maximum and minimum temperature (T+ and T-) was calculated using monthly average maximum/minimum temperature over ten years.

2.6. Statistical analysis

In order to compare the soil properties (pH, SOC, TN, and TP) and fungal richness and diversity indices among the three age groups within the same sandy land, one-way ANOVA and post-hoc Tukey tests after the normality test and the homogeneity test of variance (Data conforms to a normal distribution with uniform variance) were conducted. The effects of different sandy lands and stand age on EM fungal diversity indices were tested by two-way ANOVA with post-hoc Tukey tests. EM fungal diversity and soil properties/meteorological factor correlations were evaluated using the Pearson method. All statistical analyses were performed using SPSS 20.0 (SPSS Inc., USA), with $p < 0.05$ considered significant. The statistical analyses were performed within sandy land (local scale) and over all sandy lands (regional scale).

RDA, NMDS, ANOSIM and Mantel test were used to visualize the fungal community intergroup similarity and explain the correlation between the soil properties/climate factors and fungal community composition. Redundancy analysis (RDA) of EM fungal communities and environmental factors (meteorologic and edaphic) was performed using Canoco for Windows 5.0. EM fungal composition similarity between different samples was analyzed using non-metric multidimensional scaling (NMDS) and one-way analysis of similarity (ANOSIM). Bray–Curtis distances of EM fungal communities and Euclidean distances of soil variables and geographical distance were used to construct dissimilarity matrices for Mantel tests. NMDS, ANOSIM, and Mantel tests were performed with the vegan package in R (version 3.4.3).

Cluster heatmap and NMDS figures were generated with R (version 3.4.3). Boxplots and histograms were generated with Origin 2016 (OriginLab Corporation, USA). Network maps were drawn using Cytoscape v3.6.0.

3 Results

3.1. Diversity of EMF communities

A total of 645,186 high-quality sequences were obtained from the samples. The sequences were grouped into 2,024 OTUs. We identified 104 OTUs by filtering for ECM fungal taxa using FUNGuild v1.0.

The diversity indices based on identified OTUs (Fig. 2) showed the EMF of natural forests (NF) were more diverse than plantations. Diversity measures differed significantly among the plantations in different sandy lands ($p < 0.05$), with the highest values in the Mu Us Sandy Land and the lowest in the Hulunbuir Sandy Land. The changing laws of the EM fungal diversity variation with stand age were different among the sandy lands. In the Hulunbir Sandy Land, EM fungal alpha diversity first increased, and then decreased with stand age. However, alpha diversity decreased in the Mu Us Sandy Land and increased continuously in the Horqin Sandy Land. The EM fungal richness in the natural forest (Chao1 = 46.70 ± 4.66) was higher than those in plantations. The EM fungal richness in plantations were HB (44.32±3.39) > MU (41.67±7.11) > HQ (30.64±3.49) at regional scale.

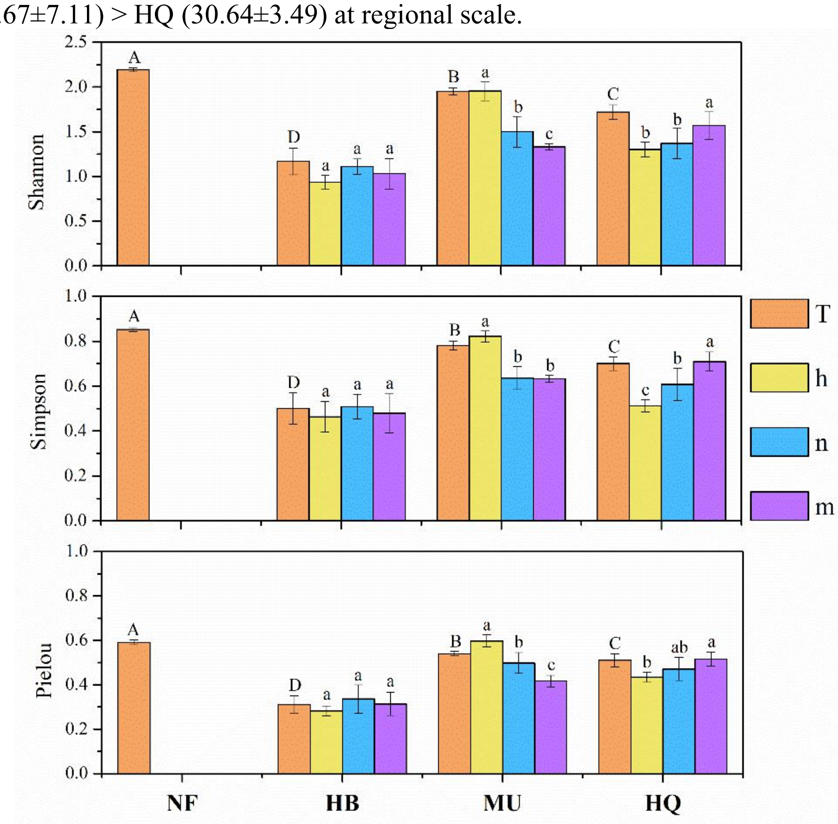

Figure 2 Diversity indices (± SE) for EM fungal communities in *P. sylvestris* natural forest and plantations in three sandy lands (n=5). **T** for the comprehensive value of each sandy lands. **h** for half-mature, **n** for nearly-mature, **m** for mature. The capital letters indicate significant differences among sandy lands (columns in orange), the lowercase letters indicate significant differences among age groups within the same sandy land, p<0.05.

Stand age and sandy land has a significant interaction effect on EM fungal diversity indices ($p < 0.05$, Table 2). There were significant differences in EMF alpha diversity indices associated with *P. sylvestris* plantations among different sandy lands ($p < 0.05$). The age main effect on EM fungal diversity was not significant ($p > 0.05$) in the regional scale. While in nested analysis, stand age had a significant effect on diversity indices ($p < 0.05$). This represented that stand age's alpha diversity difference was depending on sandy lands.

Table 2 Two-factor variance analysis of effect of stand age and sandy land on EM fungal diversity

Source	Dependent variable	Sum of the squares	Mean square	*F*	Significance
Sandy lands*Age groups	Shannon	1.233	0.308	19.551	**0.000**
	Simpson	0.218	0.054	18.429	**0.000**
	Pielou	0.101	0.025	15.189	**0.000**
Sandy lands	Shannon	2.552	1.276	80.959	**0.000**
	Simpson	0.341	0.170	57.679	**0.000**
	Pielou	0.331	0.166	99.782	**0.000**
Age groups	Shannon	0.065	0.032	2.060	0.142
	Simpson	0.003	0.002	0.551	0.581
	Pielou	0.004	0.002	1.242	0.301
Age groups(Sandy lands)	Shannon	1.298	0.216	13.721	**0.000**
	Simpson	0.221	0.037	12.470	**0.000**
	Pielou	0.105	0.017	10.540	**0.000**
Error	Shannon	0.567	0.016		
	Simpson	0.106	0.003		
	Pielou	0.060	0.002		
Total	Shannon	85.890			
	Simpson	16.677			
	Pielou	8.790			

Values in bold are statistically significant ($p < 0.05$).

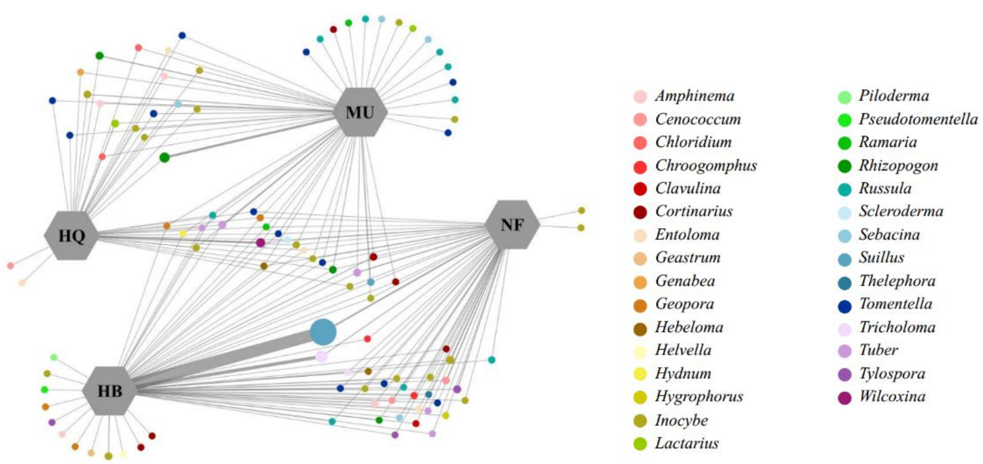

Figure 3 Network of EM fungal OTUs in each *P. sylvestris* stand across three sandy lands. Circle size represents absolute OTU abundance. Line thickness represents relative OTU abundance in sandy land.

3.2. EM fungal community composition and structure

In total, 104 EM fungal OTUs were successfully identified (Table S1). Of these, 88 belonged to *Basidiomycota* and 16 to *Ascomycota*, representing 30 EMF genera. Natural forest samples contained 50 OTUs, while the plantation samples from three sandy lands included 64 (HB), 55(MU), and 38 (HQ) OTUs. Only 8 OTUs were shared among all groups (Fig. 3). Among them, Hulunbuir Sandy Land plantations had the most OTUs similar to natural forest. Relative frequency analysis revealed *Basidiomycota* was the most abundant phylum (84%), followed by *Ascomycota* (16%) (Fig. 4). *P. sylvestris*-associated EMF in the Hulunbuir (both natural forest and plantations) and Mu Us Sandy land were mainly *Basidiomycota*. The relative abundance of *Basidiomycota* initially decreased and then increased with increasing stand age in these two sandy lands. But in the Horqin Sandy Land, EMF was mainly *Ascomycota*, with significant decreasing relative abundance ($p<0.05$, Fig. 4).

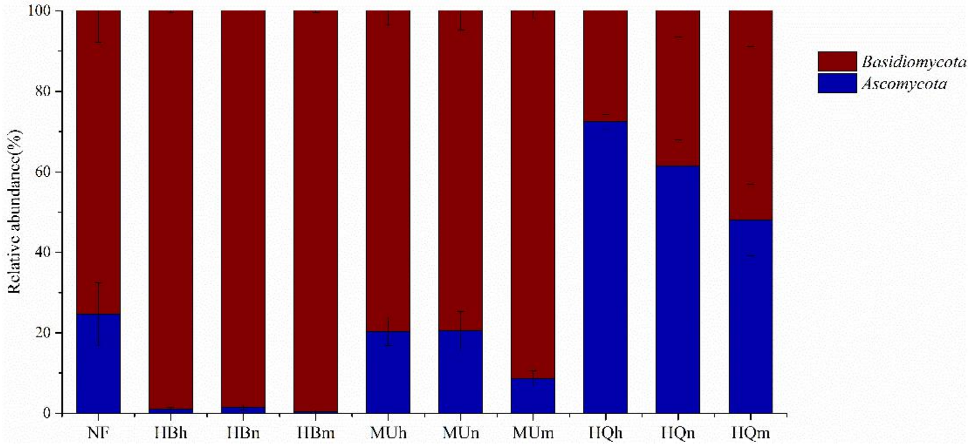

Figure 4 Relative abundance of EM fungal phyla in each *P. sylvestris* stand across three sandy lands

The relative abundances were calculated on the OTUs numbers. Of these, among *Basidiomycota*, *Suillus* was the OTU-richest genus, followed by *Tricholoma*. Among *Ascomycota*, *Wilcoxina* was the most abundant genus. A detailed analysis of the EM fungal genera in each *P. sylvestris* stand (Fig. 5) revealed that the relative fungal abundance was more balanced in natural forest, and was predominantly *Suillus* and *Inocybe*. The dominant genera of the Hulunbuir Sandy Land plantations were *Suillus* and *Tricholoma*. *Suillus* accumulated as stand age increased, but *Tricholoma* did the opposite. In Mu Us Sandy Land, *Rhizopogon* and *Tuber* were highly abundant. Relative *Rhizopogon* abundance rose with stand age, while *Tuber* decreased. In the Horqin Sandy Land, *Wilcoxina* was the major genus, and abundance decreased with stand age. Finally, *Lactarius* enrichment initially decreased and then increased as stand age increased.

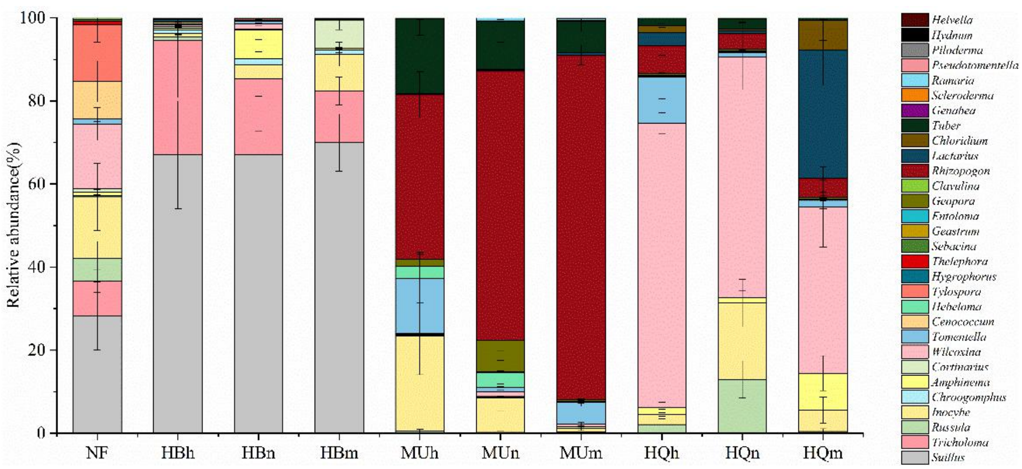

Figure 5 Relative abundances of EM fungal genera in each *P. sylvestris* stand across three sandy lands. The relative abundances were calculated as an average of 5 replicates in each stand.

The EMF community composition differed among sampling locations. Inocybe, Russula, Amphinema, Wilcoxina, Lactarius, Tomentella, Cenococcum, Hebeloma, Sebacina, Geopora, Rhizopogon and Ramaria were detected in samples from all three sandy land areas. Tricholoma, Chroogomphus, Hygrophorus, Tylospora, Thelephora, Helvella, Clavulina, Geastrum, Piloderma, and Pseudotomentella were absent in the Mu Us and Horqin Sandy Lands, while Chloridium and Genabea were not found in the Hulunbuir Sandy Land.

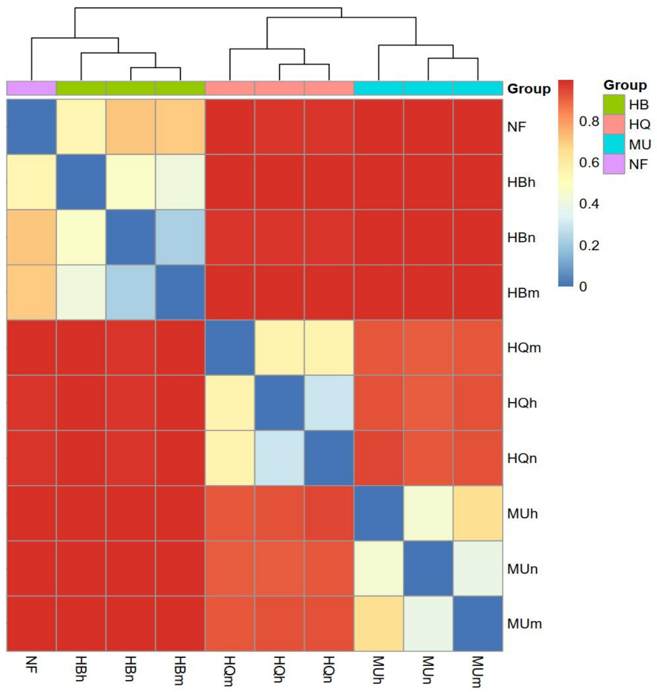

Figure 6 Bray-Curtis distance heatmap of each *P. sylvestris* stand across three sandy lands. Colour varies from blue to red, representing dissimilarities in EM fungal community composition from low (blue) to high (red).

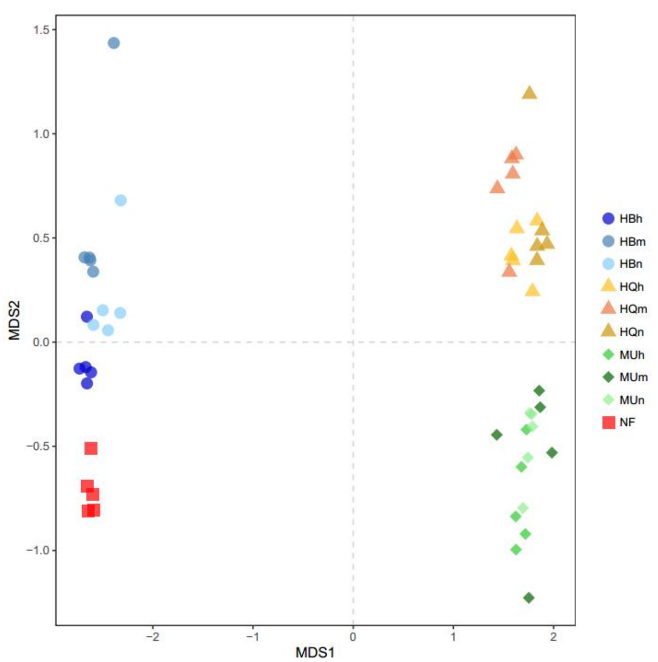

Figure 7 EM fungal community structure based on operational taxonomic units (OTUs), as determined by non-metric multidimensional scaling (NMDS), stress= 0.078.

The EM fungal communities of different age groups in the same sandy land clustered well (Fig. 6), as did natural forest samples and samples from the Hulunbuir Sandy Land plantations. The EM fungal communities from the Hulunbuir Sandy Land were the most different from the other two. The nearly-mature and mature forests showed greater similarity in the Hulunbuir and Mu Us Sandy Land. However, half mature and nearly-mature forests were more similar in the Horqin Sandy Land. NMDS analysis showed clear area separation (Fig. 7). The ANOSIM results indicated that location has significant effects on the EM fungal community structure (r = 0.977, P = 0.001).

3.3. The response of EM fungal communities to environmental variation

From Table 3, the Shannon and Simpson diversity and Pielou evenness indices had the strongest positive correlation with the mean annual sunshine times (0.592 and 0.573) and the mean annual temperature (0.506). They also had the strongest negative correlation with the total soil organic carbon content (-0.601, -0.578 and -0.742, respectively). The Shannon index was significantly correlated with the mean annual sunshine times, soil organic carbon and total nitrogen content ($p < 0.05$). The Simpson index was significantly correlated with the mean annual temperature, sunshine, minimum temperature, soil organic carbon, and total nitrogen content ($p < 0.05$). The factors that were most significantly associated with the evenness index included meteorological factors and soil organic carbon content ($p < 0.05$).

Table 3 Pearson correlation coefficients for EM fungal diversity and climate factor/soil properties

	Ta	**Pa**	**St**	**T+**	**T-**	**TSP**	**pH**	**SOC**	**TN**	**TP**
Shannon	0.270	0.192	0.592**	0.223	0.240	-0.018	0.032	-0.601**	-0.338*	0.133
Simpson	0.311*	0.226	0.573**	0.268	0.290*	0.001	0.032	-0.578**	-0.335*	0.232
Pielou	0.506**	0.448**	0.410**	0.466**	0.474**	-0.079	0.014	-0.742**	-0.212	0.217

Abbreviations: mean annual temperature (Ta), mean annual precipitation (Pa), mean annual sunshine times (St), mean maximum temperature (T+), mean minimum temperature (T-), total soil porosity (TSP), soil pH, total soil organic carbon (SOC) content, total nitrogen (TN), and total phosphorus (TP). * and ** indicate significant correlation at 0.05 and 0.01, respectively.

Table 4 Correlations between EM fungal community composition and climate factors/soil properties/stand age/geographical distance assessed by Mantel test

	Ta	**Pa**	**St**	**T+**	**T-**	**TSP**	**pH**	**SOC**	**TN**	**TP**	**Age**	**GD**
r	0.733	0.725	0.592	0.726	0.763	0.312	0.266	0.440	0.529	0.500	0.103	0.777
P	0.001	0.001	0.001	0.001	0.001	0.001	0.001	0.001	0.001	0.001	0.010	0.001

Abbreviations: mean annual temperature (Ta), mean annual precipitation (Pa), mean annual sunshine times (St), mean maximum temperature (T+), mean minimum temperature (T-), total soil porosity (TSP), soil pH, total soil organic carbon (SOC) content, total nitrogen (TN), total phosphorus (TP), stand age (Age), and geographical distance (GD).

Based on the Mantel test (Table 4), the geographical distance, the selected climate factors and soil properties (Table S2) were significantly correlated with EM fungal community composition (p = 0.001). On the regional scale, the EM fungal communities are strongly significantly affected by geographical distance (r=0.777, p=0.001). The effect of the mean minimum temperature (T-) and the mean annual temperature on EM fungal community composition was the most obvious (r = 0.763 and 0.733, respectively) among the climate factors. Soil nutrients had a more pronounced effect than other soil factors. The correlation with stand age was significant (r = 0.103, p = 0.010), though relatively weak at the regional scale. At the local scale, increasing stand age had a significant impact on EMF community structure ($p < 0.01$, Table S3), as did SOC. Moreover, the EMF community structures were strongly significantly associated with TP and TN content in different age groups in the Hulunbuir Sandy Land ($p < 0.01$). The EMF community structures were extremely significantly associated with TP content in the Mu Us Sandy Land. And they were extremely significantly associated with TSP and pH in the Horqin Sandy Land ($p < 0.01$).

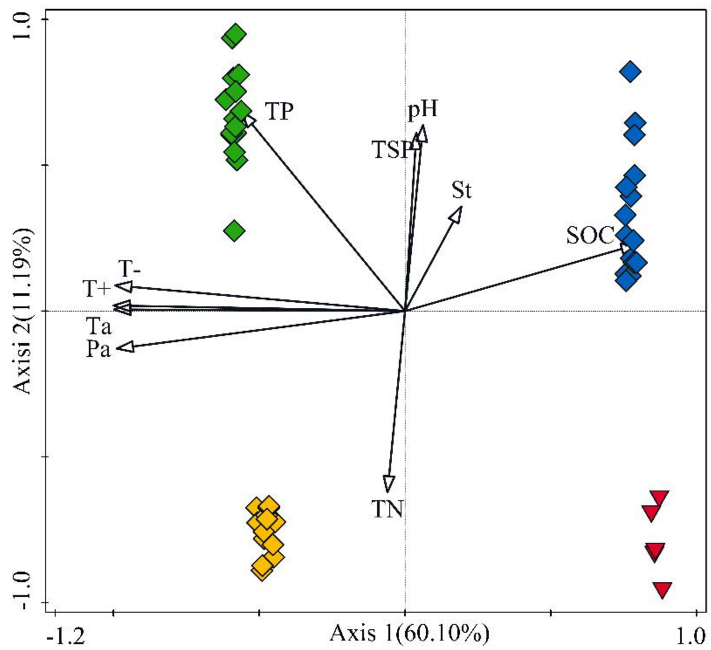

Figure 8 EM fungal community dissimilarity in each *P. sylvestris* stand across three sandy lands was tested by redundancy analysis (RDA). Red triangles represent NF (natural forest), blue diamonds represent HB (Hulunbuir Sandy Land), green diamonds represent MU (Mu Us Sandy Land), and yellow diamonds represent HQ (Horqin Sandy Land). Arrows represent environment variables.

From the redundancy analysis (Fig. 8), climatic variables and SOC content were the main factors in explaining the differences in community composition between NF+HB and MU+HQ. And the differences between NF and HB and between MU and HQ were mainly caused by differences in TN, TP content, TSP and soil pH. The difference in EMF community composition between HB and the other types (especially MU and HQ) was caused by the much higher SOC in HB. The difference in EMF community composition between MU and the other types was caused by the much higher TP in MU. Similarly, the difference between HQ and others was caused by TN.

4 Discussion

4.1 Variation in ectomycorrhizal fungal community composition with introduction

EM fungal diversity can affect the hosts growth and nitrogen uptake (Leake 2001). The highest EM fungal diversity in the natural forest partly supported our first hypothesis. Earlier observations showed that EM fungi were more adapted to the prevailing conditions in the natural forests, with higher richness and more even distribution (Grebenc et al., 2005). The natural forest was highly ecologically stable, with a diverse age group and rich under-storey vegetation (He et al., 2013). The average diversity indices of plantations among the three sandy lands were significantly different (p<0.05) as MU>HQ>HB. Prior studies noted EMF biogeographic and ecological patterns associated with host plant species. While, our research objects were the same species without notable genetic variation, but under various growth status in different sandy lands. Contrary to our expectations, the EM fungal diversity of plantations in the Hulunbuir Sandy Land was not higher than that in the Mu Us and Horqin Sandy Land, suggesting that EM fungal diversity is not positively correlated with host status (as mentioned in Tab.1, normal growth or decline). No clear relationship between EM fungal diversity and host status has been reported to date. Variation in the diversity indices according to stand age was inconsistent across the tested sandy lands. Results from previous studies on the relationship between EMF diversity and stand age varied widely, with clear differences even within one species across different regions. However, whether stand age influences fungal diversity remains controversial, this could be known through analyses of long-term soil chronosequences.

Among the 50 samples we obtained, the relative frequency of *Basidiomyceta* was higher than *Ascomycota*, which is consistent with general EM fungal distribution (Hayward et al., 2015). The relative abundance of *Basidiomyceta* was also higher except in the Horqin Sandy Land, where the dominant genus belonged to *Ascomycota*

The present genera have a wide geographical distribution, and they are commonly associated with pine[41]. During the stand ageing, some fungi appeared in the early stages, and some occur in late stages. In our study, the most dominant genera were consistent in all age groups within one sandy land area. This result is in consistent with previous data showing that Atheliaceae was always dominant in the EM fungal community of *P. sylvestris* stands in 10-80 years old stage (Bennett et al., 2020).

In native areas, both natural and planted, the dominant taxon is *Suillus*. Suilloid EMF (specifically the genera *Suillus* and *Rhizopogon*) are considered to be “pioneers” in human-introduced pine stands, and are key to understanding plantation success or failure[44]. These EMF facilitate pine seedling establishment and are important for later stage growth. *Suillus* was predominant in the three age groups in the Hulunbuir Sandy Land, with no significant fluctuation with age. In the Mu Us and Horqin Sandy Lands, the dominant genera changed with stand development, which corresponded to decreased and increased diversity. The dominant genus of the Mu Us Sand Land was *Rhizopogon*, which is a common EMF genus often observed at great distance from the host source area. *Wilcoxina* was dominant in the Horqin Sandy Land. In China, *Wilcoxina* species was first discovered in the north-eastern region, which is also the location of the Horqin Sandy Land. With the stand aging, its relative abundance was gradually reduced.

4.2. Interactions between environmental change, ectomycorrhizal fungal community composition, and stand ageing

P. sylvestris from one source were introduced into different regions, producing different stand structures under the differing hydrothermal conditions, including the EM fungal communities. At the regional scale, significant differences in geographical distribution of EM fungal community structure were detected. Among them, environmental heterogeneity mainly included climate and soil composition. Climate factors markedly impact the EM fungal diversity and community structure (Dumbrell et al., 2020). The biological distribution of terrestrial ecosystems is primary and mostly regulated by temperature and moisture (Rosinger et al., 2018). Mantel tests showed that temperature had the strongest influence on EM fungal communities. Increased EMF diversity occurs with elevated temperature based on the promoted plant productivity, as the EM fungal alpha diversity indices of plantations are correlated with the mean annual or extreme temperatures. Long-term warming studies in the Artic found an increased abundance and richness of EMF with increasing temperature. In a boreal forest, however, warming in combination with drying was found to negatively affect fungal abundance (Sterkenburg et al., 2018). The response of below-ground ecosystem to temperature changes requires more in-depth and comprehensive research. Solar radiation is an important heat source, so the mean annual sunshine time was used as a characterization index. Energy from the sun directly affects soil temperature and plant metabolic processes. The mean annual sunshine time had significant impacts on all three indices. EMF obtain carbon from the host plant for growth. We posit that sunlight indirectly influences EMF by driving photosynthesis within the host plant. Fungal species react differently to changes in temperature and moisture. Therefore, large regional climate changes substantially affect composition and regulation of EM fungal communities. Furthermore, precipitation can also influence EM fungal communities, particularly in desert regions (Zhang et al., 2017). Generally speaking, drought decreases soil microbial diversity at a global scale. However, the study on the EM colonization of pinyon pine in northern Arizona found that EM colonization was significantly higher at the much drier cinder site for 5 of 12 months than that in moist sandy-loam soils sites. Drought influenced the EMF community composition in a water-exclusion experiment on beech, and the EMF responded to drought differently in terms of their abundance. In our study, although the precipitation was HQ>MU>HB, evaporation within HQ and MU was double the evaporation of HB. We found that MU and HQ were experienced much greater drought stress than HB, after calculating the aridity index (potential evaporation/precipitation) simply. This could probably explain why fungi with large fruiting bodies (such as *Suillus*) didn’t appear in the Horqin and Mu Us Sandy Land. Hypogeous fungi, like *Wilcoxina* and *Rhizopogon*, were thought to be adapted to water scarcity, and are dominant in those sandy lands (Close et al., 2009).

Soil conditions are external abiotic factors directly affecting EM fungal communities. In our study, the total soil porosity, pH, and total phosphorus content drove EM fungal community composition, but they had no significant correlation with diversity. This was also reported in previous studies. Most EM fungi were more suitable for slightly acidic or neutral pH, and soil pH exhibited a significant effect on both EM diversity and community structures in the Beech, Pine, and Spruce Forests in both continental and global scale (Fränzle et al., 2010). At the same time, EMF had large pH adaptation range, EMF could grow in the range of pH 3-8 in both culture media and peat associated with *P.*

sylvestris seedlings. The contribution of pH to the variation of EM fungal communities was not highlighted due to the minor differences among our samples (Kennedy et al., 2010).

At the regional scale, soil organic carbon was significantly correlated with EM fungal community composition among the soil nutrient elements. Soil organic carbon in forests is mainly derived from litter, root and dead microbial cells in the soil decomposition, and is an important part of the carbon cycle. EMF mediate carbon cycling, while carbon productivity is also a driver of ectomycorrhizal abundance and diversity. The Mantel test revealed that the total nitrogen content was a major factor influencing EM fungal community structure in our study. EM fungal communities are affected by available nitrogen, and form large-scale patterns by nitrogen variation based on a European biomonitoring network of pine forest plots. Fungal diversity and total soil nitrogen content were negatively correlated in our results. Diverse fungal communities are observed by field experiment in a mixed boreal *P. sylvestris* and *Picea abies* forests in Sweden, where the organic layer is relatively nitrogen poor. Soil phosphorus content has selective influence on EM fungal community composition and ectomycorrhizal role of increasing water absorption. The relationship between nutrient content and EMF diversity are contrary to some studies. This may be due to low soil nutrients in sandy lands. The nutrient content was less variable, and our forest stand conditions were distinct from other terrestrial forest ecosystems.

At the local scale, EM fungal richness in the three sandy lands was very different according to stand age. Previous studies showed that EM fungal richness increased, decreased, or did not significantly change with the increased stand age. There was no clear pattern for the change of EM fungal diversity with stand aging, either among the different tree species or the same tree species in different regions. At the local scale, stand age was the major factor driving the composition and structure of the EMF community. It was demonstrated aging of forest soil determines the EM fungal composition in secondary stands of *P. sylvestris* in The Netherlands. The change in soil properties resulting from stand ageing were considerable factors in EM fungal community composition. The EMF communities were mainly regulated by SOC, TN and TP content in the Hulunbuir Sandy Land. The SOC and TN content increased with stand ageing, showing consistent homogeneity. Filtration and influence of soil nutrient and organic matter on EMF communities were also been reported in pine forest of California. The EM fungal community composition in Mu Us Sandy Land plantations was also affected by SOC and TP content. In this group, the TP content had more effect. The increase in soil phosphorus content promotes the growth of most EMF species, particularly *Rhizopogon*, which was consistent with our data. However, soil phosphorus has no effect on *Suillus*. Moreover, there is no strong evidence for the impact of phosphorus on EM fungal diversity. In the Horqin Sandy Land, the total soil porosity, pH, and SOC regulated EM fungal community composition. Soil acidity is a crucial factor affecting soil fungi. Our data indicate that the EMF community in the Horqin Sandy Land may be sensitive to soil pH. Soil porosity controls root and fungal mycelial growth. Several hypogeous fungi which sporulated mitotically within the soil, exist in the Horqin Sandy Land, making TSP a vital factor.

4.3. Ectomycorrhizal fungi and *P. sylvestris* plantation degradation: a supposition

The EM Fungal composition and community structure are filtered and shaped by climate and soil conditions in different sandy lands. Changes in the community structure under introduction of host plant can have consequences for ecosystem function. Community composition and structure of ectomycorrhizal fungi in declined and non-declined forests were significantly different . Considering the benefits from EMF to tree health and ecosystem service, the EM association feedback may be a causal factor of trees degradation. In the declining *Phytophthora cinnamomic*-infected *Quercus ilex* forest, the changes of the EM fungal diversity and abundance caused by human impact were involved in the *Q. ilex* decline, this counteracted the positive symbiosis effect and might lead to further tree death.

Variation in EM fungal community composition can result from nutrient cycle efficiency . At the same time, because of their extremely important role in the nutrient cycle, they would affect the host tree productivity and health in turn[80]. In addition, the loss of fungi which have strong pathogen antagonism and drought tolerance may lead to stand degradation. Host plants suffer from withering dead leaves and low pathogen resistance, likely due to the lack of essential trace elements such as manganese, zinc and Copper. The introduction of EMF which have these elements' transporters can help host plant absorb and transport the elements. This could alter trace element shortage and the low absorption rate in desert ecosystems. Simultaneously, the local reduction in the relative abundance of dominant genera may be an overlooked cause of stand decline. The dominant genus in the Hulunbuir Sandy Land was in a relatively stable state during stand evolution, while the other two had larger fluctuations. A population competition mechanism could have a non-negligible influence on EM fungal ecosystem function (Teste et al., 2009). The regeneration barriers - "able to germinate, unable to survive" are important phenomena in plantation degradation. EM may be an key point to alleviate this problem because they have critical benefits to seedling growth and survival. Especially considering that Suilloid fungi play an essential role in *P. sylvestris* invasion and seedling establishment (Migeon et al., 2010).

In the strong mutual feedback relationship between EMF, host plant, and the environment, the composition and structure of ectomycorrhizal fungi community could be used as a crucial indicator of plant health and ecosystem function. Further, this research could inform an answer to plantation degradation.

5. Conclusions

EMF associated with *P. sylvestris* are diverse with various genera and have clear regional differences. The environmental changes caused by the large-scale introduction of *P. sylvestris* strongly affected the diversity and composition of the EM fungal community. We propose that this introduction reduced the EM fungal diversity and richness of *P. sylvestris*. The original plantations were not superior to other introduced areas regarding EM fungal diversity. The variety of EM fungal diversity and richness with the age gradient had no consensus across three sandy lands.

At the regional scale, the mean annual sunshine times and the soil organic carbon content affects EMF species diversity. The EM fungal community composition and structure were more characterized by temperature and precipitation. EM fungal changes were expected to differ among the sandy lands. At the local scale, the factors which drive and modulate the EM fungal communities during stand development were significantly different among three sandy lands. In addition to the soil organic carbon content, the EM fungal community structures were closely correlated with total nitrogen and phosphorus content (Hulunbuir), the total phosphorus content (Mu Us), and the pH and total soil porosity (Horqin).

The primary relationship between EM fungal community and plantation introduction is supported by our results. The EM fungal community changes and related nutrient cycles could reflect stand status. Therefore, we highly considered that study on fungal dynamics of multi-spatial EMF could alleviate the *P. sylvestris* decline and solve the regeneration problem. Our results have the potential to guide sustainable forest management, such as cultivating specific functional mycorrhizal seedlings and mycorrhizal fungal inocula configuration.

Acknowledgments

We would like to thank Mr. Weilin Jin (Hulunbuir Forestry and Grassland Bureau), Dr. Guoping Zhao (Desert Control Research Institute of Shaanxi Province), Prof. Gang Lyu (Liaoning Technical University) and Prof. Hongda Chen (Liaoning Sand Land Amelioration and Utilization Research Institute) for their generous help with the field investigation. Special thanks to Yue Ren, Hongyu Cao and Yuxuan Chen for their help with sampling and measurements in the field and laboratory.

Reference

Steidinger, B.; Bhatnagar, J.; Vilgalys, R.; Taylor, J.; Bruns, T.; Peay, K. Global climate changes will lead to regionally divergent trajectories for ectomycorrhizal communities in North American Pinaceae forests. *bioRxiv* **2018**, 10.1101/393009, doi:10.1101/393009.

Anderson, I.C.; Cairney, J.W.G. Ectomycorrhizal fungi: exploring the mycelial frontier. *FEMS Microbiology Reviews* **2010**, *31*, 388-406, doi:10.1111/j.1574-6976.2007.00073.x.

Smith, S.E.; Read, D. 6 - Structure and development of ectomycorrhizal roots. In *Mycorrhizal Symbiosis (Third Edition)*, Smith, S.E., Read, D., Eds. Academic Press: London, 2008, 191-268.

Courty, P.E.; Buée, M.; Diedhiou, A.G.; Frey-Klett, P.; Tacon, F.L.; Rineau, F.; Turpault, M.P.; Uroz, S.; Garbaye, J. The role of ectomycorrhizal communities in forest ecosystem processes: New perspectives and emerging concepts. *Soil Biology and Biochemistry* **2010**, *42*, 679-698, doi:10.1016/j.soilbio.2009.12.006.

Tedersoo, L.; Bahram, M.; Toots, M.; Diedhiou, A.G.; Henkel, T.W.; Kjøller, R.; Morris, M.H.; Nara, K.; Nouhra, E.R.; Peay, K., et al. Towards global patterns in the diversity and community structure of ectomycorrhizal fungi. *Molecular Ecology* **2012**, *21*, 4160-4170, doi:10.1111/j.1365-294X.2012.05602.x

Glassman, S.I.; Peay, K.G.; Talbot, J.M.; Smith, D.P.; Chung, J.A.; Taylor, J.W.; Vilgalys, R.; Bruns, T.D. A continental view of pine-associated ectomycorrhizal fungal spore banks: a quiescent functional guild with a strong biogeographic pattern. *New Phytologist* **2015**, *205*, 1619-1631, doi:10.1111/nph.13240.

Reverchon, F.; del Pilar Ortega-Larrocea, M.; Bonilla-Rosso, G.; Pérez-Moreno, J. Structure and species composition of ectomycorrhizal fungal communities colonizing seedlings and adult trees of *Pinus montezumae* in Mexican neotropical forests. *FEMS Microbiology Ecology* **2012**, *80*, 479-487, doi:10.1111/j.1574-6941.2012.01314.x.

Murata, M.; Kanetani, S.; Nara, K. Ectomycorrhizal fungal communities in endangered *Pinus amamiana* forests. *PLOS ONE* **2017**, *12*, e0189957, doi:10.1371/journal.pone.0189957.

He, X.H.; Duan, Y.H.; Chen, Y.L.; Xu, M.G. A 60-year journey of mycorrhizal research in China: Past, present and future directions. *Science China-life Sciences* **2010**, *53*, 1374-1398, doi:10.1007/s11427-010-4096-z.

Li, M.; Ding, G.; Gao, G.; Zhao, Y.; Yu, M.; Wang, D. Introduction suitability of *Pinus sylvestris* var.*mongholica* in 10 northern provinces of China. *Journal of Desert Research* **2016**, *36*, 1021-1028, doi:10.7522/j.issn.1000-694x.2015.00073.

Zhu, J.J.; Kang, H.Z.; Xu, M.L.; Wu, X.Y.; Wang, W. Effects of ectomycorrhizal fungi on alleviating the decline of *Pinus sylvestris* var. *mongolica* plantations on Keerqin sandy land. *Chinese Journal of Applied Ecology* **2007**, *14*, 232-235, doi:10.13287/j.1001-9332.2007.0456.

Alberton, O.; Kuyper, T.W. Ectomycorrhizal fungi associated with *Pinus sylvestris* seedlings respond differently to increased carbon and nitrogen availability: implications for ecosystem responses to global change. *Global Change Biology* **2010**, *15*, 166-175, doi:10.1111/j.1365-2486.2008.01714.x.

Hayward, J.; Horton, T.R.; Pauchard, A.; Nuñez, M.A. A single ectomycorrhizal fungal species can enable a *Pinus* invasion. *Ecology* **2015**, *96*, 1438-1444, doi:10.1890/14-1100.1.

Zhu, J.J.; Li, F.Q.; Xu, M.L.; Kang, H.Z.; Wu, X.Y. The role of ectomycorrhizal fungi in alleviating pine decline in semiarid sandy soil of northern China: an experimental approach. *Annals of Forest Science* **2008**, *65*, 304-304, doi:10.1051/forest:2008007.

Lehto, T.; Zwiazek, J.J. Ectomycorrhizas and water relations of trees: a review. *Mycorrhiza* **2011**, *21*, 71-90, doi:10.1007/s00572-010-0348-9.

Hohmann, P.; Messmer, M.M. Breeding for mycorrhizal symbiosis: focus on disease resistance. *Euphytica* **2017**, *213*, 113, doi:10.1007/s10681-017-1900-x

Jonsson, L.; Dahlberg, A.; Nilsson, M.C.; Karen, O.; Zackrisson, O. Continuity of ectomycorrhizal fungi in self-regenerating boreal *Pinus sylvestris* forests studied by comparing mycobiont diversity on seedlings and mature trees. *New Phytologist* **1999**, *142*, 151-162, doi:10.1046/j.1469-8137.1999.00383.x.

Scott, P.; Shearer, B.; Barber, P.; St, G.; Hardy, G. Relationships between the crown health, fine root and ectomycorrhizae density of declining *Eucalyptus gomphocephala*. *Australasian Plant Pathology* **2012**, *42*, doi:10.1007/s13313-012-0152-4.

Tedersoo, L.; Bahram, M.; Põlme, S.; Kõljalg, U.; Yorou, N.S.; Wijesundera, R.; Ruiz, L.V.; Vasco-Palacios, A.M.; Thu, P.Q.; Suija, A., et al. Global diversity and geography of soil fungi. *Science* **2014**, *346*, 1256688, doi:10.1126/science.1256688.

Miao, Y.B.; Zhu, X.M.; Li, Z.J.; Jia, F.L.; Li, W. Genetic evaluation of breeding resources of *Pinus sylvestris* var. *mongolica* from different improved generations. *Journal of Beijing Forestry University* **2017**, *39*, 71-78, doi:10.13332/j.1000-1522.20170194.

Treseder, K.K.; Bent, E.; Borneman, J.; Mcguire, K.L. Shifts in fungal communities during decomposition of boreal forest litter. *Fungal Ecology* **2014**, *10*, 58-69, doi:10.1016/j.funeco.2013.02.002.

Peay, K.G.; Schubert, M.G.; Nguyen, N.H.; Bruns, T.D. Measuring ectomycorrhizal fungal dispersal: macroecological patterns driven by microscopic propagules. *Molecular Ecology* **2012**, *21*, 4122-4136, doi:10.1111/j.1365-294X.2012.05666.x.

Gao, C.; Zhang, Y.; Shi, N.N.; Zheng, Y.; Chen, L.; Tesfaye, W.; Helge, B.; Sabine, B.; Francois, B.; Ding, Q. Community assembly of ectomycorrhizal fungi along a subtropical secondary forest succession. *New Phytologist* **2015**, *205*, 771-785, doi:10.1111/nph.13068

Wurzburger, N.; Brookshire, E.N.J.; Mccormack, M.L.; Lankau, R. Mycorrhizal fungi as drivers and modulators of terrestrial ecosystem processes. *New Phytologist* **2017**, *213*, 996-999, doi:10.1111/nph.14409.

Tang, Y.; Li, X. Simulating effects of precipitation and initial planting density on population size of Mongolian pine in the Horqin Sandy Land, China. *Agroforestry Systems* **2018**, *92*, 1-9, doi:10.1007/s10457-016-0004-2.

Edgar, R.C. Search and clustering orders of magnitude faster than BLAST. *Bioinformatics* **2010**, *26*, 2460-2461, doi:10.1093/bioinformatics/btq461

Nguyen, N.H.; Song, Z.; Bates, S.T.; Branco, S.; Tedersoo, L.; Menke, J.; Schilling, J.S.; Kennedy, P.G. FUNGuild: An open annotation tool for parsing fungal community datasets by ecological guild. *Fungal Ecology* **2016**, *20*, 241-248.

Soil Survey Staff. *Soil Survey Field and Laboratory Methods Manual, Soil Survey Investigations Report, no. 51*; United States Department of Agriculture, Natural Resources Conservation Service: 2009.

Klute, A. *Methods of Soil Analysis: Part 1—Physical and Mineralogical Methods*; Agronomy Monograph, American Society of Agronomy: Madison, Wis, USA, 1986.

Walkley, A.; Black, I.A. An examination of the degtjareff method for determining soil organic matter, and a proposed modification of the chromic acid titration method. *Soil Science* **1934**, *37*, 29-38, doi:10.1097/00010694-193401000-00003.

Mason, C.; Edwards, M.; Riby, P.; Coe, G. The use of microwaves in the acceleration of digestion and colour development in the determination of total Kjeldahl nitrogen in soil. *Analyst* **1999**, *124*, 1719-1726, doi:10.1039/a903623g.

John, M. Colorimetric determination of phosphorus in soil and plant materials with ascorbic acid. *Soil Science* **1970**, *109*, 214-220, doi:10.1097/00010694-197004000-00002.

Šmilauer, P.; Lepš, J. *Multivariate Analysis of Ecological Data using CANOCO 5 (2nd Edition)*; Cambridge University Press: Cambridge, 2014.

Leake, J.R. Is diversity of ectomycorrhizal fungi important for ecosystem function? *New Phytologist* **2001**, *152*, 1-3, doi:10.2307/1353574.

Grebenc, T.; Christensen, M.; Vilhar, U.; Čater, M.; Martín, M.P.; Simončič, P.; Kraigher, H. Response of ectomycorrhizal community structure to gap opening in natural and managed temperate beech-dominated forests. *Canadian Journal of Forest Research* **2009**, *39*, 1375-1386, doi:10.1139/X09-072.

He, J.Z.; Li, J.; Zheng, Y.M. Thoughts on the microbial diversity-stability relationship in soil ecosystems. *Biodiversity Science* **2013**, *4*, 411-420, doi:10.3724/SP.J.1003.2013.10033.

Dickie, I.A.; Moyersoen, B., . Towards a global view of ectomycorrhizal ecology. *New Phytologist* **2010**, *180*, 263-265, doi:10.1111/j.1469-8137.2008.02635.x.

North, M.; Trappe, J.; Franklin, J. Standing crop and animal consumption of fungal sporocarps in Pacific northwest forests. *Ecology* **1997**, *78*, 1543-1554, doi:10.1890/0012-9658(1997)078[1543:SCAACO]2.0.CO;2.

Smith, J.E.; Molina, R.; Huso, M.M.; Luoma, D.L.; McKay, D.; Castellano, M.A.; Lebel, T.; Valachovic, Y. Species richness, abundance, and composition of hypogeous and epigeous ectomycorrhizal fungal sporocarps in young, rotation-age, and old-growth stands of Douglas-fir (*Pseudotsuga menziesii*) in the Cascade Range of Oregon, U.S.A. *Canadian Journal of Botany* **2002**, *80*, 186-204, doi:10.1139/B02-003.

Vellinga, E.C.; Wolfe, B.E.; Anne, P. Global patterns of ectomycorrhizal introductions. *New Phytologist* **2009**, *181*, 960-973, doi:10.1111/j.1469-8137.2008.02728.x

Chung, H.C.; Kim, D.H.; Cho, N.S.; Lee, S.S. Observation and distribution of ectomycorrhizal fungi in *Pinus* roots. *Mycobiology* **2003**, *31*, 1, doi:10.4489/MYCO.2003.31.1.001.

Martínez-Peña, F.; Ágreda, T.; Águeda, B.; Ortega-Martínez, P.; Fernández-Toirán, L.M. Edible sporocarp production by age class in a Scots pine stand in Northern Spain. *Mycorrhiza* **2012**, *22*, 167-174, doi:10.1007/s00572-011-0389-8.

Kyaschenko, J.; Clemmensen, K.E.; Hagenbo, A.; Karltun, E.; Lindahl, B.D. Shift in fungal communities and associated enzyme activities along an age gradient of managed *Pinus sylvestris* stands. *Isme Journal* **2017**, *11*, 863, doi:10.1038/ismej.2016.184.

Nahuel, P.; Thomas, D.B.; Rytas, V.; Martin, A.N. Suilloid fungi as global drivers of pine invasions. *New Phytologist* **2019**, *222*, 714-725, doi:10.1111/nph.15660.

Hayward, J.; Thomas R, H.; Martin A, N. Ectomycorrhizal fungal communities coinvading with Pinaceae host plants in Argentina: Gringos bajo el bosque. *New Phytologist* **2015**, *208*, 497-506, doi:10.1111/nph.13453.

Salgado, S.M.E.; Barroetaveña, C.; Rajchenberg, M. Do pine plantations provide mycorrhizal inocula for seedlings establishment in grasslands from Patagonia, Argentina? *New Forests* **2011**, *41*, 191-205, doi:10.1007/s11056-010-9220-1.

Shi, C.H.; Tolgor, B.; Li, Y. Newly recorded genus and species of *Pezizales* in China. *Mycosystema* **2016**, *35*, 1348-1356, doi:10.13346/j.mycosystema.150247.

Drigo, B.; Kowalchuk, G.; A. van Veen, J. Climate change goes underground: Effects of elevated atmospheric CO_2 on microbial community structure and activities in the rhizosphere. *Biology and Fertility of Soils* **2008**, *44*, 667-679, doi:10.1007/s00374-008-0277-3.

Bennett, A.E.; Classen, A.T. Climate change influences mycorrhizal fungal–plant interactions, but conclusions are limited by geographical study bias. *Ecology* **2020**, *n/a*, e02978, doi:10.1002/ecy.2978.

Deslippe, J.R.; Hartmann, M.; MOHN, W.W.; Simard, S. Long-term experimental manipulation alters the ectomycorrhizal community of *Betula nana* in Arctic tundra. *Global Change Biology* **2010**, *17*, 1625-1636, doi:10.1111/j.1365-2486.2010.02318.x.

Maclean, C.; Dickson, A.; Bell, G. Resource competition and adaptive radiation in a microbial microcosm. *Ecology Letters* **2004**, *8*, 38-46, doi:10.1111/j.1461-0248.2004.00689.x.

Clemmensen, K.; Michelsen, A.; Jonasson, S.; Shaver, G. Increased ectomycorrhizal fungal abundance after long-term fertilization and warming of two arctic tundra ecosystems. *The New phytologist* **2006**, *171*, 391-404, doi:10.1111/j.1469-8137.2006.01778.x.

Allison, S.; Treseder, K. Warming and drying suppress microbial activity and carbon cycling in boreal forest soils. Glob. Change Biol. 14, 2898-2909. *Global Change Biology* **2008**, *14*, 2898-2909, doi:10.1111/j.1365-2486.2008.01716.x.

Zhang, H.; Yin, Q.; Nakajima, T.; Nakata, M.; Lu, P.; He, J. Influence of changes in solar radiation on changes of surface temperature in China. *Acta Meteorologica Sinica* **2013**, *27*, 87-97, doi:10.1007/s13351-013-0109-8.

Pickles, B.J.; Egger, K.N.; Massicotte, H.B.; Green, D.S. Ectomycorrhizas and climate change. *Fungal Ecology* **2012**, *5*, 73-84, doi:10.1016/j.funeco.2011.08.009.

Arvis, S.; Woodward, S.; Alexander, I.J.; Taylor, A.F.S. Regional scale gradients of climate and nitrogen deposition drive variation in ectomycorrhizal fungal communities associated with native Scots pine. *Global Change Biology* **2013**, *19*, 1688-1696, doi:10.1111/gcb.12178.

Maestre, F.T.; Delgado-Baquerizo, M.; Jeffries, T.C.; Eldridge, D.J.; Ochoa, V.; Gozalo, B.; Quero, J.L.; García-Gómez, M.; Gallardo, A.; Ulrich, W., et al. Increasing aridity reduces soil microbial diversity and abundance in global drylands. *Proceedings of the National Academy of Sciences of the United States of America* **2015**, *112*, 15684-15689, doi:10.1073/pnas.1516684112

Swaty, R.; Gehring, C.; Ert, M.; Theimer, T.A.D.; Keim, P.; Whitham, T. Temporal variation in temperature and rainfall differentially affects ectomycorrhizal colonization at two contrasting sites. *New Phytologist* **1998**, *139*, 733-739, doi:10.1046/j.1469-8137.1998.00234.x.

Shi, L.; Guttenberger, M.; Kottke, I.; Hampp, R. The effect of drought on mycorrhizas of beech (*Fagus sylvatica* L.): changes in community structure, and the content of carbohydrates and nitrogen storage bodies of the fungi. *Mycorrhiza* **2002**, *12*, 303-311, doi:10.1007/s00572-002-0197-2.

Dumbrell, A.J.; Nelson, M.; Helgason, T.; Dytham, C.; H Fitter, A. Relative roles of niche and neutral process in structuring a soil microbial community. *The ISME journal* **2010**, *4*, 337-345, doi:10.1038/ismej.2010.48.

Rosinger, C.; Sandén, H.; Matthews, B.; Mayer, M.; Godbold, D. Patterns in Ectomycorrhizal Diversity, Community Composition, and Exploration Types in European Beech, Pine, and Spruce Forests. *Forests* **2018**, *9*, 445, doi:10.3390/f9080445.

Leho, T.; Mohammad, B.; MäRt, T.; Diédhiou, A.G.; Henkel, T.W.; Rasmus, K.; Morris, M.H.; Kazuhide, N.; Eduardo, N.; Peay, K.G. Towards global patterns in the diversity and community structure of ectomycorrhizal fungi. *Molecular Ecology* **2012**, *21*, 4160-4170.

Erland, S.; Söderström, B.; Andersson, S. Effects of liming on ectomycorrhizal fungi infecting *Pinus sylvestris* L. 2. Growth rates in pure culture at different ph values compared to growth-rates in symbiosis with the host plant. *New Phytologist* **1990**, *115*, 683-688, doi:10.1111/j.1469-8137.1990.tb00499.x.

Richter, D.D.; Markewitz, D.; Trumbore, S.E.; Wells, C.G. Rapid accumulation and turnover of soil carbon in a re-establishing forest. *Nature* **1999**, *400*, 56-58, doi:10.1038/21867.

Druebert, C.; Lang, C.; Valtanen, K.; Polle, A. Beech carbon productivity as driver of ectomycorrhizal abundance and diversity. *Plant, cell & environment* **2009**, *32*, 992-1003, doi:10.1111/j.1365-3040.2009.01983.x.

Cox, F.; Barsoum, N.; Lilleskov, E.A.; Bidartondo, M.I. Nitrogen availability is a primary determinant of conifer mycorrhizas across complex environmental gradients. *Ecology Letters* **2010**, *13*, 1103-1113, doi:10.1111/j.1461-0248.2010.01494.x.

Sterkenburg, E.; Clemmensen, K.; Ekblad, A.; Finlay, R.; Lindahl, B. Contrasting effects of ectomycorrhizal fungi on early and late stage decomposition in a boreal forest. *The ISME Journal* **2018**, *12*, 2187-2197, doi:10.1038/s41396-018-0181-2.

Cairney, J.W.G. Ectomycorrhizal fungi: the symbiotic route to the root for phosphorus in forest soils. *Plant and Soil* **2011**, *344*, 51-71, doi:10.1007/s11104-011-0731-0.

Rao, C.; Sharma, G.; Shukla, A. Distribution of ectomycorrhizal fungi in pure stands of different age groups of *Pinus* *kesiya*. *Canadian Journal of Microbiology* **2011**, *43*, 85-91, doi:10.1139/m97-012.

Zhang, T.T.; Wang, Q.; Du, C.; Zhang, D.N.; Zhang, F.; Ma, W.; Wang, Z.K.; Li, X.; Geng, Z.C. Diversity of ectomycorrhizal fungi associated with *Betula albosinensis* in Xinjiashan forest region of Qinling Mountains. *Mycosystema* **2017**, *36*, 851-860, doi:10.13346/j.mycosystema.160232.

Baar, J.; Vries, A.H.M.d. Effects of manipulation of litter and humus layers on ectomycorrhizal colonization potential in Scots pine stands of different age. *Mycorrhiza* **1995**, *5*, 267-272, doi:10.1007/BF00204960.

Glassman, S.; Wang, I.; Bruns, T. Environmental filtering by pH and soil nutrients drives community assembly in fungi at fine spatial scales. *Molecular Ecology* **2017**, *26*, doi:10.1111/mec.14414.

Hagerberg, D.; Thelin, G.; Wallander, H. The production of ectomycorrhizal mycelium in forests: Relation between forest nutrient status and local mineral sources. *Plant and Soil* **2003**, *252*, 279-290, doi:10.1023/a:1024719607740.

Bidartondo, M.; Ek, H.; Wallander, H.; Soderstrom, B. Do nutrient additions alter carbon sink strength of ectomycorrhizal fungi? *New Phytologist* **2001**, *151*, 543-550, doi:10.1046/j.1469-8137.2001.00180.x.

Bauman, J.M.; Keiffer, C.H.; Hiremath, S.; Mccarthy, B.C.; Kardol, P. Soil preparation methods promoting ectomycorrhizal colonization and American chestnut *Castanea dentata* establishment in coal mine restoration. *Journal of Applied Ecology* **2013**, *50*, 721-729, doi:10.1111/1365-2664.12070.

Horton, B.M.; Glen, M.; Davidson, N.J.; Ratkowsky, D.; Close, D.C.; Wardlaw, T.J.; Mohammed, C. Temperate eucalypt forest decline is linked to altered ectomycorrhizal communities mediated by soil chemistry. *For Ecol Manage* **2013**, *302*, 329-337, doi:10.1016/j.foreco.2013.04.006.

Close, D.C.; Davidson, N.J.; Johnson, D.W.; Abrams, M.D.; Hart, S.C.; Lunt, I.D.; Archibald, R.D.; Horton, B.; Adams, M.A. Premature decline of Eucalyptus and altered ecosystem processes in the absence of fire in some Australian forests. *The Botanical Review* **2009**, *75*, 191-202, doi:10.1007/s12229-009-9027-y.

Corcobado, T.; Moreno, G.; Azul, A.; Solla, A. Seasonal variations of ectomycorrhizal communities in declining *Quercus ilex* forests: Interactions with topography, tree health status and *Phytophthora cinnamomi* infections. *Forestry* **2015**, *88*, 257-266, doi:10.1093/forestry/cpu056.

Berner, C.; Johansson, T.; Wallander, H. Long-term effect of apatite on ectomycorrhizal growth and community structure. *Mycorrhiza* **2012**, *22*, 615-621, doi:10.1007/s00572-012-0438-y.

Twieg, B.D.; Durall, D.M.; Simard, S.W. Ectomycorrhizal fungal succession in mixed temperate forests. *New Phytologist* **2007**, *176*, 437-447, doi:10.1111/j.1469-8137.2007.02173.x.

Manoharachary, C.; Reddy, P. Plant Mineral Nutrition Through Ectomycorrhiza. In *Mycorrhizal Biology*, K.G. Mukerji, B.P. Chamola, Singh, J., Eds. Springer: Boston, MA, 2000; 10.1007/978-1-4615-4265-0_9pp. 135-141.

Fränzle, S. Autocatalytic processes and the role of essential elements in plant growth. In *Chemical Elements in Plant and Soil: Parameters Controlling Essentiality*, Springer Netherlands: Dordrecht, 2010; 10.1007/978-90-481-2752-8_2pp. 17-130.

Blaudez, D.; Chalot, M. Characterization of the ER-located zinc transporter ZnT1 and identification of a vesicular zinc storage compartment in *Hebeloma cylindrosporum*. *Fungal Genetics and Biology* **2011**, *48*, 496-503, doi:10.1016/j.fgb.2010.11.007.

Migeon, A.; Blaudez, D.; Wilkins, O.; Montanini, B.; Campbell, M.M.; Richaud, P.; Thomine, S.; Chalot, M. Genome-wide analysis of plant metal transporters, with an emphasis on poplar. *Cellular and Molecular Life Sciences* **2010**, *67*, 3763-3784, doi:10.1007/s00018-010-0445-0.

Kennedy, P. Ectomycorrhizal fungi and interspecific competition: Species interactions, community structure, coexistence mechanisms, and future research directions. *New Phytologist* **2010**, *187*, 895-910, doi:10.1111/j.1469-8137.2010.03399.x.

Teste, F.; Simard, S.; Durall, D.M.; Guy, R.D.; Jones, M.D.; Schoonmaker, A.L. Access to mycorrhizal networks and roots of trees: Importance for seedling survival and resource transfer. *Ecology* **2009**, *90*, 2808-2822, doi:10.1890/08-1884.1.

Ecological-Economic Management Technology in Eco-Fragile Region the Yellow River Basin

Shen Zhenzhou[1], Yao Wenyi[1], Rao Liangyi[2], Xiao Peiqing[1], Hou Liting[3], Chen Cheng[3],Yang Jishan[1]
1 Key Laboratory of Soil and Water Conservation on the Loess Plateau of Ministry of Water Resources, Yellow River Institute of Hydraulic Research, Zhengzhou 450003
2 School of soil and water conservation, Beijing Forestry University, Beijing 100083, China
3 Yellow River Conservancy Technical College, Kaifeng, Henan 450003, China

Abstract

The national strategy of ecological protection and high quality development of the Yellow River Basin points out that the Yellow River basin governance should adhere to the concept that green water and green mountains are golden mountains and silver mountains, and focus on strengthening ecological protection and governance, promoting the implementation of a number of major ecological protection, restoration and construction projects, among which the Pisha Sandstone Area in the middle reaches of the Yellow River is one of the areas that should focus on ecological comprehensive governance. Based on the analysis of the previous management theory and practice in Pisha Sandstone Area, this paper carried out the research and development of ecological comprehensive management technology in Pisha Sandstone area covered with sand, including slope top runoff high-efficiency storage and utilization technology, slope top economic forest fruit industry mode, block gravity erosion polymer grouting technology, slope anti erosion and promoting growth comprehensive management technology, channel flexible dam Pisha Sandstone modified material valley Through the research and development and integration of erosion control technology of the slope top and check dam, the ecological comprehensive management mode of the sand covered Pisha Sandstone Area was finally summarized: slope top ditch network vertical and horizontal water blocking, irrigation and grass mixing to improve efficiency; steep slope grouting consolidation, gentle slope protection with shrub and grass; ditch bottom modified material gufangtang dam + irrigation and grass flexible dam; gully mouth Pisha Sandstone modified check dam, sediment detention, flood reduction and silting to increase efficiency, and the project was put into practice The model of comprehensive ecological management was tested and demonstrated. The comprehensive ecological management mode of Pisha Sandstone can provide strong technical support for ecological protection and high-quality development of the Yellow River Basin.

Keywords: Pisha stone Area, Comprehensive ecological management, Model

The Yellow River is the mother river of the Chinese nation and the cradle of Chinese civilization. Ecological protection and high-quality development of the Yellow River basin are major national strategies, like the coordinated development of the Beijing-Tianjin-Hebei region, the development of the Yangtze River Economic Belt, the construction of the Guangdong-Hong Kong-Macao Greater Bay Area, and the integrated development of the Yangtze River Delta (Xi 2019).The Yellow River basin is an important region to win the battle against poverty at the present stage and plays a very important role in China's economic and social development and ecological security.The Arsenic sandstone area in the Yellow River basin is not only an important source of the coarse sediment deposited in the lower reaches of the Yellow River, but also an important battlefield for winning the battle against poverty. Therefore, the comprehensive ecological management in the Arsenic sandstone area is urgent (Yao 2019). Pisha sandstone area is located in the Ordos Plateau bordering Inner Mongolia Autonomous Region, Shaanxi Province and Shanxi Province, with a total area of 16,700 km2. It is one of the typical ecologically fragile areas in China, and also the area with the most severe erosion in the Yellow River Basin and even in the world (Wang et al., 2007).Pisha sandstone is an interbedded rock composed of sandstone, sand shale and argillaceous sandstone formed in Permian, Triassic, Jurassic and Cretaceous of Paleozoic, and belongs to the clastic sedimentary rock of continental facies. It is as firm as rock without water and as weak as mud when exposed to water, so it is extremely difficult to deal with it [4].There are many erosion factors in this area. Different erosion factors, such as wind power, water power and freeze-thaw, compound and superposition each other, making the erosion modulus of this area as high as 30,000 ~ 40,000 t/(km2·a), which is the concentrated source area of the Yellow River coarse sediment, and thus becomes the focus of national governance (Xu 2007).

In November 1985, the then minister of hydropower Qian Zhengying (Qian 1980) to the central submitted to develop seabuckthorn resources as the acceleration of the governance of the loess plateau in China - about development in Shanxi Province survey of seabuckthorn, then begun to arsenic sandstone of governance, including many scholars began to study on arsenic sandstone of governance and the management of government investment projects,For example, the World Bank loan project for soil and water conservation on the Loess Plateau (Li 2005). In scientific research, 1989 Han Xibin (Han 1989) should be according to the principle of "adjust measures to local conditions, due to harm fortification" in Liang Mao coordinated level trench of the part of the slope is steep, and scale-hole soil preparation, build pinus tabulaeformis, white elm, various of shrubbery, mixed needle, such as in the part of the slower level terrace as fixed good farmland and planting forage grass;In 1999, the Research Group of Seabuckthorn Treatment Arsenic Sandstone of the Ministry of Water Resources carried out the investigation of Seabuckthorn Treatment Arsenic Sandstone by developing Seabuckthorn, conserving water and soil, and building ecological agriculture, and achieved abundant results.Bi Cifen (Bi 2000; Bi 2003) proposed using seabuckthorn as plant flexible dam to control the channel erosion of arsenic sandstone, and carried out relevant experimental research.Tang Zhenghong et al. (Tang et al., 2001) carried out some studies on the water erosion law, the alternating features of water and wind erosion, geomorphologic features and vegetation types in this area, and initially recognized some basic features or laws in this area. Wang Yuechang et al. proposed some treatment schemes, such as biological measures for the treatment of mixed forest such as Caragana korshinskii and Pinus formulaeformis.Yao Wenyi (Yao 2018) proposed a treatment mode of three-dimensional configuration by adopting new anti-corrosion and growth promoting materials, combined with engineering measures such as slope ladder, horizontal ditch, fish-scale pit, and biological measures, and achieved good results.

Overall, despite decades for arsenic sandstone erosion treatment technology was carried out by a number of research and practice, has made certain progress, but the traditional management localization, trivializes situated, discontinuous problems, lack of the whole regional scale compound erosion resistance control, the degradation of ecological management for the integration of system integrated solutions and technology system.Recently, the national key research and development plan has specially set up the project of "Integrated Ecological Management Technology in the Pisha Sandstone Area of Ordos Plateau", aiming to make innovations in the theory, technology and practice of integrated ecological management in the Pisha Sandstone Area, and provide technical support for the restoration and reconstruction of fragile ecosystem in the Pisha Sandstone Area and the treatment of coarse sediment in the Yellow River.The integrated ecological management of erosion control and vegetation restoration will be the main development direction of soil erosion control technology research in the Pisha sandstone area.This article is based on this goal to carry out the study, carried out a lot of arsenic sandstone area topography and geomorphology, soil erosion, vegetation community characteristics, combined with the local government and the management experience of the masses, all the comprehensive control on the arsenic sandstone areas construction of the ecological slope runoff experiment plot and watershed runoff and sediment monitoring facilities, the subsequent practice of small watershed comprehensive treatment technology,Finally, a set of technical models of ecological comprehensive management in Pisha sandstone area is summarized, and the practical application of the comprehensive management model is introduced by taking the sand-covered Pisha sandstone area as an example (Fig. 1).

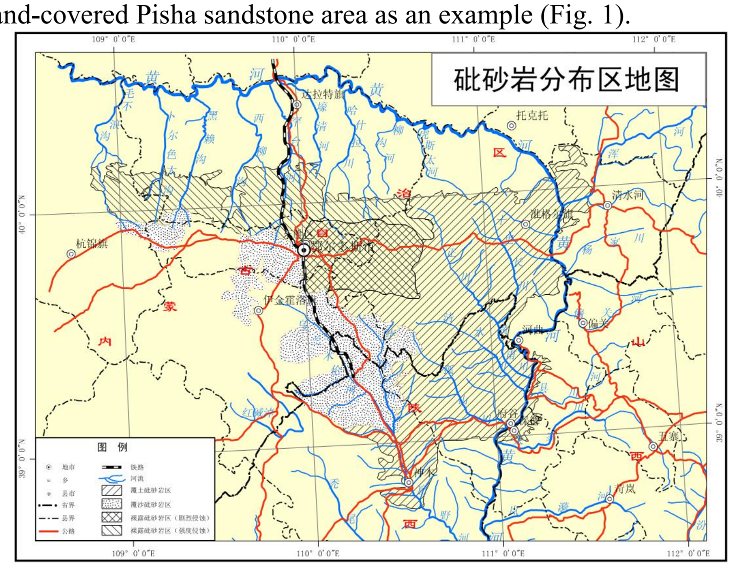

Figure 1 Distribution range of arsenic sandstone

1 Overview of integrated ecological management mode in eco-fragile region area

The comprehensive ecological management system of sand overburden Arsenic Sandstone area is established by taking measures according to local conditions and classifying measures, especially taking small watershed as the unit, following the ecological principles and using the method of system engineering to design the management mode.

Bare area based on arsenic sandstone slope slope - channel geomorphic unit combination type and structure characteristic, according to "the top hat, slope protection of the waist, foot wear boots" governance principles, developed by arsenic sandstone area slope rainfall runoff sand high efficient reservoir been technology, is proposed based on recovery is given priority to, complementary with the development of fruit industry in grass runoff utilization mode;Polymer grouting technology and construction process, such as block gravitation erosion reinforcement of steep slope of overburden sandstone, seepage prevention of rock crack and anchorage grouting, are researched and developed.The application technology of plant-generated consolidation materials on Pisha sandstone slope is researched and developed.The construction technology of modified materials of arsenic sandstone was developed.The comprehensive erosion control system and model of the ditch system, including ditch top - ditch bank - ditch bed - ditch head, are constructed (Fig. 2).

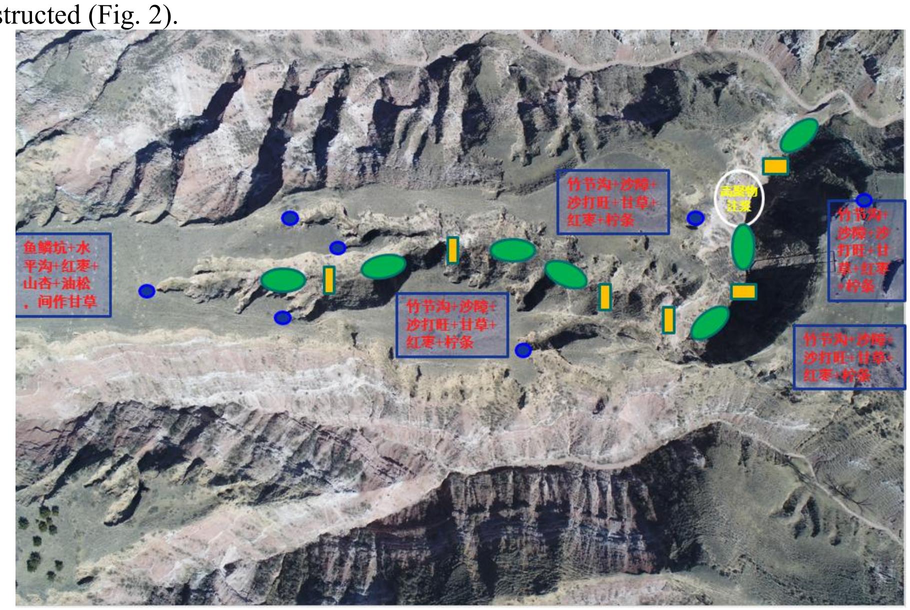

Figure 2 Design sketch of integrated ecological management mode for small watershed eco-fragile region

2 Sloping top management technology of overlying sand in eco-fragile region

On the premise of ecological management, various engineering, biological and agronomic management measures and technologies are arranged in the corresponding position. Through the effective development of land management technology and rainwater resources' production potential, the efficient and enrichment utilization of water resources can be realized, so as to provide good material conditions for the sustainable development of ecological environment and agricultural production, promote a virtuous cycle of ecological environment, and finally establish an efficient slope top ecosystem and model.

Adopts the technical route of treating drought with rain, and develops and popularizes the efficient production technology system of water collection.Natural precipitation runoff is collected and stored on a large scale, and combined with advanced micro-irrigation technology, efficient supplementary irrigation is carried out in severe drought period and critical period of water demand of vegetation, and the efficient production technology system of water collection is successfully established, which consists of rainwater collection and afforestation and grass planting technology, rainwater collection and supplementary irrigation slope vegetation efficient water use technology and rainwater collection and efficiency enhancement technology.

The conditions of the underlying surface in this area are relatively poor, so the biological measures are as follows: the mixing of apricot and peach, and the replanting of Chinese pine.According to the local suitable construction method, the original part of Chinese pine planted in the fishscale pit withered, to replace the replanting of jujube, which can not only enrich the vegetation, but also can produce economic benefits.

For the slope top with large catchment area, PVC water cellar is set with a volume of about 1.5m^3.

For the slopes with large white arsenic sandstone exposed, it is not suitable to bury water cellars, so the modified materials of arsenic sandstone can be used to build the millet to hold the rainwater and reduce the scour of the ground by runoff.A catchment tank is arranged in connection with the trench network at the top of the slope (Fig. 3). Seep prevention treatment is required for the catchment tank, and two soil mounds with a height of 1/2 of the depth of the catchment trench are built in the catchment trench connecting the inlet of the catchment tank (Fig. 4), with the purpose of precipitation of sediment before runoff enters the catchment tank as far as possible.The water in the catchment tank is led out through the siphon device, and then the drip irrigation belt is introduced into the slope.

Figure 3 The top of the slope exposed by large area white arsenic sandstone **Figure 4** Catchment pool

3 Slope control technology of overlying sand in eco-fragile region

Arsenic sandstone slope often development size of aperture, such as weathering, rain after entering gap will cause serious erosion, the massive weight force become the important source of channel erosion and sediment, the erosion of the arsenic sandstone areas watershed erosion often 60% ~ 70%, therefore, to effectively reduce arsenic sandstone areas into the yellow coarse sediment loads,Block weight erosion must be controlled.Based on this, the slope is divided into three parts for treatment according to the topography, geomorphology and structure characteristics and erosion characteristics of the slope, namely the slope of > 60°, 30° ~ 60° and < 30°.

3.1 Comprehensive treatment technology of slope > 60°

(1) Block gravity erosion treatment technology

Side of the main reason for the block of gravity erosion have two: one is influenced by the effect such as tectonics, weathering, white sandstone exist lots of vertical cracks, constitutes the channel of water infiltration, under the effect of freeze-thaw cycle and water erosion, the crack is incised, loss of fracture surface on both sides of the bite force, make the slope in the sandstone blocks and maternal separation;A layered arsenic sandstone area geological structure, lithologic differences between layers, because red arsenic sandstone weathering faster than white arsenic sandstone, lead to the upper white arsenic sandstone lost support, dangling shaped, drop, and potential energy of the capsized, when reaches a certain limit state is a sudden collapse, block shape of gravity erosion occur.

In view of the special lithology, sensitive to water, dilatation and disintegration of arsenic sandstone, the traditional method is difficult to deal with the problems.Therefore, through the idea innovation, no water grouting concept is put forward, which make full use of the new nonaqueous reaction polymer grouting materials from inflation, seepage control, Gao Ren excellent features, such as combination of arsenic sandstone block shape of gravity erosion mechanism, through the vertical fissure polymer and polymer, polymer consolidation grouting seepage grouting inhibit the massive gravity erosion.

(2) consolidation technology of weathered materials on steep slopes

In the slope > 60°, there are a lot of gravity erosion caused by weathered arsenic sandstone besides a few large lumped gravity erosion.Due to the characteristics of arsenic sandstone itself and the damage of freezing-thawing and wind to > 60° slope rock mass, arsenic sandstone will be peeledinto smaller particles and slide down. The slope soil in this part is poor and steep, and vegetation cannot grow. Therefore, HKYGJ -- 1 is adopted for consolidation in this part of steep slope to prevent erosion of this part of slope.HKYGJ-1 was mixed and stirred with water at a volume of 1：100 and then loaded into the spray tank. The spray tank used gravity flow and pressure pump to consolidate the slope rock mass greater than 60° in the small watershed (Fig. 4).

Figure 4 Construction site of consolidation on small watershed slope with a slope greater than 60°eco-fragile region

3.2 Comprehensive treatment mode for slopes of 30° ~ 60°

3.2.1 Engineering treatment measures

For the slope of 30° ~ 60°, the control engineering measures are mainly aimed at the large water and sediment erosion gullies on the slope.The engineering measures adopt a 60cm high hedgerow made of wicker, which is buried vertically in the Huishui ditch. The depth of the hedgerow is 30cm, and the width of the hedgerow is generally the same as that of the Huishui ditch.A thick sand willow strip or fine steel bar is laid every 30cm distance as the pile foundation. At the same time, some vines such as ivy and lara vine are planted in the upper and lower parts of the hedgerows to increase the sand settling effect of the hedgerows. The hedgerows need to be managed and protected within a certain period of time after completion.

In combination with vegetation measures such as shrub and grass, half-moon small fish scale pits can be set on the slopes of 30° ~ 60°. The diameter and depth of half-moon fish scale pits are generally about 30cm and about 20cm. The row spacing of fish scale pits is generally about 3m, and the plant spacing is about 1.5m.This kind of fish-scale pit can not only increase the infiltration of rainfall on the slope, but also maximize the efficiency of the storage of water in the water cellar when the weather is dry.

3.2.2 Vegetation management measures

Due to 30 ° ~ 60 ° slope steep slope, soil moisture content is low, not suitable for planting trees and other tall tree species, so the part of the slope general mixed planting strong vitality, soil and water conservation function better with alkali grass, health, flower sticks, sea buckthorn, Mongolia hedysarummaxim, mixed shrub cultivated into the engineering measures to lay half moon scale-hole, planting period twice a year,First choice in the middle and late April of each year, the end of October;At the same time, alfalfa, melilotus melilotus, sargassum, icicarpa and ceratoides with strong vitality were sown between the mixed shrub rows before and after rainfall.

Due to the poor nutrition and severe weathering of some white arsenic sandstone layers, vines such as ivy and lalla vines should be planted in the red arsenic sandstone below them according to the row spacing of 50cm and plant spacing of 50cm. The mature vines can form a good ability of preventing wind erosion and temperature difference freeze-thaw erosion to white arsenic sandstone.

In the early stage of planting, attention should be paid to the management and protection, and water should be poured every 10 days to promote the survival of vegetation.

3.2.3 Consolidation measures

Generally speaking, the consolidated plant HKYGJZS-2 material with a lower concentration is still needed to spray on the slope of 30° ~ 60° to maintain the soil moisture content in this area. A part of the infiltration water can be preserved during rainfall, and soil moisture evaporation can be reduced during non-rainfall period, so as to maintain good vegetation growth.The consolidated material HKYGJZS-2 is mixed and stirred with water at a volume of 1:150 and then loaded into the spraying tank truck. The 30 ° ~ 60° slope rock mass can be sprayed by gravity flow and pressure pump.

3.3 Comprehensive treatment mode of slope < 30°

3.3.1 Project management mode

For the < 30° slope, the pyro-sandstone debris particles formed by freeze-thaw above the slope are easy to form loose deposits at the foot of the slope. If there is no vegetation to intercept these loose deposits, they are easy to slip away.The measures to treat the erosion are modified bricks made of modified materials of arsenic sandstone, or hexagenic hollow blocks made of modified blocks to protect the slope. Grass can be planted in the hollow places to prevent the erosion materials from entering the gully.

According to previous explorations, gravity erosion of root layer will occur when there is heavy rainfall on a single planted grass. In order to prevent the occurrence of shallow gravity erosion, small zigzag drains and shrubs such as sea-buckthorn can be set to divert the slope catchment water away and reduce the occurrence of gravity erosion of root layer.In serious cases, the modified materials of arsenic sandstone can also be used to make retaining walls with trapezoidal cross sections to prevent the occurrence of gravity erosion.In addition, a half-moon fish scale pit can be set. The diameter of the fish scale pit is generally about 50cm, and the depth is about 30cm. The row spacing of the fish scale pit is generally about 3m, and the plant spacing is about 2m.This kind of fish-scale pit is slightly larger than the fish-scale pit on the slope of 30 °~ 60°, planting jujube and other economic fruits.

3.3.2 Vegetation management measures

On the slope of less than 30°, the soil moisture content is relatively high, which is suitable for planting economic fruit forest and other shrub species. Therefore, the excavation of fish-scale pit and the mixed planting of HKY-1, HKY-2 red jujube, papyriformis papyriformis and Chinese wolfberry with strong vigor and certain water and soil conservation function are good for forest irrigation trees with good economic benefits.The planting period is twice a year, the first choice is in the middle and late April of each year, and the second time is at the end of October of each year.At the same time, the mixed shrub rows were scattered with Elymus chinensis, Sargassum sargassum, Agropyrum, Mongoliae and other strong vitality grass.

In the early stage of planting, attention should be paid to the management and protection, and water should be poured every 10 days to promote the survival of vegetation.

3.2.3 Measures for consolidation of plant biomass

For the slope of less than 30°, it is generally not necessary to spray the consolidation material, but for the area where there is a loose accumulation body of arsenic sandstone, it is still necessary to spray the consolidation material with a lower concentration to prevent the erosion of the loose accumulation body.Consolidated material HKYGJZS-2 was mixed with water at a volume of 1:180 and then sprayed.

4 Channel governance model in eco-fragile region

4.1 Soft sandstone modified material Gufang

A modified material valley is set up about 50m apart in the small watershed ditch, and at the same time, it should be spaced with the plant flexible dam behind it.In general, the floor width of the floor is 3m, the ceiling width is 0.5m, and the height is about 2m.The foundation should be cleaned up during the construction of the valley.Before the dam construction, the dam foundation and bank slope should be treated first. The bank slope should be cut down to 1:1.5 after the tree roots and other debris on the dam foundation are cleaned up, and then the joint groove is excavated in the dam foundation and dam abutment.As the original material of the modified material of arsenic sandstone, the arsenic sandstone should be mined from the place not far from the dam site without affecting the stability of the project. It is better to be mined from the inundated land not far from the upstream of the dam site. After the surface debris is removed, it can be transported to the working face for use.When filling the dam foundation, the water content of the soil is required to be 15% ~ 18% and homogeneous, and the soil should be laid along the axis of the dam.Dam foundation namely for dam filling, when completed, will be prepared the original arsenic sandstone rock in proportion evenly sprayed with viscous or bentonite modified material mix bulldozers to promote working face, after each shop is 0.3 m after using artificial ramming machine or mechanical rolling to design soil dry density, then the soil surface debristling, sprinkling on the second floor shop again after filling, upwards, in turn,Adequate subsidence joints shall be left in the elevation of the dam until the maximum height of the dam is reached.For mechanical rolling less than the place available artificial tamping treatment.Modified millet after the completion of construction to plastic, local high part to scrape flat, low-lying part to fill, dam top to make a field grid planting plants to prevent soil erosion, dam back surface can also sow grass seed to prevent soil erosion;After the construction of the valley floor, the surface should be sprayed with consolidation materials for consolidation, and the consolidation material HKYGJ-1 and water should be mixed and stirred with a volume of 1:50 and then loaded into spraying. Small warping DAMS can be built in small watershed gullies with an area of more than 1km2 to create silting land.

4.2 Plant flexible dam management mode

The plant flexible dam in the gully is arranged between the valleys of arsenic sandstone modified material, and one plant flexible dam is arranged every 10m.Plant flexible dam is composed of five lines of shrubbery, mixed planting, planting into each row shrubbery "W" or "V" glyph, to meet the water first row planting distance of 3 m plant salix, can effectively reduce the kinetic energy of water, into the water the second line according to the planting distance of 2 m planting jujube and salix are arranged "product" glyph, YingShui third line according to the planting distance below 1 m planting clay and red dates are arranged "product" glyph,In the fourth row, Caragana korshinskii and Sashalix were planted with a spacing of 1m, and in the fifth row, sea-buckthorn and Caragana korshinskii were planted with a spacing of 1m.And then you do it every 5 rows.

The spacing between the rows of trees was 2m, 2m, 1m and 1m respectively, and the grass seeds such as melilotus melilotus, dagawang and lara valla were scattered among the rows in order to first reduce the flow velocity of the channel and then sedimentation.

It has a strong climbing and covering ability. It can be planted on both sides of the gully in front of the rigid dam with high water content at the bottom of the gully according to the plant spacing of 1m, which can not only prevent the lateral erosion of the gully, but also prevent the erosion and scouring of the silting ground on the slope.Can also be along the bottom of the ditch slide slope body planting a row of sand, poplar, elm and other prevention of side erosion.

4.3 Consolidated plant biomass treatment technology

In order to prevent the surface erosion of the modified material of arsenic sandstone, the consolidated material HKYGJ-1 was mixed with water at a volume of 1:50 to spray the consolidated material.At the same time, 1:100 consolidation mixture should be sprayed on the surface of the plant flexible dam.

5 Conclusion and discussion

Based on the techniques and practices of ecological comprehensive management in the Sand-overlying Arsenic Sandstone area, the ecological comprehensive management models in the Sand-overlying Arsenic Sandstone area are summarized as follows.Slope steep slope grouting consolidation, gentle slope vines grass seal slope corrosion resistance;Gully bottom modified material Gufang dam + shrub-grass flexible dam;Modified silting dam of gully mouth arsenic sandstone can increase the efficiency of silting by retaining sand and reducing flood.

Erosion intensity and governance in view of the arsenic sandstone areas, complexity and difficulty of the arsenic sandstone areas ecological comprehensive treatment need to be further in-depth study, at the same time also need to state and local government investment in ecological management, corresponding grazing prohibition of immigrants and a series of laws and regulations to ensure that effect to the preservation and development of the ecological management.

References

Xi Jinping.Speech at the symposium on ecological protection and high quality development in the Yellow River Basin [J]. Qiushi, 2019,20:1-2

Yao Wenyi.Development opportunities and scientific orientation of soil and water conservation in the Yellow River Basin in the new era [J]. Yellow River,2019,41(12):1-7

WANG Yuechang, WU Yonghong, LI Min, et al.Research on Soil and Water Loss and Its Control Approach in Soft Sandstone Area [M]. Zhengzhou: Yellow River Water Conservancy Press,2007

YAO Wenyi, XIAO Peiqing, WANG Chengchang, et al.Research progress of erosion control technology in arsenic sandstone area [J]. Advances in Science and Technology of Water Resources and Hydropower,2019,39(05):1-9

XU Jianhua, GAO Yajun, LI Xiaoyu, et al.The influence of sediment management on water resources in the Yellow River [J].Journal of Soil and Water Conservation, 2007,21 (6):47-50

Qian Zhengying.Development of sea-buckthorn resources as a breakthrough to accelerate the control of the Loess Plateau: A report on the development of sea-buckthorn resources in Shanxi Province [J].Science and Technology Information of Soil and Water Conservation,1986(02):1-4

Li Xu, Li Haikuan.Construction of a new model of World Bank loan project management: Overview of World Bank project construction of soil and water conservation in the Loess Plateau of Inner Mongolia [J].China Water Resources, 2005(12):4-6

Han Xibin.Soil and Water Conservation in China,1989(05):57-58.

Hippophae rhamnoides of the Ministry of Water Resources for the treatment of arsenic sandstone investigation group.Development of ecological agriculture for soil and water conservation of seabuckthorn: A report on treatment of arsenic sandstone [J].Seabuckthorn, 1999 (02) : 1-5

Bi Cifen, Qiao Wanglin.Experimental study on sea-buckthorn flexible dam in gully treatment in arsenic sandstone area [J]. Sea Buckthorn,2000(01):28-34

Bi Cifen, Tai Yuanlin.Study on Comprehensive Technology of Soil and Water Conservation to Preent Soil Erosion in Soft Sandstone Area [J]. Journal of Sediment Research, 2003, (3) : 63-65

TANG Zhenghong, CAI Qiangguo, LI Zhongwu, et al.Study on interaction of wind erosion, water erosion and gravity erosion in arsenic sandstone area of Inner Mongolia [J]. Journal of Soil and Water Conservation, 2001(02):25-29

WANG Yuechang, WU Yonghong, KOU Quan, et al.Science of Soil and Water Conservation in China, 2007,5 (1):14-18. (in Chinese with English abstract

Yao Wenyi, Shi Mingli, Wu Zhiren, Wang Lijiu, Yang Caiqian.Comprehensive treatment technology and demonstration effect of binary stereoscopic allocation in arsenic sandstone area [J]. Yellow River,2016,38(6):1-7;Yao Wenyi, Shi Mingli,WU Zhiren. Management Technology and Demonstration Effect on Two-Dimensional Configuration in Pisha Sandstone Area[J]. YELLOW RIVER, 2016, 38 (6) : 1-7

Yao Wenyi, Liu Hui, Liang Zhishui.A new approach to ecological restoration in arsenic sandstone area: an environmental protection technology against erosion and promoting growth [J].Bulletin of Soil and Water Conservation,2018,38(04):118-124.

Ecological rehabilitation practice of production and construction projects in ecologically fragile area
——Taking the construction of Qinghai Tibet ± 400kV DC Power Transmission Interconnection Project as an example

Jing Huang *[1,2], Xinxin Hou[1,2]
1 Key Laboratory of Soil and Water Conservation on the Loess Plateau of Ministry of Water Resources, China
2 Yellow River Institute of Hydraulic Research, China
*Corresponding Author, e-mail:huangjing_hky@163.com

Abstract

Ecological rehabilitation in ecologically fragile areas is an important part of the 14th Five-Year Plan. The Qinghai-Tibet Plateau is characterized by high and cold terrain, harsh climate, harsh natural conditions, sparse vegetation, and obvious soil erosion phenomena such as wind erosion, water erosion, frost erosion, etc. Moreover, the construction of production and construction projects is likely to destroy the surrounding ecological environment. It is too difficult to ecological rehabilitation in ecologically fragile areas. Taking Qinghai ~ Tibet ±400kV DC power transmission interconnection project as an example, this paper investigated and analyzed the impact of temporary protection of soil and water conservation, plant measures and engineering measures on ecological rehabilitation in the process of project construction, and discussed the ecological rehabilitation schemes of production and construction projects in the ecologically fragile area.

Keywords: Ecologically fragile area, ecological rehabilitation, production and construction projects

China's overall ecological environment is fragile. It is one of the countries with the largest ecological fragile areas and the most fragile ecological types in the world, and it is mainly located in areas where the economy is relatively backward and the people live in poverty[1-2]. The construction of production and construction projects has promoted the economic development of impoverished areas, but the construction process will inevitably destroy the original ecological environment, especially in areas with fragile ecological environment. Once destroyed, restoration is extremely difficult.

The Qinghai-Tibet ±400kV DC interconnection project is located on the Qinghai-Tibet Plateau. The project has a long line with an average altitude of 4,500 meters along the line. The terrain is complex, the landform is rich, and the climate environment is diverse. ecosystem. There are also Sanjiangyuan Nature Reserve, Kekexili Nature Reserve, Selincuo Black-necked Crane National Nature Reserve, Black-necked Crane Nature Reserve in the middle reaches of the Yarlung Zangbo River, and Rezhen National Forest Park near the project. It is a region in my country and South Asia. Important "sources of rivers" and "ecological sources". The natural ecological environment along the line is primitive, unique, sensitive, and fragile. Once vegetation is destroyed, recovery is very slow, and it accelerates the melting of frozen soil, causing soil desertification and soil erosion. The types of soil erosion are complex, and water erosion, wind erosion, and freeze-thaw erosion occur alternately. The task of soil and water conservation and ecological restoration is arduous.

1 Project Overview

Qinghai-Tibet ±400kV DC interconnection project passes through Golmud City, Haixi Mongolian-Tibetan Autonomous Prefecture of Qinghai Province, Qumalai and Zhiduo County of Yushu Tibetan Autonomous Prefecture, Anduo County, Naqu County, and Damxung County, Lhasa City, Naqu Prefecture, Tibet Autonomous Region Zhou County is known as the "Electric Power Road". The construction content includes the new Golmud converter station, the Lhasa converter station, the newly built Golmud converter station ~ Lhasa converter station 1 ±400kV DC line, with a total length of 1031.1km (including 608.8km in Qinghai section and 422.3km in Tibet section), transmission tower 2361 base. The grade is I grade. The project occupies a total area of 209.86hm^2, with a total excavation and filling volume of 1,791,500 m^3. The project started construction in July 2010 and was put into trial operation in December 2011.

2 Analysis on Characteristics of Soil and Water Loss in Engineering Construction

(1) Long construction line, wide range, scattered disturbance points

The construction of the project involves four cities and eight counties in Qinghai and Tibet. The length of the line is 1031.1km. The distance between adjacent tower foundations of the DC line is mostly between 300-600m, and the excavation points are scattered.

(2) Wind erosion, water erosion, freeze-thaw erosion, etc. staggered in the project area

The project area has high and cold terrain, harsh weather, harsh natural conditions, sparse vegetation. According to the report of the water and soil conservation plan of this project, the type and intensity of soil erosion along the line are shown in Table 1. It can be seen that there are obvious wind erosion, water erosion, and other soil erosion phenomena along the project area (Ebol 2008).

Table 1 Table of Soil Erosion Type and Intensity Along the Line

Administrative District		Landforms and vegetation types	Path length (km)	Type of erosion		
				Water erosion	Wind erosion	Freeze-thaw erosion
Within Qinghai	Golmud Township, Golmud City	Bare Gobi area	91.24	/	Serious	/
		Desert area	65.8	/	Serious	/
		Alpine Steppe	18.86	/	Moderate	Moderate
	Qumalai County	Alpine Steppe	95.02	/	Moderate	Mild
		Alpine Meadow	52.98	/	Moderate	Mild
	Zhiduo County	Alpine Steppe	25	/	Mild	Micro
		Alpine Meadow	56.6	/	Mild	Micro
	Tanggula Mountain Township, Golmud City	Alpine Steppe	108.8	/	Moderate	Mild
		Alpine Meadow	98.7	/	Mild	Moderate
Within the Tibet Autonomous Region	Linzhou County	Desert area	34.88	/	Serious	/
		Alpine Steppe	29.14	Mild	Moderate	Moderate
		Alpine Meadow	22.96	Mild	Moderate	Mild
		Mountain shrubland	11.48	Mild	Mild	Mild
		Farming area	5.74	Mild	Mild	Mild
	Damxung County	Desert area	5.74	Mild	Mild	/
		Alpine Meadow	30.05	Mild	/	Mild
		Mountain shrubland	2.21	Mild	/	Mild
	Nagqu County	Desert area	21.17	/	Serious	/
		Alpine Meadow	82.93	Mild	Moderate	Serious
		Mountain shrubland	15	Mild	Mild	Moderate
		Farming area	6.6	Mild	Mild	Mild
	Anduo County	Desert area	63.55	/	Serious	/
		Alpine Meadow	62.66	/	Serious	Serious
		Mountain shrubland	30.89	/	Moderate	Moderate

As the project construction area is disturbed, the native vegetation is destroyed and the surface coverage is reduced, increasing the intensity of water and wind erosion. Excavation, soil borrowing, and human activities in the ice-rich, ice-saturated, and soil-bearing ice-bearing areas along the project will expose the frozen soil to the air, which may cause thermal thawing slump and thawing mud flow after thawing. The formation of comprehensive erosion by freezing and thawing, wind and water power has exacerbated the erosion of surface water and soil.

3 Ecological restoration measures system for soil and water conservation

3.1 Temporary protection

(1)The resident and material station of the project department and the construction team should try to use the existing buildings during the construction of the railways and highways along the line. The temporary construction site should be selected in a place with sparse vegetation, and the floor area should be minimized. A large number of fences are set up around construction roads, material stacking and other areas to limit the scope of construction work. Construction machinery and vehicles are not allowed to drive outside the construction roads. Construction workers are strictly prohibited from stepping on the grass at will to reduce vegetation damage. Simple fences of 42,000m are set at the construction site along the project.

(2) In order to protect high native vegetation, palm mats are used to isolate grassland from construction machinery and appliances, and color striped cloths are used to isolate grass from construction materials. The numbers of palm mats are 8.38hm^2, and the numbers of color striped cloths are 120.47hm^2. Lay straw mats, palm mats or sleepers in the tower material stacking area, assembly area, lifting area and tool stacking area to prevent damage to the surface vegetation during the tower material placement, assembly, and lifting operations. The base areas of the DC line towers are equipped with palm mats isolation protection of 26,438m^2, and color striped cloths isolation protection of 404,672m^2. The material stations are set up with 80,000m^2 of colored striped cloths. Optimize the position of the stretch fields, and lay straw mats or palm mats and sleepers in the placement area of machines and materials to protect the surface vegetation. The stretch fields are set up with 32,463m^2 of palm mats for isolation and protection.

(3) Centrally stack the excavated temporary earthwork and construction sand and gravel, and take measures to block soil by woven bags and cover with colored striped cloth or geotextile to prevent soil erosion. Completed the project to block 133,300m^3 of soil in woven bags.

(4) The Golmud Converter Station and Lhasa Converter Station have adopted 0.3hm^2 for temporary brick paving and 1.50hm^2 gravel paving respectively due to missing the suitable greening seasons.

The temporary protective measures implemented in the project area are shown in Table 2.

Table 2 Temporary protective measures implemented

Temporary protection measures	Golmud Converter Station	Lhasa Converter Station	DC link (Qinghai section)	DC link (Tibet section)	Total
Straw bag soil block (m^3)	800	475	72400	59660	133335
Color striped cloth covering （hm^2）	2.00	1.25	3.21	1.03	7.49
Temporary drainage ditch (m)	153	198			351
Sand basin (base)	1	1			2
Topsoil stripping (hm^2)		14.76	12.85	4.12	31.73
Turf stripping maintenance (hm^2)			4.19	4.64	8.83
Shrub transplant and maintenance (Strain)				1148	1148
Temporary capping of tiles or gravel（hm^2）	0.30	1.50			1.80
Brown mat grass isolation protection (hm^2)		0.46	4.58	3.80	8.85
Color striped cloth isolation protection (hm^2)		1.84	69.30	51.16	122.31

3.2 Plant restoration

Due to long-term low temperature and short growing season, once the vegetation in the alpine region is destroyed, recovery is very slow. In order to restore vegetation along the Qinghai-Tibet DC project, a total of 68 vegetation restoration demonstration sites have been set up along the project, which mainly completed plant species screening, seed germination, soil improvement technology, and turf transplantation technology demonstration research.

(1)Planting grass in alpine grassland and alpine meadow areas

The selection and matching schemes of grass species in the alpine steppe area were Elymus nutans, Poa pratensis and Leymus chinensis, or Elymus nutans, Poa pratensis and Puccinellia tenuiflora. The species matching scheme in the alpine meadow area is Elymus nutans, Kentucky bluegrass and Puccinellia tenuiflora, or Elymus nutans, Kentucky bluegrass and Leymus chinensis. Before planting, first prepare the ground to form a loose soil layer of 10-25 cm, and fertilize with diammonium phosphate (the dosage is 75-150kg per hectare). The seeding adopts drill or broadcast method, and the seeding amount is 50-100kg/hm^2. Spray water after sowing and cover with non-woven fabric to maintain soil moisture and temperature, promote seed germination, growth and safe overwintering.

(2)Sod stripping maintenance and backing in alpine swamp meadow area

In the alpine swamp meadow area, the vegetation restoration is carried out by stripping the native turf for maintenance and back-paving. That is, the original turf in the construction area is stripped first, moved to another place and maintained. After the tower foundation is backfilled, the turf is moved back to the original place and watered and managed in time. According to the survival of the turf after transplantation, replanting is carried out in a short period of time, and the grass species is Elymus dahuricus and Trithorn grass.

(3)Shrub transplantation and replanting in mountainous shrubland

The vegetation restoration of the mountainous shrub areas in Tibet adopts shrub transplantation, replanting and grass planting. Before the construction of the project, the whole shrub should be dug out and maintained independently. After the tower base is backfilled, the shrubs shall be replanted and transplanted, and watering and management shall be carried out in time. Replant shrubs and sow grass seeds on the bare land after shrubs are replanted. The shrubs are seabuckthorn or snow-covered rhododendron, and the grass species is Kobresia or Tibet Carex.

A total of 55.31hm^2 of artificial grass planting and maintenance has been completed along the project. The vegetation coverage can reach more than 60%, and the hay output increase by 20-30kg/hm^2. The area of turf stripping, maintenance and back-paved area is 17.66hm^2, and 1149 shrubs are transplanted, maintained and planted.

See Table 3 for the plant restoration measures implemented in the project area.

Table 3 Plant restoration measures implemented

Vegetation restoration measures	Lhasa Converter Station	DC line (Qinghai section)	DC line (Tibet section)
Plant grass（hm^2）	0.43	63.59	38.88
Vegetation Tending Management（hm^2）	0.43	63.59	38.88
Sod back paving (hm^2)		4.19	4.64
Shrub transplanting back planting (Strain)			1148
Replanting shrubs (Strain)			1148

3.3 Engineering protection

(1)Topsoil stripping

The topsoil stripping measures have been implemented in the construction sections of the project except for the Gobi Desert. The topsoil is the soil that has undergone a maturation process, and the water and fertilizer conditions in it are more suitable for plant growth. The stripped topsoil and the deep raw soil are piled separately, and temporary blocking and covering measures are taken. Topsoil is used for soil replacement and land preparation for later plant restoration to ensure the survival rate of plants.

The topsoil stripping area of the tower base area of the Qinghai-Tibet DC line project is 169661m^2. The topsoil stripping area of the Lhasa converter station, grounding electrode and grounding electrode line is 150900m^2.

(2)Wind-proof and sand-fixing project

Part of the tower base of the project located in the Gobi desert adopts gravel capping and sand-fixing measures with stone grids to prevent soil erosion.

(3)Slope protection engineering

For the tower foundation, the side slope is steep and easy to collapse, or the slope between the high and low legs cannot be placed due to the small foundation, the section with poor soil stability, and the tower foundation with more waste slag, and the mortar is laid. Stone retaining wall. A total of 3535m mortar-masonry retaining walls are laid in the tower base area of the DC line. In order to prevent the erosion of the base surface by the upstream catchment of the hillside and ensure the safety of the tower foundation, 3920m drainage ditch in the tower foundation area was laid.

(4) Land consolidation

After the construction is completed, the construction site should be cleaned and renovated in time.

The engineering protection measures implemented in the project area are shown in Table 4.

4 Evaluation of Soil and Water Conservation Effect

Through on-site investigation and consulting related materials of water and soil conservation monitoring and water and soil conservation supervision of the project, after more than two years of ecological restoration in the project area, the water and soil conservation prevention and control area is 182.39hm^2, and the restored vegetation area is 111.76hm^2. According to calculations, the disturbed land remediation rate in the project area is 98.2%, the total water and soil erosion control rate is 98.0%, the average soil loss control ratio is 0.82, the slag blocking rate is about 94.5%, the forest and grass vegetation restoration rate reaches 97.6%, and the forest and grass cover The rate reached 53.3%.

Table 4 Engineering protection measures implemented

Engineering protection measures	**Golmud Converter Station**	**Lhasa Converter Station**	**DC line (Qinghai section)**	**DC line (Tibet section)**
retaining wall（m）	940	/	1152	2383
Slope protection（m）	500	1525	/	/
Land consolidation（hm^2）	11.54	10.23	108.65	53.54
gutter（m）	1335	1540	470	3450
Crushed stone capping（hm^2）	0.42		3.73	

5 Conclusions

Under the combined effects of natural restoration and manual intervention, the Qinghai-Tibet ±400kV DC interconnection project area has obvious ecological restoration effects, with high plant survival and preservation rates, good growth, and obvious improvement of the surrounding ecological environment. The ecological restoration experience of this project can be used as a reference for similar projects in similar areas.

References

Ministry of Environmental Protection of the People's Republic of China. National Plan for the Protection of Fragile Ecological Areas [EB/OL]. (2008-10-09)

Yuelong Zhao, Yanhua Liu. Distribution of Fragile Ecological Environment in China and Its Relationship with Poverty[J]. Human geography, 1996, 11(2) : 1-7

Spatio-temporal variability and driving factors of urban household water consumption in arid and semi-arid areas of Northwest China

Lin Li[1], Xiaohu Dang[1, *], Liangxin Fan[2], Peng Li[3], Xiaoshu Cao[4], Jiaxin Tian[1]
1 College of Geology and Environment, Xi'an University of Science and Technology, Xi'an 710054, China
2 Research Centre of Arable Land Protection and Urban-Rural High-Quality Development of Yellow River Basin, Henan Polytechnic University, Jiaozuo, Henan, 454003, China
3 State Key Laboratory of Eco-hydraulics in Northwest Arid Region of China, Xi'an University of Technology, Xi'an 710048, China
4 Academy of Natural Resources and Territorial Space, Shaanxi Normal University, Xi'an 710062, China
*Corresponding Author, e-mail: 1004149699@qq.com

Abstract

Given increasing water demand, cities in arid and semi-arid areas are facing increasingly severe water scarcity in China. Understanding the spatio-temporal pattern of water consumption and its socio-economic drivers is of importance to alleviate urban water crisis in arid and semi-arid areas. In this study, influencing factors of water consumption in 42 cities in Northwest China were identified by cluster tree analysis and multivariate regression. Results showed that from 2000 to 2017, the per capita domestic water consumption in Northwest China decreased by 9.5%. 17 cities out of 42 cities were low water consumption cities (<100L/d), 12 cities of which had changed significantly (8 increased cities and 4 decreased cities); 14 cities were high-consumption cities (>190L/d), 6 cities of which had changed significantly (5 increased cities and 1 decreased city); and remains were medium water-consumed. Daily water consumption per capita was found positively correlated with household income, water supply capacity, and built-up area, and negatively correlated urban population, people engaging in social services, and water saving and reuse efficiency. Among the high water-consumed cities, the expansion of built-up area is the main factor that causes high water consumption; and in low and medium water-consumed cities, residential water use is restricted by water supply and household income. The findings of this work suggested that improving water-use efficiency in high-water-consumed cities and increasing water supply capacity in low-water-consumed cities should be considered in urban water management strategies in Northwest China.

Keywords: Urban water use, Socio-economic driver; Cluster analysis, Water resource management, Arid and semi-arid area

1 Introduction

Water scarcity is becoming a threat to sustainable development, due to the growing water demand by increasing population and urbanization (Bao and Chen, 2015; Zhu and Chang, 2020). In 2000, approximately 36.2% of the China's population lived in urban areas, compared with 58.5% of urban population in 2017 (NBSC, 2016). It is estimated that by 2050, 76% of China's population (additional 279 million urban dwellers) will live in urban settlements (UN, 2015). As the urban population grows, the total amount of water demand is rising as well. Compared with rapid expansion in water demand of urban population, however, the city's water supply capacity slowly rises and is limited, and many cities in China are facing increasing water shortages. Since 2010, more than 400 cities out of the 668 cities in China experienced more or less water scarcity, and at least 100 cities were in severe conditions (Feng et al., 2017). Especially in Northwest China, where low precipitation (230 mm per year), high evaporation (1200 mm per year) (Chen et al., 2012), have limited ground water endowment (137.95 billion m^3), has suffered from severe water shortages (NBSC, 2018).

In order to meet the water demand, groundwater of many cities has been excessively overexploited, the depletion of groundwater resources, for example, has caused groundwater level in Xi'an's being dropped by 20.6 m, and the surface subsidence occurred at a maximum annual subsidence rate of approximately 146 mm/a (Li et al., 2018). The growing water demand has also led to increasing use of surface water. In the Weihe River Basin of China, the surface runoff decreased by 26.6% (about 1.92 billion m^3) due to human activities during the period 1971-2006 (Chang et al., 2015). Under this severe water resource situation, solving the water shortage caused by the growth of water demand of urban residents remains a challenge in Northwest China.

Researches on the factors affecting residential water consumption under the growing water-use pressure have received widespread attention. Several studies focus on the relationship between climate features (e.g. precipitation, temperature) and urban socioeconomic characteristic (e.g. population, water supply, and water price) and water consumption, as well as the influence of household structure (e.g. household size, income, education) and water use behavior (e.g. water-saving awareness, water appliance) on residential water consumption. On the one hand, some studies found that climate affected the water consumption behavior of urban residents and explored how climate factors, especially temperature and precipitation, influenced the domestic water consumption of urban residents.

Gato et al. (2007) found that residential water consumption increased in hot summers and decreased during cool winters in East Doncaster, Australia, and attributed to the increases in the frequency and water consumption of bathing, laundry, and courtyard water due to high temperatures in summer. Balling and Gober (2007) observed that when annual precipitation decreases by 10%, the per capita water consumption of residents would increase by 3.9% in Phoenix, Arizona, the US. On the other hand, the social and economic factors related to household water consumption determine the behavior and mode of residents' water use. Fan et al. (2017) analyzed the urban water consumption and the influencing factors of 286 cities in China and found that high-water-consumption cities were influenced by socioeconomic level, while low-water-consumption cities were restricted by water supply capacity and economic status. In cities of Germany, water consumption per capita was highly affected by price, with prices rising by 11% and consumption falling by 30% (Schleich and Hillenbrand, 2009).

Many household-based studies have focused on the changes in water consumption, which usually consider the effects of income, family structure, and educational background, and found that households with higher incomes consume more water than do households with lower incomes, and that this difference is obvious in external water use (Musolesi and Nosvelli, 2007; Chang et al., 2017). Higher income families usually have more water facilities. The proportion of households with swimming pools, for example, is identified as the main reason for the increase in total water consumption from 223 m^3 to 2823 m^3, in Phoenix, USA (Wentz and Gober, 2007). In terms of household size, there is a scale effect between household size and water consumption, that is, larger households use more water in total, but less water per capita (Bennett et al., 2013; Yu et al., 2018). In addition, the water consumption of residents has negatively correlated with their education level (Nieswiadomy, 1992; Yu et al., 2018). Households with higher education levels have positive influence on environmental awareness in general, and they are more likely to adopt modern and energy-saving behaviors (Wang et al., 2020). Water-saving equipment and water-saving subsidies are considered effective solutions to water management. Bartos and Chester (2014) investigated the benefits of water-saving measures in Arizona, USA, and showed that implementing appropriate water-saving measures can reduce regional water consumption by 1.9-15%, and the savings exceed the costs of these measures. Therefore, it is necessary to determine the domestic water use profiles and their related factors in order to establish effective water management, avoid water shortages, and meet basic water requirements.

Current relevant research on Northwest China have much more focused on the main factor of urban residential water consumption and the residential water use in single-city. For example, Yang et al. (2019) found that economic growth was the main factor for the increase of domestic water consumption in Xi'an, while Yan (2013) showed the importance of temperature in Urumqi. Comprehensive understanding of the water use, and precise identifying the key factors affecting residents' water-using behavior, however, remains insufficient. Water consumption is affected by a group of factors, and the influence varies greatly among cities. Deep understanding of urban water use in Northwest China and its influencing factors would help the implementation of urban water resources management strategies. The driving factors and spatio-temporal variations of urban residents' water consumption behavior in arid and semi-arid areas of Northwest China are largely unknown in the context of climate change and increasing urban population. The present work, therefore, explores the relationship between the urban family socio-economic factors and their water use characteristics, to understand the pattern of urban domestic water use in Northwest China. The main objectives of present research are (1) identify the influencing factors of urban domestic water use and understand the relationship between socio-economic level and urban water use, and (2) to recover the spatio-temporal pattern of urban domestic water consumption, aiming to give a new insight for the regulation of residents' water use behavior and alleviating water crisis in arid and semi-arid areas.

2 Materials and methods

2.1 Study area

The region of Northwest China (73.7°–126.0°E, 31.7°–53.4°N) is the inner part of the Eurasian continent, and includes Xinjiang, Ningxia, Shaanxi, Gansu, Qinghai, and Inner Mongolia, with an area of 3.69×10^6 km^2, or 38.4% of the nation's land. This area features a typical temperate continental climate with the driest and most vulnerable ecological environment in the country.

By the end of 2017, Northwest China has a population of 127.15 million, with an urbanization rate of 54.13 %. The total water consumption is 104.13 billion m^3, accounting for 17.23% of the national total. Among various water consumption, approximately 88.0% of the total water consumption is used for agriculture, and only 5.4% for domestic use. Urban domestic water consumption was 2.11 billion m^3, with an average annual growth rate of 3.27% from 2000 to 2017 (NBSC, 2000-2017).

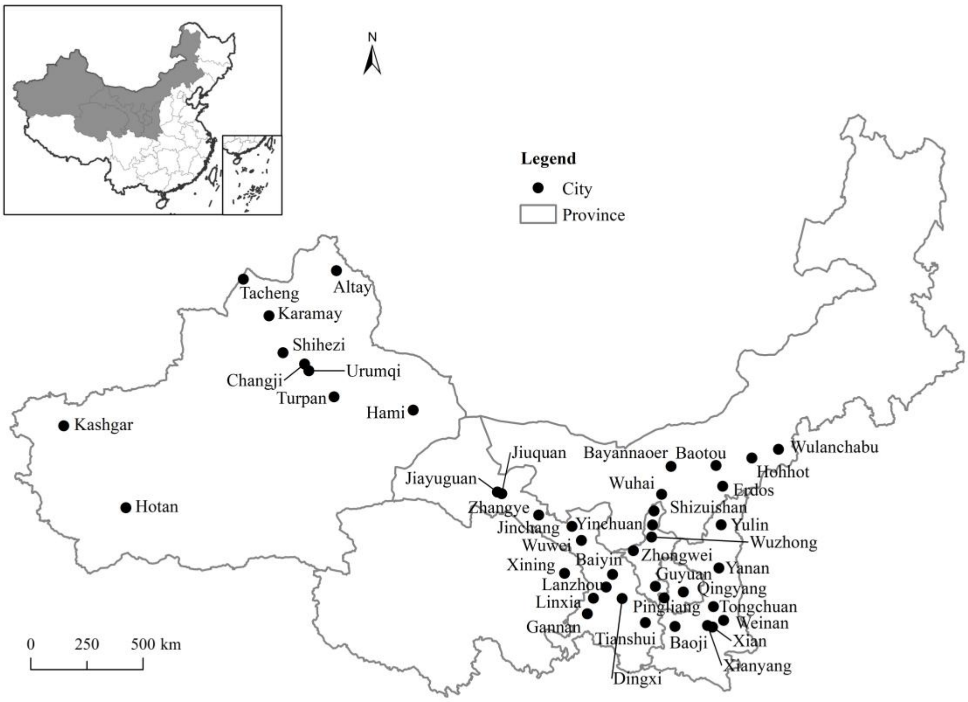

Figure 1 Location of research area

Due to the limitation of data sources, 42 major cities in Northwest China were selected as research objects, as shown in Fig. 1 The 42 cities are major consumers of water resources in Northwest China, accounting for more than 80% of the urban water use in this region (DUSS-NBSC, 2000-2017). The 42 cities selected are reliable and representative.

2.2 Variables of residents' water consumption

2.2.1 Population and socio-demographic characteristics

The accelerated urbanization of the population is considered to be the major cause for tense between demand and supply of water, as growing populations bring more water demands and intensifies competition for scarce water resources in arid and semi-arid areas (Martin-Carrasco et al., 2013; Jenerette and Larsen, 2006). Population density and growth rates are popular means of describing human demands on water resources (March and Saurí, 2010). Cities with high population density reduce the domestic water demands of residents through smaller residential areas and outdoor space (Jenerette and Larsen, 2006; Ruben and Alfredo, 2018), and these cities are more efficient in water use (Hummel and Lux, 2007).

Besides urban population, other socio-demographic determinants examined in literature are education background and water-saving awareness. Environmental attitudes increase the possibility that people undertake environmental actions. An analysis of OECD surveys in 10 countries indicated that education improves the environmental behavior of residents in their daily water use (OECD, 2011). Gilg and Barr (2006) confirmed the positive impact of education on environmental awareness, especially in water conservation. People who actively participate in environmental protection or public welfare services are expected to be more willing to take positive environmental protection actions including saving water (Millock and Nauges, 2010), because they usually have a higher awareness of environmental protection (Lubell, 2002).

2.2.2 Economic factors

Water consumption of urban residents can be seen as the demand for water commodities, and such a demand is affected by the incomes of residents (Dalhuisen et al., 2002; Lu et al., 2018). The influence of income on household water use is difficult to assess. Higher incomes enable people to buy more goods and services that have an impact on water resources, regardless of their effects on water stress. For example, water-saving appliances are relatively expensive, but operating costs are reduced in the process of using them (OECD, 2011). Conversely, the cost of taking the time to reuse water is likely to be much greater for high-income households, while low-income households are more likely to develop water-conservation habits (Martinez-Espineira and Garcia-Valiñas, 2013; Oliver, 1999).

Many studies focusing on water use consider the impact of water price on people's water demand. For a long time, the Chinese government has set low water prices to ensure the normal use of water by the people. Water charges account for a very small proportion of most households' incomes, so there are few strong economic incentives to encourage people to save water (Worthington and Hoffman, 2008; Arbués and Villanúa, 2006).

2.2.3 Urban water supply and water saving

The growth of urban total water demand promotes the construction of new water supply facilities in cities. However, urban water supply capacity is a direct restriction on water use, and the limitation of water resources greatly limits the water supply capacity of cities, especially in areas where water resources are scarce (Li et al., 2020). Water supply capacity also varies greatly across cities. Wealthier cities have sufficient resources to build more complete water supply systems, some of which even get enough water from distant places (McDonald et al., 2014).

The progress of water-saving technology has an inhibitory effect on water consumption. Government investment in water-saving education and activities can reduce the daily water demand of urban residents (Nieswiadomy, 1992; Barnett et al., 2020). Some studies have noticed the impact of water-saving equipment on residents' water use behavior, and these equipment can raise water-saving awareness and promote water-saving practices (Martinez-Espineira and Garcia-Valiñas, 2013; OECD, 2011).

2.2.4 Domestic water appliances

Household water use mainly includes toilet flushing, showering, laundry, and cooking, which correspond to the use of toilets, shower water heaters, washing machines, and faucets, respectively. Household water consumption is directly related to the quantity and frequency of use of various water appliances (Inman and Jeffrey, 2006; Gato-Trinidad et al., 2011). The use of washing machines and bathrooms has a significant impact on domestic water consumption (Lyons et al., 2010; Roshan and Kumar, 2020), with more than half of the various terminal water used for showers and laundry (Willis et al., 2013).

As mentioned above, we chose 14 factors (see Table 1 for details) that affect the daily water consumption of residents as explanatory variables. These factors can be divided into the following four categories: population and social characteristics (POP_1–POP_5), economic factors (ECO_1–ECO_3), urban water supply and water saving (UW_1–UW_4), and water appliances (WA_1, WA_2).

Table 1 Description of the data

Variables	Explanation	Data source
Water consumption		
LPCD	Liters of water consumption per capita per day (L)	DUSS–NBSC, 2000–2017
Population factors		
POP_1	Urban population number (per 10^4 persons)	DUSS–NBSC, 2000–2017 NBSC, 2000–2017
POP_2	Urban population growth rate (% y^{-1})	
POP_3	Urban population density (km^{-2})	
POP_4	Number of people engaged in social services (per 10^4 persons)	
POP_5	Number of college students (per 10^4 persons)	
Economic factors		
ECO_1	Retail sales of consumer goods per capita (10^4 yuan)	NBSC, 2000–2017
ECO_2	GDP per capita (10^4 yuan)	
ECO_3	Urban per capita household income (10^4 yuan)	
Urban water supply and water saving		
UW_1	Built-up area (km^2)	DUSS–NBSC, 2000–2017 MOHURD, 2002–2017
UW_2	Water supply capacity per capita per day (10^4 m^3)	
UW_3	Ratio of water saving and reuse (%)	
UW_4	Investment in water conservation per capita (10^4 yuan)	
Water appliances factors		
WA_1	Number of washing machines (per 100 households)	DUSS–NBSC, 2000–2017
WA_2	Number of water heaters for showering (per 100 households)	

2.3 Data analysis

To analyze the variation of residents' water consumption characteristics, we adopted the hierarchical clustering method by the SPSS version 23.0 platform to conduct cluster of 42 cities in Northwest China. In hierarchical clustering, the square Euclidean distance was used to represent the similarity between groups, and the method of intergroup connection was used to obtain the similarity gradually. Cities with similar characteristics of residential daily water consumption(liters of domestic water consumption per capita per day, LPCD) were used to group into the same cluster, the water consumption of urban residents in each group showed high internal similarity and prominent differences.

Based on the results of cluster analysis, we used the Pearson correlation analysis to analyze the relationship between residential water consumption and influencing factors. The linear correlation was determined using the Pearson coefficient (r) and its corresponding p-value. The two sets of variables were considered correlated in absolute value if the p-value was less than 0.05.

The multiple linear regression analysis was performed for each cluster in order to connect the water consumption with significantly correlated variables in a linear model. Economic variables tend to exhibit common changes over time. Multicollinearity exists between them and can result to parameter estimation errors. Thus, some explanatory variables needed to be eliminated. We further estimated the related variables using stepwise regression to find the variable with the best fitness, and then selected explanatory variables again on this basis to eliminate the unimportant variables and eliminate multicollinearity. The Durbin–Watson (DW) statistic was calculated to test for residual independence convergence at a level of 2.000 in all clusters, representing the random distribution of residuals.

3. Results

3.1 Profiles of urban domestic water consumption in Northwest China

Urban domestic water consumption in Northwest China showed overall growth from 1.22 billion m^3 in 2000 to 2.11 billion m^3 in 2017, an increase of 72.9% (Fig. 2a). Urban residents' LPCD dropped from 168.63 L in 2000 to 152.58 L in 2017, a decrease of about 9.5% (Fig. 2b). Here, 12 cities showed increased water consumption (9 cities, $p< 0.01$; 3 cities, $p< 0.05$). Among them, Ordos had the largest increase in per capita water consumption, which grew by 173.3% during the study period. Approximately10 cities showed decreased water consumption (6 cities, $p< 0.01$; 4 cities, $p< 0.05$), of which Baotou exhibited the largest decrease at 44.7%.

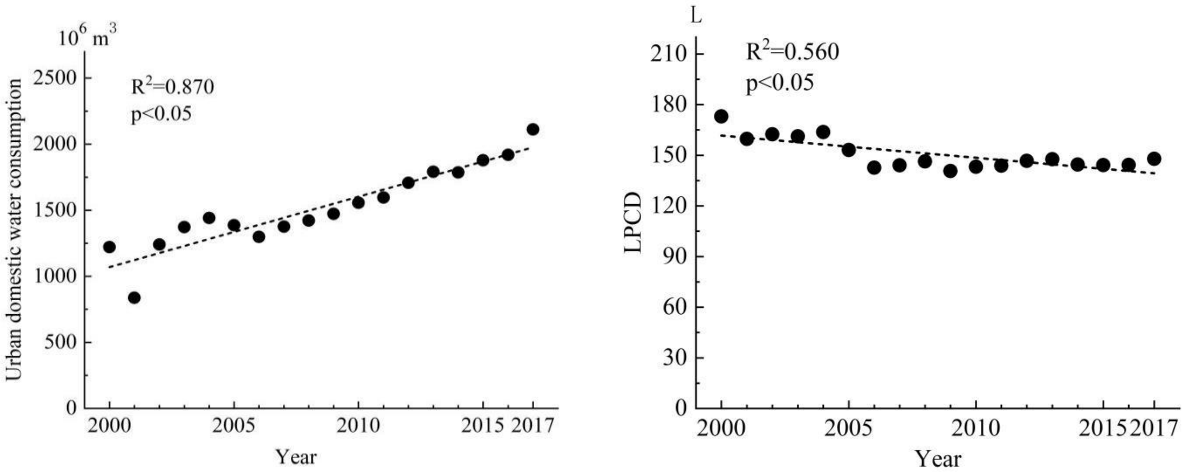

(a) Urban domestic water consumption changes (b) LPCD

Figure 2 Profiles of urban domestic water consumption in Northwest China

3.2 Characteristics of domestic water consumption in Northwest China

The systematic cluster analysis method was used to perform clustering on each city (Fig. 4). According to the residential daily water consumption per capita, 42 cities were divided into three groups with similar characteristics, including low-water-consumption cities (LC), medium-water-consumption cities (MC), and high-water-consumption cities (HC). Seventeen cities (40.5%) with average water consumption of 86.83 ± 28.84 L/d were marked LC, eleven cities (26.2%) with consumption of 148.33 ± 30.40 L/d were marked MC, and fourteen cities (33.3%) using 198.62 ± 38.47 L/d were marked HC.

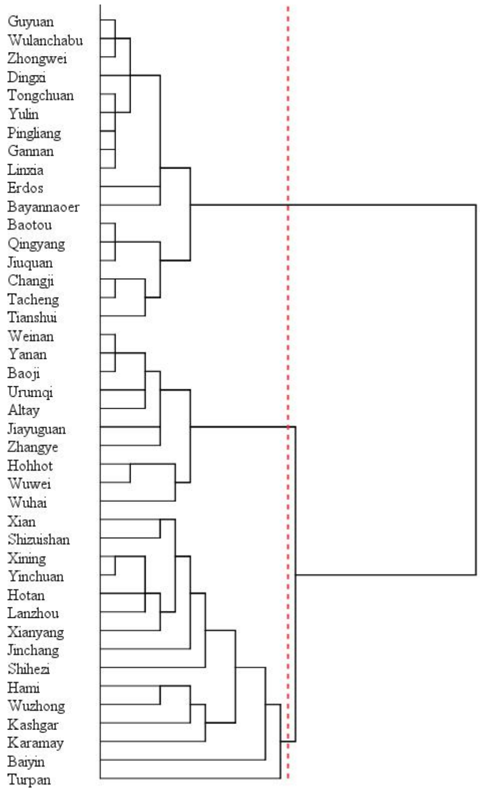

Figure 4 The hierarchical dendrograms of water consumption in 42 cities of northwest China. The dashed red line corresponds to a cut point of the classification.

The three types of cities showed significant spatial variation. LC were mainly located in the southeast of the study area, including southern Gansu, southern Ningxia and southeastern Inner Mongolia (Fig. 5a), and HC were located in the middle and northwest of the study area, consisting of Northern Xinjiang, Eastern Qinghai, central Shaanxi, central Gansu and northern Ningxia (Fig. 5c). The distribution of MCs was scattered (Figure 5b). The results of the cluster analysis of the LPCD in LC, MC, and HC areas were showed in Fig. 6. During the 2000 to 2017, the residential water consumption intensity in southeast cities (LC) was lower than that of other cities in the study area, while the water intensity in central and northwestern cities (HC) was higher. In LC, 12 cities showed significant changes, of which 8 increased (2 cities, $p<0.05$; 6 cities, $p<0.01$) and 4 decreased (1 cities, $p<0.05$; 3 cities, $p<0.01$); among HC, 6 cities experienced significant changes, of which 5 (3 cities, $p<0.05$; 2 cities, $p<0.01$) increased and 1 decreased ($p<0.01$).

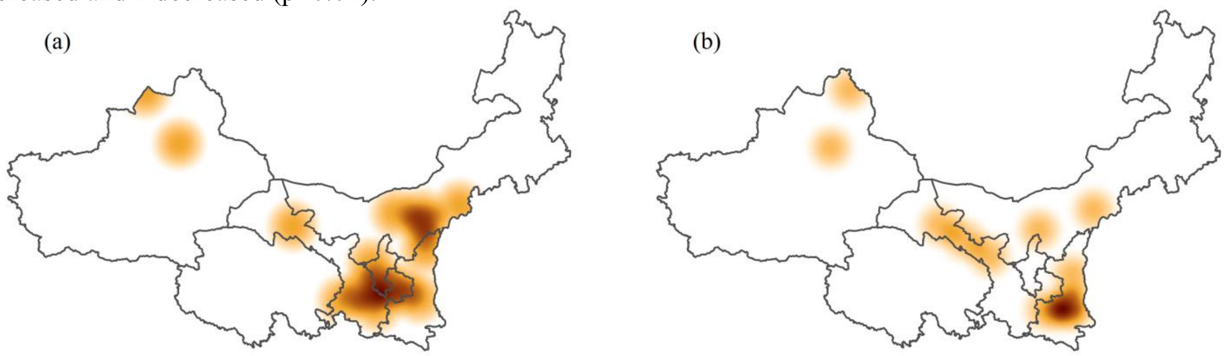

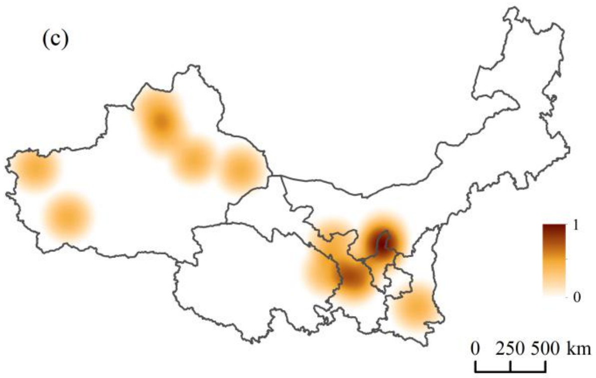

Figure 5 The spatial distribution of low-, medium- and high consumption cities. Note: (a), (b) and (c) represent cities with domestic water consumption in low-, medium- and high consumption respectively. 0 and 1 represent the city does not fall into or fall into this category respectively.

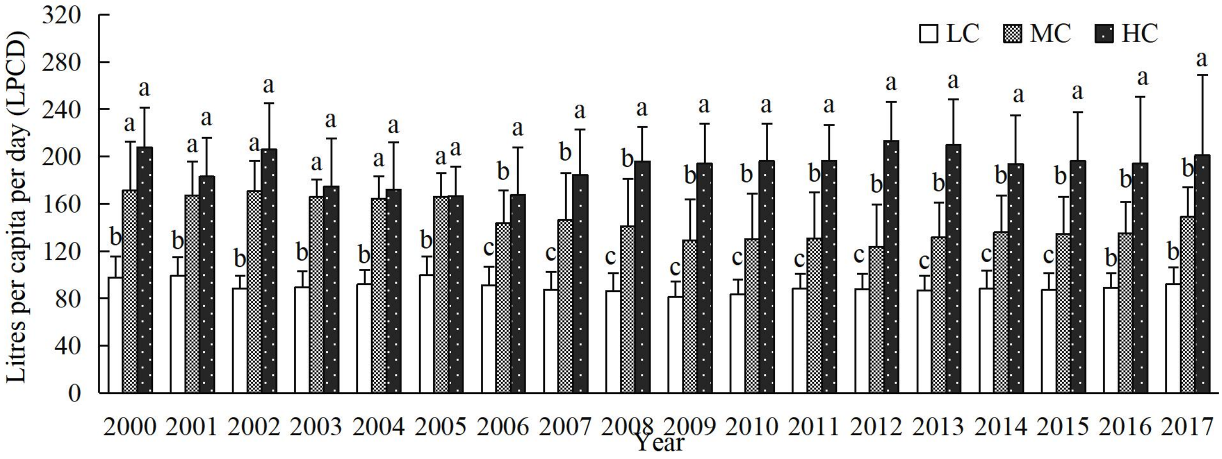

Figure 6 The LPCD in the 3 groups of the cities. Note: Mean scores that share a different letter in each column are differ significantly ($p < 0.05$) on LSD post hoc test. Bar represent the mean ± SD.

3.3 Factors influencing domestic water consumption in Northwest China

Based on the cluster analysis results of LPCD, the impacting indicators selected above were correlated with the LPCD of urban dwellers, and the results were presented in Table 2.

As indicated in Table 2, there were strong correlations among the four types of indicators affecting urban domestic water consumption in Northwest China. In MC and HC, water saving and reuse rate exerted a strong negative correlation with urban LPCD ($p < 0.01$), but the relationship was not significant in LC ($p > 0.05$). The water-saving investment and water appliances in the three types of cities had different correlations with LPCD. The correlation analysis results demonstrated that the degree of influence of each factor was different among the different groups, and that there were complex driving mechanisms in the change in urban LPCD in Northwest China.

The results of the multiple regression analysis are shown in Table 3. The DW statistics for the three groups tended to 2.000, indicating the residuals satisfied the independence test. The values of F and p-value (<0.05) allowed rejection of the null hypothesis. The three sets of regression models explained most of the variance of urban per capita water use change ($R^2 > 0.85$). The driving factors explained the changes in residential water consumption were the urban population, people engaging in social services, household disposable income, built-up area, water supply capacity, and water reuse rate (Table 3). Among the four types of indicators, there was no data to support the impact of two factors in the water appliance indicators on urban water consumption. According to the standardized coefficients, we can further judge that population, household income, and built-up area had the strongest relationship with the change of LPCD in the three groups of cities.

Table 2 Correlation coefficient between LPCD and influencing factors in three types of cities

Factors	LC	MC	HC
Urban population number	0.621**	–0.885**	0.822**
	(0.006)	(0.000)	(0.000)
Urban population growth rate	–0.092	–0.023	0.005
	(0.718)	(0.928)	(0.985)
Urban population density	0.643**	–0.873**	0.843**
	(0.004)	(0.000)	(0.000)
Number of people engaged in social services	0.537*	–0.693**	0.818**
	(0.021)	(0.001)	(0.000)
Number of college students	0.565*	–0.855**	0.766**
	(0.015)	(0.000)	(0.000)
Retail sales of consumer goods per capita	0.708**	–0.699**	0.862**
	(0.001)	(0.001)	(0.000)
GDP per capita	0.635**	–0.788**	0.850**
	(0.005)	(0.000)	(0.000)
Urban per capita household income	0.720**	–0.706**	0.860**
	(0.001)	(0.001)	(0.000)
Built-up area	0.616**	–0.773**	0.862**
	(0.006)	(0.000)	(0.000)
Water supply capacity per capita per day	0.582*	–0.878**	0.841**
	(0.011)	(0.000)	(0.000)
Water saving and reuse rate	–0.290	0.823**	–0.819**
	(0.243)	(0.000)	(0.000)
Investment in water conservation per capita	–0.296	0.418	–0.848**
	(0.232)	(0.085)	(0.000)
Washing machines per household	0.627**	–0.528*	0.046
	(0.005)	(0.024)	(0.855)
Water heaters for showering per household	0.449	–0.849**	0.817**
	(0.062)	(0.000)	(0.000)

Note: LC, low-water-consumption cities; MC, medium-water-consumption cities; HC, high-water-consumption cities, P–values are in parentheses, *Significant at P = 0.05 (bilateral); ** Significant at P =0.01 (bilateral)

Table 3 Results of regression for each influencing factor on LPCD

Group	LC			MC		HC		
Variable	POP_1	UC_2	ECO_3	POP_1	ECO_3	POP_4	UC_3	UC_1
Coefficients	-1.058	0.391	1.763	-1.72	0.926	-0.938	-0.760	1.167
t-Statistic	-2.812	4.199	4.656	-7.415	3.994	-2.425	-3.868	3.776
Sig.	0.015	0.001	0.000	0.000	0.002	0.032	0.002	0.003
R^2	0.901			0.891		0.895		
D.W	1.921			1.845		1.819		
Std. Error	2.112			6.758		6.672		
F	39.219			51.691		34.222		
p-value	0.000			0.000		0.000		

Note: LC, low-water-consumption cities; MC, medium-water-consumption cities; HC, high-water-consumption cities; POP_1, urban population; POP_4, number of people engaged in social services; ECO_3, per capita household income; UC_1, built-up area; UC_2, water supply capacity; UC3, water saving and reuse rate.

We determined the relative importance of all explanatory variables in various cities. In the low-water-consumption cites, the joint effects of urban population, household income, and water supply capacity explained 90.1% the change of LPCD, and household income explained the highest proportion of that variation. Daily urban water supply capacity had a positive influence on the change of LPCD, whereas population exhibited a negative correlation. For medium-water-consumption cities, household income still had a strong influence on LPCD, but the strongest impact was the urban population, which had a negative influence. High-consumption cities were most strongly influenced by people engaging in social services, built-up area, and water reuse rates. Built-up area displayed a strong positive influence on LPCD, while people engaging in social services and water supply capacity exhibited negative impacts on residential water use.

4 Discussion

Domestic water is an important part of urban water use. This study found that urban population, economy and water-saving measures were the main reasons for the decline of per capita water consumption. The per capita water consumption of 42 cities in Northwest China was divided into three groups with low-, medium- and high-water consumption. About two-fifths of the cities in the study area were low-water consumption cities with an average water consumption of 86.83 L/d, which did not meet the minimum domestic water demand per capita(100 L/d) determined by the World Health Organization based on family daily living needs and level of health concern (WHO, 2011). In contrast, LPCD in cities with high water consumption (198.62 L/d) was slightly higher than the national average of 190 L/d in the same period (NBSC, 2018). Given the water scarce in arid and semi-arid Northwest China, such a level of water consumption is noteworthy. The three types of urban LPCD have great spatial heterogeneity. High-water-consumption cities were concentrated in the middle and northwest of the study area, while low-water-consumption cities were located in the southeast of the study area, which was contrary to the regional water resources endowment. Such a mismatch between domestic water consumption and water resources endowment are largely determined by the urban population, people engaging in social services, household income, built-up area, water supply capacity, and water reuse rate in the middle and northwest of the arid and semi-arid Northwest China. Depending on the urban water consumption patterns, the effects of these factors on water use are varies, and the need for a conservation policy will be different.

Among high-water-consumption cities, built-up areas exhibited strong positive effect on urban residents' water use. The built-up area indirectly reflects the residential area of residents, which has been proven to strongly influence residents' consumption needs (Barnett et al., 2020). With the continuous expansion of urban areas and the improvement of residents' living conditions, urban domestic water consumption increased (Wu et al., 2015; Li et al., 2020). In this study, the area of high-water-consumption cities expanded by more than doubled, which was the main driving force for residents' highwater demand. The water supply infrastructure in these cities should be continuously improved with the expansion of the city scale to meet the living needs of urban residents. In addition, urban development cannot be contained. Therefore, policymakers must fully consider the increase in residential water demand caused by urban expansion, especially in the arid Northwest China, urban expansion must be sustained sufficient water resources.

Public participation in environmental protection activities is an effective way to encourage residents to save water. People engaged in social services should pay more attention to and participate in environmental protection activities, and they are more likely to develop the habit of saving water and more inclined to adopt water-saving technologies (Martinez-Espineira and Garcia-Valiñas, 2013; Barnett et al., 2020). This group of people usually have higher socioeconomic status, which is related to higher education and economy (Dean et al., 2016). In this study, people engaged in social services had a greater impact on cities with high water consumption than in cities with low- and medium-water consumption. They are powerful promoters of the water-saving campaign and work to persuade others to become involved (Haida et al., 2019). Meanwhile, urban residents with high water consumption have greater flexibility in water use, and it is easier to reduce their high water demand through water-saving education. Policies should focus on strengthening water-saving services and education in cities with high water consumption.

In low- and mid-water-consumption cities, urban population had a significant negative impact on water use. With the increase of urban population, the per capita water consumption in Northwest China has decreased. This is consistent with research of Tello and Ostos (2012), who studied the relationship between population and per capita water use in Barcelona. They showed argued that rapid increase in urban population has aggravated the conflict between urban water use and water resources. In addition, cities with higher population density use less water in the same population scale. Higher urban density reduces residential space, and residential households have fewer high water-consuming equipment (bathrooms, swimming pools) (March and Saurí, 2010).

Water supply factor is a strong restriction on water consumption of urban residents. Urban water supply capacity is directly related to people's living needs and adequate urban water supply and reflects the level of urban development. Since year of 1990, Chinese government has made great efforts in improving the water supply capacity. The comprehensive production capacity of urban water supply increased from 218 × 10^6 m^3 in 2000 to 305 × 10^6 m^3 in 2017 (MOHURD, 2002-2017). Studies found that the duration of urban water supply showed a significant impact on per capita water consumption (Martinez-Espineira and Garcia-Valiñas, 2013; Barnett et al., 2020). Seasonal drought and high water demand make water supply system adopt intermittent water supply mode in some areas, especially in some urban fringe areas in Northwest China (Fan et al., 2014). With guaranteed 24-hour water supply, LPCD in these areas will increase by 14.55% to 27.50% (Andey and Kelkar, 2009). This study found that the impact of urban water supply capacity on cities with low water consumption is greater than that of cities with high water consumption, because growth for water supply capacity of low water consumption cities cannot meet the growth of residents' water demand. More policy should be obtained in low consumption cities to improve their urban water supply capacity.

The impact of per capita income on low-water-consumption cities is greater than that on medium- and high-water-consumption cities. Previous studies have provided strong empirical evidence that income drives residential water demand (Arbués and Villanúa, 2006; Domene and Saurí, 2006), and our result are consistent with these findings. Household with a high per capita income often have a high standard of living, showing more water appliances and facilities, which increases household water use (Romano et al., 2014; Wang et al., 2021). Our study also found that lower water consumption cities are more responsive to income increases than higher water consumption cities. Household income should be increased in low water consumption cities to improve residential daily living level and health needs. Meanwhile, water-saving measures, such as strengthening residents' awareness of water-saving and adding water-saving equipment to improve water efficiency, should be fully considered to cope with the increase in domestic water consumption with economic development and the popularity of water-based appliances.

Going further, China has increased its investment in water conservation since 1998 when it introduced policies at the national level to encourage people to save water, including providing education and campaigns on water conservation (enterprises, schools, and communities) (Wang et al., 2007). Household water consumption can be effectively reduced through changing personal water use habits and increasing water-saving appliances use. However, the high price of water-efficient appliances discourages their widespread use. For example, the cost of residents buying water-saving washing machines will be more than twice that of ordinary washing machines (Fan et al., 2017). In Northwest China, residents with low income cannot afford expensive water-saving appliances, which makes the effect of initial water-saving investment in many cities not obvious.

The uneven temporal and spatial distribution of water use in Northwest China and the changes in its main driving factors indicate that strategies should be tailored to specific situations. In low-water-consumption cities, the first priority is to ensure the local water supply. Restricted by geographical conditions, urban development in Northwest China requires an adequate supply of water. For these cities facing water shortage challenges, long-distance water transfer through canals or pipelines is a feasible solution with financial and policy support (McDonald et al., 2014). In high-consumption cities, effective measures continue to increase subsidies for residents to use water-saving appliances. Promoting efficient water-saving appliances is a low-cost solution to achieve sustainable water resources management (Willis et al., 2013). Replacing household water appliances across the board with high-efficiency water-saving appliances can reduce indoor water consumption by more than one third (Inman and Jeffrey, 2006). This measure can spirit the development of water-saving technologies, promote the upgrading of related product technologies, and reduce manufacturing costs. At the same time, water-saving campaigns should be strengthened and residents should be encouraged to join public environmental protection organizations, so as to appeal for environmental responsibility and improve public awareness of water-saving. Encouraging urban residents to live in high-density communities and compact cities is one of the powerful measures for sustainable water resource use in the face of the future urban population growth.

5 Conclusion

In this study, we explored the spatial-temporal dynamics of urban residents' water consumption and determined the driving factors of their water use in Northwest China. From 2000 to 2017, the total amount of urban domestic water consumption in Northwest China increased by 72.9%, but the per capita water use decreases at 9.5%, and about 25% of the cities decreased significantly. Urban population, people engaging in social services, household income, built-up area, water supply capacity, and water reuse rate are recognized as the key driving factors of urban household water consumption. These factors vary greatly across three types of cities. These differences can inform water resources protection policies.

Low-water-consumption cities need to obtain policy support and financial subsidies to ensure safe water for residents, while high-water-consumption cities should promote conservation and enhancing efficiency to alleviate the growth of water consumption. Economic incentives, subsidies and raising environmental awareness together can positively contribute to household water use behavior. Therefore, in this regard, people should be encouraged to participate in public social water-saving services, environmental education, and to advocate environmental responsibility, so as to promote the water-saving society in more cities, in particular in arid and semi-arid Northwest China.

Acknowledgement

This work was supported by the National Natural Science Foundation of China (Grant No. 41671514) and the Consulting Research Project of the Chinese Academy of Engineering (Grant No. 2020-xz-15).

References

Andey, S. P., & Kelkar, P. S. (2009). Influence of Intermittent and Continuous Modes of Water Supply on Domestic Water Consumption. *Water Resources Management, 23*(12), 2555-2566.

Arbués, F., & Villanúa, I. (2006). Potential for Pricing Policies in Water Resource Management: Estimation of Urban Residential Water Demand in Zaragoza, Spain. *Urban Studies, 43*, 2421-2442.

Balling, R., & Gober, P. (2007). Climate Variability and Residential Water Use in the City of Phoenix, Arizona. *Journal of Applied Meteorology and Climatology, 46*, 1130-1137.

Bao, C., & Chen, X. (2015). The driving effects of urbanization on economic growth and water use change in China: A provincial-level analysis in 1997–2011. *Journal of Geographical Sciences, 25*(5), 530-544.

Barnett, M. J., Jackson-Smith, D., Endter-Wada, J., & Haeffner, M. (2020). A multilevel analysis of the drivers of household water consumption in a semi-arid region. *Science of The Total Environment, 712*, 136489.

Bartos, M., & Chester, M. (2014). The Conservation Nexus: Valuing Interdependent Water and Energy Savings in Arizona. *Environmental science & technology, 48*.

Bennett, C., Stewart, R. A., & Beal, C. D. (2013). ANN-based residential water end-use demand forecasting model. *Expert Systems with Applications, 40*(4), 1014-1023.

Chang, H., Bonnette, M. R., Stoker, P., Crow-Miller, B., & Wentz, E. (2017). Determinants of single family residential water use across scales in four western US cities. *Science of The Total Environment, 596-597*, 451-464.

Chang, J., Wang, Y., Istanbulluoglu, E., Bai, T., Huang, Q., Yang, D., & Huang, S. (2015). Impact of climate change and human activities on runoff in the Weihe River Basin, China. *Quaternary International, 380-381*, 169-179.

Chen, Y., Yang, q., & Luo, y. (2012). Ponder on the issues of water resources in the arid region of northwest China. *Arid Land Geography, 35*(1), 1-9.

Dalhuisen, J., Florax, R., de Groot, H. L. F., & Nijkamp, P. (2002). Price and Income Elasticities of Residential Water Demand: A Meta-Analysis. *Land Economics, 79*.

Dean, A. J., Lindsay, J., Fielding, K. S., & Smith, L. D. G. (2016). Fostering water sensitive citizenship – Community profiles of engagement in water-related issues. *Environmental Science & Policy, 55*, 238-247.

Domene, E., & Saurí, D. (2006). Urbanisation and Water Consumption: Influencing Factors in the Metropolitan Region of Barcelona. *Urban Studies, 43*, 1605-1623.

DUSS-NBSC. (2000-2017). *China City Statistical Yearbook (2000-2017)*. Beijing,China: China Statistics Press.

Fan, L., Gai, L., Tong, Y., & Li, R. (2017). Urban water consumption and its influencing factors in China: Evidence from 286 cities. *Journal of Cleaner Production, 166*, 124-133.

Fan, L., Liu, G., Wang, F., Ritsema, C. J., & Geissen, V. (2014). Domestic Water Consumption under Intermittent and Continuous Modes of Water Supply. *Water Resources Management, 28*(3), 853-865.

Feng, L., Chen, B., Hayat, T., Alsaedi, A., & Ahmad, B. (2017). The driving force of water footprint under the rapid urbanization process: a structural decomposition analysis for Zhangye city in China. *Journal of Cleaner Production, 163*, S322-S328.

Gato-Trinidad, S., Jayasuriya, N., & Roberts, P. (2011). Understanding urban residential end uses of water. *Water science and technology, 64*, 36-42.

Gato, S., Jayasuriya, N., & Roberts, P. (2007). Forecasting Residential Water Demand: Case Study. *Journal of Water Resources Planning and Management, 133*(4), 309-319.

Gilg, A., & Barr, S. (2006). Behavioural attitudes towards water saving? Evidence from a study of environmental actions. *Ecological Economics, 57*(3), 400-414.

Haida, C., Chapagain, A. K., Rauch, W., Riede, M., & Schneider, K. (2019). From water footprint to climate change adaptation: Capacity development with teenagers to save water. *Land Use Policy, 80*, 456-463.

Hummel, D., & Lux, A. (2007). Population decline and infrastructure: The case of the German water supply system. *Vienna Yearbook of Population Research, 2007*.

Inman, D., & Jeffrey, P. (2006). A review of residential water conservation tool performance and influences on implementation effectiveness. *Urban Water Journal, 3*, 127-143.

Jenerette, D. G., & Larsen, L. (2006). A global perspective on changing sustainable urban water supplies. *Global and Planetary Change, 50*(3), 202-211.

Li, H., Ma, C., Zhou, W., Yan, Q., & Song, Y. (2018). Characterizing the Evolution of Groundwater Flow Field and Its Driving Forces in Xi'an, China. *Journal of Hydrologic Engineering, 23*.

Li, W., Hai, X., Han, L., Mao, J., & Tian, M. (2020). Does urbanization intensify regional water scarcity? Evidence and implications from a megaregion of China. *Journal of Cleaner Production, 244*, 118592.

Lu, S., Gao, X., Li, W., Jiang, S., & Huang, L. (2018). A study on the spatial and temporal variability of the urban residential water consumption and its influencing factors in the major cities of China. *Habitat International, 78*.

Lubell, M. (2002). Environmental Activism as Collective Action. *Environment and Behavior, 34*(4), 431-454.

Lyons, S., O'Doherty, J., & Tol, R. S. J. (2010). Determinants of Water Connection Type and Ownership of Water-Using Appliances in Ireland. *Water Resources Management, 24*(12), 2853-2867.

March, H., & Saurí, D. (2010). The Suburbanization of Water Scarcity in the Barcelona Metropolitan Region: Sociodemographic and Urban Changes Influencing Domestic Water Consumption. *The Professional Geographer, 62*, 32-45.

Martin-Carrasco, F., Garrote, L., Iglesias, A., & Mediero, L. (2013). Diagnosing Causes of Water Scarcity in Complex Water Resources Systems and Identifying Risk Management Actions. *Water Resources Management, 27*(6), 1693-1705.

Martinez-Espineira, R., & Garcia-Valiñas, M. (2013). Adopting versus adapting: Adoption of water-saving technology versus water conservation habits in Spain. *International Journal of Water Resources Development, 29*.

McDonald, R. I., Weber, K., Padowski, J., Flörke, M., Schneider, C., Green, P. A., . . . Montgomery, M. (2014). Water on an urban planet: Urbanization and the reach of urban water infrastructure. *Global Environmental Change, 27*, 96-105.

Millock, K., & Nauges, C. (2010). Household Adoption of Water-Efficient Equipment: The Role of Socio-Economic Factors, Environmental Attitudes and Policy. *Katrin Millock, 46*.

MOHURD. (2002-2017). *China Urban Construction Statistical Yearbook* Beijing, China: China Statistics Press.

Musolesi, A., & Nosvelli, M. (2007). Dynamics of residential water consumption in a panel of Italian municipalities. *Applied Economics Letters, 14*(6), 441-444.

NBSC. (2000-2017). *China Statistical Yearbook (2000-2017)*.

Nieswiadomy, M. L. (1992). Estimating urban residential water demand: Effects of price structure, conservation, and education. *Water Resources Research, 28*(3), 609-615.

OECD. (2011). Greening Household Behaviour: the Role of Public Policy. In. OECD Publishing.

Oliver, M. (1999). Attitudes and Inaction A Case Study of the Manifest Demographics of Urban Water Conservation. *Environment and Behavior, 31*, 372-394.

Romano, G., Salvati, N., & Guerrini, A. (2014). Estimating the Determinants of Residential Water Demand in Italy. *Water, 6*(10), 2929-2945.

Roshan, A., & Kumar, M. (2020). Water end-use estimation can support the urban water crisis management: A critical review. *Journal of Environmental Management, 268*, 110663.

Ruben, V. N., & Alfredo, P. M. A. (2018). Factors Affecting Domestic Water Consumption on the Spanish Mediterranean Coastline. *The Professional Geographer*.

Schleich, J., & Hillenbrand, T. (2009). Determinants of residential water demand in Germany. *Ecological Economics, 68*(6), 1756-1769.

Tello, E., & Ostos, J. R. (2012). Water consumption in Barcelona and its regional environmental imprint: a long-term history (1717–2008). *Regional Environmental Change, 12*(2), 347-361.

UN. (2015). World Urbanization Prospects: The 2014 Revision. Retrieved from

Wang, L., Zuo, Q. T., & Gao, J. X. (2007). Study on the Connotation and Evaluation Index System of Resource-efficient Society. *Progress In Geography, 26*.

Wang, Q., Lin, J., Zhou, K., Fan, J., & Kwan, M.-P. (2020). Does urbanization lead to less residential energy consumption? A comparative study of 136 countries. *Energy, 202*, 117765.

Wentz, E. A., & Gober, P. (2007). Determinants of Small-Area Water Consumption for the City of Phoenix, Arizona. *Water Resources Management, 21*(11), 1849-1863.

WHO. (2011). Guidelines for drinking-water quality (4th ed.).

Willis, R. M., Stewart, R. A., Giurco, D. P., Talebpour, M. R., & Mousavinejad, A. (2013). End use water consumption in households: impact of socio-demographic factors and efficient devices. *Journal of Cleaner Production, 60*, 107-115.

Worthington, A., & Hoffman, M. (2008). An Empirical Survey of Residential Water Demand Modeling. *Journal of Economic Surveys, 22*, 842-871.

Wu, F., Zhan, J., & Güneralp, İ. (2015). Present and future of urban water balance in the rapidly urbanizing Heihe River Basin, Northwest China. *Ecological Modelling, 318*, 254-264.

Yan, D. (2013). Urban domestic water consumption response to climate change in Urumqi city. *International Conference on Earth Science and Environmental Protection, 189*, 897-904.

Yang, Z., Song, J., Cheng, D., Xia, J., Li, Q., & Ahamad, M. I. (2019). Comprehensive evaluation and scenario simulation for the water resources carrying capacity in Xi'an city, China. *Journal of Environmental Management, 230*, 221-233.

Zhu, D., & Chang, Y.-J. (2020). Urban water security assessment in the context of sustainability and urban water management transitions: An empirical study in Shanghai. Journal of Cleaner Production, 275, 122968.

Spatial temporal evolution pattern and driving mechanism of soil erosion in the Yellow River Basin based on LMDI model and Geodetector

Hongwei Wu[1], Cuixia Wei[1], Bing Guo[1,*]
1 School of Civil Architectural Engineering, Shandong University of Technology, Zibo 255000, Shandong, China
*Corresponding Author, e-mail:guobingjl@163.com

Abstract

Under the influences of global change, soil erosion in the Yellow River Basin has changed dramatically. However, it is a significant challenge to analyze the impacts of climate vegetation and land use as well as their combined effects on soil erosion. Based on RUSLE model and multi-source data, this study aims to retrieve the annual soil erosion modulus of the Yellow River Basin, and use LMDI model and geographic detector to identify the dominant driving factors of soil erosion evolution in different historical periods and regions at pixel scale and landscape scale. Results showed that: (1) In recent 40 years, the average soil erosion was 2,255 $t \cdot km^{-1} \cdot a^{-1}$, which belonged to mild erosion. The serious (intensive, extreme intensive and severe) erosion areas are mainly distributed in the Loess Plateau, while the slight and mild erosion areas are mainly distributed in the Hetao Plain, Ordos Plateau, Ningxia plain and Guanzhong Plain; (2) In the last 40 years, the soil erosion modulus of Loess Plateau has a decreasing trend, mainly manifested in the area of stability and reduction area in the study area is 78.63%. During the study period, the gravity center of soil erosion moved from southwest to northeast, which indicated that the increment and increasing rate of soil erosion in the northeast of the Yellow River Basin were higher than that of the southwestern areas; (3) During the past 40 years, the increased soil erosion due to the R factor (ISER) was the most widely distributed, accounting for 79.21% of the area where soil erosion increased, while the decreased soil erosion due to the C factor and the R factor was the most widely distributed, accounting for 49.15% of the area where soil erosion decreased; (4) Before 2000, precipitation, vegetation and soil types were the dominant factors affecting the evolution pattern of soil erosion in the study area. With the increase of human activities, such as returning farmland to forest or grassland, the explanatory power of land use change in the evolution pattern of soil erosion was increasing. The research results can provide important decision support for the control of soil erosion in the Yellow River Basin.

Keywords: Soil erosion, Evolution pattern, LMDI model, Geographic detector, Driving mechanism

1 Introduction

Soil erosion refers to the process that the soil and its parent material are moved away from the original position and deposited in a new position through physical and chemical processes under the comprehensive action of many external forces in nature. It is the most common form of damage to land resources (Zhu et al., 2019; Yin et al., 2021). Soil erosion will lead to a decline in soil fertility, an elevated watershed, deposits along the river course, and an increase in the occurrence of natural disasters such as debris flow, drought, flood, and landslide (Guo and Wen, 2020). The Yellow River Basin experiences the most serious soil erosion in China (Guo et al., 2020a; Ma et al., 2020). Dynamic monitoring of soil erosion and identification of dominant influencing factors in different regions are of great significance for the efficient and accurate conservation of soil and water in the Yellow River Basin (Guo et al., 2020b).

The measurement of regional soil erosion is usually completed by field investigation, which is more accurate but wastes time and energy, so it is not suitable to be applied in large-scale regions. The soil erosion model can integrate the complex relationship and interaction of soil erosion susceptibility factors and help to accurately simulate the soil erosion in a specific area. The Revised Universal Soil Loss Equation (RUSLE) model is a modification of the Universal Soil Loss Equation (USLE) model based on a large number of experiments and observation data from the USDA (U.S. Department of Agriculture), and has been widely used to predict the dynamic changes of regional soil erosion (Guo et al., 2020c; Guo et al., 2020d). In recent years, relevant scholars have simulated soil erosion changes on different scales such as basin, city, and countryside. This provides a useful reference for the prevention and control of regional soil erosion and ecological protection planning. Kebede et al. (2021) combined the RUSLE model and the geographical information system (GIS) to estimate the soil loss at the watershed level in the upper Beles of Ethiopia. Wang et al. (2020) explored the spatial distributions of water and wind erosion around Zhangjiakou City and detected the influence of soil erosion on soil quality. It is of great significance to study the spatial and temporal variation and influencing factors of soil erosion in order to determine an accurate evaluation of regional soil erosion. In the field of research regarding the driving mechanisms of soil erosion, Liu et al. (2019) investigated the influencing factors of soil erosion in the Nanbei Panjiang River Basin by using the superposition analysis method and found that the increase of vegetation coverage and the significant decrease of erosive rainfall were the main driving factors of the obvious decrease of soil erosion in the region. Quan et al. (2011) investigated the influencesof land use change on the changes of soil erosion and found that the increase in erosion intensity mainly resulted from cultivation on steep slopes and overgrazing of pastures. Perović et al. (2019) combined the EBU-POM model and InVEST model to predict the impacts of climate change and land use on soil erosion. Jin et al. (2021) utilized the correlation and wavelet coherence analysis to investigate the relationships between erosion and driving factors and then adopted the elasticity coefficient method to quantify the contribution of each factor to soil erosion. Through spatial superposition and correlation analysis, Wang (2018) revealed the impact that the direction and degree of precipitation, as well as returning farmland to forest, has on soil erosion in the Luohe River Basin of Northern Shaanxi. Chen et al. (2021) found that land use (except for bare land) has a limited influence on soil erosion when suitable land cover was established. The above research mostly adopted traditional statistical analysis and spatial analysis methods, which cannot distinguish the influence and interaction of multiple factors. However, the geographical detector can disclose the driving force behind geographical phenomena by revealing the spatial heterogeneity of those phenomena and can effectively identify the high-risk areas of geographical phenomena and the interaction between different factors. At the same time, rainfall erosivity and vegetation coverage are important indicators of soil erosion change, and the interannual change is more intense. It is of great significance to quantitatively distinguish the impact of rainfall erosivity and vegetation coverage on the evolution of soil erosion at the pixel scale. However, there are few studies that carry out the relevant work. The Yellow River Basin covers a vast area, with significant differences in topography and climate. There are also great differences in the dominant factors of soil erosion in different regions . In addition, with the continuous aggravation of global climate change and the increasing intensity of human activities, the main factors affecting soil erosion during different historical periods also differ. What are the dominant factors of the soil erosion evolution pattern in different ecological sub-regions of the Yellow River Basin during different historical periods and how should we adjust for different historical periods? The answers to the above questions need to be investigated. At the same time, due to the lack of land use data, most of the current research is conducted based on sparse time series of soil erosion intensity in order to analyze its spatial-temporal evolution patterns and driving mechanisms, which does not monitor the gradual mutation process of soil erosion .

Based on annual MODIS NDVI, meteorological station data, and land use types, this study utilizes the RUSLE model to calculate and obtain the continuous time series soil erosion dataset from 1981a to 2019a, and then analyzes and discusses the spatial and temporal evolution patterns of soil erosion to determine the dominant driving factors in different historical periods and regions at the pixel scale and landscape scale. Combined with the LMDI model, the study quantitatively distinguishes the impact of rainfall erosivity and vegetation coverage on the evolution process of soil erosion at the pixel scale for different study periods and then applies the geographical detector model to determine the dominant influencing factors of different ecological sub-regions during the period 1981-2019a.

2 Materials and methods

2.1 Study area

The Yellow River Basin, located at 95° E-120° E and 32° N-42° N, includes Qinghai, Sichuan, Gansu, the Ningxia Hui Autonomous Region, the Inner Mongolia Autonomous Region, Shaanxi, Shanxi, Henan and Shandong provinces. This region covers a total area of about 7.95 × 10^5 km^2. The altitude of the study area ranges from 0 to 6255m (Chen et al., 2020). From west to east, the terrain includes the Qinghai Tibet Plateau, Loess Plateau, and North China Plain. In general, the climate is arid in the west and humid in the east. There are significant differences in the seasonal characteristics within the basin, with the temperature gradient in the east-west direction being higher than that in the north-south direction. The annual average precipitation is 438 mm, which is unevenly distributed, with most of the precipitation occurring in summer, and the interannual variation being large (Chen et al., 2019). Generally, the basin has low humidity, high evaporation and a short frost-free period. The main land cover types are grass, crops, broad-leaved forest, and sparse vegetation, which account for 69.18%, 19.79%, 6% and 2.73% of the total study area, respectively. (Fig. 1)

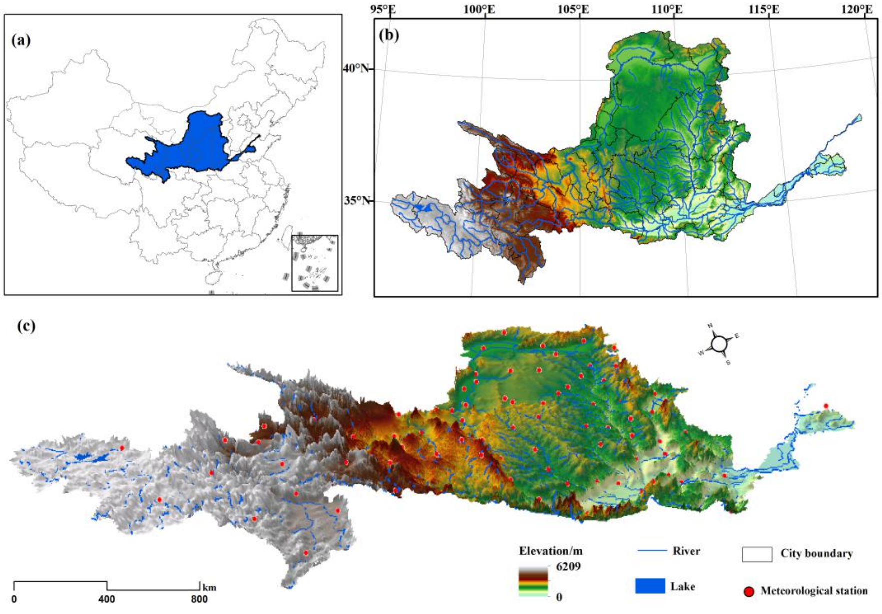

Figure 1 Location of the Yellow River Basin and its terrain

2.2 Data sources and processing

The land use data with a spatial scale of 1:100,000 in 1980a, 1985a, 1990a, 1995a, 2000a, 2005a, 2010a, 2015a, and 2018a were obtained from the Institute of Remote Sensing and Digital Earth of the Chinese Academy of Sciences through a human-computer interaction method based on Landsat TM and ETM + images. The land use datasets of the other years were produced with the satellite image data of corresponding years based on the above datasets, and the overall accuracy reached 80%, which meets the research needs. Meteorological data of 121 meteorological stations from 1981-2019 were obtained from the National Meteorological Center of China (http://data.cma.cn/) and mainly included precipitation (0.1 mm), sunshine hours (0.1 hour), and daily average temperature (0.1 ℃). The meteorological data was then interpolated by using the kriging method with ArcGIS 10.2 to obtain the grid datasets with a spatial resolution of 1000m and the projection type of Krasovsky_1940_Albers. DEM data were derived from the SRTM3 with a 90m resolution. These data can be downloaded from the Geospatial Data Cloud. Soil attribute data were obtained from the ISSAS (Institute of Soil Science, Chinese Academy of Sciences) with a scale of 1:1,000,000. The dataset mainly included soil texture, sand content, silt content, and clay content. The NDVI data used in the study were derived from MOD13A2, with a spatial resolution of 1000m, a temporal resolution of 16 d, and a projection type of SIN (Li et al., 2019). The dataset was preprocessed with MRT tools for data format conversion, projection type conversion, and splicing.

2.3 Methods

2.3.1 RUSLE model

RUSLE is one of the most widely used soil erosion models. The annual soil loss was obtained with RUSLE by multiplying the factors manifested in the following equation:

$$A = C \times R \times LS \times K \times P \tag{1}$$

where A is the amount of soil erosion $(t/(hm^2 \cdot a))$; C refers to the vegetation cover factor (dimensionless); R is the rainfall erosivity factor $(MJ \cdot mm/(hm^2 \cdot h \cdot a))$. LS refers to the topographic factor (dimensionless). K refers to the soil erodibility factor $(t \cdot hm^2 \cdot h/(hm^2 \cdot MJ \cdot mm))$. P refers to the support practice factor (dimensionless), (Fayas et al., 2019).

2.3.2 Contributions of the influencing factors to the variation of soil erosion with the LMDI model

The LMDI model, which can divide the research object into several influencing factors, is a logarithmic decomposition method proposed by Ang (2005). Due to the fact that the method does not produce a decomposable residual and has a wide range of applications, the influence degree and driving force of different influencing factors on the research object can be measured.

The LMDI model has been introduced to quantitatively analyze the contribution values of the C factor and R factor to the evolution process of the soil erosion. The equation is as Eq. (2):

$$\Delta A_{\mathrm{C}} = \sum_{i}^{n} L\left(A_i^{\mathrm{m}}, A_i^{\mathrm{n}}\right) \ln\left(\frac{\mathrm{C}_{k,i}^{\mathrm{m}}}{\mathrm{C}_{k,i}^{\mathrm{n}}}\right) = \sum_{i}^{n} \frac{A_i^{\mathrm{m}} - A_i^{\mathrm{n}}}{\ln A_i^{\mathrm{m}} - \ln A_i^{\mathrm{n}}} \ln\left(\frac{\mathrm{C}_{k,i}^{\mathrm{m}}}{\mathrm{C}_{k,i}^{\mathrm{n}}}\right) \tag{2}$$

where ΔA_{C} refers to the contribution value of the C factor $(t/(hm^2 \cdot a))$; A_i^m refers to the soil erosion modulus in year m $(t/(hm^2 \cdot a))$; A_i^n refers to the soil erosion modulus in year n $(t/(hm^2 \cdot a))$; $\mathrm{C}_{k,i}^m$ refers to the vegetation cover factor in year m; and $\mathrm{C}_{k,i}^n$ refers to the vegetation cover factor in year n. The C factor would aggravate the soil erosion when the ΔA_{C} >0, and the C factor would alleviate soil erosion when the ΔA_{C} <0.

The contribution of the R factor was calculated by the following Eq. (3):

$$\Delta A_{\mathrm{R}} = \sum_{i}^{n} L\left(A_i^{m}, A_i^{m}\right) \ln\left(\frac{\mathrm{R}_{k,i}^{m}}{\mathrm{R}_{k,i}^{n}}\right) = \sum_{i}^{n} \frac{A_i^{m} - A_i^{n}}{\ln A_i^{2015} - \ln A_i^{n}} \ln\left(\frac{\mathrm{R}_{k,i}^{m}}{\mathrm{R}_{k,i}^{n}}\right) \tag{3}$$

where ΔA_{R} refers to the contribution value of the R factor $(t/(hm^2 \cdot a))$; $\mathrm{R}_{k,i}^m$ refers to the rainfall erosivity factor in year m; and $\mathrm{R}_{k,i}^n$ refers to the rainfall erosivity factor in year n. The R factor would aggravate the soil erosion when the ΔA_{R} >0 and the R factor would alleviate the soil erosion when the ΔA_{R} <0.

2.3.3 Geodetector model

The geographical detector model proposes that "factor force" indicators based on spatial differentiation theory can be used to identify the interaction between multiple elements. The geographical detector model includes four forms of detection: differentiation and factor detection, interaction detection, risk area detection, and ecological detection.

Factor detection can be used to detect the spatial differentiation of the dependent variable and the degree of interpretation of the dependent variable by the explanatory factor, which is measured by the q-statistic (Eqs.(4)-(6)).

$$q = 1 - \frac{\sum_{h=1}^{L} N_h \sigma_h^2}{N\sigma^2} = 1 - \frac{W_{\mathrm{SS}}}{T_{\mathrm{SS}}} \tag{4}$$

$$W_{\mathrm{SS}} = \sum_{h=1}^{L} N_h \sigma_h^2 \tag{5}$$

$$T_{\mathrm{ss}} = N\sigma^2 \tag{6}$$

where h refers to the classification of variable Y or X; N_h and N refer to the number of units in layer h and the unit number of the whole region, respectively; σ_h^2 and σ^2 refer to the variance of the Y value of layer h and the variance of the y value of the whole region, respectively; W_{ss} is the sum of variance within the layer; T_{ss} is the total variance of the whole region; $q \in [0,1]$, with the larger the q-statistic, the stronger the explanatory power of X to Y; the smaller the q-statistic, the weaker the explanatory power of X to Y.

Interaction detectors can be used to identify interactions between different factors. By comparing the single factor q value and the double factor q value, this method determines the direction and mode of interaction between the two factors.

2.3.4 Gravity center model

The mitigation distance and direction of the gravity center can reflect the degrees of the change trend of soil erosion. The formula is as follows:

$$\bar{x} = \frac{\sum_{i=1}^{n} Z_i x_i}{\sum_{i=1}^{n} Z_i} \tag{7}$$

$$\bar{y} = \frac{\sum_{i=1}^{n} Z_i y_i}{\sum_{i=1}^{n} Z_i} \tag{8}$$

where Z_i is the attribute value of the i-th plane space unit; (x_i, y_i) is the coordinate value of the i-th plane space unit; the point (x, j) is the spatial mean value of n plane space units.

3 Results

Based on the RUSLE model, this study calculated the annual soil erosion modulus of the Yellow River Basin from 1981 to 2019. Following this, the classification and grading standard of soil erosion was used to divide the soil erosion modulus into seven grades: <1,000 $t \cdot km^{-1} \cdot a^{-1}$ as slight erosion, 1,000-2,500 $t \cdot km^{-1} \cdot a^{-1}$ as mild erosion, 2,500-5,000 $t \cdot km^{-1} \cdot a^{-1}$ as moderate erosion, 5,000-8,000 $t \cdot km^{-1} \cdot a^{-1}$ as intensive erosion, 8,000-15,000 $t \cdot km^{-1} \cdot a^{-1}$ as extreme intensive erosion, and >15,000 $t \cdot km^{-1} \cdot a^{-1}$ as severe erosion.

3.1 Average soil erosion during 1981-2019

As shown in Fig. 2, the average soil erosion modulus in the Yellow River Basin during the period 1981-2019 is 2,255 $t \cdot km^{-1} \cdot a^{-1}$, which is categorized as mild erosion. However, there are significant differences in the area and spatial distribution of soil erosion modulus among different grades. The slight erosion area is mainly distributed in the source area of the Yellow River, Hetao Plain, Ordos Plateau, Ningxia Plain, and Guanzhong Plain, accounting for 53.84% of the total area. Mild and moderate erosion areas are mainly distributed in the mountainous and hilly areas of the upper reaches of the Yellow River, such as the eastern part of Guoluo Tibetan Autonomous Prefecture, the northern part of Aba Tibetan and Qiang Autonomous Prefecture, and Haidong Prefecture, accounting for 16.75% and 14.14% of the total area. The regions of intensive, extreme intensive, and severe erosion are mainly distributed in Linxia Hui Autonomous Prefecture in the upper reaches, Jincheng in the middle and lower reaches, and the Shangluo and Loess Plateau areas, such as Yan'an, Luliang, Xinzhou, Western Linfen, Western Taiyuan, and Qingyang (Fig. 3).

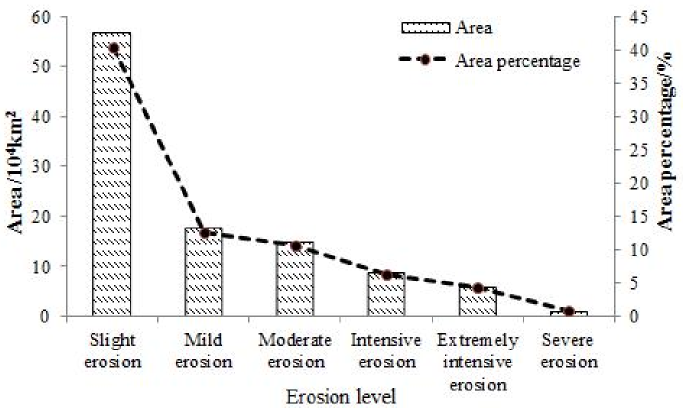

Figure 2 Area and area percentages of different erosion grades

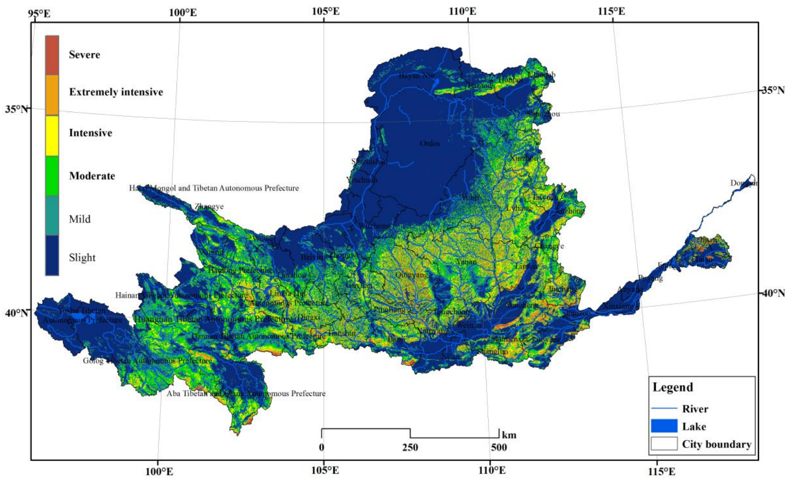

Figure 3 Spatial distribution of different grades of soil erosion in the Yellow River Basin during the period 1981-2019.

3.2 Gravity centers of soil erosion during 1981-2019

In this study, the gravity center model was utilized to calculate the gravity center of soil erosion in the Yellow River Basin at 1-year, 5-year and 10-year scales. In order to better analyze the non-uniformity of growth and increment of soil erosion in the study area during the period 1981-2019, this study took the gravity center coordinates of the average soil erosion modulus during the past 40 years as the origin, and took the mitigation distance from the gravity center of the annual soil erosion modulus to the origin as the polar diameter in order to establish the gravity center polar coordinate system of soil erosion. As shown in Fig. 4, the majority of gravity centers were distributed in the northeast quadrant, accounting for 48.72% of the total; followed by that of the southwest quadrant, accounting for 33.33% of the total; the gravity centers in the northwest quadrant and southeast quadrant were the fewest, both accounting for 10.26% of the total. The results indicated that the growth rate and increment of soil erosion in the southwest of the Yellow River Basin from 1981 to 2000 were higher than those in other regions, while the growth rate and increment of soil erosion in the northeast of the Yellow River Basin from 2001 to 2019 were the largest.

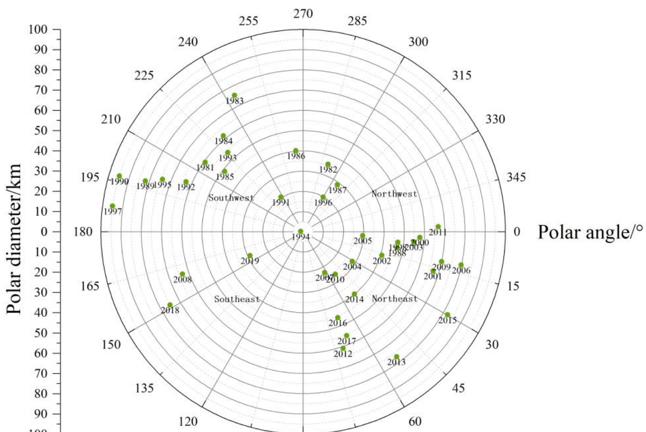

Figure 4 Distributions of gravity centers in different quadrants during the period 1981-2019

In order to show and analyze the change patterns of the gravity center of soil erosion modulus in the Yellow River Basin in the past 40 years, this paper calculated the migration trajectory of the gravity center at different time scales. As seen in Fig. 5, the gravity center of soil erosion intensity in the Yellow River Basin moved from southwest to northeast during the period 1981-2019. This shift indicates that the growth rate and increment of soil erosion in the northeast of the study area were higher than those in other regions, which was consistent with the above analysis results. According to the analysis of the gravity center migration trajectory, the change of gravity center of soil erosion in the past 40 years can be divided into two stages: 1981-2000 and 2001-2019. The gravity center of soil erosion in 1981-2000 moved to the north, which indicates that during the period 1981-2000, the increment of soil erosion in the northern part of the study area was higher than that of the south; the gravity center soil erosion in 2001-2019 moved to the northwest, which indicates that during the period 2001-2019, the increment of soil erosion in the northwestern part of the study area was higher than that of the southeast. Around 2000, the gravity center of soil erosion moved to the northeast, indicating that the increment and growth rate of soil erosion in the northeast of the Yellow River Basin was higher than that of the northwest.

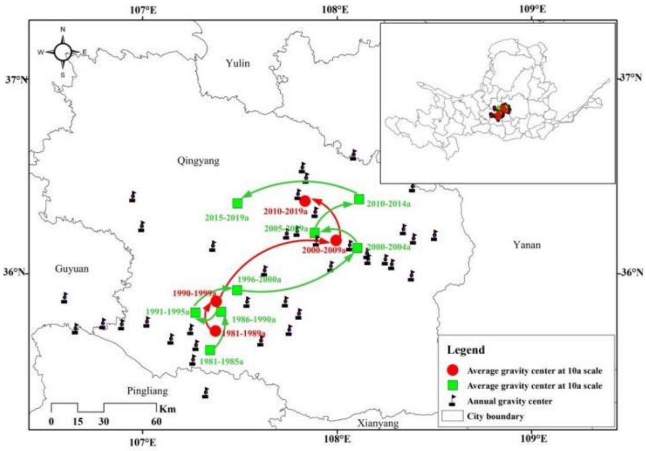

Figure 5 Migration trajectory of gravity center of soil erosion in the Yellow River Basin at different time scales.

3.3 Quantitative distinguishment of impacts of rainfall and vegetation during different historical periods

This study quantitatively distinguished the effects of rainfall erosivity and vegetation coverage on soil erosion in the Yellow River Basin in the past 40 years, based on the LMDI model (Eq. (3)) and Table 1. Fig. 6 shows that, the increased soil erosion due to the R factor (ISER) was the most widely distributed, accounting for 79.21% of the area where soil erosion increased, which was mainly distributed in northern Qingyang, Lanzhou, Linxia Hui Autonomous Prefecture, northern Dingxi, Zhongwei, Baiyin, and northern Guyuan. The increased soil erosion due to the C factor and R factor had the second largest area, accounting for 17.20% (increased area of soil erosion), which were mainly distributed in northern Bayan Nur, Hainan Tibetan Autonomous Prefecture, southern Golog Tibetan Autonomous Prefecture, and the central area of Jincheng. The increased soil erosion due to the C factor had the smallest area, accounting for 3.60% (increased area of soil erosion), which was mostly concentrated in Bayan Nur and southern Hohhot. The decreased soil erosion due to the C factor and R factor was the most widely distributed, accounting for 49.15% of the area where soil erosion decreased, which was mainly concentrated in Yanan, Baoji, Xianyang, the junction of Yulin-Linfen-Lvliang, Golog Tibetan Autonomous Prefecture, and Yushu Tibetan Autonomous Prefecture. The decreased soil erosion due to the C factor had the second largest area, accounting for 31.50% (decreased area of soil erosion), which was mostly distributed in northern Yulin, southern Xinzhou, and eastern Jinzhou. The decreased soil erosion due to the R factor occupied the smallest area, accounting for 19.35%, which was mostly distributed in Yushu Tibetan Autonomous Prefecture, Golog Tibetan Autonomous Prefecture, and Zhangye.

Table 1 Criteria for assessing the relative effects of the C factor and R factor on the change of soil erosion

ΔA	ΔA_C	ΔA_R	**Description**
	>0	>0	C factor and R factor both increased soil erosion (ISECR)
>0	>0	<0	C factor increased soil erosion (ISEC)
	<0	>0	R factor increased soil erosion (ISER)
	<0	<0	C factor and R factor both decreased soil erosion (DSECR)
<0	<0	>0	C factor decreased soil erosion (DSEC)
	>0	<0	R factor decreased soil erosion (DSER)

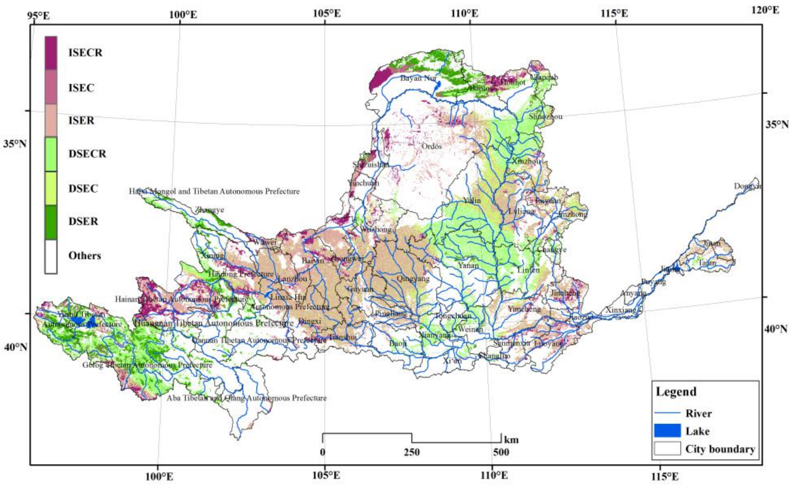

Figure 6. Spatial distribution of relative effects of the C factor and R factor on the change of soil erosion during the period 1981-2019a

Coupled with the influences of global climate change and the increase of human activity in the area, there were also significant differences in the effects of rainfall erosivity and vegetation coverage in the change of soil erosion for different historical periods. Therefore, this study quantitatively distinguished the effects of rainfall erosivity and vegetation coverage on soil erosion in the Yellow River Basin during four time periods: 1981-1990, 1991-2000, 2001-2010 and 2011-2019.

As is shown in Fig. 7 (a) (1981-1989), the increased soil erosion due to the C factor and R factor was the most widely distributed, accounting for 82.47% of the area where soil erosion increased, which was mainly distributed in Baiyin, northern Qiangyang, Lanzhou, Dingxi, northern Tianshui, the junction of Hainan Tibetan Autonomous Prefecture- Haidong Prefecture- Huangnan Tibetan Autonomous Prefecture, Lüliang, Taiyuan, Jinzhong, Jiaozuo, Jincheng, and northern Luoyang. The increased soil erosion due to the C factor accounted for 17.20% of the increased area of soil erosion, which was mainly concentrated in northern Hainan Tibetan Autonomous Prefecture, southern Zhongwei, northern Yulin, and northern Baotou. The decreased soil erosion due to the C factor and R factor was the most widely distributed, accounting for 82.47% of the area where soil erosion decreased, which was mainly concentrated in Yushu Tibetan Autonomous Prefecture, southern Qingyang, Pingliang, Yanan, Xianyang, Tongchuan, Baoji, Linfen, the junction of Ordos-Xinzhou-Shuozhou, Baotou, northern Bayan Nur, Xining, and Zhangye. The decreased soil erosion due to the C factor accounted for 17.53% (decreased area of soil erosion), which was mostly distributed in middle of Yulin, the junction of Yuncheng-Linfen-Jincheng, and eastern Ordos.

As is shown in Fig.7 (b) (1990-1999), increased soil erosion due to the R factor (ISER) was the most widely distributed, accounting for 64.66% of the area where soil erosion increased, which was mainly distributed in Golog Tibetan Autonomous Prefecture, southern Yushu Tibetan Autonomous Prefecture, southern Hainan Tibetan Autonomous Prefecture, Xining, Zhangye, southern Wuwei, northern Weinan, and eastern Jincheng. The increased soil erosion due to the C factor and R factor had the second largest area, accounting for 34.24% (increased area of soil erosion), which was mainly distributed in Luoyang, Shangluo, Jiaozuo, eastern Yuncheng, and northern Tongchun. The increased soil erosion due to the C factor had the smallest area, accounting for 1.10% (increased area of soil erosion), which was only concentrated in the middle of Haidong Prefecture and southeastern Linfen. The decreased soil erosion due to the C factor and R factor was the most widely distributed, accounting for 54.89% of the area where soil erosion decreased, which was mainly concentrated in Zhongwei, Wuzhong, southern Qiangyang, northern Lanzhou, Dingxi, western Tongchuan, and eastern Ordos (Thomas et al., 2018). The decreased soil erosion due to the R factor had the second largest area, accounting for 43.72% (decreased area of soil erosion), which was mostly distributed in Baotou, Hohhot, Shuozhou, Xinzhou, eastern Yulin, western Lüliang, western Taiyuan, northern Yanan, the junction of Qingyang-Yulin-Yanan, and the middle of Tianshui. The decreased soil erosion due to the C factor occupied the smallest area, accounting for 1.39%, which was mostly distributed in northern Hainan Tibetan Autonomous Prefecture.

As is shown in Fig. 7 (c) (2000-2009), increased soil erosion due to the R factor (ISER) was the most widely distributed, accounting for 63.90% of the area where soil erosion increased, which was mainly distributed in Shuozhou, Xinzhou, eastern Ordos, eastern Yulin, northern Yanan, western Lüliang, and the junction of Qingyang-Yulin-Yanan. The increased soil erosion due to the C factor and R factor occupied the second largest area, accounting for 32.88% (increased area of soil erosion), which was mainly distributed in Yushu Tibetan Autonomous Prefecture, Hainan Tibetan Autonomous Prefecture, Golog Tibetan Autonomous Prefecture, northern Gannan Tibetan Autonomous Prefecture, northern Guyuan, western Qingyang, and western Bayan Nur. The increased soil erosion due to the C factor had the smallest area, accounting for 3.22% (increased area of soil erosion), which was only concentrated in eastern Wuzhong. The decreased soil erosion due to the R factor was the most widely distributed, accounting for 49.06% of the area where soil erosion decreased, which was mainly concentrated in Lanzhou, Baiyin, Zhongwei, northern Haidong Prefecture, and northern Pingliang. The decreased soil erosion due to the C factor and R factor had the second largest area, accounting for 45.63% (decreased area of soil erosion), which was mostly distributed in the middle of Dingxi, Tianshui, Pingliang, southern Qiangyang, western Xiangyang, and the junction of Linfen-Jincheng-Yuncheng. The decreased soil erosion due to the C factor occupied the smallest area, accounting for 5.31%, which was mostly distributed in northeastern Qingyang.

As is shown in Fig. 7 (d) (2010-2019), increased soil erosion due to the R factor (ISER) was the most widely distributed, accounting for 63.45% of the area where soil erosion increased, which was mainly distributed in Lanzhou, Baiyin, Zhongwei, southern Wuzhong, northern Qingyang, Guyuan, northern Dingxi, northern Tianshui, northwestern Yanan, and eastern Yulin. The increased soil erosion due to the C factor and R factor occupied the second largest area, accounting for 32.98% (increased area of soil erosion), which was mainly distributed in northern Golog Tibetan Autonomous Prefecture, Hainan Tibetan Autonomous Prefecture, the junction of Yulin-Yanan-Lüliang-Linfen, Yuncheng, and Jincheng. The increased soil erosion due to the C factor had the smallest area, accounting for 3.56% (increased area of soil erosion), which was only concentrated in the junction of Yulin-Ordos -Xinzhou-Shuozhou. The decreased soil erosion due to the R factor was the most widely distributed, accounting for 36.61% of the area where soil erosion decreased, which was mainly concentrated in Yushu Tibetan Autonomous Prefecture, Shizuishan, and northern Bayan Nur. The decreased soil erosion due to the C factor and R factor had the second largest area, accounting for 33.42% (decreased area of soil erosion), which was widely distributed in the middle of the Loess Plateau. The decreased soil erosion due to the C factor and R factor occupied the smallest area, accounting for 29.97%, which was mostly distributed in northern Golog Tibetan Autonomous Prefecture, Zhangye, and the junction of Ordos-Shuozhou- Xinzhou-Yulin.

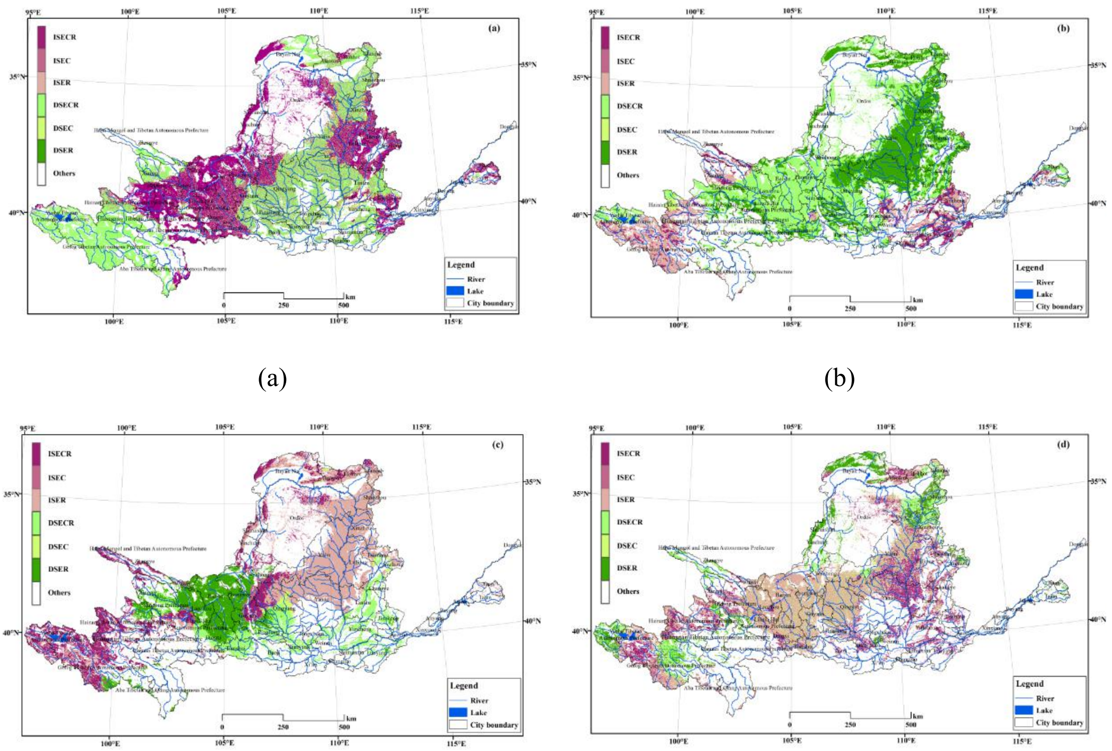

(a) (b)

(c) (d)

Figure 7. Spatial distributions of relative effects of the C factor and R factor on the change of soil erosion for different historical periods (a) 1981-1990a;(b)1991-2000a;(c) 2001-2010a;(d) 2011-2019a.

3.4 Dominant and interactive dominant factors in different ecological sub-regions for different periods

There are significant differences in the effects of slope, precipitation, land use, soil type and vegetation coverage on soil erosion in different historical periods and ecological zones. In this study, the geographical detector model was utilized to determine the dominant and interactive dominant factors of different ecological zones in the Yellow River Basin in 1981, 1990, 1999, 2008 and 2019 (Table 2).

As shown in Fig. 8(a) and Fig. 8(b) (1981), soil type was the dominant factor in ecological zones, including: the Fenwei Plain warm temperate agriculture ecological zone, the Hetao Plain grassland ecological region, the Loess Hills warm temperate broad-leaved deciduous forest, and the Taihang Mountain warm temperate broad-leaved deciduous forest ecological zones. However, the *q* values of the above sub-regions differed. Among these sub-regions, elevation impacted the Taihang Mountain warm temperate broad-leaved deciduous forest ecological zone the most significantly, with a *q* value of 0.875. In addition, the interactive dominant factor of this zone was slope aspect ∩ soil type, with a *q* value of 0.928. Land use was the dominant factor of the upper reaches of the Yellow River alpine shrub ecological zone, Alpine meadow ecological region, the Qilian Mountain temperate mountain meadow-mountain shrub ecological zone, Sijiangyuan Plateau frigid sub-frigid meadow steppe, and the Yinshan and the north of Yinshan middle temperate grassland ecological zones (Diwediga et al., 2018). Among these sub-regions, land use impacted the Yinshan and the north of Yinshan middle temperate grassland ecological zones the most significantly, with a *q* value of 0.856. In addition, the interactive dominant factor of these zones was vegetation coverage ∩ slope, with a *q* value of 0.999. Precipitation was the dominant factor of the Gansu Qin and Jin warm temperate broad-leaved deciduous forest, the middle of the Gansu temperate desert, and the Huanghuai Plain warm temperate agriculture ecological zones. Among these sub-regions, precipitation impacted the Gansu Qin and Jin warm temperate broad-leaved deciduous forest ecological zone the most significantly, with a *q* value of 0.478. The interactive dominant factor of these zones was land use ∩ precipitation, with a *q* value of 0.624. The interactive dominant factor in the middle of the Gansu temperate desert ecological zone was slope ∩ soil type, with a *q* value of 0.972. The interactive dominant factor in the middle of the Huanghuai Plain warm temperate agriculture ecological zone was vegetation coverage ∩ land use, with a *q* value of 0.974. Vegetation coverage was the dominant factor of the Ordos Plateau middle temperate desert and the Alxa Plateau temperate desert ecological zones. Among these sub-regions, vegetation coverage impacted the Ordos Plateau middle temperate desert ecological zone the most significantly, with a *q* value of 0.574. The interactive dominant factor of these zones was slope ∩ precipitation, with a *q* value of 0.931. The interactive dominant factor in the Alxa Plateau temperate desert ecological zone was vegetation coverage ∩ soil type, with a *q* value of 0.998 (Han et al., 2021; Jin et al., 2021).

As shown in Fig. 8(c) and Fig. 8(d) (1990), soil type was the dominant factor in ecological zones, including: the Alxa Plateau temperate desert, the Ordos Plateau middle temperate desert, the Fenwei Plain warm temperate agriculture ecological zone, the Huanghuai Plain warm temperate agriculture ecological zone, the Gansu Qin and Jin warm temperate broad-leaved deciduous forest, the Taihang Mountain warm temperate broad-leaved deciduous forest, and the Sijiangyuan Plateau frigid sub-frigid meadow steppe. However, the *q* values of the above sub-regions differed. Among these sub-regions, soil type impacted the Fenwei Plain warm temperate agriculture ecological zone the most significantly, with a *q* value of 0.965. The interactive dominant factor for this ecological region was land use ∩ soil type, with a *q* value of 0.882. Vegetation coverage was the dominant factor of the Hetao Plain grassland, the middle of the Huanghuai Plain warm temperate agriculture ecological zone, the Qilian Mountain temperate mountain meadow-mountain shrub ecological zone, and the Yinshan and the north of Yinshan middle temperate grassland ecological zone. Among these sub-regions, vegetation coverage impacted the Hetao Plain grassland ecological zones the most significantly, with a *q* value of 0.853. The interactive dominant factor for this ecological region was vegetation coverage ∩ soil type, with a *q* value of 0.999. Precipitation was the dominant factor of the Loess Hills warm temperate broad-leaved deciduous forest, with a *q* value of 0.057 (Zhao et al., 2019). The interactive dominant factor in this region was vegetation coverage ∩ land use, with a *q* value of 0.681. Land use was the dominant factor of the upper reaches of the Yellow River alpine shrub ecological zone. The interactive dominant factor in this ecological zone was slope ∩ soil type, with a *q* value of 0.892.

As shown in Fig. 8(e) and Fig. 8(f) (1999), vegetation coverage was the dominant factor in ecological zones, including: the Alxa Plateau temperate desert, the Ordos Plateau middle temperate desert, the Fenwei Plain warm temperate agriculture ecological zone, the middle of the Gansu temperate desert, the Qilian Mountain temperate mountain meadow-mountain shrub ecological zone, and the Sijiangyuan Plateau frigid sub-frigid meadow steppe. Among these sub-regions, vegetation coverage impacted the Qilian Mountain temperate mountain meadow-mountain shrub ecological zone the most significantly, with a *q* value of 0.997. Soil type was the dominant factor of the Hetao Plain grassland, the Huanghuai Plain warm temperate agriculture ecological zone, the Loess Hills warm temperate broad-leaved deciduous forest, and the Gansu Qin and Jin warm temperate broad-leaved deciduous forest. Among these sub-regions, soil type impacted the Huanghuai Plain warm temperate agriculture ecological zone the most significantly, with a *q* value of 0.895. The interactive dominant factor for this ecological region was soil type ∩ precipitation, with a *q* value of 0.998. Land use was the dominant factor of the upper reaches of the Yellow River alpine shrub ecological zone and the Yinshan and the north of Yinshan middle temperate grassland ecological zone. However, the *q* values and interactive dominant factors of the above sub-regions differed. The dominant factor *q* of the former was 0.956, and the interactive dominant factor was precipitation ∩ slope. The dominant factor *q* of the latter was 0.720, and the interactive dominant factor was vegetation coverage ∩ slope. Precipitation was the dominant factor of the Taihang Mountain warm temperate broad-leaved deciduous forest. The interactive dominant factor in this ecological zone was slope ∩ soil type, with a *q* value of 0.779.

As shown in Fig. 8(g) and Fig. 8(h) (2008), soil type was the dominant factor in ecological zones, including: the Fenwei Plain warm temperate agriculture ecological zone, the Hetao Plain grassland, the Loess Hills warm temperate broad-leaved deciduous forest, the Gansu Qin and Jin warm temperate broad-leaved deciduous forest, the Taihang Mountain warm temperate broad-leaved deciduous forest, and the Sijiangyuan Plateau frigid sub-frigid meadow steppe. Among these sub-regions, soil type impacted the Hetao Plain grassland ecological zone the most significantly, with a *q* value of 0.893. The interactive dominant factor in this ecological zone was land use ∩ soil type, with a *q* value of 0.999. Vegetation coverage was the dominant factor of the Alxa Plateau temperate desert, the Huanghuai Plain warm temperate agriculture ecological zone, the middle of the Gansu temperate desert, and the Qilian Mountain temperate mountain meadow-mountain shrub ecological zone. Among these sub-regions, vegetation coverage impacted the Huanghuai Plain warm temperate agriculture ecological zone the most significantly, with a *q* value of 0.887. The interactive dominant factor for this ecological region was land use ∩ soil type, with a *q* value of 0.999. Land use was the dominant factor of the Ordos Plateau middle temperate desert, the upper reaches of the Yellow River alpine shrub ecological zone, and the Yinshan and the north of Yinshan middle temperate grassland ecological zone. However, the interactive dominant factors of the above sub-regions differed. Among these sub-regions, land use impacted the upper reaches of the Yellow River alpine shrub ecological zone the most significantly, with a *q* value of 0.974.

As shown in Fig. 8(i) and Fig. 8(j) (2019), precipitation was the dominant factor in ecological zones, including: the Alxa Plateau temperate desert, the Fenwei Plain warm temperate agriculture ecological zone, the Gansu Qin and Jin warm temperate broad-leaved deciduous forest, the Qilian Mountain temperate mountain meadow-mountain shrub ecological zone, the Taihang Mountain warm temperate broad-leaved deciduous forest, and the Sijiangyuan Plateau frigid sub-frigid meadow steppe. Among these sub-regions, precipitation impacted the Gansu Qin and Jin warm temperate broad-leaved deciduous forest ecological zone the most significantly, with a *q* value of 0.970. The interactive dominant factor in this ecological zone was vegetation coverage ∩ soil type, with a *q* value of 0.670. Land use was the dominant factor of the Ordos Plateau middle temperate desert, the upper reaches of the Yellow River alpine shrub ecological zone, and the Loess Hills warm temperate broad-leaved deciduous forest ecological zone. Among these sub-regions, land use impacted the upper reaches of the Yellow River alpine shrub ecological zone the most significantly, with a *q* value of 0.630. Vegetation coverage was the dominant factor of the middle of the Gansu temperate desert and the Yinshan and the north of Yinshan middle temperate grassland ecological zone. However, the interactive dominant factors of the above sub-regions differed. The *q* value of the former was 0.602, and the interactive dominant factor was slope ∩ soil type. The *q* value of the latter was 0.910, and the interactive dominant factor was slope ∩ vegetation coverage, with a *q* value of 0.997.

Table 2 The q value of dominant factors and interactive dominant factors for different ecological sub-regions of the Yellow River Basin.

Ecological sub-region		A	B	C	D	E	F	G	H	I	J	K	L	M
Dominant factor	1981	VC	VC	ST	ST	LU	PR	ST	PR	PR	LU	ST	LU	LU
	1990	ST	ST	ST	VC	LU	ST	PR	ST	VC	VC	ST	ST	VC
	1999	VC	VC	VC	ST	LU	ST	ST	ST	VC	VC	PR	VC	LU
	2008	VC	LU	ST	ST	LU	VC	ST	ST	VC	VC	ST	ST	LU
	2019	PR	LU	PR	ST	LU	ST	LU	PR	VC	PR	PR	PR	VC
q	19	0.48	0.57	0.83	0.79	0.708	0.231	0.058	0.487	0.235	0.629	0.875	0.831	0.856

	81	4	4	4	0									
	1990	0.504	0.592	0.965	0.853	0.477	0.875	0.057	0.865	0.700	0.797	0.927	0.054	0.667
	1999	0.921	0.928	0.938	0.706	0.956	0.895	0.014	0.913	0.767	0.967	0.809	0.292	0.720
	2008	0.521	0.610	0.683	0.893	0.974	0.887	0.030	0.859	0.343	0.880	0.848	0.524	0.745
	2019	0.355	0.383	0.920	0.858	0.630	0.992	0.100	0.97	0.602	0.700	0.935	0.423	0.910
Interactive dominant factor	1981	VC∩ST	SO∩PR	SO∩PR	SO∩LU	SO∩PR	VC∩LU	LU∩PR	Lu∩PR	SO∩ST	SO∩ST	SO∩ST	SO∩PR	VC∩SO
	1990	VC∩ST	SO∩LU	LU∩ST	VC∩ST	SO∩ST	VC∩SO	VC∩LU	VC∩LU	SO∩PR	SO∩ST	SO∩ST	SO∩PR	SO∩LU
	1999	St∩LU	ST∩LU	PR∩LU	SO∩ST	SO∩PR	ST∩PR	ST∩PR	VC∩LU	VC∩SO	SO∩ST	SO∩ST	VC∩SO	VC∩SO
	2008	PR∩ST	SO∩PR	LU∩ST	LU∩ST	VC∩SO	LU∩ST	VC∩LU	LU∩ST	SO∩ST	SO∩ST	VC∩LU	VC∩SO	VC∩SO
	2019	LU∩PR	SO∩ST	SO∩ST	LU∩ST	SO∩VC	LU∩ST	SO∩VC	VC∩ST	SO∩ST	SO∩VC	LU∩SO	SO∩VC	SO∩VC
q	1981	0.998	0.931	0.962	0.999	0.836	0.974	0.793	0.624	0.972	0.995	0.928	0.866	0.999
	1990	0.998	0.870	0.882	0.999	0.892	0.995	0.681	0.670	0.965	0.942	0.840	0.868	0.973
	1999	0.988	0.887	0.909	0.999	0.543	0.998	0.587	0.683	0.921	0.921	0.921	0.983	0.998
	2008	0.997	0.847	0.761	0.999	0.833	0.999	0.578	0.552	0.934	0.993	0.957	0.844	0.998
	2019	0.998	0.782	0.787	0.999	0.793	0.999	0.418	0.670	0.746	0.834	0.788	0.983	0.997

Note: A refers to the Alxa Plateau temperate desert ecological zone; B refers to the Ordos Plateau middle temperate desert ecological zone; C refers to the Fenwei Plain warm temperate agriculture ecological zone; D refers to the Hetao Plain grassland ecological region; E refers to the upper reaches of the Yellow River alpine shrub ecological zone; F refers to the Huanghuai Plain warm temperate agriculture ecological zone; G refers to the Loess Hills warm temperate broad-leaved deciduous forest ecological zone; H refers to the Gansu Qin and Jin warm temperate broad-leaved deciduous forest ecological zone; I refers to the middle of the Gansu temperate desert ecological zone; J refers to the Qilian Mountain temperate mountain meadow-mountain shrub ecological zone; K refers to the Taihang Mountain warm temperate broad-leaved deciduous forest ecological zone; L refers to the Sijiangyuan Plateau frigid sub-frigid meadow steppe ecological zone; M refers to the Yinshan and the north of Yinshan middle temperate grassland ecological zone. VC refers to vegetation coverage; PR refers to precipitation; ST refers to soil type; LU refers to land use; SO refers to slope.

4. Discussion

4.1 Advantages of the research methods

In this paper, the LMDI model is used to distinguish the influences of the rainfall erosion force factor and the vegetation coverage factor on soil erosion in the Yellow River Basin. Compared with the traditional regression model, the LMDI method can distinguish the influences of the driving factors and then determines the contribution of each factor to the variation of soil erosion on pixel scale, which would better demonstrate the spatial distribution differences of the contribution fordominant factors.

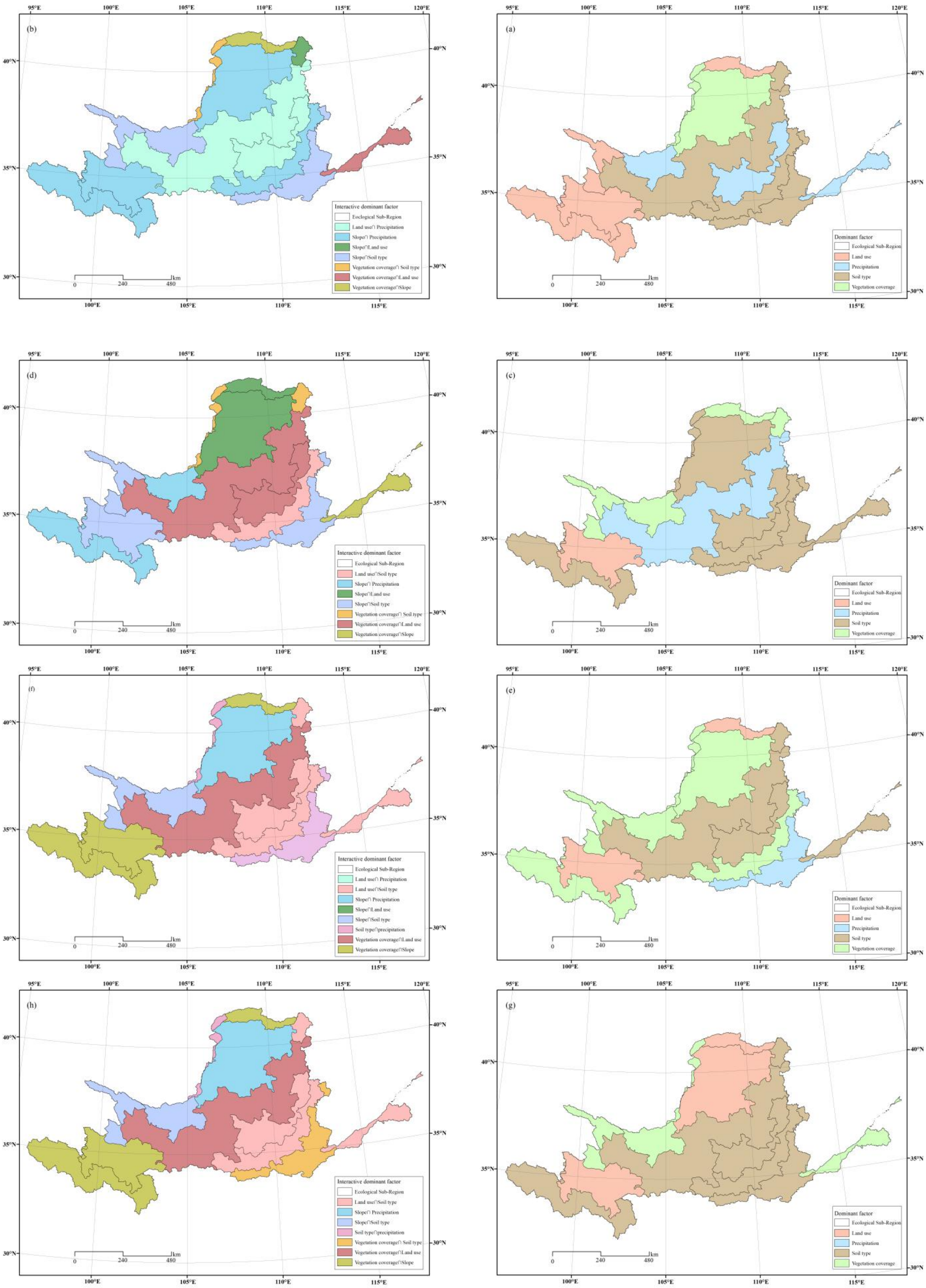
(b)
Interactive dominant factor
Ecological Sub-Region
Land use∩ Precipitation
Slope∩ Precipitation
Slope∩Land use
Slope∩Soil type
Vegetation coverage∩ Soil type
Vegetation coverage∩Land use
Vegetation coverage∩Slope
(a)
Dominant factor
Ecological Sub-Region
Land use
Precipitation
Soil type
Vegetation coverage
(d)
Interactive dominant factor
Ecological Sub-Region
Land use∩Soil type
Slope∩ Precipitation
Slope∩Land use
Slope∩Soil type
Vegetation coverage∩ Soil type
Vegetation coverage∩Land use
Vegetation coverage∩Slope
(c)
(f)
Interactive dominant factor
Ecological Sub-Region
Land use∩ Precipitation
Land use∩Soil type
Slope∩ Precipitation
Slope∩Land use
Slope∩Soil type
Soil type∩precipitation
Vegetation coverage∩Land use
Vegetation coverage∩Slope
(e)
(h)
Interactive dominant factor
Ecological Sub-Region
Land use∩Soil type
Slope∩ Precipitation
Slope∩Soil type
Soil type∩precipitation
Vegetation coverage∩ Soil type
Vegetation coverage∩Land use
Vegetation coverage∩Slope
(g)
0 240 480 km

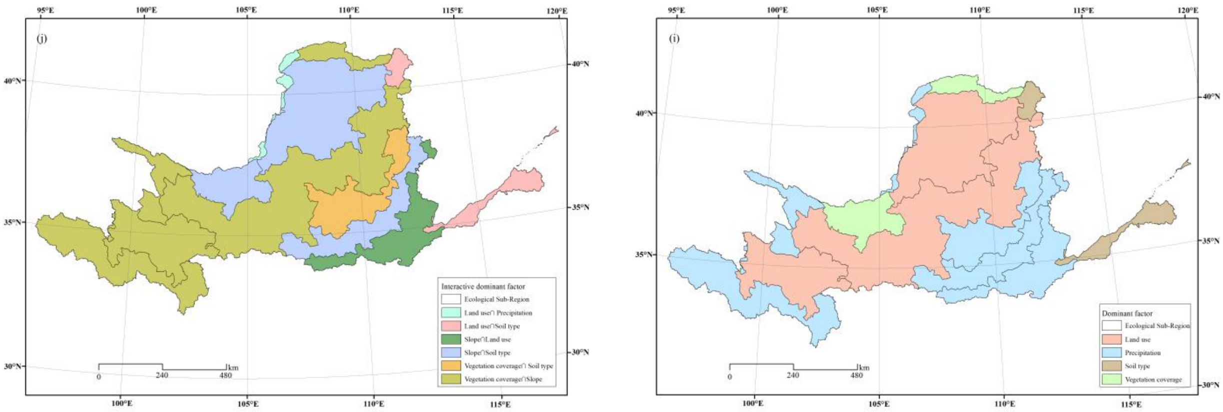

Figure 8 Main influential factors of soil erosion in different ecological subregions of the Yellow River Basin (a) interactive dominant factors of 1981; (b) dominant factors of 1981; (c) interactive dominant factors of 1990; (d) dominant factors of 1990; (e) interactive dominant factors of 1999; (f) dominant factors of 1999; (g) interactive dominant factors of 2008; (h) dominant factors of 2008; (i) interactive dominant factors of 2019; (j) dominant factors of 2019.

In addition, the calculation processes of the contributions of the C factor and R factor were independent . Moreover, the whole process of quantitative distinguishment of the effects of the R factor and C factor on soil erosion was not dependent on experimental or statistical data that were difficult to obtain. Therefore, this method has better applicability in these regions with scare observation data (Cai et al., 2019). Different factors have comprehensive influences on the change process of soil erosion. However, using the traditional analysis model of driving factors ignores interactions between factors. Utilizing the geographical detector model can better determine the dominant single and interaction factors on the landscape scale by identifying the interactions between multiple factors (Chen et al., 2021).

4.2 Dominant influencing factors of spatial distribution of soil erosion in the Yellow River Basin

Intensive and severe erosion zones in the Yellow River Basin were mainly concentrated in the Loess Plateau. This is due to the long-term cultivation and utilization of the area by human society, especially during the Ming and Qing dynasties. During these dynasties, problems such as land reclamation, grazing, and war resulted in the natural forest and grassland vegetation of the Loess Plateau to be nearly destroyed (Guo et al., 2020d). The ecological environment was severely damaged, with serious soil erosion occurring in Shaanxi, Gansu, and other northwest regions. During the past several decades, desertification has become the geomorphic feature of the gully and barren mountain in the Loess Plateau. The soil erosion modulus in most areas of the Loess Plateau was higher than 1,000 $t \cdot km^{-1} \cdot a^{-1}$. In hill and gully areas, soil erosion was very severe, with a soil erosion modulus higher than 5,000 $t \cdot km^{-1} \cdot a^{-1}$. In summary, it was found that the main causes of severe soil erosion in the Loess Plateau were topography, human activities, and special soil texture. The soil erosion modulus in the source region of the Yellow River, Hetao Plain, Guanzhong Plain, and Ningxia Plain was relatively small. The reason being that the source area of the Yellow River is an important part of the Three-River Source Region Nature Reserve. After decades of ecological restoration and management (afforestation, returning farmlands to forests and grasslands, etc.), its ecological environment has been greatly improved and the vegetation coverage has increased to a certain extent (Han et al., 2021). For the Hetao Plain, Guanzhong Plain, and Ningxia Plain, the terrain is flat and there are abundant water resources and high vegetation coverage. Thus, the overall soil erosion intensity was slight. In the middle and upper reaches of the Yellow River, the soil erosion modulus belonged to mild and moderate erosion. The main reason being that in these regions the low mountains and hills are widely distributed, the relief is large, and the vegetation coverage is low. Therefore, a large amount of soil erosion occurred in this area. Precipitation as the dominant factor of soil erosion was mainly concentrated in the source region of the Yellow River and Hetao Plain. Vegetation coverage as the dominant factor of soil erosion was mainly distributed in the middle and upper reaches of the Yellow River.

4.3 Dominant influencing factors of soil erosion change in the Yellow River Basin

The erosion intensity and total amount of soil erosion in the Yellow River Basin showed a decreasing trend over the past 40 years. They main reason being that many soil and water conservation measures, such as small watershed management and the construction of the Three-North Shelterbelt, were carried out in the region by the government from the 1980s to the 1990s (Ran et al., 2020). Since 2000, projects for converting farmlands to forests or grasslands, improving steep slope cultivated land, and constructing ditch land have been conducted (Xu et al., 2021). In 2016, the Loess Plateau was the first area to receive ecological protection and restoration projects in China. This was due to the Loes Plateau having the most severe erosion in the Yellow River Basin. The projects included restoration of mountains, rivers, forests, fields and lakes, allowing the Loess Plateau to enter a new stage in soil erosion control. From 2000 to 2015, zones of returning farmlands to forests on the Loess Plateau covered about $581.12\times10^5 hm^2$, among which $215.07\times10^5 hm^2$ were returning farmlands to forests, $328.65\times10^5 hm^2$ were afforestation of barren mountains, and $37.5\times10^5 hm^2$ were closing hillsides for afforestation. However, there are significant differences in the spatial and temporal evolution of soil erosion in different historical periods and regions. Before 2000, the spatial and temporal distribution of soil erosion in more ecological sub-regions was more significantly affected by precipitation, vegetation, and soil types. But with the increase of human intervention, for example, returning farmland to forest and grassland, the Three-North Shelterbelt Project, returning grazing land to grassland, and the implementation of various types of soil and water conservation measures, the explanatory power of land use change in the evolution pattern of soil erosion also increased.

5. Conclusion

Based on the RUSLE model, the annual soil erosion modulus of the Yellow River Basin from 1981 to 2019 was calculated and the temporal and spatial evolution pattern of soil erosion in the past 40 years was analyzed. Furthermore, the dominant factors of the Yellow River Basin in different historical periods were quantitatively analyzed from the pixel scale and landscape scale utilizing the LMDI model and Geodetector model. The main conclusions are as follows:

(1) In the past 40 years, the average soil erosion modulus of the Yellow River Basin is 2,255 $t\cdot km^{-1}\cdot a^{-1}$, which belongs to mild erosion. Among them, the severe (intensive, extremely intensive, and severe) erosion areas are mainly distributed in the Loess Plateau, while the micro and mild erosion areas are mainly distributed in the Hetao Plain, Ordos Plateau, Ningxia Plain, and Guanzhong Plain.

(2) In the past 40 years, the gravity center of soil erosion intensity in the Yellow River Basin moved from southwest to northeast. The results show that the growth rate and increment of soil erosion in the northeast of the Yellow River Basin are higher than those in other areas.

(3) During the past 40 years, the increased soil erosion due to the R factor (ISER) was the most widely distributed, accounting for 79.21% of the area where soil erosion increased, while the decreased soil erosion due to the C factor and R factor was the most widely distributed, accounting for 49.15% of the area where soil erosion decreased.

(4) Before 2000, precipitation, vegetation, and soil types were the main factors affecting the evolution pattern of soil erosion in the Yellow River Basin. However, with the increase of human intervention, including returning farmland to forest and grassland, the Three-North Shelterbelt Project, returning grazing land to grassland, and the implementation of various types of soil and water conservation measures, the explanatory power of land use change in the evolution pattern of soil erosion has increased.

Acknowledgments

This work was supported by the Open Fund of Key Laboratory of National Geographic Census and Monitoring, MNR (grant no. 2020NGCM02).

References

Ang, B.W. (2005). “The LMDI approach to decomposition analysis: A practical guide”. Energy Policy, 33(7), 867–871.

Cai, J.Y., Zhou, Z.H., Liu, J.J., Wang, H., Jia, Y.W., Xu, C.Y. (2019). “A three-process-based distributed soil erosion model at catchment scale on the Loess Plateau of China”. J Hydrol, 578, 124005.

Chen, J., Li, Z.W., Xiao, H.B., Ning, K., Tang, C.J. (2021). “Effects of land use and land cover on soil erosion control in southern China: Implications from a systematic quantitative review”. J Environ Mange, 282, 111924.

Chen, P., Yi, P., Xiong, L., Yu, Z.B., Aldahan, A., Muscheler, R., Jin, H.J., Luo, D.L., Possnert, G., Wu, M., Wan, C.W., Zheng, M.J. (2019). “Use of 10Be isotope to predict landscape development in the source area of the Yellow River (SAYR), northeastern Qinghai-Tibet Plateau”. J Environ Radioactiv, 203, 187-199.

Chen, S.T., Guo, B., Zhang, R., Zang, W.Q., Wei, C.X., Wu, H.W., Yang, X., Zhen, X.Y., Li, X., Zhang, D.F., Han, B.M., Zhang, H.L. (2021). "Quantitatively determine the dominant driving factors of the spatial–temporal changes of vegetation NPP in the Hengduan Mountain area during 2000-2015". J Mt Sci, 18(2), 427-445.

Chen, Y.P., Fu, B.J., Zhao, Y., Wang, K.B., Zhao, M.M., Ma, J.F., Wu, J.H., Xu, C., Liu, W.G., Wang, H. (2020). "Sustainable development in the Yellow River Basin: Issues and strategies". J Clean Prod, 263, 121223.

Chen, P., Yi, P., Xiong, L., Yu, Z.B., Aldahan, A., Muscheler, R., Jin, H.J., Luo, D.L., Possnert, G., Wu, M., Wan, C.W., Zheng, M.J. (2019). "Use of 10Be isotope to predict landscape development in the source area of the Yellow River (SAYR), northeastern Qinghai-Tibet Plateau". J Environ Radioactiv, 203, 187-199.

Chen, S.T., Guo, B., Zhang, R., Zang, W.Q., Wei, C.X., Wu, H.W., Yang, X., Zhen, X.Y., Li, X., Zhang, D.F., Han, B.M., Zhang, H.L. (2021). "Quantitatively determine the dominant driving factors of the spatial–temporal changes of vegetation NPP in the Hengduan Mountain area during 2000-2015". J Mt Sci, 18(2), 427-445.

Diwediga, B., Quang, B.L., Sampson K.A., Lulseged D.T., Wala, K. (2018). "Modelling soil erosion response to sustainable landscape management scenarios in the Mo River Basin (Togo, West Africa)". Sci Total Environ, 625, 1309-1320.

Fayas, C.M., Abeysingha, N.S., Nirmanee, K.G.S., Samaratunga, D., Mallawatantri, A. (2019). "Soil loss estimation using rusle model to prioritize erosion control in KELANI river basin in Sri Lanka". Int Soil Water Conse, 7(2), 130-137.

Guo, B., Wen, Y. (2020). "An Optimal Monitoring Model of Desertification in Naiman Banner Based on Feature Space Utilizing Landsat8 OLI Image". IEEE Access, 8, 4761-4768.

Guo, B., Zang, W.Q., Luo, W. (2020a). "Spatial-temporal shifts of ecological vulnerability of Karst Mountain ecosystem-impacts of global change and anthropogenic interference". Sci Total Environ, 74, 140256.

Guo, B., Zang, W.Q., Luo, W., Wen, Y., Yang, F., Han, B.M., Fan, Y.W., Chen, X., Qi, Z., Wang, Z., Chen, S.T., Yang, X. (2020b). "Detection model of soil salinization information in the Yellow River Delta based on feature space models with typical surface parameters derived from Landsat8 OLI image". Geomat Nat Haz Risk, 11(1), 288-300.

Guo, B., Wen, Y. (2020). "An Optimal Monitoring Model of Desertification in Naiman Banner Based on Feature Space Utilizing Landsat8 OLI Image". IEEE Access, 8, 4761-4768.

Guo, B., Zang, W.Q., Yang, F., Han, B.M., Chen, S.T., Liu, Y., Yang, X., He, T.L., Chen, X., Liu, C.T., Gong, R. (2020c). "Spatial and temporal change patterns of net primary productivity and its response to climate change in the Qinghai–Tibet Plateau of China from 2000 to 2015". J Arid Land, 12(1), 1-17.

Guo, B., Zang, W.Q., Yang, X., Huang, X.Z., Zhang, R., Wu, H.W., Yang, L.A., Wang, Z., Sun, G.Q., Zhang, Y. (2020d). "Improved evaluation method of the soil wind erosion intensity based on the cloud–AHP model under the stress of global climate change". Sci Total Environ, 746, 141271.

Guo, B., Wen, Y. (2020). "An Optimal Monitoring Model of Desertification in Naiman Banner Based on Feature Space Utilizing Landsat8 OLI Image". IEEE Access, 8, 4761-4768.

Han, X.X., Xiao, J., Wang, L.Q., Tian, S.H., Liang, T., Liu, Y.J. (2021). "Identification of areas vulnerable to soil erosion and risk assessment of phosphorus transport in a typical watershed in the Loess Plateau". Sci Total Environ, 758, 143661.

Jin, F.M., Yang, W.C., Fu, J.X., Li, Z. (2021). "Effects of vegetation and climate on the changes of soil erosion in the Loess Plateau of China". Sci Total Environ, 773, 145514.

Kebede, Y.S., Endalamaw, N.T., Sinshaw, B.G., Sinshaw, H.B. (2021). "Modeling soil erosion using RUSLE and GIS at watershed level in the upper beles, Ethiopia". Environmental Challenges, 2, 100009.

Li, Y., Zhang, H.B., Fu, C.C., Tu, C., Luo, Y.M., Christie, P. (2019). "A red clay layer in soils of the Yellow River Delta: Occurrence, properties and implications for elemental budgets and biogeochemical cycles". Catena, 172, 469-479.

Liu, L.L., Cao., W., He T. (2019). Analysis on spatial-temporal variation of soil loss and its driving factors in north-south pan river watershed". Science of Soil and Water Conservation, 17(6), 69-77.

Ma, X.F., Zhu, J.T., Yan, W., Zhao, C.Y. (2020). "Assessment of soil conservation services of four river basins in Central Asia under global warming scenarios". Geoderma, 375, 114533.

Quan, B., Römkens, M.J.M., Li, R., Wang, F., Chen, J. (2011). "Effect of land use and land cover change on soil erosion and the spatio-temporal variation in Liupan Mountain Region, southern Ningxia, China". Front Environ Sci En, 5, 564–572.

Perović, V., Kadović, R., Djurdjević, V., Braunović, S., Čakmak, D., Mitrović, M., Pavlović, P. (2019). "Effects of changes in climate and land use on soil erosion: a case study of the Vranjska Valley, Serbia". Reg Environ Change, 19,1035–1046.

Ran, Q.H., Zong, X.Y., Ye, S., Gao, J.H., Hong, Y.Y. (2020). "Dominant mechanism for annual maximum flood and sediment events generation in the Yellow River basin". Catena, 187, 104376.

Thomas, J., Joseph, S., Thrivikramji, K.P. (2018). "Assessment of soil erosion in a tropical mountain river basin of

the southern Western Ghats, India using RUSLE and GIS". Geosci Front, 9 (3), 893-906.
Wang T. (2018). "Quantitative analysis on influencing factors of soil erosion using RUSLE: a case sudy of the Luohe Basin in northem Shanxi Province". Environ Sci Technol, 41(8), 170-177.
Wang, W., Zhang, Y.Y., Tang, Q.H. (2020). "Impact assessment of climate change and human activities on streamflow signatures in the Yellow River Basin using the Budyko hypothesis and derived differential equation". J Hydrol, 591, 125460.
Yin, L.C., Feng, X.M., Fu, B.J., Wang, S., Wang, X.F., Chen, Y.Z., Tao, F.L., Hu, J. (2021). "A coupled human-natural system analysis of water yield in the Yellow River basin, China". Sci Total Environ, 762, 143141.
Zhu, M.Y., He, W., Zhang, Q.F., Xiong, Y.Z., Tan, S.D., He, H.M. (2019). "Spatial and temporal characteristics of soil conservation service in the area of the upper and middle of the Yellow River, China". Heliyon, 5(12), e02985

Research on mining method of spatial and temporal distribution information of soil erosion in small watershed

Jing Huang *[1,2], Xinxin Hou[1,2]
1 Key Laboratory of Soil and Water Conservation on the Loess Plateau of Ministry of Water Resources, China
2 Yellow River Institute of Hydraulic Research, China
*Corresponding Author, e-mail:huangjing_hky@163.com

Abstract

The process of soil erosion in small watershed is a typical nonlinear dynamic processes, its internal erosion development and evolution process is very complex, so spatial and time distribution information of soil erosion in small watershed need to be mined, but using current algorithms for mining the information of small watershed soil erosion, only focus on the space distribution information mining of soil erosion, which results in the inefficient minting of spatial and time information. This paper proposes a space-time distribution information mining method for small watershed soil erosion based on density track clustering. The method firstly use water and soil loss equation to form the model for small watershed soil erosion, calculate rainfall erosivity, soil erodibility factor, slope length factor of small watershed area, on the basis of spatial and temporal information included in small watershed soil erosion trajectory, spatial and time neighborhood density of soil erosion is clustered to dig out the temporal and spatial distribution pattern information of soil erosion. The simulation proved that spatial and time distribution information mining method for small watershed soil erosion based on the density cluster of tracks has a high value in the field of soil erosion.

Keywords: Small watershed, Soil erosion, Data mining

1 Introduction

Soil erosion is a global environment problem, which is a serious threat to the survival and development of human beings (Liang et al., 2014; Xu et al., 2013; Liu et al., 2013). It is of great significance to study the spatial distribution of soil erosion in small watershed, and to study the temporal and spatial distribution of soil erosion in small watershed. However, most of the existing methods for the spatial and temporal distribution of soil erosion in small watershed only focus on spatial information, so it is not effective in mining of the temporal and spatial distribution of watershed erosion (Wang et al., 2013; Yue et al., 2015; Ju et al., 2015). Therefore, how to effectively carry out the temporal and spatial distribution information mining of soil erosion in small watershed is the main problem to be solved in this field.

At present, the main stream of time and space information mining methods include the method based on genetic algorithm, ant colony algorithm and neural network algorithm (Liang et al., 2015). Among them, the method of spatial and temporal information mining based on genetic algorithm is often used. But this method can only start mining from the spatial position, and it cannot effectively excavate the temporal and spatial distribution of soil erosion in small watershed.

Aiming at these problems, this paper proposes a space-time distribution information mining method for small watershed soil erosion based on density track clustering. The method firstly use water and soil loss equation to form the model for small watershed soil erosion, calculate rainfall erosivity, soil erodibility factor, slope length factor of small watershed area, on the basis of spatial and temporal information included in small watershed soil erosion trajectory, spatial and time neighborhood density of soil erosion is clustered to dig out the temporal and spatial distribution pattern information of soil erosion. The simulation proved that spatial and time distribution information mining method for small watershed soil erosion based on the density cluster of tracks has a high application value in the field of soil erosion.

2 Temporal and spatial distribution information mining principle of soil erosion in small watershed

During the process of spatial and temporal distribution information mining of soil erosion in small watershed, the spatial location of soil erosion in small watershed within each sampling period is clustered to obtain cluster regions, and the regions are connected according to the time sequence of soil erosion in small watershed, the temporal and spatial track summarizing the soil erosion in small watershed is obtained, through the cumulative probability distribution of time distance of soil erosion to determine the threshold, the time distance between time segment of soil erosion is calculated, in the end, counting the temporal and spatial distribution region of soil erosion in small watershed to complete the mining. Specific steps are as follows:

In the process of spatial and temporal distribution information mining of soil erosion in small watershed, the time weighted method is used to calculate the spatial and temporal clustering center of soil erosion in small watershed represented by :

$$\mathrm{wight}_i=\frac{\mathrm{stay}_{i\cdot\Delta t}}{r_{j\cdot\Delta t}} \quad (1)$$

In the equation, $stay_{i\cdot\Delta t}$ is time weight of soil erosion in small watershed.

3 Optimization of spatial and temporal distribution information mining of soil erosion in small watershed

3.1 Establishment of soil erosion model in small watershed

In the optimized mining process of spatial and temporal distribution information of soil erosion in small watershed, the water and soil loss equation can be used to establish a small watershed soil erosion model, described as below:

$$A=R\cdot K\cdot LS\cdot C\cdot P \quad (2)$$

Wherein, A is soil erosion amount of unit area, R is the rainfall erosion factor, K is the soil erosion factor, L is the slope length factor, S is the slope factor, C is the vegetation cover factor, P is the tillage measure factor.

In the optimized mining process of spatial and temporal distribution information of soil erosion in small watershed, the regional total erosion amount As can be expressed in the following formula:

$$A_s=\sum_{i=1}^{n} a_i A_i \quad (3)$$

In the formula: A_i is the erosion amount of the i unit, and a_i is the area of the unit i.

In the optimized mining process of spatial and temporal distribution information of soil erosion in small watershed, the rainfall erosivity represented by (R) is defined as the index which reflects the ability of rainfall on soil detachment and carrying capacity, which is related to rainfall amount, rainfall kinetic energy, rainfall intensity, rainfall duration, rainfall type and other factors. Rainfall erosion in small watershed is calculated with the following equation:

$$R=\alpha F^{\beta} \quad (4)$$

$$F=N^{-1}\sum_{i=1}^{N}\left[\left(\sum_{j=1}^{12} p_{i,j}^2\right)\cdot\left(\sum_{j=1}^{12} p_{i,j}\right)^{-1}\right] \quad (5)$$

In the formula, $p_{i,j}$ is the rainfall amount of i -th year and j -th month, N is number of years, and R is the average rainfall erosion force for many years, P is the model parameters.

In the optimized mining process of spatial and temporal distribution information of soil erosion in small watershed, the soil erosion factor represented by (K) is defined as the sensitivity of soil to erosion, and the following equation can be used to calculate soil erosion factors:

$$K=0.1317\left(\frac{S_i}{S_i\times C_l}\right)\times\left(1.0-\frac{S_n}{S_n+\exp}\right) \quad (6)$$

In the formula, S_i on behalf of sand content, S_n is silt content, C_l is clay content:

In the optimized mining process of spatial and temporal distribution information of soil erosion in small watershed, (S) is defined as the slope factor, and can be calculated by the following gradient factor formula:

$$S=\sin\theta+0.03\leq\theta\leq\gamma \quad (7)$$

3.2 The realization of optimal mining of spatial and temporal distribution information of soil erosion in small watershed

In the optimized mining process of spatial and temporal distribution information of soil erosion in small watershed, the soil erosion tracks should be labeled as a line segment based on certain rules, and the relative position between the segments is determined by the relative distance, relative length and relative angle of soil erosion, which is explained by the following equation:

$$J(A,B)=1-\frac{|A\cap B|}{|A\cup B|} \tag{8}$$

In the equation, (A,B) is the relative position relationship of the soil erosion trace line segment in the small watershed.

In the optimized mining process of spatial and temporal distribution information of soil erosion in small watershed, assuming that the time span of soil erosion trace line segments in small watershed is T_i and T_j , the time difference (ΔT_{ij}) of soil erosion time zone in small watershed is defined by the following equation:

$$\left(\Delta T_{ij}\right)=\max\left(t_{si},t_{sj}\right)-\min(t_{ei},t_{ej}) \tag{9}$$

In the optimized mining process of spatial and temporal distribution information of soil erosion in small watershed, the time difference represented by $\left(\Delta T_{ij}\right)$ can only reflect difference between the 2 time intervals of soil erosion in small watershed, so it is needed to consider the whole time difference and time span of soil erosion in small watershed, the following equation is used to define the time distance of soil erosion trace space:

$$\begin{cases} T_i=t_{ei}-t_{si} \\ T_j=t_{ej}-t_{sj} \\ disT_{ij}=\Delta T/(T_i+T_j) \end{cases} \tag{10}$$

In the optimized mining process of spatial and temporal distribution information of soil erosion in small watershed, time distance is determined by the time span and time difference of soil erosion spatial and temporal segments in small watershed. The spatial and temporal neighborhood of soil erosion in small watershed is determined as space-time range determined by combing space neighborhood and time neighborhood of soil erosion, thus, the neighborhood range need to be determined from the space and time aspect, and then to be combined. Therefore, the optimized mining of spatial and temporal distribution information of soil erosion in small watershed is determined by using the following equation:

$$\Delta T_{ij}^{'}=\min\frac{(\Delta T_{ij},T_p-T_i-T_j-\Delta T_{ij})}{\varepsilon_s} \tag{11}$$

In the upper, ε_s represents the spatial neighborhood threshold of soil erosion in small watershed.

4 Experiment and simulation

In order to prove the validity of this method, we need to carry out an experiment, and use C++ to build the simulation platform of the temporal and spatial distribution of soil erosion in small watershed.

By using the improved algorithm and the traditional algorithm, the mining experiment for time and space distribution of soil erosion in small watershed is conducted. The accuracy, error rate and stability of two algorithms are compared under different experiment times to measure the overall validity of different algorithms on time and space distribution of soil erosion in small watershed. The results are shown in Table 1 and table 2.

From table 1 and table 2 it can be seen that the overall superiority of the improved algorithm is higher than the traditional algorithm. This is mainly because the improved method uses water and soil loss equation to form the model for small watershed soil erosion, calculates rainfall erosivity, soil erodibility factor, slope length factor of small watershed area, on the basis of spatial and temporal information included in small watershed soil erosion trajectory, spatial and time neighborhood density of soil erosion is clustered to dig out the temporal and spatial distribution pattern information of soil erosion, so as to ensure the effectiveness of improved algorithm for spatial and temporal distribution and has a high application value.

Table 1 The overall effectiveness of temporal and spatial distribution of soil erosion in small watershed of traditional algorithm

Experiment times	Information mining accuracy of traditional algorithm（%）	Information mining error rate of traditional algorithm（%）	Information mining stability of traditional algorithm (%)
15	70	0.5	75
25	70	0.5	75
35	70	0.5	75
45	70	0.5	75
55	70	0.5	75
65	70	0.5	75

Table 2 The overall effectiveness of temporal and spatial distribution of soil erosion in small watershed of improved algorithm

Experiment times	Information mining accuracy of improved algorithm（%）	Information mining error rate of improved algorithm（%）	Information mining stability of improved algorithm (%)
15	96	0.01	98
25	96	0.01	98
35	96	0.01	98
45	96	0.01	98
55	96	0.01	98
65	96	0.01	98

5 Conclusion

Using current algorithms for mining the information of small watershed soil erosion, only focus on the space distribution information mining of soil erosion, which results in the inefficient minting of spatial and time information. This paper proposes a space-time distribution information mining method for small watershed soil erosion based on density track clustering. The method firstly use water and soil loss equation to form the model for small watershed soil erosion, calculate rainfall erosivity, soil erodibility factor, slope length factor of small watershed area, on the basis of spatial and temporal information included in small watershed soil erosion trajectory, spatial and time neighborhood density of soil erosion is clustered to dig out the temporal and spatial distribution pattern information of soil erosion. The simulation proved that spatial and time distribution information mining method for small watershed soil erosion based on the density cluster of tracks has a high value in the field of soil erosion.

Reference

Liang Jiawei,Dai Quanhou,Zhang Xi,et al.Study on Soil Erosion Features of Small Catchment of Karst Plateau Wetland by 137 Cs Tracing Technology[J].Journal of Nuclear Agricultural Sciences.2014,28,137(01):116-122.

Xu Guoce,Li Zhanbin,Li Peng,et al.Quantitative analysis of soil erosion and nutrient loss in Yingwugou watershed of the Dan River[J].Transactions of the Chinese Society of Agricultural Engineering,2013,29(10):160-167.

Liu Wei,Zhang Shaoliang,Zhang Xingyi,et al.Spatial Pattern Prediction of Soil Erosion in Small Typical Watersheds in Black Earth Region[J].Bulletin of Soil and Water Conservation,2013,33(04):224-227.

Wang Chieh,Huang Ying,Huang Songbai,et al.Spatial Difference of Soil Erosion in the Small Watershed of Songhuaba Water Source Area in Kunming City[J].Journal of Yangtze River Scientific Research Institute.2013,(4):21-24.

Yue Dapeng,Li Kui,Liu Peng,et al.Study on soil erosion and soil and water conservation of Huangtuwa watershed based on RUSLE[J].Journal of Shaanxi Normal University(Natural Science Edition),2015,(2):85-91.

Ju Zhansheng,Wen Anbang,Yan Dongchun,Shi Zhonglin,Wang Binyan,Wang Yongyan.Evaluation of Soil Erosion in Small Watershed of the Three Gorges Reservoir Region by Using 137Cs,210Pb and CSLE[J].Journal of soil and water conservation,2015,29(03):75-80.

Liang Zonghua.The application of data mining in precipitation data in Sichuan[J].Western Education Research,2015,(1):123-132.

Spatial distribution characteristics of gravity erosion on Loess Gully Slope

ShiJiao Dong[1], XiangZhou Xu[1]
1 Institute of water environment, Dalian University of technology, Dalian 116024, China
*Corresponding Author, e-mail: xzxu@dlut.edu.cn

Abstract

To explore the influence of rainfall and geomorphic factors on the spatial distribution characteristics of gully slope gravity erosion can provide the basis for monitoring and controlling the gravity erosion disaster in the Loess Plateau. Based on the rainfall simulation experiment of gravity erosion on loess gully slope, the distribution law of collapse, landslide and mud flow erosion on the gully slope and near the gully edge line under the influence of different rainfall and underlying surface was analyzed. The sensitivity analysis method based on variable growth rate was used to analyze the geomorphology and rainfall influencing the gravity erosion near the gully edge line. The results show that. (1) The top of the gully slope is the erosion prone area, the middle of the gully slope is the second, and the slope toe is the weakest. The average ratio of the erosion volume at the top, middle and toe of the gully slope to the total erosion volume is 48%, 33% and 19% respectively. (2) The spatial distribution characteristics of collapse, landslide and mud flow on the loess gully slope are closely related to rainfall and underlying surface. With the increase of rainfall duration, the distribution of landslide erosion on the top and middle of the gully slope increases, which aggravates the development degree of landslide erosion on the top and middle of the slope, and expands the scope of mud flow erosion from the upper part of the gully slope to all parts of the gully slope. With the increase of slope, the volume of collapse erosion increases in the middle and toe of the slope, which aggravates the collapse in the middle and lower part of the gully slope, and the mud flow is mainly concentrated on the top of the slope, which aggravates the development degree of the mud flow on the top of the slope. With the increase of slope height, the erosion volume of collapse and landslide increases at the toe of slope, which intensifies the development degree of collapse and landslide at the toe of slope. The erosion volume of mud flow increases at the top of slope, which intensifies the development of mud flow at the top of slope （3) The sensitivity of different gravity erosion types near the gully edge line to rainfall duration and gully slope geomorphic change is different. In terms of the total amount of gully edge line erosion, collapse, landslide and mudflow are the most sensitive to rainfall duration, and the corresponding sensitivity coefficients are 0.6, 34.2 and 9.1. From the maximum single collapse of the gully edge line, the landslide and mud flow are most sensitive to the rainfall duration change, and the sensitive corresponding sensitivity coefficient is 13.8 and 6.5, and the collapse is the most sensitive to the change of slope height, and the sensitivity coefficient is 0.6.

Key words: Gravity erosion, Rainfall simulation test, Loess gully sidewall, Sensitivity analysis, Gully edge line

1 Introduction

Gravity erosion refers to the process of rock and soil mass losing balance and moving under the action of gravity, including landslide, collapse, mud flow and other forms (Tang 2004). Gravity erosion is serious in the Loess Plateau, which is one of the most serious areas of soil erosion in China. It is also the main source of sediment in the Yellow River. In 2019, the area of soil and water loss in the Loess Plateau of Northwest China will be 2.1×10^5 km^2, accounting for 36.56% of the total land area. Although compared with 2018, the area of soil and water loss will be reduced by 3.6×10^3 km^2, by 1.69%, the soil erosion is still serious (Bulletin 2019). Prevention and control of soil erosion are the main contents and fundamental measures of ecological protection in the Yellow River Basin. In 2019, General Secretary Xi gave rich instructions to the Yellow River Basin, and proposed to promote the ecological protection and high-quality development of the Yellow River Basin (Yang et al., 2019). The loess gully region is an important part of the Loess Plateau. The loess gully is divided into two parts: gully land and ridge land, and the ridge land is divided into gully slope and gully channel (Yu et al., 2018). The slope of gully slope is broken, the slope is steep and the erosion is serious. It is the main slope section of gravity erosion and the main area of sediment production in the basin. At present, most scholars focus on the contribution of erosion and sediment in gully slope system, but few on the spatial distribution characteristics of gully slope system (Cao et al., 2017). The Loess Hilly and gully region is an important natural geography research area (Zhu et al., 2014; Jiang et al., 1966). The study of the geomorphic characteristics of the Loess Plateau can not only explore the relationship between gravity erosion and geomorphic morphology, but also be conducive to the study of soil and water loss. Among them, the gully edge line is an important structural line of loess landform. Taking the gully edge line as the boundary, splash erosion and sheet erosion occur above the gully edge line, and gully cutting and gravity erosion occur below the gully edge line. The research of gully edge line started in 1960s by domestic scholars. The research on the edge line mainly lies in the determination of the location, type division and automatic extraction of the edge line (Jiang et al., 1966; Xiao et al., 2007; Zhou et al., 2010). There are few studies on the evolution characteristics and influencing factors of gully edge line. The causes of gravity erosion are complex, and the influencing factors can be divided into two categories, one is internal, including the physical and chemical properties of loess, topography, the other is external, including climate change, vegetation, human activities (Yang et al., 2010). Among them, slope is the most typical influencing factor of gravity erosion in topography, and the occurrence frequency, scale and spatial distribution characteristics of gravity erosion are related to slope (Liu and Wu 1993). Field survey results of a typical small watershed in the Loess Plateau show that collapses mostly occur on gully slopes above 55°. Landslides have a wide range of slopes, mostly between 35°-55° (Zhao et al., 2020). Rainfall is another important factor inducing gravity erosion. Most of gravity erosion occurs in the process of rainfall or shortly after the end of rainfall (Xu et al., 2015). Rainfall infiltration increases soil moisture content, bulk density, shear strength and sliding resistance, which leads to instability. The analysis of influencing factors of gully slope gravity erosion is not only conducive to the study of evolution characteristics of gravity erosion, but also of great significance to the planning of soil and water conservation in small watershed.

In this paper, the distribution of gravity erosion on loess gully slope is analyzed through the rainfall simulation test of gravity erosion under different slope height, slope, rainfall duration and other specific conditions. The influence of rainfall and underlying surface on the distribution of erosion amount of collapse, landslide and mudflow is analyzed. The sensitivity of gravity erosion to slope, slope height and rainfall duration was evaluated. The results provide a scientific basis for early warning of gravity erosion disaster and planning of soil and water conservation in the Loess Plateau.

2 Materials and methods

The rainfall simulation experiment of gravity erosion on loess gully slope was carried out in the soil erosion Joint Laboratory of Tsinghua University, Dalian University of technology from June 2012 to September 2012. According to the literature and field investigation, the Loess Gully Slope test model is constructed. The model consists of gentle slope, steep slope and gully. The gentle slope is 3°. The steep slope is 60°, 70°, 80°. The vertical projection of the model gully slope is 300 cm long and 300 cm wide. The soil sample of the model test is loess below 2 m of the surface, and the dry bulk density of loess is 1.56×10^3 kg/m^3, and the average particle size of loess is D50. When shaping the terrain, it is constructed by hand. The test equipment used in the test mainly includes rainfall simulator, topography meter and automatic moisture detector. The rainfall simulator developed by Dalian University of technology mainly provides rainfall for gully slope gravity erosion. The rainfall coverage is 3.5 m×3.5 m. The rainfall uniformity is over 80%. Rainfall intensity is 0.8 mm/min. A total of seven groups of terrain, each terrain for 5 rainfall, each rainfall interval of 12 hours. The change of steep slope topography in the process of rainfall was monitored in real time by using a topography meter. According to the volume difference before and after the occurrence of gravity erosion, the volume of gravity erosion is calculated quantitatively. The automatic moisture detector is used to monitor the soil water content at different depth of gully slope in real time. The type, location and degradation process of gravity erosion were determined by the combination of manual observation and video check of topography meter. Different from the traditional contact observation tools, the topography meter can make real-time dynamic quantitative observation of the random gravity erosion on the gully slope. A set of horizontal laser lines are emitted by topography meter on the steep slope of the model, and the recorder on the upper part of the model can record the change process of terrain and contour during rainfall. By using R2V software to vectorize the terrain contour and modeling in Arc GIS, the model volume at any time can be obtained. By calculating the volume difference before and after the occurrence of gravity erosion, the collapse amount of any gravity erosion can be obtained.

In order to analyze the distribution law of gravity erosion in loess gully slope, the photos of gravity erosion and landslide taken by topography meter camera are imported into CAD, and the gully slope is divided into nine areas by CAD. The distribution of the gully slope is shown in Fig. 1, and the area where the landslide occurs is analyzed. When the volume of a gravity erosion is small, the occurrence area accounts for one of the nine areas, then which area occurs and which area is recorded. When the volume of a gravity erosion is large, the occurrence area is two or more of nine areas, so it is necessary to divide the gravity erosion. Take G as the parameter of gravity erosion, unit 10^3 cm^3. Describe the area of gravity erosion, and divide the gravity erosion. Firstly, the area M_i of gully slope area is calculated by CAD. Then the erosion area E_i is calculated. Then the ratio of erosion area E_i to gully slope area M_i was calculated.

$$P_i = E_i/M_i \tag{1}$$

Then the sum $\sum P_i$ of the ratio of the erosion area E_i to the gully slope area M_i is calculated

$$\sum P_i = \sum\left(\frac{E_i}{M_i}\right) \tag{2}$$

Finally, the gravity erosion is divided according to the proportion.

$$G_i = G \times \left(\frac{E_i}{M_i}\right) \div \sum(E_i/M_i) \quad (3)$$

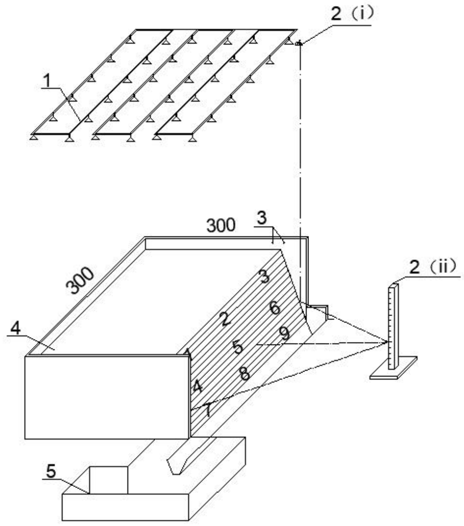

Note: 1) rainfall simulator; 2) topography meter r (I camera with sighting instrument, II host machine); 3) Control points; 4) Model slope; 5) Catchment basin

Figure 1 Experimental layout of gravity erosion process of gully slope.

Table 1 Division process of gravity erosion.

	Zone 1	Zone 2	Zone 3	Zone 4	Zone 5	Zone 6	Zone 7	Zone 8	Zone 9
Gully slope area M_i	M_1	M_2	M_3	M_4	M_5	M_6	M_7	M_8	M_9
Erosion area E_i	E_1	E_2	E_3	E_4	E_5	E_6	E_7	E_8	E_9
E_i/M_i	E_1/M_1	E_2/M_2	E_3/M_3	E_4/M_4	E_5/M_5	E_6/M_6	E_7/M_7	E_8/M_8	E_9/M_9

$$\sum\left(\frac{E_i}{M_i}\right) \quad (4)$$

$$G_i = G \times \left(\frac{E_i}{M_i}\right) \div \sum(E_i/M_i) \quad (5)$$

The slide body is located in yellow in Fig. 2, and the erosion volume G is $43.7\times10^3 cm^3$. The erosion occurred in areas 1, 2, 4 and 5. The gravity erosion is divided. According to CAD calculation, the M_1 area of region 1 is 117.5, the M_2 area of region 2 is 120.5, the M_4 area of region 4 is 105.0, and the M_5 area of region 5 is 113.9. According to the classification of the erosion volume, the area E_1 occurring in region 1 is 39.4, the area E_2 occurring in region 2 is 59.6, the area E_4 occurring in region 4 is 28.0, and the area E_5 occurring in region 5 is 61.4. The ratio of erosion area E to gully slope area M is calculated E_i/M_i. Then calculate all ratios and $\sum(E_i/M_i)$. Finally, the gravity erosion is divided according to the proportion, $G_i = G \times \left(\frac{E_i}{M_i}\right) \div \sum(E_i/M_i)$.

Table 2 Division process of gravity erosion case - Case 1.

Zone	1	2	3	4	5	6	7	8	9
Gully slope area M_i	117.5	120.5		105.0	113.9				
Erosion area E_i	39.4	59.6		28.0	61.4				
E_i/M_i	0.3	0.5		0.3	0.5				
$\sum\left(\frac{E_i}{M_i}\right)$				1.6					
$G_i = G \times \left(\frac{E_i}{M_i}\right) \div \sum(E_i/M_i)$	9.0	13.2		7.1	14.4				

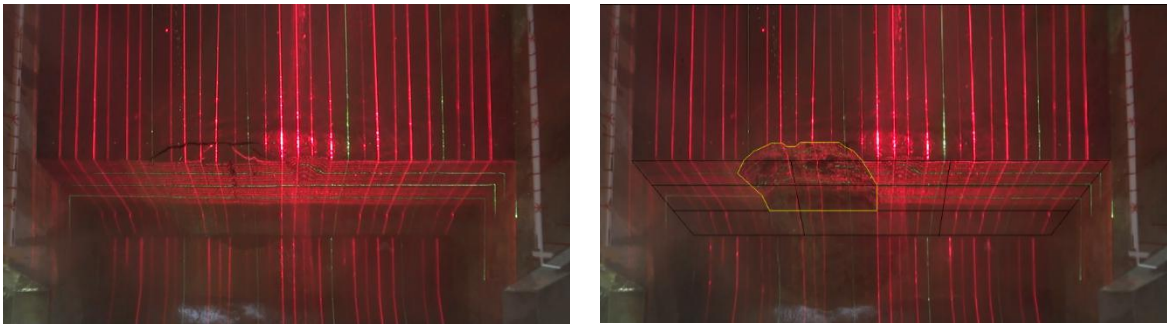

(a) Before landslide (b) After landslide

Figure 2 A landslide event in the test

In order to analyze the influence of rainfall duration, slope gradient and slope height on the distribution of gravity erosion in gully and slope, the experiment was divided into the following groups: M_1 (L30-1-70d, L30-1-80d) vs M_2 (L60-1-70d, L60-1-80d). The former group rainfall duration was 30min, and the latter group rainfall duration was 60min. M_3 (L60-1-70d, L60-1.5-70d) vs M_4 (L60-1-80d, L60-1.5-80d). The slope of the former group is 70°, the slope of the latter group is 80°. M_5（L60-1-70d, L60-1-80d）vs M_6（L60-1.5-70d, L60-1.5-80d. The slope height of the former group is 1 m, and that of the latter group is 1.5 m. L30-1-70d is rainfall duration of 30 min, slope height of 1 m and slope of 70°. The sensitivity analysis method based on growth rate is proposed by Xu (Xu et al., 2015). Through the independent variable rate of change compared with dependent variable change rate, the sensitivity of independent variable to dependent variable is quantitatively analyzed. The steps are as follows:

Firstly, the average values of the maximum single landslide amount and total erosion amount of each group of tests are calculated. Then, the independent variable growth rate is calculated under a single variable. That is, with the increase of rainfall duration, slope and slope height, the growth rate of gravity erosion R_g. The formula is as follows:

$$R_g = (g_2 - g_1)/g_1 \tag{6}$$

where g_1 is the amount of gravity erosion before the change of influencing factors. g_2 is the amount of gravity erosion after the change of influencing factors.

Then calculate the growth rate of influencing factors R_t. The formula is as follows:

$$R_t = (t_2 - t_1)/t_1 \tag{7}$$

where t_1 is the value before the change of influence factor, t_2 is the value after the change of influence factor. Finally, the sensitivity parameter S of gravity erosion volume to influence factors is calculated. The formula is as follows:

$$S = R_g/R_t \tag{8}$$

3 Results

3.1 Spatial distribution of gravity erosion on Loess Gully Slope

The scale and frequency of gravity erosion on gully slope of loess are related to its location. The experiments show that the average erosion volume at the top, middle and foot of gully slope is 230.5×10^3 cm^3, 156.0×10^3 cm^3 and 92.0×10^3 cm^3, respectively. The average erosion volume ratio of the top, middle and foot of the gully slope to the total volume ratio of erosion was 48%, 33% and 19%, respectively. It can be seen from Table 3 that the maximum and minimum erosion volume ratio of area 1, 2 and 3 at the top of the gully slope to the total erosion volume ratio is 55% and 41% respectively, which is greater than the erosion volume of the middle and foot of the gully slope. The average frequency of gravity erosion at the top, middle and foot of the slope was 19, 7 and 5, respectively. The average ratio of gravity erosion at the top of slope, middle slope and toe to total erosion times was 63%, 22% and 15%, respectively. That is, the probability of erosion at the top of the gully slope is greater than that at the middle and foot of the gully slope. Combined with the erosion volume distribution in Fig. 2, it can be found that the top of the gully slope is the erosion prone area, followed by the middle of the gully slope, and the erosion at the foot of the gully slope is the weakest, indicating that the higher topography of the upper gully slope is more conducive to the occurrence

Table 3 Distribution of secondary gravity erosion in gully and slope

Terrain group	Ratio of erosion volume of each part of slope to total erosion volume / (%)			Ratio of erosion times of each part of slope to total erosion times / (%)		
	Top of gully slope	Middle of gully slope	Toe of gully slope	Top of gully slope	Middle of gully slope	Toe of gully slope
L60-1-60d	43%	32%	25%	49%	29%	22%
L60-1-70d	51%	40%	9%	49%	27%	23%
L60-1-80d	55%	31%	13%	57%	28%	15%
L60-1.5-70d	48%	32%	20%	64%	18%	18%
L60-1.5-80d	41%	31%	27%	90%	6%	4%
L30-1-70d	53%	29%	18%	68%	24%	8%
L30-1-80d	48%	31%	21%	80%	17%	3%
Average value	48%	33%	19%	63%	22%	15%

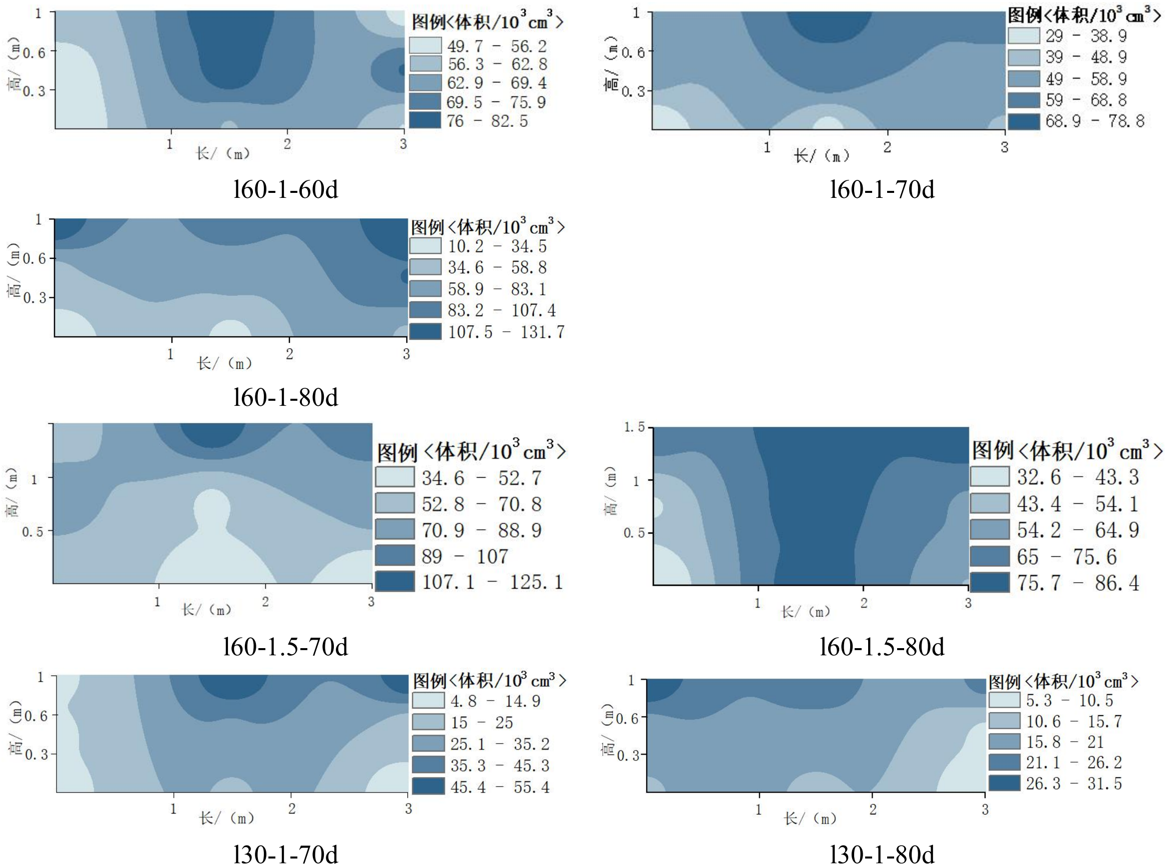

Figure 3 Distribution of erosion volume.

of erosion events. Relying on the Soil and Water Loss Laboratory, Yang analyzed the phylogenetic process of gully slope from a spatial perspective, and concluded that the lower part of slope to the upper part of gully slope was the area prone to erosion (Yang et al., 2018). The average frequency of gravity erosion on the left, the middle and the right side of the gully slope was 11, 11 and 8, respectively, which indicated that there was little difference in the erosion frequency at each position in the same horizontal direction of the slop.

3.2 Distribution law of gully slope collapse, landslide and mudflow erosion in loess

The distribution of three erosion phenomena of collapse, landslide and mudflow on gully slope under the influence of rainfall and underlying surface was analyzed. When the rainfall duration increased from 30 min to 60 min, the amount of erosion by collapse, landslide and mudflow increased, among which the amount of erosion by collapse, landslide and mudflow increased by 0.3 times, 25.6 times and 16.1 times. The data of collapses, landslides and corresponding rainfall in Shaanxi Loess Plateau show that landslides need more rainfall than collapses. With the increase of rainfall duration, the ratio of collapse erosion volume at the top of slope to the total erosion volume increased from 51% to 62%, and the ratio of collapse erosion volume at the foot of slope to the total erosion volume decreased from 19% to 12%. The ratio of erosion volume of slope top to total erosion volume increased from 42% to 52%, and that of slope toe decreased from 21% to 9%. The proportion of erosion volume of mud flow at the top of slope to the total erosion volume decreased from 100% to 42%, the proportion of erosion volume of mud flow at the middle of slope to the total erosion volume increased from 0% to 33%, and the proportion of erosion volume of mud flow at the foot of slope to the total erosion volume increased from 0% to 25%. It can be seen from Figure 4 that with the increase of rainfall duration, the occurrence of collapse erosion on the top of slope is intensified, the distribution of landslide erosion on the top and in the slope is increased, and the development degree of erosion on the top and in the slope is aggravated. The scope of mud flow erosion is expanding from the upper part of gully slope to all parts of gully slope.

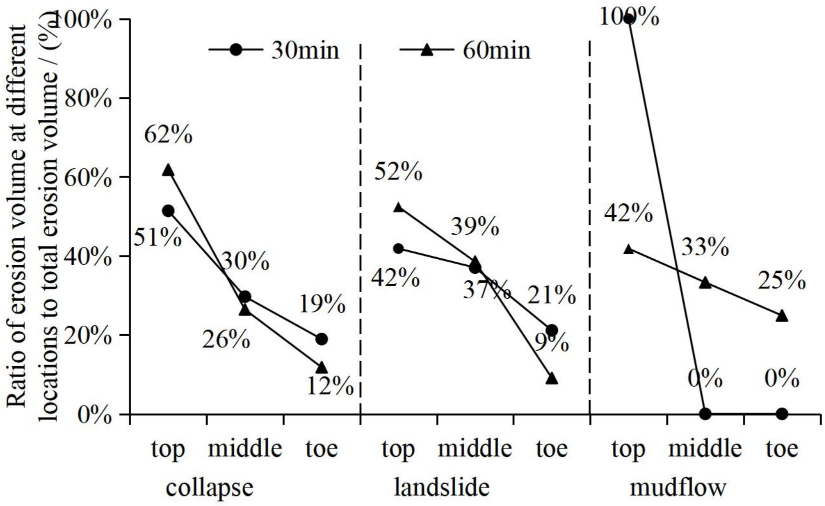

Figure 4 Relationship between distribution of collapse, landslide, mud flow erosion and rainfall.

The underlying surface is another important factor affecting the gravity erosion. The slope not only affects the frequency of collapse, landslide and mud flow, but also affects its scale and distribution. When the slope changes from 70° Increase to 80°, the results show that the erosion volume ratio of the top of the slope to the total erosion volume decreases from 58% to 49%, that of the toe of the slope increases from 14% to 22%, that of the top of the slope increases from 43% to 47%, that of the middle of the slope decreases from 44% to 34%, and that of the toe of the slope increases from 13% to 19%. When the slope is 70° The volume of soil erosion was distributed in all parts of gully slope. When the slope is 80° The mud flow only occurs at the top of the slope. With the increase of slope, it is conducive to the occurrence of landslide and weaken the occurrence of collapse and mudflow, in which the amount of collapse and mudflow erosion decreases by 0.3 times and 0.8 times respectively, and the amount of landslide erosion increases by 0.6 times. It can be seen from Fig. 5 that with the increase of slope, the development degree of collapse in the middle and lower part of gully slope is intensified, the development degree of collapse in the upper part of gully slope is slowed down, the development degree of landslide at the top and toe of gully slope is increased, the development degree of landslide in the middle part of gully slope is weakened, and the development degree of mud flow at the top of slope is intensified.

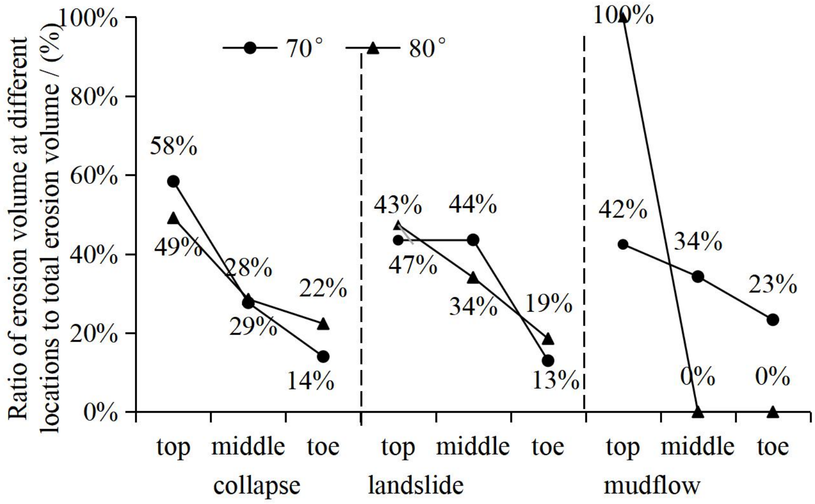

Figure 5 Relationship between distribution of collapse, landslide, mud flow erosion and slope.

The slope height also has an important effect on the gravity erosion. When the slope height is 1.0 m, the volume ratio of collapse erosion at the top, middle and toe of the slope is 62%, 26% and 12%, respectively, and when the slope height is 1.5 m, the volume ratio of collapse erosion at the top, middle and toe of the slope is 50%, 29% and 21%, respectively. When the slope height increases from 1.0 m to 1.5 m, the ratio of the erosion volume of the top slope to the total erosion volume decreases from 52% to 35%, the ratio of the erosion volume of the middle slope to the total erosion volume decreases from 39% to 36%, and the ratio of the erosion volume of the foot slope to the total erosion volume increases from 9% to 29%. The ratio of the erosion volume of the top of the slope to the total erosion volume increased from 42% to 89%, the ratio of the erosion volume of the middle slope to the total erosion volume decreased from 33% to 11%, and the ratio of the erosion volume of the foot of the slope to the total erosion volume decreased from 26% to 0%. With the increase of slope height, it is conducive to the occurrence of collapse, and the amount of landslide and mudflow erosion decreases. The amount of collapse erosion increases by 0.6 times, while the amount of landslide and mudflow erosion decreases by 0.4 times and 0.7 times respectively. Fig. 6 shows that with the increase of slope height, the distribution of collapse and landslide erosion volume increases at the toe of the gully slope, and the distribution of mud flow erosion volume at the top of the slope increases, which aggravates the collapse and development degree of slope toe and the development of mud flow at the top of the slope.

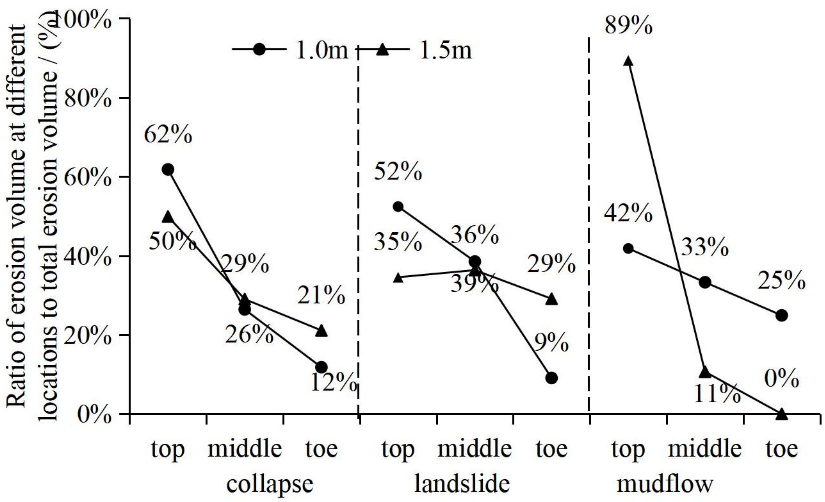

Figure 6 Relationship between distribution of collapse, landslide, mud flow erosion and slope heigh

3.3 Erosion distribution law of gully edge line

A total of 214 landslides occurred in the rainfall simulation test of gully slope of loess, among which 125 erosion occurred near gully margin, accounting for 58% of the total erosion. In the erosion near the gully edge, the frequency of collapse, landslide and mudflow erosion accounted for 62%, 33% and 6% of the total frequency of gully edge erosion, respectively. The erosion of landslide, landslide and mudflow accounted for 54%, 44% and 2% of the total erosion of gully margin, respectively. The gully margin line is the dividing line between slope surface and gully slope, with large elevation difference and easy to collapse. Collapse is the direct separation of soil from the parent body, which happens quickly, and will not only cause property losses, but also cause casualties.

Different types of gravity erosion near the gully margin have different sensitivity to rainfall duration and gully slope topography. As can be seen from Fig. 7, the sensitivity coefficients of total erosion of landslide, landslide and mudflow to rainfall duration in a test were all positive, 0.6, 34.2 and 9.1, respectively. The results showed that with the increase of rainfall duration, the volume of landslide, landslide and mudflow erosion along the gully margin increased, and the change of rainfall duration had a significant effect on the total erosion of landslide and mudflow along the gully margin. For the maximum single landslide amount near the gully margin in an experiment, the sensitivity coefficients of maximum landslide and mudflow erosion amount to rainfall duration were 13.8 and 6.5 respectively, indicating that the variation of rainfall duration was more likely to trigger large-scale landslides and mudflow. From the perspective of total erosion of gully edge, landslide and mudflow are more sensitive to slope change, and their sensitivity coefficients are 3.7 and -2.5, respectively. The sensitivity coefficient of landslide and mudflow to slope was 1.6 and 0.7, respectively, for the maximum single slide amount near the gully edge line in one test. It shows that the higher the slope is, the more conducive to the occurrence of landslide near the gully margin, and the less conducive to the occurrence of mudflow near the gully margin. Sensitivity coefficients of total erosion of collapse, landslide and mudflow near the gully margin to slope height are all negative, which are -0.3, -1.6 and -1.7, respectively. It is shown that the increase of slope height has a certain inhibitory effect on the amount of erosion by collapse, landslide and mudflow near the gully margin. In general, for the landslide erosion near the gully margin, the duration of rainfall has the greatest influence and is a promoting effect, while the slope height has a small influence and is a inhibiting effect. For the mudflow, rainfall duration is the biggest influencing factor, the longer the rainfall duration is, the more conducive to the mudflow, while the topography factor has less influence. For the collapse near the gully edge line, rainfall duration is the biggest influencing factor of the collapse, and it is the promoting effect.

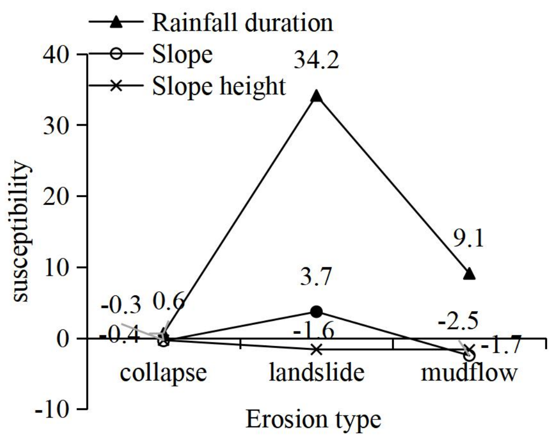

Figure 7. Sensitivity analysis of total erosion amount near gully edge line.

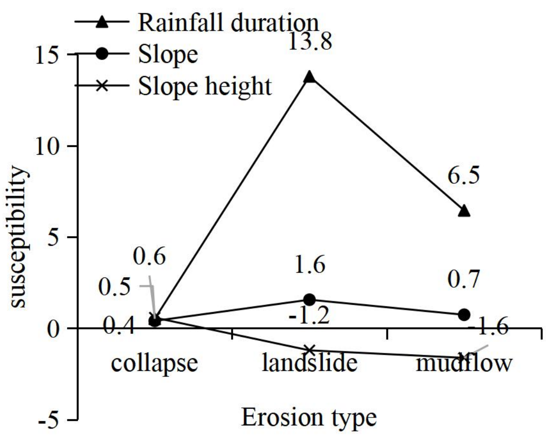

Figure 8. Sensitivity analysis of single erosion maximum near gully edge.

4 Discussion and analysis

The results show that the erosion volume and frequency in different horizontal directions are quite different, but in the same horizontal direction, the erosion volume and frequency in different parts of the slope are almost the same. The erosion at the top of the gully slope is the most severe, and the erosion at the foot of the slope is the weakest. Relying on the laboratory of soil and water loss, Yang (Yang et al., 2017) analyzed the erosion development process of gully slope system from the perspective of space, and concluded that the lower part of slope to the upper part of gully slope is the erosion prone area. Yang (Yang 2007) obtained that the intensity of slope erosion is basically similar in the horizontal direction through the indoor artificial rainfall simulation test. In the total volume of gravity erosion, the erosion volume ratio of slope top, slope middle and slope toe are 48%, 33% and 19% respectively, which indicates that slope top erosion has significant contribution to gully slope gravity erosion. Therefore, more attention should be paid to gully slope top erosion in the study of gravity erosion.

Precipitation is the main cause of gravity erosion. When the sliding force of slope soil is greater than the shear strength of soil, the phenomenon of gravity erosion is caused. Landslides are most sensitive to rainfall duration, and a long period of rainfall will lead to large-scale landslides. According to literature statistics, about 70% of the total number of landslides are caused by rainfall, and up to 95% of landslides occur in the rainy season (Zhong 2015). The rainfall duration has an important impact on the distribution of landslide on the gully slope. With the increase of rainfall duration, the amount of landslide erosion increases on the top and middle of the gully slope respectively, which intensifies the degree of erosion development on the top and middle of the slope. Although the landslide occurs slowly, it has a large volume and will cause property losses. In the medium intensity rainstorm on the Loess Plateau, we should pay special attention to the occurrence of the landslide in the middle and upper part of the gully slope. Slope is one of the important factors of landform. When the slope degree of gully is large, the shear force on soil increases, and the slope Angle where gravity erosion occurs is easy to reach the internal friction Angle, resulting in material movement (Yu et al., 2019). The experimental results show that the higher the slope is, the lower the volume of collapse erosion and the higher the volume of landslide erosion. Jin Xin (Jin et al., 2020) simulated complex terrain by $FLAC_{3D}$, analyzed the distribution process of slope gravity erosion, and concluded that the gravity erosion increased with the increase of slope. Slope not only affects the scale and frequency of gravity erosion, but also has a certain impact on the spatial distribution characteristics of gravity erosion. With the increase of slope, the development degree of collapse in the middle and lower part of gully slope is intensified, the development degree of collapse in the upper part of gully slope is slowed down, the development degree of landslide at the top and toe of gully slope is increased, the development degree of landslide in the middle part of gully slope is weakened, and the development degree of mud flow at the top of slope is intensified. Although the slope height has no obvious effect on the total volume of gravity erosion, the volume of collapse erosion increases and the volume of landslide erosion decreases with the increase of slope height. According to literature statistics [23-24], most collapses occur at the slope height of more than 20 m, and the probability of collapse increases with the increase of slope height. The slope height also had a certain influence on the distribution of gravity erosion. With the increase of slope height, the erosion volume of collapse and landslide moved from the distribution of gully slope to the foot of gully slope, which intensified the erosion development in the middle and lower part of gully slope and slowed down the erosion development in the upper part of gully slope (Xu et al., 1999).

In this paper, the sensitivity analysis method based on variable growth rate is used to evaluate the impact of rainfall and geomorphic factors on gully edge erosion. This method can quantitatively and accurately describe the sensitivity of gully edge erosion to influencing factors and avoid the influence of gravity erosion randomness. For the total amount of gully erosion, the rainfall duration has the greatest impact on the gully collapse, landslide and mud flow, and it is the promoting effect, followed by the slope, and the slope height has the least impact. For the single maximum erosion amount of gully edge line, rainfall duration has the greatest impact on landslide and mud flow, and slope height has the greatest impact on collapse. For the Loess Plateau region, we should pay special attention to long-term rainfall, which may lead to large landslides.

5 Conclusion

(1) The top of the gully slope is the most prone area to erosion, the middle of the gully slope is the second, and the foot of the gully slope is the weakest. In the rainfall simulation test of loess gully slope, the average erosion volume ratio at the top, middle and toe of gully slope to the total volume ratio of erosion is 48%, 33% and 19%, respectively.

(2) The distribution of erosion volume of collapse, landslide and mudflow on gully slope of loess is closely related to rainfall and underlying surface. When the rainfall duration increased from 30min to 60min, the distribution of landslide erosion in the top and middle of the gully slope increased, which aggravated the degree of landslide erosion at the top and middle of the gully slope, and the range of mudflow erosion expanded from the upper part of the gully slope to all parts of the gully slope. With the slope increasing, the volume of collapse erosion increases in the middle and foot of the gully slope respectively, which aggravates the collapse in the middle and lower slopes. The mudflow mainly concentrates on the top of the gully slope, which aggravates the development of mudflow on the top of the gully slope. When the slope height increased from 1.0m to 1.5m, the erosion volume of collapse and landslide increased at the toe of the slope, which intensified the degree of collapse and landslide development. The erosion volume of mudflow increased at the top of the slope, which accelerated the development of mudflow.

(3) In terms of the total amount of gully edge erosion, collapse, landslide and mudflow are the most sensitive to rainfall duration, and the corresponding sensitivity coefficients are 0.6, 34.2 and 9.1, respectively. For the single maximum erosion of gully edge, rainfall duration has the greatest impact on landslide and mudflow, with sensitivity

coefficients of 13.8 and 6.5, and slope height has the greatest impact on collapse, with sensitivity coefficient of 0.6.

This study is based on the loess gully slope rainfall simulation experiment. It is suggested that more experimental studies on the spatial distribution of gravity erosion should be carried out in the future, the spatial and temporal distribution characteristics of gully slope system should be deeply analyzed, and more comparative experiments should be carried out to reduce the influence of test error and gravity erosion randomness on accuracy.

Reference

Tang K-L. (2004). “Soil and water conservation in China”. Beijing: Science Press.

Bulletin of China on Soil and water conservation in 2019. (2020). Bulletin of Ministry of water resources of the people's Republic of China, 1-47.

Hu C-H, Zhang X-H. (2020). “Soil erosion control on the Loess Plateau and the change of water and sediment in the Yellow River”. Water conservancy and hydropower technology, 51 (01): 1-11.

Yang H-Y, Zhang G-H, Zhang B-J. (2019) “Growth characteristics of typical plant communities on gully slope in Loess Hilly and Gully Region”. Soil and water conservation research, 26 (02): 62-67.

Yu T, Zhang X, Li Z-B, Li P, Li C. (2018). “Difference of erosion and sediment yield of slope gully system under different grass coverage”. Journal of soil and water conservation, 32 (06): 22-27.

Cao J-J, Fang X, Na J-M, Tang G-A. (2017). “Study on the undulation characteristics along the gully in different geomorphic types of the Loess Plateau Based on multifractal”. Geography and geographic information science, 33 (04): 51-56.

Zhu T-X. (2012). “Gully and tunnel erosion in the hilly Loess Plateau region, China”. Geomorphology, 153-154:

Wang W-L, Lei Alin, Li Z-B, et al. (2004). “Experimental study on spatial and temporal distribution of slope erosion and water inflow from uphill in Loess Area”. Journal of water conservancy, (05): 25-30.

Jiang D-Q, Zhao C-X, Chen Z-L. (1966). “Preliminary analysis of runoff and sediment sources in small watershed of Middle Yellow River”. Journal of Geographical Sciences, (01): 20-36

Xiao C-C, Tang G-A. (2007). “Classification of types along loess landform gully”. Geography of arid area, (05): 646-653.

Zhou Y, Tang G-A, Wang C, et al. (2010). “Automatic segmentation of positive and negative terrain of loess landform based on high resolution DEM”. Geoscience, 30 (02): 261-266

Shi Y-C. (2012). “GIS / RS based evaluation of influencing factors and erosion risk along the gully in Pi sha Sandstone Area “. China University of Geosciences (Beijing).

Gao C-D, Yao Z-Q, Li P-F, et al. (2020). “Research progress of gravity erosion on Loess Plateau”. Yellow River, 42 (06): 99-105

Yang J-S, Yao W-Y, Ma S-H, Ma S-P, Shen Z-Z. (2010). “Analysis on Influence Factors of small scale gravity erosion in gully region of Loess Plateau”. Soil and water conservation research, 17 (06): 5-8.

Liu B-Z, Wu F-Q. (1993). “Gully erosion and development in Loess Plateau”. Journal of Northwest Forestry University, (02): 7-15.

Zhao X-Y, Xu X-Z, Jiang Y-Z, Gao H, Zhang H-W. (2020). “Effect of vegetation on gravity erosion of loess gully slope under rainstorm”. Journal of soil and water conservation, 34 (01): 58-63.

Xu X-Z, Liu Z-Y, Xiao P-Q, et al. (2015). “Gravity erosion on the steep loess slope: Behavior, trigger and sensitivity”. Catena, 135:231-239.

Yang C-X, Li L, Wang J-X, et al. (2017). “Experimental study on temporal and spatial distribution characteristics of erosion in slope gully system”. Yellow River, 39 (01): 95-97.

Yang L. (2007). “Study on soil erosion law of different slope shapes”. Shenyang Agricultural University.

Zhong S. (2015). “Study on permeability of landslide soil under rainfall”. Chengdu University of technology.

Yu L, Xu X-Z, Zhang M-S, Liu G-Q. (2019). “Sensitivity analysis of gravity erosion to geomorphic factors in Loess Plateau”. Journal of soil and water conservation, 33 (04): 119-125.

Jin X, Liu Z, Wang C-Z, et al. (2020). “Numerical simulation of gravity erosion on artificial loess slope”. China Rural Water Conservancy and hydropower, (08): 40-45.

Li P-F. (2017). “Study on development characteristics and stability evaluation of bank slope collapse of Hong Shi Yan water control project”. Jilin University.

Xu Y-N, Kuang S-F, Li W-W. (1999). “Influence of slope shape on collapse”. Sediment research, (05): 69-75

LASOSU2021:International Forum on Land Degradation, Soil Conservation and Sustainable Development, 2021